Chemistry Council
OF NEW JERSEY

December 21, 2020

**VIA ELECTRONIC MAIL**
watersupply@dep.nj.gov
cooper@aesop.rutgers.edu

**RE: 1,4-DIOXANE PUBLIC COMMENT**

To Dr. Keith Cooper:

On behalf of our members, the Chemistry Council of New Jersey (CCNJ) and the Site Remediation Industry Network (SRIN) appreciate the opportunity to provide comments to the Drinking Water Quality Institute (DWQI) pursuant to the Institute's request for public input regarding the recently released subcommittee reports on 1,4-dioxane. CCNJ/SRIN have long advocated for greater transparency and public input with respect to DWQI's activities, and we appreciate this opportunity.

Below is a summary of our key points; CCNJ/SRIN recommend that DWQI conduct:

- Full consideration of the implications of the conclusions of the November 2020 United Stated Environmental Protection Agency (USEPA) Toxic Substances Control Act (TSCA) *Draft Supplemental Analysis to the Draft Risk Evaluation for 1,4-Dioxane*, which concluded that all consumer uses present no unreasonable health risk to consumers and bystanders;
    - In addition, the USEPA evaluated acute and chronic incidental exposures via oral and dermal routes from recreational swimming in ambient water and determined that this activity presents no unreasonable risk to the general population.
- Thorough review of the latest research and guidance on ***how*** to use the best available science;
- A cost/benefit analysis of treating 1,4-dioxane via Advanced Oxidation in addition to other treatment techniques to achieve perfluorinated Maximum Contaminant Level (MCL) requirements in order to ensure the full economic burden of multiple treatment trains is fully understood for communities; and
- Professional reevaluation of the latest peer-reviewed mode of action (MOA) science, focused on 2013 to present, to ensure the carcinogenic potential of 1,4-dioxane is understood and properly corrected to reflect the known threshold required for mammals to develop liver cancer.

CCNJ/SRIN agree with, and incorporate by reference, the additional comments from the American Chemistry Council dated December 21, 2020 (attached as Appendix A) without duplicating the detailed and extensive underlying supporting scientific themes.

## General Comments

Overly (unnecessarily) restricting the content of 1,4-dioxane in drinking water has significant economic implications for New Jersey's future. While toxicology research continues to explore the difficult and multifaceted biokinetic mechanisms behind human metabolism of 1,4-dioxane, CCNJ/SRIN members are particularly concerned that DWQI is relying on "others" to weigh the health risks (but not conduct a cost-benefit analysis) of 1,4-dioxane. This concern highlights the need to fill the expertise gaps on the DWQI board, particularly with an environmental health expert on 1,4-dioxane and a water purveyor who has evaluated the unique technical challenges and costs associated with removing 1,4-dioxane from water. From a toxicology perspective, New Jersey is following the (outdated) USEPA and the state of California precedents, for the most part, without robust or transparent review of the updated science. Relying on these other policy-driven agency conclusions leaves little scientific basis; foundationally, the front (science) end of the 1,4-dioxane limit ***must*** be sound, particularly where policy demands mathematic protection against a 1E-06 excess risk associated with a lifetime of hypothetical exposure. In other words, precautionary lowering to a 1 in 1 million hypothetical risk already ensures a healthy "safety factor" such that all available quality science should be fully considered, including that from 2013 to present, to ensure the most robust and scientifically accurate foundation is laid for this potentially costly 1,4-dioxane limit.

Recent precedents around the world[1] incorporate the subject updated science, and CCNJ/SRIN encourage DWQI to do the same. Currently, the 2019 California notification level (NL) is 1 microgram per liter (µg/L), as is the more recent New York MCL issued on August 26, 2020. California set the state NL to 1 µg/L in November 2010, as the USEPA revised its 1,4-dioxane risk evaluation to a 1E-06 risk level of 0.35 µg/L. California's NL was slightly greater than the *de minimis* 1E-06 level commonly used as a target for notification levels based on cancer risk, reflecting difficulty in monitoring 1,4-dioxane at very low concentrations. The present-day 2020 assessment in NJ suggests no remaining "difficulty" in monitoring 1,4-dioxane below 1 µg/L, but also fails to consider (1) the incremental cost-benefit of reporting lower levels of 1,4-dioxane and whether a difference between 3E-06 and 1E-06 incremental cancers (mathematically) is of significant economic value to the state of NJ and (2) the important foundational science on the mode of action of 1,4-dioxane toxicity at low levels, which would suggest that the present (2013) USEPA cancer potency factor results in a severe overstatement of realistic cancer risk.

Failure to consider all available science, including the advances of 2013 – 2020 publications and conclusions by the USEPA and others could cause NJ to set a limit that puts its citizens at a disadvantage. Citizens of New Jersey will have to pay more for water than those in states across the nation whose scientists went the extra mile to incorporate extensive new science on liver regeneration. Researchers and regulators in Canada and the Netherlands have realized that linear, mathematical extrapolation of risk below 1 µg/L to 0.3 µg/L is not what happens when animals (including people) drink water. Low-level 1,4-dioxane exposure is biologically *de minimis*; a failure to consider what "de minimis" means in an economic frame is a disservice to the citizens of New Jersey. As a result, the proposed 1,4-dioxane limit is willfully arbitrary and capricious, and clearly not in the best interests of the NJ citizenry.

### *Relevant Updates from the USEPA 2019 – 2020: 1,4-Dioxane Under the TSCA Risk Evaluation Program*

The Lautenberg *Chemical Safety for the 21st Century Act* amended TSCA, the nation's primary chemicals management law, in June 2016. Under the amended statute, the USEPA is required, under TSCA §6(b),

---

[1] See positions taken by Heath Canada (2018) and the Health Council of the Netherlands (2015) as examples.

to conduct risk evaluations to determine whether a chemical substance presents unreasonable risk of injury to health or the environment, under the conditions of use, without consideration of costs or other non-risk factors, including an unreasonable risk to potentially exposed or susceptible subpopulations, identified as relevant to the risk evaluation. Also, as required by TSCA §(6)(b), the USEPA established, by rule, a process to conduct these risk evaluations, *Procedures for Chemical Risk Evaluation Under the Amended Toxic Substances Control Act* (82 FR 79 33726) (Risk Evaluation Rule).

In June 2019, the USEPA followed the Risk Evaluation Rule procedures and released the draft risk evaluation for 1,4-dioxane; in November 2020, the Agency released a supplemental analysis. In this *Draft Supplemental Analysis to the Draft Risk Evaluation for 1,4-Dioxane*, the USEPA evaluated the risk to consumers and bystanders from 1,4-dioxane in consumer products, and the general population exposed to 1,4-dioxane in ambient surface water. The ethoxylation of other chemicals produces 1,4-dioxane as a ***byproduct***. ***Residual concentrations*** of 1,4-dioxane may also be present in commercial and consumer products that contain ethoxylated chemicals.

The Draft Supplemental Analysis presents draft determinations suggesting no unreasonable risk for the following eight (8) consumer uses for 1,4-dioxane: surface cleaners, anti-freeze, dish soap, dishwater detergent, laundry detergent, paint and floor lacquer, textile dye, and spray polyurethane foam. For each of these eight (8) uses, the USEPA evaluated non-cancer effects to consumers from acute inhalation and dermal exposures. For four (4) of the products with longer-term use potential, based on the exposure assessment, the USEPA also evaluated cancer risks to consumers from chronic inhalation and dermal exposures.

The USEPA concluded that all consumer conditions of use do not present an unreasonable risk of injury to the health of consumers and bystanders. In addition, the Agency evaluated acute and chronic incidental exposures via oral and dermal routes from recreational swimming in ambient water and preliminarily determined that this activity presents no unreasonable risk to the general population from all conditions of use. CCNJ/SRIN support the USEPA's draft exposure assessment portion of the risk evaluation of 1,4-dioxane, with the caveat that the implications of low-dose linear chronic (lifetime) excess risk extrapolation were not pivotal for the use cases explored in the TSCA risk determinations. In contrast, if the USEPA were to conduct robust daily **ingestion** pathway evaluations for a chronic drinking water exposure, the low-dose mode of action would be the pivotal scientific turning point in a decision on acceptable risk, and additional pharmacokinetic considerations (such as those extensively reviewed in the ACC comments presented in Appendix A) would have been front and center in the assessment.

The opportunity for expert CCNJ/SRIN stakeholders to collaborate with DWQI on a balanced weight-of-the-evidence approach, involving chemists, toxicologists, and/or pharmacologists is essential to managing these (and other health-related) issues effectively and efficiently in New Jersey and beyond. An appropriate, science-based regulation that embraces the "dose makes the poison" tenet of fact-based toxicology weighing both the risks and benefits of 1,4-dioxane is necessary for New Jersey to continue to be the powerhouse of the United States.

If DWQI or the New Jersey Department of Environmental Protection (NJDEP) cannot assemble the appropriate experts for these very advanced judgments based on sound science, then a professional third-party external and transparent peer review by, for example, the National Academies of Science and Medicine is warranted. At the heart of the issue is whether the full body of scientific evidence on 1,4-dioxane suggests that 1,4-dioxane acts via a threshold or nonlinear mechanism. The threshold concept is based on the idea that there is a dose of 1,4-dioxane below which protective mechanisms (such as reversible, non-neoplastic liver foci cause liver cell regeneration and replacement) are in place, up to a certain concentration. This is particularly unique for liver carcinogen MOA because the **liver is the unique organ that can regenerate cells** and is the organ known to have the greatest ability to recover from toxic injury (whether it be from alcohol ingestion, medication overdose, or chronic chemical exposure). At or above the threshold concentration, liver cells may no longer be able to compensate and adverse effects—in this case, progression to liver cancer—may be exhibited. In the case of 1,4-dioxane, insisting on fitting a linear curve through zero risk ignores the available modern (post-2013) toxicology, pharmacology, and physiology unique to the chemical and unique to the mammalian liver, and would be scientifically incorrect. Scientific error in this case will lead to a wasteful, unnecessary and costly regulation borne by New Jersey citizens.

## Technical Comments

### *Health Effects Subcommittee Report on 1,4-Dioxane*

*Mode of Action (MOA): Updated 1,4-Dioxane Understanding*

DWQI's draft MCL recommendation of 0.33 µg/L for 1,4-dioxane is based on the 2013 USEPA Integrated Risk Information System (IRIS) oral cancer slope factor, derived using linear, low-dose extrapolation from a mouse liver tumor study (Kano et al., 2009). As such, the toxicity value assumes that 1,4-dioxane induces liver carcinogenesis through an assumed linear, non-threshold mode of action (MOA). While the weight of the evidence presented in the literature do not support a genotoxic/mutagenic (and thus linear) MOA (USEPA, 2005, 2013), the USEPA in 2013 (and subsequently, the NJDEP and DWQI) had to assume a linear MOA because, at the time in 2013, it remained the default approach recommended for quantifying chemical carcinogenicity in the absence of evidence to the contrary, per USEPA cancer risk assessment guidelines (USEPA, 2005). The pre-2013 scientific understanding of 1,4-dioxane MOA has been updated in the intervening years, with significant advanced contributions by numerous pathologists and toxicologists. As a result, alternative evaluations and assessments are possible, as acknowledged in the scientific peer-reviewed literature from 2013 – 2020, as well as in the USEPA Draft Supplement to the risk determinations for 1,4-dioxane under TSCA released in November 2020. This warrants careful reconsideration by the NJDEP and DWQI so as not to overlook 20 more years of robust science.

The NJDEP and DWQI may no longer claim that the MOA for 1,4-dioxane is unknown in 2020. The 1,4-dioxane peer-reviewed toxicology literature does not support for a linear, non-threshold MOA; scientists have been exploring the best approach to illustrate that the weight of the evidence supports a non-linear threshold-based MOA. For 1,4-dioxane (as well as in cancer bioassays conducted in past decades such as those in 1978 mentioned below), it was common for pathologists (over 40 years ago) to only record primary lesions associated with chemical exposures. As a result, in cases where tumors were present as the primary lesion, less substantial histopathology findings that can be indicative of a non-genotoxic cancer MOA (cell hyperplasia) often went unrecorded. For this very reason, significant effort was made in the last 20 years to improve the methods and record for each piece of scientific information that helps establish "how" a chemical exerts its toxicity, so that appropriate conclusions about "how" to regulate exposures can be drawn. Without considering this recent body of work, the NJDEP and DWQI would be willfully ignoring the best available science and modern methods.

To better inform the NJDEP and DWQI on 1,4-dioxane MOA, several recent efforts – each a significant undertaking – were published in the peer-reviewed literature. In the first of the two pivotal MOA studies on 1,4-dioxane, modern pathologists (during September through November 2012) reviewed the

NCI (1978) mouse liver sections at the Experimental Pathology Laboratories (EPL), Research Triangle Park, NC. The objective (made possible by staff of the National Toxicology Program for assistance in the evaluation of data from the NCI [1978] slide re-read) was to determine if any non-neoplastic lesions in the liver were present, but not previously recorded in the report, in an effort to understand the sequence of events that may have contributed to the MOA of the observed liver tumors in mice. Another reason for the slide review was because at the time of the original slide review (i.e. 1978), the NCI typically recorded only the most severe diagnosis on a given slide, such that, if an (benign) adenoma, carcinoma, and evidence of chronic toxicity (e.g. hepatocellular hypertrophy) were all present on a given slide, only the tumor response was typically recorded. Thus, it was unclear whether non-neoplastic lesions were present in the livers of mice but were not recorded in the NCI carcinogenicity study report.

In 2018, DWQI refused to accept these scientific efforts – three months of tedious 2012 pathology re-examination and documentation – that were written up in 2013, submitted in June 2013 to a peer-review panel selected by the journal, revised and made available online by February 2014, and published in final form in April 2014 in *Regulatory Pharmacology and Toxicology*. In conducting this 2012 mouse liver slide re-read, the modern pathologists reported "dose-related non-neoplastic changes in the liver; specifically, a dose-related increase in the hypertrophic response of hepatocytes, followed by necrosis, inflammation and hyperplastic hepatocellular foci." The weight of the evidence thus suggests that 1,4-dioxane causes liver tumors in rodents via cytotoxicity followed by regenerative hyperplasia, allowing a potential "off ramp" to carcinogenesis when regeneration of the cells could overcome the low dose exposure.

To be clear, the *Regulatory Pharmacology and Toxicology* publication in 2014 was no small feat; working with the U.S. government's National Toxicology Program to locate the National Cancer Institute mouse liver slides archived in 1978 and arranging for 40 years of updated science to be applied to answer this pivotal question of MOA was a serious commitment. Critics of the work all focus on the fact that the 2014 effort was fully funded by industry. This 2012 – 2014 economic contribution to science was necessary, and its meritless rejection is all the more disappointing. Industry funding necessity is a sad reflection on the fact that neither state nor federal governments had appropriate levels of funding or in-house scientific expertise to prioritize revisiting pathology slides to test such a key hypothesis. Although the data collection started in 1978, proper application of MOA-reliant risk management policy could not be completely concluded until the re-read publication in 2014, and has not been fully informed until now, with the addition of the extensive 2018 – 2019 additional work summarized in Appendix A (see ACC comments).

In 2017, the *Regulatory Pharmacology and Toxicology* journal published an update to the previous 2014 analysis, in which pathologists, toxicologists, and regulators (including from Kentucky and with input from Texas) revisited the results of the Kano et al. (2008, 2009) rodent subchronic and chronic drinking water studies. Since the chronic study (Kano et al., 2009) forms the basis of the USEPA (and the NJDEP and DWQI) oral cancer slope factor, this re-analysis is critical to elucidating the 1,4-dioxane MOA. It turns out that Kano et al. (2008, 2009) are based on Japanese assays conducted in the late 1980s, whose reports were issued in 1990 (JBRC, 1990a,b). The authors of the *Regulatory Pharmacology and Toxicology* update (2017) requested and received the laboratory reports for these studies (JBRC, 1990a,b), and conducted their evaluation based on report translations. Not only were the evaluations transparent and publicly available, all the underlying data is available for public re-analysis on the journal's website as supplemental information.

The authors of the *Regulatory Pharmacology and Toxicology* update (2017) found that the pooled incidence of centrilobular swelling and single cell liver necrosis from the 13-week studies preceded the development of development of liver adenomas and carcinomas in the chronic studies in both dose and time. Specifically, they report:

> *"…liver cell swelling, hypertrophy and liver weight increase occur at doses of 42-55 mg/kg-day; this precedes necrosis at doses of 94-219 mg/kg-day; which has a lower overlapping range of hyperplasia and foci development found at 55-389 mg/kg day; which precedes in dose the development of adenomas and carcinomas at doses of 274-1015 mg/kg-day."*

The authors of the *Regulatory Pharmacology and Toxicology* update (2017) note that the mouse data are less clear on the sequence of histological events, as tumors appear at lower doses in the chronic studies than the liver swelling and necrosis do in the subchronic studies. The authors note that the lack of noncancer histopathology in the chronic mouse study is inconsistent with reported changes in liver enzymes in the same study, inconsistent with the precursor liver injury histopathology findings in the subchronic study mouse study, and inconsistent with their prior re-read observations in the 1978 NCI study. The authors consulted several pathologists about the contrasting findings of the chronic mouse bioassays, reporting that the collective pathology opinion supported the hypothesized MOA considered by the USEPA (2013) and supported by Dourson et al. (2014), namely that "the liver tumors from oral exposure to 1,4-dioxane occur after metabolic saturation, accumulation of the parent 1,4-dioxane molecule, liver toxicity and a regenerative hyperplasia."

Even more evidence regarding proof that metabolic saturation must occur for the carcinogenic pathway to proceed has been accumulated via scientific studies in 2018 – 2019, as summarized in Appendix A (see ACC comments). In summary:

> *"reanalysis of data from two chronic mouse cancer bioassays on 1,4-dioxane, one 13-week mouse study, seven rat cancer bioassays, coupled with other data such as 1,4-dioxane's negative mutagenicity, its lack of up-regulated DNA repair, and the appearance of liver tumors with a high background incidence, support the conclusion that rodent liver tumors, including those in mice, are evoked by a regenerative hyperplasia MOA. The initiating event for this MOA is metabolic saturation of 1,4-dioxane."*

These recent findings further strengthen the weight of evidence that liver tumors resulting in rodents orally exposed to 1,4-dioxane over a chronic time-period are the result of a threshold-based MOA. In accordance with the 2005 USEPA Cancer Guidelines, these findings should compel the USEPA, the NJDEP, and DWQI to revisit their assumptions on 1,4-dioxane MOA and derive a threshold-based cancer value. The use of the *Regulatory Pharmacology and Toxicology* updates (2014, 2017) is consistent with the "best available science". Finally, it should be noted that this approach would be in keeping with prior risk assessments by others (Health Canada, 2005; Neumann et al., 1997; NICNAS, 1998; Netherlands, 1999; and Stickney et al., 2003), and as recently updated and reaffirmed (Health Canada 2018; Netherlands 2015) in international limit setting efforts by regulatory bodies.

New Jersey citizens and DWQI should be relieved to know that popular scientific press coverage of liver regeneration as a protective mechanism against cancer has gained a growing audience and interest from scientists in recent years. The American Association for the Advancement of Science journal *Science* (in August 2018) published "*Setting Liver Regeneration Free*" to introduce a breakthrough study that discovered a way to inhibit a liver growth factor in order to accelerate liver cell regeneration. Researchers inhibited this growth factor to increase mouse survival, thus interrupting the carcinogenesis pathway and giving additional insight into MOA that could yield clues to reversing liver injury long before a malignant liver tumor would ever develop. This August 2018 peer-reviewed scientific article took a year in revision (from March 2017 submittal to March 2018 acceptance, finally coming to print in August 2018), reflecting the complexity of the topic and rigor of scientific publications in the modern era. The underlying conclusions of this work further bolster the weight of evidence explained in the 2014 and 2017 publications on 1,4-dioxane threshold MOA, and is yet one more piece of the liver carcinogenesis science that suggests absolutely no need, in modern scientific understanding, to ignore low-level regenerative and recuperative pathways that are expected to work in favor of setting a threshold-based drinking water limit for 1,4-dioxane. Although this journal article in *Science* magazine is not specific to the 1,4-dioxane MOA, it supports a greater understanding of the function of the liver. Therefore, CCNJ/SRIN recommend that DWQI review this study and reconsider the MOA.

In conclusion, it will be a costly mistake if New Jersey ignores the ACC comments and this scientific input, and continues to assume that 1,4-dioxane cancer potency remains linear at low doses. DWQI insists that the cancer MOA "is not established" and remains based on linear low-dose extrapolation (following policy set by the USEPA in 2005). For cancer, in modern assessments, it is only required to extrapolate linearly if mutagenic MOA is proven; 1,4-dioxane is unanimously <u>not</u> a mutagen according to any health agency and, therefore, non-linear extrapolation should still be part of the discussion. Requiring the drawing of the slope factor line through zero is an unnecessary, unscientific default that should be properly, professionally replaced with the known MOA science. The *Regulatory Pharmacology and Toxicology* study (2017) was not available when USEPA (2013) or California (2019) previously did their most recent cancer potency assessments, and a complete and thorough assessment of the MOA points made in 2014 and 2017 (as well as the updated 2020 understanding of liver injury and regeneration pathways, including 2018 – 2020 research) is warranted:

- Liver tumors caused in rodents is by a MOA based on cytotoxicity and subsequent regenerative hyperplasia;
- Periodic cytotoxicity in the liver induces an adaptive (i.e. not ultimately adverse) effect, particularly at low doses; the toxicity of 1,4-dioxane was not shown to be tumorigenic until metabolic saturation (at high doses) occurs based on the detailed re-assessment of all available (mouse and rat liver) pathology slides; and
- A non-linear approach to dose-response assessment will safely protect against these potential 1,4-dioxane tumorigenic effects.

Thus, even though New Jersey argued against the body of nonlinear MOA evidence in 2018, these studies (and Appendix A) support the updated MOA understanding and remain the key piece of toxicology and carcinogen science that must be understood and used for setting a health-based MCL.

### ***Treatment Subcommittee Report on 1,4-Dioxane***

The chemical-specific evaluation that solely focuses on 1,4-dioxane overlooks the "big picture" real world challenges that public water systems (PWS) may face. Advanced Oxidation Processes (AOPs, such as UV/H2O2) will not address other emerging contaminants, such as perfluorinated compounds (e.g. PFNA, PFOA, PFOS). Thus, NJ water purveyors forced to treat for 1,4-dioxane with AOPs will be looking at a separate and additional treatment train if they are, for example, already complying with PFAS MCLs. The economic impact assessment and burden on the receiving communities are likely to be a "double whammy" and may encourage selection of non-AOP systems (e.g. Reverse Osmosis (RO)) or non-treatment options (such as taking sources offline, for blending solutions) if multiple emerging contaminants are present in raw water. Based on DWQI's report, Granular Activated Carbon (GAC) is only 18% effective in treating 1,4-dioxane, while AOP is ineffective on PFAS; therefore, in systems trying to treat both 1,4-dioxane and PFAS, a supply may be pushed to select RO as the only cost-effective treatment for both types of emerging contaminants. Waste stream management is likely for 1,4-dioxane via RO (or sorbent methods) where selected due to presence of co-contaminants.

The conclusion that "reliable and feasible" removal of 1,4-dioxane can be achieved below the draft MCL of 0.33 µg/L via "carefully designed AOP treatment" does not acknowledge the reality that the systems requiring 1,4-dioxane treatment will also need to treat for other co-contaminants, as detailed in the assessment below.

In order to allow the public to transparently assess whether this is a valid economic/feasibility concern, we request that DWQI respond to the following table:

| **From DWQI Treatment Subcommittee Presentation on 1,4-Dioxane, Slide 5 of 14 (9/30/2020)** | | | |
|---|---|---|---|
| **Range Concentration (parts per billion (ppb))** | **# of New Jersey Systems** | **CCNJ/SRIN Detailed Analysis** | **Comments** |
| 6 to 3 | 4 | **(3):** NJ American Co. – Washington/Oxford, Merchantville Pennsauken, & Aqua NJ – Eastern | **Please explain difference in the number of NJ systems identified.** |
| 3 to 2 | 3 | **(3):** Merchantville Pennsauken, Collingswood, & Fair Lawn | |
| 2 to 1 | 5 | **(7):** Sparta Township – Lake Mohawk, Merchantville Pennsauken, Camden City, Livingston Township, East Hanover, South Brunswick, & Collingswood | **Please explain the difference the number of NJ systems identified.** |
| 1 to 0.5 | 9 | **(11):** NJ American Co. – Raritan, Pennsville, Aqua – Phillipsburg, West Deptford, West Caldwell, Woodbury City, South Brunswick, Merchantville Pennsauken, Garfield, Gloucester City, & Southeast Morris County Municipal Utilities Authority (MUA) | **Please explain the difference the number of NJ systems identified.** |
| 0.5 to 0.4 | 8 | **(10):** Point Pleasant, Pompton Lakes, Monroe Township, Maple Shade, Merchantville Pennsauken, Aqua – Blackwood, Oakland, Parsippany-Troy Hills, Livingston, & Southeast Morris County MUA | **Please explain the difference the number of NJ systems identified.** |
| 0.4 | 3 | **(??) None identified in CCNJ/SRIN analysis with public data** | **Please identify the NJ systems.** |

| | | | |
|---|---|---|---|
| **> 0.33** | | ***(19): Point Pleasant, Pompton Lakes, West Deptford (0.31 ppb), East Windsor (0.32058 ppb), Livingston, East Hanover (0.32 ppb), Madison (0.32 ppb), Perth Amboy, Willingboro (0.31745 ppb), Maple Shade, Moorestown (0.30531 ppb), Burlington Twp., Oakland, Ramsey, Parsippany-Troy Hills (0.32 ppb), Southeast Morris County MUA, NJ American Co. – Atlantic County, NJ American Co. – Raritan (0.32 ppb), & NJ American Co. – Western*** | **NJ PWS in *red* trigger the existing NJDEP groundwater standard for 1,4-dioxane; therefore, a total of ten (10) additional NJ PWS would require treatment systems for 1,4-dioxane.** |

Notes:

- Collingswood is in two (2) range concentration categories: 3 to 2 and 2 to 1 ppb.
- South Brunswick is in two (2) range concentration categories: 2 to 1 and 1 to 0.5 ppb.
- Merchantville Pennsauken is in five (5) range concentration categories: 6 to 3, 3 to 2, 2 to 1, 1 to 0.5, and 0.5 to 0.4 ppb.
- Southeast Morris County MUA is in two (2) range concentration categories: 1 to 0.5 and 0.5 to 0.4 ppb.
- East Hanover is in two (2) range concentration categories: 2 to 1 and 0.5 to 0.4 ppb.
- Livingston is in two (2) range concentration categories: 2 to 1 and 0.5 to 0.4 ppb.

The proposed MCL of 0.33 µg/L (ppb) for 1,4-dioxane would trigger an additional ten (10) NJ PWS, including public water supplies that are close to or slightly below this number. Mathematically, New Jersey states it relies on "new" (updated) exposure parameters that require 2.4 liters per day (L/day) and 80 kilograms (kg) body weight for a calculation of a new 0.33 µg/L draft MCL, keeping in mind the 0.35 µg/L previously rounded to 0.4 µg/L as New Jersey claimed "one significant figure" was used. The concept of "significant figures" is rife with interpretation in risk calculations because there would be the argument about the significance of the "new" exposure parameters (e.g. 2.4 L with one significant figure is the same as 2 L if you look at the underlying data set) and whether or not certain suppliers would be out of compliance depending on what the final value is. Therefore, a total of 35 NJ PWS are identified above the proposed MCL for 1,4-dioxane based on the data from the USEPA's Third Unregulated Contaminated Monitoring Rule (UCMR3), which does not require all New Jersey public water supplies to conduct sampling.

CCNJ/SRIN conducted an analysis of the UCMR3 data for PFNA, PFOA, and PFOS above the 0.02 ppb minimum reporting limit to compare to the proposed MCL of 0.33 ppb for 1,4-dioxane. Since the UCMR3 data **released,** the NJDEP has issued MCLs for PFNA, PFOA, and PFOS below 0.02 ppb, which may trigger additional NJ public water supplies.

Below is a table based on the UCMR3 data results:

| **1,4 Dioxane + PFNA/PFOA/PFOS Treatment Systems Triggered for Nine (9) NJ PWS** | |
|---|---|
| Point Pleasant | PFOA |
| West Deptford | PFNA |
| Woodbury City | PFNA |
| Gloucester City | PFNA |
| Aqua NJ – Blackwood | PFOA |
| Fair Lawn | PFOA & PFOS |
| Oakland | PFOA |
| Garfield | PFOA |
| NJ American Co. – Raritan | PFOA |

As a follow-up to the above comments, CCNJ/SRIN request that DWQI respond to the following question:

- Have any of the NJ PWS already found a solution to the UCMR3 2013-2015 1,4-dioxane data, such that an updated accounting (i.e. 2020 data) of the “real” list of PWS with a need to address 1,4-dioxane is essential to better inform a 2021 MCL decision?

A cost/benefit analysis of treating 1,4-dioxane via AOP in addition to GAC or other techniques to achieve PFAS MCL requirements should be undertaken to ensure the full economic burden of multiple treatment trains (if any) is fully understood for the communities seeking to get 1 in 1,000,000 lifetime reductions on the chance of a potential cancer due to a lifetime of low-level 1,4-dioxane in the water. Basing an MCL decision and regulatory burden on outdated 2013 – 2015 detections would not be prudent, nor would recommending an AOP treatment when others will be required for co-contaminants be fully transparent to the public or to the regulated entities.

Alternative models to reduce levels of 1,4-dioxane, such as blending source water, to achieve compliance with such a low draft MCL should also be pursued in the cost/benefit discussion, to ensure health improvement (i.e. risk reduction) measures and any associated treatment train waste streams are fully optimized.

We would like the record to reflect our support of any comments submitted by CCNJ and SRIN members, as well as the American Chemistry Council (Appendix A).

Thank you for your consideration of our comments on this very important issue. We look forward to continuing to work with DWQI and the NJDEP on this and other matters of critical importance to CCNJ and SRIN members. If I can be of further assistance, please let me know.

Sincerely,

Dennis Hart
Executive Director

Attachment

*References:*

Dourson M, Reichard J, Nance P, Burleigh-Flayer H, Parker A, Vincent M, McConnell EE. 2014. Mode of action analysis for liver tumors from oral 1,4-dioxane exposures and evidence-based dose response assessment. Regul Toxicol Pharmacol. 68(3):387-401.

Dourson M, Higginbotham J, Crum J, Burleigh-Flayer H, Nance P, Forsberg N, Lafranconi M. 2017. Update: Mode of action (MOA) for liver tumors induced by oral exposure to 1,4-dioxane. Regul Toxicol Pharmacol. Epub date: 2017 Mar 30. doi: 10.1016/j.yrtph.2017.02.025. PubMed PMID: 28366800.

Health Canada. 2005. Drinking Water Guidance Value for 1,4-Dioxane, August 23.

Health Canada. 2018. 1,4-Dioxane in Drinking Water Guideline Technical Document for Public Consultation, September 7.

Health Council of the Netherlands. 2015. 1,4-Dioxane - Re-Evaluation of the Carcinogenicity and genotoxicity, November 13.

Japan Bioassay Research Center (JBRC). 1990a. Report of Carcinogenicity Study by Oral Administration of 1,4-Dioxane (Mixed with Water) to Rats and Mice. Japan Industrial Safety and Health Association. December 28.

Japan Bioassay Research Center (JBRC). 1990b. Report of Preliminary Carcinogenicity Studies (Acute, Two-Week, and Thirteen-Week Studies) by Oral Administration of 1,4-Dioxane (Mixed with Water) to Rats and Mice. Japan Industrial Safety and Health Association. December 28.

Kano H, Umeda Y, Saito M, Senoh H, Ohbayashi H, Aiso S, Yamazaki K, Nagano K, Fukushima S. 2008. Thirteen-week oral toxicity of 1,4-dioxane in rats and mice. J Toxicol Sci. 33(2):141-53.

Kano H, Umeda Y, Kasai T, Sasaki T, Matsumoto M, Yamazaki K, Nagano K, Arito H, Fukushima S. 2009. Carcinogenicity studies of 1,4-dioxane administered in drinking-water to rats and mice for 2 years. Food Chem Toxicol. 47(11):2776-84.

National Cancer Institute (NCI). 1978. Bioassay of 1,4-dioxane for possible carcinogenicity. (78-1330 NCICGTR-80). Bethesda, MD. (124 pp).

Neumann HG, Thielmann HW, Filser JG, Gelbke HP, Greim H, Kappus H, Norpoth KH, Reuter U, Vamvakas S, Wardenbach P, Wichmann HE. 1997. Proposed changes in the classification of carcinogenic chemicals in the work area. Regul Toxicol Pharmacol. 1997 Dec;26(3):288-95.

Netherlands. 1999. Risk Assessment: 1, 4-Dioxane. Netherlands Organization for Applied Scientific Research (TNO) and the National Institute of Public Health and the Environment (RIVM). Chemical Substances Bureau, Ministry of Housing, Spatial Planning and the Environment (VROM), Netherlands, Final Version, 5 November, EINECS-No.: 204-661-8.

NICNAS (National Industrial Chemicals Notification and Assessment Scheme). 1998. Priority Existing Chemical Assessment Reports: 1,4-dioxane. Sydney, Australia: Australia Department of Health and Ageing. June.

Stickney JA, Sager SL, Clarkson JR, Smith LA, Locey BJ, Bock MJ, Hartung R, Olp SF. 2003. An updated evaluation of the carcinogenic potential of 1,4-dioxane. Regul Toxicol Pharmacol. 38(2):183-95.

USEPA. 2005. Guidelines for carcinogen risk assessment. Washington, D.C. EPA/630/P-03/001B.

USEPA. 2013. Toxicological review of 1,4-Dioxane (with inhalation update) (CAS No. 123-91-1) in support of summary information on the Integrated Risk Information System (IRIS) [EPA Report]. Washington, D.C. EPA-551 635/R-11/003-F.

USEPA. 2020. Draft Supplemental Analysis to the Draft Risk Evaluation for 1,4-Dioxane. Washington, D.C. EPA-740-R1-8007.

American Chemistry Council

BY ELECTRONIC MAIL

December 21, 2020

Jessie A. Gleason, MSPH, Chair
Health Effects Subcommittee Drinking Water Quality Institute
NJDEP – Division of Water Supply & Geoscience
Mail Code 401-04Q 401
East State Street
Trenton, NJ 08625

Re: Health-based Maximum Contaminant Level Support Document: 1,4-Dioxane (CAS # 123-91-1; Chemical Formula $C_4H_8O_2$) – Public Review Draft, July 2020

Dear Ms. Gleason:

The American Chemistry Council's 1,4-Dioxane Panel (the Panel) appreciates the opportunity to comment on the draft report of the Health Effects Subcommittee (the Subcommittee) on 1,4-dioxane (1,4-DX). The Panel represents a number of companies with a strong interest in the science used to develop regulatory standards for 1,4-DX such as the maximum contaminant level (MCL) under consideration within the New Jersey Drinking Water Quality Institute. The Panel urges the Subcommittee to update its analysis to incorporate the latest information and conclusions on the mode of action (MOA) for tumor formation before moving ahead with a recommendation for a drinking water standard.

The Subcommittee recommendation of 0.4 milligrams per liter (mg/L) is based on the application of the default linear, low-dose extrapolation of liver tumors in female mice reported by Kano *et al.* (2009) – per the 2013 analysis by the US Environmental Protection Agency for the Integrated Risk Information System (IRIS). In rejecting the threshold mode of action (MOA) accepted by authoritative bodies around the world, the Subcommittee focuses its analysis on the work by Dourson *et al.* (2014, 2017) with only passing reference to information that has been developed since the Department's previous review of the substance. Among these developments is the release of Health Canada's 2018 consultation document recommending a maximum allowable concentration of 50 mg/L for drinking water.

In addition we'd like to call your attention to the recent publication of Lafranconi *et al.* (2020)[1] presenting the results of a 90-day MOA subchronic study in female mice which provides evidence of a mitogenic response consistent with a threshold MOA for liver tumors. A transcriptomic analysis of the mouse livers from this study, currently in press, observed minimal gene expression at concentrations below 600 parts per million and a lack of enrichment of genes related to DNA damage.[2] At higher concentrations, genes involved in phase II metabolism and mitotic cell cycle checkpoints were significantly upregulated providing further support for a non-mutagenic, threshold MOA.

As discussed in the enclosed comment, the metabolism of 1,4-dioxane in animals and humans is well established, clearly indicating saturation of the cytochrome P450 pathway at higher doses that is consistent with the occurrence of toxic effects in liver and nasal tissue in the animal studies that lead to tumors. Although this progression was not reported in the female mice in the Kano *et al.* bioassay, preneoplastic effects were observed in the subchronic study by the same researchers. The latest study by Lafranconi *et al.,* moreover, provides further support for the conclusion that tumors in the animals occur only after the dose exceeds metabolic saturation.

Based on the overwhelming evidence, ACC strongly recommends that the Institute base its recommendation for a drinking water standard on a threshold MOA that is consistent with that approach taken by Health Canada. Please contact me at srisotto@americanchemistry.com or at 202-249-6727 if you have questions about the enclosed information or if you would like to discuss it further.

Sincerely,

**Steve Risotto**

Stephen P. Risotto
Senior Director

Enclosures

---

[1] The publication is inlcuded with the ACC comments. The lab report from the study was previously submitted to USEPA is available from the Agency's docket at https://www.regulations.gov/document?D=EPA-HQ-OPPT-2019-0238-0059.

[2] Chappell GA *et al.* Transcriptomic analyses of livers from mice exposed to 1,4-dioxane for up to 90 days to assess potential mode(s) of action underlying liver tumor development. (In Press).

1,4-Dioxane Panel of the American Chemistry Council
Comment to the New Jersey Drinking Water Quality Institute
On the Health-Based Maximum Contaminant Level
Support Document for 1,4-Dioxane

December 21, 2020

# Contents

## Executive Summary

In the support document for a maximum contaminant level (MCL) for 1,4-dioxane (1,4-DX), the Health Effects Subcommittee concludes that the evidence for a threshold mode of action (MOA) is not sufficiently robust and assumes a default linear/low dose assumption for a genotoxic MOA in characterizing risk from 1,4-DX exposure. Unfortunately the Subcommittee fails to fully consider the considerable evidence for the key events supporting a threshold for carcinogenic response in animals exposed to 1,4-DX.

Based on the available evidence, the application of the default genotoxic MOA is inappropriate since 1,4-DX is neither genotoxic nor mutagenic and is not able to produce mutations that would merit consideration of the more conservative, linear approach to assessing carcinogenic risk. There is no evidence that 1,4-DX is bioactivated to reactive intermediate metabolites capable of alkylating DNA resulting in known base-pair alterations that produce mutations. Instead, 1,4-DX's metabolism is well-documented to proceed to a stable, non-genotoxic/non-mutagenic metabolite, 2-hydroxyethoxyacetic acid (HEAA). Furthermore, 1,4-DX itself is chemically stable and unable to alkylate DNA. This conclusion also is based on extensive testing with *in vitro* assay systems with prokaryotic organisms, non-mammalian eukaryotic organisms, mammalian cells, and *in vivo* genotoxicity assays. In addition, there is ample evidence that the development of tumors only occurs when dosing exceeds the threshold of metabolic saturation (Figure 1).

Metabolism studies confirm that, while the substance is readily metabolized and quickly eliminated from the body, the metabolic pathway becomes saturated at higher exposure levels of 1,4-DX. Moreover, available evidence demonstrates that toxicity occurs only after the clearance pathway becomes saturated and the parent compound accumulates in the blood.

Although 1,4-DX has been reported to evoke multiple tumors, the increased tumor incidences tend to occur at the highest dose only, and all are consistent with a threshold-based non-mutagenic MOA. This finding is supported by extensive histopathology for both liver and nasal tissue providing a robust set of key event, pre-cancerous changes consistent with tissue injury and a threshold, regenerative repair MOA for 1,4-DX-induced tumors. Chronic and subchronic studies in laboratory animals exposed to levels above metabolic saturation have consistently demonstrated a threshold response to tumor formation from 1,4-DX exposure. This has been recognized by authoritative bodies worldwide and has led authorities in Australia, Canada, Europe, the World Health Organization (WHO), and Japan to apply threshold assumptions when characterizing risk, resulting in a drinking water guideline of 50 ug/L. Despite this abundance of information and precedence for the threshold approach, the support document employs a default linear low- dose extrapolation to develop a unit risk estimate and cancer slope factor based on benchmark dose modeling for multiple tumor sites, resulting in a drinking water guideline of 0.4 ug/L.

A recently competed 90-day MOA study by Lafranconi *et al.* (2020)[1], described below, adds significantly to our understanding of the dose-response for 1,4-DX by demonstrating a clear threshold for adverse effects in the liver. The results of this study are consistent with previous animal evidence that the metabolism of 1,4-DX shifts from linear, first-order metabolism to a zero-order kinetics with increasing dose indicating metabolic saturation. Once saturated, increased exposures result in a disproportional increase in circulating levels of parent 1,4-DX compound (**Figure 1**). As discussed elsewhere, this study also included an evaluation of toxicogenomics, which shows a clear threshold for any biological activity in the mouse liver.

The available evidence overwhelmingly points to the non-DNA reactive parent 1,4-DX as the toxic species. While the evidence for a threshold effect caused by accumulation of the parent compound is strongest for liver tumors, there is clear evidence to suggest that observed nasal tumors similarly occur only after an exposure threshold is exceeded along with a constellation of tissue injury, regenerative repair nasal mucosal changes consistent with a threshold carcinogen. Other reported tumors did not exhibit a statistically significant increase or, based on evidence of their spontaneous occurrence in rats, should not be considered biologically significant and lacking human relevance.

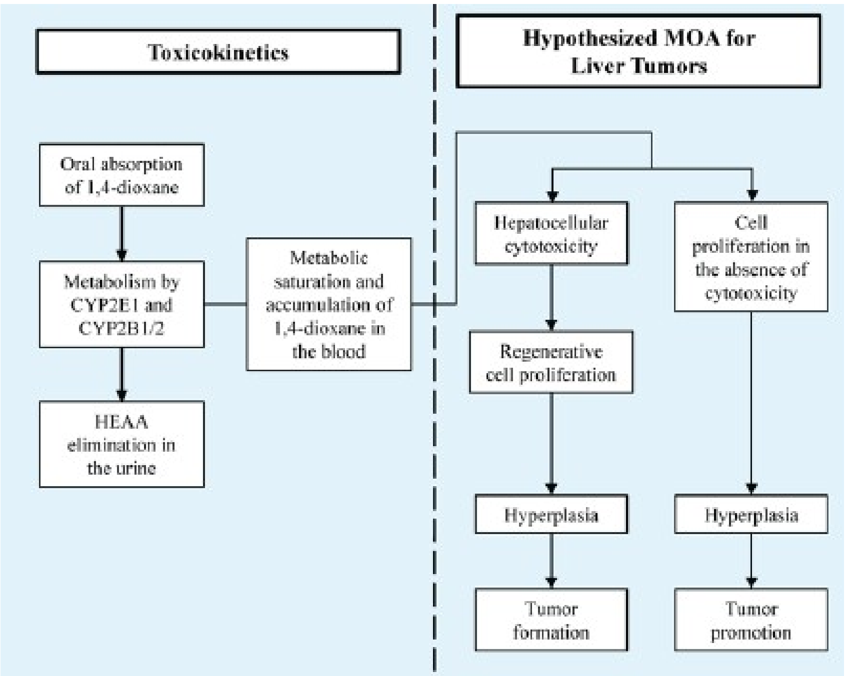

**Figure 1. Identification of key events in tumor formation following exposure to 1,4-dioxane[2]**

---

[1] ` See Attachment 1.

[2] USEPA. Toxicological Review of 1,4-Dioxane (with Inhalation Update). In Support of Summary Information on the Integrated Risk Information System (IRIS). Washington, DC (2013).

## Genotoxicity Data

1,4-DX has been tested for genotoxicity using *in vitro* and *in vivo* testing with prokaryotic organisms, non-mammalian eukaryotic organisms, and mammalian cells, both with and without metabolic activation. Based on the data presented in USEPA's 2013 IRIS assessment, all fifteen mutagenicity tests reported were negative.[3] In addition, 22 *in vitro* genotoxicity assays and nine *in vivo* genotoxicity assays were negative. Although eight assays were noted to be positive, genotoxicity was only observed at high and cytotoxic doses. Such genotoxicity outcomes at cytotoxic doses, such as increased micronuclei, are the result of cell injury and not test-material-induced mutation.[4] Based on these result, the IRIS assessment concluded that 1,4-DX is not genotoxic in the absence of cytotoxicity. The 2019 draft risk evaluation supports the conclusion that 1,4-DX is not genotoxic and does not induce tumors via a mutagenic MOA. However, the Subcommittee's support document suggests that recent studies concerning the genetic toxicity of the substance at elevated exposures may be indicative of DNA damage. As described below, this is an incorrect interpretation of EPA's own evaluation. In addition recent MOA data collected from high-throughput sampling does not provide evidence of DNA damage and repair.

While it is recognized that 1,4-DX appears to stimulate DNA synthesis in rats at elevated exposure levels, $\geq$ 1000 mg/kg/day, this does not represent a genotoxic event. Rather, the DNA synthesis appears to be a key event for either a direct mitogenic, proliferative response that proceeds overt tissue injury (e.g., hepatoxocity) or a regenerative cell proliferation mode-of-action secondary to 1,4-DX-induced tissue injury, or both, that work in concert to drive a threshold based tumor promotion outcome.[5] The DNA synthesis evidence supports the conclusion that 1,4-DX promotes cell proliferation, through mitogenesis and/or cytotoxicity depending on the dose and target organ.

### Recent Genetic Toxicity Results

Recent reports of a marginal increase in GPT-delta mutations Gi *et al.* (2018),[6] while of interest, do not provide evidence for a mutagenic cancer MoA, and certainly not one associated with low-dose exposures. This is particularly evident as the doses used in the study exceed the saturation kinetics of the pathway for metabolism of 1,4-DX in the rat – estimated to occur

---

[3] Ibid, at 73.

[4] Roy SK *et al.* Chromosome breakage is primarily responsible for the micronuclei induced by 1,4-dioxane in the bone marrow and liver of young CD-1 mice. *Mutat Res* 586(1):28–37 (2005).

[5] Goldsworthy TL *et al.* Examination of potential mechanisms of carcinogenicity of 1,4-dioxane in rat nasal epithelial cells and hepatocytes. *Arch Toxicol* 65: 1-9 (1991).

[6] Gi M *et al. In vivo* positive mutagenicity of 1,4-dioxane and quantitative analysis of its mutagenicity and carcinogenicity in rats. *Arch Toxicol* 92:3207-3221 (2018).

between 30 and 100 milligrams per kilogram body weight (mg/kg) per day – Gi *et al.* estimated the dose at 440 mg/kg/day.[7] A significant inconsistency in the Gi *et al.* (2018) study was the absence of a positive mutagenic response at the *Spi* locus. In fact, the authors stress the presence of no-effect levels for both mutagenicity and carcinogenicity of 1,4-DX.

Multiple lines of evidence from the Gi *et al.* (2018), Furihata *et al.* (2018),[8] and Itoh and Hattori (2019)[9] corroborate a threshold, tumor promotion MOA driven by increased cell proliferation. For one, Gi *et al.* (2018) is a non-conventional GPT-delta assay that went beyond the typical timeframe authorized in the guideline study thereby facilitating the direct, increased proliferative response induced by high dosages of 1,4-DX in driving a slight increase in GPT-delta mutations only at the high dose. Increased cell proliferation is demonstrated by a concomitant increase in GSTP+ foci in the rat livers that further illustrates 1,4-DX acting as a tumor promoter, not a mutagenic substance. Furthermore, the near exceedance of a maximally tolerated dose (high dose rats exhibiting an almost 10% reduction in body weight compared to controls) shows the high dose nature of the indirect, increased proliferative response in the elevated GPT-delta mutations.

When Furihata *et al.* (2018) further examined the genomic profile of 1,4-DX they observed biomarker gene changes that were in between those of classic mutagenic hepatic carcinogens, DEN and DMB and a non-genotoxic carcinogen, DEHP. Thus, the “in between” genomic biomarker profile of 1,4-DX is more consistent with a tumor promoter that drives the accumulation of naturally occurring background mutations and genomic damage. Finally, Itoh and Hattori (2019) reported that 1,4-DX failed to induce Pig-A mutation in rat blood. While they found increases in hepatic micronuclei with high dose 1,4-DX, this occurred following a partial hepatectomy that not only drives cell proliferation, but would be augmented by 1,4-DX’s known mitogenic stimuli.

Increased mutation is a common result of exposures to non-genotoxic carcinogens that exceed the threshold for effects.[10] Earlier work with the same transgenic rat strain used by Gi *et al.* noted that the length of exposure required for preneoplastic hepatic foci formation “may increase the risk of false-positive results of mutations due to nongenotoxic mechanisms caused

---

[7] The doses in the study by Gi *et al*. (2018) were 250 and 1250 mg/kg; Itoh and Hattori (2019) dosed the animals at 1000 to 3000 mg/kg.

[8] Furihata C *et al.* Using RNA-Seq with 11 marker genes to evaluate 1,4-dioxane compared with typical genotoxic and non-genotoxic rat hepatocarcinogens. *Mutat Res Genetic Toxicol Environ Mutagen* 834:51-55 (2018).

[9] Itoh S Hattori C. In vivo genotoxicity of 1,4-dioxane evaluated by liver and bone marrow micronucleus tests and Pig-a assay in rats. *Mutat Res Genetic Toxicol Environ Mutagen* 837:8-14 (2019).

[10] Singh VK *et al.* Comparison of the mutant frequencies and mutation spectra of three non-genotoxic carcinogens, oxazepam, phenobarbital, and Wyeth 14,643, at the λcII locus in Big Blue® transgenic mice. *Biochem Pharmacol* 62(6):685-92 (2001).

by chronic toxicity."[11] This effect is exacerbated by the high doses of 1,4-DX required to generate genotoxicity which have been shown to interfere with cell proliferation in the liver.[12] As a result, Morita and Hayashi (1998) concluded that "[i]t is also conceivable that the positive result in mouse liver micronucleus assay was due to a nongenotoxic mechanism, i.e., errors in genetic repair following enhancement of hepatocyte proliferation."[13] This same mechanism – increased regenerative proliferation leading to a higher background level of clastogenic effects, has also been shown to be at play for compounds triggering haematotoxin effects, signifying it as indirect, non-DNA reactive genotoxicity that have a threshold, as is the case for 1,4-DX.[14]

As described above, neither 1,4-DX or its metabolite, HEAA, are reactive compounds capable of alkylating DNA in the first place. This alone makes it entirely inconsistent to conclude that 1,4-DX has a mutagenic MOA behind its carcinogenic potential. Overall, the weight of evidence is not consistent with a mutagenic MOA that could raise the need for linear treatment of the cancer risk. The evidence is, however, much more consistent with a high dose, metabolism saturation-dependent tumor promotion MOA whereby direct cell proliferation occurring early on is subsequently augmented by regenerative repair. This is more appropriately treated as a threshold MOA.

## ToxCast Results

As part of its Toxicity Forecaster (ToxCast) program,[15] USEPA reports negative results of all 113 high-throughput screening assays that it has run for 1.4-DX, including five sequential assays for evaluating transcriptional activity of the p53 tumor suppressor protein. For the analysis, p53 transcriptional activity is evaluated in five sequential assays,[16] done over six sequential months to evaluate the stability of the test plates over time.[17] While the CompTox dashboard indicates a "hit" in the fourth of the five sequential assays, it is accompanied with a data quality flag. The data is flagged since only one data point suggests a response while all the other points indicate no response. There is no basis to interpret this single point finding in the middle of a sequential series of repeated assays as evidence of relevant biological activity associated with DNA

---

[11] Thybaud V *et al.* In vivo transgenic mutation assays. *Mutat Res* 540:141–151 (2003).

[12] Roy *et al.* Chromosome breakage is primarily responsible for the micronuclei induced by 1,4-dioxane in the bone marrow and liver of young CD-1 mice. *Mut Res Gen Toxicol Environ Mut* 586(1):28-37 (2005).

[13] Morita T and Hayashi M. 1,4-dioxane is not mutagenic in five *in vitro* assays and mouse blood micronucleus assay, but is in mouse liver micronucleus assay. *Environ Molec Mut* 32(3):269-280 (1998).

[14] Tweats DJ *et al.* Report of the IWGT working group on strategy/interpretation for regulatory *in vivo* tests: II. Identification of *in-vivo* only positive compounds in the bone marrow micronucleus test. *Mutat Res* 627(1):78-91 (2007).

[15] https://www.epa.gov/chemical-research/toxicity-forecasting

[16] The assays are identified as p53_BLA_p1_ratio, p2, p3, p4 and p5.

[17] Personal communication from Richard Judson, USEPA, April 29, 2019.

damage and repair.

## Metabolism & Toxicokinetics

Metabolism of 1,4-DX in humans and experimental animals is well characterized and extensive. In both rodents and humans, 1,4-DX is metabolized by cytochrome P-450 (P450) to β-hydroxyethoxy acetic acid (HEAA) in a linear, first-order process.[18] This metabolic transformation is responsible for the rapid clearance of 1,4-DX and elimination in the urine. Induction of P450 isoforms has been observed in the liver, kidney, and nasal mucosa in rats exposed either by gavage (acute) or in drinking water (chronic).[19]

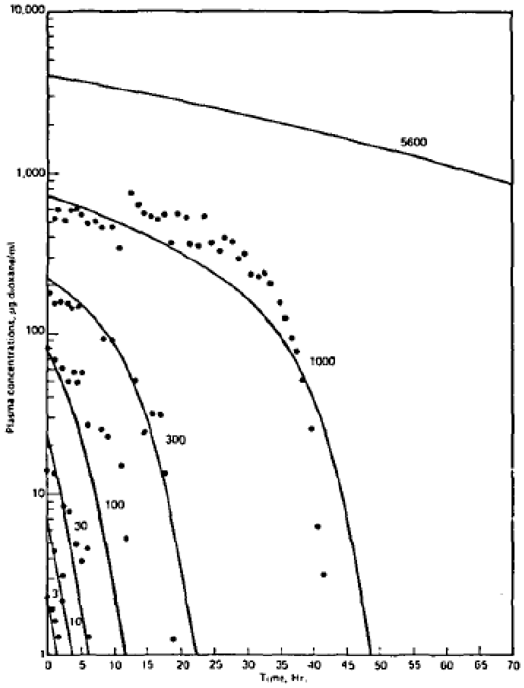

**Figure 2. Plasma concentrations over time for various intravenous doses from 3 to 1000 mg/kg of 1,4-dioxane administered to rats[20]**

Workers exposed to 1,4-DX at concentrations up to 50 parts per million (ppm) for 6 hours by inhalation showed a linear elimination of 1,4-DX in both plasma and urine leading to the

---

[18] Young JD *et al.* The dose-dependent fate of 1,4-dioxane in rats. *J Environ Pathol Toxicol* 2:263-282 (1978).

[19] Nannelli A *et al.* Effects of dioxane on cytochrome P450 enzymes in liver, kidney, lung and nasal mucosa of rat. *Arch Toxicol* 79, 74-82 (2005).

[20] Young JD *et al.* Dose-dependent fate of 1,4-dioxane in rats. *J Toxicol Environ Health* 4:709-726 (1978).

metabolite HEAA.[21] Studies in rats dosed by gavage up to 1000 mg/kg did not detect another suggested metabolite, 1,4-dioxane-2-one, leading the researchers to conclude that it was not formed or that it quickly hydrolyzed to HEAA.[22]

At higher doses of 1,4-DX in experimental animals the metabolism of 1,4-DX shifts from linear, first-order metabolism to a zero-order kinetics indicating metabolic saturation. This kinetic pattern has been demonstrated directly by monitoring plasma levels after intravenous (IV) administration of 1,4-DX and indirectly from studies monitoring the elimination of HEAA in the urine.[23] Rats given IV 1,4-DX demonstrated a dose-related shift from linear to saturation metabolism of 1,4-DX at 30 to 100 mg/kg/day resulting in an increase in 1,4-DX blood levels (**Figure 2**). Similarly, rats given gavage doses of 10, 100, or 1000 mg/kg showed that the plasma clearance rate decreased with dose, while the fraction excreted as HEAA decreased and the fraction excreted as the parent compound increased. For mice, saturation of the P450 pathway appears to start at 200 mg/kg.[24] Saturation of the metabolic pathway also has been observed in human hepatocytes exposed to up to 25 mg/ml of 1,4-DX (**Figure 3**).

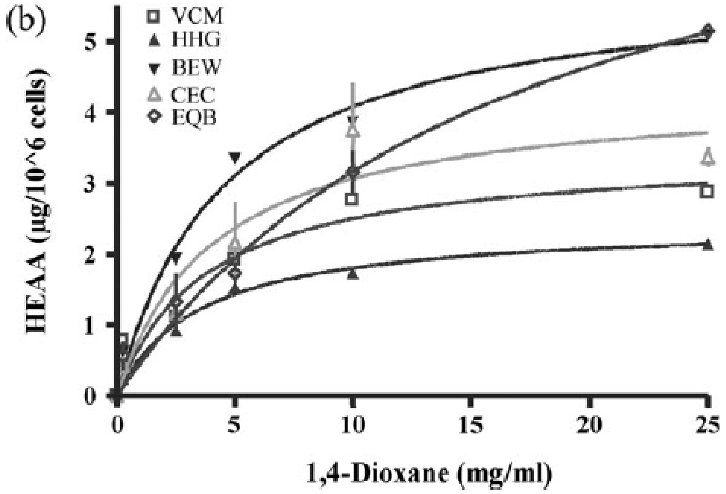

**Figure 3. Production of β-hydroxyethoxy acetic acid (HEAA) in hepatocytes from human donors incubated with initial concentration of 1,4-dioxane from 0.25 to 25 mg/ml[25]**

---

[21] Young JD *et al.* (1977). Pharmacokinetics of 1,4-dioxane in humans. *J Toxicol Environ Health* 3:507-520 (1977).

[22] US Army Public Health Command. Studies on metabolism of 1,4-dioxane. Toxicology Report No. 87-XE-08WR-09. Aberdeen Proving Ground, MD (March 2010).

[23] Nannelli *et al.* 2005.

[24] Sweeney LM *et al.* Physiologically based pharmacokinetic modeling of 1,4-dioxane in rats, mice, and humans. *Tox Sci* 101(1):32-50 (2008).

[25] Ibid, at 38.

Once saturated, increased exposures result in a disproportional increase in circulating levels of 1,4-DX. This saturation phenomenon was observed in female mice exposed to up to 6000 ppm (1000 mg/kg/day) in drinking water for up to 90 days in a recently completed subchronic study sponsored by ACC and described in greater detail below (**Figure 4**).

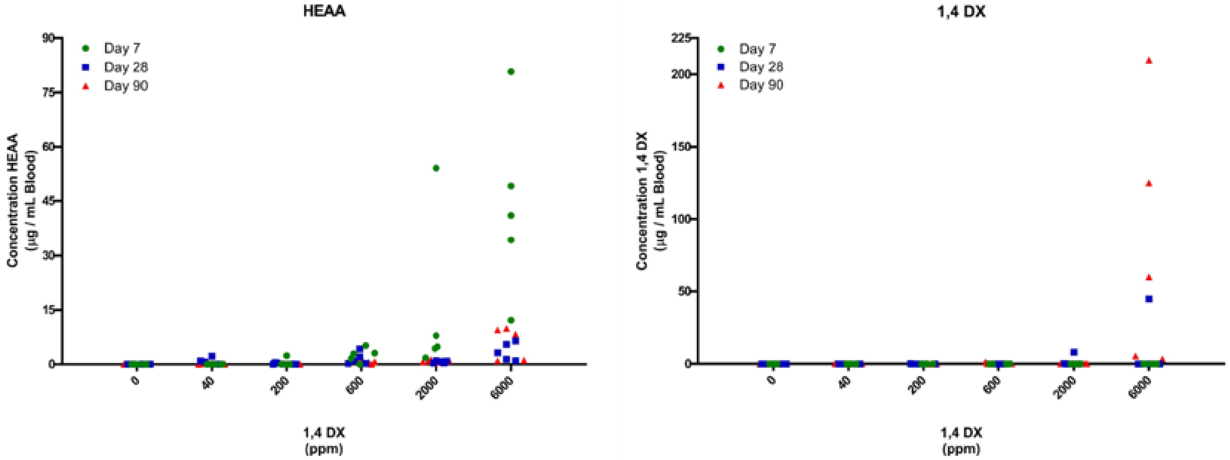

**Figure 4. Blood concentrations of β-hydroxyethoxy acetic acid (HEAA) metabolite and 1,4-dioxane (1,4 DX) after 7, 28, and 90 days of exposure to 1,4-dioxane in drinking water**[26]

At days 7 and 28, 1,4-DX blood concentrations were near or below the limit of detection. By day 90, blood levels of the parent compound increased significantly – but only at the highest dosage. At the same time, HEAA blood concentrations declined from day 7 to day 28, and by day 90, remained suppressed indicating a shift downward in the oxidative metabolism of 1,4-DX to HEAA. The results from the ACC sponsored study are summarized below. They are consistent with changing metabolic competency of the female mice as a critical key event in 1,4-DX toxicity.[27]

## Toxicokinetics

Studies have been conducted to determine whether 1,4-DX or one or more of its metabolites contributes to the chemical's reported toxicity. A study investigating the role of CYP450 isozymes in the liver toxicity of 1,4-DX reported no change in plasma alanine aminotransferase (ALT) activity or hepatic glutathione content even after inducing CYP with phenobarbital or by

---

[26] Lafranconi M *et al.* A 90-day drinking water study in mice to characterize early events in the cancer mode of action of 1,4-dioxane. *Reg Tox Pharma* 104819 (2020). (Attachment 1 - Article is available Open Access)

[27] According to EPA's Guidelines for Carcinogen Risk Assessment, a key event is defined as "an empirically observable precursor step that is itself a necessary element of the mode of action or is a biologically based marker for such an element." EPA/630/P-03/001F (March 2005) at 1-10.

fasting – indicating that HEAA or any potentially highly reactive intermediates do not play a role in the liver toxicity of 1,4-DX.[28] Pretreatment with inducers of mixed-function oxidases also did not significantly change the extent of covalent binding in subcellular fractions, supporting the conclusion that the metabolites are not toxicologically active.[29]

Taken together, these data support the hypothesis that the parent compound, 1,4-DX, and not a metabolite, is the toxic moiety. The observations in rat studies, and most of the studies in mice, support the conclusion that liver toxicity only occurs at exposures that exceed the metabolic threshold.[30,31]. It is therefore reasonable to conclude that metabolic saturation is an essential early key event to enable the subsequent sequence of events leading to tumor formation.[32,33]

This is the position taken by Heath Canada,[34] the World Health Organization,[35] the Australian National Industrial Chemicals Notification and Assessment Scheme,[36] and the Health Council of the Netherlands[37] in their assessments of health risks from 1,4-DX exposure, supporting a drinking water guideline of 50 ug/L.

---

[28] Nannelli *et al.* 2005.

[29] Woo Y *et al.* Metabolism in vivo of dioxane: effect of inducers and inhibitors of hepatic mixed-function oxidases. *Biochem Pharmacol* 26:1539-1542 (1977).

[30] Dourson M *et al.* Mode of action analysis for liver tumors from oral 1,4-dioxane exposures and evidence-based dose response assessment. *Regul Toxicol Pharma* 68:387-401 (2014).

[31] Dourson M *et al.* Update: Mode of action (MOA) for liver tumors induced by oral exposure to 1,4-dioxane. *Regul Toxicol Pharma* 88:45-55 (2017).

[32] Julien E *et al.* The key events dose-response framework: a cross-disciplinary mode-of-action based approach to examining dose-response and thresholds. *Critical Rev Food Sci Nutr 49*(8), 682–689 (2009).

[33] Boobis AR *et al.* Application of key events analysis to chemical carcinogens and noncarcinogens. *Crit. Rev. Food Sci Nutr* 49:690–707 (2009).

[34] Health Canada. 1,4-Dioxane in drinking water. Guideline Technical Document for Public Consultation (2018).

[35] WHO. 1,4-Dioxane in Drinking Water. Background document for development of WHO Guideline for Drinking Water Quality. WHO/SDE/WSH/05.08/120 (2005).

[36] NICNAS. Priority Existing Chemical Assessment Reports: 1,4-dioxane. Australia Department of Health and Ageing, Sydney, Australia. June (1998).

[37] Health Council of the Netherlands. 1,4-Dioxane – re-evaluation of the carcinogenicity and genotoxicity (2015). https://www.healthcouncil.nl/documents/advisory-reports/2015/11/13/14-dioxane-re-evaluation-of-the-carcinogenicity-and-genotoxicity

**Discussion of Cancer Bioassay Results**

The support document reviews data available from three studies in drinking water in laboratory animals and one inhalation study in male rats for its analysis of the potential carcinogenicity of 1,4-DX. The results of the study by Kano *et al.* (2009)[38] in BDF1 mice were selected as the basis for the derivation of a recommended MCL over the data from DuCrj rats in the same study or from the other drinking water studies by Kociba *et al.* (1974)*[39]* in rats and the National Cancer Institute (1978)[40] in rats and mice. The inhalation study by Kasai *et al.* (2009)*[41]* also was considered in the Subcommittee's analysis. Even though EPA selected specific findings from the study by Kano *et al.*, important key event and MOA information is available in the other cancer bioassays. Furthermore, a number of mechanistic studies looking at increased DNA synthesis and tumor promotion, add additional evidence supporting key events involving increased cell proliferation and tissue injury.

US EPA's 2005 Guidelines for Carcinogen Risk Assessment emphasize that –

> [r]ather than viewing default options as the starting point from which departures may be justified by new scientific information, these cancer guidelines view a critical analysis of all of the available information that is relevant to assessing the carcinogenic risk as the starting point from which a default option may be invoked if needed to address uncertainty or the absence of critical information.[42]

Yet, this is <u>not</u> what has been done in summary report or in the 2013 IRIS assessment of 1,4-DX. The weight of evidence clearly supports that the MOA for rodent tumors associated with high doses of 1,4-DX does not include the potential for mutagenicity, and the science clearly supports a threshold for both noncancer and cancer effects.

In the description of the potential cancer MOA, the summary document suggests that "while many of the genotoxicity studies . . . were negative, others provide evidence for mutagenicity

---

[38] Kano H et al. Carcinogenicity studies of 1,4-dioxane administered in drinking-water to rats and mice for 2 years. *Food Chem Toxicol* 47: 2776-2784 (2009).

[39] Kociba RJ *et al.* 1,4-dioxane. I. Results of a 2-year ingestion study in rats. *Toxicol Appl Pharmacol* 30: 275-286 (1974).

[40] National Cancer Institute (NCI). Bioassay of 1,4-dioxane for possible carcinogenicity. 78-1330 NCICGTR-80. Bethesda, MD (1978).

[41] Kasai T *et al.* Two-year inhalation study of carcinogenicity and chronic toxicity of 1,4-dioxane in male rats. *Inhal Toxicol* 21: 889-897 (2009).

[42] USEPA. Guidelines for Carcinogen Risk Assessment, at 1-7.

and chromosomal damage."[43] In fact, as described above, there is substantial evidence that 1,4-DX is *not* genotoxic at the low and mid doses in the rodent bioassays, and the possibility that there could be a genotoxic component to the mode of action associated with extremely high doses (e.g., 5000 ppm) is not relevant to the lower doses. Rather than a critical evaluation of the science and underlying biology, the Subcommittee provides the modeling results for all three of the drinking water studies and then chosen the most conservative number.\

In the support report, the Subcommittee presents modeling information for four tumor types reported in the animal bioassays – hepatocellular adenoma or carcinoma, nasal squamous cell carcinoma (SCC), peritoneal mesothelioma, mammary gland adenomas. An increase in liver cells adenomas and carcinomas was reported in all of the studies considered by the Subcommittee, except for the inhalation study by Torkelson *et al.* (1974).[44] With the exception of the liver tumors in female mice in the study by Kano *et al.*, tumors were only observed at doses that exceeded 200 milligrams per kilogram (mg/kg) per day. Similarly, the nasal SCCs reported by rats in the NCI, Kano *et al.*, and Kasai *et al.* studies only occurred in the highest dose group.[45] The increases in peritoneal mesotheliomas and mammary gland adenomas were only reported by among rats in highest dose group in the study by Kano *et al.* The results of the studies are summarized in **Tables 1 and 2**.

## Hepatocellular Adenomas and Carcinomas

In experimental animals, 1,4-DX exposures caused liver toxicity as evidenced by several histological and/or biochemical changes (e.g., liver enzyme changes, centrilobular swelling, and/or necrosis) as early as 13 weeks of treatment,[46] and in a dose-related manner in both sexes of rats.[47] The available studies also show that this liver toxicity precedes tumors temporally in both sexes of rats with liver histopathology preceding tumors and liver toxicity. [48]

Kano *et al.* (2009) report that "[a] significant increase in the incidence of hepatocellular foci was observed in the 1000 and 5000 ppm exposed males and the 5000 ppm-exposed females" in their rat study. While there was a statistically significant increase in mixed cell foci at the mid-

---

[43] Summary document, at 36.

[44] Torkelson *et al.* 1,4-Dioxane. II. Results of a 2-year inhalation study in rats. *Toxicol Appl Pharmacol* 30: 287-298 (1974).

[45] Contrary to the suggestion in the summary document that Torkelson *et al.* did not evaluate the incidence of nasal SCC, the authors note that no nasal tumors were observed in any of the rats.

[46] Kano H *et al.* Thirteen-week oral toxicity of 1,4-dioxane in rats and mice. *J Toxicol Sci* 33: 141-153 (2008).

[47] USEPA 2013; USEPA. Draft Risk Evaluation for 1,4-Dioxane. EPA-740-R1-8007. Office of Chemical Safety and Pollution Prevention (2019).

[48] USEPA 2013, at 85.

**Table 1. Tumor results in cancer studies of rats and mice exposed to 1,4-dioxane in drinking water**

| Study | Species/strain /sex | Dose (mg/kg) | Liver | Nasal Cavity | Peritoneal | Mammary Gland |
|---|---|---|---|---|---|---|
| Kociba *et al.* 1974 | Sherman rats - male + female | 0 | 2 | 0 | -- | -- |
| | | 14 | 0 | 0 | -- | -- |
| | | 121 | 1 | 0 | -- | -- |
| | | 1307 | 12** | 3 | -- | -- |
| NCI 1978 | Osborne-Mendel rats - male | 0 | 2 | 0 | 0 | 0 |
| | | 240 | 2 | 12 | 3 | 3 |
| | | 530 | 1 | 16** | 2 | 0 |
| | Osborne-Mendel rats - female | 0 | 0 | 0 | -- | 4 |
| | | 350 | 10** | 10** | -- | 3 |
| | | 640 | 11** | 8** | -- | 1 |
| | B6C3F1 mice - male | 0 | 8 | 0 | -- | -- |
| | | 720 | 19* | 0 | -- | -- |
| | | 830 | 28** | 1 | -- | -- |
| | B6C3F1 mice - female | 0 | 0 | 0 | 1 | -- |
| | | 380 | 21** | 1 | 0 | -- |
| | | 860 | 35** | 0 | 0 | -- |
| Kano et al. 2009 | Male F344/ DuCrj rats – male | 0 | 3 | 0 | 2 | 1 |
| | | 11 | 4 | 0 | 2 | 2 |
| | | 55 | 7 | 0 | 5 | 2 |
| | | 274 | 39** | 3 | 28** | 6 |
| | Male F344/ DuCrj rats - female | 0 | 3 | 0 | 1 | 8 |
| | | 18 | 1 | 0 | 0 | 8 |
| | | 83 | 6 | 0 | 0 | 11 |
| | | 429 | 48** | 7** | 0 | 18* |
| | Male Crj:BDF1 mice – male | 0 | 23 | 0 | -- | -- |
| | | 49 | 31 | 0 | -- | -- |
| | | 191 | 37* | 0 | -- | -- |
| | | 677 | 40** | 1 | -- | -- |
| | Male Crj:BDF1 mice – female | 0 | 5 | 0 | -- | -- |
| | | 66 | 35** | 0 | -- | -- |
| | | 278 | 41** | 0 | -- | -- |
| | | 964 | 46** | 1 | -- | -- |

* - Significantly different from control at $p<0.05$ by Fisher's exact test

** - Significantly different from control at $p<0.01$ by Fisher's exact test.

-- - Data not reported.

**Table 2. Tumor results in cancer studies of rats exposed to 1,4-dioxane via inhalation**

| Study | Species/strain /sex | Dose (mg/kg) | Liver | Nasal Cavity | Peritoneal | Mammary Gland |
|---|---|---|---|---|---|---|
| Torkelson et al. 1974 | Wistar rats – male | 0 | 0 | 0 | n/a | 0 |
| | | 70 | 0 | 0 | n/a | 0 |
| | Wistar rats – female | 0 | 0 | 0 | n/a | 24 |
| | | 70 | 0 | 0 | n/a | 45 |
| Kasai et al. 2009 | F344/ DuCrj rats – male | 0 | 1 | 0 | 2 | 1 |
| | | 33 | 2 | 0 | 4 | 2 |
| | | 165 | 4 | 1 | 14** | 3 |
| | | 826 | 23** | 6* | 41** | 6 |

* - Significantly different from control at $p<0.05$ by Fisher's exact test
** - Significantly different from control at $p<0.01$ by Fisher's exact test.
n/a – data not available.

dose (1000 ppm), there was a *decreased* incidence of acidophilic foci (7/50) in the same dose group compared to controls (12/50), such that overall there was no overall increase in altered hepatocellular foci until the high dose. Kano *et al.* also report a significant increase in liver weight in mid- and high-dose male rats, with no effect in the low-dose. There were similar findings in the female rat liver, with effects (liver weight, preneoplastic foci, and hepatocellular tumors) being observed only at the highest dose, providing further evidence for a threshold for the liver tumors.

These exposures result in doses that exceed the limit of metabolic saturation in the rat which has been estimated to be between 30 and 100 mg/kg/day. In the earlier subchronic study, moreover, the same research group observed liver lesions (including single cell necrosis and centrilobular swelling) in rats and mice at exposures of 1600 ppm and higher.[49]

Similarly, data from Kociba *et al.* described a number of important key events supporting a regenerative repair and/or direct mitogenic response to 1,4-DX exposure that is correlated with saturation of the metabolic pathway 4-DX metabolism at 100 mg/kg/day (**Figure 5**). For example, increased foci occur at a greater frequency and earlier than do liver tumors. This phenomena was also observed for vacuolar degeneration and necrosis, with both occurring with greater frequency and lower doses than the high-dose liver tumor (HCA) response. This illustrates a good dose-concordance for key events explaining a tumor promotion apical outcome.

---

[49] Kano *et al.* 2008, at 2781.

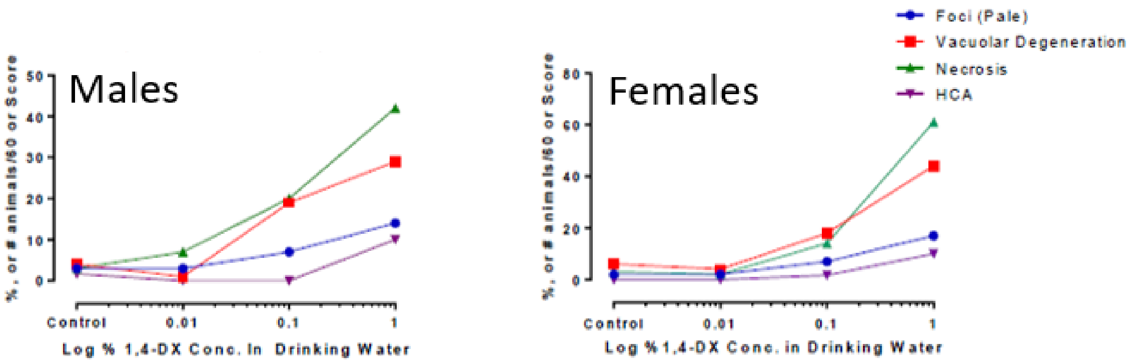

**Figure 5. Liver effects from Kociba *et al.* with Sherman rats**[50]
(Vacuolar degeneration was scored from 1 (minimal) to 3 (severe).

Kasai *et al.* also reported a number of histopathological observations that illustrate cell proliferation consistent with tumor promotion (**Figure 6**).

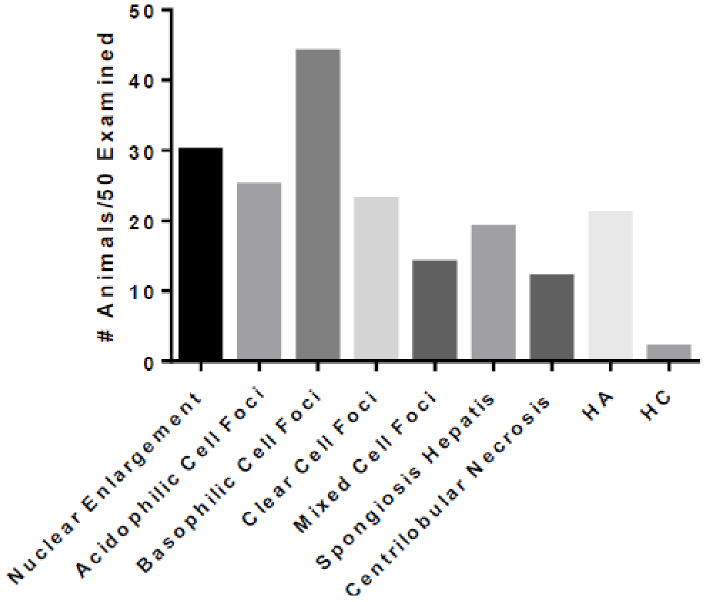

**Figure 6. Histological findings in rats exposed to 1250 ppm 1,4-dioxane in Kasai *et al.* (HA- adenomas, HC – carcinomas)**[51]

---

[50] Estimated doses were 0, 9.6(0.01%), 94 (0.1%) and 1015 (1.0%) mg/kg/day for males and 0, 19, 148 and 1599 mg/kg/day for females. The unpublished results from Kociba *et al.* are included as Attachment 2 to this comment.

[51] Kasai *et al.* 2009, at 893 (Table 3).

The various focal lesions shown in Figure 8 represent hyperplasia induced by either direct stimulation of proliferation or indirectly stimulated by regenerative repair.

In reviewing the liver data, the peer reviewers of EPA's 2013 IRIS assessment noted the inconsistency in the appearance of liver toxicity prior to tumor occurrence in the mouse studies and suggested that standard reporting practices at the time may have led to underreporting in the dose response in cytotoxicity.[52] As a consequence Dourson *et al.* (2014) reevaluated the histopathology slides from the NCI bioassay and reported evidence of dose-related, non-cancer changes in rat and mouse livers preceding the occurrence of tumors.[53] Dourson *et al.* (2017)[54] subsequently reviewed translated reports from the second bioassay[55] in hopes of resolving the inconsistencies in the animal data between the bioassay, the findings of the Dourson *et al.* 2014 review of the NCI study, and the results of a 13-week study by the researchers of the second bioassay.[56] As Dourson *et al.* noted in the paper –

> the lack of noncancer histopathology in the chronic mouse study is not consistent with the changes in liver enzymes in this same chronic study, nor is this lack of noncancer findings expected based on the histopathology of the precursor 13-week study. Nor does the tumor response in the low dose female mice of JBRC . . . match the tumor findings in the [Dourson *et al.* 2014] re-read of NCI (1978).[57]

Dourson *et al.* also noted that –

> While the non-neoplastic lesions found in the NCI (1978) slide reread that we

---

[52] Specifically: "The EPA should explore the possibility that slides from the NCI studies on 1,4-dioxane are available and in adequate condition to evaluate possible linkages between toxic effects and tumor outcome in the drinking water carcinogenicity studies in rats and mice." PEER REVIEWER COMMENTS. External Peer Review on the Toxicological Review of 1,4-Dioxane (CASRN No. 123-91-1). Versar, Inc. Contract No. EP-C-07-025 Task Order 118 (May 2012).

[53] Dourson ML *et al.* 2014. Mode of action analysis for liver tumors from oral 1,4-dioxane exposures and evidence-based dose response assessment. *Reg Toxicol Pharma* 68:387-401.

[54] Dourson ML *et al.* 2017. Update: Mode of action (MOA) for liver tumors induced by oral exposure to 1,4-dioxane. *Reg Toxicol Pharma* 88:45-55.

[55] Japan Bioassay Research Center (JBRC). Report of carcinogenicity study by oral administration of 1,4-dioxane (mixed with water) to rats and mice. Japan Industrial Safety and Health Association. Results reported in Kano *et al.* 2009.

[56] JBRC. Report of preliminary carcinogenicity studies (acute, two-week, and thirteen-week studies) by oral administration of 1,4-dioxane (mixed with water) to rats and mice. Japan Industrial Safety and Health Association. Results reported in Kano H *et al.* 2008.

[57] Dourson *et al.* 2017, at 49.

> show in this paper were not reported in mice from one long-term study (Kano *et al.* 2009), the same Japanese investigators did report hepatic hyperplasia (later changed to altered hepatocellular foci) in an earlier report of this same 2- year study . . . Moreover, mice in the Kano *et al.* (2009) study showed hepatocellular injury as evidence by an enhanced cytolytic release of liver enzymes . . . at doses of about 140-1400 mg/kg/day [unpublished results].[58]

In comparing the reported findings from the various studies, Dourson *et al.* (2017) concluded that "dose response and temporal concordance for noncancer precursors to tumors are clearly evident in rats . . . and generally supportive in mice." The authors noted that interpretation of the JBRC bioassay data was complicated by an absence of histopathological evidence and confusion about changes made in the diagnosis of liver effects in Kano *et al.* (2009).[59]

## Results of New Subchronic Study in Female Mice

To better define the key events associated with tumor formation in the laboratory animals, Lafranconi et al. conducted a subchronic drinking water study in female mice.[60] Mice consumed drinking water containing 0, 40, 200, 600, 2000 or 6000 ppm 1,4-DX (approximately 0, 10, 40, 120, 360 and 1,000 mg/kg/day, respectively) for 90-days. Interim sacrifices were conducted after 7 and 28 days of exposure. Standard in-life measurements, clinical chemistries, H&E, biomarkers including BrdU, Caspase 3, GSTP+, blood levels of 1,4-DX and HEAA, and mRNA were evaluated.

There was an increase in liver weights in animals exposed to 2000 and 6000 ppm 1,4-DX for 90 days with insignificant changes in liver weights at lower exposures. H&E observations of glycogen-accumulation-related vacuolization, centrilobular hypertrophy, and centrilobular GST-P staining, panlobular increase in proliferation (BrdU), and elevated Caspase 3, were all tightly linked to the accumulation of 1,4-DX in the blood, especially at the 90-day time point. There was no evidence of liver injury, either from clinical chemistry endpoints or histopathology unlike what was observed in a previous 2-year bioassay. However, the researchers did observe an early-phase increase in BrdU incorporation consistent with a direct mitogenic stimulus at exposures that exceeded the demonstrated metabolic saturation levels after 90- days of exposure. No such stimulus was observed at lower exposures at 90 days or at any exposure at the earlier time points. The threshold observed in this study was 2000 ppm. The increase in the BrdU response correlates with an approximate 4.5 fold increase in 1,4-DX blood levels after

---

[58] Dourson *et al.* 2014, at 399.

[59] Dourson *et al.* 2017, at 49.

[60] Lafranconi M *et al.* 2020 (Attachmenbt 1).

90-days of exposure at 6000 ppm (**Figure 7**).

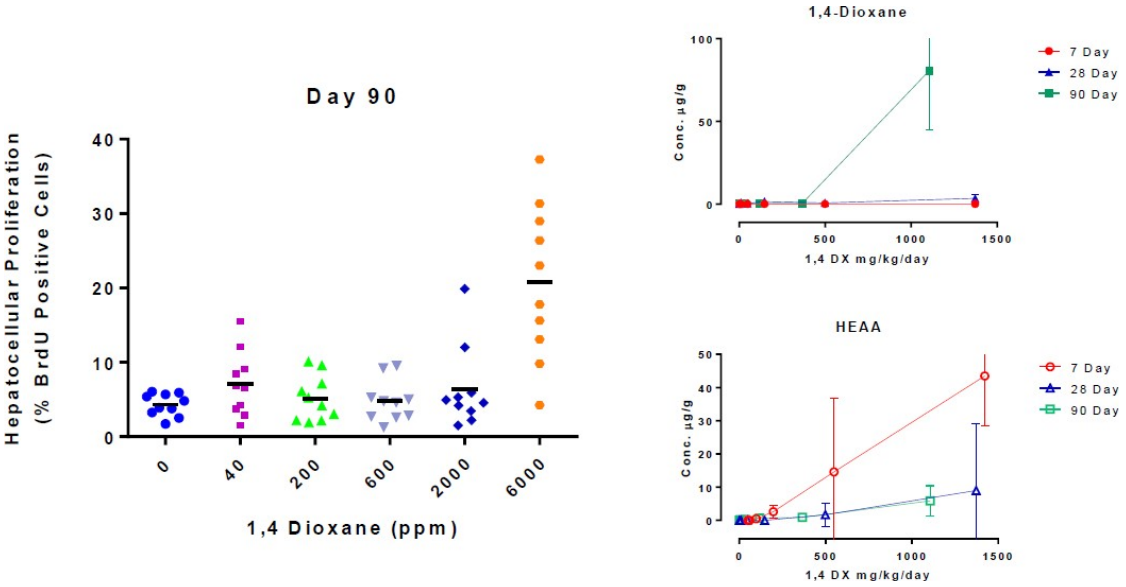

**Figure 7. Increase cell proliferation in female mice correlates with an increase in blood 1,4-dioxane concentrations**[61]

As part of the study, ACC also sponsored a transcriptomics analysis of the livers using the TempO-Seq platform (BioSpyder Technologies). **[62]** The results of this analysis demonstrate an increase in xenobiotic metabolism, a subtle yet significant dose- and time-responsive increase in mitotic cell cycle and cellular proliferation, and a decrease in complement cascade processes and lipid metabolism. The signals for proliferative response only occur at exposures of 2000 ppm or greater, while alterations related to xenobiotic metabolism occur as low as 600 ppm. Activation of DNA damage response and/or repair mechanisms was not evident at any of the concentrations and time points evaluated. As illustrated in **Figure 8**, there are no significant changes in signaling pathways/gene sets at the transcriptomic level at concentrations below 600 ppm.

---

[61] Ibid.

[62] Chappell *et al.* Transcriptomic analyses of livers from mice exposed to 1,4-dioxane for up to 90 days to assess potential mode(s) of action underlying liver tumor development. (In Press). Report submitted to USEPA included as Attachment 2. (https://www.regulations.gov/document?D=EPA-HQ-OPPT-2019-0238-0059)

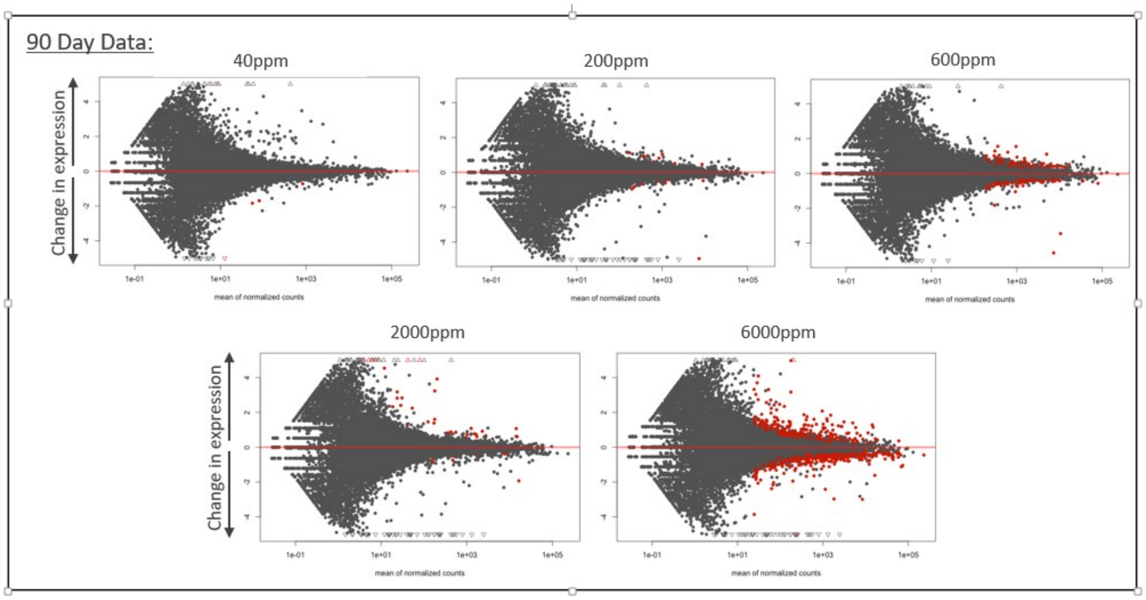

**Figure 8. Differential gene expression data after 90 days of exposure in female rats (Chappell *et al.*) (red dots designate significant up- or down-regulation of individual genes.)**

Mitogenic MOA

The results from this latest 90-day study add significantly to our understanding of the dose-response for 1,4-DX by demonstrating a clear threshold for any effect in the liver at a genomic level and supporting a mitogenic MOA for mouse liver tumors. The mitogenic response reported by Lafranconi *et al.* was characterized by a pronounced increase in lobule-wide BrdU incorporation in the 6000 ppm exposure group after 90-days of exposure. Accompanying the onset of high dose centrilobular single cell apoptosis and cell proliferation in the late-phase response was a loss of glycogen-like vacuolation and increased centrilobular staining for GST-P. A similar pattern of hepatocyte proliferation was reported in rats.[63] Notably, the late phase responses in this current study occurred at exposures that exceeded the metabolic clearance threshold although some mild changes in the liver were seen at lower exposures.

This mitogenic response occurs early and likely adds to the regenerative repair that is suggested from the increase in single cell necrosis (apoptosis) reported. Although these responses are small, they occur in a target organ (liver) in a mouse strain that is highly susceptible to the

---

[63] Goldsworthy TL *et al.* Examination of potential mechanisms of carcinogenicity of 1,4-dioxane in rat nasal epithelial cells and hepatocytes. *Arch Toxicol* 65:1-9 (1991)

induction of liver cancer.[64]

This relationship has been described previously from data generated in both rats and mice. Importantly, the mitogenic stimulation observed by Lagfranconi *et al.*, approximately a five-fold increase in liver proliferation (labeling index) in the 6000 ppm exposure group after 90 days, occurs prior to the development of cytotoxicity and the regenerative repair that is a cornerstone of the regenerative hyperplasia MOA. In this new study, 1,4-DX exposure stimulated hepatic proliferation as a result of an apparent direct mitogenic response which is recognized as a carcinogenic MOA.[65] The magnitude of the proliferative response reported is comparable to other mitogenic, non-genotoxic hepatocarcinogens.[66,67]

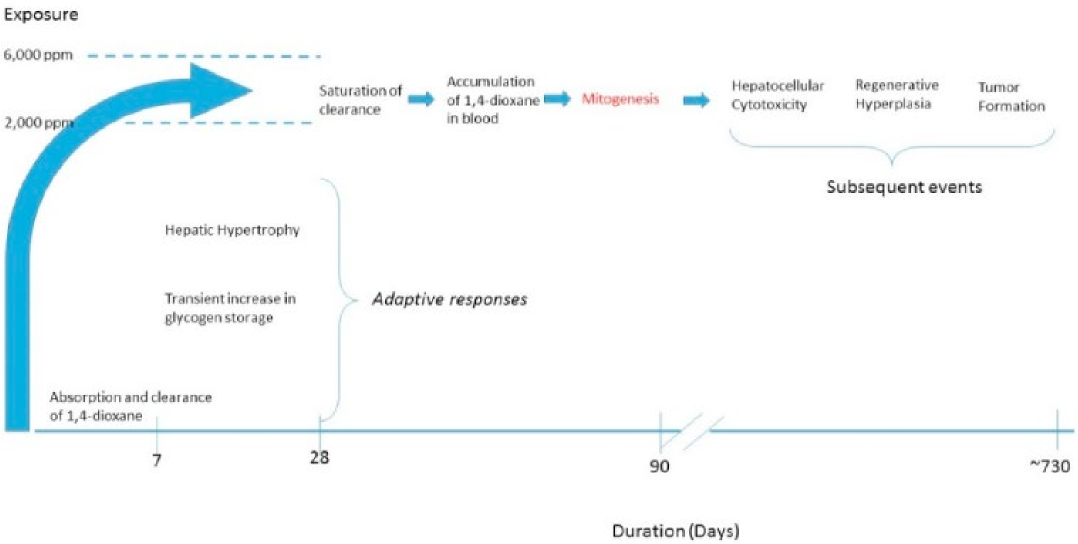

**Figure 9. Updated MOA of 1,4-DX induced development of hepatic tumors[68]**

The results reported by Lafranconi *et al.* are consistent with those in the 13-week drinking water study reported by Kano *et al.* (2008) in which BDF1 mice were exposed to up to 25,000

---

[64] Holsapple, MP *et al.* Mode of action in relevance of rodent liver tumors to human cancer risk. *Toxicol Sci* 89, 51–56 (2006).

[65] USEPA 2005.

[66] Geter DR *et al.* Dose-response modeling of early molecular and cellular key events in the CAR-mediated hepatocarcinogenesis pathway. *Toxicol Sci* 138:425–445 (2014).

[67] LaRocca JL *et al.* 2017. Integration of novel approaches demonstrates simultaneous metabolic inactivation and CAR-mediated hepatocarcinogenesis of a nitrification inhibitor. *Toxicol Reports* 4:586–597 (2017).

[68] Lafranconi *et al.* 2020.

ppm of 1,4-DX in drinking water.[69] The doses required to cause liver effects in the two 13-week study are considerably higher than those reported to cause liver tumors in female mice in the 2-year bioassay by Kano *et al.* (2009)[70] which has caused some to question the significance of these tumors. In considering the results of the bioassay by Kano *et al.*, for example, Health Canada concluded that --

> The absence of non-cancer histopathological changes and the concomitant increase in liver enzymes in the [Kano *et al.* bioassay] despite the presence of both endpoints in the subchronic studies from the same group . . . lend credence to the uncertainty surrounding the development of tumors at this low dose.[71]

USEPA's Risk Evaluation under the Toxic Substances Control Act

In its most recent review of the female mouse liver tumor data, USEPA expressed the following concerns about the use of these data for risk characterization –

> Female mouse hepatocellular carcinoma data from Kano et al. (2009) were not modeled due to the difficulties that were previously noted in the U.S. EPA (2013c) IRIS assessment. Specifically, this endpoint exhibited a low control group incidence, and a high (70% incidence) response rate at the lowest dose followed by a plateau. While the U.S. EPA (2013c) IRIS assessment did perform BMD modeling on these data, it was necessary to increase the BMR, omit the highest dose group, and apply a non-multistage model.[72]

Although this latest evaluation by USEPA continues to use the default linear low-dose (no-threshold) extrapolation in estimating the potential carcinogenic risk, it dismisses the mouse liver tumors that are the Subcommittee's key rational for rejecting the threshold MOA.

### Nasal Cavity Squamous Cell Carcinoma

A small, but statistically significant, increase in nasal cavity squamous cell carcinoma (SCC) has been reported in studies of rats exposed to 1,4-DX in drinking water studies (NCI 1978, Kano *et al. 2009*) and by inhalation (Kasai *et al.*)[73] SCC was not observed in the drinking water study by

---

[69] Kano H *et al.* 2008.

[70] Kano H et al. 2009.

[71] Health Canada 2018, at 30.

[72] USEPA 2019, at 334.

[73] An additional study by Hoch-Ligeti et al. (1970) reported nasal tumors in rats but was not included in the

Kociba et al. at doses up to 1307 mg/kg per day.  In all cases, the reported increase in nasal tumors was limited to animals in the highest dose group which exceeded the estimated metabolic saturation threshold of 100 mg/kg/day (**Figure 9**).

Kasai *et al.* also reported a significant increase in non-carcinogenic and pre-neoplastic lesions in the nose cavity at all doses (~33 to 826 mg/kg/day) (**Figure 10**).  Similar lesions were elevated at the highest dose in the 2009 bioassay by Kano *et al.* (~274 mg/kg/day in males and 429 mg/kg/day in females).[74]

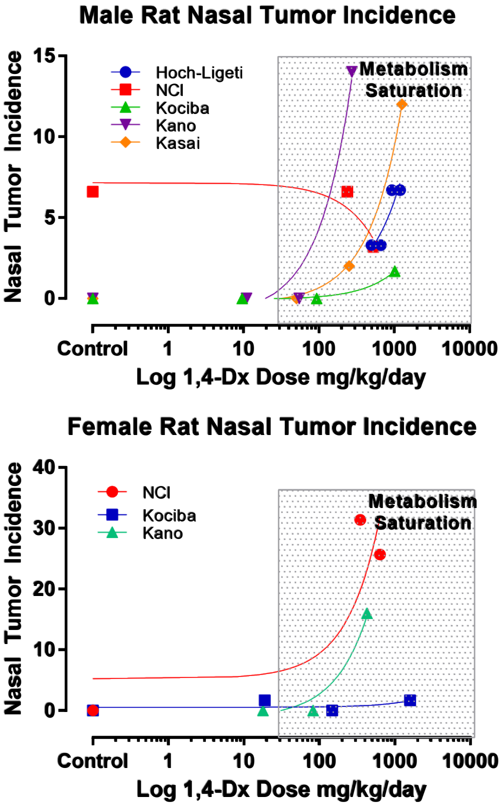

**Figure 9. Nasal tumor data from available bioassays.**

The available evidence clearly indicate a threshold for a carcinogenic response in the nasal cavity, similar to that observed in the liver.  In fact, it is not uncommon for nasal tumors to arise from regenerative processes.  There are several substances that cause SCC in the nasal cavity in rats via a proliferative MOA.  Perhaps the most notable of these substances is formaldehyde,

---

Subcommittee's quantitative analysis.  Hoch-Ligeti C *et al.* Induction of carcinomas in the nasal cavity of rats by dioxane. *Brit J Cancer* 24:164-167 (1970).

[74] Kano *et al.* 2009, at 2780.

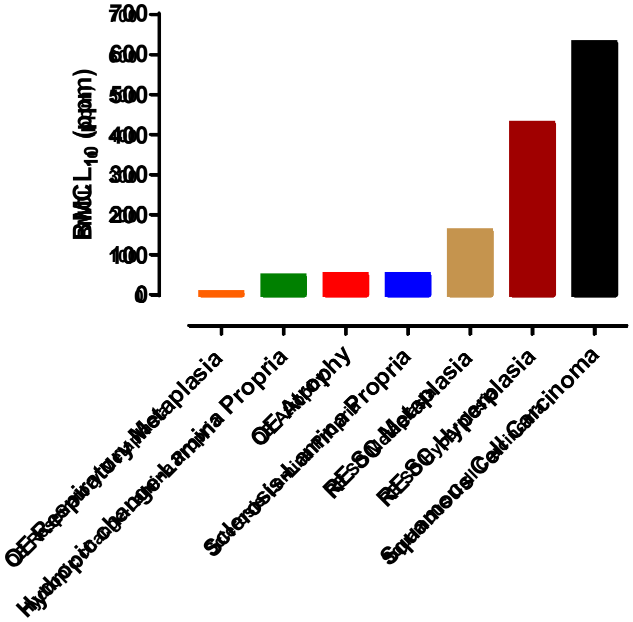

**Figure 10. Benchmark dose, lower 95% confidence limit at 10% extra risk ($BMDL_{10}$) for key events in formation of nasal tumors (from USEPA analysis of data from Kasai *et al.* 2009)[75]**

which the European Commission (EC) and the World Health Organization have concluded will not cause SCC at exposures below those that result in chronic injury in the nasal cavity. In developing its worker protection standard for formaldehyde, the EC's Scientific Committee on Occupational Exposure Limit Values concluded that --

> Mechanistic studies have provided strong evidence that tumour induction in the nasal mucosa of rats and mice is the result of chronic proliferative processes caused by the cytotoxic effects of the substance in combination with DNA alterations by endogenous and exogenous [formaldehyde]. The dose-response relationships for all parameters investigated, such as damage to the nasal epithelium, cell proliferation, tumour incidence, the formation of [DNA-protein crosslinks, DPX] and DNA-adducts, is very flat for low level exposures and becomes much steeper at higher concentrations. For these endpoints no-effect concentrations were demonstrated with the exception of the formation of DPX and DNA-adducts.[76]

---

[75] USEPA 2019, at 114 and 116.

[76] Scientific Committee on Occupational Exposure limits. SCOEL/REC/125 Formaldehyde (2017). https://publications.europa.eu/en/publication-detail/-/publication/7a7ae0c9-c03d-11e6-a6db-01aa75ed71a1/language-en

Thus, there is clear evidence to suggest that nasal SCC (and other nasal tumors) only occur after an exposure threshold is exceeded.

**Significance of Other Tumors**

In addition to hepatic cellular tumors and nasal SCC, the summary document presents information on the incidence of peritoneal mesothelioma and mammary gland fibroadenoma in its review. Of these tumors, only peritoneal mesothelioma showed a statistically significant increase at the highest dose in male rats in the study by Kano *et al.* and in the two highest doses in the study by Kasai *et al.* Similarly, mammary gland adenomas were significantly increased in the female rats in the highest dose group in the Kano et al. study. In the case of both tumor types, there is significant evidence that these also are spontaneous tumors and likely not appropriate for inclusion in the risk evaluation. This evidence is described further below.

Peritoneal Mesothelioma

Peritoneal mesothelioma is well-recognized as a common, age-related spontaneous tumor in the male F344 rat,[77] clearly acknowledged by Kano *et al.* who explain that "[i]t has been recognized that the peritoneal mesothelioma is a commonly observed, spontaneous neoplasm of male F344 rats arising from the tunica vaginalis."[78] The only statistically-significant increase seen in the bioassay was in males at the highest dose of 5000 ppm (~ 274 mg/kg/day). It is also noted that this tumor type was *not* increased in the drinking water bioassay in male rats by Kociba *et al.* (1974).[79] This provides clear evidence for a threshold for this tumor type and indicate that default, low-dose extrapolation is not supported by the science.

The incidence of peritoneal mesothelioma seldom occurs directly in toxicological studies.[80] Rather it occurs as a result of changes in other organ systems. Accordingly, Kasai *et al.* reported a statistically significant increase in peritoneal mesotheliomas in male, but not female, F344 rats at the two high doses. This sex difference is likely due to the occurrence of tunica vaginalis mesotheliomas (TVM) which grow into the peritoneal cavity. TVMs are a commonly occurring

---

[77] Haseman *et al*. 1984; Hall WC. Peritoneum, retroperitoneum, mesentery, and abdominal cavity. Chapter 6:63-69. In Boorman GA, Eustis SL, Elwell MR, Montgomery CA, MacKenzie WF (Eds). Pathology of the Fischer Rat: Reference and Atlas. San Diego, CA: Academic Press (1990).

[78] Kano H *et al.* (2009), at 2783.

[79] Unpublished data from the study by Kociba *et al.* are included as Attachment 3.

[80] Zimmerman B. Peritoneum, retroperitoneum, mesentery, and abdominal cavity. Chapter 8:71-77. In Suttie AW (Ed). Boorman's Pathology of the Rat: Reference and Atlas. Second Edition. Academic Press (2015).

tumor in these male rats, but are rare in humans, and likely are not relevant to this risk evaluation.[81]

Mammary Gland Adenoma

While not observed in the male rats, Kano *et al.* (2009) reported a statistically significant increase in mammary gland adenomas in female rats at high doses. Adenomas were not observed in female rats in the drinking water studies conducted by the National Cancer Institute[82] and Kociba *et al.* Mammary gland tumors were not significantly increased in male rats in any of the bioassays. Mammary gland adenomas are a benign, commonly observed, and spontaneous neoplasm of F344 rats.[83]

### Alternative MOAs

Although the Subcommittee and USEPA recognize that a mutagenic MOA is unlikely for the carcinogenicity of 1,4-dioxane, both maintain that use of a non-threshold (linear, low dose extrapolation) is appropriate since a cancer MOA "has not been conclusively established." While a proliferative response involving a threshold is wholly consistent with the available data, the Subcommittee appears to suggest – without evidence – that a non-threshold MOA other than genotoxicity can explain the observations in the animal bioassays.

Other MOAs such as infection, oxidative damage, and receptor-mediated processes have been identified for other substances. None of the available studies reported infections, however, and since the studies show a dose-related response in tumors infection is not the likely MOA.[84] Similarly data on oxidative stress are limited, but negative, with enhanced metabolism of 1,4-DX not showing any greater toxicity. Receptor mediated MOAs, such as the peroxisome proliferator-activated receptor -alpha (PPARα) [85] and the constitutive androstane receptor (CAR),[86] can also play a role in the developments of liver tumors in rodents exposed to non-genotoxic carcinogens. However, the pattern of responses in rodents resulting from 1,4-DX

---

[81] Haber LT *et al.* Assessment of human relevance and mode of action for tunica vaginalis mesotheliomas resulting from oral exposure to acrylamide. *Regul Toxicol Pharmacol* 53(2):134–149 (2009).

[82] NCI 1978.

[83] Boorman GA *et al.* Mammary gland. pp. 295–313. In: Boorman GA, Eustis SL, Elwell MR, Montgomery CA, MacKenzie WF (Eds). Pathology of the Fischer Rat. Academic Press, San Diego, CA (1990).

[84] Dourson et al. 2017, at 53.

[85] Klaunig JE *et al.* PPARα agonist-induced rodent tumors: modes of action and human relevance. Crit. Rev. Toxicol. 33, 655–780 (2003).

[86] Elcombe CR *et al.* Mode of action and human relevance analysis for nuclear receptor-mediated liver toxicity: a case study with phenobarbital as a model constitutive androstane receptor (CAR) activator. *Crit Rev Toxicol* 44:64–82 (2014).

exposure do not completely align with the MOA. Peroxisome proliferation is a key observation observed from PPARα activity and CAR activation generally leads to inhibition of apoptosis.[87] Neither of these are observed in 1,4-DX exposed rodent liver. Furthermore, whole transcriptome analyses of mRNA of liver tissues from ACC's 90 mouse study shows no evidence of PAPRα or CAR activity.[88] Specifically, there was no change in the expression of individual CYP-encoding genes that are considered markers of activation of such nuclear receptors, nor enrichment of gene-level changes in the signaling pathways relevant to these nuclear receptors.

---

[87] Felter SP *et al.* Human relevance of rodent liver tumors: key insights from a Toxicology Forum workshop on nongenotoxic modes of action. *Reg Toxicol and Pharma* 92:1-7 (2018).

[88] Chappell *et al.* (In Press)

Regulatory Toxicology and Pharmacology 119 (2021) 104819

Contents lists available at ScienceDirect

Regulatory Toxicology and Pharmacology

journal homepage: www.elsevier.com/locate/yrtph

# A 90-day drinking water study in mice to characterize early events in the cancer mode of action of 1,4-dioxane

Mark Lafranconi [a,*], Robert Budinsky [b], Lisa Corey [c], Joanna Klapacz [b], James Crissman [d], Matthew LeBaron [b], Rachel Golden [b], Richard Pleus [c]

[a] *Environmental Resources Management, Cincinnati, OH, USA*
[b] *Toxicology and Environmental Research and Consulting, The Dow Chemical Company, Midland, MI, USA*
[c] *Intertox, Seattle, WA, USA*
[d] *StageBio, Mason, OH, USA*

ARTICLE INFO

*Keywords:*
1,4-Dioxane
Mouse liver
Mode of action
Mitogenesis

ABSTRACT

Studies demonstrate that with sufficient dose and duration, 1,4-dioxane (1,4-DX) induces liver tumors in laboratory rodent models. The available evidence aligns with a threshold-dependent, tumor promotion mode of action (MOA). The MOA and key events (KE) in rats are well developed but less so in the mouse. Therefore, we conducted a 90-day drinking water study in female mice to evaluate early KE at 7, 28, and 90 days. Female B6D2F1/Crl mice consumed drinking water containing 0, 40, 200, 600, 2000 or 6000 ppm 1,4-DX. 1,4-DX was detected in blood at 90-days of exposure to 6000 ppm, but not in the other exposure groups, indicating a metabolic clearance threshold between 2000 and 6000. Early events identified in this study include glycogen-like vacuolization, centrilobular hypertrophy, centrilobular GST-P staining, apoptosis, and pan-lobular increase in cell proliferation observed after 90-days of exposure to 6000 ppm 1,4-DX. There was minimal evidence of hepatotoxicity over the duration of this study. These findings demonstrate a previously unreported direct mitogenic response following exposures exceeding the metabolic clearance threshold of 1,4-DX. Collectively, the information generated in this study supports a threshold MOA for the development of liver tumors in mice after exposure to 1,4-DX.

## 1. Introduction

Lifetime inhalation or oral exposure to 1,4-dioxane (1,4-DX) causes liver and other organ tumors in laboratory animals (Argus et al., 1973; Argus MF, Arcos JC, 1965; International Center for Medical Research et al., 1988; Kano et al., 2009; Kasai et al., 2009; Kociba et al., 1974; NCI, 1978). Tumor development in these studies generally occurs only at or near the maximum tolerated dose.

Currently available information from both chronic and sub-chronic rodent studies by various routes of administration is consistent with a threshold regenerative hyperplasia Mode of Action (MOA) as proposed by Dourson et al. (2014, 2017). While there is abundant information for characterizing the MOA for tumor development in rats, the evidence in mice is less developed. Earlier Japanese and NCI cancer bioassays, and their sub-chronic companion studies, provided only limited details concerning KE in the mouse model (Kano et al., 2009, 2008; NCI, 1978). In two recent analyses of the rodent liver tumor evidence, the 2-year NCI cancer bioassay in mice was re-evaluated with updated pathology standards to better characterize both the tumor and non-tumor lesions (Dourson et al., 2014). While this effort greatly expanded our understanding of the MOA for 1,4-DX in mice, there were still information gaps for characterizing early events in the development of hepatic tumors in mice exposed to 1,4-DX.

In this publication we present evaluations of clinical chemistry, biochemical and histological hepatic effects in female B6D2F1/Crl mice after exposure to 1,4-DX in drinking water for 7, 28, and 90 days. In addition, we related these findings to blood concentrations of 1,4-DX and its primary metabolite, hydroxyethoxy acetic acid (HEAA).

## 2. Materials and methods

This study was conducted in compliance with Good Laboratory Practice Standards and designed to generate information that would be relevant for interpreting the results from previous studies with 1,4-DX.

---

[*] Corresponding author
*E-mail address:* mark.lafranconi@erm.com (M. Lafranconi).

https://doi.org/10.1016/j.yrtph.2020.104819
Received 5 June 2020; Received in revised form 23 September 2020; Accepted 3 November 2020

Female B6D2F1 mice were selected to match as closely as possible the mouse strain used by Kano et al. (Kano et al, 2008, 2009). Drinking water concentrations were selected to reproduce the critical outcomes from previous studies, such as metabolic saturation, cytotoxicity, cell proliferation, apoptosis, and GSTP expression.

### 2.1. *Chemicals*

1,4-DX was obtained from Sigma-Aldrich (Lot SHBJ7415), St. Louis MO and was determined to be 99.98% pure. Reagents for BrdU (BD Biosciences:BD Pharmigen™ BrdU In-Situ detection Kit BD Biosciences, San Diego, CA; #551321) were obtained from Dako, (Carpenteria, CA). Caspase-3 reagents and antibodies were obtained from Dako (Carpenteria, CA and Biocare Medical (Concord, CA). GST-P (placental) (+ reagents and antibodies were obtained from Dako (Carpenteria, CA), Biocare Medical (Concord, CA), Biogenex, Fremont, CA), and Vector Labs (Burlingame, CA). A Provantis data collection system (Instem PLC, UK) was used to record information from the study.

### 2.2. *Animals*

Female B6D2F1/Crl mice, between the ages of 5 and 8 weeks old, were obtained from Charles River Laboratories, Inc. (Raleigh, NC). Initiation of treatment groups (i.e., 7-, 28-, or 90-day duration) were staggered to more closely align animal age at necropsy and to minimize growth-related hepatocellular proliferation. Animal care was in full accordance with applicable animal welfare standards including the U.S. Department of Agriculture's Animal Welfare Act (9) Code of Federal Regulations (CFR) Parts 1, 2 and 3, National Research Council Guide for the Care and Use of Laboratory Animals. Washington, DC (NRC, 2011), and the American Veterinary Medical Association (AVMA) Guidelines for the Euthanasia of Animals (AVMA, 2013).

Mice were implanted with transponders (BioMedic Data Systems, Seaford, DE) and acclimated for one week prior to continuous exposure to 1,4-DX in drinking water during which time they were pair-housed and provided with a Shephard Shack for enrichment purposes. The mice were fed LabDiet Certified Rodent Diet #5002 (PMI Nutrition International, St. Louis MO) ad libitum. All study animals were implanted with mini-osmotic pumps model 2ML1 (Alzet Corporation, Palo Alto, CA) eight days prior to scheduled necropsy for BrdU delivery. After pump implantation animals were housed individually.

### 2.3. *Route of administration and exposure levels*

Six groups of animals were treated with 1,4-DX in drinking water at 0 (control), 40, 200, 600, 2000 and 6000 ppm to achieve targeted dose levels of 0, 10, 50, 150, 500 and 1500 mg/kg/day. Final estimates of doses delivered were calculated utilizing concentrations of 1,4-DX in the drinking water, average water consumption, and body weights for each group.

### 2.4. *Study design*

Ten mice per exposure group were treated for 7, 28, or 90 days. At 7, 28, and 90 days of exposure, gross pathology, liver weights, histopathology and biomarkers were determined in all 10 animals per group at each time point. In addition, blood levels of 1,4-DX, and HEAA were assessed in five animals from each exposure group.

### 2.5. *Liver histopathology, biomarkers, and microscopic evaluations*

At 7, 28, and 90 days of exposure, non-fasted mice were anesthetized with isoflurane and $CO_2$, blood was collected and the mice were euthanized by decapitation. After weighing the liver, cross sections of the liver through the middle of the left lateral lobe, middle of the right medial lobe, and through the right lateral lobe were taken and preserved in neutral, phosphate-buffered 10% formalin. These liver sections were used for histopathological examination. The formalin fixed liver was processed for light microscopy which includes histochemical (hematoxylin and eosin; H&E) and immunohistochemical (BrdU)-labeled cells, caspase-3, and placental glutathione S-transferase (GST-P) staining. Further information on the biomarker assessments is provided in supplemental information.

### 2.6. *1,4-DX and HEAA analysis of whole blood*

Blood samples were collected via the retro-orbital sinus from five non-fasted mice/dose/exposure duration at necropsy following anesthesia at the time of terminal sacrifice. Each blood sample was collected into pre-weighed vials containing methanol and 1% formic acid and stored at −80 °C until analyzed by via GC/MS methods. The limit of quantification in blood was determined to be 0.05 μg/mL for HEAA and 0.2 μg/mL for 1,4-DX.

## 3. Results

The approximate doses of 1,4-DX estimated for each exposure group were 0, 7.2 (±0.624), 37.3 (±2.59), 116 (±10.2), 364 (±27.0) and 979 (±83.9) mg/kg/day for animals consuming drinking water containing 0, 40, 200, 600, 2,000, and 6000 ppm 1,4-DX, respectively. Values are means for each group (± Standard Deviation).

There were no treatment related effects in clinical signs, body weights, or clinical chemistry parameters in any of the 7-, 28-, or 90-day 1,4-DX treated groups compared to their respective controls. There were no early deaths; all animals survived to scheduled necropsy.

During the 7-day treatment period, animals exposed to 6000 ppm 1,4-DX had a slight transient decrease in water consumption from test days 1–4 (14%), but this was not statistically different from test day 4–8, when compared to their respective control group. There were no treatment-related differences in water consumption in any 1,4-DX treated animals during the 28-day treatment period when compared to their respective control group. During most intervals in the 90-day treatment period, animals exposed to 6000 ppm 1,4-DX had treatment-related decreases in water consumption ranging from 12 to 29% compared to their respective control. There were no differences in feed consumption.

### 3.1. *Liver weights*

After 7, 28, and 90 days there was a modest increase in relative liver weights of 8.7%, 10.7% and 8.9%, respectively, of animals exposed to 6000 ppm 1,4-DX with sporadic increases in relative liver weights in the 2000 ppm exposure group. No changes in relative liver weights were observed in groups exposed to 1,4-DX at less than 2000 ppm – see Supplemental Information Table 3

### 3.2. *Microscopic observations*

Histopathological (H&E) findings are briefly summarized in Table 1. After 7 days of exposure, minimal to mild vacuolation consistent with glycogen deposition was observed in the centrilobular regions of the liver in animals exposed to drinking water concentrations of 600 ppm and higher. By day 28, the centrilobular vacuolation was largely resolved.

Minimal to mild centrilobular hypertrophy, appearing as granular eosinophilic cytoplasm, appeared after 7 days of exposure. At 90-days of exposure, there was increased severity of eosinophilic, slightly granular cytoplasmic hypertrophy in the livers of mice exposed to 6000 ppm 1,4-DX – see Fig. 1. Single cell necrosis (interpreted as apoptosis) was increased at 6000 ppm with all mice showing evidence of minimal or mild single-cell necrosis at 90 days of exposure. No evidence of single cell necrosis was observed in mice exposed at or below 600 ppm 1,4-DX

**Table 1**
Incidence of liver histopathology findings.

| Finding: Observation | 1,4-DX Concentration (ppm) | | | | | |
|---|---|---|---|---|---|---|
| | 0 | 40 | 200 | 600 | 2000 | 6000 |
| Day 7 Number of Mice Examined | 10 | 10 | 10 | 10 | 10 | 10 |
| Centrilobular Vacuolation Minimal | 0 | 0 | 0 | 2 | 6 | 0 |
| Mild | 0 | 0 | 0 | 0 | 4 | 10 |
| Day 28 Number of Mice Examined | 10 | 10 | 10 | 10 | 10 | 10 |
| Centrilobular Vacuolation Minimal | 0 | 0 | 0 | 3 | 6 | 1 |
| Mild | 0 | 0 | 0 | 0 | 3 | 9 |
| Centrilobular Hypertrophy Minimal | 0 | 0 | 0 | 0 | 0 | 6 |
| Mild | 0 | 0 | 0 | 0 | 0 | 4 |
| Centrilobular Apoptosis Minimal | 0 | 0 | 0 | 0 | 0 | 7 |
| Mild | 0 | 0 | 0 | 0 | 0 | 1 |
| Day 90 Number of Mice Examined | 10 | 10 | 10 | 10 | 10 | 10 |
| Centrilobular Vacuolation Minimal | 0 | 0 | 0 | 0 | 8 | 1 |
| Mild | 0 | 0 | 0 | 0 | 1 | 1 |
| Centrilobular Hypertrophy Minimal | 0 | 0 | 0 | 0 | 1 | 0 |
| Mild | 0 | 0 | 0 | 0 | 0 | 1 |
| Moderate | 0 | 0 | 0 | 0 | 0 | 9 |
| Centrilobular Apoptosis Minimal | 0 | 0 | 0 | 0 | 1 | 6 |
| Mild | 0 | 0 | 0 | 0 | 0 | 4 |

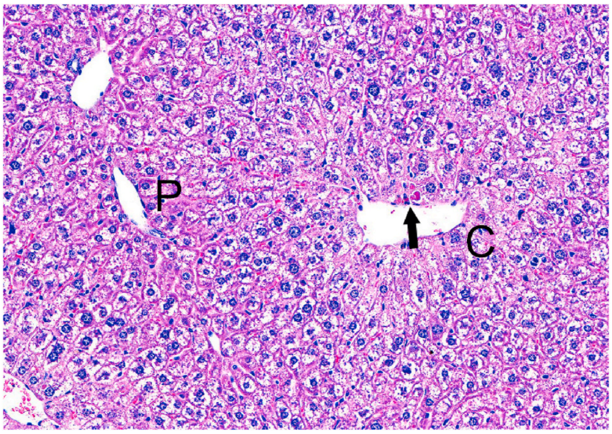

**Fig. 1.** Liver, 90-day, 6000 ppm. Moderate centrilobular hepatocyte hypertrophy and minimal vacuolation. There is also mild centrilobular hepatocyte apoptosis (arrow); note densely eosinophilic condensed cell bodies and lack of inflammation. "P" denotes Periportal while "C" marks the Centrilobular region. See supplemental information for additional photomicrographs of liver sections from this study.

(see Fig. 2).

### 3.3Biomarkers of Liver response

There were no consistent, treatment-related changes in hepatocellular proliferation in any dose group at 7 or 28 days. There was a treatment-related increase in hepatocellular proliferation as measured by BrdU incorporation at 90-days in animals exposed to 6000 ppm 1,4-DX. The BrdU incorporation was pan-lobular with a 4.3% and 20.8% labeling index in control and 6000 ppm group after 90 days of exposure. This increase in BrdU incorporation corresponds with the increase in relative liver weights as well as blood levels of 1,4-DX.

Consistent with the histopathological assessment, the 28-day and 90-day animals exposed to 6000 ppm 1,4-DX had statistically significant increases in apoptosis as measured by Caspase-3 positive cells compared to controls (0.08 and 0.46 for 28-day animals, and 0.04 and 1.08 for 90-day animals per 10,000 cells in control and high dose, respectively). There were no treatment-related differences in any other treatment group of the 28-day or 90-day treated animals when compared to their respective controls – see Supplemental Information Table 4.

GST-P+ labeling area was evaluated in the animals exposed to 6000 ppm 1,4-DX for 90 days. Earlier time points and exposures were not evaluated based on reports from prior 90-day studies (Kasai et al., 2008). GST-P+ captures possible altered hepatic foci but instead of focal collections of cells representing the clonal expansion of pre-neoplastic hepatocytes, an enhanced centrilobular staining of zone 3 hepatocytes was observed following exposures to 1,4-DX. Quantitative morphometry was not done, but visual inspection revealed that the GST-P+ centriblobular expression was greater in the 6000 ppm 1,4-DX treated group than the controls, as evidenced by a larger number of stained hepatocytes radiating away from the central vein (Fig. 3).

### 3.4. Blood concentrations of 1,4-DX and HEAA

Blood levels of HEAA exhibited linear, dose-proportional concentrations across all dose groups at all treatment durations. There was only sporadic detection of 1,4-DX in animals from the lower exposure groups (<2000 ppm) demonstrating that at these lower levels of exposure, metabolism of 1,4-DX was complete. Blood levels of 1,4-DX showed an abrupt increase in animals exposed to 6000 ppm 1,4-DX for 90-days. The appearance of 1,4-DX was biphasic, increasing in greater proportion relative to the exposure) at 6000 ppm after 90 days of exposure. This pattern is consistent with saturation of metabolic clearance pathways of 1,4-DX after prolonged exposures between 2000 ppm (approximately 400 mg/kg/day) and 6000 ppm (approximately 1000 mg/kg/day) 1,4-DX (Fig. 4).

## 4. Discussion

Identifying the MOA and its KE framework is an important element in modeling the cancer risk from rodent carcinogenicity data (Simon

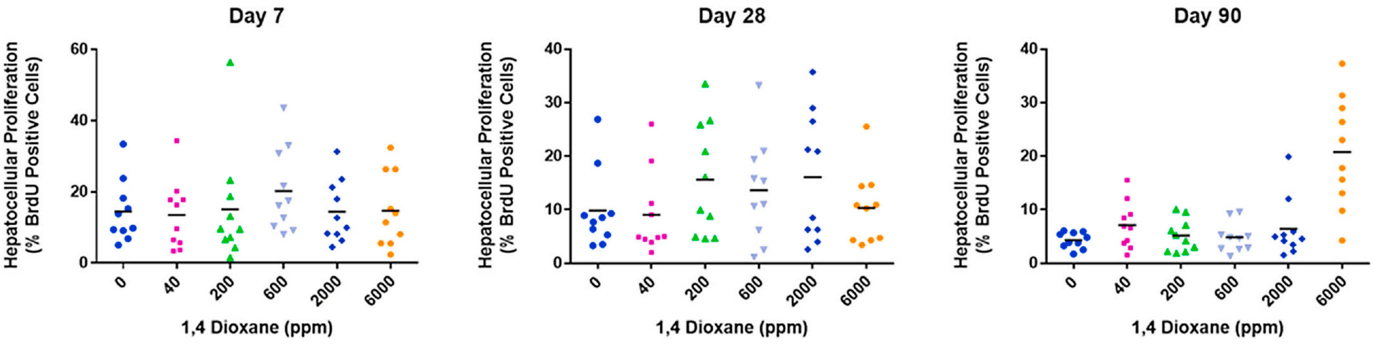

**Fig. 2.** Individual BrDU values after 7, 28, and 90 days of exposure to 1,4-DX in drinking water. Bars indicate means.

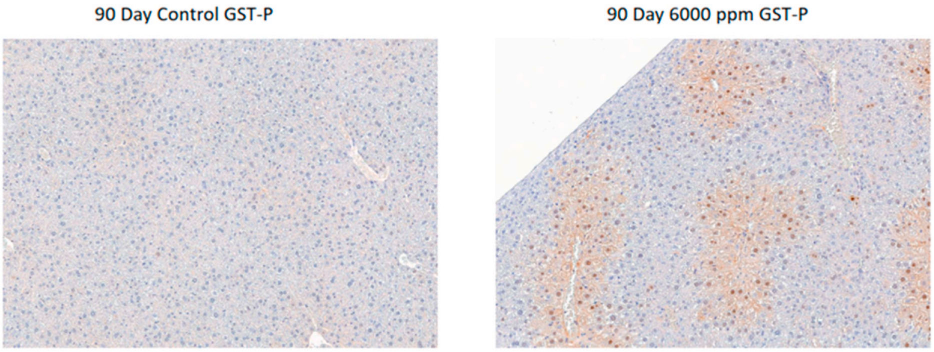

**Fig. 3.** Hepatic GST-P + Staining after 90 days of exposure to 1,4-DX in drinking water.

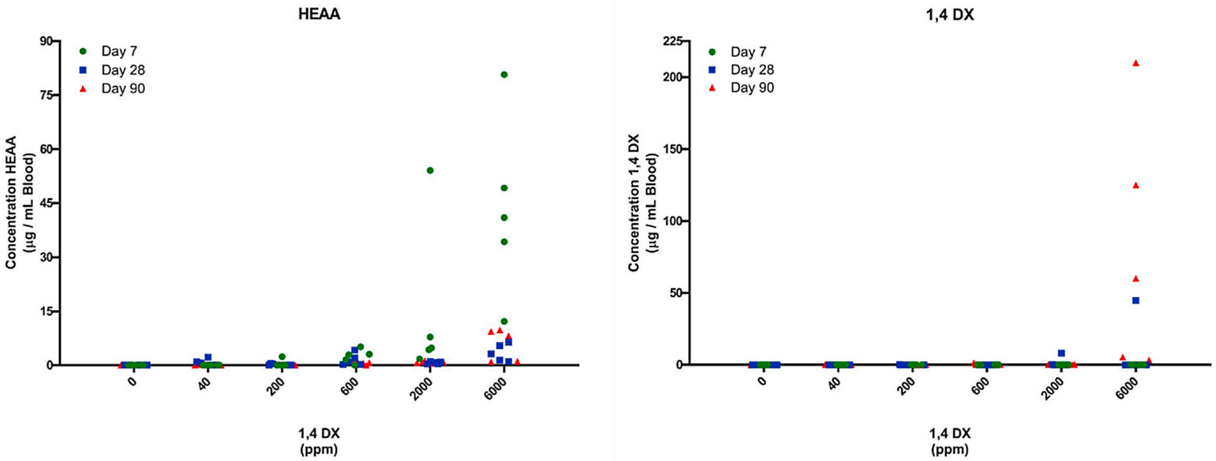

**Fig. 4.** Blood concentrations of HEAA metabolite and 1,4-DX after 7, 28, and 90 days of exposure to 1,4-DX in drinking water.

et al., 2014; US EPA, 2005a). For most carcinogens that are not mutagens, a threshold MOA establishes safe exposure level below which there is no adverse outcome (Bevan and Harrison, 2017; US EPA, 2005a). However, to support a threshold effect under the US EPA's 2005 Cancer Risk Assessment Guidelines (US EPA, 2005a), the MOA must be established. The elimination of a mutagenic MOA does not default to a threshold approach. To date, there are only a few chemicals with carcinogenic potential assessed in EPA's IRIS, database, (e.g., chloroform, perchlorate, and 2-butoxyethanol) that have met the standard for a threshold MOA (US EPA, 2010a; 2005, 2001). This study establishes that histological and biomarker responses are linked to saturation metabolisms of 1,4-DX thus providing additional KE information supporting a threshold approach for 1,4-DX cancer risk assessments.

Under the conditions of this study, there appeared to be two phases of response of female B6D2F1/Crl mice to 1,4-DX exposure from drinking water. The early phase consisted of increased liver weights, interpreted as hepatic hypertrophy, and transient increases in hepatic glycogen content. Both of these responses were adaptive and observed in the first 28-days of exposure to 1,4-DX. The late phase responses included a mitogenic response of hepatocellular proliferation, an increase in single-cell necrosis (or apoptosis) and a loss of stored glycogen. The late phase responses appeared between 28 days and 90-days of exposure to 1,4-DX and correlated with the appearance of 1,4-DX in the blood.

The mitogenic response was characterized by a pronounced increase in lobule-wide BrdU incorporation in the 6000 ppm exposure group after 90-days of exposure. Accompanying the onset of high dose centrilobular single cell apoptosis and cell proliferation in the late-phase response was a loss of glycogen-like vacuolation and increased centrilobular staining for GST-P. A similar pattern of hepatocyte proliferation was reported in rats (Goldsworthy et al., 1991). After two weeks of continuous administration of drinking water containing 1% (10,000 ppm) 1,4-DX there was a doubling of the labeling index of 3H thymidine incorporation in the rat liver. However, administration of approximately 1000 mg/kg in a single bolus dose by oral gavage did not increase the labelling index in rats at either 24 or 48 h after administration.

Notably, the late phase responses in this current study occurred at exposures that exceeded the metabolic clearance threshold although some mild changes in the liver were seen at lower exposures. The results from this study indicate there is a mitogenic response which appears to be a KE in the mouse liver tumor MOA. This mitogenic response precedes the later-developing cytotoxicity observed in longer-term studies in mice (Dourson et al., 2014, 2017).

### 4.1. *Blood concentrations of 1,4-DX and HEAA*

The dose dependent increase in the appearance of blood levels of HEAA is consistent with current understanding of its metabolism in rodents and humans. In both rodents and humans, 1,4-DX is metabolized by cytochrome P-450 (primarily Cyp2b1/2 and Cyp2e1) to HEAA in a linear, first-order process (Nannelli et al., 2005; Sweeney et al., 2008; Young et al, 1977, 1978). This kinetic pattern has been demonstrated directly by monitoring plasma levels after intravenous administration of 1,4-DX, indirectly from studies monitoring the elimination of HEAA in the urine, and from studies with rodent and human hepatocytes. This metabolic transformation is responsible for the rapid clearance of 1,4-DX and elimination in the urine. However, higher levels of exposure saturate the biotransformation of 1,4-DX which transitions to zero-order kinetics resulting in the appearance of circulating levels of parent 1,4-DX (Sweeney et al., 2008; Young et al., 1978).

The results from this current study demonstrate a biphasic kinetic profile and saturation. Blood levels of HEAA decline with an associated appearance of measurable levels of 1,4-DX after 90-days of exposure. This late onset of measurable levels of 1,4-DX in the presence of falling HEAA concentrations directly correlates with the appearance of late KE (apoptosis and increased DNA synthesis) observed at 90-days. Average blood levels of 1,4-DX were less than 1 μg/mL in mice exposed for 90 days in drinking water at 2000 ppm 1,4-DX (limit of detection 0.2 μg/mL) but increased to an average blood concentration of 81 μg/mL in mice exposed to 6000 ppm 1,4-DX. At the same time, the ratio of 1,4-DX to HEAA in blood increased from 0.38 in the 2000 ppm group to 13.7 in the 6000 ppm group. The increase in circulating levels of 1,4-DX and the role in hepatic injury, including development of liver tumors after a lifetime of exposure in rats and mice, has been well documented (ATSDR, 2012; Dourson et al., 2014, 2017; US EPA, 2019; 2013).

There is good evidence that metabolism of 1,4-DX does not generate reactive intermediates capable of causing cytotoxicity. Investigations into the formation of reactive intermediates have failed to generate evidence of DNA reactivity and repair, protein binding, or enhancement of cytotoxicity after induction of xenobiotic biotransformation (Goldsworthy et al., 1991; Stott et al., 1981; Woo et al., 1977). Although the specific molecular initiating event causing toxicity from 1,4-DX exposure is unknown, the available evidence points to the accumulation of parent 1,4-DX as the toxic species. The toxicologically-relevant events observed in this study, cell proliferation and apoptosis, correlated with the appearance of circulating blood levels of 1,4-DX.

In this study, the threshold for metabolic saturation was between 2000 and 6000 ppm of 1,4-DX in drinking water which is equivalent to approximately 400 and 1000 mg/kg/day respectively, after 90-days of exposure to 1,4-DX. Sweeney et al. (2008) estimated a metabolic saturation threshold in male B6C3F1 mice of approximately 200 mg/kg/day after a single oral gavage. The difference in the threshold estimate from this current study may be related to the strain and sex differences between studies. Female mice have a pronounced enhancement of expression of mRNA from the Cyp 2 b subfamily compared to males with some isoforms expressed more than 100-fold in female mouse liver compared to males (Renaud et al., 2011). Other sub-families of Cyp also show higher expression in females. These differences could account for the increased capacity for biotransformation of 1,4-DX and the increased metabolic threshold observed in this study. In addition, the method of dosing may have influenced the observed metabolic threshold in this study compared to estimates from previous studies. Sweeney et al. dosed 1,4-DX in a single bolus oral dose. In this current study 1,4-DX was administered ad libitum in drinking water.

Blood samples obtained at day 7 consistently show higher concentrations of HEAA than either the 28 or 90-day samples. The declining HEAA concentrations with later time points could indicate a shift in metabolic capability between 7 and 28 days of exposure favoring a competing metabolic pathway, such as conjugation, resulting in lower total HEAA blood levels at the later time points. Studies by Woo et al. (1977) demonstrated that 1,4-DX may induce its own metabolism via mixed function oxidases. However, the 1,4-DX-induced changes in metabolism may be more complex than simple induction of one system and with different time courses for reaching steady-state in the presence of 1,4-DX.

### 4.2. Cytotoxicity

There were no consistent statistical or treatment-related differences in the serum liver enzymes measured in the blood in any of the 7-, 28-, or 90-day 1,4-DX-treated animals when compared to their respective controls. This is consistent with results from previous 90-day studies in mice (Kano et al., 2008; Kasai et al., 2008). In both of these studies, there were significant increases in circulating levels of ALT and AST in the highest exposure groups but no changes in groups exposed to 1,4-DX at exposure levels comparable to the exposures used in this current study.

Likewise, there were no histopathological findings to indicate cytotoxicity in livers from animals exposed to less than 2000 ppm at any time point. There was some minimal to mild centrilobular vacuolation which appeared at 7 and 28 days from exposures of 600 ppm and greater. This vacuolation was judged to be an increase in glycogen and considered an adaptive response. At 90-days of exposure, the vacuolation resolved in the 600 ppm 1,4-DX exposure group and only appeared in the higher dose groups. This is similar to findings from previous studies in which glycogen storage was reduced after exposure to 1,4-DX (Dourson et al., 2014; Stott et al., 1981). It is difficult to determine the significance of these observations but the role of glycogen storage modulation has shown to be relevant in the progression of hepatic tumors (Bannasch et al., 1997; Nayak et al., 1996).

There was also a time and concentration dependent increase in single-cell necrosis in liver sections from mice exposed to 2000 and 6000 ppm 1,4-DX for 28 and 90 days in this study. Similar findings of single-cell necrosis at higher doses were reported in other mouse studies (Kano et al., 2008; NCI, 1978). Single-cell necrosis is generally interpreted as an indication of apoptosis (Elmore et al., 2016). The apoptosis interpretation is also supported by the increase in caspase-3 positive hepatocytes noted in livers from mice exposure to 6000 ppm 1,4-DX for 28 and 90 days. Premature loss of hepatocytes due to 1,4-DX-triggered apoptosis could contribute to a regenerative response as evidenced by increased BrdU (discussed below) and the slight hepatic hypertrophy that was observed.

The findings from this study reveal no evidence of cytotoxicity below 2000 ppm and only limited evidence of hepatic injury based on the increase in apoptosis at higher exposure levels. This is in contrast to the observations from the two-year NCI study (1978) where evidence of cytotoxicity was observed from clinical chemistry and histologic pathology (Dourson et al., 2014, 2017). The difference between the findings from this current study, and those obtained from chronic mouse studies is likely due to the time course of exposure. It appears the development of cytotoxicity requires exposures greater than the 90 days employed in this study.

### 4.3. Biomarkers

In this study we did not observe the emergence of pre-neoplastic foci including basophilic, eosinophilic, clear cell or mixed cell foci, or a clear expression of GST-P foci as was observed in chronic studies of rats (Dourson et al., 2014; Kasai et al., 2009). GST-P foci have been used as a pre-neoplastic biomarker in rats (Satoh et al., 1985) but the absence of foci in this study is not surprising. Mice express high levels of GST-P constitutively in the liver which can mask the appearance of foci (Hayes and Pulford, 1995).

### 4.4. Mode of Action

Establishing the MOA is important in determining the appropriate model for evaluating cancer risk (US EPA, 2005a). The current prevailing MOA for 1,4-DX is the regenerative hyperplasia model (Dourson et al., 2014, 2017). Evidence supporting this model was largely derived from chronic rodent bioassays and shorter-term studies (primarily 90-day studies) with limited information available to characterize early events in the MOA. In this study we have attempted to characterize the earlier time course of events involved in the induction of mouse liver tumors.

The results from this study provide further evidence for the metabolic saturation of clearance pathways as a KE leading to accumulation of systemic 1,4-DX. There was a time- and dose-dependent threshold for this saturation and the development of the subsequent KE. In the cancer studies with 1,4-DX, exposures above the metabolic threshold led to the development of hepatic tumors (Kano et al., 2009; Kociba et al., 1974;

NCI, 1978). This relationship has been described previously from data generated in both rats and mice (Dourson et al., 2017). Importantly, the mitogenic stimulation observed in this study, approximately a five-fold increase in liver proliferation (labeling index) in the 6000 ppm exposure group after 90 days, occurs prior to the development of cytotoxicity and the regenerative repair that is a cornerstone of the regenerative hyperplasia MOA. In this study, 1,4-DX exposure stimulated hepatic proliferation as a result of an apparent direct mitogenic response which is recognized as a carcinogenic MOA (US EPA, 2005a). We note that magnitude of the proliferative response observed is comparable to other mitogenic, non-genotoxic hepatocarcinogens (Geter et al., 2014; LaRocca et al., 2017).

While the essentiality of the metabolic clearance threshold relationship for subsequent tumor development has been demonstrated in numerous rodent studies, we recognize that in one study (Kano et al., 2009), hepatic tumors in female mice have been reported at exposures predicted to be below the estimated metabolic saturation. In the Kano bioassay study, there was a significant increase in combined hepatocellular adenomas and carcinomas in female mice exposed to 500 ppm (approximately 66 mg/kg/d) 1,4-DX in drinking water for two years. The estimated metabolic threshold for mice is 200 mg/kg/day (Sweeney et al., 2008). However, this was determined in male mice from a different mouse strain (B6C3F1). It is possible that the metabolic threshold in female mice is lower than that the male mice used by Sweeney et al. However, it is unlikely to account for the three-fold difference between the dose leading to tumor formation in the low dose females from the Kano bioassay study and the dose estimated to achieve metabolic saturation in either female or male mice. Thus, the observations of tumors in female mice in the Kano et al. studies at doses below presumed metabolic saturation is inconsistent with the weight of evidence from other rodent cancer bioassays or with information generated in this 90-day study.

The weight of evidence supports the conclusion that 1,4-DX is not likely to be genotoxic (ATSDR, 2012; US EPA, 2019, 2010). Numerous in vitro and in vivo studies have reported no genotoxicity with only sporadic reports of genotoxicity observed in rats exposed to 1,4-DX (Morita and Hayashi, 1998; Roy et al., 2005) and more recently (Gi et al., 2018; Itoh and Hattori, 2019; Totsuka et al., 2020). 1,4-DX-induced cytotoxicity has already been associated with weak genotoxicity outcomes before, but this was not considered relevant MOA for 1,4-DX-induced tumorigenesis (IRIS, 2013). The positive findings from in vivo studies occurred at doses that exceed the threshold for metabolic clearance and lend further support to the threshold nature of the tumor response to 1,4-DX.

Receptor mediated MOAs, such as the peroxisome proliferator-activated receptor -alpha (PPARα) and the constitutive androstane receptor (CAR), can also play a role in the developments of tumors in rodents exposed to non-genotoxic carcinogens (Elcombe et al., 2014; Klaunig et al., 2003). However, the pattern of responses in rodents resulting from 1,4-DX exposure do not completely align with the MOA. Peroxisome proliferation is a key observation observed from PPARa activity and CAR activation generally leads to inhibition of apoptosis (Felter et al., 2018). Neither of these are observed in 1,4-DX exposed rodent liver. Furthermore, whole transcriptome analyses of mRNA of liver tissues from our 90 mouse study shows no evidence of PAPRα or CAR activity (Chappell et al. manuscript in preparation). Specifically, there was no change in the expression of individual CYP-encoding genes that are considered markers of activation of such nuclear receptors, nor enrichment of gene-level changes in the signaling pathways relevant to these nuclear receptors.

The observations from this current study support the regenerative hyperplasia model with one important additional modification – inclusion of an early onset, direct mitogenic stimulus occurring prior to the development of cytotoxicity, necrosis and the regenerative processes as described in previous MOA rodent hepatic tumor models (Dourson et al., 2017) and depicted in Fig. 5. This mitogenic response occurs early and likely adds to the regenerative repair that is suggested from the increase in single cell necrosis (apoptosis) seen in this study. Although these responses are small, they occur in a target organ (liver) in a mouse strain that is highly susceptible to the induction of liver cancer (Holsapple et al., 2006; Katagiri et al., 1998; Yamate et al., 1990). Importantly, there is a clear threshold of these effects which only occur at exposures that exceed the metabolic clearance threshold and only after 90-days of exposure.

The mitogenic event is presented in red to indicate the new finding from this study. All other events have been reported previously.

## 5. Conclusion

When 1,4-DX was administered via the drinking water to female B6D2F1/Crl mice for up to 90 days, there was a strong time- and exposure-dependent threshold for hepatic effects. These effects progressed from an early phase of adaptive effects to a late phase of adverse effects. The molecular and apical treatment-induced biological changes correlated with increased quantifiable concentrations of 1,4-DX in the blood. Within the first 90 days of drinking water exposure to 1,4-DX the

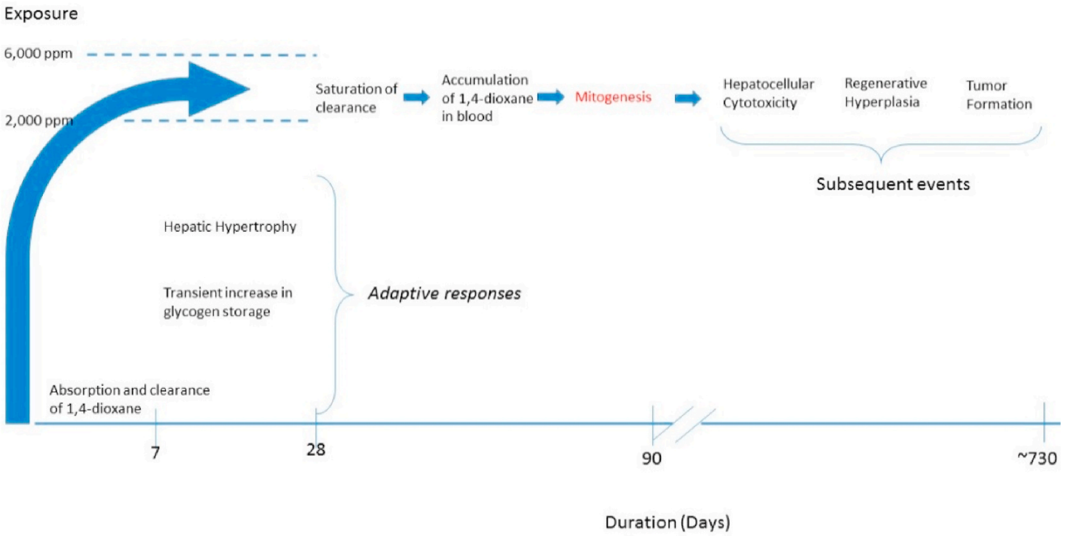

**Fig. 5.** Updated MOA of 1,4-DX induced development of hepatic tumors.

absence of evidence of significant hepatic cytotoxicity and the increase in cell proliferation indicate that a cytotoxicity/regenerative MOA alone does not account for the subsequent sequence of events leading to tumor formation. Collectively, these data indicate that after 90 days of exposure, at metabolically saturating doses of 1,4-DX, a mitogenic response is triggered in the liver of a sensitive strain of female mice that precedes the development of cytotoxicity and regenerative hyperplasia, ultimately leading to tumor development. This mitogenic response may be considered a KE in support of the threshold MOA for development of liver tumors in female mice after exposure to 1,4-DX.

The findings from this study extend the understanding of the MOA for 1,4-DX-induced hepatic tumors in mice. This is important in that the MOA of an environmental agent is key to the appropriate application of the most up-to-date cancer risk assessment approaches (Boobis et al., 2006; Cohen et al., 2019; Holsapple et al., 2006; Wolf et al., 2019).

## Funding

This work was supported by the American Chemistry Council (ACC) 1,4-Dioxane Panel and its member companies.

## Declaration of competing interest

The authors declare that they have no known competing financial interests or personal relationships that could have appeared to influence the work reported in this paper

## Acknowledgements

The authors wish to thank the American Chemistry Council (ACC) 1,4-Dioxane Panel and member companies for supporting this research. We thank our many colleagues who assisted with critical reviews including Alex Howard and Nadine Weinberg (ERM) as well as those who assisted in the conduct of the study including Kathy Kleinert, Dr. Fagen Zhang, Eric Nelson and the rest of the staff of the Toxicology and Environmental Research and Consulting Department of the Dow Chemical Company.

## Appendix A. Supplementary data

Supplementary data to this article can be found online at https://doi.org/10.1016/j.yrtph.2020.104819.

## References

Argus, M.F., Sohal, R.S., Bryant, G.M., Hoch-Ligeti, C., Arcos, J.C., 1973. Dose-response and ultrastructural alterations in dioxane carcinogenesis. Eur. J. Canc. 9, 237–243. https://doi.org/10.1016/0014-2964(73)90088-1.

Argus, M.F., Arcos Jc, H.C., 1965. Studies on the carcinogenic activity of protein-denaturing agents: hepatocarcinogenicity of dioxane. J Natl Cancer Inst 35, 949–958.

ATSDR, 2012. HEALTH EFFECTS - Toxicological Profile for 1,4-Dioxane - NCBI Bookshelf, NCBI. Atlanta.

AVMA, 2013. AVMA Guidelines for the Euthanasia of Animals: 2013 Edition Members of the Panel on Euthanasia. American Veterninary Medical Association, Schaumburge, IL.

Bannasch, P., Klimek, F., Mayer, D., 1997. Early bioenergetic changes in hepatocarcinogenesis: preneoplastic phenotypes mimic responses to insulin and thyroid hormone. J. Bioenerg. Biomembr. 29, 303–313. https://doi.org/10.1023/a:1022438528634.

Bevan, R.J., Harrison, P.T.C., 2017. Threshold and non-threshold chemical carcinogens: a survey of the present regulatory landscape. Regul. Toxicol. Pharmacol. 88, 291–302. https://doi.org/10.1016/j.yrtph.2017.01.003.

Boobis, A.R., Cohen, S.M., Dellarco, V., McGregor, D., Meek, M.E., Vickers, C., Willcocks, D., Farland, W., 2006. IPCS framework for analyzing the relevance of a cancer mode of action for humans. Crit. Rev. Toxicol. https://doi.org/10.1080/10408440600977677.

Cohen, S.M., Boobis, A.R., Dellarco, V.L., Doe, J.E., Fenner-Crisp, P.A., Moretto, A., Pastoor, T.P., Schoeny, R.S., Seed, J.G., Wolf, D.C., 2019. Chemical carcinogenicity revisited 3: risk assessment of carcinogenic potential based on the current state of knowledge of carcinogenesis in humans. Regul. Toxicol. Pharmacol. https://doi.org/10.1016/j.yrtph.2019.01.017.

Dourson, M., Reichard, J., Nance, P., Burleigh-Flayer, H., Parker, A., Vincent, M., McConnell, E.E., 2014. Mode of action analysis for liver tumors from oral 1,4-dioxane exposures and evidence-based dose response assessment. Regul. Toxicol. Pharmacol. 68, 387–401. https://doi.org/10.1016/j.yrtph.2014.01.011.

Dourson, M.L., Higginbotham, J., Crum, J., Burleigh-Flayer, H., Nance, P., Forsberg, N. D., Lafranconi, M., Reichard, J., 2017. Update: mode of action (MOA) for liver tumors induced by oral exposure to 1,4-dioxane. Regul. Toxicol. Pharmacol. 88, 45–55. https://doi.org/10.1016/J.YRTPH.2017.02.025.

Elcombe, C.R., Peffer, R.C., Wolf, D.C., Bailey, J., Bars, R., Bell, D., Cattley, R.C., Ferguson, S.S., Geter, D., Goetz, A., Goodman, J.I., Hester, S., Jacobs, A., Omiecinski, C.J., Schoeny, R., Xie, W., Lake, B.G., 2014. Mode of action and human relevance analysis for nuclear receptor-mediated liver toxicity: a case study with phenobarbital as a model constitutive androstane receptor (CAR) activator. Crit. Rev. Toxicol. 44, 64–82. https://doi.org/10.3109/10408444.2013.835786.

Elmore, S.A., Dixon, D., Hailey, J.R., Harada, T., Herbert, R.A., Maronpot, R.R., Nolte, T., Rehg, J.E., Rittinghausen, S., Rosol, T.J., Satoh, H., Vidal, J.D., Willard-Mack, C.L., Creasy, D.M., 2016. Recommendations from the INHAND apoptosis/necrosis working group. Toxicol. Pathol. 44, 173–188. https://doi.org/10.1177/0192623315625859.

Felter, S.P., Foreman, J.E., Boobis, A., Corton, J.C., Doi, A.M., Flowers, L., Goodman, J., Haber, L.T., Jacobs, A., Klaunig, J.E., Lynch, A.M., Moggs, J., Pandiri, A., 2018. Human relevance of rodent liver tumors: key insights from a Toxicology Forum workshop on nongenotoxic modes of action. Regulatory Toxicology and Pharmacology. https://doi.org/10.1016/j.yrtph.2017.11.003.

Geter, D.R., Bhat, V.S., Gollapudi, B.B., Sura, R., Hester, S.D., 2014. Dose-response modeling of early molecular and cellular key events in the CAR-mediated hepatocarcinogenesis pathway. Toxicol. Sci. 138, 425–445. https://doi.org/10.1093/toxsci/kfu014.

Gi, M., Fujioka, M., Kakehashi, A., Okuno, T., Masumura, K., Nohmi, T., Matsumoto, M., Omori, M., Wanibuchi, H., Fukushima, S., 2018. In vivo positive mutagenicity of 1,4-dioxane and quantitative analysis of its mutagenicity and carcinogenicity in rats. Arch. Toxicol. 92, 3207–3221. https://doi.org/10.1007/s00204-018-2282-0.

Goldsworthy, T.L., Monticello, T.M., Morgan, K.T., Bermudez, E., Wilson, D.M., Jäckh, R., Butterworth, B.E., 1991. Examination of potential mechanisms of carcinogenicity of 1,4-dioxane in rat nasal epithelial cells and hepatocytes. Arch. Toxicol. https://doi.org/10.1007/BF01973495.

Hayes, J.D., Pulford, D.J., 1995. The glut athione S-transferase supergene family: regulation of GST and the contribution of the lsoenzymes to cancer chemoprotection and drug resistance Part I. Crit. Rev. Biochem. Mol. Biol. 30, 445–520. https://doi.org/10.3109/10409239509083491.

Holsapple, M.P., Pitot, H.C., Cohen, S.H., Boobis, A.R., Klaunig, J.E., Pastoor, T., Dellarco, V.L., Dragan, Y.P., 2006. Mode of action in relevance of rodent liver tumors to human cancer risk. Toxicol. Sci. 89, 51–56. https://doi.org/10.1093/toxsci/kfj001.

International Center for Medical Research, Y., 1988. Asia-pacific symposium on environmental and occupational Toxicology, 4-7 october, 1987, Singapore proceedings. In: Proceedings of the ICMR Seminar (International Center for Medical Research). International Center for Medical Research, Kobe University School of Medicine.

Itoh, S., Hattori, C., 2019. In vivo genotoxicity of 1,4-dioxane evaluated by liver and bone marrow micronucleus tests and Pig-a assay in rats. Mutat. Res. Genet. Toxicol. Environ. Mutagen 837, 8–14. https://doi.org/10.1016/j.mrgentox.2018.09.004.

Kano, H., Umeda, Y., Kasai, T., Sasaki, T., Matsumoto, M., Yamazaki, K., Nagano, K., Arito, H., Fukushima, S., 2009. Carcinogenicity studies of 1,4-dioxane administered in drinking-water to rats and mice for 2years. Food Chem. Toxicol. 47, 2776–2784. https://doi.org/10.1016/j.fct.2009.08.012.

Kano, H., Umeda, Y., Saito, M., Senoh, H., Ohbayashi, H., Aiso, S., Yamazaki, K., Nagano, K., Fukushima, S., 2008. Thirteen-week oral toxicity of 1,4-dioxane in rats and mice. J. Toxicol. Sci. 33, 141–153. https://doi.org/10.2131/jts.33.141.

Kasai, T., Kano, H., Umeda, Y., Sasaki, T., Ikawa, N., Nishizawa, T., Nagano, K., Arito, H., Nagashima, H., Fukushima, S., 2009. Two-year inhalation study of carcinogenicity and chronic toxicity of 1,4-dioxane in male rats 2-yr inhalation study of 1,4-dioxane in rats Tatsuya Kasai et al. Inhal. Toxicol. 21, 889–897. https://doi.org/10.1080/08958370802629610.

Kasai, T., Saito, M., Senoh, H., Umeda, Y., Aiso, S., Ohbayashi, H., Nishizawa, T., Nagano, K., Fukushima, S., 2008. Thirteen-week inhalation toxicity of 1,4-dioxane in rats. Inhal. Toxicol. 20, 961–971. https://doi.org/10.1080/08958370802105397.

Katagiri, T., Nagano, K., Aiso, S., Senoh, H., Sakura, Y., Takeuchi, T., Okudaira, M., 1998. A pathological study on spontaneous hepatic neoplasms in BDF1 mice. J. Toxicol. Pathol. 11 https://doi.org/10.1293/tox.11.21, 21–21.

Klaunig, J.E., Babich, M.A., Baetcke, K.P., Cook, J.C., Corton, J.C., David, R.M., DeLuca, J.G., Lai, D.Y., McKee, R.H., Peters, J.M., Roberts, R.A., Fenner-Crisp, P.A., 2003. PPARα agonist-induced rodent tumors: modes of action and human relevance. Crit. Rev. Toxicol. 33, 655–780. https://doi.org/10.1080/713608372.

Kociba, R.J., McCollister, S.B., Park, C., Torkelson, T.R., Gehring, P.J., 1974. 1,4-Dioxane. I. Results of a 2-year ingestion study in rats. Toxicol. Appl. Pharmacol. 30, 275–286. https://doi.org/10.1016/0041-008X(74)90099-4.

LaRocca, J.L., Rasoulpour, R.J., Gollapudi, B.B., Eisenbrandt, D.L., Murphy, L.A., LeBaron, M.J., 2017. Integration of novel approaches demonstrates simultaneous metabolic inactivation and CAR-mediated hepatocarcinogenesis of a nitrification inhibitor. Toxicol. reports 4, 586–597. https://doi.org/10.1016/j.toxrep.2017.10.007.

Morita, T., Hayashi, M., 1998. 1,4-Dioxane is not mutagenic in five in vitro assays and mouse peripheral blood micronucleus assay, but is in mouse liver micronucleus assay. Environ. Mol. Mutagen. 32, 269–280. https://doi.org/10.1002/(SICI)1098-2280.

Nannelli, A., De Rubertis, A., Longo, V., Gervasi, P.G., 2005. Effects of dioxane on cytochrome P450 enzymes in liver, kidney, lung and nasal mucosa of rat. Arch. Toxicol. 79, 74–82. https://doi.org/10.1007/s00204-004-0590-z.

Nayak, N.C., Sathar, S.A., Mughal, S., Duttagupta, S., Mathur, M., Chopra, P., 1996. The nature and significance of liver cell vacuolation following hepatocellular injury - an analysis based on observations on rats rendered tolerant to hepatotoxic damage. Virchows Arch. https://doi.org/10.1007/BF00202202.

Nci, 1978. Bioassay of 1,4-Dioxane for Possible Carcinogenicity CAS No. 123-91-1. Technical Report Series Number 80.

NRC, 2011, eighth ed.. Guide for the Care and use of Laboratory Animals Eighth Edition. National Academies Press.

Renaud, H.J., Cui, J.Y., Khan, M., Klaassen, C.D., 2011. Tissue distribution and gender-divergent expression of 78 cytochrome p450 mRNAs in mice. Toxicol. Sci. vol. 124, 261–277. https://doi.org/10.1093/toxsci/kfr240.

Roy, S.K., Thilagar, A.K., Eastmond, D.A., 2005. Chromosome breakage is primarily responsible for the micronuclei induced by 1,4-dioxane in the bone marrow and liver of young CD-1 mice. Mutat. Res. Genet. Toxicol. Environ. Mutagen 586, 28–37. https://doi.org/10.1016/j.mrgentox.2005.05.007.

Satoh, K., Kitahara, A., Soma, Y., Inaba, Y., Hatayama, I., 1985. Purification, induction, and distribution of placental glutathione transferase: a new marker enzyme for preneoplastic cells in the rat chemical hepatocarcinogenesis. Proc. Natl. Acad. Sci. U. S.A. 82, 3964–3968. https://doi.org/10.1073/pnas.82.12.3964.

Simon, T.W., Stoney Simons Jr., S., Julian Preston, R., Boobis, A.R., Cohen, S.M., Doerrer, N.G., Fenner-Crisp, P.A., McMullin, T.S., McQueen, C.A., Craig Rowlands, J., 2014. Critical Reviews in Toxicology the use of mode of action information in risk assessment: quantitative key events/dose-response framework for modeling the dose-response for key events the use of mode of action information in risk assessment: quantitative key events/dose-response framework for modeling the dose-response for. Crit. Rev. Toxicol. 44, 17–43. https://doi.org/10.3109/10408444.2014.931925.

Stott, W.T., Quast, J.F., Watanabe, P.G., 1981. Differentiation of the mechanisms of oncogenicity of 1,4-dioxane and 1,3-hexachlorobutadiene in the rat. Toxicol. Appl. Pharmacol. 60, 287–300. https://doi.org/10.1016/0041-008X(91)90232-4.

Sweeney, L.M., Thrall, K.D., Poet, T.S., Corley, R.A., Weber, T.J., Locey, B.J., Clarkson, J., Sager, S., Gargas, M.L., 2008. Physiologically based pharmacokinetic modeling of 1,4-dioxane in rats, mice, and humans. Toxicol. Sci. 101, 32–50. https://doi.org/10.1093/toxsci/kfm251.

Totsuka, Y., Maesako, Y., Ono, H., Nagai, M., Kato, M., Gi, M., Wanibuchi, H., Fukushima, S., Shiizaki, K., Nakagama, H., 2020. Comprehensive analysis of DNA adducts (DNA adductome analysis) in the liver of rats treated with 1,4-dioxane. Proc. Jpn. Acad. Ser. B Phys. Biol. Sci. 96, 180–187. https://doi.org/10.2183/pjab.96.015.

US EPA, 2019. Draft Risk Evaluation for 1,4-Dioxane CASRN: 123-91-1 EPA Document 740-R1-8007. Washington, DC.

US EPA, 2013. Toxicological Review of 1,4-Dioxane (With Inhalation Update). EPA/635/R-11/003F. Washington, DC. https://cfpub.epa.gov/ncea/iris/iris_documents/documents/toxreviews/0326tr.pdf.

US EPA, 2010a. Ethylene Glycol Monobutyl Ether (EGBE) (2-Butoxyethanol); CASRN 111-76-2. Integrated Risk Information System (IRIS) Chemical Assessment Summary, Washington, DC.

US EPA, 2010b. Toxicological Review of 1,4-Dioxane (CAS No. 123-91-1) in Support of Summary Information on the Integrated Risk Information System (IRIS) [EPA Report]. (EPA-635/r-09-005-F). Washington, DC.

US EPA, 2005a. Guidelines for Carcinogen Risk Assessment [EPA Report]. (EPA/630/P-03/001F). Washington, DC.

US EPA, 2005b. Perchlorate (ClO4-) and Perchlorate Salts: Integrated Risk Informaiton System. IRIS) chemical Assessment Summary, Washington, DC.

US EPA, 2001. Toxicological Review of Chloroform (CAS No. 67-66-3) in Support of Summary Information on the Integrated Risk Infomation System. IRIS), Washington, DC. EPA/635/R-01/001.

Wolf, D.C., Cohen, S.M., Boobis, A.R., Dellarco, V.L., Fenner-Crisp, P.A., Moretto, A., Pastoor, T.P., Schoeny, R.S., Seed, J.G., Doe, J.E., 2019. Chemical carcinogenicity revisited 1: a unified theory of carcinogenicity based on contemporary knowledge. Regul. Toxicol. Pharmacol. 103, 86–92. https://doi.org/10.1016/j.yrtph.2019.01.021.

Woo, Y., Argus, M.F., Arcos, J.C., 1977. Metabolism in vivo of dioxane: effect of inducers and inhibitors of hepatic mixed-function oxidases. Biochem. Pharmacol. https://doi.org/10.1016/0006-2952(77)90431-2.

Yamate, J., Tajima, M., Kudow, S., Sannai, S., 1990. Background pathology in BDF1 mice allowed to live out their life-span. Lab. Anim. 24, 332–340. https://doi.org/10.1258/002367790780865976.

Young, J.D., Braun, W.H., Gehring, P.J., 1978. Dose-dependent fate of 1,4-dioxane in rats. J. Toxicol. Environ. Health 4, 709–726. https://doi.org/10.1080/15287397809529693.

Young, J.D., Braun, W.H., Rampy, L.W., Chenoweth, M.B., Blau, G.E., 1977. Pharmacokinetics of 1,4-dioxane in humans. J. Toxicol. Environ. Health 3, 507–520. https://doi.org/10.1080/15287397709529583.

# Transcriptomic analyses of the liver in female mice exposed to 1,4-dioxane in drinking water: summary of findings

AUGUST 27, 2019

ToxStrategies

Innovative solutions
Sound science

# Transcriptomic analyses of the liver in female mice exposed to 1,4-dioxane in drinking water: summary of findings

**AUGUST 27, 2019**

**PREPARED FOR:**
Stephen Risotto
American Chemistry Council

**PREPARED BY:**
ToxStrategies, Inc.
31 College Place
Suite B118
Asheville, NC 28801

# Table of Contents

# 1 Background

ToxStrategies, Inc. reviewed gene expression data from livers collected from female B6D2F1(BDF1)/Crl mice exposed to 0, 40, 200, 600, 2000, or 6000 ppm 1,4-dioxane in the drinking water for 7, 28, or 90 days in support of an investigation of the mode of action for 1,4-dioxane-induced murine liver tumors. Transcriptomic responses in 1,4-dioxane-exposed mice were compared to time-matched control mice. Pathway analysis based on altered genes, as well as benchmark dose modeling and functional classification were conducted, and a summary of the results of these analyses is presented herein.

# 2 Analysis Methods

Liver tissues collected from female mice were formalin-fixed, paraffin-embedded and sectioned on to slides. Tissue was scraped from these sections and processed for RNA sequencing using the TempO-Seq platform (BioSpyder Technologies, Carlsbad, CA). RNA sequencing data were processed, and comparative analyses were conducted to identify genes that were significantly differentially expressed for each treatment group compared to appropriate controls for the same timepoint. Samples that did not pass quality control metrics intended to ensure a successful sequencing experiment were removed from the analysis. The differential expression analysis results were then applied to identify enriched gene sets and signaling pathways among the treatment-related alterations in transcriptomic signaling. Gene set enrichment analysis was conducted two ways: 1.) genes that were significantly differentially expressed according using the criterion of a p-value adjusted for multiple hypothesis testing of <0.1 (i.e., a false discovery rate (FDR) < 10%) were queried for significant enrichment of known gene sets and signaling pathways using a hypergeometric test and known gene sets from the Molecular Signature Database (MSigDB)[1]; 2.) all genes were included in enrichment analysis using a ranked list based on statistical significance according to the method published by Subramanian et al., 2005[2]. A fold change filter was not applied; in other words, genes with consistent altered expression compared to controls for a certain treatment group were carried forward to pathway analysis even if they demonstrated a small magnitude of change. Additionally, gene expression data were applied in benchmark dose (BMD) modeling and results were used to identify enriched gene sets and signaling pathways among the significantly dose-responsive genes. This analysis was conducted using the BMDExpress software, v2.2[3].

## 2.1 RNA Sequencing

A single 4-6 μm section was microtomed from one formalin-fixed paraffin embedded (FFPE) block per liver sample (one per animal) for 5 animals per treatment group (study

---

[1] http://software.broadinstitute.org/gsea/msigdb

[2] Subramanian, A et al., 2005. Gene set enrichment analysis: a knowledge-based approach for interpreting genome-wide expression profiles. *PNAS*

[3] https://github.com/auerbachs/BMDExpress-2/wiki

day and concentration). Sections were mounted on a glass slide (uncovered), yielding a total of 40 samples for RNA sequencing. Slides were shipped to BioSpyder Technologies (Carlsbad, CA) where liver tissue was scraped from each unstained slide into lysis buffer. The resulting cell lysates were processed according to the TempO-Seq protocol, as previously described (Yeakley et al., 2017). Briefly, mRNA targets were hybridized with a detector oligomer probe mix. Nuclease digestion of excess oligomers was conducted, followed by ligation to result in a pool of amplification templates sharing PCR primer "landing sites." Following PCR, clean-up, and pooling (all libraries have a unique adapter barcode such that all data may be appropriately separated by individual sample following sequencing), the DNA libraries from each liver sample from each animal were sequenced using a HiSeq 2500 Ultra-High-Throughput Sequencing System (Illumina, San Diego, CA). There was no sample pooling for analytical purposes, nor were technical replicates run.

## 2.2 Data processing and analysis

Sequencing data were analyzed using multiple packages in the R software, v3.5.2 (cran.r-project.org/). The number of sequenced reads per probe were extracted from FASTQ files generated from the sequencing experiment, with each probe representing a gene-specific sequence. Some genes are targeted with multiple probes to detect important alternative splicing variants. An alignment step was not required because the gene-specific probe sequences are known. A "counts file" was generated that includes the number of counts for each probe, for each sample. The number of counts represents the number of times the probe was read by the sequencer, and each sample represents a FFPE liver section from an individual animal. Samples with an overall sequencing depth (total reads across all probes) lower than two standard deviations below the mean sequencing depth across all samples were excluded from the comparative analysis. A total of 7 samples were removed from the analysis based on this data quality criterion. The DESeq2 R package (v.122.2) (Love, Huber, & Anders, 2014) was used to normalize data such that sample-to-sample variation in sequencing depth was considered.

## 2.3 Identification of genes with significant differential expression across concentrations

Statistical methods within DESeq2 were used to identify differentially expressed of genes associated with exposure by conducting comparisons between groups that share a characteristic (i.e., test agent concentration), with betaPrior set to "false." (Love et al., 2014). In the present study, the various treatment groups were compared to controls of the same sex. The DESeq2 method is based on the calculation of shrunken logarithmic fold changes in expression (representing ratio of exposure over unexposed samples), which are then divided by their standard errors to conduct Wald tests for differential expression. These tests produce z-statistics that are compared against standard normal distribution curves, resulting in Wald test p-values, that are then adjusted for multiple testing using the Benjamini and Hochberg (BH) procedure (Love et al., 2014). Differentially expressed probes (DEPs) were defined as those with false discovery rate (FDR) <10% for any chosen comparison between treatment groups, based on a BH-adjusted p-values, paralleling methods previously used to analyze RNA sequencing data (Chappell et al., 2017; Rooney et al., 2017). All samples that share an assigned characteristic, in this case the concentration of 1,4-dioxane, are grouped together to evaluate the differences between each group. The expression level of each probe is averaged across the samples that are commonly classified before statistical tests are conducted between the various groups. Unique differentially expressed genes (DEGs) were identified from respective DEPs.

## 2.4 Identification of pathway-level alterations across concentrations

Biological pathways that were associated with the transcriptomic response profiles were identified using gene set enrichment analysis. For the genes for which multiple probes were used to measure expression, the probe with the highest sequencing count (total number of reads) across all samples was selected as the representative gene to be used in the enrichment analysis. Mouse gene identifiers were converted into human identifiers, when available, using the R package biomaRt (v2.38.0) based on the Ensembl genome database[4]. Human gene identifiers were then queried for enrichment of gene sets within the Canonical Pathways sub-collection several curated genesets available through the Molecular Signatures Database (MSigDB)[5]. Specifically, the following collections were used: Hallmark gene sets, Curated gene sets (Chemical and genetic perturbations and Canonical pathways), and Gene Ontology (GO) gene sets. The sub-collection Canonical Pathways was used as the primary source for evaluation, because this collection provides a well-characterized and well-maintained (i.e., updated) list of genesets and pathways. The Canonical Pathways sub-collection includes gene sets from several pathway databases, including the BioCarta online maps of metabolic and signaling pathways (BIOCARTA) (Nishimura, 2001), the Kyoto Encyclopedia of Genes and Genomes (KEGG) (Ogata et al., 1999), the Pathway Interaction Database (PID) (Schaefer et al., 2009), and the Reactome database of reactions, pathways, and biological processes (REACTOME) (Croft et al., 2011)). The other collections were included for confirmation of geneset enrichment profiles and to identify any novel genesets that may only be represented in one collection. More information regarding the various collections can be found within the Broad Institute's GSEA Molecular Signatures Database website: http://software.broadinstitute.org/gsea/msigdb/index.jsp.

Enrichment of gene sets and pathways was evaluated by two different methods: 1) GSEA computational method - employed the GSEA platform made available by the Broad Institute (Subramanian et al., 2005), 2) general hypergeometric method - employed a more simple hypergeometric test. The GSEA computational method[6] determines whether sets of genes (e.g., a molecular signaling pathway) are significantly concordant between various defined groups (in the case presented herein, different doses) based on a ranking all genes evaluated according to a designated metric (in this, the statistical measure of significance of expression differences between treated and control mice). An enrichment score is

---

[4] http://uswest.ensembl.org/index.html

[5] http://software.broadinstitute.org/gsea/msigdb/index.jsp

[6] http://software.broadinstitute.org/gsea/index.jsp

calculated for each gene set in the defined list, which reflects the degree to which a gene set is overrepresented at either end of the ranked list (i.e. down- vs. up-regulated genes. The GSEA statistical method was applied within the Platform for Integrative Analysis of Omics data (PIANO) R package (v1.22.0) (Varemo, Nielsen, & Nookaew, 2013) (the GSEA R package was not used because it has not been maintained since 2005). Genes were first ranked according to Wald statistical values generated during the DESeq2 analysis, where genes with the greatest magnitude of significant increases in expression having the highest positive Wald statistical value, and genes showing the greatest magnitude of a significant decrease in expression having the lowest negative Wald statistical value. Genes with minimal expression changes (i.e., low or no change associated with treatment) had Wald statistical values near zero. The GSEA method was then used to determine whether the defined set of genes in each pathway were randomly distributed throughout the ranked gene list, representing a non-significant pathway enrichment; conversely, if the defined set of genes were primarily present at the top/bottom of the ranked list, this represented a significant pathway enrichment with distinct directionality (i.e., primarily up- or down-regulated). Gene set enrichment significance was calculated using permutation-based nominal p-values based on weighted Kolmogorov Smirnov test enrichment scores, and adjusted for multiple hypothesis testing by calculating FDRs using the BH method, as previously described (Subramanian et al., 2005). Gene sets with an FDR <10% were considered to be significantly enriched. A requirement was set that at least 5 and no more than 500 genes from each gene set queried must also been included in the experimental data being evaluated for enrichment (slightly more inclusive than the minimums of 15 and 25 in the original GSEA article (Subramanian et al., 2005) and the current GSEA online User's Guide, respectively).

For the hypergeometric method, all DEGs for each treatment group (i.e., an FDR of <10% as described above) were tested for over-representation among the gene sets in the Canonical Pathways sub-collection using Fisher's combined probability test function with the PIANO package. The magnitude of induction/reduction of the genes was not used a limiter in this approach; i.e., no fold-change filter was applied. Gene sets with an FDR <10% were considered to be significantly enriched. As stated above, a requirement was set that at least 5 and no more than 500 genes from each gene set queried must also been included in the experimental data being evaluated for enrichment.

The results of both gene set enrichment analysis methods were evaluated to inform and understand treatment-related effects. The results of the hypergeometric test for overrepresentation were the focus of the results described in the main body of this report as the pre-ranked GSEA method was determined to not be as robust of a method based on the fact that minimal change was seen at the lower doses. Although the top-most significantly enriched gene sets were similar across the two methods, the nature of the algorithm resulted in significant enrichment of some gene sets for which no members (individual genes) were differentially expressed in the lower dose groups.

To investigate enrichment of gene sets related to DNA damage response and repair further than looking at relevant gene sets within the Canonical Pathways collection, a collection of gene sets was curated by searching all gene sets in MSigDB for key words related to

DNA damage response. A hypergeometric test was used to test enrichment of this specific curated list of 77 gene sets related to DNA damage response.

### 2.5 Benchmark Dose Analysis

Dose–response modeling of the DEGs was conducted using the BMDExpress software (v2.2) (Phillips et al., 2019). Briefly, probe IDs from the TempO-Seq experiment were translated into Ensembl IDs using the biomaRt R package (v2.38.0). Normalized expression data as generated using DESeq2 were then loaded into BMDExpress without transformation. A Williams trend test (with p-value cutoff = 0.05) was used to identify genes altered by exposure to 1,4-dioxane. No fold-change filters or correction for multiple tests were applied. BMD analysis was conducted using the following models: linear, power, Hill, 2° and 3° polynomial models, and exponential models 2-5. The models were run assuming constant variance and a benchmark response (BMR) of 1 standard deviation.

## 3 Results

### 3.1 Identification of differentially expressed genes and enrichment of gene sets (signaling pathways)

Results of these analyses demonstrate that there is an overall lack of transcriptomic response at the 40 and 200 ppm concentrations. Using the criterion detailed above for the gene set enrichment analysis, very few genes were changed in the mice exposed to these concentrations relative to the time-matched controls. At 90 days, only 20 genes were altered by 200 ppm 1,4-dioxane, with fewer genes altered by this concentration at the earlier timepoints, and practically no response at any timepoints for 40 ppm (only one gene was differentially expressed in the 40 ppm group at 28 and 90 days, none at 7 days). Pathway enrichment analysis of significantly differentially expressed genes, thus, did not yield any significantly enriched gene sets/pathways using the hypergeometric test.

At the 600 ppm concentration, a general stress response to the treatment was observed at 7 days, indicated by the down-regulation of a broad range of normal metabolic and cellular processes (e.g., citric acid cycle, metabolism of amino acids, and glucose metabolism, among others), with up-regulation of only 5 gene sets (e.g., ribosome biogenesis and translational regulation). The same response was not observed at 28 days. At 90 days, the signal shifted to a response that is similar to what is seen at the higher concentrations (described below) in regard to up-regulation of xenobiotic metabolism, particularly phase I metabolism (e.g., KEGG “Metabolism of xenobiotics by cytochrome P450” enriched by the up-regulation of *Cyp3a4* and several *Ugt2b* isoforms). Down-regulation of complement and coagulation cascade-related gene sets was observed at both 7 and 90 days, which is discussed further in the following paragraphs for the higher concentrations.

At both the 2000 and 6000 ppm concentrations, genes that were significantly differentially expressed reflected up-regulation of xenobiotic metabolism pathways at all timepoints. This signal was seen at a higher degree at 6000 than at 2000 ppm, and increased over the timepoints evaluated, both in the number of significantly differentially expressed genes within the gene sets (which confers a greater level of statistical significance), as well as the number of gene sets/pathways that were significantly enriched between the treatment groups and time points. In other words, the enrichment of these xenobiotic metabolism gene sets appears to increase with both dose and time. Gene sets related to xenobiotic metabolism were significantly enriched (up-regulated), for example KEGG “Metabolism of xenobiotics by cytochrome P450”, Reactome “Biological oxidations” and Reactome “Phase II conjugation”, among others. The enrichment of these gene sets was driven by genes that encode relevant glutathione transferases, UDP-glucuronosyltransferases, and CYPs.

Another major signal at these two higher concentrations is the enrichment of the complement and coagulation cascade gene set, and related gene sets, in the negative direction (loss of signal), owing to the down-regulation of genes encoding proteolytic subunits in the complement system and gene members of the serpin family (serine protease inhibitors), relative to controls. Deficiency in certain serpins (e.g., *Serpina1*) has been observed in relation to liver damage[7], and the complement system is related to innate immune responses. Down-regulation of genes involved in lipid metabolism was also observed, which is a signal aligned with a liver injury at these higher concentrations. These down-regulated signals were observed at a greater degree in the 6000 vs. the 2000 ppm treatment group.

At the 90-day timepoint, gene sets related to mitotic cell cycle and DNA synthesis were also significantly enriched, indicating a proliferative response and mitosis. This was seen primarily in the 6000 ppm treatment group, but also minimally in the 2000 ppm group. This proliferative response was not evident at earlier time points.

Gene sets related to DNA damage response and repair were not significantly enriched when utilizing the Canonical Pathways collection of gene sets available in the MSigDB. Additionally, using the more extensive collection of gene sets that was curated to identify all gene sets related to DNA damage response as described in the Methods (2.4), no treatments had any significant enrichment at 7 or 28 days. At 90 days, some of these gene sets were significantly enriched; however, the enrichment of these gene sets was due to up-regulation of genes involved in apoptotic signaling, while DNA damage repair genes were not up-regulated.

## 3.2 Benchmark dose modeling analysis

Benchmark dose modeling analysis and functional classification of the gene-level BMD results confirmed the gene set enrichment results detailed above that were obtained from analysis of each individual concentration separately. For example, at 90 days, the Reactome[8] gene set “Glutathione conjugation” was significantly enriched (median BMD for the gene set >1500 ppm). Also at 90 days, “Innate immune system” was down-regulated (median BMD >3200 ppm), which is related to the down-regulation of

---

[7] Law, RHP et al., 2006. An overview of the serpin superfamily. *Genome Biol*

[8] https://reactome.org/

complement and coagulation cascade signal as discussed above. Gene sets related to cell cycle and mitosis were also up-regulated and enriched according to the BMD analysis (median BMDs for these gene sets were 3400 ppm or higher). A single "DNA repair" gene set was significantly enriched among dose-responsive genes (median BMD >4000 ppm). The genes within this gene set that were identified as dose-responsive are primarily histone- and polymerase-encoding genes involved in DNA synthesis. The *Rad51* repair gene was identified as dose-responsive, although it should be noted that this gene was not significantly differentially expressed at any of the doses when compared to the controls and had a low level of expression across all of the samples.

At 28 days, the phase II metabolism gene sets were significantly enriched similar to 90 days, with similar BMD values. Gene sets related to cell cycle or mitosis were up-regulated according to the BMD analysis at 28 days, and down-regulation of fatty acid metabolism and immune responses was observed, all of which had a lower level of statistical significance compared to results from 90 day data. At 7 days, the phase II metabolism-related gene sets were also enriched among dose-responsive genes, although the BMD median values were higher compared to those at 28 and 90 days. At 7 days, the same "DNA repair" gene set was enriched as discussed above for 90 days, with histone and ubiquination genes underlying the enrichment, which are involved in DNA synthesis and may be related to cellular proliferation. Results of the BMDExpress Functional Classification analysis can be found in Appendix I.

# 4 Summary

In summary, the findings from the transcriptomics analyses of livers from female mice exposed to 1,4-dioxane in drinking water demonstrate an increase in xenobiotic metabolism, a subtle yet significant dose- and time-responsive increase in mitotic cell cycle and cellular proliferation, and a decrease in complement cascade processes and lipid metabolism. The proliferative response appears to only occur at concentrations above 2000 ppm, while xenobiotic metabolism alterations occur as low as 600 ppm. The lack of significant changes in signaling pathways/gene sets at the transcriptomic level at concentrations below 600 ppm indicates that 600 ppm represents a threshold between a lack of response and a response. However, the response at 600 ppm appears to be temporally sensitive with a transient non-specific cellular stress response after one week of exposure and with up-regulation of xenobiotic metabolism at the 90 day timepoint. Thus, a threshold for transcriptomic responses related to adverse effects may in fact be higher than 600 ppm, as enrichment of gene sets related to a proliferative response appears at higher concentrations, and BMDs for all enriched genesets are > 600 ppm according to BMD analysis. Importantly, activation of DNA damage response and/or repair mechanisms was not evident at the concentrations and time points evaluated.

# 5 References

Chappell, G. A., Israel, J. W., Simon, J. M., Pott, S., Safi, A., Eklund, K., . . . Furey, T. S. (2017). Variation in DNA-Damage Responses to an Inhalational Carcinogen (1,3-Butadiene) in Relation to Strain-Specific Differences in Chromatin Accessibility and Gene Transcription Profiles in C57BL/6J and CAST/EiJ Mice. *Environmental Health Perspectives, 125*(10), 107006. doi:10.1289/EHP1937

Croft, D., O'Kelly, G., Wu, G., Haw, R., Gillespie, M., Matthews, L., . . . Stein, L. (2011). Reactome: a database of reactions, pathways and biological processes. *Nucleic Acids Research, 39*(Database issue), D691-697. doi:10.1093/nar/gkq1018

Love, M. I., Huber, W., & Anders, S. (2014). Moderated estimation of fold change and dispersion for RNA-seq data with DESeq2. *Genome Biology, 15*(12), 550. doi:10.1186/s13059-014-0550-8

Nishimura, D. (2001). BioCarta. *Biotech Softw Internet Rep, 2*, 117-120.

Ogata, H., Goto, S., Sato, K., Fujibuchi, W., Bono, H., & Kanehisa, M. (1999). KEGG: Kyoto Encyclopedia of Genes and Genomes. *Nucleic Acids Research, 27*(1), 29-34. doi:10.1093/nar/27.1.29

Phillips, J. R., Svoboda, D. L., Tandon, A., Patel, S., Sedykh, A., Mav, D., . . . Auerbach, S. S. (2019). BMDExpress 2: enhanced transcriptomic dose-response analysis workflow. *Bioinformatics, 35*(10), 1780-1782. doi:10.1093/bioinformatics/bty878

Rooney, J. P., Ryan, N., Chorley, B. N., Hester, S. D., Kenyon, E. M., Schmid, J. E., . . . Corton, J. C. (2017). From the Cover: Genomic Effects of Androstenedione and Sex-Specific Liver Cancer Susceptibility in Mice. *Toxicological Sciences, 160*(1), 15-29. doi:10.1093/toxsci/kfx153

Schaefer, C. F., Anthony, K., Krupa, S., Buchoff, J., Day, M., Hannay, T., & Buetow, K. H. (2009). PID: the Pathway Interaction Database. *Nucleic Acids Research, 37*(Database issue), D674-679. doi:10.1093/nar/gkn653

Subramanian, A., Tamayo, P., Mootha, V. K., Mukherjee, S., Ebert, B. L., Gillette, M. A., . . . Mesirov, J. P. (2005). Gene set enrichment analysis: a knowledge-based approach for interpreting genome-wide expression profiles. *Proceedings of the National Academy of Sciences of the United States of America, 102*(43), 15545-15550. doi:10.1073/pnas.0506580102

Varemo, L., Nielsen, J., & Nookaew, I. (2013). Enriching the gene set analysis of genome-wide data by incorporating directionality of gene expression and combining statistical hypotheses and methods. *Nucleic Acids Research, 41*(8), 4378-4391. doi:10.1093/nar/gkt111

Yeakley, J. M., Shepard, P. J., Goyena, D. E., VanSteenhouse, H. C., McComb, J. D., & Seligmann, B. E. (2017). A trichostatin A expression signature identified by TempO-Seq targeted whole transcriptome profiling. *PloS One, 12*(5), e0178302. doi:10.1371/journal.pone.0178302

# Appendix I

BMD analysis results for functional classification based on dose-responsive genes, using the Reactome database for gene sets within BMDExpress2.2 software.

BMD analysis results for functional classification based on dose-responsive genes, using the Reactome database for gene sets in BMDExpress2.2 software.

| Study Day | Gene Set Name | Fisher's Exact Left P-Value | Fisher's Exact Right P-Value | Fisher's Exact Two Tail | Gene Symbols | BMD Mean | BMD Median | BMD Minimum | BMD Standard Deviation | BMD wMean | BMD wSD | Overall Direction | Percent Genes With Overall Direction Up | Percent Genes With Overall Direction Down |
|---|---|---|---|---|---|---|---|---|---|---|---|---|---|---|
| 90Day | Signal Transduction | 2.17E-50 | 1 | 4.31E-50 | hnrnpf;gpnmb;klb;notum;arhgef6;tmed5;cenpu;fmnl2;rhou;hist1h4h;tubb6;ppid;gng11;lpar3;ranbp9;iqgap2;hgfac;rdh7;ccnc;cbx6;irs2;c5ar2;hist1h4i;hist1h3c;pdk4;adh4;nr5a2;mapk14;aldh1a7;olfr1033;ift52;wasf2;pin1;apob;aldh8a1;gatad2b;pdk1;tubb4b;yy1;ywhaz;fgd4;vav1;ube2m;tubb2a;tuba1b;ttr;tnfrsf10b;tln1;tiam1;rasa1;tgfa;tek;wwc1;nrg1;sdc4;kntc1;camkk2;sos1;sh3gl3;rxrg;rtkn;rock2;rock1;rbp1;rarg;psen2;psap;pml;plg;pcsk5;gpr143;nudc;ntrk2;nfkbia;myo9b;mtnr1a;rdh11;mdm2;il1rap;ikbkg;hsp90aa1;h2afx;hebp1;hdac2;gnai3;gfra1;gab1;fn1;fgf1;opn3;dll1;ddx5;cdkn1a;cdc42;cbfb;ctnnb1;casr;c3;btrc;areg;ar;apoe;apoc3;ap2m1;adra1b;adora1;abca4;sec13;cenpf;lgr4 | 3180.5077 | 3387.63 | 74.8133 | 1774.83128 | 3292.92402 | 1816.33815 | CONFLICT | 0.545454545 | 0.454545455 |
| 90Day | Signaling by GPCR | 2.00E-36 | 1 | 4.31E-36 | arhgef6;gng11;lpar3;rdh7;c5ar2;olfr1033;apob;ttr;sdc4;camkk2;sos1;rock2;rock1;rbp1;psap;gpr143;mtnr1a;rdh11;hebp1;gnai3;opn3;cdc42;casr;c3;apoe;apoc3;adra1b;adora1;abca4 | 3497.3139 | 3874.11 | 98.0082 | 2108.92646 | 3964.51885 | 2022.13737 | CONFLICT | 0.551724138 | 0.448275862 |
| 90Day | GPCR downstream signalling | 6.06E-36 | 1 | 1.27E-35 | arhgef6;gng11;lpar3;rdh7;olfr1033;apob;ttr;sdc4;camkk2;sos1;rock2;rock1;rbp1;psap;gpr143;mtnr1a;rdh11;hebp1;gnai3;opn3;cdc42;casr;c3;apoe;apoc3;adra1b;adora1;abca4 | 3443.04833 | 3718.565 | 98.0082 | 2126.90737 | 3953.14582 | 2031.24843 | CONFLICT | 0.535714286 | 0.464285714 |
| 7Day | Signal Transduction | 2.94E-35 | 1 | 5.38E-35 | akr1c6;clasp2;ranbp10;tmed5;rps6kb1;myh14;rgs12;reep6;hist1h4h;rraga;hist1h2bc;ppid;cenpk;ranbp9;gsk3b;vps29;ptges3;metap2;kalrn;iqgap2;hgfac;avpr1a;suz12;tax1bp1;nckap1;dlc1;hist2h2ac;pdhx;mapk3;polr2h;klhl12;pebp1;apob;lingo1;sept7;tubb4b;ywhaz;yes1;pak2;uba52;tubb2a;tuba4a;ttr;rasa1;tgfbr1;tfdp1;rdh16f2;sdc3;stat1;sox6;smpd2;sel1l;rgs9;ptpn11;flna;pten;prkar2a;ppp2cb;prkcz;prkci;pfn2;pfn1;pcsk5;ncoa2;ncoa1;myh9;mdk;lrp5;lrp1;kras;kif2a;jak1;itpr2;il1rap;hsp90aa1;hist2h2aa1;hebp1;gnai3;gfra1;fgf1;f2;adgre1;eif4ebp1;dld;csnk2b;cdkn1a;cdc42;ccnk;ctnnb1;casp9;calm3;calm2;cab39;btrc;bmi1;cxcr5;atp6v1e1;apoe;xiap;abl1;wwp1;akr1c14;xpo1;brk1 | 3316.45352 | 3443.57 | 54.5232 | 1516.89313 | 3318.4404 | 1535.54406 | CONFLICT | 0.596153846 | 0.403846154 |
| 90Day | G alpha (s) signalling events | 6.28E-35 | 1 | 9.68E-35 | gng11;olfr1033 | 4747.235 | 4747.235 | 4640.23 | 151.327922 | 4677.79404 | 115.134904 | UP | 1 | 0 |
| 7Day | G alpha (s) signalling events | 3.63E-30 | 1 | 7.07E-30 | reep6 | 2593.62 | 2593.62 | 2593.62 | | 2593.62 | | DOWN | 0 | 1 |
| 90Day | Olfactory Signaling Pathway | 3.68E-29 | 1 | 6.68E-29 | olfr1033 | 4640.23 | 4640.23 | 4640.23 | | 4640.23 | | UP | 1 | 0 |

BMD analysis results for functional classification based on dose-responsive genes, using the Reactome database for gene sets in BMDExpress2.2 software.

| Study Day | Gene Set Name | Fisher's Exact Left P-Value | Fisher's Exact Right P-Value | Fisher's Exact Two Tail | Gene Symbols | BMD Mean | BMD Median | BMD Minimum | BMD Standard Deviation | BMD wMean | BMD wSD | Overall Direction | Percent Genes With Overall Direction Up | Percent Genes With Overall Direction Down |
|---|---|---|---|---|---|---|---|---|---|---|---|---|---|---|
| 28Day | Signal Transduction | 1.44E-28 | 1 | 2.25E-28 | phlpp1;akr1c6;atp6v0e2;arhgap45;pygo2;zwilch;ppid;nts;akr1c12;cysltr1;ranbp9;dynll1;iqgap2;tax1bp1;reep1;dlc1;akr1c19;cenpt;hist1h4i;adh4;map3k11;olfr378;apob;aldh8a1;sept7;a2m;cdc14a;tubb4b;stradb;ube2m;tubb2a;tnfrsf10b;tfdp1;rdh16f2;cx3cl1;polr2a;arhgdia;ppp3cb;pfn1;pdpk1;p4hb;sqstm1;notch1;cxcl9;mdm2;mapkapk2;lrp1;il1rap;ikbkg;hgs;hbegf;gpc4;gnb5;fn1;fgf1;f2;cdc42;ccnk;c3;bmi1;atp6v1e1;app;apoe;birc2;agt;adora1;adcy9;mylk;akr1c14;brk1 | 3861.86604 | 4068.31 | 160.43 | 1724.51206 | 3869.25966 | 1672.47843 | CONFLICT | 0.542857143 | 0.457142857 |
| 7Day | Signaling by GPCR | 3.11E-28 | 1 | 4.70E-28 | akr1c6;rgs12;reep6;metap2;kalrn;avpr1a;mapk3;apob;ttr;rdh16f2;sdc3;rgs9;prkar2a;ppp2cb;lrp1;kras;itpr2;hebp1;gnai3;f2;adgre1;cdc42;calm3;calm2;cxcr5;apoe;akr1c14 | 3241.27322 | 3627.04 | 113.316 | 1726.92825 | 3070.17697 | 1684.78312 | DOWN | 0.37037037 | 0.62962963 |
| 7Day | GPCR downstream signalling | 6.03E-28 | 1 | 9.20E-28 | akr1c6;rgs12;reep6;metap2;kalrn;avpr1a;mapk3;apob;ttr;rdh16f2;sdc3;rgs9;prkar2a;ppp2cb;lrp1;kras;itpr2;hebp1;gnai3;f2;cdc42;calm3;calm2;cxcr5;apoe;akr1c14 | 3252.61296 | 3638.015 | 113.316 | 1760.10274 | 3079.1862 | 1745.97574 | DOWN | 0.384615385 | 0.615384615 |
| 7Day | Olfactory Signaling Pathway | 5.14E-24 | 1 | 1.15E-23 | reep6 | 2593.62 | 2593.62 | 2593.62 |  | 2593.62 |  | DOWN | 0 | 1 |
| 28Day | G alpha (s) signalling events | 1.35E-17 | 1 | 2.01E-17 | reep1;olfr378;gnb5;adcy9 | 3762.577 | 4079.355 | 953.648 | 2070.66227 | 3627.58322 | 2285.46734 | UP | 0.75 | 0.25 |
| 28Day | Signaling by GPCR | 4.40E-17 | 1 | 1.01E-16 | akr1c6;nts;akr1c12;cysltr1;reep1;akr1c19;olfr378;apob;rdh16f2;cx3cl1;pdpk1;cxcl9;lrp1;hbegf;gpc4;gnb5;f2;cdc42;c3;app;apoe;agt;adora1;adcy9;akr1c14 | 3394.649 | 3361.03 | 192.988 | 1888.93514 | 3334.38703 | 1842.60481 | CONFLICT | 0.44 | 0.56 |
| 28Day | GPCR downstream signalling | 2.05E-16 | 1 | 4.44E-16 | akr1c6;nts;akr1c12;cysltr1;reep1;akr1c19;olfr378;apob;rdh16f2;cx3cl1;pdpk1;cxcl9;lrp1;hbegf;gpc4;gnb5;f2;cdc42;c3;app;apoe;agt;adora1;adcy9;akr1c14 | 3394.649 | 3361.03 | 192.988 | 1888.93514 | 3334.38703 | 1842.60481 | CONFLICT | 0.44 | 0.56 |
| 28Day | Olfactory Signaling Pathway | 9.77E-16 | 1 | 2.30E-15 | reep1;olfr378 | 4938.03 | 4938.03 | 3938.11 | 1414.10043 | 4908.99441 | 1413.50411 | UP | 1 | 0 |
| 90Day | Immune System | 1.49E-15 | 1 | 2.44E-15 | erap1;irak3;defb30;tmem173;fbxo22;ist1;cpn2;fbxo9;anapc10;fbxw9;arel1;ndufc2;tubb6;fbxo32;pnp2;serpinb1a;asb2;tbk1;iqgap2;irf7;dctn3;prdx4;ube2k;keap1;znrf2;irs2;c5ar2;hist1h3c;sh2d1b1;slc27a2;mapk14;ceacam2;eda2r;kbtbd8;wasf2;usp18;abce1;pin1;apob;mgam;tubb4b;ywhaz;vtn;vav1;ube2m;txn1;tubb2a;tuba1b;ttr;cdc34;pdxk;tap2;stx3;serpina1e;sos1;snap23;siah2;rock1;psap;pnp;plaur;nfkbia;myo9b;myo10;mme;man2b1;lifr;lamp1;il9r;il1rap;il15ra;ikbkg;cd74;il18bp;ifngr2;ifnar1;icam1;hsp90aa1;h2-aa;gstp2;lilr4b;gm2a;ftl1;fcgr2b;ctsh;ctsd;csf1;crp;crlf1;cdc42;cd1d1;ctnnb1;c3;btrc;ap2m1;prdx6;ahsg;sec13;mlec | 2850.84586 | 3115.46 | 45.5307 | 1738.85671 | 2772.30212 | 1757.02643 | CONFLICT | 0.424242424 | 0.575757576 |

BMD analysis results for functional classification based on dose-responsive genes, using the Reactome database for gene sets in BMDExpress2.2 software.

| Study Day | Gene Set Name | Fisher's Exact Left P-Value | Fisher's Exact Right P-Value | Fisher's Exact Two Tail | Gene Symbols | BMD Mean | BMD Median | BMD Minimum | BMD Standard Deviation | BMD wMean | BMD wSD | Overall Direction | Percent Genes With Overall Direction Up | Percent Genes With Overall Direction Down |
|---|---|---|---|---|---|---|---|---|---|---|---|---|---|---|
| 90Day | Metabolism of proteins | 6.94E-14 | 1 | 1.44E-13 | eif3m;trappc6b;notum;crebrf;spp2;fbxo22;fbxo9;lman1;hist1h4h;fbxw9;mrpl58;babam1;tomm20;tubb6;rps27l;fbxo32;stx17;mrps18b;eid3;gng11;mrpl54;asb2;mrps30;ngly1;park7;mrps31;psmd8;sae1;pigp;rnf5;dctn3;ube2k;mcrs1;st6galnac6;keap1;etfbkmt;hist1h4i;tomm70a;mbtps2;nr5a2;ceacam2;kbtbd8;dcaf10;usp18;psmc4;apob;wdtc1;galnt12;psmf1;tubb4b;yy1;ino80c;ube2m;txn1;tubb2a;tuba1b;trf;tnc;nup153;tgfa;mrpl22;cdc34;serpina1e;st3gal3;siah2;exoc4;rps12;rad23a;pml;plaur;nfkbia;mmp2;mme;mdm2;man1a;ly6d;large1;itih2;inhbc;ikbkg;igfbp4;hdac2;gpld1;gnai3;fn1;fem1b;f7;ddx5;ctsh;ctsd;csf1;c3;btrc;areg;ar;apoe;ahsg;sec13;adamts6;golm1;dcun1d2;spon2 | 2997.59553 | 3416.655 | 25.9884 | 1655.12855 | 2813.87591 | 1586.10242 | CONFLICT | 0.558823529 | 0.441176471 |
| 7Day | GPCR ligand binding | 6.50E-13 | 1 | 1.12E-12 | avpr1a;hebp1;f2;adgre1;cxcr5 | 2128.7362 | 836.92 | 156.627 | 2363.42894 | 2282.45635 | 2381.44419 | DOWN | 0.4 | 0.6 |
| 90Day | Transport of small molecules | 1.14E-11 | 1 | 2.55E-11 | abcb8;afg3l2;micu2;gng11;slc29a1;rnf5;ces3a;abcg2;apob;trf;slc17a8;slc22a1;slc1a2;pcsk5;lipc;slc6a12;ftl1;ces3b;slc26a2;bmp1;apoe;apoc3;ap2m1;abca4;ano10;slco2b1 | 2834.34404 | 3070.33 | 175.96 | 1661.76142 | 2873.32404 | 1665.68923 | CONFLICT | 0.423076923 | 0.576923077 |
| 90Day | Post-translational protein modification | 2.08E-11 | 1 | 3.47E-11 | trappc6b;notum;spp2;fbxo22;fbxo9;lman1;hist1h4h;fbxw9;babam1;tomm20;tubb6;fbxo32;stx17;eid3;asb2;ngly1;park7;psmd8;sae1;pigp;rnf5;dctn3;ube2k;mcrs1;st6galnac6;keap1;etfbkmt;hist1h4i;tomm70a;nr5a2;ceacam2;kbtbd8;dcaf10;usp18;psmc4;apob;wdtc1;galnt12;psmf1;tubb4b;yy1;ino80c;ube2m;tubb2a;tuba1b;trf;tnc;nup153;tgfa;cdc34;serpina1e;st3gal3;siah2;rad23a;pml;plaur;nfkbia;mdm2;man1a;ly6d;large1;itih2;ikbkg;igfbp4;hdac2;gpld1;fn1;fem1b;f7;ddx5;csf1;c3;btrc;areg;ar;apoe;ahsg;sec13;adamts6;golm1;dcun1d2;spon2 | 2865.16206 | 3148.415 | 25.9884 | 1695.01582 | 2730.17627 | 1650.65443 | CONFLICT | 0.536585366 | 0.463414634 |
| 90Day | Gene expression (Transcription) | 2.98E-11 | 1 | 5.70E-11 | smarcd2;cstf2t;ints11;pcgf6;ints14;hist1h4h;srsf6;thoc7;zfp110;trp53inp1;ccnc;txnrd1;cbx6;hist1h4i;hist1h3c;zfp354b;eloa;zfp747;nr5a2;mapk14;esrrg;pin1;zfp445;gatad2b;ywhaz;txn1;plk2;smarcb1;rxrg;rarg;pml;mdm2;h2afx;hdac2;gsr;brd2;cdkn1a;cdk7;ccng1;cbfb;ctnnb1;btg2;bax;ar | 3176.22566 | 3346.45 | 137.958 | 1715.77322 | 2934.0987 | 1739.14829 | UP | 0.659090909 | 0.340909091 |
| 90Day | GPCR ligand binding | 1.04E-10 | 1 | 2.05E-10 | gng11;lpar3;c5ar2;psap;gpr143;mtnr1a;hebp1;opn3;casr;c3;adra1b;adora1 | 3750.93167 | 4062.31 | 639.57 | 1767.18456 | 4075.34824 | 1848.47526 | CONFLICT | 0.583333333 | 0.416666667 |
| 7Day | Class A/1 (Rhodopsin-like receptors) | 1.01E-09 | 1 | 1.67E-09 | avpr1a;hebp1;f2;cxcr5 | 1924.31025 | 813.537 | 156.627 | 2677.52286 | 2048.17584 | 2811.26815 | CONFLICT | 0.5 | 0.5 |
| 28Day | Biological oxidations | 1 | 7.17E-09 | 7.17E-09 | ugt1a6a;sult2a8;abhd14b;ugt2a3;bphl;sult2a7;cyp3a25;ugt1a1;ugt1a6b;ahcy;adh4;ugt2b35;ces2e;ces2c;ces2b;ugt2b36;ugt3a2;ugt2b5;ugdh;gstz1;gstp1;gstp2;gstm4;gsta2;gsta1;gclm;gclc;fdxr;ces3b;cyp4a12b;cyp3a11;cyp2e1;cyp2c37;cyp2c29;cyp2a5;cyp2a4;aldh2;gm4737;glyat;ces2a;ugt2b34;gm3776;cyp3a59;cyp3a41b | 2625.72486 | 2131.875 | 309.913 | 1866.42956 | 2525.80954 | 1748.51695 | CONFLICT | 0.5 | 0.5 |

BMD analysis results for functional classification based on dose-responsive genes, using the Reactome database for gene sets in BMDExpress2.2 software.

| Study Day | Gene Set Name | Fisher's Exact Left P-Value | Fisher's Exact Right P-Value | Fisher's Exact Two Tail | Gene Symbols | BMD Mean | BMD Median | BMD Minimum | BMD Standard Deviation | BMD wMean | BMD wSD | Overall Direction | Percent Genes With Overall Direction Up | Percent Genes With Overall Direction Down |
|---|---|---|---|---|---|---|---|---|---|---|---|---|---|---|
| 28Day | Phase II - Conjugation of compounds | 1 | 9.28E-09 | 9.28E-09 | ugt1a6a;sult2a8;abhd14b;ugt2a3;sult2a7;ugt1a1;ugt1a6b;ahcy;ugt2b35;ugt2b36;ugt3a2;ugt2b5;ugdh;gstz1;gstp1;gstp2;gstm4;gsta2;gsta1;gclm;gclc;gm4737;glyat;ugt2b34;gm3776 | 2355.13768 | 1902.72 | 309.913 | 1709.63218 | 2343.74456 | 1632.88604 | CONFLICT | 0.56 | 0.44 |
| 90Day | RNA Polymerase II Transcription | 8.39E-09 | 1 | 1.71E-08 | smarcd2;cstf2t;ints11;pcgf6;ints14;hist1h4h;srsf6;thoc7;zfp110;trp53inp1;ccnc;txnrd1;cbx6;hist1h4i;hist1h3c;zfp354b;eloa;zfp747;nr5a2;mapk14;esrrg;pin1;zfp445;gatad2b;ywhaz;txn1;plk2;smarcb1;rxrg;rarg;pml;mdm2;h2afx;hdac2;gsr;brd2;cdkn1a;cdk7;ccng1;cbfb;ctnnb1;btg2;bax;ar | 3176.22566 | 3346.45 | 137.958 | 1715.77322 | 2934.0987 | 1739.14829 | UP | 0.659090909 | 0.340909091 |
| 90Day | Ion channel transport | 1.40E-08 | 1 | 2.25E-08 | ano10 | 3679.83 | 3679.83 | 3679.83 |  | 3679.83 |  | UP | 1 | 0 |
| 90Day | Innate Immune System | 1.49E-08 | 1 | 2.81E-08 | defb30;tmem173;ist1;cpn2;ndufc2;pnp2;serpinb1a;tbk1;iqgap2;irf7;prdx4;c5ar2;slc27a2;mapk14;ceacam2;wasf2;pin1;apob;mgam;tubb4b;vtn;vav1;ube2m;txn1;ttr;cdc34;pdxk;serpina1e;sos1;snap23;rock1;psap;pnp;plaur;nfkbia;myo9b;myo10;mme;man2b1;lamp1;ikbkg;hsp90aa1;gstp2;lilr4b;gm2a;ftl1;fcgr2b;ctsh;ctsd;crp;cdc42;ctnnb1;c3;btrc;prdx6;ahsg;mlec | 2919.02877 | 3265.56 | 45.5307 | 1818.52597 | 3022.94114 | 1759.58219 | DOWN | 0.368421053 | 0.631578947 |
| 90Day | Muscle contraction | 6.83E-08 | 1 | 1.07E-07 | scn3b;tln1 | 5174.92 | 5174.92 | 4478.93 | 984.278497 | 5430.61984 | 915.444886 | CONFLICT | 0.5 | 0.5 |
| 90Day | Vesicle-mediated transport | 7.40E-08 | 1 | 1.37E-07 | trappc6b;st5;lman1;tubb6;stx17;ubap1;scoc;dctn3;dennd1b;pacsin2;apob;stx16;dennd1a;tubb4b;ywhaz;tubb2a;tuba1b;trf;tgfa;fnbp1l;serpina1e;snap23;sh3gl3;man1a;acbd3;gjb2;ftl1;areg;apoe;ap2m1;sec13;kifc1 | 2897.27012 | 2871.225 | 137.958 | 1820.06836 | 2727.44092 | 1716.12068 | UP | 0.625 | 0.375 |
| 90Day | Class A/1 (Rhodopsin-like receptors) | 1.02E-07 | 1 | 1.65E-07 | lpar3;c5ar2;psap;gpr143;mtnr1a;hebp1;opn3;c3;adra1b;adora1 | 3429.046 | 3191.495 | 639.57 | 1751.93278 | 3783.39488 | 1859.83665 | CONFLICT | 0.5 | 0.5 |
| 7Day | Extracellular matrix organization | 3.71E-07 | 1 | 5.96E-07 | ttr;sdc3;p3h3;dst;ctsb;bgn | 3854.32833 | 3795.99 | 2968.59 | 996.379375 | 3842.1728 | 882.542529 | DOWN | 0.333333333 | 0.666666667 |
| 90Day | Membrane Trafficking | 3.99E-07 | 1 | 7.84E-07 | trappc6b;st5;lman1;tubb6;stx17;ubap1;scoc;dctn3;dennd1b;pacsin2;apob;stx16;dennd1a;tubb4b;ywhaz;tubb2a;tuba1b;trf;tgfa;fnbp1l;serpina1e;snap23;sh3gl3;man1a;acbd3;gjb2;ftl1;areg;ap2m1;sec13;kifc1 | 2934.28465 | 2983.55 | 137.958 | 1837.87014 | 2750.4141 | 1730.22063 | UP | 0.64516129 | 0.35483871 |
| 90Day | Generic Transcription Pathway | 4.15E-07 | 1 | 8.80E-07 | smarcd2;pcgf6;hist1h4h;zfp110;trp53inp1;ccnc;txnrd1;cbx6;hist1h4i;hist1h3c;zfp354b;eloa;zfp747;nr5a2;mapk14;esrrg;pin1;zfp445;gatad2b;ywhaz;txn1;plk2;smarcb1;rxrg;rarg;pml;mdm2;h2afx;hdac2;gsr;brd2;cdkn1a;cdk7;ccng1;cbfb;ctnnb1;btg2;bax;ar | 3028.63664 | 3141.48 | 137.958 | 1706.73482 | 2793.28915 | 1770.54293 | UP | 0.666666667 | 0.333333333 |
| 90Day | SLC-mediated transmembrane transport | 1.09E-06 | 1 | 1.74E-06 | slc29a1;slc17a8;slc22a1;slc1a2;slc6a12;slc26a2;slco2b1 | 2125.06986 | 1935.84 | 777.189 | 1245.83306 | 2249.01564 | 1085.52979 | DOWN | 0.142857143 | 0.857142857 |
| 28Day | Glucuronidation | 1 | 1.76E-06 | 1.76E-06 | ugt1a6a;ugt2a3;ugt1a1;ugt1a6b;ugt2b35;ugt2b36;ugt3a2;ugt2b5;ugdh;ugt2b34 | 1940.1023 | 1092.105 | 309.913 | 1847.24982 | 1885.83694 | 1683.87445 | CONFLICT | 0.5 | 0.5 |
| 28Day | Fatty acid metabolism | 1 | 2.16E-06 | 2.69E-06 | echs1;akr1c6;acox3;fads1;crot;ndufab1;gpx4;akr1c12;hacd3;hacl1;fads2;elovl2;acaa2;akr1c19;hacd1;acsf2;decr2;slc25a17;mapkapk2;lta4h;phyh;hsd17b4;hsd17b3;acsl1;cyp4a12b;cyp2c37;cyp2c29;elovl3;aldh3a2;acox1;acadl;akr1c14;acly | 3239.48033 | 3384.83 | 250.729 | 1654.88681 | 3150.22605 | 1637.35895 | DOWN | 0.333333333 | 0.666666667 |

BMD analysis results for functional classification based on dose-responsive genes, using the Reactome database for gene sets in BMDExpress2.2 software.

| Study Day | Gene Set Name | Fisher's Exact Left P-Value | Fisher's Exact Right P-Value | Fisher's Exact Two Tail | Gene Symbols | BMD Mean | BMD Median | BMD Minimum | BMD Standard Deviation | BMD wMean | BMD wSD | Overall Direction | Percent Genes With Overall Direction Up | Percent Genes With Overall Direction Down |
|---|---|---|---|---|---|---|---|---|---|---|---|---|---|---|
| 90Day | Adaptive Immune System | 1.57E-06 | 1 | 2.83E-06 | erap1;fbxo22;fbxo9;anapc10;fbxw9;arel1;tubb6;fbxo32;asb2;dctn3;ube2k;keap1;znrf2;sh2d1b1;kbtbd8;tubb4b;ywhaz;vav1;ube2m;tubb2a;tuba1b;cdc34;tap2;sos1;snap23;siah2;nfkbia;ikbkg;cd74;icam1;h2-aa;fcgr2b;ctsh;ctsd;cdc42;cd1d1;c3;btrc;ap2m1;sec13 | 2636.00384 | 2957.615 | 61.8554 | 1682.14578 | 2493.82028 | 1680.89375 | CONFLICT | 0.55 | 0.45 |
| 90Day | Keratinization | 1.99E-06 | 1 | 4.01E-06 | krt8;krt18;dsg2 | 3414.55333 | 3788.19 | 2496.49 | 799.638993 | 3214.23654 | 807.558939 | UP | 0.666666667 | 0.333333333 |
| 90Day | Peptide ligand-binding receptors | 2.55E-06 | 1 | 5.69E-06 | c5ar2;psap;hebp1;c3 | 2739.995 | 2651.83 | 639.57 | 1828.98707 | 1834.41241 | 1622.50456 | DOWN | 0.25 | 0.75 |
| 90Day | Cardiac conduction | 3.96E-06 | 1 | 6.69E-06 | scn3b | 5870.91 | 5870.91 | 5870.91 | | 5870.91 | | UP | 1 | 0 |
| 28Day | Developmental Biology | 3.07E-06 | 1 | 6.86E-06 | ranbp9;pkp4;tubb4b;tubb2a;pkp1;pfn1;krt8;krt18;epha7;dag1;cdc42 | 3672.83427 | 3208.19 | 856.847 | 1664.0307 | 3542.36692 | 1536.76528 | UP | 0.909090909 | 0.090909091 |
| 28Day | Generic Transcription Pathway | 4.20E-06 | 1 | 7.64E-06 | meaf6;tmem219;med4;e2f7;txnrd1;nr1d2;hist1h4i;cnot1;tfdp1;tal1;polr2a;rorc;nrbp1;notch1;mdm2;ccnk;ccng1;bnip3l;bmi1;zfp729b | 3648.58815 | 3712.885 | 908.573 | 1588.07557 | 3410.62998 | 1553.99857 | UP | 0.65 | 0.35 |
| 7Day | Generic Transcription Pathway | 5.72E-06 | 1 | 1.01E-05 | zfp266;pcgf5;zfp248;pcgf6;med6;hist1h4h;zfp707;rraga;hist1h2bc;kmt5a;suz12;txnrd1;hist2h2ac;polr2h;taf10;cnot1;ywhaz;uba52;tfdp1;prdx2;rorc;ptpn11;ppp2cb;kras;hist2h2aa1;csnk2b;cdkn1a;ccnk;ccng1;ccne2;ctnnb1;bmi1;abl1 | 3385.01173 | 3489.14 | 54.5232 | 1214.8211 | 3339.00094 | 1237.87958 | UP | 0.787878788 | 0.212121212 |
| 90Day | G alpha (q) signalling events | 6.88E-06 | 1 | 1.20E-05 | gng11;lpar3;sos1;gpr143;casr;adra1b | 4881.85833 | 5115.43 | 2444.64 | 1269.0783 | 5128.17895 | 1044.67841 | UP | 0.666666667 | 0.333333333 |
| 7Day | Neuronal System | 8.01E-06 | 1 | 1.51E-05 | gria3;slc22a1;slc1a2;ptprf;ptprd;prkar2a;il1rap;gnai3;flot2;calm3;calm2 | 2866.22582 | 3050.32 | 131.024 | 1799.35932 | 2447.31331 | 1656.36542 | DOWN | 0.272727273 | 0.727272727 |
| 90Day | G alpha (i) signalling events | 7.08E-06 | 1 | 1.51E-05 | gng11;lpar3;rdh7;apob;ttr;sdc4;camkk2;rbp1;psap;mtnr1a;rdh11;hebp1;gnai3;opn3;casr;c3;apoe;apoc3;adora1;abca4 | 3406.20521 | 3416.7 | 98.0082 | 2098.44064 | 3924.51046 | 2055.30073 | CONFLICT | 0.5 | 0.5 |
| 28Day | GPCR ligand binding | 7.31E-06 | 1 | 1.63E-05 | nts;cysltr1;cx3cl1;cxcl9;gnb5;f2;c3;agt;adora1 | 3717.326 | 4610.42 | 907.506 | 2243.2963 | 3524.29581 | 2164.64592 | CONFLICT | 0.555555556 | 0.444444444 |
| 7Day | Glucuronidation | 1 | 3.01E-05 | 3.01E-05 | ugt1a6a;ugt2b1;ugt1a1;ugt1a9;ugt2b35;ugt2b36;ugt3a2;ugt2b5;ugdh;ugt2b34 | 1506.85551 | 1187.735 | 70.0701 | 1427.5697 | 1573.89544 | 1419.673 | UP | 0.6 | 0.4 |
| 28Day | Metabolism | 0.99998 | 2.35E-05 | 3.73E-05 | dpyd;ugt1a6a;echs1;akr1c6;acox3;sult2a8;abhd14b;fads1;ippk;crot;phykpl;ugt2a3;ndufab1;ndufaf1;fitm1;pmvk;adipor2;ndufc2;bphl;nudt12;atp5g2;dgat2;pnpla8;pi4k2b;ormdl2;etfdh;ormdl3;asrgl1;tnfaip8l1;dpys;sult2a7;gpx4;akr1c12;hacd3;atp5j2;hacl1;tdo2;nme4;fads2;serinc1;cyp3a25;prodh2;elovl2;nudt5;acaa2;txnrd1;akr1c19;ugt1a1;ugt1a6b;agmo;hacd1;slc25a10;ahcy;adh4;acsf2;decr2;hsd17b13;ugt2b35;hs2st1;apob;phospho1;ces2e;ces2c;ces2b;pla2g4c;sds;ugt2b36;coq3;pi4ka;ugt3a2;ugt2b5;ugdh;etnk2;aldh4a1;suclg2;slc25a17;slc22a1;slc10a1;sardh;ptdss1;pnp;pfkl;enpp1;pcx;pck1;otc;odc1;oat;me1;mapkapk2;man2b2;man2b1;amacr;lta4h;lrp1;phyh;ldha;khk;hyal1;hsd17b4;hsd17b3;hsd11b1;hprt;hpd;guk1;gstz1;gstp1;gstp2;gstm4;gsta2;gsta1;gpi1;gpc4;got2;gnb5;glul;gclm;gclc;gc;gaa;fech;fdxr;acsl1;ces3b;ddc;cyp4a12b;cyp3a11;cyp2e1;cyp2c37;cyp2c29;cyp2a5;cyp2a4;elovl3;entpd5;bpgm;ass1;apoe;aldh3a2;aldh2;gm4737;adss;adk;adcy9;acp5;acox1;acadl;aldh7a1;cyb5a;haao;glyat; | 3000.7126 | 3049.42 | 67.9262 | 1681.12043 | 2868.78683 | 1654.39784 | DOWN | 0.333333333 | 0.666666667 |

BMD analysis results for functional classification based on dose-responsive genes, using the Reactome database for gene sets in BMDExpress2.2 software.

| Study Day | Gene Set Name | Fisher's Exact Left P-Value | Fisher's Exact Right P-Value | Fisher's Exact Two Tail | Gene Symbols | BMD Mean | BMD Median | BMD Minimum | BMD Standard Deviation | BMD wMean | BMD wSD | Overall Direction | Percent Genes With Overall Direction Up | Percent Genes With Overall Direction Down |
|---|---|---|---|---|---|---|---|---|---|---|---|---|---|---|
| 28Day | Gene expression (Transcription) | 2.26E-05 | 0.99999 | 3.93E-05 | iws1;meaf6;ints14;tmem219;med4;wdr61;e2f7;cpsf2;txnrd1;nr1d2;hist1h4i;ell3;cnot1;rpap2;u2af2;tfdp1;tal1;polr2a;polr1a;rorc;nrbp1;papola;notch1;mdm2;ccnk;ccng1;bnip3l;bmi1;srsf1;thoc5;zfp729b;bc005561 | 3686.92147 | 3663.77 | 860.451 | 1575.79133 | 3554.92322 | 1521.43705 | CONFLICT | 0.59375 | 0.40625 |
| 7Day | Phase II - Conjugation of compounds | 0.99999 | 4.11E-05 | 4.11E-05 | ugt1a6a;gstk1;ugt2b1;ugt1a1;ugt1a9;ahcy;ugt2b35;ugt2b36;ugt3a2;ugt2b5;ugdh;gstp1;gstp2;gstm4;gsta1;gss;gclc;esd;acsm1;gm4737;glyat;ugt2b34;gm3776 | 2296.24338 | 2300.86 | 49.8526 | 1616.27738 | 2443.34515 | 1490.30542 | UP | 0.695652174 | 0.304347826 |
| 7Day | Degradation of the extracellular matrix | 3.16E-05 | 1 | 5.82E-05 | ctsb | 3881.76 | 3881.76 | 3881.76 |  | 3881.76 |  | UP | 1 | 0 |
| 28Day | Peroxisomal lipid metabolism | 0.99999 | 6.75E-05 | 6.75E-05 | acox3;crot;hacl1;decr2;slc25a17;phyh;hsd17b4;aldh3a2;acox1 | 2908.42444 | 3304.47 | 702.63 | 1027.3398 | 2984.9316 | 1073.13485 | DOWN | 0.333333333 | 0.666666667 |
| 28Day | Glutathione conjugation | 0.99999 | 6.75E-05 | 6.75E-05 | gstz1;gstp1;gstp2;gstm4;gsta2;gsta1;gclm;gclc;gm3776 | 2302.22322 | 1681.57 | 691.166 | 1795.00689 | 2140.16119 | 1723.20689 | UP | 0.777777778 | 0.222222222 |
| 90Day | Phospholipid metabolism | 4.38E-05 | 0.99999 | 9.74E-05 | osbpl10;dgat2;tnfaip8l1;tnfaip8l3;pi4ka;plekha1 | 2875.24333 | 2893.34 | 1984.74 | 584.157484 | 2906.28296 | 452.413567 | DOWN | 0.333333333 | 0.666666667 |
| 7Day | Peptide ligand-binding receptors | 5.85E-05 | 0.99999 | 1.14E-04 | avpr1a;hebp1;f2;cxcr5 | 1924.31025 | 813.537 | 156.627 | 2677.52286 | 2048.17584 | 2811.26815 | CONFLICT | 0.5 | 0.5 |
| 7Day | Potassium Channels | 6.43E-05 | 1 | 1.39E-04 |  |  |  |  |  |  |  |  |  |  |
| 90Day | Developmental Biology | 8.12E-05 | 0.99996 | 1.51E-04 | tubb6;pdlim7;ranbp9;stx1b;irs2;mapk14;tubb4b;tubb2a;tuba1b;tln1;tiam1;rasa1;sos1;siah2;rock2;rock1;myo9b;msn;mmp2;mef2a;krt8;krt18;hsp90aa1;gfra1;gab1;dsg2;cdc42;ctnnb1;ap2m1;itga9 | 2629.31194 | 2740.02 | 74.8133 | 1896.9482 | 2353.19076 | 1962.87938 | DOWN | 0.4 | 0.6 |
| 90Day | Glycerophospholipid biosynthesis | 1.09E-04 | 0.99999 | 1.75E-04 | osbpl10;dgat2 | 3115.43 | 3115.43 | 2903.14 | 300.223397 | 3131.64681 | 299.346151 | CONFLICT | 0.5 | 0.5 |
| 90Day | Stimuli-sensing channels | 7.44E-05 | 0.99999 | 1.77E-04 | ano10 | 3679.83 | 3679.83 | 3679.83 |  | 3679.83 |  | UP | 1 | 0 |
| 90Day | Neuronal System | 1.08E-04 | 0.99996 | 2.03E-04 | gng11;gria3;kcns3;lin7c;unc13b;camkk2;slc22a1;slc1a2;ptprd;mdm2;kcnj8;il1rap;gnai3;glul;slc6a12;gabrb3;epb41l1;ap2m1 | 3104.37596 | 3426.16 | 98.0082 | 1699.98764 | 3065.72998 | 1557.98412 | CONFLICT | 0.555555556 | 0.444444444 |
| 90Day | Signaling by WNT | 9.30E-05 | 0.99997 | 2.04E-04 | tmed5;gng11;ywhaz;ctnnb1;btrc;ap2m1;lgr4 | 3715.97257 | 4087.04 | 137.958 | 1800.60819 | 4216.23304 | 1751.83661 | UP | 0.714285714 | 0.285714286 |
| 7Day | Biological oxidations | 0.99991 | 1.86E-04 | 2.68E-04 | ugt1a6a;gstk1;ugt2b1;bphl;cyp3a25;ptges3;cyp39a1;ugt1a1;ugt1a9;ahcy;ugt2b35;ces2c;ugt2b36;ugt3a2;ugt2b5;ugdh;nqo2;ncoa2;ncoa1;gstp1;gstp2;gstm4;gsta1;gss;gclc;ces3b;esd;cyp3a11;cyp2e1;cyp2c37;cyp2c29;arnt;acsm1;aldh2;gm4737;maob;acy1;glyat;ces2a;ugt2b34;gm3776;cyp3a41b | 2411.07542 | 2474.22 | 46.9364 | 1694.49369 | 2395.23376 | 1587.12073 | CONFLICT | 0.547619048 | 0.452380952 |
| 28Day | Biosynthesis of specialized proresolving mediators (SPMs) | 0.99995 | 2.79E-04 | 2.79E-04 | gpx4;cyp3a25;lta4h;gstm4;cyp3a11;cyp2e1;cyp2c37;cyp2c29;cyp3a59;cyp3a41b | 3195.6493 | 3231.855 | 792.488 | 2077.75928 | 2840.57897 | 1887.92444 | DOWN | 0.4 | 0.6 |
| 90Day | Biosynthesis of specialized proresolving mediators (SPMs) | 0.99993 | 2.85E-04 | 2.85E-04 | gpx4;cyp3a25;cyp3a41a;cyp2c54;hpgd;gstm4;cyp2e1;cyp2d9;cyp2c38;cyp2c37;cyp1a2;cyp2c69;cyp3a41b | 2473.49 | 1703.57 | 343.937 | 1801.37161 | 2020.27981 | 1623.45474 | DOWN | 0.384615385 | 0.615384615 |
| 7Day | G alpha (q) signalling events | 1.71E-04 | 0.99996 | 2.88E-04 | kalrn;avpr1a;mapk3;kras;itpr2;f2 | 2907.75617 | 3747.02 | 156.627 | 1931.77903 | 2394.3639 | 2163.35543 | DOWN | 0.333333333 | 0.666666667 |
| 28Day | Alpha-oxidation of phytanate | 0.99999 | 2.95E-04 | 2.95E-04 | hacl1;slc25a17;phyh;aldh3a2 | 3412.465 | 3374.64 | 3193.99 | 221.321757 | 3438.51723 | 213.47785 | CONFLICT | 0.5 | 0.5 |
| 7Day | G alpha (i) signalling events | 1.37E-04 | 0.99994 | 2.96E-04 | akr1c6;rgs12;metap2;apob;ttr;rdh16f2;sdc3;rgs9;prkar2a;ppp2cb;lrp1;hebp1;gnai3;calm3;calm2;cxcr5;apoe;akr1c14 | 3329.54889 | 3638.015 | 113.316 | 1810.61245 | 3201.8182 | 1665.41903 | DOWN | 0.388888889 | 0.611111111 |
| 7Day | Keratinization | 1.93E-04 | 0.99996 | 3.22E-04 | dsg1c;krt8;krt18;dsp | 1895.05825 | 2157.095 | 240.593 | 1294.67509 | 1764.83129 | 1510.73684 | DOWN | 0.25 | 0.75 |

BMD analysis results for functional classification based on dose-responsive genes, using the Reactome database for gene sets in BMDExpress2.2 software.

| Study Day | Gene Set Name | Fisher's Exact Left P-Value | Fisher's Exact Right P-Value | Fisher's Exact Two Tail | Gene Symbols | BMD Mean | BMD Median | BMD Minimum | BMD Standard Deviation | BMD wMean | BMD wSD | Overall Direction | Percent Genes With Overall Direction Up | Percent Genes With Overall Direction Down |
|---|---|---|---|---|---|---|---|---|---|---|---|---|---|---|
| 7Day | RNA Polymerase II Transcription | 1.70E-04 | 0.9999 | 3.39E-04 | zfp266;pcgf5;rprd2;zfp248;ints13;pcgf6;rprd1b;med6;hist1h4h;zfp707;ssu72;rraga;hist1h2bc;kmt5a;fip1l1;wdr61;zc3h8;phax;suz12;cpsf2;txnrd1;hist2h2ac;polr2h;taf10;cnot1;ywhaz;uba52;tfdp1;prdx2;rorc;ell2;ptpn11;ppp2cb;kras;hist2h2aa1;csnk2b;cdkn1a;ccnk;ccng1;ccne2;ctnnb1;bmi1;lsm10;abl1;srsf1;cstf2;thoc5 | 3442.55505 | 3489.14 | 54.5232 | 1139.09255 | 3375.29713 | 1101.08632 | UP | 0.85106383 | 0.14893617 |
| 90Day | Neutrophil degranulation | 1.89E-04 | 0.9999 | 3.58E-04 | tmem173;ist1;ndufc2;pnp2;serpinb1a;iqgap2;prdx4;slc27a2;mapk14;ceacam2;mgam;tubb4b;ttr;pdxk;serpina1e;snap23;rock1;psap;pnp;plaur;mme;man2b1;lamp1;hsp90aa1;gstp2;lilr4b;gm2a;ftl1;fcgr2b;ctsh;ctsd;c3;prdx6;ahsg;mlec | 2753.85175 | 3055.31 | 82.4742 | 1474.67171 | 2821.24407 | 1305.88853 | DOWN | 0.371428571 | 0.628571429 |
| 28Day | RNA Polymerase II Transcription | 2.00E-04 | 0.9999 | 3.83E-04 | iws1;meaf6;ints14;tmem219;med4;wdr61;e2f7;cpsf2;txnrd1;nr1d2;hist1h4i;ell3;cnot1;rpap2;u2af2;tfdp1;tal1;polr2a;rorc;nrbp1;papola;notch1;mdm2;ccnk;ccng1;bnip3l;bmi1;srsf1;thoc5;zfp729b;bc005561 | 3616.72345 | 3638.56 | 860.451 | 1550.14331 | 3507.41064 | 1499.7423 | UP | 0.612903226 | 0.387096774 |
| 90Day | Hemostasis | 2.25E-04 | 0.99988 | 3.98E-04 | spp2;tubb6;gng11;hist1h3c;mapk14;ceacam2;apob;tubb4b;ywhaz;vav1;tubb2a;tuba1b;trf;tnfrsf10b;tln1;tek;sdc4;serpina1e;sos1;psap;plg;plaur;p2rx4;cd74;hdac2;gnai3;fn1;f7;ecm1;cdc42;cbx5;anxa5;ahsg;rad51c;actn1;sccpdh;dock9;kifc1 | 2387.51566 | 2155.07 | 82.4742 | 1820.18781 | 2556.03108 | 1826.9623 | DOWN | 0.394736842 | 0.605263158 |
| 7Day | Muscle contraction | 3.02E-04 | 0.99993 | 5.12E-04 | pak2;itpr2;dmpk;calm3;calm2 | 3620.406 | 3498.74 | 2538.2 | 924.565079 | 3509.03511 | 789.214299 | DOWN | 0.4 | 0.6 |
| 90Day | Glutathione conjugation | 0.99988 | 6.16E-04 | 6.16E-04 | gstk1;gstz1;gstp2;gstm4;gsta2;gsta1;gclm;gclc;gm10639;gm3776 | 1778.8786 | 1547.73 | 677.965 | 988.928952 | 1714.96755 | 984.223276 | UP | 0.8 | 0.2 |
| 90Day | Biosynthesis of DHA-derived SPMs | 0.99985 | 6.52E-04 | 6.52E-04 | cyp3a25;cyp3a41a;cyp2c54;gstm4;cyp2e1;cyp2d9;cyp2c38;cyp2c37;cyp1a2;cyp2c69;cyp3a41b | 2180.32818 | 1652.41 | 343.937 | 1636.92385 | 1867.89167 | 1633.37688 | DOWN | 0.363636364 | 0.636363636 |
| 7Day | Integrin cell surface interactions | 4.29E-04 | 1 | 6.93E-04 | | | | | | | | | | |
| 28Day | Post-translational protein phosphorylation | 0.9998 | 5.51E-04 | 7.24E-04 | spp2;ano8;apob;trf;serpina1e;serpina1b;proc;p4hb;lgals1;itih2;fn1;f5;c4b;c3;serpinc1;app;apoe;qsox1;dnajc3 | 2829.69116 | 3089.4 | 248.527 | 1710.17032 | 2629.9656 | 1660.03367 | DOWN | 0.052631579 | 0.947368421 |
| 7Day | Glutathione conjugation | 0.99986 | 7.46E-04 | 7.46E-04 | gstk1;gstp1;gstp2;gstm4;gsta1;gss;gclc;esd;gm3776 | 2296.99696 | 2305 | 49.8526 | 1013.50727 | 2334.47548 | 657.20068 | UP | 0.888888889 | 0.111111111 |
| 28Day | Signaling by Receptor Tyrosine Kinases | 3.94E-04 | 0.99985 | 8.05E-04 | atp6v0e2;ranbp9;polr2a;pdpk1;mapkapk2;hgs;hbegf;fn1;fgf1;cdc42;atp6v1e1;brk1 | 3384.483 | 3188.36 | 192.988 | 1944.65333 | 3245.43064 | 1786.19736 | CONFLICT | 0.5 | 0.5 |
| 90Day | Biosynthesis of maresins | 0.99982 | 8.47E-04 | 8.47E-04 | cyp3a25;cyp3a41a;cyp2c54;cyp2e1;cyp2d9;cyp2c38;cyp2c37;cyp1a2;cyp2c69;cyp3a41b | 2318.9941 | 1677.99 | 343.937 | 1655.96869 | 1958.81693 | 1674.89027 | DOWN | 0.3 | 0.7 |
| 90Day | Biosynthesis of maresin-like SPMs | 0.99982 | 8.47E-04 | 8.47E-04 | cyp3a25;cyp3a41a;cyp2c54;cyp2e1;cyp2d9;cyp2c38;cyp2c37;cyp1a2;cyp2c69;cyp3a41b | 2318.9941 | 1677.99 | 343.937 | 1655.96869 | 1958.81693 | 1674.89027 | DOWN | 0.3 | 0.7 |
| 28Day | Class A/1 (Rhodopsin-like receptors) | 4.53E-04 | 0.99985 | 9.00E-04 | nts;cysltr1;cx3cl1;cxcl9;f2;c3;agt;adora1 | 4062.78575 | 5060.73 | 907.506 | 2126.91495 | 4031.3968 | 1978.73091 | CONFLICT | 0.5 | 0.5 |
| 7Day | Gene expression (Transcription) | 4.45E-04 | 0.99973 | 9.33E-04 | sf3b1;zfp266;pcgf5;rprd2;zfp248;brf1;ints13;pcgf6;rprd1b;med6;hist1h4h;zfp707;ssu72;rraga;hist1h2bc;kmt5a;gtf3c6;fip1l1;wdr61;zc3h8;phax;gsk3b;ddx21;suz12;cpsf2;txnrd1;hist2h2ac;mapk3;polr2h;taf10;cnot1;ywhaz;uba52;tfdp1;prdx2;ubtf;rorc;ell2;ptpn11;ppp2cb;mybbp1a;kras;hist2h2aa1;csnk2b;cdkn1a;ccnk;ccng1;ccne2;ctnnb1;bmi1;lsm10;abl1;srsf1;cstf2;thoc5 | 3402.4114 | 3439.85 | 54.5232 | 1123.11133 | 3377.49701 | 1067.07644 | UP | 0.836363636 | 0.163636364 |

BMD analysis results for functional classification based on dose-responsive genes, using the Reactome database for gene sets in BMDExpress2.2 software.

| Study Day | Gene Set Name | Fisher's Exact Left P-Value | Fisher's Exact Right P-Value | Fisher's Exact Two Tail | Gene Symbols | BMD Mean | BMD Median | BMD Minimum | BMD Standard Deviation | BMD wMean | BMD wSD | Overall Direction | Percent Genes With Overall Direction Up | Percent Genes With Overall Direction Down |
|---|---|---|---|---|---|---|---|---|---|---|---|---|---|---|
| 7Day | DNA Repair | 5.13E-04 | 0.9998 | 9.63E-04 | ube2n;ube2v2;rnf168;hist1h4h;babam1;hist1h2bc;prpf19;polr2h;ino80c;uba52;rad51ap1;abl1 | 3633.865 | 3506.09 | 2423.08 | 669.512277 | 3532.19041 | 654.342441 | UP | 0.833333333 | 0.166666667 |
| 7Day | Transport of small molecules | 5.11E-04 | 0.99971 | 9.87E-04 | nipa2;npc2;abcg8;apoa5;angptl8;slc2a8;slc5a3;rab11a;abca3;abca8b;eif2s3x;abcg2;abcc4;apob;erlin1;uba52;slc39a2;slc22a12;slc22a1;slc20a1;slc1a2;slc12a7;sel1l;prkar2a;abcb4;pcsk5;slc8b1;ldlr;ftl1;ces3b;calm3;calm2;azgp1;atp6v1e1;apoe;apoc1;slc12a6;wwp1 | 3538.88745 | 3773.925 | 73.2912 | 1364.89803 | 3640.53279 | 1213.94278 | CONFLICT | 0.5 | 0.5 |
| 7Day | Ion channel transport | 5.47E-04 | 0.99986 | 9.95E-04 | uba52;calm3;calm2;atp6v1e1;wwp1 | 3867.372 | 3782.92 | 2825.5 | 956.630939 | 3563.6266 | 953.816092 | UP | 0.8 | 0.2 |
| 28Day | Regulation of Insulin-like Growth Factor (IGF) transport and uptake by Insulin-like Growth Factor Binding Proteins (IGFBPs) | 0.99964 | 9.39E-04 | 9.98E-04 | spp2;ano8;apob;trf;serpina1e;serpina1b;proc;p4hb;lgals1;itih2;igfals;fn1;f5;c4b;c3;serpinc1;app;apoe;qsox1;dnajc3 | 2871.6611 | 3122.7 | 248.527 | 1675.10638 | 2655.29964 | 1645.63506 | DOWN | 0.05 | 0.95 |
| 7Day | Antimicrobial peptides | 6.40E-04 | 1 | 0.0010497 |  |  |  |  |  |  |  |  |  |  |
| 7Day | Transmission across Chemical Synapses | 5.59E-04 | 0.99983 | 0.0010874 | gria3;slc22a1;slc1a2;prkar2a;gnai3;calm3;calm2 | 3232.68 | 3853.21 | 794.2 | 1484.36012 | 2849.44233 | 1488.84375 | CONFLICT | 0.428571429 | 0.571428571 |
| 7Day | Rho GTPase cycle | 6.59E-04 | 0.99987 | 0.0010984 | kalrn;dlc1;cdc42 | 4559.47 | 4595.9 | 3395.83 | 1145.85941 | 4811.71558 | 1012.23125 | UP | 0.666666667 | 0.333333333 |
| 90Day | Collagen formation | 6.35E-04 | 0.99991 | 0.0011489 | p4ha2;bmp1 | 2145.7695 | 2145.7695 | 190.369 | 2765.35391 | 1594.97401 | 2653.38103 | CONFLICT | 0.5 | 0.5 |
| 90Day | DNA Repair | 5.45E-04 | 0.99976 | 0.0011858 | hist1h4h;babam1;pole4;ppp4c;mcrs1;hist1h4i;polk;fto;yy1;ino80c;rad51;rad23a;h2afx;cdk7;brca2;rad51c | 3859.97325 | 4046.18 | 513.022 | 1448.58378 | 3617.74544 | 1504.7569 | UP | 0.625 | 0.375 |
| 90Day | Signaling by Receptor Tyrosine Kinases | 5.90E-04 | 0.9997 | 0.0012067 | hnrnpf;klb;ranbp9;hgfac;irs2;mapk14;wasf2;vav1;rasa1;tgfa;nrg1;sos1;sh3gl3;rock2;rock1;plg;pcsk5;ntrk2;hsp90aa1;gab1;fn1;fgf1;cdc42;ctnnb1;areg;ap2m1 | 2763.39574 | 3252.06 | 74.8133 | 1805.74442 | 2948.55441 | 1886.20894 | CONFLICT | 0.423076923 | 0.576923077 |
| 28Day | alpha-linolenic acid (ALA) metabolism | 0.99993 | 0.0012318 | 0.0012318 | fads1;fads2;elovl2;acsl1 | 1638.0815 | 624.2485 | 250.729 | 2289.62951 | 1272.53137 | 1821.15387 | DOWN | 0 | 1 |
| 28Day | Aflatoxin activation and detoxification | 0.99983 | 0.0012792 | 0.0012792 | cyp3a25;cyp3a11;cyp2a5;cyp2a4;cyp3a59;cyp3a41b | 3035.18083 | 3021.61 | 850.005 | 1889.46966 | 2281.79161 | 1423.31367 | UP | 0.666666667 | 0.333333333 |
| 28Day | Biosynthesis of DHA-derived SPMs | 0.99972 | 0.0014083 | 0.0014083 | cyp3a25;gstm4;cyp3a11;cyp2e1;cyp2c37;cyp2c29;cyp3a59;cyp3a41b | 2780.31038 | 2051.215 | 792.488 | 2075.65676 | 2333.1099 | 1699.7196 | CONFLICT | 0.5 | 0.5 |
| 90Day | Class I MHC mediated antigen processing & presentation | 8.32E-04 | 0.99961 | 0.0014986 | erap1;fbxo22;fbxo9;anapc10;fbxw9;arel1;fbxo32;asb2;ube2k;keap1;znrf2;kbtbd8;ube2m;cdc34;tap2;snap23;siah2;btrc;sec13 | 2775.44492 | 3141.94 | 61.8554 | 1900.69805 | 2661.07984 | 1851.57464 | CONFLICT | 0.578947368 | 0.421052632 |
| 90Day | Biotin transport and metabolism | 0.99987 | 0.0015353 | 0.0015353 | mccc2;pccb;pcx;hlcs;pcca | 1945.4304 | 2782.05 | 410.825 | 1405.20854 | 2135.89599 | 1343.93766 | DOWN | 0 | 1 |
| 90Day | RAB geranylgeranylation | 6.64E-04 | 1 | 0.0015594 |  |  |  |  |  |  |  |  |  |  |
| 7Day | RHO GTPases activate PAKs | 0.99973 | 0.0016643 | 0.0016643 | myh14;pak2;flna;myh9;cdc42;calm3;calm2 | 3764.03571 | 4226.97 | 2152.51 | 1159.16425 | 3589.38581 | 1087.60247 | CONFLICT | 0.428571429 | 0.571428571 |
| 90Day | Potassium Channels | 7.78E-04 | 0.99988 | 0.0017298 | kcns3;kcnj8 | 4052.335 | 4052.335 | 2260.22 | 2534.43334 | 3944.41493 | 2529.83376 | UP | 1 | 0 |
| 28Day | Muscle contraction | 9.86E-04 | 0.9998 | 0.0017546 | scn7a;cald1;mylk | 3957.77667 | 3855.8 | 2735.83 | 1275.99488 | 3761.01133 | 1144.21517 | UP | 1 | 0 |
| 28Day | Cell-Cell communication | 0.001123 | 1 | 0.0018011 |  |  |  |  |  |  |  |  |  |  |
| 28Day | Potassium Channels | 9.73E-04 | 1 | 0.00183 |  |  |  |  |  |  |  |  |  |  |
| 7Day | ISG15 antiviral mechanism | 0.9996 | 0.0020109 | 0.0020109 | ube2n;flnb;eif4e2;mapk3;arih1;stat1;jak1;eif4a2 | 3537.26625 | 3499.555 | 2513.13 | 705.438918 | 3463.21926 | 677.179951 | UP | 0.75 | 0.25 |
| 28Day | Translation | 0.0010478 | 0.99984 | 0.0020817 | eif3m;eif1ax | 2737.81 | 2737.81 | 1517.45 | 1725.84966 | 2423.68091 | 1667.69388 | CONFLICT | 0.5 | 0.5 |
| 28Day | alpha-linolenic (omega3) and linoleic (omega6) acid metabolism | 0.99985 | 0.0020974 | 0.0020974 | fads1;fads2;elovl2;acsl1 | 1638.0815 | 624.2485 | 250.729 | 2289.62951 | 1272.53137 | 1821.15387 | DOWN | 0 | 1 |
| 90Day | Formation of the cornified envelope | 9.32E-04 | 0.99982 | 0.0021022 | krt8;krt18;dsg2 | 3414.55333 | 3788.19 | 2496.49 | 799.638993 | 3214.23654 | 807.558939 | UP | 0.666666667 | 0.333333333 |
| 90Day | Antigen processing: Ubiquitination & Proteasome degradation | 0.0012151 | 0.99946 | 0.00213 | fbxo22;fbxo9;anapc10;fbxw9;arel1;fbxo32;asb2;ube2k;keap1;znrf2;kbtbd8;ube2m;cdc34;siah2;btrc | 2820.54156 | 3593.5 | 61.8554 | 2028.69844 | 2574.69183 | 2056.51767 | UP | 0.6 | 0.4 |
| 28Day | Cardiac conduction | 0.0011772 | 0.99989 | 0.002189 | scn7a | 3855.8 | 3855.8 | 3855.8 |  | 3855.8 |  | UP | 1 | 0 |
| 90Day | Ion transport by P-type ATPases | 0.0013661 | 1 | 0.0021949 |  |  |  |  |  |  |  |  |  |  |
| 7Day | Bile acid and bile salt metabolism | 0.99932 | 0.0022724 | 0.0022724 | akr1c6;cyp39a1;slc27a5;osbpl2;slc10a2;slc10a1;ncoa2;ncoa1;hsd17b4;baat;akr1c14;hsd3b7 | 2666.15472 | 3187.835 | 86.7986 | 1621.14041 | 2952.23825 | 1161.96383 | CONFLICT | 0.583333333 | 0.416666667 |

BMD analysis results for functional classification based on dose-responsive genes, using the Reactome database for gene sets in BMDExpress2.2 software.

| Study Day | Gene Set Name | Fisher's Exact Left P-Value | Fisher's Exact Right P-Value | Fisher's Exact Two Tail | Gene Symbols | BMD Mean | BMD Median | BMD Minimum | BMD Standard Deviation | BMD wMean | BMD wSD | Overall Direction | Percent Genes With Overall Direction Up | Percent Genes With Overall Direction Down |
|---|---|---|---|---|---|---|---|---|---|---|---|---|---|---|
| 90Day | Extracellular matrix organization | 0.0011863 | 0.99945 | 0.0023215 | tmprss6;ceacam2;vtn;ttr;tnc;sdc4;plg;p4ha2;mmp2;lum;icam1;fn1;ctsd;capn5;bmp1;bgn;itga9 | 3394.45092 | 4015.56 | 45.5307 | 1921.99598 | 3238.19909 | 2041.89909 | CONFLICT | 0.470588235 | 0.529411765 |
| 28Day | Adaptive Immune System | 0.0012343 | 0.99934 | 0.002344 | ube2n;btbd1;fbxo22;ube2v2;ube2g1;asb3;dynll1;ube2k;arih2;tubb4b;ube2m;tubb2a;traip;cdc27;tap1;ppp3cb;pdpk1;ikbkg;cd74;h2-q7;h2-d1;h2-ab1;h2-aa;ctss;cdc42;capza2;c3 | 3873.11733 | 4034.64 | 192.988 | 1566.20625 | 3957.75089 | 1415.04046 | CONFLICT | 0.555555556 | 0.444444444 |
| 90Day | Intra-Golgi and retrograde Golgi-to-ER traffic | 0.0011518 | 0.99959 | 0.0024086 | tubb6;scoc;dctn3;stx16;tubb4b;tubb2a;tuba1b;man1a;kifc1 | 2824.6 | 1951.01 | 713.489 | 1853.06003 | 2202.43718 | 1832.87711 | UP | 0.777777778 | 0.222222222 |
| 28Day | Histidine, lysine, phenylalanine, tyrosine, proline and tryptophan catabolism | 0.99936 | 0.0025802 | 0.0025802 | phykpl;asrgl1;tdo2;prodh2;aldh4a1;hpd;gstz1;aldh7a1;haao | 3115.98467 | 3472.64 | 726.97 | 1756.35475 | 3039.82171 | 1764.54756 | DOWN | 0.222222222 | 0.777777778 |
| 90Day | Antimicrobial peptides | 0.0014525 | 0.99986 | 0.0026026 | defb30 | 5550.64 | 5550.64 | 5550.64 |  | 5550.64 |  | UP | 1 | 0 |
| 28Day | Biosynthesis of maresins | 0.99944 | 0.0028635 | 0.0028635 | cyp3a25;cyp3a11;cyp2e1;cyp2c37;cyp2c29;cyp3a59;cyp3a41b | 3064.285 | 2751.06 | 850.005 | 2067.30614 | 2498.90637 | 1713.63668 | CONFLICT | 0.428571429 | 0.571428571 |
| 28Day | Biosynthesis of maresin-like SPMs | 0.99944 | 0.0028635 | 0.0028635 | cyp3a25;cyp3a11;cyp2e1;cyp2c37;cyp2c29;cyp3a59;cyp3a41b | 3064.285 | 2751.06 | 850.005 | 2067.30614 | 2498.90637 | 1713.63668 | CONFLICT | 0.428571429 | 0.571428571 |
| 28Day | Activation of C3 and C5 | 0.9999 | 0.0028994 | 0.0028994 | c4b;c3;c2 | 2076.44167 | 2572.88 | 520.995 | 1376.11119 | 1715.75301 | 1348.31746 | DOWN | 0 | 1 |
| 28Day | Synthesis of very long-chain fatty acyl-CoAs | 0.99952 | 0.0029475 | 0.0029475 | hacd3;elovl2;hacd1;hsd17b3;acsl1;elovl3 | 3076.84583 | 3507.97 | 411.194 | 2078.36776 | 2875.43094 | 2178.50476 | UP | 0.666666667 | 0.333333333 |
| 28Day | Axon guidance | 0.0015283 | 0.99949 | 0.0029929 | ranbp9;tubb4b;tubb2a;pfn1;epha7;dag1;cdc42 | 4242.08286 | 4831.18 | 2359.45 | 1599.75749 | 4046.43703 | 1604.36544 | UP | 0.857142857 | 0.142857143 |
| 28Day | Immune System | 0.0017057 | 0.99883 | 0.0030996 | ube2n;btbd1;atp6v0e2;fbxo22;arhgap45;ube2v2;c8g;ndufc2;npc2;cmtm6;ube2g1;ormdl3;psmd6;serpinb1a;asb3;golga7;dynll1;hebp2;methig1;iqgap2;ube2k;tax1bp1;map2k4;arih2;arih1;apob;clec12a;tubb4b;vtn;ube2m;tubb2a;traip;tnfrsf1b;cdc27;eea1;tap1;serpina1e;serpina1b;s100a11;rab18;ppp3cb;ppm1b;pnp;pa2g4;pkp1;pfkl;pdpk1;p4hb;sqstm1;mme;mapkapk2;man2b1;ly96;lta4h;lifr;lbp;anpep;il1rap;ikbkg;cd74;h2-q7;h2-d1;h2-ab1;h2-aa;gstp1;gstp2;gpi1;gaa;ftl1;f2;ctss;clu;cdc42;capza2;c4b;c3;c2;bcl2l1;atp6v1e1;app;birc2;atad3a;acly;qsox1;brk1;dnajc3 | 3327.97043 | 3366.84 | 160.43 | 1870.47727 | 3301.38018 | 1889.66471 | DOWN | 0.360465116 | 0.639534884 |
| 90Day | Chemokine receptors bind chemokines | 0.0022101 | 1 | 0.0033521 |  |  |  |  |  |  |  |  |  |  |
| 90Day | Ion homeostasis | 0.0019597 | 1 | 0.0033635 |  |  |  |  |  |  |  |  |  |  |
| 7Day | RHO GTPases activate IQGAPs | 0.99925 | 0.0033771 | 0.0033771 | iqgap2;tubb4b;tubb2a;tuba4a;cdc42;ctnnb1;calm3;calm2 | 2412.54115 | 1973.755 | 54.5232 | 1690.41653 | 2378.45461 | 1691.48367 | UP | 0.625 | 0.375 |
| 90Day | Signaling by TGF-beta family members | 0.0021282 | 0.99965 | 0.0034639 | ccnc;ube2m | 2361.655 | 2361.655 | 678.11 | 2380.89217 | 2437.24834 | 2378.49087 | UP | 1 | 0 |
| 28Day | Signaling by WNT | 0.0020461 | 0.99948 | 0.0038217 | pygo2;ppp3cb;pfn1;gnb5 | 3454.282 | 4016.15 | 953.648 | 1712.02807 | 2868.89238 | 1933.14079 | UP | 0.75 | 0.25 |
| 90Day | Assembly of collagen fibrils and other multimeric structures | 0.0022364 | 0.99978 | 0.0038267 | bmp1 | 190.369 | 190.369 | 190.369 |  | 190.369 |  | DOWN | 0 | 1 |
| 7Day | Association of TriC/CCT with target proteins during biosynthesis | 0.99968 | 0.0040199 | 0.0040199 | tcp1;cct7;cct4;cct2 | 3408.39 | 3368.435 | 2526.48 | 892.357141 | 3029.35461 | 739.844083 | UP | 1 | 0 |
| 28Day | Mitochondrial translation elongation | 0.0023034 | 1 | 0.0041003 |  |  |  |  |  |  |  |  |  |  |

BMD analysis results for functional classification based on dose-responsive genes, using the Reactome database for gene sets in BMDExpress2.2 software.

| Study Day | Gene Set Name | Fisher's Exact Left P-Value | Fisher's Exact Right P-Value | Fisher's Exact Two Tail | Gene Symbols | BMD Mean | BMD Median | BMD Minimum | BMD Standard Deviation | BMD wMean | BMD wSD | Overall Direction | Percent Genes With Overall Direction Up | Percent Genes With Overall Direction Down |
|---|---|---|---|---|---|---|---|---|---|---|---|---|---|---|
| 90Day | Metabolism | 0.0021658 | 0.99836 | 0.0041136 | mccc2;abhd14b;gstk1;pank1;osbpl10;dmgdh;nmnat3;aldh1b1;acad10;amdhd1;osbpl3;ndufab1;cyp4f16;slc52a3;ndufc2;dgat2;hoga1;sdha;pccb;ormdl2;etfdh;ndufaf3;pnp2;rpe;asrgl1;tnfaip8l1;ndufb9;gng11;dpys;gpx4;hacl1;serinc1;cyp3a25;sult1b1;ivd;pdss1;cyp39a1;fmo2;slc23a2;cyp3a41a;nudt5;acaa2;acsl4;txnrd1;cyp2c54;ces3a;dnph1;agmo;cyp4a12a;pdk4;omd;pon3;ahcy;adh4;slc27a5;slc27a2;aldh1a7;tnfaip8l3;ugt2b35;ppm1l;bpnt1;kcns3;apob;scap;ces2e;ces2c;blvrb;acer2;gmps;fitm2;pdk1;tkfc;pi4ka;ugdh;txn1;ttr;tst;tk1;slc25a21;pdxk;nudt15;nudt18;suox;sdc4;suclg2;sptlc2;slc25a17;slc22a1;slc10a1;st3gal3;scd1;rbp1;sardh;psap;pnp;pcx;oat;mut;mthfd2;minpp1;rdh11;man2b1;amacr;pfkfb3;lum;hyal1;hsp90aa1;hsd17b7;hsd11b1;hpgd;hpd;hdac3;gstz1;gstp2;gstm4;gsta2;gsta1;gsr;gm2a;glul;gclm;gclc;slc6a12;acsl1;ces3b;ephx2;ephx1;slc26a2;cyp4a12b;cyp2f2;cyp2e1;cyp2d9;cyp2c38;cyp2c37;cyp1a2;elovl3;cdo1;car5a;car3;bgn;atp5k;arg2;apoe;apoc3;aox1;ak2;gm4737;agxt;adk;hlcs;pcca;c | 2932.49559 | 3114.2 | 54.2263 | 1542.94627 | 2914.92808 | 1498.55712 | CONFLICT | 0.422360248 | 0.577639752 |
| 28Day | Mitochondrial translation termination | 0.0019953 | 1 | 0.0042487 | | | | | | | | | | |
| 7Day | Glyoxylate metabolism and glycine degradation | 0.99901 | 0.0042857 | 0.0042857 | lias;lipt2;prodh2;pdhx;hao1;gnmt;dld;bckdha | 3387.13525 | 3613.145 | 174.982 | 1576.32093 | 3520.08702 | 1185.48464 | DOWN | 0.375 | 0.625 |
| 28Day | Mitochondrial translation | 0.001857 | 1 | 0.0043724 | | | | | | | | | | |
| 90Day | TCF dependent signaling in response to WNT | 0.0024797 | 0.99937 | 0.0044298 | ywhaz;ctnnb1;btrc;lgr4 | 3673.517 | 4619.87 | 137.958 | 2419.23728 | 4348.60793 | 2076.6021 | CONFLICT | 0.5 | 0.5 |
| 90Day | Cell Cycle | 0.0022398 | 0.99865 | 0.0045451 | haus7;esco2;cenpu;smc4;hist1h4h;gins1;anapc10;babam1;tubb6;mastl;pole4;cables1;nek6;arpp19;psmd8;orc6;dctn3;hist1h4i;gtse1;dbf4;cntrl;e2f2;psmc4;psmf1;tubb4b;ywhaz;cep76;tubb2a;tuba1b;nup153;kntc1;nudc;mdm2;hsp90aa1;h2afx;cdkn1a;cdk7;btrc;sec13;cenpf | 3118.54895 | 3428.245 | 137.958 | 1566.85982 | 3124.02404 | 1524.03414 | UP | 0.85 | 0.15 |
| 90Day | Metabolism of carbohydrates | 0.0025551 | 0.99891 | 0.0045761 | rpe;omd;tkfc;sdc4;st3gal3;pcx;man2b1;pfkfb3;lum;hyal1;slc26a2;bgn | 2540.08853 | 2757.255 | 54.2263 | 2081.88494 | 2560.24861 | 1934.45153 | DOWN | 0.333333333 | 0.666666667 |
| 28Day | TCF dependent signaling in response to WNT | 0.0025538 | 0.99973 | 0.0046402 | pygo2 | 3936.43 | 3936.43 | 3936.43 | | 3936.43 | | DOWN | 0 | 1 |
| 90Day | Integration of energy metabolism | 0.0028652 | 0.99951 | 0.0049959 | gng11;kcns3 | 5349.345 | 5349.345 | 4854.24 | 700.184206 | 5679.2676 | 522.072862 | UP | 1 | 0 |
| 7Day | Antiviral mechanism by IFN-stimulated genes | 0.9987 | 0.0053711 | 0.0053711 | ube2n;flnb;eif4e2;mapk3;arih1;stat1;jak1;eif4a2 | 3537.26625 | 3499.555 | 2513.13 | 705.438918 | 3463.21926 | 677.179951 | UP | 0.75 | 0.25 |
| 7Day | Ribosomal scanning and start codon recognition | 0.9981 | 0.0059113 | 0.0059113 | eif3m;eif3j1;rps25;eif1ax;eif3b;rps3;eif2s3x;eif3l;eif5;rps12;eif4a2 | 3192.10478 | 3441.48 | 84.8066 | 1709.32291 | 3140.99651 | 1569.93197 | UP | 0.909090909 | 0.090909091 |
| 28Day | Signaling by Rho GTPases | 0.0033816 | 0.99837 | 0.0060711 | arhgap45;zwilch;dynll1;iqgap2;dlc1;cenpt;hist1h4i;a2m;tubb4b;tubb2a;arhgdia;pfn1;pdpk1;cdc42;mylk;brk1 | 3832.71738 | 4199.195 | 160.43 | 1861.07466 | 4147.03993 | 1520.25385 | UP | 0.6875 | 0.3125 |
| 90Day | Biological oxidations | 0.99788 | 0.0036741 | 0.0061525 | abhd14b;gstk1;aldh1b1;cyp4f16;cyp3a25;sult1b1;cyp39a1;fmo2;cyp3a41a;cyp2c54;ces3a;cyp4a12a;ahcy;adh4;aldh1a7;ugt2b35;bpnt1;ces2e;ces2c;ugdh;gstz1;gstp2;gstm4;gsta2;gsta1;gclm;gclc;ces3b;ephx1;slc26a2;cyp4a12b;cyp2f2;cyp2e1;cyp2d9;cyp2c38;cyp2c37;cyp1a2;gm4737;cbr3;cyp2c69;gm10639;gm3776;cyp3a41b | 2400.17416 | 2740.9 | 343.937 | 1365.07959 | 2332.53303 | 1350.22841 | CONFLICT | 0.581395349 | 0.418604651 |
| 90Day | Rab regulation of trafficking | 0.0035212 | 0.99907 | 0.0061619 | trappc6b;st5;dennd1b;dennd1a | 2873.6475 | 3095.14 | 1239.12 | 1313.98598 | 2663.10414 | 1396.8076 | DOWN | 0.25 | 0.75 |

BMD analysis results for functional classification based on dose-responsive genes, using the Reactome database for gene sets in BMDExpress2.2 software.

| Study Day | Gene Set Name | Fisher's Exact Left P-Value | Fisher's Exact Right P-Value | Fisher's Exact Two Tail | Gene Symbols | BMD Mean | BMD Median | BMD Minimum | BMD Standard Deviation | BMD wMean | BMD wSD | Overall Direction | Percent Genes With Overall Direction Up | Percent Genes With Overall Direction Down |
|---|---|---|---|---|---|---|---|---|---|---|---|---|---|---|
| 28Day | RA biosynthesis pathway | 0.99859 | 0.0061718 | 0.0061718 | akr1c6;akr1c12;akr1c19;adh4;aldh8a1;rdh16f2;akr1c14 | 3658.91614 | 3384.83 | 912.843 | 1735.94718 | 3406.08354 | 1417.35316 | DOWN | 0.285714286 | 0.714285714 |
| 90Day | Asparagine N-linked glycosylation | 0.0028362 | 0.99863 | 0.0063049 | trappc6b;lman1;tubb6;stx17;ngly1;rnf5;dctn3;st6galnac6;tubb4b;tubb2a;tuba1b;tgfa;serpina1e;st3gal3;man1a;areg;sec13 | 3308.12882 | 3728.57 | 779.791 | 1531.93311 | 2970.25226 | 1582.05092 | UP | 0.647058824 | 0.352941176 |
| 7Day | Recycling of bile acids and salts | 0.99882 | 0.0063795 | 0.0063795 | slc27a5;slc10a2;slc10a1;ncoa2;ncoa1;baat | 2355.2856 | 3155.67 | 86.7986 | 1775.40354 | 2943.36028 | 1379.88539 | UP | 0.666666667 | 0.333333333 |
| 90Day | Metabolism of RNA | 0.0032681 | 0.9981 | 0.0065211 | hnrnpf;cstf2t;rbm17;nop14;riok1;cd2bp2;ppil3;srsf6;u2surp;rps27l;thoc7;wtap;rcl1;adar;exosc9;usp39;smg5;ywhaz;zrsr1;paip1;nup153;utp4;snrpc;rps12;prpf8;nxf7;emg1;fbl;ddx5;cdk7;sec13;tsr1 | 3550.62872 | 3439.425 | 137.958 | 1654.74194 | 3435.96135 | 1519.75857 | UP | 0.84375 | 0.15625 |
| 90Day | Chromatin modifying enzymes | 0.0029179 | 0.99879 | 0.0066241 | smarcd2;msl1;hist1h4h;atf7ip;mcrs1;hist1h4i;hist1h3c;gatad2b;smarcb1;hdac3;hdac2 | 3140.10673 | 3951.81 | 157.333 | 2193.96801 | 2787.1216 | 2259.85147 | CONFLICT | 0.545454545 | 0.454545455 |
| 90Day | Chromatin organization | 0.0029179 | 0.99879 | 0.0066241 | smarcd2;msl1;hist1h4h;atf7ip;mcrs1;hist1h4i;hist1h3c;gatad2b;smarcb1;hdac3;hdac2 | 3140.10673 | 3951.81 | 157.333 | 2193.96801 | 2787.1216 | 2259.85147 | CONFLICT | 0.545454545 | 0.454545455 |
| 90Day | Cellular responses to external stimuli | 0.0032481 | 0.99817 | 0.006991 | hist1h4h;anapc10;tubb6;gabarapl1;dnaja2;dctn3;atg13;gm45902;txnrd1;nox4;cbx6;hist1h4i;hist1h3c;mapk14;tubb4b;txn1;tubb2a;tuba1b;nup153;mdm2;hsp90aa1;h2afx;gstp2;gsr;cdkn1a;ar;prdx6;sec13 | 2607.38339 | 2450.705 | 190.561 | 1617.05587 | 2227.99324 | 1672.21833 | UP | 0.642857143 | 0.357142857 |
| 28Day | Phase I - Functionalization of compounds | 0.99774 | 0.0051178 | 0.0071459 | bphl;cyp3a25;adh4;ces2e;ces2c;ces2b;fdxr;ces3b;cyp4a12b;cyp3a11;cyp2e1;cyp2c37;cyp2c29;cyp2a5;cyp2a4;aldh2;ces2a;cyp3a59;cyp3a41b | 2981.76063 | 2751.06 | 350.258 | 2046.75807 | 2781.49392 | 1915.8218 | CONFLICT | 0.421052632 | 0.578947368 |
| 7Day | Chylomicron clearance | 0.99964 | 0.0072088 | 0.0072088 | apob;ldlr;apoe | 2349.262 | 1999.21 | 113.316 | 2429.95644 | 3125.65168 | 2337.73998 | DOWN | 0.333333333 | 0.666666667 |
| 28Day | Xenobiotics | 0.99788 | 0.0072153 | 0.0072153 | cyp3a25;cyp3a11;cyp2e1;cyp2c37;cyp2c29;cyp2a5;cyp2a4;cyp3a59;cyp3a41b | 3093.69278 | 2751.06 | 850.005 | 1842.88683 | 2606.14147 | 1498.04441 | CONFLICT | 0.555555556 | 0.444444444 |
| 90Day | Transport of bile salts and organic acids, metal ions and amine compounds | 0.0034891 | 0.99939 | 0.0073768 | slc22a1;slc6a12 | 2247.86 | 2247.86 | 1050.57 | 1693.22376 | 3017.91745 | 1296.54531 | DOWN | 0 | 1 |
| 28Day | Chromatin modifying enzymes | 0.0043301 | 0.99867 | 0.0074139 | msl1;meaf6;hist1h4i;kat7;hcfc1 | 4539.96 | 5043.8 | 2859.88 | 1234.05187 | 4409.47817 | 1273.01653 | DOWN | 0.4 | 0.6 |
| 28Day | Chromatin organization | 0.0043301 | 0.99867 | 0.0074139 | msl1;meaf6;hist1h4i;kat7;hcfc1 | 4539.96 | 5043.8 | 2859.88 | 1234.05187 | 4409.47817 | 1273.01653 | DOWN | 0.4 | 0.6 |
| 28Day | MAPK1/MAPK3 signaling | 0.0039223 | 0.9988 | 0.0074381 | ranbp9;map3k11;hbegf;fn1;fgf1 | 3061.3016 | 3156 | 919.738 | 1930.82326 | 2739.58196 | 1684.15141 | DOWN | 0.4 | 0.6 |
| 7Day | Synthesis of bile acids and bile salts | 0.99786 | 0.0074777 | 0.0074777 | akr1c6;cyp39a1;osbpl2;ncoa2;ncoa1;hsd17b4;baat;akr1c14;hsd3b7 | 2767.57018 | 3262.32 | 86.7986 | 1601.414 | 3020.5072 | 1045.00713 | UP | 0.666666667 | 0.333333333 |
| 28Day | Plasma lipoprotein assembly | 0.99872 | 0.007777 | 0.007777 | apob;a2m;p4hb;bmp1;apoe | 3319.623 | 3212.68 | 939.205 | 2365.92573 | 3060.50873 | 2554.9319 | DOWN | 0.4 | 0.6 |
| 90Day | Cytokine Signaling in Immune system | 0.0038609 | 0.99787 | 0.007985 | irak3;tbk1;irs2;hist1h3c;mapk14;eda2r;usp18;abce1;ywhaz;vav1;ube2m;stx3;sos1;nfkbia;lifr;il9r;il1rap;il15ra;ikbkg;il18bp;ifngr2;ifnar1;csf1;crlf1;btrc | 2954.53897 | 3265.56 | 74.8133 | 1829.65475 | 2691.21189 | 2022.46377 | DOWN | 0.36 | 0.64 |
| 28Day | Metabolism of proteins | 0.0039509 | 0.99721 | 0.0080175 | obsl1;eif3m;c1galt1;ube2n;btbd1;spp2;asxl2;fbxo22;ube2v2;tomm20;nanp;ube2g1;lman2;psmd6;wdr61;eif1ax;asb3;ngly1;psmd8;dynll1;rab9;pigp;rab11a;ube2k;ppp6r3;uchl3;gne;ano8;hist1h4i;abca3;pign;apob;psmf1;tubb4b;sbspon;rab29;ino80c;usp12;ube2m;tubb2a;trf;mgat2;sec22c;serpina1e;serpina1b;exoc4;rad21;rab18;proc;polb;p4hb;mme;mdm2;man1a;ly6d;psmb8;lgals1;itih2;ikbkg;igfals;hgs;hcfc1;gnb5;gfpt1;fn1;f7;f5;f2;dag1;cct4;capza2;c4b;c3;brca1;bmi1;blm;bet1;serpinc1;asgr1;app;apoe;birc2;agt;tpr;gbf1;qsox1;dnajc3 | 3626.36022 | 3669.42 | 185.394 | 1741.86203 | 3614.166 | 1793.76577 | CONFLICT | 0.482758621 | 0.517241379 |

BMD analysis results for functional classification based on dose-responsive genes, using the Reactome database for gene sets in BMDExpress2.2 software.

| Study Day | Gene Set Name | Fisher's Exact Left P-Value | Fisher's Exact Right P-Value | Fisher's Exact Two Tail | Gene Symbols | BMD Mean | BMD Median | BMD Minimum | BMD Standard Deviation | BMD wMean | BMD wSD | Overall Direction | Percent Genes With Overall Direction Up | Percent Genes With Overall Direction Down |
|---|---|---|---|---|---|---|---|---|---|---|---|---|---|---|
| 90Day | Hedgehog 'on' state | 0.0040315 | 1 | 0.0080428 | | | | | | | | | | |
| 7Day | Protein localization | 0.99711 | 0.0074555 | 0.0081628 | gstk1;pitrm1;pex14;ldhd;decr2;pex6;uba52;pex7;phyh;hsd17b4;hao1;ephx2;baat;pecr | 2498.93566 | 3180.375 | 49.8526 | 1711.27218 | 2785.82251 | 1473.67705 | DOWN | 0.357142857 | 0.642857143 |
| 90Day | Toll-like Receptor Cascades | 0.0047 | 0.99832 | 0.0082625 | tbk1;irf7;mapk14;apob;nfkbia;ikbkg;btrc | 3315.05286 | 3601.1 | 175.96 | 2038.92263 | 3429.19726 | 2034.27276 | DOWN | 0.285714286 | 0.714285714 |
| 90Day | Synthesis of (16-20)-hydroxyeicosatetraenoic acids (HETE) | 0.9981 | 0.0083924 | 0.0083924 | cyp2c54;cyp4a12a;cyp4a12b;cyp2c38;cyp2c37;cyp1a2;cyp2c69 | 2799.36286 | 3033.17 | 928.37 | 1542.29973 | 3147.62503 | 1313.47036 | CONFLICT | 0.428571429 | 0.571428571 |
| 7Day | The role of GTSE1 in G2/M progression after G2 checkpoint | 0.99799 | 0.0085659 | 0.0085659 | gtse1;tubb4b;uba52;tubb2a;tuba4a;hsp90aa1;cdkn1a | 2535.598 | 2094.04 | 919.856 | 1523.88877 | 2300.31657 | 1444.24257 | UP | 1 | 0 |
| 28Day | Beta-oxidation of pristanoyl-CoA | 0.99935 | 0.0091429 | 0.0091429 | acox3;crot;hsd17b4 | 2619.01667 | 3528.55 | 702.63 | 1660.35273 | 2925.08461 | 1487.54404 | DOWN | 0.333333333 | 0.666666667 |
| 90Day | Cell Cycle, Mitotic | 0.0052181 | 0.99679 | 0.0094389 | haus7;esco2;cenpu;smc4;hist1h4h;gins1;anapc10;tubb6;mastl;pole4;cables1;nek6;arpp19;psmd8;orc6;dctn3;hist1h4i;gtse1;dbf4;cntrl;e2f2;psmc4;psmf1;tubb4b;cep76;tubb2a;tuba1b;nup153;kntc1;nudc;hsp90aa1;h2afx;cdkn1a;cdk7;btrc;sec13;cenpf | 3115.37568 | 3413.71 | 186.178 | 1486.03554 | 3109.35872 | 1497.91195 | UP | 0.837837838 | 0.162162162 |
| 90Day | Signaling by Rho GTPases | 0.0048127 | 0.99715 | 0.0096762 | arhgef6;cenpu;fmnl2;rhou;hist1h4h;tubb6;iqgap2;hist1h4i;hist1h3c;mapk14;wasf2;pin1;tubb4b;ywhaz;fgd4;vav1;tubb2a;tuba1b;tiam1;kntc1;sos1;rtkn;rock2;rock1;nudc;myo9b;h2afx;cdc42;ctnnb1;ar;sec13;cenpf | 3399.93459 | 3912.96 | 137.958 | 1760.34923 | 3285.51236 | 1887.004 | CONFLICT | 0.59375 | 0.40625 |
| 28Day | Fatty acyl-CoA biosynthesis | 0.99744 | 0.010089 | 0.010089 | hacd3;elovl2;hacd1;hsd17b3;acsl1;elovl3;acly | 3230.915 | 4155.33 | 411.194 | 1940.57679 | 2990.77125 | 2086.85335 | CONFLICT | 0.571428571 | 0.428571429 |
| 28Day | RAF/MAP kinase cascade | 0.0052703 | 0.99835 | 0.0101 | ranbp9;map3k11;hbegf;fn1;fgf1 | 3061.3016 | 3156 | 919.738 | 1930.82326 | 2739.58196 | 1684.15141 | DOWN | 0.4 | 0.6 |
| 28Day | Synthesis of bile acids and bile salts via 7alpha-hydroxycholesterol | 0.99769 | 0.010474 | 0.010474 | akr1c6;akr1c12;akr1c19;amacr;hsd17b4;akr1c14 | 3924.225 | 4373.23 | 702.63 | 2036.02025 | 3237.11114 | 1777.52258 | DOWN | 0.333333333 | 0.666666667 |
| 90Day | RNA Polymerase II Pre-transcription Events | 0.005158 | 0.99906 | 0.010493 | eloa;cdk7 | 4445.455 | 4445.455 | 3130.16 | 1860.10803 | 4242.37403 | 1837.80252 | UP | 1 | 0 |
| 90Day | MAPK family signaling cascades | 0.0050676 | 0.99762 | 0.010791 | klb;ranbp9;irs2;tln1;rasa1;tgfa;tek;nrg1;sos1;gfra1;fn1;fgf1;cdc42;areg | 2357.87524 | 2148.075 | 74.8133 | 1925.27039 | 2446.17276 | 2054.34489 | CONFLICT | 0.428571429 | 0.571428571 |
| 7Day | Cap-dependent Translation Initiation | 0.99716 | 0.0079707 | 0.010827 | eif3m;eif3j1;rps25;eif1ax;eif3b;rps3;eif2s3x;eif3l;eif5;rps12;eif4ebp1;eif4a2 | 3185.84438 | 3420.48 | 84.8066 | 1629.91973 | 3140.44345 | 1545.3292 | UP | 0.833333333 | 0.166666667 |
| 28Day | Metabolism of amino acids and derivatives | 0.99648 | 0.0069866 | 0.010909 | phykpl;ndufab1;asrgl1;tdo2;serinc1;prodh2;txnrd1;ahcy;sds;aldh4a1;sardh;otc;odc1;oat;hpd;gstz1;got2;glul;ddc;ass1;gm4737;aldh7a1;haao;aldh6a1 | 2751.13308 | 2763.68 | 726.832 | 1404.8189 | 2691.14141 | 1183.04341 | DOWN | 0.125 | 0.875 |
| 28Day | Neuronal System | 0.0064015 | 0.99707 | 0.01134 | gria3;lin7c;slc22a1;slc1a2;ptprd;mdm2;il1rap;gnb5;glul;slc6a13;epb41l3;adcy9 | 2791.34417 | 2159.59 | 151.142 | 1749.21816 | 2627.92103 | 1560.6028 | DOWN | 0.25 | 0.75 |
| 7Day | Eukaryotic Translation Initiation | 0.99668 | 0.0091338 | 0.011719 | eif3m;eif3j1;rps25;eif1ax;eif3b;rps3;eif2s3x;eif3l;eif5;rps12;eif4ebp1;eif4a2 | 3185.84438 | 3420.48 | 84.8066 | 1629.91973 | 3140.44345 | 1545.3292 | UP | 0.833333333 | 0.166666667 |
| 90Day | E3 ubiquitin ligases ubiquitinate target proteins | 0.0073511 | 1 | 0.011932 | | | | | | | | | | |
| 90Day | Chylomicron clearance | 0.99927 | 0.011973 | 0.011973 | apob;lipc;apoe | 1672.98333 | 1749.82 | 175.96 | 1460.12207 | 2324.5335 | 1324.11035 | DOWN | 0 | 1 |
| 90Day | Propionyl-CoA catabolism | 0.99927 | 0.011973 | 0.011973 | pccb;mut;pcca | 1622.02567 | 1339.27 | 412.607 | 1372.81254 | 1859.85519 | 1369.88864 | DOWN | 0 | 1 |
| 90Day | Transport of inorganic cations/anions and amino acids/oligopeptides | 0.0054226 | 0.9985 | 0.012233 | slc17a8;slc1a2;slc6a12;slc26a2 | 2689.32225 | 3008.81 | 777.189 | 1397.86912 | 3063.38493 | 929.405967 | DOWN | 0.25 | 0.75 |
| 90Day | Collagen chain trimerization | 0.0057811 | 1 | 0.012545 | | | | | | | | | | |
| 7Day | Developmental Biology | 0.0062483 | 0.99629 | 0.012789 | ranbp9;gsk3b;kalrn;sdcbp;mapk3;tubb4b;yes1;pak2;vasp;uba52;tubb2a;tuba4a;rasa1;dsg1c;sema4d;sema4a;reln;ptpn11;pfn2;pfn1;krt8;krt18;kras;hsp90aa1;gfra1;csnk2b;cdc42;ctnnb1;abl1;dsp | 3184.11607 | 3381.94 | 54.5232 | 1578.02548 | 3131.41453 | 1822.62673 | CONFLICT | 0.566666667 | 0.433333333 |
| 7Day | Neurotransmitter receptors and postsynaptic signal transmission | 0.0056358 | 0.99824 | 0.013063 | gria3;prkar2a;gnai3;calm3;calm2 | 3336.17 | 3853.21 | 794.2 | 1568.57851 | 2915.53749 | 1584.96901 | UP | 0.6 | 0.4 |

BMD analysis results for functional classification based on dose-responsive genes, using the Reactome database for gene sets in BMDExpress2.2 software.

| Study Day | Gene Set Name | Fisher's Exact Left P-Value | Fisher's Exact Right P-Value | Fisher's Exact Two Tail | Gene Symbols | BMD Mean | BMD Median | BMD Minimum | BMD Standard Deviation | BMD wMean | BMD wSD | Overall Direction | Percent Genes With Overall Direction Up | Percent Genes With Overall Direction Down |
|---|---|---|---|---|---|---|---|---|---|---|---|---|---|---|
| 7Day | Synthesis of bile acids and bile salts via 7alpha-hydroxycholesterol | 0.99662 | 0.013068 | 0.013068 | akr1c6;ncoa2;ncoa1;hsd17b4;baat;akr1c14;hsd3b7 | 2647.49451 | 3301.55 | 86.7986 | 1828.06574 | 2920.91192 | 1357.03567 | UP | 0.714285714 | 0.285714286 |
| 7Day | Cardiac conduction | 0.0056277 | 0.99843 | 0.013118 | itpr2;dmpk;calm3;calm2 | 3890.9575 | 3798.475 | 3050.32 | 807.324813 | 3574.7767 | 786.454883 | DOWN | 0.25 | 0.75 |
| 28Day | Transcriptional regulation by RUNX1 | 0.0068842 | 0.9983 | 0.013262 | hist1h4i;tal1;bmi1 | 3730.3 | 3918.46 | 1424.03 | 2218.18343 | 3823.03545 | 2379.05883 | DOWN | 0.333333333 | 0.666666667 |
| 7Day | Alpha-oxidation of phytanate | 0.99899 | 0.013412 | 0.013412 | slc25a17;phyh;pecr | 2478.42 | 2689.11 | 1604.15 | 790.277396 | 2367.9245 | 757.002727 | DOWN | 0.333333333 | 0.666666667 |
| 7Day | Choline catabolism | 0.99899 | 0.013412 | 0.013412 | dmgdh;sardh;aldh7a1 | 1098.06733 | 408.564 | 233.368 | 1348.82647 | 1115.83937 | 1385.41342 | DOWN | 0 | 1 |
| 7Day | Regulation of PTEN localization | 0.99899 | 0.013412 | 0.013412 | uba52;pten;xiap | 4270.09 | 4761.56 | 3174.68 | 950.318197 | 4222.95249 | 979.246287 | UP | 0.666666667 | 0.333333333 |
| 28Day | Proline catabolism | 0.99968 | 0.013472 | 0.013472 | prodh2;aldh4a1 | 2205.51 | 2205.51 | 1092.57 | 1573.93484 | 1975.64572 | 1539.99861 | DOWN | 0 | 1 |
| 28Day | Beta oxidation of lauroyl-CoA to decanoyl-CoA-CoA | 0.99968 | 0.013472 | 0.013472 | echs1;acadl | 2016.1655 | 2016.1655 | 802.301 | 1716.66364 | 1538.10672 | 1577.92701 | DOWN | 0 | 1 |
| 28Day | Biosynthesis of E-series 18(S)-resolvins | 0.99968 | 0.013472 | 0.013472 | gpx4;lta4h | 4857.005 | 4857.005 | 3909.63 | 1339.79057 | 4832.85644 | 1339.35525 | DOWN | 0 | 1 |
| 28Day | Keratinization | 0.0067684 | 0.99805 | 0.013805 | pkp4;pkp1;krt8;krt18 | 2676.64925 | 2807.215 | 856.847 | 1425.57491 | 2794.74322 | 1223.74793 | UP | 1 | 0 |
| 7Day | SLC-mediated transmembrane transport | 0.0063227 | 0.99712 | 0.013918 | slc2a8;slc5a3;slc39a2;slc22a12;slc22a1;slc20a1;slc1a2;slc12a7;slc8b1;calm3;calm2;slc12a6 | 3720.52333 | 3445.645 | 1710.87 | 1322.53874 | 3757.00214 | 1300.02822 | CONFLICT | 0.416666667 | 0.583333333 |
| 7Day | Activation of the mRNA upon binding of the cap-binding complex and eIFs, and subsequent binding to 43S | 0.99679 | 0.0093065 | 0.014498 | eif3m;eif3j1;rps25;eif1ax;eif3b;rps3;eif2s3x;eif3l;rps12;eif4ebp1;eif4a2 | 3166.42296 | 3441.48 | 84.8066 | 1708.01734 | 3102.15628 | 1658.7131 | UP | 0.818181818 | 0.181818182 |
| 90Day | Metabolism of lipids | 0.0080643 | 0.99453 | 0.014787 | osbpl10;acad10;osbpl3;ndufab1;cyp4f16;dgat2;pccb;ormdl2;tnfaip8l1;gpx4;hacl1;cyp3a25;cyp39a1;cyp3a41a;acaa2;acsl4;cyp2c54;agmo;cyp4a12a;pon3;slc27a5;slc27a2;tnfaip8l3;ppm1l;scap;acer2;fitm2;pi4ka;sptlc2;slc25a17;slc10a1;scd1;psap;mut;amacr;hsd17b7;hsd11b1;hpgd;hdac3;gstm4;gm2a;acsl1;ephx2;cyp4a12b;cyp2e1;cyp2d9;cyp2c38;cyp2c37;cyp1a2;elovl3;pcca;plekha1;osbpl9;cyp2c69;cyp3a41b | 3102.0314 | 3327.72 | 105.476 | 1472.79105 | 3064.34323 | 1368.45951 | DOWN | 0.381818182 | 0.618181818 |
| 28Day | Cell junction organization | 0.0062884 | 1 | 0.014873 |  |  |  |  |  |  |  |  |  |  |
| 90Day | Purine catabolism | 0.99665 | 0.015029 | 0.015029 | pnp2;nudt5;dnph1;nudt15;nudt18;pnp | 3648.29167 | 3600.91 | 2714.47 | 612.548675 | 3618.05393 | 423.693132 | CONFLICT | 0.5 | 0.5 |
| 28Day | Formation of Fibrin Clot (Clotting Cascade) | 0.99567 | 0.015564 | 0.015564 | f12;a2m;proc;f7;f5;f2;serpinc1 | 2447.52357 | 2170.26 | 362.714 | 2004.60325 | 2068.01102 | 2112.87601 | DOWN | 0.142857143 | 0.857142857 |
| 90Day | Golgi-to-ER retrograde transport | 0.008227 | 0.99711 | 0.015588 | tubb6;dctn3;tubb4b;tubb2a;tuba1b;kifc1 | 1779.45667 | 1751.94 | 713.489 | 1092.46087 | 1506.31085 | 1127.69973 | UP | 0.833333333 | 0.166666667 |
| 90Day | Epigenetic regulation of gene expression | 0.0082858 | 0.99761 | 0.016478 | hist1h4h;hist1h4i;hist1h3c;h2afx | 3214.00725 | 3979.26 | 811.859 | 1602.37406 | 2298.31583 | 1843.92338 | CONFLICT | 0.5 | 0.5 |
| 7Day | Regulation of Complement cascade | 0.99436 | 0.016933 | 0.016933 | c8g;c1rb;c1s1;cfhr1;f2;cfh;c4b;c2;c1qb | 2570.38667 | 1971.95 | 56.713 | 2036.81442 | 2209.89729 | 2181.8838 | DOWN | 0 | 1 |
| 28Day | Retinoid metabolism and transport | 0.99449 | 0.017403 | 0.017403 | akr1c6;akr1c12;akr1c19;apob;lrp1;gpc4;apoe;akr1c14 | 3304.12688 | 3286.855 | 939.205 | 1587.30096 | 2770.81203 | 1466.02632 | DOWN | 0.25 | 0.75 |
| 28Day | Intrinsic Pathway of Fibrin Clot Formation | 0.99624 | 0.017932 | 0.017932 | f12;a2m;proc;f2;serpinc1 | 2868.5328 | 2357.81 | 362.714 | 2225.23577 | 2689.94892 | 2345.22346 | DOWN | 0.2 | 0.8 |
| 7Day | Peroxisomal protein import | 0.9932 | 0.017045 | 0.018615 | gstk1;pex14;decr2;pex6;uba52;pex7;phyh;hsd17b4;hao1;ephx2;baat;pecr | 2289.21328 | 2985.61 | 49.8526 | 1767.76367 | 2628.16399 | 1537.73308 | CONFLICT | 0.416666667 | 0.583333333 |
| 90Day | mTOR signalling | 0.0093469 | 1 | 0.018812 |  |  |  |  |  |  |  |  |  |  |
| 90Day | Class B/2 (Secretin family receptors) | 0.0080143 | 0.99905 | 0.019003 | gng11 | 4854.24 | 4854.24 | 4854.24 |  | 4854.24 |  | UP | 1 | 0 |
| 7Day | Peptide hormone metabolism | 0.011259 | 0.99858 | 0.019019 | mme | 2165.57 | 2165.57 | 2165.57 |  | 2165.57 |  | DOWN | 0 | 1 |
| 7Day | Collagen biosynthesis and modifying enzymes | 0.011259 | 0.99858 | 0.019019 | p3h3 | 3788.93 | 3788.93 | 3788.93 |  | 3788.93 |  | DOWN | 0 | 1 |
| 90Day | Organelle biogenesis and maintenance | 0.0096732 | 0.99535 | 0.01929 | haus7;cep89;tubb6;dctn3;cntrl;ift52;tubb4b;cep76;tubb2a;tuba1b;exoc4;hsp90aa1;atp5k | 2333.235 | 1951.01 | 135.802 | 1719.06723 | 2342.66599 | 1539.02207 | UP | 0.769230769 | 0.230769231 |
| 7Day | Collagen degradation | 0.0094696 | 0.99884 | 0.019465 | ctsb | 3881.76 | 3881.76 | 3881.76 |  | 3881.76 |  | UP | 1 | 0 |

BMD analysis results for functional classification based on dose-responsive genes, using the Reactome database for gene sets in BMDExpress2.2 software.

| Study Day | Gene Set Name | Fisher's Exact Left P-Value | Fisher's Exact Right P-Value | Fisher's Exact Two Tail | Gene Symbols | BMD Mean | BMD Median | BMD Minimum | BMD Standard Deviation | BMD wMean | BMD wSD | Overall Direction | Percent Genes With Overall Direction Up | Percent Genes With Overall Direction Down |
|---|---|---|---|---|---|---|---|---|---|---|---|---|---|---|
| 28Day | Metabolism of lipids | 0.9921 | 0.011728 | 0.01968 | echs1;akr1c6;acox3;fads1;crot;ndufab1;fitm1;pmvk;dgat2;pnpla8;pi4k2b;ormdl2;ormdl3;tnfaip8l1;gpx4;akr1c12;hacd3;hacl1;fads2;cyp3a25;elovl2;acaa2;akr1c19;agmo;hacd1;acsf2;decr2;hsd17b13;phospho1;pla2g4c;pi4ka;etnk2;slc25a17;slc10a1;ptdss1;mapkapk2;amacr;lta4h;phyh;hsd17b4;hsd17b3;hsd11b1;gstm4;gc;fdxr;acsl1;cyp4a12b;cyp3a11;cyp2e1;cyp2c37;cyp2c29;elovl3;aldh3a2;acox1;acadl;abhd4;akr1c14;acly;cyp3a59;cyp3a41b | 3157.27265 | 3343.195 | 67.9262 | 1675.85824 | 2996.35377 | 1613.26151 | DOWN | 0.35 | 0.65 |
| 7Day | Class C/3 (Metabotropic glutamate/pheromone receptors) | 0.01042 | 1 | 0.01969 | | | | | | | | | | |
| 90Day | Transport of connexons to the plasma membrane | 0.99589 | 0.020553 | 0.020553 | tubb6;tubb4b;tubb2a;tuba1b;gjb2 | 1916.9702 | 1781.5 | 779.791 | 922.579865 | 1733.98302 | 1064.65299 | UP | 0.6 | 0.4 |
| 90Day | Biosynthesis of the N-glycan precursor (dolichol lipid-linked oligosaccharide, LLO) and transfer to a nascent protein | 0.012219 | 0.99751 | 0.021009 | st6galnac6;st3gal3 | 4683.725 | 4683.725 | 4143.19 | 764.431928 | 4469.98451 | 702.129746 | DOWN | 0 | 1 |
| 90Day | The role of GTSE1 in G2/M progression after G2 checkpoint | 0.99384 | 0.021721 | 0.021721 | tubb6;gtse1;tubb4b;tubb2a;tuba1b;hsp90aa1;cdkn1a | 1386.23586 | 1722.38 | 426.32 | 664.868459 | 1289.25247 | 639.31966 | UP | 0.857142857 | 0.142857143 |
| 28Day | Metabolism of fat-soluble vitamins | 0.99278 | 0.021803 | 0.021803 | akr1c6;akr1c12;akr1c19;apob;lrp1;gpc4;apoe;akr1c14 | 3304.12688 | 3286.855 | 939.205 | 1587.30096 | 2770.81203 | 1466.02632 | DOWN | 0.25 | 0.75 |
| 90Day | Immunoregulatory interactions between a Lymphoid and a non-Lymphoid cell | 0.012425 | 0.99581 | 0.02183 | sh2d1b1;icam1;fcgr2b;cd1d1;c3 | 2316.7788 | 2931.68 | 639.57 | 1458.85717 | 1731.86105 | 1388.39031 | DOWN | 0.4 | 0.6 |
| 90Day | Alpha-oxidation of phytanate | 0.99801 | 0.021952 | 0.021952 | hacl1;slc27a2;slc25a17 | 3683.26 | 3419.78 | 2910.82 | 932.527616 | 3761.45897 | 916.721686 | DOWN | 0.333333333 | 0.666666667 |
| 7Day | Initial triggering of complement | 0.99526 | 0.02224 | 0.02224 | c1rb;c1s1;c4b;c2;c1qb | 2024.1086 | 1939.15 | 56.713 | 1811.39163 | 1363.19794 | 1399.09444 | DOWN | 0 | 1 |
| 90Day | Neddylation | 0.010736 | 0.99445 | 0.022272 | fbxo22;fbxo9;fbxw9;fbxo32;asb2;psmd8;keap1;kbtbd8;dcaf10;psmc4;wdtc1;psmf1;ube2m;fem1b;btrc;dcun1d2 | 2496.52815 | 2234.2 | 61.8554 | 1776.88051 | 2535.86014 | 1738.28033 | UP | 0.625 | 0.375 |
| 90Day | M Phase | 0.012715 | 0.99265 | 0.022967 | haus7;cenpu;smc4;hist1h4h;anapc10;tubb6;mastl;nek6;arpp19;dctn3;hist1h4i;cntrl;tubb4b;cep76;tubb2a;tuba1b;nup153;kntc1;nudc;hsp90aa1;h2afx;sec13;cenpf | 3187.91661 | 3442.78 | 426.32 | 1395.97387 | 3224.94305 | 1447.49908 | UP | 0.869565217 | 0.130434783 |
| 7Day | Signaling by Receptor Tyrosine Kinases | 0.011577 | 0.99319 | 0.023051 | ranbp10;ranbp9;hgfac;nckap1;mapk3;polr2h;yes1;pak2;uba52;rasa1;stat1;ptpn11;ppp2cb;prkcz;pcsk5;kras;hsp90aa1;fgf1;cdc42;ctnnb1;calm3;calm2;atp6v1e1;wwp1;brk1 | 3378.37149 | 3629.67 | 54.5232 | 1564.98066 | 3325.71149 | 1661.08608 | UP | 0.64 | 0.36 |
| 7Day | Collagen formation | 0.013014 | 0.99657 | 0.023576 | p3h3;dst;ctsb | 3551.01 | 3788.93 | 2982.34 | 494.665067 | 3542.51101 | 520.283197 | UP | 0.666666667 | 0.333333333 |
| 7Day | O-linked glycosylation | 0.011254 | 0.99709 | 0.02407 | c1galt1;large1;adamts7 | 3186.34333 | 3416.43 | 2525.28 | 581.242416 | 3214.36703 | 621.324607 | DOWN | 0.333333333 | 0.666666667 |
| 28Day | Cytokine Signaling in Immune system | 0.011395 | 0.99427 | 0.024423 | ube2n;map2k4;arih1;ube2m;tnfrsf1b;ppm1b;p4hb;sqstm1;mapkapk2;lifr;il1rap;ikbkg;app;birc2 | 4008.77721 | 4948.59 | 727.581 | 1908.57018 | 3795.96088 | 2055.80587 | CONFLICT | 0.428571429 | 0.571428571 |
| 90Day | MAPK1/MAPK3 signaling | 0.011593 | 0.99435 | 0.024694 | klb;ranbp9;irs2;tln1;rasa1;tgfa;tek;nrg1;sos1;gfra1;fn1;fgf1;areg | 2527.21279 | 2162.51 | 74.8133 | 1892.25992 | 2550.28585 | 2041.691 | DOWN | 0.384615385 | 0.615384615 |
| 90Day | Deubiquitination | 0.012722 | 0.99322 | 0.024698 | babam1;tomm20;psmd8;mcrs1;keap1;tomm70a;usp18;psmc4;psmf1;yy1;ino80c;siah2;rad23a;nfkbia;mdm2;ikbkg;ar | 2829.23253 | 3031.27 | 143.029 | 1847.34956 | 2769.53306 | 1729.64448 | UP | 0.705882353 | 0.294117647 |
| 90Day | Synthesis of epoxy (EET) and dihydroxyeicosatrienoic acids (DHET) | 0.99367 | 0.024729 | 0.024729 | cyp2c54;ephx2;cyp2c38;cyp2c37;cyp1a2;cyp2c69 | 2656.36667 | 2368.37 | 928.37 | 1639.96321 | 2875.04451 | 1661.73435 | DOWN | 0.166666667 | 0.833333333 |
| 7Day | Proline catabolism | 0.99917 | 0.02494 | 0.02494 | prodh2;aldh4a1 | 1154.5437 | 1154.5437 | 84.5274 | 1513.23156 | 1587.65602 | 1383.72584 | DOWN | 0 | 1 |
| 7Day | VLDL assembly | 0.99917 | 0.02494 | 0.02494 | apob;apoc1 | 2882.07 | 2882.07 | 1999.21 | 1248.55259 | 3387.19612 | 1024.00135 | DOWN | 0 | 1 |
| 28Day | G2/M Transition | 0.014424 | 0.99612 | 0.025215 | dynll1;tubb4b;tubb2a | 3684.67667 | 2903.04 | 2359.45 | 1844.72961 | 3931.15502 | 1868.40338 | UP | 1 | 0 |
| 28Day | Mitotic G2-G2/M phases | 0.012997 | 0.99655 | 0.0254 | dynll1;tubb4b;tubb2a | 3684.67667 | 2903.04 | 2359.45 | 1844.72961 | 3931.15502 | 1868.40338 | UP | 1 | 0 |
| 28Day | Cell Cycle, Mitotic | 0.013065 | 0.99256 | 0.025703 | zwilch;psmd6;nek6;arpp19;pole3;psmd8;dynll1;set;cnep1r1;cenpt;hist1h4i;cdc6;cdc14a;psmf1;tubb4b;tubb2a;tfdp1;cdc27;rad21;psmb8;tpr | 3817.7681 | 3638.67 | 748.272 | 1660.67406 | 3936.11963 | 1582.40173 | UP | 0.80952381 | 0.19047619 |

BMD analysis results for functional classification based on dose-responsive genes, using the Reactome database for gene sets in BMDExpress2.2 software.

| Study Day | Gene Set Name | Fisher's Exact Left P-Value | Fisher's Exact Right P-Value | Fisher's Exact Two Tail | Gene Symbols | BMD Mean | BMD Median | BMD Minimum | BMD Standard Deviation | BMD wMean | BMD wSD | Overall Direction | Percent Genes With Overall Direction Up | Percent Genes With Overall Direction Down |
|---|---|---|---|---|---|---|---|---|---|---|---|---|---|---|
| 28Day | Neurotransmitter uptake and metabolism In glial cells | 0.99878 | 0.025721 | 0.025721 | slc1a2;glul | 1856.72 | 1856.72 | 1774.78 | 115.880659 | 1827.3371 | 108.174014 | DOWN | 0 | 1 |
| 28Day | Astrocytic Glutamate-Glutamine Uptake And Metabolism | 0.99878 | 0.025721 | 0.025721 | slc1a2;glul | 1856.72 | 1856.72 | 1774.78 | 115.880659 | 1827.3371 | 108.174014 | DOWN | 0 | 1 |
| 28Day | Lysosomal oligosaccharide catabolism | 0.99878 | 0.025721 | 0.025721 | man2b2;man2b1 | 1624.9215 | 1624.9215 | 240.253 | 1958.21697 | 1298.07952 | 1902.88264 | DOWN | 0 | 1 |
| 28Day | Scavenging by Class B Receptors | 0.99878 | 0.025721 | 0.025721 | apob;scarb1 | 2108.7525 | 2108.7525 | 939.205 | 1653.98994 | 2000.86534 | 1646.93759 | DOWN | 0 | 1 |
| 28Day | Advanced glycosylation endproduct receptor signaling | 0.99878 | 0.025721 | 0.025721 | capza2;app | 5033.45 | 5033.45 | 4630.47 | 569.899781 | 5168.55413 | 536.916667 | DOWN | 0 | 1 |
| 28Day | Resolution of AP sites via the single-nucleotide replacement pathway | 0.99878 | 0.025721 | 0.025721 | polb;lig3 | 5622.33 | 5622.33 | 5391.42 | 326.556054 | 5616.5595 | 326.454068 | CONFLICT | 0.5 | 0.5 |
| 28Day | Regulation of Complement cascade | 0.99198 | 0.02576 | 0.02576 | c8g;vtn;f2;clu;c4b;c3;c2 | 1813.981 | 2305.72 | 447.762 | 1052.00591 | 1683.33373 | 944.640074 | DOWN | 0 | 1 |
| 90Day | Degradation of the extracellular matrix | 0.015163 | 0.99395 | 0.025961 | tmprss6;plg;mmp2;fn1;ctsd;capn5;bmp1 | 3225.71843 | 3885.66 | 190.369 | 2242.46386 | 2534.03961 | 2382.64934 | DOWN | 0.285714286 | 0.714285714 |
| 90Day | Formation of TC-NER Pre-Incision Complex | 0.016612 | 0.99779 | 0.026276 | cdk7 | 3130.16 | 3130.16 | 3130.16 |  | 3130.16 |  | UP | 1 | 0 |
| 7Day | Translation initiation complex formation | 0.99196 | 0.021558 | 0.027293 | eif3m;eif3j1;rps25;eif1ax;eif3b;rps3;eif2s3x;eif3l;rps12;eif4a2 | 3171.36726 | 3842.8 | 84.8066 | 1800.32538 | 3101.75382 | 1689.54617 | UP | 0.9 | 0.1 |
| 7Day | Pink/Parkin Mediated Mitophagy | 0.99362 | 0.027905 | 0.027905 | tomm20;mfn1;mterf3;tomm7;uba52 | 4096.692 | 4048.88 | 2384.74 | 1205.41607 | 3628.23874 | 1042.88808 | UP | 0.6 | 0.4 |
| 7Day | G1/S DNA Damage Checkpoints | 0.99362 | 0.027905 | 0.027905 | cop1;uba52;cdkn1a;cdc25a;ccne2 | 4336.77 | 4598.19 | 2818.63 | 1165.22018 | 4198.65867 | 1079.35895 | UP | 1 | 0 |
| 90Day | Fanconi Anemia Pathway | 0.017035 | 1 | 0.027972 |  |  |  |  |  |  |  |  |  |  |
| 90Day | RNA Polymerase III Transcription | 0.015109 | 1 | 0.028398 |  |  |  |  |  |  |  |  |  |  |
| 90Day | RNA Polymerase III Transcription Initiation | 0.015109 | 1 | 0.028398 |  |  |  |  |  |  |  |  |  |  |
| 90Day | Translation | 0.013037 | 0.99435 | 0.029248 | eif3m;mrpl58;rps27l;mrps18b;mrpl54;mrps30;mrps31;mrpl22;rps12 | 3118.28833 | 3479.94 | 958.825 | 1389.80948 | 2899.04688 | 1530.79325 | UP | 0.777777778 | 0.222222222 |
| 7Day | Elastic fibre formation | 0.018923 | 1 | 0.029507 |  |  |  |  |  |  |  |  |  |  |
| 7Day | MET promotes cell motility | 0.018923 | 1 | 0.029507 |  |  |  |  |  |  |  |  |  |  |
| 7Day | L13a-mediated translational silencing of Ceruloplasmin expression | 0.99069 | 0.024407 | 0.029599 | eif3m;eif3j1;rps25;eif1ax;eif3b;rps3;eif2s3x;eif3l;rps12;eif4a2 | 3171.36726 | 3842.8 | 84.8066 | 1800.32538 | 3101.75382 | 1689.54617 | UP | 0.9 | 0.1 |
| 28Day | Resolution of D-loop Structures through Synthesis-Dependent Strand Annealing (SDSA) | 0.99281 | 0.029601 | 0.029601 | rmi1;rad51d;rad51;brca1;blm | 3513.5312 | 3769.36 | 692.086 | 1790.07678 | 3877.73216 | 1143.86555 | UP | 1 | 0 |
| 90Day | Macroautophagy | 0.016192 | 0.99657 | 0.030007 | gabarapl1;atg13 | 2761.14 | 2761.14 | 841.06 | 2715.40318 | 2873.17968 | 2710.77639 | CONFLICT | 0.5 | 0.5 |
| 90Day | Collagen biosynthesis and modifying enzymes | 0.016192 | 0.99657 | 0.030007 | p4ha2;bmp1 | 2145.7695 | 2145.7695 | 190.369 | 2765.35391 | 1594.97401 | 2653.38103 | CONFLICT | 0.5 | 0.5 |
| 7Day | Transport of vitamins, nucleosides, and related molecules | 0.015511 | 1 | 0.03008 |  |  |  |  |  |  |  |  |  |  |
| 7Day | Cilium Assembly | 0.014981 | 0.99339 | 0.030189 | atat1;hspb11;cep89;rab11a;tubb4b;tubb2a;tuba4a;nedd1;hsp90aa1 | 2775.07956 | 3074.7 | 919.856 | 1351.62912 | 2688.13639 | 1362.55383 | UP | 0.888888889 | 0.111111111 |
| 90Day | RAF/MAP kinase cascade | 0.016523 | 0.99171 | 0.030915 | klb;ranbp9;irs2;tln1;rasa1;tgfa;tek;nrg1;sos1;gfra1;fn1;fgf1;areg | 2527.21279 | 2162.51 | 74.8133 | 1892.25992 | 2550.28585 | 2041.691 | DOWN | 0.384615385 | 0.615384615 |
| 7Day | Amine ligand-binding receptors | 0.014043 | 1 | 0.030975 |  |  |  |  |  |  |  |  |  |  |
| 7Day | Voltage gated Potassium channels | 0.014043 | 1 | 0.030975 |  |  |  |  |  |  |  |  |  |  |
| 7Day | Collagen chain trimerization | 0.014043 | 1 | 0.030975 |  |  |  |  |  |  |  |  |  |  |
| 90Day | Beta-catenin independent WNT signaling | 0.018823 | 0.99484 | 0.031028 | gng11;ctnnb1;ap2m1 | 3974.94333 | 4087.04 | 2983.55 | 940.369351 | 4048.13013 | 972.884127 | UP | 0.666666667 | 0.333333333 |
| 7Day | Biosynthesis of DHA-derived SPMs | 0.9901 | 0.031269 | 0.031269 | cyp3a25;gstm4;cyp3a11;cyp2e1;cyp2c37;cyp2c29;cyp3a41b | 3229.52186 | 2813.51 | 529.743 | 1691.38457 | 3004.89739 | 1441.18311 | CONFLICT | 0.428571429 | 0.571428571 |
| 90Day | Clathrin-mediated endocytosis | 0.017292 | 0.99264 | 0.031366 | pacsin2;apob;trf;tgfa;fnbp1l;sh3gl3;areg;ap2m1 | 3270.33713 | 3476.97 | 175.96 | 2233.63372 | 3101.83853 | 2159.25523 | UP | 0.625 | 0.375 |
| 28Day | Ion transport by P-type ATPases | 0.019778 | 1 | 0.031599 |  |  |  |  |  |  |  |  |  |  |
| 28Day | Signaling by PDGF | 0.018412 | 1 | 0.031667 |  |  |  |  |  |  |  |  |  |  |
| 28Day | Signaling by Interleukins | 0.016557 | 0.99258 | 0.031743 | ube2n;map2k4;p4hb;sqstm1;mapkapk2;lifr;il1rap;ikbkg;app | 4350.48344 | 5266.71 | 727.581 | 1708.00819 | 4616.0705 | 1618.62408 | DOWN | 0.333333333 | 0.666666667 |
| 90Day | Neurotransmitter receptors and postsynaptic signal transmission | 0.015105 | 0.99365 | 0.031749 | gng11;gria3;camkk2;mdm2;gnai3;gabrb3;epb41l1;ap2m1 | 3313.27228 | 3683.79 | 98.0082 | 1910.30946 | 2834.02861 | 1761.68773 | UP | 0.75 | 0.25 |
| 90Day | Cell-Cell communication | 0.013627 | 0.99583 | 0.031822 | arhgef6;afdn;ctnnb1;actn1 | 4037.9335 | 4700.81 | 797.214 | 2295.03793 | 4190.02407 | 2312.13407 | DOWN | 0.25 | 0.75 |
| 90Day | CYP2E1 reactions | 0.99 | 0.032075 | 0.032075 | cyp2c54;cyp2f2;cyp2e1;cyp2d9;cyp2c38;cyp2c37;cyp2c69 | 3014.61429 | 3033.17 | 1493.96 | 1482.51701 | 3137.40638 | 1452.81272 | CONFLICT | 0.428571429 | 0.571428571 |
| 90Day | RHO GTPases activate IQGAPs | 0.99 | 0.032075 | 0.032075 | tubb6;iqgap2;tubb4b;tubb2a;tuba1b;cdc42;ctnnb1 | 1826.00971 | 1781.5 | 156.487 | 1241.69399 | 1394.27274 | 939.491167 | CONFLICT | 0.571428571 | 0.428571429 |

BMD analysis results for functional classification based on dose-responsive genes, using the Reactome database for gene sets in BMDExpress2.2 software.

| Study Day | Gene Set Name | Fisher's Exact Left P-Value | Fisher's Exact Right P-Value | Fisher's Exact Two Tail | Gene Symbols | BMD Mean | BMD Median | BMD Minimum | BMD Standard Deviation | BMD wMean | BMD wSD | Overall Direction | Percent Genes With Overall Direction Up | Percent Genes With Overall Direction Down |
|---|---|---|---|---|---|---|---|---|---|---|---|---|---|---|
| 7Day | Formation of the ternary complex, and subsequently, the 43S complex | 0.9933 | 0.019565 | 0.032278 | eif3m;eif3j1;rps25;eif1ax;eif3b;rps3;eif2s3x;eif3l;rps12 | 3141.35473 | 4244.12 | 84.8066 | 1906.87819 | 3022.06387 | 1878.99333 | UP | 0.888888889 | 0.111111111 |
| 7Day | Formation of the cornified envelope | 0.016975 | 0.99463 | 0.032346 | dsg1c;krt8;krt18;dsp | 1895.05825 | 2157.095 | 240.593 | 1294.67509 | 1764.83129 | 1510.73684 | DOWN | 0.25 | 0.75 |
| 7Day | Cytokine Signaling in Immune system | 0.015231 | 0.99116 | 0.033182 | ube2n;flnb;eif4e2;mapk3;map2k3;arih1;ywhaz;yes1;uba52;hsp90b1;stat1;ptpn11;prlr;ppp2cb;jak1;il1rap;ifng;ghr;eif4a2;csf1r;csf1;btrc | 3311.8225 | 3628.355 | 131.024 | 1176.84533 | 3240.75029 | 1258.651 | UP | 0.772727273 | 0.227272727 |
| 28Day | G alpha (i) signalling events | 0.01787 | 0.99016 | 0.033324 | akr1c6;akr1c12;akr1c19;apob;rdh16f2;cx3cl1;cxcl9;lrp1;gpc4;gnb5;c3;app;apoe;agt;adora1;adcy9;akr1c14 | 3526.57288 | 3361.03 | 907.506 | 1788.0793 | 3033.72803 | 1754.35763 | DOWN | 0.294117647 | 0.705882353 |
| 90Day | Cellular Senescence | 0.018706 | 0.9913 | 0.033465 | hist1h4h;anapc10;cbx6;hist1h4i;hist1h3c;mapk14;txn1;mdm2;h2afx;cdkn1a | 3184.5738 | 3979.26 | 744.949 | 1679.62346 | 2343.34957 | 1756.05903 | UP | 0.6 | 0.4 |
| 90Day | Phase I - Functionalization of compounds | 0.98821 | 0.021181 | 0.033481 | aldh1b1;cyp4f16;cyp3a25;cyp39a1;fmo2;cyp3a41a;cyp2c54;ces3a;cyp4a12a;adh4;aldh1a7;ces2e;ces2c;ces3b;ephx1;cyp4a12b;cyp2f2;cyp2e1;cyp2d9;cyp2c38;cyp2c37;cyp1a2;cbr3;cyp2c69;cyp3a41b | 2739.95376 | 3047.49 | 343.937 | 1449.41888 | 2790.68439 | 1406.00101 | CONFLICT | 0.56 | 0.44 |
| 90Day | Cilium Assembly | 0.018346 | 0.99095 | 0.034529 | haus7;cep89;tubb6;dctn3;cntrl;ift52;tubb4b;cep76;tubb2a;tuba1b;exoc4;hsp90aa1 | 2516.35442 | 2032.085 | 154.682 | 1657.79703 | 2395.61575 | 1520.47541 | UP | 0.833333333 | 0.166666667 |
| 90Day | Transmission across Chemical Synapses | 0.017635 | 0.9909 | 0.034877 | gng11;gria3;lin7c;unc13b;camkk2;slc22a1;slc1a2;mdm2;gnai3;glul;slc6a12;gabrb3;epb41l1;ap2m1 | 2977.32694 | 3490.115 | 98.0082 | 1763.18318 | 2750.88314 | 1506.44157 | CONFLICT | 0.571428571 | 0.428571429 |
| 28Day | Chylomicron assembly | 0.99508 | 0.035072 | 0.035072 | apob;p4hb;apoe | 3294.26833 | 3212.68 | 939.205 | 2396.89917 | 2832.04742 | 2711.32472 | DOWN | 0 | 1 |
| 28Day | Gamma-carboxylation of protein precursors | 0.99508 | 0.035072 | 0.035072 | proc;f7;f2 | 2700.24 | 2170.26 | 1340.75 | 1688.07416 | 1850.85737 | 1335.69078 | DOWN | 0 | 1 |
| 28Day | Transport of gamma-carboxylated protein precursors from the endoplasmic reticulum to the Golgi apparatus | 0.99508 | 0.035072 | 0.035072 | proc;f7;f2 | 2700.24 | 2170.26 | 1340.75 | 1688.07416 | 1850.85737 | 1335.69078 | DOWN | 0 | 1 |
| 90Day | MASTL Facilitates Mitotic Progression | 0.99857 | 0.035205 | 0.035205 | mastl;arpp19 | 2369.5705 | 2369.5705 | 577.791 | 2533.95887 | 3023.16335 | 2359.36015 | UP | 1 | 0 |
| 90Day | STAT6-mediated induction of chemokines | 0.99857 | 0.035205 | 0.035205 | tmem173;tbk1 | 2558.24 | 2558.24 | 1058.39 | 2121.10821 | 2553.28861 | 2121.09665 | DOWN | 0 | 1 |
| 90Day | Vitamins B6 activation to pyridoxal phosphate | 0.99857 | 0.035205 | 0.035205 | pdxk;aox1 | 3825.07 | 3825.07 | 3196.71 | 888.635234 | 3853.28022 | 887.739233 | CONFLICT | 0.5 | 0.5 |
| 28Day | Estrogen-dependent gene expression | 0.01453 | 0.99691 | 0.035289 | hist1h4i;polr2a | 5444.54 | 5444.54 | 5040.67 | 571.158431 | 5494.50555 | 566.770537 | CONFLICT | 0.5 | 0.5 |
| 7Day | Metabolism of RNA | 0.98477 | 0.022287 | 0.035762 | sf3b1;rps25;sf3a3;fcf1;utp14a;gm49336;dcp2;snrpa1;dnajc8;zcrb1;fip1l1;riok3;crnkl1;wdr61;pno1;ppih;sf3b6;utp3;hbs1l;adar;ddx21;nop58;bysl;hnrnpa2b1;cpsf2;prpf19;rps3;polr2h;pcbp1;cnot1;hnrnpul1;prpf38a;ywhaz;uba52;zrsr2;utp18;snrpc;rps12;utp14b;ncl;hnrnpc;fbl;eif4a2;dhx9;lsm10;pwp2;srsf1;tpr;cstf2;thoc5;snrpd2;utp15;xpo1;sf3b3 | 3495.79884 | 3404.94 | 84.8066 | 1271.25282 | 3331.61405 | 1190.08518 | UP | 0.962962963 | 0.037037037 |
| 7Day | Microtubule-dependent trafficking of connexons from Golgi to the plasma membrane | 0.99287 | 0.036389 | 0.036389 | tubb4b;tubb2a;tuba4a;gja1 | 2276.434 | 1954.85 | 919.856 | 1424.18025 | 1763.60227 | 985.706882 | UP | 0.75 | 0.25 |
| 7Day | Protein methylation | 0.99287 | 0.036389 | 0.036389 | prmt3;etfbkmt;calm3;calm2 | 3358.08 | 3253.69 | 2008.38 | 1204.86006 | 3326.34795 | 937.160808 | UP | 0.75 | 0.25 |
| 28Day | Pink/Parkin Mediated Mitophagy | 0.99222 | 0.037302 | 0.037302 | tomm20;mterf3;sqstm1;atg5 | 4818.665 | 4936.54 | 3654.44 | 1058.71114 | 5368.53606 | 825.784265 | UP | 1 | 0 |
| 90Day | Platelet activation, signaling and aggregation | 0.017245 | 0.99031 | 0.037349 | spp2;gng11;mapk14;ywhaz;vav1;trf;tln1;serpina1e;sos1;psap;plg;gnai3;fn1;ecm1;cdc42;anxa5;ahsg;actn1;sccpdh | 2864.74343 | 3112.61 | 82.4742 | 2024.71146 | 3226.11939 | 2006.99711 | DOWN | 0.263157895 | 0.736842105 |
| 28Day | G alpha (q) signalling events | 0.021376 | 0.99105 | 0.037825 | nts;cysltr1;hbegf;gnb5;f2;app;agt | 3372.78514 | 4610.42 | 919.738 | 2192.42274 | 3223.5604 | 2239.60151 | CONFLICT | 0.571428571 | 0.428571429 |
| 28Day | Plasma lipoprotein assembly, remodeling, and clearance | 0.98989 | 0.027121 | 0.038276 | lmf1;npc2;apob;a2m;scarb1;p4hb;ces3b;bmp1;apoe | 2909.28044 | 3007.97 | 614.079 | 1893.95297 | 2560.18225 | 2078.39985 | DOWN | 0.222222222 | 0.777777778 |
| 90Day | Inositol phosphate metabolism | 0.022604 | 0.99683 | 0.038377 | minpp1 | 3256.99 | 3256.99 | 3256.99 |  | 3256.99 |  | UP | 1 | 0 |
| 90Day | Aquaporin-mediated transport | 0.022604 | 0.99683 | 0.038377 | gng11 | 4854.24 | 4854.24 | 4854.24 |  | 4854.24 |  | UP | 1 | 0 |

BMD analysis results for functional classification based on dose-responsive genes, using the Reactome database for gene sets in BMDExpress2.2 software.

| Study Day | Gene Set Name | Fisher's Exact Left P-Value | Fisher's Exact Right P-Value | Fisher's Exact Two Tail | Gene Symbols | BMD Mean | BMD Median | BMD Minimum | BMD Standard Deviation | BMD wMean | BMD wSD | Overall Direction | Percent Genes With Overall Direction Up | Percent Genes With Overall Direction Down |
|---|---|---|---|---|---|---|---|---|---|---|---|---|---|---|
| 90Day | Phase II - Conjugation of compounds | 0.9849 | 0.029403 | 0.038413 | abhd14b;gstk1;sult1b1;ahcy;ugt2b35;bpnt1;ugdh;gstz1;gstp2;gstm4;gsta2;gsta1;gclm;gclc;slc26a2;gm4737;gm10639;gm3776 | 1928.25806 | 1651.995 | 444.891 | 1110.11588 | 1817.12238 | 1102.15486 | UP | 0.611111111 | 0.388888889 |
| 28Day | CYP2E1 reactions | 0.98953 | 0.039535 | 0.039535 | cyp2e1;cyp2c37;cyp2c29;cyp2a5;cyp2a4 | 3205.078 | 2751.06 | 1326.21 | 1639.97523 | 3044.33339 | 1332.90059 | UP | 0.6 | 0.4 |
| 90Day | O-linked glycosylation | 0.022915 | 0.99171 | 0.039618 | galnt12;st3gal3;large1;adamts6;spon2 | 4039.772 | 3858.6 | 2622.31 | 1467.17891 | 3285.15745 | 1267.22913 | DOWN | 0.4 | 0.6 |
| 7Day | Organelle biogenesis and maintenance | 0.01998 | 0.9903 | 0.040352 | atat1;hspb11;cep89;rab11a;idh2;tubb4b;tubb2a;tuba4a;nedd1;hsp90aa1;atp5j | 2968.22145 | 3074.7 | 919.856 | 1379.36573 | 2958.11122 | 1455.38031 | UP | 0.818181818 | 0.181818182 |
| 7Day | Class B/2 (Secretin family receptors) | 0.022325 | 0.99684 | 0.040401 | adgre1 | 2946.44 | 2946.44 | 2946.44 |  | 2946.44 |  | DOWN | 0 | 1 |
| 28Day | Peptide ligand-binding receptors | 0.023615 | 0.9906 | 0.04093 | nts;cx3cl1;cxcl9;f2;c3;agt | 4497.39333 | 5577.235 | 1340.75 | 2013.82097 | 4077.79891 | 2113.96356 | DOWN | 0.333333333 | 0.666666667 |
| 28Day | Chylomicron clearance | 0.9971 | 0.040936 | 0.040936 | apob;apoe | 2075.9425 | 2075.9425 | 939.205 | 1607.58959 | 1295.41266 | 1168.71324 | DOWN | 0 | 1 |
| 28Day | Synthesis of PIPs at the ER membrane | 0.9971 | 0.040936 | 0.040936 | pi4k2b;pi4ka | 4418.385 | 4418.385 | 4173.55 | 346.248978 | 4399.97266 | 345.268484 | CONFLICT | 0.5 | 0.5 |
| 28Day | Biosynthesis of EPA-derived SPMs | 0.9971 | 0.040936 | 0.040936 | gpx4;lta4h | 4857.005 | 4857.005 | 3909.63 | 1339.79057 | 4832.85644 | 1339.35525 | DOWN | 0 | 1 |
| 90Day | Rho GTPase cycle | 0.021123 | 0.99082 | 0.040965 | arhgef6;rhou;fgd4;vav1;tiam1;sos1;myo9b;cdc42 | 4424.12838 | 4948.215 | 156.487 | 1937.7847 | 4628.92188 | 1600.97466 | DOWN | 0.375 | 0.625 |
| 90Day | Xenobiotics | 0.99034 | 0.024355 | 0.040967 | cyp3a25;cyp3a41a;cyp2c54;cyp2f2;cyp2e1;cyp2d9;cyp2c38;cyp2c37;cyp1a2;cyp2c69;cyp3a41b | 2462.65645 | 1703.57 | 343.937 | 1641.65669 | 2118.08842 | 1691.54269 | DOWN | 0.363636364 | 0.636363636 |
| 28Day | Mitotic Prometaphase | 0.02168 | 0.99146 | 0.040976 | zwilch;dynll1;cenpt;tubb4b;tubb2a;rad21 | 3719.56667 | 3563.05 | 2359.45 | 1186.01958 | 3809.00797 | 1244.66079 | UP | 1 | 0 |
| 7Day | Regulation of insulin secretion | 0.018837 | 0.99741 | 0.041757 | itpr2 | 4098.21 | 4098.21 | 4098.21 |  | 4098.21 |  | DOWN | 0 | 1 |
| 90Day | Cellular responses to stress | 0.02194 | 0.98647 | 0.042092 | hist1h4h;anapc10;tubb6;dnaja2;dctn3;gm45902;txnrd1;nox4;cbx6;hist1h4i;hist1h3c;mapk14;tubb4b;txn1;tubb2a;tuba1b;nup153;mdm2;hsp90aa1;h2afx;gstp2;gsr;cdkn1a;ar;prdx6;sec13 | 2595.55596 | 2450.705 | 190.561 | 1589.68108 | 2181.3073 | 1642.29523 | UP | 0.653846154 | 0.346153846 |
| 90Day | Protein ubiquitination | 0.023445 | 0.99475 | 0.042432 | ube2k;cdc34 | 2429.116 | 2429.116 | 569.072 | 2630.49945 | 1344.2356 | 2136.72563 | UP | 1 | 0 |
| 7Day | MAPK6/MAPK4 signaling | 0.98693 | 0.042839 | 0.042839 | kalrn;sept7;pak2;uba52;cdc42;xpo1 | 3485.07167 | 3161.305 | 2538.2 | 970.390702 | 3606.55949 | 978.996491 | UP | 0.833333333 | 0.166666667 |
| 90Day | Inactivation, recovery and regulation of the phototransduction cascade | 0.027528 | 1 | 0.042907 |  |  |  |  |  |  |  |  |  |  |
| 90Day | ROS, RNS production in phagocytes | 0.027528 | 1 | 0.042907 |  |  |  |  |  |  |  |  |  |  |
| 90Day | Negative regulation of MAPK pathway | 0.027528 | 1 | 0.042907 |  |  |  |  |  |  |  |  |  |  |
| 90Day | Transcription-Coupled Nucleotide Excision Repair (TC-NER) | 0.024293 | 0.99311 | 0.042967 | pole4;polk;cdk7 | 4212.22333 | 3652.71 | 3130.16 | 1445.45671 | 3760.17242 | 830.658559 | UP | 0.666666667 | 0.333333333 |
| 28Day | Synthesis of bile acids and bile salts | 0.98645 | 0.043067 | 0.043067 | akr1c6;akr1c12;akr1c19;amacr;hsd17b4;akr1c14 | 3924.225 | 4373.23 | 702.63 | 2036.02025 | 3237.11114 | 1777.52258 | DOWN | 0.333333333 | 0.666666667 |
| 90Day | The phototransduction cascade | 0.024416 | 1 | 0.043154 |  |  |  |  |  |  |  |  |  |  |
| 28Day | HDACs deacetylate histones | 0.021566 | 0.99693 | 0.043507 | hist1h4i | 5848.41 | 5848.41 | 5848.41 |  | 5848.41 |  | DOWN | 0 | 1 |
| 28Day | Synthesis of Prostaglandins (PG) and Thromboxanes (TX) | 0.9902 | 0.044178 | 0.044178 | akr1c6;akr1c12;akr1c19;akr1c14 | 4259.3975 | 4373.23 | 2669.87 | 1456.14239 | 3630.29862 | 1225.99018 | CONFLICT | 0.5 | 0.5 |
| 90Day | Lysosome Vesicle Biogenesis | 0.021656 | 1 | 0.044245 |  |  |  |  |  |  |  |  |  |  |
| 90Day | RAF activation | 0.021656 | 1 | 0.044245 |  |  |  |  |  |  |  |  |  |  |
| 28Day | Removal of aminoterminal propeptides from gamma-carboxylated proteins | 0.99302 | 0.044436 | 0.044436 | proc;f7;f2 | 2700.24 | 2170.26 | 1340.75 | 1688.07416 | 1850.85737 | 1335.69078 | DOWN | 0 | 1 |
| 28Day | Phenylalanine and tyrosine catabolism | 0.99302 | 0.044436 | 0.044436 | asrgl1;hpd;gstz1 | 3495.52 | 4526.39 | 726.97 | 2423.54016 | 2552.46734 | 2448.54772 | DOWN | 0.333333333 | 0.666666667 |
| 7Day | Protein ubiquitination | 0.98815 | 0.028649 | 0.04453 | ube2n;ube2v2;rraga;hist1h2bc;wdr61;pex14;ube2k;ube2a;ube2e3;uba52;cdc34 | 3107.84909 | 3225.73 | 1018.89 | 955.142118 | 3165.74946 | 728.022569 | UP | 1 | 0 |
| 7Day | Activation of Matrix Metalloproteinases | 0.028161 | 1 | 0.044944 |  |  |  |  |  |  |  |  |  |  |
| 7Day | Complement cascade | 0.98554 | 0.037255 | 0.044985 | c8g;c1rb;c1s1;cfhr1;f2;cfh;c4b;c2;c1qb | 2570.38667 | 1971.95 | 56.713 | 2036.81442 | 2209.89729 | 2181.8838 | DOWN | 0 | 1 |
| 7Day | Scavenging by Class A Receptors | 0.9933 | 0.045455 | 0.045455 | apob;hsp90b1;apoe | 1321.822 | 1852.94 | 113.316 | 1049.14908 | 1545.13646 | 906.344871 | DOWN | 0.333333333 | 0.666666667 |
| 7Day | alpha-linolenic (omega3) and linoleic (omega6) acid metabolism | 0.9933 | 0.045455 | 0.045455 | fads1;elovl5;fads2 | 108.1313 | 56.7644 | 55.2305 | 90.301734 | 95.258529 | 83.000013 | DOWN | 0 | 1 |
| 7Day | Classical antibody-mediated complement activation | 0.9933 | 0.045455 | 0.045455 | c1rb;c1s1;c1qb | 2315.66433 | 1939.15 | 56.713 | 2468.83611 | 1154.21203 | 1850.07688 | DOWN | 0 | 1 |

BMD analysis results for functional classification based on dose-responsive genes, using the Reactome database for gene sets in BMDExpress2.2 software.

| Study Day | Gene Set Name | Fisher's Exact Left P-Value | Fisher's Exact Right P-Value | Fisher's Exact Two Tail | Gene Symbols | BMD Mean | BMD Median | BMD Minimum | BMD Standard Deviation | BMD wMean | BMD wSD | Overall Direction | Percent Genes With Overall Direction Up | Percent Genes With Overall Direction Down |
|---|---|---|---|---|---|---|---|---|---|---|---|---|---|---|
| 7Day | Biotin transport and metabolism | 0.9933 | 0.045455 | 0.045455 | mccc2;pccb;btd | 1104.77653 | 199.112 | 77.8976 | 1674.72876 | 1310.70042 | 1721.84718 | DOWN | 0 | 1 |
| 7Day | Prolactin receptor signaling | 0.9933 | 0.045455 | 0.045455 | prlr;ghr;btrc | 4091.75333 | 4207.06 | 3805.67 | 249.302999 | 4180.66283 | 184.775987 | UP | 1 | 0 |
| 28Day | MAPK family signaling cascades | 0.02001 | 0.99125 | 0.045906 | ranbp9;map3k11;sept7;cdc14a;hbegf;fn1;fgf1;cdc42 | 3036.8275 | 2809.745 | 748.272 | 1999.5176 | 3062.10703 | 1936.95559 | UP | 0.625 | 0.375 |
| 7Day | Transport of connexons to the plasma membrane | 0.99012 | 0.046029 | 0.046029 | tubb4b;tubb2a;tuba4a;gja1 | 2276.434 | 1954.85 | 919.856 | 1424.18025 | 1763.60227 | 985.706882 | UP | 0.75 | 0.25 |
| 7Day | Molecules associated with elastic fibres | 0.023085 | 1 | 0.046043 | | | | | | | | | | |
| 7Day | Fatty acids | 0.023085 | 1 | 0.046043 | | | | | | | | | | |
| 90Day | TBC/RABGAPs | 0.019207 | 1 | 0.046173 | | | | | | | | | | |
| 7Day | Lysosomal oligosaccharide catabolism | 0.9969 | 0.046779 | 0.046779 | man2c1;man2b1 | 1950.9045 | 1950.9045 | 420.579 | 2164.20708 | 1897.9567 | 2162.91131 | DOWN | 0 | 1 |
| 7Day | Conjugation of benzoate with glycine | 0.9969 | 0.046779 | 0.046779 | acsm1;glyat | 5641.24 | 5641.24 | 5478.46 | 230.205684 | 5548.95276 | 189.633298 | UP | 1 | 0 |
| 7Day | Long-term potentiation | 0.9969 | 0.046779 | 0.046779 | calm3;calm2 | 3983.44 | 3983.44 | 3050.32 | 1319.63096 | 3556.9103 | 1173.69957 | CONFLICT | 0.5 | 0.5 |
| 28Day | Epigenetic regulation of gene expression | 0.026675 | 0.99378 | 0.047002 | hist1h4i;polr1a | 5855.735 | 5855.735 | 5848.41 | 10.3591143 | 5854.78856 | 10.27228 | DOWN | 0 | 1 |
| 28Day | RNA Polymerase I Transcription | 0.026675 | 0.99378 | 0.047002 | hist1h4i;polr1a | 5855.735 | 5855.735 | 5848.41 | 10.3591143 | 5854.78856 | 10.27228 | DOWN | 0 | 1 |
| 28Day | RHO GTPase Effectors | 0.02313 | 0.98824 | 0.047786 | zwilch;dynll1;iqgap2;cenpt;hist1h4i;tubb4b;tubb2a;pfn1;pdpk1;cdc42;mylk;brk1 | 3790.08567 | 3563.05 | 192.988 | 1713.23873 | 4051.71855 | 1407.6109 | UP | 0.666666667 | 0.333333333 |
| 28Day | Semaphorin interactions | 0.024512 | 1 | 0.048786 | | | | | | | | | | |
| 28Day | Ion homeostasis | 0.024512 | 1 | 0.048786 | | | | | | | | | | |
| 90Day | Mitotic Spindle Checkpoint | 0.026683 | 0.98938 | 0.048991 | cenpu;anapc10;kntc1;nudc;sec13;cenpf | 3803.32333 | 3370.595 | 2758.9 | 1092.35219 | 4013.06255 | 1256.89861 | UP | 1 | 0 |
| 7Day | Biosynthesis of maresins | 0.98414 | 0.049876 | 0.049876 | cyp3a25;cyp3a11;cyp2e1;cyp2c37;cyp2c29;cyp3a41b | 3329.52217 | 3098.075 | 529.743 | 1830.01027 | 3082.0157 | 1591.6575 | DOWN | 0.333333333 | 0.666666667 |
| 7Day | Biosynthesis of maresin-like SPMs | 0.98414 | 0.049876 | 0.049876 | cyp3a25;cyp3a11;cyp2e1;cyp2c37;cyp2c29;cyp3a41b | 3329.52217 | 3098.075 | 529.743 | 1830.01027 | 3082.0157 | 1591.6575 | DOWN | 0.333333333 | 0.666666667 |
| 7Day | Signaling by Interleukins | 0.02756 | 0.98488 | 0.050003 | ube2n;mapk3;map2k3;ywhaz;yes1;uba52;hsp90b1;stat1;ptpn11;ppp2cb;jak1;il1rap;csf1r;csf1;btrc | 3196.85567 | 3627.04 | 131.024 | 1352.57627 | 3093.02479 | 1434.87479 | UP | 0.733333333 | 0.266666667 |
| 7Day | Sulfur amino acid metabolism | 0.98625 | 0.050013 | 0.050013 | bhmt2;txn2;ahcy;cdo1;gm4737 | 3841.228 | 3770.5 | 2019.09 | 1397.48618 | 4067.90229 | 1087.77839 | DOWN | 0.4 | 0.6 |
| 7Day | Major pathway of rRNA processing in the nucleolus and cytosol | 0.98176 | 0.035177 | 0.050016 | rps25;fcf1;utp14a;riok3;pno1;utp3;ddx21;nop58;bysl;rps3;utp18;rps12;utp14b;ncl;fbl;pwp2;utp15 | 3102.57074 | 3078.47 | 84.8066 | 1347.77261 | 3073.59348 | 1240.79203 | UP | 0.941176471 | 0.058823529 |
| 7Day | rRNA processing | 0.98176 | 0.035177 | 0.050016 | rps25;fcf1;utp14a;riok3;pno1;utp3;ddx21;nop58;bysl;rps3;utp18;rps12;utp14b;ncl;fbl;pwp2;utp15 | 3102.57074 | 3078.47 | 84.8066 | 1347.77261 | 3073.59348 | 1240.79203 | UP | 0.941176471 | 0.058823529 |
| 7Day | rRNA processing in the nucleus and cytosol | 0.98176 | 0.035177 | 0.050016 | rps25;fcf1;utp14a;riok3;pno1;utp3;ddx21;nop58;bysl;rps3;utp18;rps12;utp14b;ncl;fbl;pwp2;utp15 | 3102.57074 | 3078.47 | 84.8066 | 1347.77261 | 3073.59348 | 1240.79203 | UP | 0.941176471 | 0.058823529 |

BMD analysis results for functional classification based on dose-responsive genes, using the Reactome database for gene sets in BMDExpress2.2 software.

| Study Day | Gene Set Name | Fisher's Exact Left P-Value | Fisher's Exact Right P-Value | Fisher's Exact Two Tail | Gene Symbols | BMD Mean | BMD Median | BMD Minimum | BMD Standard Deviation | BMD wMean | BMD wSD | Overall Direction | Percent Genes With Overall Direction Up | Percent Genes With Overall Direction Down |
|---|---|---|---|---|---|---|---|---|---|---|---|---|---|---|
| 7Day | Immune System | 0.026219 | 0.97912 | 0.050692 | ube2n;btbd1;rbsn;faf2;rnf6;cotl1;fbxo22;ist1;cul2;fuca1;fbxo9;trim69;ube2v2;tmem30a;c8g;arl8a;ndufc2;npc2;ilf2;pycard;c1rb;psmd6;9130409i23rik;golga7;iqgap2;sdcbp;ube2k;tax1bp1;hgsnat;c1s1;nckap1;cfhr1;flnb;eif4e2;ecsit;mapk3;map2k3;arih1;apob;mgam;tubb4b;ywhaz;yes1;pak2;ube3a;ube2a;ube2e3;uba52;tubb2a;tuba4a;ttr;hsp90b1;cdc27;cdc34;tap2;nhlrc3;dsg1c;stat1;sec22b;rab6a;rab18;rab10;ptpn11;pten;psmc2;prlr;ppp2cb;pa2g4;pgam1;neu1;myh9;mme;man2b1;lbp;lamp1;kras;kif2a;jak1;itpr2;kpnb1;il1rap;cd74;igf2r;ifng;hsp90aa1;h2-t23;h2-q10;h2-ab1;h2-aa;trip12;gstp1;gstp2;gpi1;ghr;ftl1;ubox5;f2;ube2j2;eif4a2;dhx9;ddx3x;ctsb;csnk2b;csf1r;csf1;chil1;cfh;cdc42;cd34;cd1d1;cct2;ccnf;ctnnb1;casp9;capza2;calm3;calm2;cab39;c4b;c2;c1qb;btrc;atp6v1e1;arsb;ahsg;aga;abl1;dsp;mlec;atad3a;wwp1;qsox1;brk1;cd300ld5 | 3279.47269 | 3395.925 | 34.2395 | 1366.28184 | 3196.67903 | 1377.65291 | CONFLICT | 0.567164179 | 0.432835821 |
| 28Day | IKK complex recruitment mediated by RIP1 | 0.98785 | 0.051715 | 0.051715 | ube2n;ly96;ikbkg;birc2 | 5276.735 | 5342.195 | 4560.3 | 540.392733 | 5309.42215 | 615.334604 | UP | 0.75 | 0.25 |
| 28Day | Common Pathway of Fibrin Clot Formation | 0.98785 | 0.051715 | 0.051715 | proc;f5;f2;serpinc1 | 1728.22875 | 980.2455 | 362.714 | 1952.05792 | 1110.89183 | 1146.81353 | DOWN | 0 | 1 |
| 90Day | Phosphate bond hydrolysis by NUDT proteins | 0.99228 | 0.051747 | 0.051747 | nudt5;nudt15;nudt18 | 3590.63333 | 3566.76 | 2714.47 | 888.340623 | 3657.31499 | 576.537187 | UP | 1 | 0 |
| 7Day | Formation of a pool of free 40S subunits | 0.98754 | 0.03497 | 0.052102 | eif3m;eif3j1;rps25;eif1ax;eif3b;rps3;eif3l;rps12 | 2913.68783 | 3791.07 | 84.8066 | 1903.28872 | 2870.95152 | 1872.08436 | UP | 0.875 | 0.125 |
| 7Day | E3 ubiquitin ligases ubiquitinate target proteins | 0.98754 | 0.03497 | 0.052102 | ube2n;ube2v2;rraga;hist1h2bc;wdr61;pex14;ube2a;uba52 | 3390.1375 | 3322.065 | 2423.08 | 715.376565 | 3236.66725 | 711.86911 | UP | 1 | 0 |
| 7Day | Adaptive Immune System | 0.025479 | 0.98215 | 0.052709 | ube2n;btbd1;rnf6;fbxo22;cul2;fbxo9;trim69;ube2v2;ube2k;tubb4b;ywhaz;yes1;pak2;ube3a;ube2a;ube2e3;uba52;tubb2a;tuba4a;cdc27;cdc34;tap2;sec22b;ptpn11;pten;ppp2cb;kras;kif2a;itpr2;cd74;h2-t23;h2-q10;h2-ab1;h2-aa;trip12;ubox5;ube2j2;ctsb;cdc42;cd34;cd1d1;ccnf;capza2;calm3;calm2;btrc;wwp1;cd300ld5 | 3457.34388 | 3406.92 | 919.856 | 1060.09485 | 3503.7595 | 994.489345 | UP | 0.729166667 | 0.270833333 |
| 28Day | SLC-mediated transmembrane transport | 0.024323 | 0.98869 | 0.052729 | slc35d2;slc9a5;slc25a10;slc13a5;slc17a8;slc22a1;slc1a2;slc6a13;slco2b1 | 2711.97578 | 2439.34 | 151.142 | 1429.62145 | 3126.28699 | 1139.43816 | CONFLICT | 0.555555556 | 0.444444444 |
| 28Day | M Phase | 0.028485 | 0.98488 | 0.052962 | zwilch;nek6;arpp19;dynll1;set;cnep1r1;cenpt;hist1h4i;tubb4b;tubb2a;cdc27;rad21;tpr | 4083.04308 | 3638.67 | 2359.45 | 1315.31392 | 4033.02415 | 1271.14938 | UP | 0.923076923 | 0.076923077 |
| 90Day | COPI-mediated anterograde transport | 0.03082 | 0.98844 | 0.053014 | tubb6;dctn3;tubb4b;tubb2a;tuba1b | 1992.6502 | 1781.5 | 779.791 | 1072.82446 | 1774.95351 | 1190.4266 | UP | 0.8 | 0.2 |
| 28Day | Gamma-carboxylation, transport, and amino-terminal cleavage of proteins | 0.99046 | 0.054904 | 0.054904 | proc;f7;f2 | 2700.24 | 2170.26 | 1340.75 | 1688.07416 | 1850.85737 | 1335.69078 | DOWN | 0 | 1 |
| 90Day | Ub-specific processing proteases | 0.030835 | 0.98405 | 0.055005 | tomm20;psmd8;keap1;tomm70a;usp18;psmc4;psmf1;siah2;nfkbia;mdm2;ikbkg;ar | 2352.46525 | 2515.11 | 143.029 | 1666.82412 | 2357.30515 | 1496.66069 | UP | 0.75 | 0.25 |
| 90Day | Signaling by Interleukins | 0.028367 | 0.98346 | 0.055418 | irak3;tbk1;irs2;hist1h3c;mapk14;ywhaz;vav1;stx3;sos1;nfkbia;lifr;il9r;il1rap;il15ra;ikbkg;il18bp;csf1;crlf1;btrc | 3161.05565 | 3485.11 | 74.8133 | 1873.72768 | 3010.55942 | 2106.53889 | DOWN | 0.263157895 | 0.736842105 |
| 90Day | Phase 0 - rapid depolarisation | 0.033923 | 0.99487 | 0.055974 | scn3b | 5870.91 | 5870.91 | 5870.91 |  | 5870.91 |  | UP | 1 | 0 |
| 90Day | Positive epigenetic regulation of rRNA expression | 0.032716 | 0.98882 | 0.056631 | hist1h4h;hist1h4i;hist1h3c;h2afx | 3214.00725 | 3979.26 | 811.859 | 1602.37406 | 2298.31583 | 1843.92338 | CONFLICT | 0.5 | 0.5 |
| 90Day | B-WICH complex positively regulates rRNA expression | 0.032716 | 0.98882 | 0.056631 | hist1h4h;hist1h4i;hist1h3c;h2afx | 3214.00725 | 3979.26 | 811.859 | 1602.37406 | 2298.31583 | 1843.92338 | CONFLICT | 0.5 | 0.5 |

BMD analysis results for functional classification based on dose-responsive genes, using the Reactome database for gene sets in BMDExpress2.2 software.

| Study Day | Gene Set Name | Fisher's Exact Left P-Value | Fisher's Exact Right P-Value | Fisher's Exact Two Tail | Gene Symbols | BMD Mean | BMD Median | BMD Minimum | BMD Standard Deviation | BMD wMean | BMD wSD | Overall Direction | Percent Genes With Overall Direction Up | Percent Genes With Overall Direction Down |
|---|---|---|---|---|---|---|---|---|---|---|---|---|---|---|
| 7Day | p53-Dependent G1 DNA Damage Response | 0.98673 | 0.056948 | 0.056948 | cop1;uba52;cdkn1a;ccne2 | 3951.5225 | 4112.95 | 2818.63 | 906.024201 | 3955.42276 | 894.012085 | UP | 1 | 0 |
| 7Day | p53-Dependent G1/S DNA damage checkpoint | 0.98673 | 0.056948 | 0.056948 | cop1;uba52;cdkn1a;ccne2 | 3951.5225 | 4112.95 | 2818.63 | 906.024201 | 3955.42276 | 894.012085 | UP | 1 | 0 |
| 90Day | Synthesis of PIPs at the plasma membrane | 0.027711 | 0.99597 | 0.057216 | plekha1 | 2516.3 | 2516.3 | 2516.3 |  | 2516.3 |  | UP | 1 | 0 |
| 90Day | Class C/3 (Metabotropic glutamate/pheromone receptors) | 0.027711 | 0.99597 | 0.057216 | casr | 5866.48 | 5866.48 | 5866.48 |  | 5866.48 |  | UP | 1 | 0 |
| 90Day | RAB GEFs exchange GTP for GDP on RABs | 0.028006 | 0.99063 | 0.057278 | trappc6b;st5;dennd1b;dennd1a | 2873.6475 | 3095.14 | 1239.12 | 1313.98598 | 2663.10414 | 1396.8076 | DOWN | 0.25 | 0.75 |
| 7Day | Phospholipid metabolism | 0.02631 | 0.98729 | 0.05765 | hadha;pla1a;dgat2;crls1;tnfaip8l1;stard10;mtmr7;mtmr6;pten;ptdss1 | 3178.6217 | 3586.9 | 197.056 | 1571.67918 | 3422.43941 | 1330.86292 | CONFLICT | 0.5 | 0.5 |
| 7Day | NRAGE signals death through JNK | 0.033995 | 0.99481 | 0.058402 | kalrn | 3395.83 | 3395.83 | 3395.83 |  | 3395.83 |  | DOWN | 0 | 1 |
| 28Day | Choline catabolism | 0.9945 | 0.058652 | 0.058652 | sardh;aldh7a1 | 3179.325 | 3179.325 | 2886.01 | 414.810051 | 3034.05808 | 360.364295 | DOWN | 0 | 1 |
| 28Day | Lipid particle organization | 0.9945 | 0.058652 | 0.058652 | fitm1;hsd17b13 | 2514.165 | 2514.165 | 1978.91 | 756.96488 | 2305.84445 | 697.281093 | UP | 1 | 0 |
| 28Day | Vitamin B2 (riboflavin) metabolism | 0.9945 | 0.058652 | 0.058652 | enpp1;acp5 | 1661.4965 | 1661.4965 | 201.213 | 2065.15273 | 1473.8792 | 2048.03694 | DOWN | 0 | 1 |
| 7Day | O-linked glycosylation of mucins | 0.031268 | 0.9953 | 0.058786 | c1galt1 | 3617.32 | 3617.32 | 3617.32 |  | 3617.32 |  | UP | 1 | 0 |
| 7Day | GABA receptor activation | 0.031268 | 0.9953 | 0.058786 | gnai3 | 794.2 | 794.2 | 794.2 |  | 794.2 |  | UP | 1 | 0 |
| 90Day | RNA Polymerase II Promoter Escape | 0.025032 | 0.99643 | 0.058865 | cdk7 | 3130.16 | 3130.16 | 3130.16 |  | 3130.16 |  | UP | 1 | 0 |
| 90Day | RNA Polymerase II Transcription Pre-Initiation And Promoter Opening | 0.025032 | 0.99643 | 0.058865 | cdk7 | 3130.16 | 3130.16 | 3130.16 |  | 3130.16 |  | UP | 1 | 0 |
| 90Day | RNA Polymerase II Transcription Initiation | 0.025032 | 0.99643 | 0.058865 | cdk7 | 3130.16 | 3130.16 | 3130.16 |  | 3130.16 |  | UP | 1 | 0 |
| 90Day | RNA Polymerase II Transcription Initiation And Promoter Clearance | 0.025032 | 0.99643 | 0.058865 | cdk7 | 3130.16 | 3130.16 | 3130.16 |  | 3130.16 |  | UP | 1 | 0 |
| 7Day | Stimuli-sensing channels | 0.032698 | 0.98875 | 0.058987 | uba52;calm3;calm2;wwp1 | 3888.485 | 3905.94 | 2825.5 | 1103.27631 | 3548.17172 | 1016.84299 | UP | 0.75 | 0.25 |
| 7Day | Signaling by ROBO receptors | 0.98285 | 0.059141 | 0.059141 | vasp;uba52;pfn2;pfn1;abl1 | 3693.962 | 3557.63 | 3106.36 | 634.460751 | 3898.36452 | 786.373572 | UP | 0.6 | 0.4 |
| 7Day | Mitophagy | 0.98285 | 0.059141 | 0.059141 | tomm20;mfn1;mterf3;tomm7;uba52 | 4096.692 | 4048.88 | 2384.74 | 1205.41607 | 3628.23874 | 1042.88808 | UP | 0.6 | 0.4 |
| 28Day | Platelet degranulation | 0.97624 | 0.04583 | 0.059523 | spp2;cdc37l1;ola1;abcc4;a2m;trf;serpina1e;serpina1b;itih4;fn1;f5;clu;app;anxa5;qsox1 | 2860.33287 | 3086.6 | 248.527 | 1738.11813 | 2807.32881 | 1831.76681 | DOWN | 0.2 | 0.8 |
| 90Day | Synthesis of substrates in N-glycan biosythesis | 0.030815 | 0.99279 | 0.060348 | st6galnac6;st3gal3 | 4683.725 | 4683.725 | 4143.19 | 764.431928 | 4469.98451 | 702.129746 | DOWN | 0 | 1 |
| 90Day | Signaling by TGF-beta Receptor Complex | 0.030815 | 0.99279 | 0.060348 | ccnc;ube2m | 2361.655 | 2361.655 | 678.11 | 2380.89217 | 2437.24834 | 2378.49087 | UP | 1 | 0 |
| 7Day | CS/DS degradation | 0.98966 | 0.060503 | 0.060503 | hyal1;bgn;arsb | 2697.2565 | 2968.59 | 34.2395 | 2538.25052 | 3151.98547 | 2691.86356 | DOWN | 0 | 1 |
| 7Day | MAPK3 (ERK1) activation | 0.98966 | 0.060503 | 0.060503 | mapk3;ptpn11;jak1 | 3994.74333 | 3629.67 | 3554.32 | 698.597213 | 3930.59598 | 681.24112 | UP | 0.666666667 | 0.333333333 |
| 90Day | Regulation of insulin secretion | 0.028144 | 0.99351 | 0.061417 | gng11;kcns3 | 5349.345 | 5349.345 | 4854.24 | 700.184206 | 5679.2676 | 522.072862 | UP | 1 | 0 |
| 90Day | Opioid Signalling | 0.026426 | 0.99241 | 0.061441 | gng11;camkk2;gnai3 | 3618.4394 | 4854.24 | 98.0082 | 3093.55588 | 2681.47556 | 3196.16742 | UP | 0.666666667 | 0.333333333 |
| 90Day | RNA polymerase II transcribes snRNA genes | 0.026426 | 0.99241 | 0.061441 | ints11;ints14;cdk7 | 3135.72 | 3130.16 | 3119.18 | 19.9109919 | 3137.13707 | 22.4959562 | UP | 0.666666667 | 0.333333333 |
| 90Day | mRNA Splicing - Major Pathway | 0.032589 | 0.9835 | 0.061856 | hnrnpf;cstf2t;rbm17;cd2bp2;ppil3;srsf6;u2surp;usp39;snrpc;prpf8;ddx5 | 4253.12818 | 3853.08 | 2671.37 | 1163.84413 | 4046.45743 | 1233.71041 | UP | 0.727272727 | 0.272727273 |
| 28Day | RUNX1 regulates genes involved in megakaryocyte differentiation and platelet function | 0.032968 | 0.99493 | 0.061995 | hist1h4i | 5848.41 | 5848.41 | 5848.41 |  | 5848.41 |  | DOWN | 0 | 1 |
| 28Day | Antimicrobial peptides | 0.032968 | 0.99493 | 0.061995 | clu | 2374.31 | 2374.31 | 2374.31 |  | 2374.31 |  | DOWN | 0 | 1 |
| 7Day | Assembly of collagen fibrils and other multimeric structures | 0.033275 | 0.99204 | 0.06253 | dst;ctsb | 3432.05 | 3432.05 | 2982.34 | 635.985981 | 3506.38147 | 627.238259 | UP | 1 | 0 |
| 7Day | Cell death signalling via NRAGE, NRIF and NADE | 0.030877 | 0.99271 | 0.063183 | kalrn;uba52 | 4078.695 | 4078.695 | 3395.83 | 965.716944 | 4279.32804 | 923.093701 | CONFLICT | 0.5 | 0.5 |
| 7Day | Histidine, lysine, phenylalanine, tyrosine, proline and tryptophan catabolism | 0.98044 | 0.05064 | 0.063353 | amdhd1;kyat1;prodh2;gcdh;uroc1;aldh4a1;dld;aldh7a1 | 2910.94218 | 2817.09 | 84.5274 | 1574.94437 | 2781.21537 | 1295.61683 | DOWN | 0.125 | 0.875 |
| 28Day | Neurotransmitter receptors and postsynaptic signal transmission | 0.027895 | 0.99052 | 0.063696 | gria3;mdm2;gnb5;adcy9 | 2373.357 | 2159.59 | 953.648 | 1359.18843 | 1905.88243 | 938.033043 | UP | 0.75 | 0.25 |
| 90Day | Microtubule-dependent trafficking of connexons from Golgi to the plasma membrane | 0.98493 | 0.063829 | 0.063829 | tubb6;tubb4b;tubb2a;tuba1b | 1558.67025 | 1751.94 | 779.791 | 528.216289 | 1311.72381 | 614.22224 | UP | 0.75 | 0.25 |
| 90Day | Toll Like Receptor 4 (TLR4) Cascade | 0.035256 | 0.98549 | 0.064505 | tbk1;irf7;mapk14;nfkbia;ikbkg;btrc | 3838.235 | 3931.53 | 1058.39 | 1639.93973 | 3671.64014 | 1885.92371 | DOWN | 0.333333333 | 0.666666667 |

BMD analysis results for functional classification based on dose-responsive genes, using the Reactome database for gene sets in BMDExpress2.2 software.

| Study Day | Gene Set Name | Fisher's Exact Left P-Value | Fisher's Exact Right P-Value | Fisher's Exact Two Tail | Gene Symbols | BMD Mean | BMD Median | BMD Minimum | BMD Standard Deviation | BMD wMean | BMD wSD | Overall Direction | Percent Genes With Overall Direction Up | Percent Genes With Overall Direction Down |
|---|---|---|---|---|---|---|---|---|---|---|---|---|---|---|
| 28Day | Resolution of D-loop Structures through Holliday Junction Intermediates | 0.98003 | 0.064836 | 0.064836 | rmi1;rad51d;rad51;brca1;blm | 3513.5312 | 3769.36 | 692.086 | 1790.07678 | 3877.73216 | 1143.86555 | UP | 1 | 0 |
| 7Day | mRNA Splicing | 0.97865 | 0.036516 | 0.064842 | sf3b1;sf3a3;snrpa1;dnajc8;zcrb1;fip1l1;crnkl1;ppih;sf3b6;hnrnpa2b1;cpsf2;prpf19;polr2h;pcbp1;hnrnpul1;prpf38a;zrsr2;snrpc;hnrnpc;dhx9;srsf1;cstf2;snrpd2;sf3b3 | 3686.87979 | 3515.895 | 730.51 | 1347.52896 | 3478.96033 | 1311.30014 | UP | 0.958333333 | 0.041666667 |
| 28Day | ESR-mediated signaling | 0.037651 | 0.9884 | 0.0649 | ppid;hist1h4i;polr2a | 5538.30333 | 5725.83 | 5040.67 | 435.299512 | 5566.6399 | 427.807411 | UP | 0.666666667 | 0.333333333 |
| 28Day | Regulation of TP53 Activity | 0.035848 | 0.98904 | 0.064932 | meaf6;mdm2;ccng1 | 2083.91333 | 2266.61 | 1125.25 | 881.628529 | 2174.62481 | 822.305509 | UP | 0.666666667 | 0.333333333 |
| 90Day | Neurotransmitter uptake and metabolism In glial cells | 0.99477 | 0.065183 | 0.065183 | slc1a2;glul | 1166.9995 | 1166.9995 | 777.189 | 551.275296 | 1473.12635 | 341.287501 | DOWN | 0 | 1 |
| 90Day | Astrocytic Glutamate-Glutamine Uptake And Metabolism | 0.99477 | 0.065183 | 0.065183 | slc1a2;glul | 1166.9995 | 1166.9995 | 777.189 | 551.275296 | 1473.12635 | 341.287501 | DOWN | 0 | 1 |
| 90Day | SOS-mediated signalling | 0.99477 | 0.065183 | 0.065183 | irs2;sos1 | 2984.87165 | 2984.87165 | 74.8133 | 4115.44399 | 2818.21844 | 4108.68989 | DOWN | 0 | 1 |
| 90Day | Cell Cycle Checkpoints | 0.031431 | 0.98232 | 0.065604 | cenpu;hist1h4h;anapc10;babam1;orc6;hist1h4i;gtse1;dbf4;ywhaz;kntc1;nudc;mdm2;h2afx;cdkn1a;sec13;cenpf | 3407.30362 | 3474.395 | 137.958 | 1484.96682 | 3335.48346 | 1502.62347 | UP | 0.875 | 0.125 |
| 90Day | RNA Polymerase III Transcription Initiation From Type 1 Promoter | 0.03945 | 1 | 0.066006 | | | | | | | | | | |
| 90Day | RNA Polymerase III Transcription Initiation From Type 2 Promoter | 0.03945 | 1 | 0.066006 | | | | | | | | | | |
| 90Day | Insulin receptor recycling | 0.03945 | 1 | 0.066006 | | | | | | | | | | |
| 90Day | RNA Polymerase III Transcription Initiation From Type 3 Promoter | 0.034992 | 1 | 0.067066 | | | | | | | | | | |
| 90Day | Synthesis of IP3 and IP4 in the cytosol | 0.034992 | 1 | 0.067066 | | | | | | | | | | |
| 28Day | RNA Polymerase I Promoter Clearance | 0.029733 | 0.99294 | 0.067702 | hist1h4i;polr1a | 5855.735 | 5855.735 | 5848.41 | 10.3591143 | 5854.78856 | 10.27228 | DOWN | 0 | 1 |
| 7Day | Lysosome Vesicle Biogenesis | 0.0419 | 1 | 0.068637 | | | | | | | | | | |
| 7Day | G alpha (z) signalling events | 0.0419 | 1 | 0.068637 | | | | | | | | | | |
| 7Day | Glucagon-type ligand receptors | 0.0419 | 1 | 0.068637 | | | | | | | | | | |
| 28Day | Hydrolysis of LPE | 1 | 0.068645 | 0.068645 | pla2g4c | 3475.05 | 3475.05 | 3475.05 | | 3475.05 | | UP | 1 | 0 |
| 28Day | Metabolism of ingested MeSeO2H into MeSeH | 1 | 0.068645 | 0.068645 | txnrd1 | 3178.52 | 3178.52 | 3178.52 | | 3178.52 | | UP | 1 | 0 |
| 28Day | Mitophagy | 0.98207 | 0.068745 | 0.068745 | tomm20;mterf3;sqstm1;atg5 | 4818.665 | 4936.54 | 3654.44 | 1058.71114 | 5368.53606 | 825.784265 | UP | 1 | 0 |
| 90Day | mRNA Splicing | 0.036444 | 0.98085 | 0.069003 | hnrnpf;cstf2t;rbm17;cd2bp2;ppil3;srsf6;u2surp;usp39;zrsr1;snrpc;prpf8;ddx5 | 4254.3025 | 3986.9 | 2671.37 | 1109.68929 | 4054.34502 | 1207.21286 | UP | 0.75 | 0.25 |
| 7Day | Striated Muscle Contraction | 0.037939 | 1 | 0.069208 | | | | | | | | | | |
| 90Day | Energy dependent regulation of mTOR by LKB1-AMPK | 0.031037 | 1 | 0.069347 | | | | | | | | | | |
| 90Day | DNA Double-Strand Break Repair | 0.038624 | 0.9807 | 0.069444 | hist1h4h;babam1;pole4;ppp4c;hist1h4i;polk;rad51;h2afx;brca2;rad51c | 4045.4582 | 4046.18 | 513.022 | 1470.8127 | 3606.13368 | 1521.5189 | UP | 0.7 | 0.3 |
| 28Day | Ion channel transport | 0.037393 | 0.98428 | 0.070119 | atp6v0e2;ano8;clcn6;sgk3;clcn2;atp6v1e1 | 3380.89167 | 3205.75 | 2316.49 | 1106.33568 | 3092.31363 | 862.148298 | DOWN | 0.333333333 | 0.666666667 |
| 7Day | Metabolism of steroids | 0.97615 | 0.043092 | 0.070347 | akr1c6;cyp39a1;idi1;slc27a5;osbpl2;slc10a2;slc10a1;ncoa2;ncoa1;kpnb1;hsd17b4;hsd17b2;hsd11b1;gc;ebp;baat;acat2;akr1c14;hsd3b7 | 2531.59187 | 3113.35 | 41.196 | 1699.49847 | 2585.28128 | 1582.14086 | CONFLICT | 0.526315789 | 0.473684211 |
| 90Day | COPI-dependent Golgi-to-ER retrograde traffic | 0.041162 | 0.98396 | 0.070583 | tubb6;tubb4b;tubb2a;tuba1b;kifc1 | 1389.634 | 1722.38 | 713.489 | 593.401723 | 1135.0221 | 585.08693 | UP | 0.8 | 0.2 |
| 7Day | Amino acid transport across the plasma membrane | 0.034351 | 1 | 0.070641 | | | | | | | | | | |
| 90Day | Amplification of signal from the kinetochores | 0.03565 | 0.98637 | 0.071014 | cenpu;kntc1;nudc;sec13;cenpf | 3685.894 | 3327.48 | 2758.9 | 1178.18473 | 3996.4277 | 1307.65387 | UP | 1 | 0 |
| 90Day | Amplification of signal from unattached kinetochores via a MAD2 inhibitory signal | 0.03565 | 0.98637 | 0.071014 | cenpu;kntc1;nudc;sec13;cenpf | 3685.894 | 3327.48 | 2758.9 | 1178.18473 | 3996.4277 | 1307.65387 | UP | 1 | 0 |
| 90Day | Processing of Capped Intron-Containing Pre-mRNA | 0.034152 | 0.98035 | 0.071077 | hnrnpf;cstf2t;rbm17;cd2bp2;ppil3;srsf6;u2surp;thoc7;wtap;usp39;zrsr1;nup153;snrpc;prpf8;nxf7;ddx5;sec13 | 4322.11 | 4120.72 | 2671.37 | 1161.73757 | 4241.09977 | 1205.1784 | UP | 0.823529412 | 0.176470588 |

BMD analysis results for functional classification based on dose-responsive genes, using the Reactome database for gene sets in BMDExpress2.2 software.

| Study Day | Gene Set Name | Fisher's Exact Left P-Value | Fisher's Exact Right P-Value | Fisher's Exact Two Tail | Gene Symbols | BMD Mean | BMD Median | BMD Minimum | BMD Standard Deviation | BMD wMean | BMD wSD | Overall Direction | Percent Genes With Overall Direction Up | Percent Genes With Overall Direction Down |
|---|---|---|---|---|---|---|---|---|---|---|---|---|---|---|
| 28Day | Arachidonic acid metabolism | 0.97806 | 0.049681 | 0.071247 | akr1c6;gpx4;akr1c12;akr1c19;mapkapk2;lta4h;cyp4a12b;cyp2c37;cyp2c29;akr1c14 | 4519.911 | 5064.1 | 2669.87 | 1231.38753 | 4043.78048 | 1238.22292 | DOWN | 0.4 | 0.6 |
| 28Day | Resolution of D-Loop Structures | 0.97696 | 0.072301 | 0.072301 | rmi1;rad51d;rad51;brca1;blm | 3513.5312 | 3769.36 | 692.086 | 1790.07678 | 3877.73216 | 1143.86555 | UP | 1 | 0 |
| 28Day | Plasma lipoprotein clearance | 0.97696 | 0.072301 | 0.072301 | npc2;apob;scarb1;ces3b;apoe | 2145.8648 | 2685.06 | 614.079 | 1276.09083 | 1637.02007 | 1293.32598 | DOWN | 0 | 1 |
| 7Day | Activation of C3 and C5 | 0.99279 | 0.073159 | 0.073159 | c4b;c2 | 1586.775 | 1586.775 | 1201.6 | 544.719709 | 1722.75787 | 509.643877 | DOWN | 0 | 1 |
| 7Day | VLDL clearance | 0.99279 | 0.073159 | 0.073159 | apob;apoc1 | 2882.07 | 2882.07 | 1999.21 | 1248.55259 | 3387.19612 | 1024.00135 | DOWN | 0 | 1 |
| 7Day | Autodegradation of the E3 ubiquitin ligase COP1 | 0.99279 | 0.073159 | 0.073159 | cop1;uba52 | 4194.635 | 4194.635 | 3627.71 | 801.753024 | 4115.83314 | 793.970052 | UP | 1 | 0 |
| 7Day | Ubiquitin Mediated Degradation of Phosphorylated Cdc25A | 0.99279 | 0.073159 | 0.073159 | uba52;cdc25a | 5319.66 | 5319.66 | 4761.56 | 789.272589 | 5256.30284 | 784.170237 | UP | 1 | 0 |
| 7Day | p53-Independent DNA Damage Response | 0.99279 | 0.073159 | 0.073159 | uba52;cdc25a | 5319.66 | 5319.66 | 4761.56 | 789.272589 | 5256.30284 | 784.170237 | UP | 1 | 0 |
| 7Day | p53-Independent G1/S DNA damage checkpoint | 0.99279 | 0.073159 | 0.073159 | uba52;cdc25a | 5319.66 | 5319.66 | 4761.56 | 789.272589 | 5256.30284 | 784.170237 | UP | 1 | 0 |
| 28Day | Class C/3 (Metabotropic glutamate/pheromone receptors) | 0.037645 | 1 | 0.073531 |  |  |  |  |  |  |  |  |  |  |
| 28Day | Extracellular matrix organization | 0.03597 | 0.98094 | 0.074512 | phykpl;tmprss6;a2m;vtn;p4hb;fn1;dag1;ctss;col8a1;capn5;bmp1;app | 3794.45175 | 4482.905 | 182.399 | 2111.69959 | 4236.00406 | 1783.26918 | CONFLICT | 0.416666667 | 0.583333333 |
| 28Day | Intracellular signaling by second messengers | 0.034485 | 0.98403 | 0.074767 | phlpp1;pdpk1;mdm2;il1rap;hbegf;fgf1;bmi1;adcy9 | 2544.8045 | 2966.785 | 192.988 | 1545.1028 | 2305.79205 | 1239.28447 | DOWN | 0.375 | 0.625 |
| 90Day | Transcriptional Regulation by TP53 | 0.040542 | 0.97599 | 0.076145 | trp53inp1;txnrd1;eloa;mapk14;pin1;gatad2b;ywhaz;txn1;plk2;pml;mdm2;hdac2;gsr;cdkn1a;cdk7;ccng1;btg2;bax | 2834.12133 | 3114.78 | 137.958 | 1666.56665 | 2532.14033 | 1686.2547 | UP | 0.833333333 | 0.166666667 |
| 90Day | Transport to the Golgi and subsequent modification | 0.038186 | 0.97936 | 0.076399 | trappc6b;lman1;tubb6;stx17;dctn3;tubb4b;tubb2a;tuba1b;tgfa;serpina1e;man1a;areg;sec13 | 2916.88077 | 2758.9 | 779.791 | 1508.82177 | 2494.78053 | 1441.67815 | UP | 0.692307692 | 0.307692308 |
| 90Day | Gene Silencing by RNA | 0.044395 | 0.98415 | 0.076419 | hist1h4h;hist1h4i;hist1h3c;h2afx | 3214.00725 | 3979.26 | 811.859 | 1602.37406 | 2298.31583 | 1843.92338 | CONFLICT | 0.5 | 0.5 |
| 90Day | TRAF6 mediated induction of NFkB and MAP kinases upon TLR7/8 or 9 activation | 0.044395 | 0.98415 | 0.076419 | mapk14;nfkbia;ikbkg;btrc | 4070.33 | 3931.53 | 3265.56 | 831.881085 | 4282.38479 | 1027.24106 | DOWN | 0.25 | 0.75 |
| 28Day | Cell-cell junction organization | 0.03263 | 1 | 0.076553 |  |  |  |  |  |  |  |  |  |  |
| 90Day | Cellular response to heat stress | 0.038147 | 0.98668 | 0.077106 | gm45902;nup153;hsp90aa1;sec13 | 1801.33125 | 1592.61 | 339.755 | 1680.72509 | 1453.56222 | 1669.59061 | UP | 1 | 0 |
| 7Day | Interleukin-6 signaling | 0.98494 | 0.077544 | 0.077544 | stat1;ptpn11;jak1 | 3700.28667 | 3629.67 | 3554.32 | 191.312992 | 3689.86935 | 200.012264 | UP | 1 | 0 |
| 7Day | Tetrahydrobiopterin (BH4) synthesis, recycling, salvage and regulation | 0.98494 | 0.077544 | 0.077544 | hsp90aa1;calm3;calm2 | 2990.83 | 3050.32 | 1005.61 | 1956.15357 | 2746.7427 | 1679.58489 | UP | 0.666666667 | 0.333333333 |
| 7Day | MET activates RAS signaling | 0.98494 | 0.077544 | 0.077544 | ranbp10;ranbp9;kras | 2634.76333 | 2966.85 | 778.73 | 1714.28626 | 2764.00121 | 1370.47238 | UP | 0.666666667 | 0.333333333 |
| 7Day | Chylomicron remodeling | 0.98494 | 0.077544 | 0.077544 | apoa5;apob;apoe | 1991.362 | 1999.21 | 113.316 | 1874.13432 | 2561.84919 | 1735.71019 | DOWN | 0 | 1 |
| 7Day | Growth hormone receptor signaling | 0.98494 | 0.077544 | 0.077544 | mapk3;prlr;ghr | 4289.48 | 4262.53 | 3805.67 | 497.8324 | 4384.06501 | 412.716182 | UP | 0.666666667 | 0.333333333 |
| 7Day | Regulation of IFNG signaling | 0.98494 | 0.077544 | 0.077544 | stat1;jak1;ifng | 3909.44667 | 3916.87 | 3554.32 | 351.473799 | 3908.88068 | 370.332739 | UP | 1 | 0 |
| 28Day | HDL assembly | 0.99086 | 0.078456 | 0.078456 | a2m;bmp1 | 3357.655 | 3357.655 | 1023.63 | 3300.80981 | 3295.67976 | 3299.64597 | UP | 1 | 0 |
| 28Day | Pyrimidine catabolism | 0.99086 | 0.078456 | 0.078456 | dpyd;dpys | 1501.205 | 1501.205 | 744.72 | 1069.83135 | 1904.56626 | 905.062701 | DOWN | 0 | 1 |
| 28Day | APEX1-Independent Resolution of AP Sites via the Single Nucleotide Replacement Pathway | 0.99086 | 0.078456 | 0.078456 | polb;lig3 | 5622.33 | 5622.33 | 5391.42 | 326.556054 | 5616.5595 | 326.454068 | CONFLICT | 0.5 | 0.5 |
| 28Day | Complement cascade | 0.9826 | 0.048344 | 0.078722 | c8g;vtn;f2;clu;c4b;c3;c2 | 1813.981 | 2305.72 | 447.762 | 1052.00591 | 1683.33373 | 944.640074 | DOWN | 0 | 1 |
| 7Day | Clathrin-mediated endocytosis | 0.03818 | 0.98306 | 0.079444 | ubqln1;slc2a8;apob;picalm;uba52;ldlr;igf2r | 3609.88 | 3459.74 | 1999.21 | 993.723225 | 3580.2941 | 733.778551 | CONFLICT | 0.571428571 | 0.428571429 |
| 7Day | Plasma lipoprotein remodeling | 0.97439 | 0.080039 | 0.080039 | apoa5;angptl8;apob;pcsk5;apoe | 2984.1052 | 3861.56 | 113.316 | 1899.27994 | 3554.8157 | 1538.66448 | DOWN | 0.2 | 0.8 |
| 90Day | Intracellular signaling by second messengers | 0.038431 | 0.97801 | 0.080435 | klb;cbx6;irs2;gatad2b;vav1;tgfa;nrg1;camkk2;pml;mdm2;il1rap;hdac2;gab1;fgf1;cdkn1a;areg | 2088.97309 | 2423.43 | 74.8133 | 1676.16302 | 1953.69573 | 1554.09745 | CONFLICT | 0.5 | 0.5 |
| 90Day | TNF signaling | 0.050596 | 0.99171 | 0.081519 | ikbkg | 3265.56 | 3265.56 | 3265.56 |  | 3265.56 |  | UP | 1 | 0 |
| 90Day | DAP12 interactions | 0.045813 | 0.99265 | 0.081616 | sos1 | 5894.93 | 5894.93 | 5894.93 |  | 5894.93 |  | DOWN | 0 | 1 |
| 90Day | PCP/CE pathway | 0.045813 | 0.99265 | 0.081616 | ap2m1 | 2983.55 | 2983.55 | 2983.55 |  | 2983.55 |  | UP | 1 | 0 |
| 90Day | Vasopressin regulates renal water homeostasis via Aquaporins | 0.045813 | 0.99265 | 0.081616 | gng11 | 4854.24 | 4854.24 | 4854.24 |  | 4854.24 |  | UP | 1 | 0 |
| 90Day | SUMOylation of DNA replication proteins | 0.045813 | 0.99265 | 0.081616 | nup153 | 3680.35 | 3680.35 | 3680.35 |  | 3680.35 |  | UP | 1 | 0 |
| 90Day | trans-Golgi Network Vesicle Budding | 0.04337 | 0.98657 | 0.081624 | snap23;acbd3;ftl1 | 1950.35 | 1733.37 | 544.33 | 1526.12279 | 2829.99571 | 1312.61691 | UP | 1 | 0 |
| 90Day | Clathrin derived vesicle budding | 0.04337 | 0.98657 | 0.081624 | snap23;acbd3;ftl1 | 1950.35 | 1733.37 | 544.33 | 1526.12279 | 2829.99571 | 1312.61691 | UP | 1 | 0 |

BMD analysis results for functional classification based on dose-responsive genes, using the Reactome database for gene sets in BMDExpress2.2 software.

| Study Day | Gene Set Name | Fisher's Exact Left P-Value | Fisher's Exact Right P-Value | Fisher's Exact Two Tail | Gene Symbols | BMD Mean | BMD Median | BMD Minimum | BMD Standard Deviation | BMD wMean | BMD wSD | Overall Direction | Percent Genes With Overall Direction Up | Percent Genes With Overall Direction Down |
|---|---|---|---|---|---|---|---|---|---|---|---|---|---|---|
| 90Day | Collagen degradation | 0.04337 | 0.98657 | 0.081624 | tmprss6;mmp2;ctsd | 4985.37667 | 5410.11 | 3885.66 | 960.566929 | 4770.14505 | 1031.26455 | DOWN | 0.333333333 | 0.666666667 |
| 7Day | Regulation of PTEN stability and activity | 0.97776 | 0.082518 | 0.082518 | uba52;pten;csnk2b;xiap | 3909.985 | 3968.12 | 2829.67 | 1058.66531 | 4009.38925 | 1028.42097 | UP | 0.75 | 0.25 |
| 90Day | Metabolism of steroid hormones | 0.041464 | 0.99348 | 0.08265 | hsd11b1 | 2402.05 | 2402.05 | 2402.05 |  | 2402.05 |  | DOWN | 0 | 1 |
| 28Day | Antigen processing: Ubiquitination & Proteasome degradation | 0.044019 | 0.9768 | 0.083401 | ube2n;btbd1;fbxo22;ube2v2;ube2g1;asb3;ube2k;arih2;ube2m;traip;cdc27 | 4026.69273 | 4043.68 | 1308.55 | 1279.87107 | 4058.69399 | 1282.071 | UP | 0.727272727 | 0.272727273 |
| 90Day | O-linked glycosylation of mucins | 0.048155 | 0.98783 | 0.084068 | galnt12;st3gal3 | 3923.285 | 3923.285 | 2622.31 | 1839.85649 | 2887.75239 | 1113.7398 | CONFLICT | 0.5 | 0.5 |
| 90Day | GABA receptor activation | 0.048155 | 0.98783 | 0.084068 | gnai3;gabrb3 | 5052.49 | 5052.49 | 4201.91 | 1202.90177 | 4597.44422 | 1016.28704 | CONFLICT | 0.5 | 0.5 |
| 28Day | Bile acid and bile salt metabolism | 0.9782 | 0.058006 | 0.084336 | akr1c6;akr1c12;akr1c19;slc10a1;amacr;hsd17b4;akr1c14 | 3774.80714 | 3384.83 | 702.63 | 1900.2005 | 3180.23039 | 1613.96855 | DOWN | 0.285714286 | 0.714285714 |
| 90Day | Cargo recognition for clathrin-mediated endocytosis | 0.04626 | 0.98029 | 0.084492 | apob;trf;tgfa;sh3gl3;areg;ap2m1 | 2487.8495 | 2573.03 | 175.96 | 2005.2704 | 2731.82978 | 2101.53961 | UP | 0.666666667 | 0.333333333 |
| 90Day | Formation of RNA Pol II elongation complex | 0.044085 | 0.98903 | 0.084585 | eloa;cdk7 | 4445.455 | 4445.455 | 3130.16 | 1860.10803 | 4242.37403 | 1837.80252 | UP | 1 | 0 |
| 90Day | RNA Polymerase II Transcription Elongation | 0.044085 | 0.98903 | 0.084585 | eloa;cdk7 | 4445.455 | 4445.455 | 3130.16 | 1860.10803 | 4242.37403 | 1837.80252 | UP | 1 | 0 |
| 90Day | Voltage gated Potassium channels | 0.037512 | 0.99422 | 0.084601 | kcns3 | 5844.45 | 5844.45 | 5844.45 |  | 5844.45 |  | UP | 1 | 0 |
| 7Day | HDMs demethylate histones | 0.047364 | 0.99227 | 0.084619 | hist1h4h | 3406.55 | 3406.55 | 3406.55 |  | 3406.55 |  | DOWN | 0 | 1 |
| 28Day | Peroxisomal protein import | 0.96752 | 0.075485 | 0.085152 | acox3;crot;hacl1;decr2;amacr;phyh;hsd17b4;acox1 | 3167.76875 | 3416.51 | 702.63 | 1508.40439 | 3080.59607 | 1290.58284 | DOWN | 0.125 | 0.875 |
| 90Day | Deadenylation-dependent mRNA decay | 0.040338 | 0.99012 | 0.085816 | exosc9;paip1 | 1508.701 | 1508.701 | 212.512 | 1833.08806 | 1967.17266 | 1714.59013 | UP | 1 | 0 |
| 7Day | Chemokine receptors bind chemokines | 0.040149 | 0.99366 | 0.086831 | cxcr5 | 5913.54 | 5913.54 | 5913.54 |  | 5913.54 |  | UP | 1 | 0 |
| 7Day | Nuclear Receptor transcription pathway | 0.040149 | 0.99366 | 0.086831 | rorc | 3619.39 | 3619.39 | 3619.39 |  | 3619.39 |  | DOWN | 0 | 1 |
| 7Day | ECM proteoglycans | 0.040149 | 0.99366 | 0.086831 | bgn | 2968.59 | 2968.59 | 2968.59 |  | 2968.59 |  | DOWN | 0 | 1 |
| 7Day | Integration of energy metabolism | 0.037343 | 0.98862 | 0.087195 | adipor2;prkar2a;itpr2 | 4454.89333 | 4098.21 | 4066.56 | 645.397401 | 4344.19833 | 587.600135 | DOWN | 0 | 1 |
| 7Day | Macroautophagy | 0.044736 | 0.98874 | 0.087793 | rraga;atg4c | 2173.4 | 2173.4 | 1121.07 | 1488.21936 | 1903.38488 | 1438.39512 | UP | 1 | 0 |
| 28Day | Glycosaminoglycan metabolism | 0.050344 | 0.98375 | 0.088142 | hs2st1;hyal1;gpc4 | 3615.18667 | 3361.03 | 2376.85 | 1383.04188 | 3530.52442 | 1515.30949 | DOWN | 0 | 1 |
| 90Day | Transcriptional regulation by RUNX1 | 0.043363 | 0.97806 | 0.088197 | smarcd2;hist1h4h;cbx6;hist1h4i;hist1h3c;smarcb1;pml;h2afx;cdk7;cbfb | 3413.5568 | 3961.185 | 744.949 | 1540.06894 | 3185.71409 | 1878.69661 | UP | 0.6 | 0.4 |
| 28Day | PRC2 methylates histones and DNA | 0.053101 | 0.991 | 0.088515 | hist1h4i | 5848.41 | 5848.41 | 5848.41 |  | 5848.41 |  | DOWN | 0 | 1 |
| 28Day | Miscellaneous substrates | 0.96992 | 0.088569 | 0.088569 | cyp3a25;cyp4a12b;cyp3a11;cyp3a59;cyp3a41b | 3316.883 | 3712.65 | 850.005 | 2173.66024 | 2761.60256 | 2036.23554 | UP | 0.6 | 0.4 |
| 7Day | Chromatin modifying enzymes | 0.047242 | 0.97441 | 0.088759 | prmt3;hist1h4h;hist1h2bc;kmt5a;suz12;hist2h2ac;setd2;kmt5b;kat7;ncoa2;ncoa1;hist2h2aa1 | 3245.81155 | 3379.33 | 86.7986 | 1266.28832 | 3462.68653 | 875.789942 | UP | 0.75 | 0.25 |
| 7Day | Chromatin organization | 0.047242 | 0.97441 | 0.088759 | prmt3;hist1h4h;hist1h2bc;kmt5a;suz12;hist2h2ac;setd2;kmt5b;kat7;ncoa2;ncoa1;hist2h2aa1 | 3245.81155 | 3379.33 | 86.7986 | 1266.28832 | 3462.68653 | 875.789942 | UP | 0.75 | 0.25 |
| 28Day | RMTs methylate histone arginines | 0.047179 | 0.9922 | 0.089 | hist1h4i | 5848.41 | 5848.41 | 5848.41 |  | 5848.41 |  | DOWN | 0 | 1 |
| 28Day | Class I MHC mediated antigen processing & presentation | 0.044183 | 0.97508 | 0.089031 | ube2n;btbd1;fbxo22;ube2v2;ube2g1;asb3;ube2k;arih2;ube2m;traip;cdc27;tap1;h2-q7;h2-d1 | 3927.14 | 4039.16 | 1188.24 | 1453.58963 | 3938.47646 | 1379.20359 | UP | 0.642857143 | 0.357142857 |
| 28Day | Signaling by NTRKs | 0.04446 | 0.99274 | 0.08976 | mapkapk2 | 5375 | 5375 | 5375 |  | 5375 |  | DOWN | 0 | 1 |
| 28Day | Response to elevated platelet cytosolic Ca2+ | 0.96802 | 0.059452 | 0.09007 | spp2;cdc37l1;ola1;abcc4;a2m;trf;serpina1e;serpina1b;itih4;fn1;f5;clu;app;anxa5;qsox1 | 2860.33287 | 3086.6 | 248.527 | 1738.11813 | 2807.32881 | 1831.76681 | DOWN | 0.2 | 0.8 |
| 7Day | Deactivation of the beta-catenin transactivating complex | 0.97342 | 0.069179 | 0.09008 | ywhaz;uba52;sox6;ctnnb1;btrc;xiap;xpo1 | 2782.26174 | 2726.98 | 54.5232 | 2027.05359 | 2693.73177 | 2180.76333 | CONFLICT | 0.571428571 | 0.428571429 |
| 7Day | ABC-family proteins mediated transport | 0.97559 | 0.057572 | 0.091567 | abcg8;abca3;abca8b;eif2s3x;abcc4;erlin1;uba52;sel1l;abcb4 | 3839.74111 | 4054.31 | 2076.62 | 897.839237 | 3799.09245 | 727.748929 | UP | 0.777777778 | 0.222222222 |
| 28Day | ABC-family proteins mediated transport | 0.97306 | 0.06878 | 0.0916 | abcb8;abca3;abca8b;abcc4;abcd3;abcb4;abcb1b | 2657.01729 | 2494.49 | 870.176 | 1735.83727 | 2567.92033 | 1880.30238 | UP | 0.714285714 | 0.285714286 |
| 7Day | Negative regulation of FGFR3 signaling | 0.96928 | 0.091781 | 0.091781 | mapk3;uba52;ptpn11;ppp2cb;fgf1 | 3893.254 | 3629.67 | 2647.76 | 903.905503 | 3770.28016 | 910.359639 | UP | 0.6 | 0.4 |
| 28Day | Cell death signalling via NRAGE, NRIF and NADE | 0.039465 | 0.99371 | 0.092288 | sqstm1 | 5683.98 | 5683.98 | 5683.98 |  | 5683.98 |  | UP | 1 | 0 |
| 28Day | Senescence-Associated Secretory Phenotype (SASP) | 0.043248 | 0.98906 | 0.092915 | hist1h4i;cdc27 | 5814.585 | 5814.585 | 5780.76 | 47.8357737 | 5810.29652 | 47.4497544 | CONFLICT | 0.5 | 0.5 |

BMD analysis results for functional classification based on dose-responsive genes, using the Reactome database for gene sets in BMDExpress2.2 software.

| Study Day | Gene Set Name | Fisher's Exact Left P-Value | Fisher's Exact Right P-Value | Fisher's Exact Two Tail | Gene Symbols | BMD Mean | BMD Median | BMD Minimum | BMD Standard Deviation | BMD wMean | BMD wSD | Overall Direction | Percent Genes With Overall Direction Up | Percent Genes With Overall Direction Down |
|---|---|---|---|---|---|---|---|---|---|---|---|---|---|---|
| 90Day | Post-translational modification: synthesis of GPI-anchored proteins | 0.050888 | 0.97958 | 0.093455 | pigp;ceacam2;plaur;ly6d;gpld1 | 2543.714 | 3011.39 | 957.7 | 1198.12357 | 2837.1885 | 1182.21116 | UP | 0.6 | 0.4 |
| 90Day | Sulfur amino acid metabolism | 0.96915 | 0.093461 | 0.093461 | ahcy;tst;suox;cdo1;gm4737 | 2041.1644 | 1627.86 | 683.252 | 1216.09608 | 2221.12793 | 1306.03286 | DOWN | 0.2 | 0.8 |
| 90Day | Degradation of cysteine and homocysteine | 0.98073 | 0.093577 | 0.093577 | tst;suox;cdo1 | 2386.53067 | 2669.27 | 683.252 | 1580.98573 | 2390.34461 | 1507.50488 | DOWN | 0.333333333 | 0.666666667 |
| 7Day | Synthesis of CL | 1 | 0.094226 | 0.094226 | crls1 | 4148.47 | 4148.47 | 4148.47 | | 4148.47 | | UP | 1 | 0 |
| 7Day | Metabolism of ingested MeSeO2H into MeSeH | 1 | 0.094226 | 0.094226 | txnrd1 | 2303.89 | 2303.89 | 2303.89 | | 2303.89 | | UP | 1 | 0 |
| 7Day | Respiratory electron transport | 0.97248 | 0.063582 | 0.094851 | ndufaf1;ndufaf4;ndufc2;coq10b;ndufa13;ndufa6;ndufa1;ecsit;ndufa2 | 3811.92444 | 3920.07 | 2874.39 | 543.291647 | 3626.07299 | 550.830133 | CONFLICT | 0.555555556 | 0.444444444 |
| 28Day | Signaling by Retinoic Acid | 0.97021 | 0.074587 | 0.095831 | akr1c6;akr1c12;akr1c19;adh4;aldh8a1;rdh16f2;akr1c14 | 3658.91614 | 3384.83 | 912.843 | 1735.94718 | 3406.08354 | 1417.35316 | DOWN | 0.285714286 | 0.714285714 |
| 28Day | Protein localization | 0.97332 | 0.061121 | 0.096131 | acox3;crot;hacl1;decr2;otc;amacr;phyh;hsd17b4;acox1 | 2896.55356 | 3304.47 | 702.63 | 1628.77023 | 2979.17912 | 1351.26373 | DOWN | 0.111111111 | 0.888888889 |
| 7Day | Biosynthesis of specialized proresolving mediators (SPMs) | 0.96942 | 0.077367 | 0.09629 | cyp3a25;gstm4;cyp3a11;cyp2e1;cyp2c37;cyp2c29;cyp3a41b | 3229.52186 | 2813.51 | 529.743 | 1691.38457 | 3004.89739 | 1441.18311 | CONFLICT | 0.428571429 | 0.571428571 |
| 7Day | Creation of C4 and C2 activators | 0.97907 | 0.096415 | 0.096415 | c1rb;c1s1;c1qb | 2315.66433 | 1939.15 | 56.713 | 2468.83611 | 1154.21203 | 1850.07688 | DOWN | 0 | 1 |
| 7Day | Lysine catabolism | 0.97907 | 0.096415 | 0.096415 | gcdh;dld;aldh7a1 | 3385.63 | 2652.27 | 2360.99 | 1529.42277 | 3078.93481 | 1351.60319 | DOWN | 0.333333333 | 0.666666667 |
| 7Day | Sodium/Calcium exchangers | 0.97907 | 0.096415 | 0.096415 | slc8b1;calm3;calm2 | 3614.55333 | 3050.32 | 2876.78 | 1130.90453 | 3353.96535 | 932.818439 | DOWN | 0.333333333 | 0.666666667 |
| 7Day | Spry regulation of FGF signaling | 0.97907 | 0.096415 | 0.096415 | mapk3;uba52;ppp2cb | 4396.28 | 4761.56 | 3627.04 | 666.462054 | 4245.99731 | 706.330246 | UP | 0.666666667 | 0.333333333 |
| 7Day | eNOS activation | 0.97907 | 0.096415 | 0.096415 | hsp90aa1;calm3;calm2 | 2990.83 | 3050.32 | 1005.61 | 1956.15357 | 2746.7427 | 1679.58489 | UP | 0.666666667 | 0.333333333 |
| 28Day | Cytochrome P450 - arranged by substrate type | 0.97128 | 0.060135 | 0.097005 | cyp3a25;fdxr;cyp4a12b;cyp3a11;cyp2e1;cyp2c37;cyp2c29;cyp2a5;cyp2a4;cyp3a59;cyp3a41b | 3430.53864 | 3712.65 | 850.005 | 1812.48495 | 3087.89317 | 1642.84983 | CONFLICT | 0.545454545 | 0.454545455 |
| 7Day | Aflatoxin activation and detoxification | 0.97209 | 0.097081 | 0.097081 | cyp3a25;cyp3a11;acy1;cyp3a41b | 3841.9025 | 3960.035 | 1896.11 | 1766.87506 | 3524.50363 | 1681.78694 | DOWN | 0.25 | 0.75 |
| 7Day | LDL clearance | 0.97209 | 0.097081 | 0.097081 | npc2;apob;ldlr;ces3b | 3506.2275 | 3545.22 | 1999.21 | 1199.64641 | 3611.77033 | 990.151608 | DOWN | 0.25 | 0.75 |
| 7Day | Immunoregulatory interactions between a Lymphoid and a non-Lymphoid cell | 0.048382 | 0.9806 | 0.09709 | h2-t23;h2-q10;cd34;cd1d1;cd300ld5 | 3924.828 | 3860.24 | 2584.12 | 940.924578 | 3546.12557 | 828.629454 | DOWN | 0 | 1 |
| 28Day | Nucleobase catabolism | 0.96592 | 0.097358 | 0.097358 | dpyd;dpys;nudt5;pnp;entpd5 | 2268.334 | 2257.69 | 744.72 | 1176.9016 | 2216.14255 | 788.510641 | DOWN | 0.4 | 0.6 |
| 7Day | Hemostasis | 0.050837 | 0.96385 | 0.098814 | rbsn;tmx3;mfn1;cdc37l1;f12;clec1b;mapk3;abcc4;apob;tubb4b;ywhaz;yes1;vps45;tubb2a;tuba4a;itpk1;sdc3;serpinb8;sod1;ptpn11;flna;prkar2a;ppp2cb;lgals3bp;kras;kif2a;kif1c;itpr2;cd74;gnai3;f5;f2;ecm1;cdc42;cbx5;capza2;calm3;calm2;serpinc1;ahsg;qsox1 | 3154.79004 | 3443.96 | 85.9375 | 1572.6713 | 2971.60322 | 1609.82206 | CONFLICT | 0.43902439 | 0.56097561 |
| 7Day | Vesicle-mediated transport | 0.053146 | 0.96143 | 0.099614 | rab3gap2;trappc6b;chmp5;trappc8;cog6;ubap1;trappc13;plin3;0610009b22rik;copz1;rab9;ubqln1;slc2a8;rab11a;dennd4c;ppp6r1;cog5;apob;picalm;tubb4b;ywhaz;vps45;uba52;tubb2a;tuba4a;hsp90b1;arcn1;sec22b;rab6a;rab18;rab10;rab1a;hps4;cyth1;lrp1;ldlr;kif2a;kif1c;igf2r;gja1;ftl1;f5;capza2;apoe;ap3b1;gbf1 | 3104.59324 | 3330.605 | 113.316 | 1364.54785 | 2985.00112 | 1255.31101 | UP | 0.673913043 | 0.326086957 |
| 28Day | Glutathione synthesis and recycling | 0.98611 | 0.099978 | 0.099978 | gclm;gclc | 3489.155 | 3489.155 | 1604.65 | 2665.09253 | 3468.9264 | 2664.93899 | CONFLICT | 0.5 | 0.5 |
| 28Day | Terminal pathway of complement | 0.98611 | 0.099978 | 0.099978 | c8g;clu | 2340.015 | 2340.015 | 2305.72 | 48.5004541 | 2340.47809 | 48.4960323 | DOWN | 0 | 1 |
| 90Day | RHO GTPases Activate ROCKs | 0.98803 | 0.10066 | 0.10066 | rock2;rock1 | 2068.101 | 2068.101 | 262.092 | 2554.08242 | 1087.57877 | 2144.87514 | UP | 1 | 0 |
| 90Day | Regulation of cytoskeletal remodeling and cell spreading by IPP complex components | 0.98803 | 0.10066 | 0.10066 | arhgef6;actn1 | 5633.74 | 5633.74 | 5314.58 | 451.360401 | 5440.61636 | 359.350429 | DOWN | 0 | 1 |
| 7Day | Mitotic Prometaphase | 0.049565 | 0.97369 | 0.10071 | clasp2;pds5a;cenpk;tubb4b;tubb2a;tuba4a;ppp2cb;nedd1;kif2a;hsp90aa1;xpo1 | 2843.69691 | 3074.7 | 919.856 | 1251.43972 | 2823.11876 | 1256.13876 | UP | 0.909090909 | 0.090909091 |
| 90Day | Trafficking and processing of endosomal TLR | 0.063726 | 1 | 0.10162 | | | | | | | | | | |
| 90Day | RAF-independent MAPK1/3 activation | 0.063726 | 1 | 0.10162 | | | | | | | | | | |
| 90Day | Miscellaneous transport and binding events | 0.063726 | 1 | 0.10162 | | | | | | | | | | |

BMD analysis results for functional classification based on dose-responsive genes, using the Reactome database for gene sets in BMDExpress2.2 software.

| Study Day | Gene Set Name | Fisher's Exact Left P-Value | Fisher's Exact Right P-Value | Fisher's Exact Two Tail | Gene Symbols | BMD Mean | BMD Median | BMD Minimum | BMD Standard Deviation | BMD wMean | BMD wSD | Overall Direction | Percent Genes With Overall Direction Up | Percent Genes With Overall Direction Down |
|---|---|---|---|---|---|---|---|---|---|---|---|---|---|---|
| 90Day | Intrinsic Pathway of Fibrin Clot Formation | 0.063726 | 1 | 0.10162 | | | | | | | | | | |
| 90Day | Basigin interactions | 0.056527 | 1 | 0.1024 | | | | | | | | | | |
| 90Day | Activation of G protein gated Potassium channels | 0.056527 | 1 | 0.1024 | | | | | | | | | | |
| 90Day | G protein gated Potassium channels | 0.056527 | 1 | 0.1024 | | | | | | | | | | |
| 90Day | Inhibition of voltage gated Ca2+ channels via Gbeta/gamma subunits | 0.056527 | 1 | 0.1024 | | | | | | | | | | |
| 90Day | Scavenging of heme from plasma | 0.056527 | 1 | 0.1024 | | | | | | | | | | |
| 90Day | Interleukin-20 family signaling | 0.056527 | 1 | 0.1024 | | | | | | | | | | |
| 90Day | Regulation of Hypoxia-inducible Factor (HIF) by oxygen | 0.056527 | 1 | 0.1024 | | | | | | | | | | |
| 90Day | Cellular response to hypoxia | 0.056527 | 1 | 0.1024 | | | | | | | | | | |
| 90Day | DNA Damage/Telomere Stress Induced Senescence | 0.059766 | 0.97768 | 0.10256 | hist1h4h;hist1h4i;h2afx;cdkn1a | 3239.47 | 3979.26 | 913.71 | 1551.47947 | 2461.37301 | 1789.8706 | CONFLICT | 0.5 | 0.5 |
| 7Day | Downregulation of ERBB4 signaling | 0.98659 | 0.10303 | 0.10303 | uba52;wwp1 | 3793.53 | 3793.53 | 2825.5 | 1369.00115 | 3538.42374 | 1320.6081 | UP | 1 | 0 |
| 7Day | SUMOylation of RNA binding proteins | 0.98659 | 0.10303 | 0.10303 | nop58;hnrnpc | 2026.5925 | 2026.5925 | 852.825 | 1659.95792 | 1763.7452 | 1617.80187 | UP | 1 | 0 |
| 7Day | Amino Acid conjugation | 0.98659 | 0.10303 | 0.10303 | acsm1;glyat | 5641.24 | 5641.24 | 5478.46 | 230.205684 | 5548.95276 | 189.633298 | UP | 1 | 0 |
| 7Day | Conjugation of carboxylic acids | 0.98659 | 0.10303 | 0.10303 | acsm1;glyat | 5641.24 | 5641.24 | 5478.46 | 230.205684 | 5548.95276 | 189.633298 | UP | 1 | 0 |
| 7Day | Synthesis of bile acids and bile salts via 27-hydroxycholesterol | 0.98659 | 0.10303 | 0.10303 | ncoa2;ncoa1 | 1694.1743 | 1694.1743 | 86.7986 | 2273.17251 | 2801.46736 | 1647.76134 | UP | 1 | 0 |
| 7Day | CaMK IV-mediated phosphorylation of CREB | 0.98659 | 0.10303 | 0.10303 | calm3;calm2 | 3983.44 | 3983.44 | 3050.32 | 1319.63096 | 3556.9103 | 1173.69957 | CONFLICT | 0.5 | 0.5 |
| 7Day | CREB1 phosphorylation through the activation of CaMKII/CaMKK/CaMKIV cascasde | 0.98659 | 0.10303 | 0.10303 | calm3;calm2 | 3983.44 | 3983.44 | 3050.32 | 1319.63096 | 3556.9103 | 1173.69957 | CONFLICT | 0.5 | 0.5 |
| 7Day | Activation of RAC1 downstream of NMDARs | 0.98659 | 0.10303 | 0.10303 | calm3;calm2 | 3983.44 | 3983.44 | 3050.32 | 1319.63096 | 3556.9103 | 1173.69957 | CONFLICT | 0.5 | 0.5 |
| 7Day | Cation-coupled Chloride cotransporters | 0.98659 | 0.10303 | 0.10303 | slc12a7;slc12a6 | 3111.555 | 3111.555 | 1978.78 | 1601.98577 | 3132.11975 | 1601.72176 | DOWN | 0 | 1 |
| 7Day | Cam-PDE 1 activation | 0.98659 | 0.10303 | 0.10303 | calm3;calm2 | 3983.44 | 3983.44 | 3050.32 | 1319.63096 | 3556.9103 | 1173.69957 | CONFLICT | 0.5 | 0.5 |
| 90Day | Platelet homeostasis | 0.051563 | 0.98118 | 0.10328 | gng11;mapk14;apob;p2rx4 | 2369.51675 | 2223.9335 | 175.96 | 2538.70268 | 1809.3576 | 2470.75618 | DOWN | 0.25 | 0.75 |
| 28Day | Metabolism of nucleotides | 0.96452 | 0.07196 | 0.10334 | dpyd;dpys;nme4;nudt5;txnrd1;pnp;hprt;guk1;entpd5;adss;adk | 3159.96182 | 3178.52 | 744.72 | 1467.89082 | 3186.11742 | 1457.13635 | CONFLICT | 0.545454545 | 0.454545455 |
| 7Day | mRNA Splicing - Major Pathway | 0.96395 | 0.059869 | 0.10446 | sf3b1;sf3a3;snrpa1;dnajc8;fip1l1;crnkl1;ppih;sf3b6;hnrnpa2b1;cpsf2;prpf19;polr2h;pcbp1;hnrnpul1;prpf38a;snrpc;hnrnpc;dhx9;srsf1;cstf2;snrpd2;sf3b3 | 3595.37659 | 3427.05 | 730.51 | 1370.35259 | 3371.18239 | 1327.35734 | UP | 0.954545455 | 0.045454545 |
| 7Day | Membrane Trafficking | 0.054441 | 0.96083 | 0.10487 | rab3gap2;trappc6b;chmp5;trappc8;cog6;ubap1;trappc13;plin3;0610009b22rik;copz1;rab9;ubqln1;slc2a8;rab11a;dennd4c;ppp6r1;cog5;apob;picalm;tubb4b;ywhaz;vps45;uba52;tubb2a;tuba4a;arcn1;sec22b;rab6a;rab18;rab10;rab1a;hps4;cyth1;ldlr;kif2a;kif1c;igf2r;gja1;ftl1;f5;capza2;ap3b1;gbf1 | 3244.84867 | 3440.38 | 244.081 | 1283.89474 | 3021.55737 | 1239.2098 | UP | 0.697674419 | 0.302325581 |
| 90Day | Phase 2 - plateau phase | 0.050141 | 1 | 0.10497 | | | | | | | | | | |
| 90Day | Glycogen metabolism | 0.050141 | 1 | 0.10497 | | | | | | | | | | |
| 7Day | Laminin interactions | 0.062332 | 1 | 0.10517 | | | | | | | | | | |
| 28Day | Cilium Assembly | 0.052992 | 0.97536 | 0.10557 | dynll1;rab11a;bbs9;tubb4b;tubb2a;exoc4;ttbk2 | 3279.51 | 2439.57 | 2192.92 | 1463.62755 | 3319.79576 | 1526.59776 | UP | 0.714285714 | 0.285714286 |
| 28Day | PIP3 activates AKT signaling | 0.051027 | 0.97638 | 0.10598 | phlpp1;pdpk1;mdm2;il1rap;hbegf;fgf1;bmi1 | 2305.40514 | 2266.61 | 192.988 | 1500.10686 | 2194.9304 | 1181.7772 | CONFLICT | 0.428571429 | 0.571428571 |
| 28Day | Regulation of TLR by endogenous ligand | 0.97447 | 0.10675 | 0.10675 | apob;ly96;lbp | 3768.84833 | 4560.3 | 939.205 | 2528.5868 | 2672.56284 | 2422.36232 | DOWN | 0.333333333 | 0.666666667 |
| 90Day | Miscellaneous substrates | 0.96259 | 0.091867 | 0.10698 | cyp4f16;cyp3a25;cyp3a41a;cyp4a12a;cyp4a12b;cyp2d9;cyp3a41b | 2835.82871 | 3568.65 | 343.937 | 1557.03688 | 2518.38923 | 1605.17351 | UP | 0.714285714 | 0.285714286 |
| 7Day | Regulation of TP53 Activity through Acetylation | 0.051106 | 1 | 0.10869 | | | | | | | | | | |
| 7Day | MET activates PTK2 signaling | 0.051106 | 1 | 0.10869 | | | | | | | | | | |
| 7Day | Inwardly rectifying K+ channels | 0.051106 | 1 | 0.10869 | | | | | | | | | | |

BMD analysis results for functional classification based on dose-responsive genes, using the Reactome database for gene sets in BMDExpress2.2 software.

| Study Day | Gene Set Name | Fisher's Exact Left P-Value | Fisher's Exact Right P-Value | Fisher's Exact Two Tail | Gene Symbols | BMD Mean | BMD Median | BMD Minimum | BMD Standard Deviation | BMD wMean | BMD wSD | Overall Direction | Percent Genes With Overall Direction Up | Percent Genes With Overall Direction Down |
|---|---|---|---|---|---|---|---|---|---|---|---|---|---|---|
| 28Day | NCAM signaling for neurite out-growth | 0.066671 | 1 | 0.10974 | | | | | | | | | | |
| 7Day | RAF/MAP kinase cascade | 0.056309 | 0.96894 | 0.11005 | ranbp9;mapk3;pebp1;uba52;rasa1;ppp2cb;kras;jak1;gfra1;fgf1;calm3;calm2 | 3875.345 | 4115.2 | 778.73 | 1302.5301 | 3869.35753 | 1169.20014 | CONFLICT | 0.583333333 | 0.416666667 |
| 90Day | Signaling by Hedgehog | 0.05644 | 0.97531 | 0.11042 | notum;tubb6;ift52;tubb4b;tubb2a;tuba1b | 1737.39717 | 1751.94 | 154.682 | 1322.79012 | 1507.29711 | 1099.23869 | CONFLICT | 0.5 | 0.5 |
| 28Day | Cell Cycle | 0.053704 | 0.96428 | 0.11057 | ube2n;ube2v2;zwilch;psmd6;cenpw;nek6;arpp19;pole3;psmd8;dynll1;set;cnep1r1;cenpt;hist1h4i;cdc6;cdc14a;psmf1;tubb4b;tubb2a;tfdp1;cdc27;cenpx;rad21;mdm2;psmb8;brca1;tpr | 3957.53704 | 4060.76 | 748.272 | 1598.51598 | 3945.41887 | 1554.10871 | UP | 0.740740741 | 0.259259259 |
| 90Day | Dual incision in TC-NER | 0.064637 | 0.97861 | 0.11114 | pole4;polk;cdk7 | 4212.22333 | 3652.71 | 3130.16 | 1445.45671 | 3760.17242 | 830.658559 | UP | 0.666666667 | 0.333333333 |
| 90Day | Regulation of HSF1-mediated heat shock response | 0.064637 | 0.97861 | 0.11114 | gm45902;nup153;sec13 | 2259.66833 | 2758.9 | 339.755 | 1725.34574 | 1626.35697 | 1830.96796 | UP | 1 | 0 |
| 7Day | Neurexins and neuroligins | 0.046275 | 1 | 0.11223 | | | | | | | | | | |
| 7Day | G alpha (12/13) signalling events | 0.046275 | 1 | 0.11223 | | | | | | | | | | |
| 90Day | Aromatic amines can be N-hydroxylated or N-dealkylated by CYP1A2 | 1 | 0.11268 | 0.11268 | cyp1a2 | 928.37 | 928.37 | 928.37 | | 928.37 | | DOWN | 0 | 1 |
| 90Day | Synthesis of IPs in the ER lumen | 1 | 0.11268 | 0.11268 | minpp1 | 3256.99 | 3256.99 | 3256.99 | | 3256.99 | | UP | 1 | 0 |
| 90Day | Metabolism of ingested MeSeO2H into MeSeH | 1 | 0.11268 | 0.11268 | txnrd1 | 3099.4 | 3099.4 | 3099.4 | | 3099.4 | | UP | 1 | 0 |
| 7Day | Cyclin E associated events during G1/S transition | 0.96559 | 0.11275 | 0.11275 | uba52;cdkn1a;cdc25a;ccne2 | 4514.035 | 4679.875 | 2818.63 | 1265.23972 | 4350.66448 | 1194.57246 | UP | 1 | 0 |
| 7Day | Transcriptional Regulation by TP53 | 0.058571 | 0.96559 | 0.11358 | rraga;kmt5a;txnrd1;polr2h;taf10;cnot1;ywhaz;uba52;prdx2;ppp2cb;csnk2b;cdkn1a;ccnk;ccng1;ccne2 | 3177.14533 | 3225.73 | 1234.63 | 933.644194 | 3252.70841 | 970.863606 | UP | 0.933333333 | 0.066666667 |
| 7Day | Post-translational protein modification | 0.056421 | 0.95458 | 0.11405 | dcaf8;c1galt1;ube2n;btbd1;trappc6b;dcun1d5;plet1;usp16;fbxo22;prmt3;gm49336;cul2;fuca1;fbxo9;ube2v2;pigw;rnf168;hist1h4h;rraga;babam1;hist1h2bc;tomm20;cog6;psmd5;psmd6;wdr61;apoa5;0610009b22rik;ngly1;copz1;rab9;pex14;hdac7;nop58;gnpnat1;rab11a;rab25;ube2k;suz12;uba2;etfbkmt;hist2h2ac;cop1;ppp6r1;dcaf10;taf10;fem1c;psmc4;cog5;apob;nae1;tubb4b;ino80c;vdac3;vdac2;ube2a;ube2e3;uba52;tubb2a;tuba4a;hsp90b1;top2b;tgfbr1;cdc34;arcn1;sel1l;sec22b;rab6a;rab18;rab10;rab1a;pten;psmc2;nucb1;neu1;ncoa1;commd1;ly6e;ly6d;large1;igfbp5;hnrnpc;hist2h2aa1;gpaa1;gfpt1;f5;f2;csf1;cdc25a;ccnf;capza2;calm3;calm2;c4b;btrc;bmi1;serpinc1;asgr1;arsb;apoe;ahsg;afp;uhrf2;tpr;adamts7;gbf1;qsox1;alg9 | 3307.63049 | 3411.49 | 34.2395 | 1357.1012 | 3224.0202 | 1322.09714 | UP | 0.740740741 | 0.259259259 |
| 90Day | RHO GTPase Effectors | 0.055097 | 0.964 | 0.11439 | cenpu;fmnl2;hist1h4h;tubb6;iqgap2;hist1h4i;hist1h3c;mapk14;wasf2;pin1;tubb4b;ywhaz;tubb2a;tuba1b;kntc1;rtkn;rock2;rock1;nudc;h2afx;cdc42;ctnnb1;ar;sec13;cenpf | 2942.45468 | 3327.48 | 137.958 | 1666.76604 | 2729.46778 | 1791.72597 | UP | 0.68 | 0.32 |
| 7Day | Detoxification of Reactive Oxygen Species | 0.97326 | 0.075011 | 0.11691 | txn2;txnrd1;prdx2;sod1;gstp1;gstp2 | 3067.77167 | 2364.315 | 1934.11 | 1407.64818 | 2638.24246 | 1004.62892 | UP | 0.666666667 | 0.333333333 |
| 7Day | VEGFR2 mediated cell proliferation | 0.97197 | 0.11693 | 0.11693 | rasa1;prkcz;kras | 5247.51333 | 5786.08 | 4158.71 | 942.9494 | 5500.44753 | 766.132962 | DOWN | 0.333333333 | 0.666666667 |
| 7Day | TGF-beta receptor signaling in EMT (epithelial to mesenchymal transition) | 0.97197 | 0.11693 | 0.11693 | uba52;tgfbr1;prkcz | 5403.78667 | 5652.05 | 4761.56 | 560.935327 | 5505.00175 | 513.773786 | UP | 0.666666667 | 0.333333333 |
| 7Day | Attenuation phase | 0.97197 | 0.11693 | 0.11693 | hsbp1;ptges3;hsp90aa1 | 2555.69 | 3138.45 | 1005.61 | 1356.10936 | 2112.59176 | 1392.19616 | UP | 0.666666667 | 0.333333333 |
| 7Day | Apoptotic cleavage of cell adhesion proteins | 0.97197 | 0.11693 | 0.11693 | dsg1c;ctnnb1;dsp | 1106.8554 | 240.593 | 54.5232 | 1664.15427 | 1209.2455 | 1689.05741 | DOWN | 0 | 1 |

BMD analysis results for functional classification based on dose-responsive genes, using the Reactome database for gene sets in BMDExpress2.2 software.

| Study Day | Gene Set Name | Fisher's Exact Left P-Value | Fisher's Exact Right P-Value | Fisher's Exact Two Tail | Gene Symbols | BMD Mean | BMD Median | BMD Minimum | BMD Standard Deviation | BMD wMean | BMD wSD | Overall Direction | Percent Genes With Overall Direction Up | Percent Genes With Overall Direction Down |
|---|---|---|---|---|---|---|---|---|---|---|---|---|---|---|
| 90Day | Nucleobase catabolism | 0.95647 | 0.10353 | 0.11693 | pnp2;dpys;nudt5;dnph1;nudt15;nudt18;pnp | 3360.77571 | 3566.76 | 1635.68 | 944.106911 | 3216.17975 | 938.174015 | CONFLICT | 0.428571429 | 0.571428571 |
| 28Day | Transcriptional Regulation by TP53 | 0.061662 | 0.96723 | 0.1172 | meaf6;tmem219;e2f7;txnrd1;cnot1;polr2a;mdm2;ccnk;ccng1;bnip3l | 3457.676 | 3155.34 | 1125.25 | 1517.32818 | 3021.67977 | 1410.8717 | UP | 0.6 | 0.4 |
| 90Day | Glucose metabolism | 0.068194 | 0.98159 | 0.11762 | pcx;pfkfb3 | 2690.7375 | 2690.7375 | 410.825 | 3224.28318 | 1569.96174 | 2807.79725 | CONFLICT | 0.5 | 0.5 |
| 90Day | Heparan sulfate/heparin (HS-GAG) metabolism | 0.062565 | 0.98339 | 0.11811 | sdc4;bgn | 2581.783 | 2581.783 | 630.216 | 2759.93252 | 3403.41741 | 2503.40993 | DOWN | 0 | 1 |
| 28Day | Amine ligand-binding receptors | 0.046646 | 1 | 0.11817 |  |  |  |  |  |  |  |  |  |  |
| 90Day | HDR through Single Strand Annealing (SSA) | 0.067968 | 0.98812 | 0.11824 | rad51 | 513.022 | 513.022 | 513.022 |  | 513.022 |  | UP | 1 | 0 |
| 90Day | Base Excision Repair | 0.067968 | 0.98812 | 0.11824 | pole4 | 5853.8 | 5853.8 | 5853.8 |  | 5853.8 |  | DOWN | 0 | 1 |
| 90Day | Resolution of Abasic Sites (AP sites) | 0.067968 | 0.98812 | 0.11824 | pole4 | 5853.8 | 5853.8 | 5853.8 |  | 5853.8 |  | DOWN | 0 | 1 |
| 90Day | Chylomicron assembly | 0.97238 | 0.11831 | 0.11831 | apob;apoe;apoc3 | 2494.08667 | 1749.82 | 175.96 | 2766.39631 | 3075.73574 | 2798.82787 | DOWN | 0 | 1 |
| 90Day | Chylomicron remodeling | 0.97238 | 0.11831 | 0.11831 | apob;apoe;apoc3 | 2494.08667 | 1749.82 | 175.96 | 2766.39631 | 3075.73574 | 2798.82787 | DOWN | 0 | 1 |
| 28Day | Neddylation | 0.053985 | 0.97174 | 0.1186 | obsl1;btbd1;fbxo22;psmd6;asb3;psmd8;uchl3;psmf1;ube2m;psmb8 | 3801.796 | 4283.805 | 1308.55 | 1505.91358 | 3880.67917 | 1590.21422 | DOWN | 0.4 | 0.6 |
| 90Day | NCAM signaling for neurite out-growth | 0.061629 | 0.98946 | 0.11928 | sos1 | 5894.93 | 5894.93 | 5894.93 |  | 5894.93 |  | DOWN | 0 | 1 |
| 90Day | GABA B receptor activation | 0.061629 | 0.98946 | 0.11928 | gnai3 | 5903.07 | 5903.07 | 5903.07 |  | 5903.07 |  | UP | 1 | 0 |
| 90Day | Activation of GABAB receptors | 0.061629 | 0.98946 | 0.11928 | gnai3 | 5903.07 | 5903.07 | 5903.07 |  | 5903.07 |  | UP | 1 | 0 |
| 90Day | Transcriptional activity of SMAD2/SMAD3:SMAD4 heterotrimer | 0.061629 | 0.98946 | 0.11928 | ccnc | 4045.2 | 4045.2 | 4045.2 |  | 4045.2 |  | UP | 1 | 0 |
| 90Day | Golgi Associated Vesicle Biogenesis | 0.057368 | 0.98502 | 0.1195 | acbd3;ftl1 | 2653.36 | 2653.36 | 1733.37 | 1301.06234 | 3063.20902 | 1164.8222 | UP | 1 | 0 |
| 90Day | Formation of Fibrin Clot (Clotting Cascade) | 0.055854 | 0.99065 | 0.12154 | f7 | 3350.52 | 3350.52 | 3350.52 |  | 3350.52 |  | DOWN | 0 | 1 |
| 90Day | Cargo trafficking to the periciliary membrane | 0.055854 | 0.99065 | 0.12154 | exoc4 | 2113.16 | 2113.16 | 2113.16 |  | 2113.16 |  | UP | 1 | 0 |
| 28Day | Initial triggering of complement | 0.96891 | 0.12189 | 0.12189 | c4b;c3;c2 | 2076.44167 | 2572.88 | 520.995 | 1376.11119 | 1715.75301 | 1348.31746 | DOWN | 0 | 1 |
| 28Day | Deposition of new CENPA-containing nucleosomes at the centromere | 0.96891 | 0.12189 | 0.12189 | cenpw;cenpt;cenpx | 4594.13333 | 4682.29 | 3567.21 | 985.805758 | 4633.05174 | 1140.90633 | DOWN | 0.333333333 | 0.666666667 |
| 28Day | Nucleosome assembly | 0.96891 | 0.12189 | 0.12189 | cenpw;cenpt;cenpx | 4594.13333 | 4682.29 | 3567.21 | 985.805758 | 4633.05174 | 1140.90633 | DOWN | 0.333333333 | 0.666666667 |
| 28Day | Endosomal Sorting Complex Required For Transport (ESCRT) | 0.96046 | 0.12198 | 0.12198 | vps36;ubap1;vps37a;hgs | 3411.59 | 3333.065 | 2396.85 | 901.917258 | 3368.7906 | 1032.57673 | UP | 0.75 | 0.25 |
| 28Day | RHO GTPases activate IQGAPs | 0.96046 | 0.12198 | 0.12198 | iqgap2;tubb4b;tubb2a;cdc42 | 2737.835 | 2683.265 | 2359.45 | 401.419857 | 2783.09066 | 384.123954 | UP | 0.75 | 0.25 |
| 28Day | Immunoregulatory interactions between a Lymphoid and a non-Lymphoid cell | 0.052807 | 0.98282 | 0.12262 | h2-q7;h2-d1;c3 | 4023.66 | 3718.12 | 2572.88 | 1625.23494 | 3626.7901 | 1367.74163 | DOWN | 0.333333333 | 0.666666667 |
| 7Day | Plasma lipoprotein clearance | 0.96873 | 0.084731 | 0.12267 | npc2;apob;ldlr;ces3b;apoe;apoc1 | 2983.85933 | 3545.22 | 113.316 | 1688.72845 | 3495.51574 | 1115.58326 | DOWN | 0.166666667 | 0.833333333 |
| 28Day | Scavenging by Class A Receptors | 0.98021 | 0.12289 | 0.12289 | apob;apoe | 2075.9425 | 2075.9425 | 939.205 | 1607.58959 | 1295.41266 | 1168.71324 | DOWN | 0 | 1 |
| 28Day | mitochondrial fatty acid beta-oxidation of saturated fatty acids | 0.98021 | 0.12289 | 0.12289 | echs1;acadl | 2016.1655 | 2016.1655 | 802.301 | 1716.66364 | 1538.10672 | 1577.92701 | DOWN | 0 | 1 |
| 28Day | Urea cycle | 0.98021 | 0.12289 | 0.12289 | otc;ass1 | 899.061 | 899.061 | 726.832 | 243.568588 | 953.614934 | 231.026824 | DOWN | 0 | 1 |
| 7Day | Hedgehog 'on' state | 0.06055 | 0.98958 | 0.12381 | uba52 | 4761.56 | 4761.56 | 4761.56 |  | 4761.56 |  | UP | 1 | 0 |
| 7Day | HDR through Homologous Recombination (HRR) | 0.055652 | 0.98542 | 0.12452 | uba52;rad51ap1 | 4319.445 | 4319.445 | 3877.33 | 625.245029 | 4260.9519 | 619.748708 | UP | 1 | 0 |
| 28Day | Fcgamma receptor (FCGR) dependent phagocytosis | 0.07272 | 0.97971 | 0.12599 | cdc42;brk1 | 3960.63 | 3960.63 | 2463.49 | 2117.27569 | 4417.2828 | 2016.38111 | CONFLICT | 0.5 | 0.5 |
| 7Day | DNA Damage Bypass | 0.055808 | 0.99057 | 0.12605 | uba52 | 4761.56 | 4761.56 | 4761.56 |  | 4761.56 |  | UP | 1 | 0 |
| 28Day | RNA Polymerase I Chain Elongation | 0.0691 | 0.98092 | 0.12613 | hist1h4i;polr1a | 5855.735 | 5855.735 | 5848.41 | 10.3591143 | 5854.78856 | 10.27228 | DOWN | 0 | 1 |
| 7Day | PI5P, PP2A and IER3 Regulate PI3K/AKT Signaling | 0.072147 | 0.96934 | 0.1265 | mapk3;ptpn11;ppp2cb;il1rap;fgf1 | 2967.1468 | 3627.04 | 131.024 | 1759.27735 | 2795.99089 | 1795.89908 | DOWN | 0.4 | 0.6 |
| 28Day | Positive epigenetic regulation of rRNA expression | 0.065647 | 0.98205 | 0.1266 | hist1h4i;polr1a | 5855.735 | 5855.735 | 5848.41 | 10.3591143 | 5854.78856 | 10.27228 | DOWN | 0 | 1 |
| 28Day | B-WICH complex positively regulates rRNA expression | 0.065647 | 0.98205 | 0.1266 | hist1h4i;polr1a | 5855.735 | 5855.735 | 5848.41 | 10.3591143 | 5854.78856 | 10.27228 | DOWN | 0 | 1 |
| 28Day | Regulation of PLK1 Activity at G2/M Transition | 0.065647 | 0.98205 | 0.1266 | dynll1;tubb4b | 4075.495 | 4075.495 | 2359.45 | 2426.85411 | 4561.33816 | 2327.55961 | UP | 1 | 0 |
| 28Day | Regulation of insulin secretion | 0.075401 | 0.98617 | 0.12674 | gnb5 | 953.648 | 953.648 | 953.648 |  | 953.648 |  | UP | 1 | 0 |
| 28Day | PTEN Regulation | 0.071153 | 0.98713 | 0.12686 | bmi1 | 3918.46 | 3918.46 | 3918.46 |  | 3918.46 |  | UP | 1 | 0 |

BMD analysis results for functional classification based on dose-responsive genes, using the Reactome database for gene sets in BMDExpress2.2 software.

| Study Day | Gene Set Name | Fisher's Exact Left P-Value | Fisher's Exact Right P-Value | Fisher's Exact Two Tail | Gene Symbols | BMD Mean | BMD Median | BMD Minimum | BMD Standard Deviation | BMD wMean | BMD wSD | Overall Direction | Percent Genes With Overall Direction Up | Percent Genes With Overall Direction Down |
|---|---|---|---|---|---|---|---|---|---|---|---|---|---|---|
| 7Day | Signaling by Rho GTPases | 0.061713 | 0.95755 | 0.12707 | clasp2;myh14;hist1h4h;hist1h2bc;cenpk;kalrn;iqgap2;nckap1;dlc1;hist2h2ac;mapk3;tubb4b;ywhaz;pak2;tubb2a;tuba4a;flna;ppp2cb;pfn2;pfn1;ncoa2;myh9;kif2a;hist2h2aa1;cdc42;ctnnb1;calm3;calm2;abl1;xpo1;brk1 | 3262.95283 | 3406.55 | 54.5232 | 1403.85221 | 3312.88593 | 1415.442 | UP | 0.612903226 | 0.387096774 |
| 90Day | Glycosaminoglycan metabolism | 0.061178 | 0.97137 | 0.12723 | omd;sdc4;st3gal3;lum;hyal1;slc26a2;bgn | 3214.985 | 3962.48 | 144.869 | 1997.4444 | 3545.10983 | 1689.16138 | DOWN | 0.285714286 | 0.714285714 |
| 7Day | Cyclin A:Cdk2-associated events at S phase entry | 0.95823 | 0.12945 | 0.12945 | uba52;cdkn1a;cdc25a;ccne2 | 4514.035 | 4679.875 | 2818.63 | 1265.23972 | 4350.66448 | 1194.57246 | UP | 1 | 0 |
| 7Day | Synaptic adhesion-like molecules | 0.95823 | 0.12945 | 0.12945 | gria3;ptprf;ptprd;flot2 | 3155.4775 | 3050.285 | 1019.97 | 1947.22982 | 3207.00014 | 1360.83163 | DOWN | 0.25 | 0.75 |
| 7Day | Death Receptor Signalling | 0.071486 | 0.96566 | 0.12966 | kalrn;tax1bp1;lingo1;uba52;smpd2;prkci;xiap | 4109.23286 | 3409.24 | 3247.44 | 1023.33552 | 4183.22777 | 1041.92089 | CONFLICT | 0.571428571 | 0.428571429 |
| 28Day | PKMTs methylate histone lysines | 0.059727 | 0.98962 | 0.12992 | hist1h4i | 5848.41 | 5848.41 | 5848.41 |  | 5848.41 |  | DOWN | 0 | 1 |
| 28Day | p75 NTR receptor-mediated signalling | 0.056218 | 0.98508 | 0.12999 | arhgdia;sqstm1 | 5327.91 | 5327.91 | 4971.84 | 503.559023 | 5342.98982 | 503.107233 | UP | 1 | 0 |
| 28Day | Synthesis of PS | 0.99529 | 0.13259 | 0.13259 | ptdss1 | 3854.48 | 3854.48 | 3854.48 |  | 3854.48 |  | DOWN | 0 | 1 |
| 28Day | Biosynthesis of DHA-derived sulfido conjugates | 0.99529 | 0.13259 | 0.13259 | gstm4 | 792.488 | 792.488 | 792.488 |  | 792.488 |  | UP | 1 | 0 |
| 28Day | Biosynthesis of maresin conjugates in tissue regeneration (MCTR) | 0.99529 | 0.13259 | 0.13259 | gstm4 | 792.488 | 792.488 | 792.488 |  | 792.488 |  | UP | 1 | 0 |
| 28Day | Abasic sugar-phosphate removal via the single-nucleotide replacement pathway | 0.99529 | 0.13259 | 0.13259 | polb | 5853.24 | 5853.24 | 5853.24 |  | 5853.24 |  | UP | 1 | 0 |
| 28Day | TP53 Regulates Transcription of Death Receptors and Ligands | 0.99529 | 0.13259 | 0.13259 | tmem219 | 5589.83 | 5589.83 | 5589.83 |  | 5589.83 |  | DOWN | 0 | 1 |
| 28Day | Transfer of LPS from LBP carrier to CD14 | 0.99529 | 0.13259 | 0.13259 | lbp | 5807.04 | 5807.04 | 5807.04 |  | 5807.04 |  | DOWN | 0 | 1 |
| 28Day | Linoleic acid (LA) metabolism | 0.99529 | 0.13259 | 0.13259 | elovl2 | 829.671 | 829.671 | 829.671 |  | 829.671 |  | DOWN | 0 | 1 |
| 7Day | Complex I biogenesis | 0.96275 | 0.085569 | 0.13293 | ndufaf1;ndufaf4;ndufc2;ndufa13;ndufa6;ndufa1;ecsit;ndufa2 | 3765.34375 | 3870.965 | 2874.39 | 561.261806 | 3563.34922 | 546.182095 | CONFLICT | 0.5 | 0.5 |
| 7Day | Interferon Signaling | 0.95694 | 0.088503 | 0.13324 | ube2n;flnb;eif4e2;mapk3;arih1;stat1;ptpn11;jak1;ifng;eif4a2 | 3618.495 | 3591.995 | 2513.13 | 662.008597 | 3584.68031 | 664.910743 | UP | 0.8 | 0.2 |
| 7Day | HSF1 activation | 0.97816 | 0.13551 | 0.13551 | ptges3;hsp90aa1 | 2072.03 | 2072.03 | 1005.61 | 1508.14563 | 1840.5494 | 1472.18772 | UP | 1 | 0 |
| 7Day | Heme degradation | 0.97816 | 0.13551 | 0.13551 | ugt1a1;blvrb | 2545.203 | 2545.203 | 178.786 | 3346.61902 | 2903.10937 | 3308.12105 | CONFLICT | 0.5 | 0.5 |
| 7Day | Aryl hydrocarbon receptor signalling | 0.97816 | 0.13551 | 0.13551 | ptges3;arnt | 3306.16 | 3306.16 | 3138.45 | 237.177757 | 3272.82664 | 232.445828 | CONFLICT | 0.5 | 0.5 |
| 90Day | PI Metabolism | 0.069124 | 0.97357 | 0.13757 | tnfaip8l1;tnfaip8l3;pi4ka;plekha1 | 2755.15 | 2699.92 | 1984.74 | 693.540876 | 2789.32817 | 510.939159 | DOWN | 0.25 | 0.75 |
| 28Day | LDL clearance | 0.9627 | 0.13775 | 0.13775 | npc2;apob;ces3b | 1412.78133 | 939.205 | 614.079 | 1113.75333 | 1033.23597 | 853.388406 | DOWN | 0 | 1 |
| 90Day | Mitotic Anaphase | 0.067819 | 0.96392 | 0.13843 | cenpu;anapc10;tubb6;tubb4b;tubb2a;tuba1b;kntc1;nudc;sec13;cenpf | 2905.4621 | 2971.72 | 779.791 | 1448.96614 | 2908.06114 | 1718.42046 | UP | 0.9 | 0.1 |
| 90Day | Mitotic Metaphase and Anaphase | 0.064222 | 0.96605 | 0.13931 | cenpu;anapc10;tubb6;tubb4b;tubb2a;tuba1b;kntc1;nudc;sec13;cenpf | 2905.4621 | 2971.72 | 779.791 | 1448.96614 | 2908.06114 | 1718.42046 | UP | 0.9 | 0.1 |
| 90Day | Fibronectin matrix formation | 0.97805 | 0.14001 | 0.14001 | ceacam2;fn1 | 2935.755 | 2935.755 | 2110.06 | 1167.70907 | 3438.7646 | 926.016822 | CONFLICT | 0.5 | 0.5 |
| 90Day | Choline catabolism | 0.97805 | 0.14001 | 0.14001 | dmgdh;sardh | 2153.1035 | 2153.1035 | 562.177 | 2249.90983 | 1709.48348 | 2160.67045 | DOWN | 0 | 1 |
| 90Day | Activated NTRK2 signals through FRS2 and FRS3 | 0.97805 | 0.14001 | 0.14001 | sos1;ntrk2 | 4819.635 | 4819.635 | 3744.34 | 1520.69677 | 5019.62489 | 1494.16424 | DOWN | 0 | 1 |
| 7Day | RAB GEFs exchange GTP for GDP on RABs | 0.9416 | 0.10767 | 0.14025 | rab3gap2;trappc6b;trappc8;trappc13;0610009b22rik;rab9;dennd4c;rab6a;rab18;rab10;rab1a;hps4 | 3354.70917 | 3549.365 | 1046.66 | 987.765335 | 3158.49338 | 802.748125 | UP | 0.833333333 | 0.166666667 |
| 7Day | p75 NTR receptor-mediated signalling | 0.077514 | 0.96959 | 0.14053 | kalrn;lingo1;uba52;prkci | 3703.5175 | 3402.535 | 3247.44 | 709.16182 | 3635.7194 | 714.955261 | UP | 0.75 | 0.25 |
| 90Day | Regulation of TP53 Activity | 0.077647 | 0.96078 | 0.14176 | trp53inp1;mapk14;pin1;gatad2b;pml;mdm2;hdac2;ccng1 | 2852.982 | 3338.28 | 202.162 | 1639.26752 | 2701.54097 | 1741.80736 | UP | 0.75 | 0.25 |
| 7Day | mRNA Splicing - Minor Pathway | 0.95332 | 0.10269 | 0.14284 | sf3b1;zcrb1;sf3b6;polr2h;zrsr2;srsf1;snrpd2;sf3b3 | 4178.27875 | 3958.2 | 3209.5 | 845.527167 | 3976.3674 | 617.723557 | UP | 1 | 0 |
| 90Day | Ethanol oxidation | 0.96217 | 0.14514 | 0.14514 | aldh1b1;adh4;aldh1a7 | 2948.69667 | 2828.04 | 2740.9 | 287.766466 | 2839.44943 | 213.108444 | UP | 1 | 0 |
| 90Day | Phenylalanine and tyrosine catabolism | 0.96217 | 0.14514 | 0.14514 | asrgl1;hpd;gstz1 | 2010.449 | 1889.08 | 932.277 | 1143.69662 | 1847.96643 | 1180.88947 | DOWN | 0 | 1 |
| 7Day | Cooperation of PDCL (PhLP1) and TRiC/CCT in G-protein beta folding | 0.95214 | 0.11779 | 0.14595 | tcp1;rgs9;gnai3;cct7;cct4;cct2 | 3317.08333 | 3368.435 | 794.2 | 1639.67521 | 2488.37326 | 1531.66786 | UP | 0.833333333 | 0.166666667 |
| 7Day | MAPK1/MAPK3 signaling | 0.074403 | 0.95679 | 0.14615 | ranbp9;mapk3;pebp1;uba52;rasa1;ptpn11;ppp2cb;kras;jak1;gfra1;fgf1;calm3;calm2 | 3856.44692 | 4071.69 | 778.73 | 1248.9377 | 3857.71942 | 1137.75892 | UP | 0.615384615 | 0.384615385 |
| 28Day | Organic anion transporters | 0.97315 | 0.1469 | 0.1469 | slc25a10;slc17a8 | 3022.865 | 3022.865 | 2312.64 | 1004.40983 | 3208.50484 | 969.492034 | UP | 1 | 0 |

BMD analysis results for functional classification based on dose-responsive genes, using the Reactome database for gene sets in BMDExpress2.2 software.

| Study Day | Gene Set Name | Fisher's Exact Left P-Value | Fisher's Exact Right P-Value | Fisher's Exact Two Tail | Gene Symbols | BMD Mean | BMD Median | BMD Minimum | BMD Standard Deviation | BMD wMean | BMD wSD | Overall Direction | Percent Genes With Overall Direction Up | Percent Genes With Overall Direction Down |
|---|---|---|---|---|---|---|---|---|---|---|---|---|---|---|
| 7Day | Metabolism of proteins | 0.071932 | 0.94033 | 0.14698 | eif3m;dcaf8;c1galt1;mrpl16;mrpl1;ube2n;btbd1;eif3j1;trappc6b;dcun1d5;plet1;rps25;mrpl47;usp16;fbxo22;prmt3;gm49336;cul2;fuca1;fbxo9;ube2v2;pigw;rnf168;hist1h4h;rraga;babam1;hist1h2bc;tomm20;cog6;psmd5;psmd6;wdr61;mrps17;eif1ax;mrps36;apoa5;0610009b22rik;ngly1;mrps31;copz1;rab9;pex14;hdac7;nop58;gnpnat1;rab11a;rab25;ube2k;suz12;uba2;etfbkmt;hist2h2ac;eif3b;abca3;mrpl2;msrb1;rps3;eif2s3x;cop1;ppp6r1;dcaf10;taf10;fem1c;psmc4;cog5;apob;nae1;tubb4b;ino80c;eif3l;vdac3;vdac2;ube2a;ube2e3;uba52;tubb2a;tuba4a;hsp90b1;top2b;tgfbr1;eif5;cdc34;tcp1;arcn1;sel1l;sec22b;rps12;rgs9;rab6a;rab18;rab10;rab1a;pten;psmc2;nucb1;neu1;ncoa1;commd1;mme;ly6e;ly6d;large1;igfbp5;hnrnpc;hist2h2aa1;gspt1;gpaa1;gnai3;gfpt1;f5;f2;eif4ebp1;eif4a2;csf1;cdc25a;cct7;cct4;cct2;ccnf;capza2;calm3;calm2;c4b;btrc;bmi1;serpinc1;asgr1;arsb;apoe;ahsg;afp;uhrf2;tpr;adamts7;gbf1;qsox1;alg9 | 3331.02157 | 3418.4 | 34.2395 | 1365.20864 | 3221.59993 | 1326.52158 | UP | 0.744525547 | 0.255474453 |
| 7Day | Glycerophospholipid biosynthesis | 0.070324 | 0.96809 | 0.14754 | hadha;pla1a;dgat2;crls1;stard10;ptdss1 | 2781.72283 | 3586.9 | 197.056 | 1878.288 | 3280.41818 | 1631.32008 | DOWN | 0.333333333 | 0.666666667 |
| 7Day | Regulation of TP53 Activity | 0.066684 | 0.96997 | 0.14872 | kmt5a;taf10;uba52;ppp2cb;csnk2b;ccng1 | 3216.805 | 3423.965 | 1234.63 | 1159.98087 | 3098.48255 | 1211.00302 | UP | 1 | 0 |
| 7Day | Cell Cycle, Mitotic | 0.077549 | 0.9444 | 0.14877 | clasp2;gm49336;pds5a;hist1h4h;hist1h2bc;kmt5a;psmd5;psmd6;cenpk;nek6;arpp19;hist2h2ac;gtse1;mapk3;psmc4;tubb4b;uba52;tubb2a;tuba4a;tfdp1;cdc27;rab1a;psmc2;prim2;ppp2cb;nedd1;kif2a;hsp90aa1;hist2h2aa1;cdkn1a;cdc25a;ccne2;btrc;abl1;tpr;xpo1 | 3338.59217 | 3521.41 | 707.264 | 1286.77305 | 3294.11171 | 1260.15661 | UP | 0.861111111 | 0.138888889 |
| 90Day | Cap-dependent Translation Initiation | 0.088041 | 0.96918 | 0.15091 | eif3m;rps27l;rps12 | 2578.52 | 2517.83 | 1662.63 | 947.693586 | 2378.76706 | 980.623942 | UP | 1 | 0 |
| 90Day | Eukaryotic Translation Initiation | 0.08157 | 0.97186 | 0.15108 | eif3m;rps27l;rps12 | 2578.52 | 2517.83 | 1662.63 | 947.693586 | 2378.76706 | 980.623942 | UP | 1 | 0 |
| 90Day | Costimulation by the CD28 family | 0.069891 | 0.97655 | 0.15399 | vav1;h2-aa;cdc42 | 2439.569 | 3001.17 | 156.487 | 2060.5043 | 2705.98577 | 1639.34757 | DOWN | 0.333333333 | 0.666666667 |
| 90Day | Gap-filling DNA repair synthesis and ligation in TC-NER | 0.069891 | 0.97655 | 0.15399 | pole4;polk;cdk7 | 4212.22333 | 3652.71 | 3130.16 | 1445.45671 | 3760.17242 | 830.658559 | UP | 0.666666667 | 0.333333333 |
| 90Day | Cleavage of Growing Transcript in the Termination Region | 0.069891 | 0.97655 | 0.15399 | cstf2t;srsf6;thoc7 | 5120.03333 | 5843.41 | 3549.69 | 1361.36044 | 5319.43866 | 1251.94412 | UP | 0.666666667 | 0.333333333 |
| 90Day | RNA Polymerase II Transcription Termination | 0.069891 | 0.97655 | 0.15399 | cstf2t;srsf6;thoc7 | 5120.03333 | 5843.41 | 3549.69 | 1361.36044 | 5319.43866 | 1251.94412 | UP | 0.666666667 | 0.333333333 |
| 28Day | Glucose metabolism | 0.94696 | 0.12572 | 0.154 | slc25a10;pfkl;pcx;pck1;gpi1;bpgm | 3791.51 | 3857.705 | 3056.49 | 619.406093 | 3535.2427 | 522.694369 | DOWN | 0.333333333 | 0.666666667 |
| 7Day | Chaperonin-mediated protein folding | 0.94557 | 0.13006 | 0.15556 | tcp1;rgs9;gnai3;cct7;cct4;cct2 | 3317.08333 | 3368.435 | 794.2 | 1639.67521 | 2488.37326 | 1531.66786 | UP | 0.833333333 | 0.166666667 |
| 7Day | Protein folding | 0.94557 | 0.13006 | 0.15556 | tcp1;rgs9;gnai3;cct7;cct4;cct2 | 3317.08333 | 3368.435 | 794.2 | 1639.67521 | 2488.37326 | 1531.66786 | UP | 0.833333333 | 0.166666667 |
| 7Day | Signaling by FGFR3 | 0.94557 | 0.13006 | 0.15556 | mapk3;uba52;ptpn11;ppp2cb;kras;fgf1 | 3937.49667 | 3894.19 | 2647.76 | 815.708654 | 3810.92898 | 853.996178 | UP | 0.666666667 | 0.333333333 |
| 90Day | Unblocking of NMDA receptors, glutamate binding and activation | 0.10292 | 1 | 0.15748 |  |  |  |  |  |  |  |  |  |  |
| 90Day | Oxygen-dependent proline hydroxylation of Hypoxia-inducible Factor Alpha | 0.10292 | 1 | 0.15748 |  |  |  |  |  |  |  |  |  |  |
| 90Day | Lagging Strand Synthesis | 0.091296 | 1 | 0.15755 |  |  |  |  |  |  |  |  |  |  |
| 90Day | Downregulation of SMAD2/3:SMAD4 transcriptional activity | 0.091296 | 1 | 0.15755 |  |  |  |  |  |  |  |  |  |  |
| 90Day | Endosomal/Vacuolar pathway | 0.091296 | 1 | 0.15755 |  |  |  |  |  |  |  |  |  |  |
| 90Day | Synthesis of Prostaglandins (PG) and Thromboxanes (TX) | 0.091296 | 1 | 0.15755 |  |  |  |  |  |  |  |  |  |  |

BMD analysis results for functional classification based on dose-responsive genes, using the Reactome database for gene sets in BMDExpress2.2 software.

| Study Day | Gene Set Name | Fisher's Exact Left P-Value | Fisher's Exact Right P-Value | Fisher's Exact Two Tail | Gene Symbols | BMD Mean | BMD Median | BMD Minimum | BMD Standard Deviation | BMD wMean | BMD wSD | Overall Direction | Percent Genes With Overall Direction Up | Percent Genes With Overall Direction Down |
|---|---|---|---|---|---|---|---|---|---|---|---|---|---|---|
| 28Day | Post-translational protein modification | 0.081087 | 0.93575 | 0.15772 | obsl1;c1galt1;ube2n;btbd1;spp2;asxl2;fbxo22;ube2v2;tomm20;nanp;ube2g1;lman2;psmd6;wdr61;asb3;ngly1;psmd8;dynll1;rab9;pigp;rab11a;ube2k;ppp6r3;uchl3;gne;ano8;hist1h4i;pign;apob;psmf1;tubb4b;sbspon;rab29;ino80c;usp12;ube2m;tubb2a;trf;mgat2;sec22c;serpina1e;serpina1b;rad21;rab18;proc;polb;p4hb;mdm2;man1a;ly6d;psmb8;lgals1;itih2;ikbkg;hgs;hcfc1;gfpt1;fn1;f7;f5;f2;dag1;capza2;c4b;c3;brca1;bmi1;blm;bet1;serpinc1;asgr1;app;apoe;birc2;tpr;gbf1;qsox1;dnajc3 | 3694.92401 | 3767.265 | 185.394 | 1724.89683 | 3702.88491 | 1735.81921 | CONFLICT | 0.487179487 | 0.512820513 |
| 90Day | Death Receptor Signalling | 0.072611 | 0.96227 | 0.15868 | arhgef6;fgd4;vav1;tnfrsf10b;tiam1;sos1;psen2;nfkbia;ikbkg | 4469.39778 | 4161.05 | 3135.19 | 1146.137 | 4336.11238 | 1140.0596 | DOWN | 0.333333333 | 0.666666667 |
| 7Day | Transcription-Coupled Nucleotide Excision Repair (TC-NER) | 0.067874 | 0.97718 | 0.1597 | prpf19;polr2h;uba52 | 3815.36333 | 3964.6 | 2719.93 | 1028.96402 | 3913.27434 | 885.21152 | UP | 1 | 0 |
| 90Day | CTLA4 inhibitory signaling | 0.080986 | 1 | 0.16022 | | | | | | | | | | |
| 90Day | NCAM1 interactions | 0.080986 | 1 | 0.16022 | | | | | | | | | | |
| 90Day | Metal ion SLC transporters | 0.080986 | 1 | 0.16022 | | | | | | | | | | |
| 90Day | Common Pathway of Fibrin Clot Formation | 0.080986 | 1 | 0.16022 | | | | | | | | | | |
| 7Day | DNA Double-Strand Break Repair | 0.086304 | 0.95393 | 0.16049 | ube2n;ube2v2;rnf168;hist1h4h;babam1;hist1h2bc;uba52;rad51ap1;abl1 | 3610.97889 | 3444.79 | 2423.08 | 647.933214 | 3488.58257 | 659.371908 | UP | 0.777777778 | 0.222222222 |
| 28Day | mRNA Splicing - Minor Pathway | 0.94199 | 0.13475 | 0.16108 | rnpc3;sf3b6;snrpd1;polr2a;prpf8;srsf1 | 3946.6835 | 4993.735 | 131.831 | 2170.39278 | 3775.10545 | 2384.96324 | UP | 0.666666667 | 0.333333333 |
| 90Day | RNA Polymerase I Chain Elongation | 0.082007 | 0.96466 | 0.16141 | hist1h4h;hist1h4i;hist1h3c;h2afx;cdk7 | 3197.2378 | 3951.81 | 811.859 | 1388.20317 | 2385.19446 | 1713.34211 | UP | 0.6 | 0.4 |
| 7Day | Role of phospholipids in phagocytosis | 0.10238 | 1 | 0.16152 | | | | | | | | | | |
| 7Day | Cobalamin (Cbl, vitamin B12) transport and metabolism | 0.10238 | 1 | 0.16152 | | | | | | | | | | |
| 7Day | G beta:gamma signalling through PI3Kgamma | 0.092711 | 1 | 0.16186 | | | | | | | | | | |
| 7Day | ADP signalling through P2Y purinoceptor 1 | 0.092711 | 1 | 0.16186 | | | | | | | | | | |
| 7Day | Basigin interactions | 0.092711 | 1 | 0.16186 | | | | | | | | | | |
| 7Day | Activation of G protein gated Potassium channels | 0.092711 | 1 | 0.16186 | | | | | | | | | | |
| 7Day | G protein gated Potassium channels | 0.092711 | 1 | 0.16186 | | | | | | | | | | |
| 7Day | Inhibition of voltage gated Ca2+ channels via Gbeta/gamma subunits | 0.092711 | 1 | 0.16186 | | | | | | | | | | |
| 28Day | O-linked glycosylation | 0.07683 | 0.97333 | 0.162 | c1galt1;sbspon;dag1 | 5078.49333 | 5312.69 | 4256.3 | 733.685912 | 5100.20972 | 728.91463 | UP | 0.666666667 | 0.333333333 |
| 90Day | Mitotic Prometaphase | 0.084425 | 0.9487 | 0.16285 | haus7;cenpu;smc4;tubb6;dctn3;cntrl;tubb4b;cep76;tubb2a;tuba1b;kntc1;nudc;hsp90aa1;sec13;cenpf | 3001.67807 | 3184.54 | 426.32 | 1482.71675 | 3068.64721 | 1625.21055 | UP | 0.933333333 | 0.066666667 |
| 28Day | PI5P, PP2A and IER3 Regulate PI3K/AKT Signaling | 0.073366 | 0.97474 | 0.16325 | il1rap;hbegf;fgf1 | 2030.93933 | 1467.57 | 919.738 | 1475.86252 | 1887.6209 | 1368.24713 | DOWN | 0.333333333 | 0.666666667 |
| 90Day | Nucleotide Excision Repair | 0.073511 | 0.96474 | 0.16365 | pole4;mcrs1;polk;yy1;ino80c;rad23a;cdk7 | 3814.86 | 3652.71 | 1252.26 | 1612.71329 | 3703.59993 | 1422.1654 | CONFLICT | 0.571428571 | 0.428571429 |
| 90Day | DNA Damage Bypass | 0.08799 | 0.97497 | 0.16415 | pole4;polk | 4753.255 | 4753.255 | 3652.71 | 1556.40567 | 3884.77714 | 955.97646 | CONFLICT | 0.5 | 0.5 |
| 90Day | Toll Like Receptor 9 (TLR9) Cascade | 0.071745 | 0.96972 | 0.16448 | irf7;mapk14;nfkbia;ikbkg;btrc | 4394.204 | 4261.96 | 3265.56 | 1021.51429 | 4535.14678 | 1084.60939 | DOWN | 0.4 | 0.6 |
| 90Day | Processing of DNA double-strand break ends | 0.071745 | 0.96972 | 0.16448 | hist1h4h;babam1;ppp4c;hist1h4i;h2afx | 4313.072 | 4006.71 | 3721.17 | 842.236755 | 4116.8701 | 738.037657 | UP | 0.6 | 0.4 |
| 28Day | Organelle biogenesis and maintenance | 0.086545 | 0.95352 | 0.16513 | atp5g2;atp5j2;dynll1;rab11a;bbs9;tubb4b;tubb2a;exoc4;ttbk2 | 3784.97556 | 2903.04 | 2192.92 | 1616.78928 | 3801.04188 | 1646.66451 | UP | 0.666666667 | 0.333333333 |
| 90Day | CD28 dependent PI3K/Akt signaling | 0.07184 | 1 | 0.1653 | | | | | | | | | | |
| 90Day | mTORC1-mediated signalling | 0.07184 | 1 | 0.1653 | | | | | | | | | | |
| 90Day | Cellular hexose transport | 0.07184 | 1 | 0.1653 | | | | | | | | | | |
| 90Day | CD209 (DC-SIGN) signaling | 0.07184 | 1 | 0.1653 | | | | | | | | | | |
| 90Day | Transcriptional regulation by the AP-2 (TFAP2) family of transcription factors | 0.07184 | 1 | 0.1653 | | | | | | | | | | |
| 28Day | Transmission across Chemical Synapses | 0.083771 | 0.9552 | 0.16537 | gria3;lin7c;slc22a1;slc1a2;mdm2;gnb5;glul;slc6a13;adcy9 | 2263.17889 | 1938.66 | 151.142 | 1586.36418 | 2350.06997 | 1505.23149 | DOWN | 0.333333333 | 0.666666667 |

BMD analysis results for functional classification based on dose-responsive genes, using the Reactome database for gene sets in BMDExpress2.2 software.

| Study Day | Gene Set Name | Fisher's Exact Left P-Value | Fisher's Exact Right P-Value | Fisher's Exact Two Tail | Gene Symbols | BMD Mean | BMD Median | BMD Minimum | BMD Standard Deviation | BMD wMean | BMD wSD | Overall Direction | Percent Genes With Overall Direction Up | Percent Genes With Overall Direction Down |
|---|---|---|---|---|---|---|---|---|---|---|---|---|---|---|
| 90Day | Cell-cell junction organization | 0.080873 | 0.9774 | 0.16571 | afdn;ctnnb1 | 2442.127 | 2442.127 | 797.214 | 2326.25827 | 1451.95914 | 1857.58251 | CONFLICT | 0.5 | 0.5 |
| 7Day | Signaling by FGFR4 | 0.93847 | 0.14291 | 0.16599 | mapk3;uba52;ptpn11;ppp2cb;kras;fgf1 | 3937.49667 | 3894.19 | 2647.76 | 815.708654 | 3810.92898 | 853.996178 | UP | 0.666666667 | 0.333333333 |
| 90Day | Detoxification of Reactive Oxygen Species | 0.93844 | 0.1444 | 0.16606 | txnrd1;nox4;txn1;gstp2;gsr;prdx6 | 3570.695 | 3583.44 | 1676.13 | 1519.56913 | 3616.58845 | 1660.04604 | CONFLICT | 0.5 | 0.5 |
| 7Day | Translation | 0.9369 | 0.10073 | 0.16622 | eif3m;mrpl16;mrpl1;eif3j1;rps25;mrpl47;mrps17;eif1ax;mrps36;mrps31;eif3b;mrpl2;rps3;eif2s3x;eif3l;eif5;rps12;gspt1;eif4ebp1;eif4a2 | 3607.17663 | 3885.79 | 84.8066 | 1418.08335 | 3571.07351 | 1295.32571 | UP | 0.85 | 0.15 |
| 28Day | Digestion and absorption | 0.10232 | 1 | 0.16716 |  |  |  |  |  |  |  |  |  |  |
| 7Day | SUMOylation of intracellular receptors | 0.076021 | 1 | 0.1678 |  |  |  |  |  |  |  |  |  |  |
| 7Day | Integrin alphaIIb beta3 signaling | 0.076021 | 1 | 0.1678 |  |  |  |  |  |  |  |  |  |  |
| 7Day | Integrin signaling | 0.076021 | 1 | 0.1678 |  |  |  |  |  |  |  |  |  |  |
| 7Day | TNFs bind their physiological receptors | 0.076021 | 1 | 0.1678 |  |  |  |  |  |  |  |  |  |  |
| 7Day | Cytosolic sulfonation of small molecules | 0.076021 | 1 | 0.1678 |  |  |  |  |  |  |  |  |  |  |
| 7Day | Ion transport by P-type ATPases | 0.097922 | 0.97125 | 0.1679 | calm3;calm2 | 3983.44 | 3983.44 | 3050.32 | 1319.63096 | 3556.9103 | 1173.69957 | CONFLICT | 0.5 | 0.5 |
| 7Day | Histidine catabolism | 0.96746 | 0.16983 | 0.16983 | amdhd1;uroc1 | 3016.64 | 3016.64 | 2981.91 | 49.115637 | 3019.12941 | 48.9892991 | DOWN | 0 | 1 |
| 7Day | Mitochondrial protein import | 0.96746 | 0.16983 | 0.16983 | pitrm1;ldhd | 3757.27 | 3757.27 | 3743.17 | 19.9404112 | 3753.77075 | 19.3165876 | DOWN | 0 | 1 |
| 7Day | alpha-linolenic acid (ALA) metabolism | 0.96746 | 0.16983 | 0.16983 | fads1;fads2 | 55.99745 | 55.99745 | 55.2305 | 1.08463109 | 56.0557676 | 1.08149097 | DOWN | 0 | 1 |
| 7Day | Synthesis of UDP-N-acetyl-glucosamine | 0.96746 | 0.16983 | 0.16983 | gnpnat1;gfpt1 | 3426.45 | 3426.45 | 3132.03 | 416.372757 | 3435.4841 | 416.176697 | UP | 1 | 0 |
| 7Day | Glutathione synthesis and recycling | 0.96746 | 0.16983 | 0.16983 | gss;gclc | 2729.28 | 2729.28 | 2300.86 | 605.877374 | 2748.44746 | 605.270691 | UP | 1 | 0 |
| 7Day | Stabilization of p53 | 0.96746 | 0.16983 | 0.16983 | cop1;uba52 | 4194.635 | 4194.635 | 3627.71 | 801.753024 | 4115.83314 | 793.970052 | UP | 1 | 0 |
| 7Day | SCF-beta-TrCP mediated degradation of Emi1 | 0.96746 | 0.16983 | 0.16983 | uba52;btrc | 4484.31 | 4484.31 | 4207.06 | 392.09071 | 4446.04923 | 388.339223 | UP | 1 | 0 |
| 28Day | RNA Polymerase III Transcription | 0.082597 | 1 | 0.17117 |  |  |  |  |  |  |  |  |  |  |
| 28Day | RNA Polymerase III Transcription Initiation | 0.082597 | 1 | 0.17117 |  |  |  |  |  |  |  |  |  |  |
| 28Day | Activation of NMDA receptors and postsynaptic events | 0.082597 | 1 | 0.17117 |  |  |  |  |  |  |  |  |  |  |
| 28Day | Rho GTPase cycle | 0.080681 | 0.96483 | 0.17162 | arhgap45;dlc1;a2m;arhgdia;cdc42 | 3661.188 | 4971.84 | 160.43 | 2311.53571 | 4076.2988 | 2025.40877 | UP | 0.8 | 0.2 |
| 28Day | Purine salvage | 0.96493 | 0.17175 | 0.17175 | hprt;adk | 2990.7 | 2990.7 | 2420.29 | 806.681558 | 3160.53958 | 770.093613 | CONFLICT | 0.5 | 0.5 |
| 28Day | Tryptophan catabolism | 0.96493 | 0.17175 | 0.17175 | tdo2;haao | 2669.151 | 2669.151 | 887.232 | 2520.01402 | 3576.30393 | 2169.01308 | DOWN | 0 | 1 |
| 28Day | Synthesis of PE | 0.96493 | 0.17175 | 0.17175 | phospho1;etnk2 | 3830.44 | 3830.44 | 2962.74 | 1227.11311 | 3824.40463 | 1227.08342 | DOWN | 0 | 1 |
| 28Day | Chylomicron remodeling | 0.96493 | 0.17175 | 0.17175 | apob;apoe | 2075.9425 | 2075.9425 | 939.205 | 1607.58959 | 1295.41266 | 1168.71324 | DOWN | 0 | 1 |
| 28Day | Translocation of ZAP-70 to Immunological synapse | 0.96493 | 0.17175 | 0.17175 | h2-ab1;h2-aa | 3461.14 | 3461.14 | 3245.73 | 304.635743 | 3292.13505 | 188.885132 | DOWN | 0 | 1 |
| 90Day | Metalloprotease DUBs | 0.090885 | 0.98296 | 0.17186 | babam1 | 5800.02 | 5800.02 | 5800.02 |  | 5800.02 |  | UP | 1 | 0 |
| 90Day | Amino acid transport across the plasma membrane | 0.090885 | 0.98296 | 0.17186 | slc6a12 | 3445.15 | 3445.15 | 3445.15 |  | 3445.15 |  | DOWN | 0 | 1 |
| 90Day | Gamma carboxylation, hypusine formation and arylsulfatase activation | 0.090885 | 0.98296 | 0.17186 | f7 | 3350.52 | 3350.52 | 3350.52 |  | 3350.52 |  | DOWN | 0 | 1 |
| 90Day | Separation of Sister Chromatids | 0.079661 | 0.95679 | 0.17297 | cenpu;anapc10;tubb6;tubb4b;tubb2a;tuba1b;kntc1;nudc;sec13;cenpf | 2905.4621 | 2971.72 | 779.791 | 1448.96614 | 2908.06114 | 1718.42046 | UP | 0.9 | 0.1 |
| 7Day | Synthesis of Leukotrienes (LT) and Eoxins (EX) | 0.068838 | 1 | 0.17319 |  |  |  |  |  |  |  |  |  |  |
| 28Day | DNA Damage/Telomere Stress Induced Senescence | 0.09833 | 0.97078 | 0.17338 | acd;hist1h4i | 5109.845 | 5109.845 | 4371.28 | 1044.48864 | 5169.31387 | 1041.09722 | DOWN | 0 | 1 |
| 90Day | GRB2 events in EGFR signaling | 0.9501 | 0.17371 | 0.17371 | tgfa;sos1;areg | 4009.27667 | 3970.39 | 2162.51 | 1866.51383 | 3698.23096 | 2070.13409 | UP | 0.666666667 | 0.333333333 |
| 28Day | Activation of Matrix Metalloproteinases | 0.076906 | 1 | 0.17426 |  |  |  |  |  |  |  |  |  |  |
| 28Day | RHO GTPases activate PKNs | 0.089004 | 0.97411 | 0.17434 | hist1h4i;pdpk1 | 3020.699 | 3020.699 | 192.988 | 3998.98725 | 4607.8042 | 3309.69684 | DOWN | 0 | 1 |
| 28Day | Platelet homeostasis | 0.089004 | 0.97411 | 0.17434 | apob;gnb5 | 946.4265 | 946.4265 | 939.205 | 10.2127432 | 947.355903 | 10.1278105 | CONFLICT | 0.5 | 0.5 |
| 90Day | Activation of NMDA receptors and postsynaptic events | 0.08254 | 0.98489 | 0.17441 | camkk2 | 98.0082 | 98.0082 | 98.0082 |  | 98.0082 |  | DOWN | 0 | 1 |
| 7Day | Dual Incision in GG-NER | 0.10608 | 0.9791 | 0.17526 | uba52 | 4761.56 | 4761.56 | 4761.56 |  | 4761.56 |  | UP | 1 | 0 |
| 7Day | Cargo trafficking to the periciliary membrane | 0.10608 | 0.9791 | 0.17526 | rab11a | 4542.35 | 4542.35 | 4542.35 |  | 4542.35 |  | UP | 1 | 0 |

BMD analysis results for functional classification based on dose-responsive genes, using the Reactome database for gene sets in BMDExpress2.2 software.

| Study Day | Gene Set Name | Fisher's Exact Left P-Value | Fisher's Exact Right P-Value | Fisher's Exact Two Tail | Gene Symbols | BMD Mean | BMD Median | BMD Minimum | BMD Standard Deviation | BMD wMean | BMD wSD | Overall Direction | Percent Genes With Overall Direction Up | Percent Genes With Overall Direction Down |
|---|---|---|---|---|---|---|---|---|---|---|---|---|---|---|
| 7Day | DAP12 interactions | 0.090553 | 0.98287 | 0.17665 | kras | 4158.71 | 4158.71 | 4158.71 |  | 4158.71 |  | UP | 1 | 0 |
| 7Day | Homologous DNA Pairing and Strand Exchange | 0.090553 | 0.98287 | 0.17665 | rad51ap1 | 3877.33 | 3877.33 | 3877.33 |  | 3877.33 |  | UP | 1 | 0 |
| 28Day | Recruitment of mitotic centrosome proteins and complexes | 0.080487 | 0.97708 | 0.17691 | dynll1;tubb4b | 4075.495 | 4075.495 | 2359.45 | 2426.85411 | 4561.33816 | 2327.55961 | UP | 1 | 0 |
| 28Day | Centrosome maturation | 0.080487 | 0.97708 | 0.17691 | dynll1;tubb4b | 4075.495 | 4075.495 | 2359.45 | 2426.85411 | 4561.33816 | 2327.55961 | UP | 1 | 0 |
| 28Day | Gene Silencing by RNA | 0.080487 | 0.97708 | 0.17691 | hist1h4i;polr2a | 5444.54 | 5444.54 | 5040.67 | 571.158431 | 5494.50555 | 566.770537 | CONFLICT | 0.5 | 0.5 |
| 28Day | Signaling by FGFR | 0.080487 | 0.97708 | 0.17691 | polr2a;fgf1 | 3254.12 | 3254.12 | 1467.57 | 2526.56324 | 2657.99173 | 2381.76069 | CONFLICT | 0.5 | 0.5 |
| 7Day | Synthesis of PS | 0.99113 | 0.17958 | 0.17958 | ptdss1 | 3684.01 | 3684.01 | 3684.01 |  | 3684.01 |  | DOWN | 0 | 1 |
| 7Day | Pre-NOTCH Transcription and Translation | 0.99113 | 0.17958 | 0.17958 | prkci | 3409.24 | 3409.24 | 3409.24 |  | 3409.24 |  | UP | 1 | 0 |
| 7Day | Signaling by NOTCH4 | 0.99113 | 0.17958 | 0.17958 | ywhaz | 2726.98 | 2726.98 | 2726.98 |  | 2726.98 |  | UP | 1 | 0 |
| 7Day | Biosynthesis of DHA-derived sulfido conjugates | 0.99113 | 0.17958 | 0.17958 | gstm4 | 2629.52 | 2629.52 | 2629.52 |  | 2629.52 |  | UP | 1 | 0 |
| 7Day | Biosynthesis of maresin conjugates in tissue regeneration (MCTR) | 0.99113 | 0.17958 | 0.17958 | gstm4 | 2629.52 | 2629.52 | 2629.52 |  | 2629.52 |  | UP | 1 | 0 |
| 7Day | NOTCH4 Activation and Transmission of Signal to the Nucleus | 0.99113 | 0.17958 | 0.17958 | ywhaz | 2726.98 | 2726.98 | 2726.98 |  | 2726.98 |  | UP | 1 | 0 |
| 7Day | mRNA Editing: A to I Conversion | 0.99113 | 0.17958 | 0.17958 | adar | 3802.37 | 3802.37 | 3802.37 |  | 3802.37 |  | UP | 1 | 0 |
| 7Day | C6 deamination of adenosine | 0.99113 | 0.17958 | 0.17958 | adar | 3802.37 | 3802.37 | 3802.37 |  | 3802.37 |  | UP | 1 | 0 |
| 7Day | Formation of editosomes by ADAR proteins | 0.99113 | 0.17958 | 0.17958 | adar | 3802.37 | 3802.37 | 3802.37 |  | 3802.37 |  | UP | 1 | 0 |
| 7Day | Regulation of Glucokinase by Glucokinase Regulatory Protein | 0.99113 | 0.17958 | 0.17958 | gckr | 3375.32 | 3375.32 | 3375.32 |  | 3375.32 |  | DOWN | 0 | 1 |
| 7Day | Synthesis of bile acids and bile salts via 24-hydroxycholesterol | 0.99113 | 0.17958 | 0.17958 | cyp39a1 | 3113.35 | 3113.35 | 3113.35 |  | 3113.35 |  | DOWN | 0 | 1 |
| 7Day | Biogenic amines are oxidatively deaminated to aldehydes by MAOA and MAOB | 0.99113 | 0.17958 | 0.17958 | maob | 46.9364 | 46.9364 | 46.9364 |  | 46.9364 |  | DOWN | 0 | 1 |
| 7Day | Transfer of LPS from LBP carrier to CD14 | 0.99113 | 0.17958 | 0.17958 | lbp | 5240.82 | 5240.82 | 5240.82 |  | 5240.82 |  | DOWN | 0 | 1 |
| 7Day | Beta oxidation of myristoyl-CoA to lauroyl-CoA | 0.99113 | 0.17958 | 0.17958 | hadha | 197.056 | 197.056 | 197.056 |  | 197.056 |  | DOWN | 0 | 1 |
| 7Day | Linoleic acid (LA) metabolism | 0.99113 | 0.17958 | 0.17958 | elovl5 | 212.399 | 212.399 | 212.399 |  | 212.399 |  | DOWN | 0 | 1 |
| 90Day | Cell surface interactions at the vascular wall | 0.087018 | 0.95537 | 0.17982 | ceacam2;apob;tnfrsf10b;tek;sdc4;sos1;cd74;fn1 | 2382.25025 | 2162.38 | 175.96 | 2004.49059 | 3360.58389 | 1812.67216 | DOWN | 0.25 | 0.75 |
| 7Day | Peroxisomal lipid metabolism | 0.95716 | 0.11773 | 0.18006 | decr2;slc25a17;phyh;hsd17b4;pecr | 2226.2346 | 2689.11 | 185.683 | 1346.51069 | 2493.92571 | 1080.16661 | DOWN | 0.4 | 0.6 |
| 7Day | Synthesis of active ubiquitin: roles of E1 and E2 enzymes | 0.95716 | 0.11773 | 0.18006 | ube2k;ube2a;ube2e3;uba52;cdc34 | 2978.584 | 3066.12 | 1018.89 | 1374.41615 | 3333.18209 | 1060.44253 | UP | 1 | 0 |
| 7Day | Negative regulation of FGFR4 signaling | 0.95716 | 0.11773 | 0.18006 | mapk3;uba52;ptpn11;ppp2cb;fgf1 | 3893.254 | 3629.67 | 2647.76 | 903.905503 | 3770.28016 | 910.359639 | UP | 0.6 | 0.4 |
| 28Day | O-linked glycosylation of mucins | 0.10632 | 0.97876 | 0.18091 | c1galt1 | 4256.3 | 4256.3 | 4256.3 |  | 4256.3 |  | UP | 1 | 0 |
| 28Day | GABA receptor activation | 0.10632 | 0.97876 | 0.18091 | adcy9 | 4220.6 | 4220.6 | 4220.6 |  | 4220.6 |  | DOWN | 0 | 1 |
| 28Day | NoRC negatively regulates rRNA expression | 0.10046 | 0.98022 | 0.18113 | hist1h4i | 5848.41 | 5848.41 | 5848.41 |  | 5848.41 |  | DOWN | 0 | 1 |
| 28Day | Regulation of TP53 Activity through Phosphorylation | 0.10046 | 0.98022 | 0.18113 | mdm2 | 2266.61 | 2266.61 | 2266.61 |  | 2266.61 |  | UP | 1 | 0 |
| 90Day | RUNX3 regulates p14-ARF | 0.96476 | 0.18192 | 0.18192 | brd2;cbfb | 4716.23 | 4716.23 | 4070.59 | 913.072844 | 4385.61638 | 784.277557 | UP | 1 | 0 |
| 28Day | Signaling by NTRK1 (TRKA) | 0.094894 | 0.98159 | 0.18193 | mapkapk2 | 5375 | 5375 | 5375 |  | 5375 |  | DOWN | 0 | 1 |
| 90Day | The canonical retinoid cycle in rods (twilight vision) | 0.95413 | 0.12548 | 0.18201 | rdh7;ttr;rbp1;rdh11;abca4 | 4303.324 | 4135.51 | 2528.1 | 1361.66594 | 4808.5251 | 1316.78938 | UP | 0.8 | 0.2 |
| 7Day | Metabolism of amino acids and derivatives | 0.92825 | 0.10769 | 0.18209 | lias;mccc2;dmgdh;amdhd1;kyat1;lipt2;bhmt2;txn2;prodh2;txnrd1;pdhx;gcdh;ahcy;uroc1;aldh4a1;sardh;nqo1;hao1;gnmt;dld;cdo1;bckdha;amd1;gm4737;aldh7a1 | 2749.40854 | 2981.91 | 84.5274 | 1675.36876 | 2767.1782 | 1542.25177 | DOWN | 0.32 | 0.68 |
| 90Day | Toll Like Receptor 10 (TLR10) Cascade | 0.091835 | 0.96316 | 0.1821 | mapk14;nfkbia;ikbkg;btrc | 4070.33 | 3931.53 | 3265.56 | 831.881085 | 4282.38479 | 1027.24106 | DOWN | 0.25 | 0.75 |
| 90Day | Toll Like Receptor 5 (TLR5) Cascade | 0.091835 | 0.96316 | 0.1821 | mapk14;nfkbia;ikbkg;btrc | 4070.33 | 3931.53 | 3265.56 | 831.881085 | 4282.38479 | 1027.24106 | DOWN | 0.25 | 0.75 |
| 90Day | MyD88 cascade initiated on plasma membrane | 0.091835 | 0.96316 | 0.1821 | mapk14;nfkbia;ikbkg;btrc | 4070.33 | 3931.53 | 3265.56 | 831.881085 | 4282.38479 | 1027.24106 | DOWN | 0.25 | 0.75 |

BMD analysis results for functional classification based on dose-responsive genes, using the Reactome database for gene sets in BMDExpress2.2 software.

| Study Day | Gene Set Name | Fisher's Exact Left P-Value | Fisher's Exact Right P-Value | Fisher's Exact Two Tail | Gene Symbols | BMD Mean | BMD Median | BMD Minimum | BMD Standard Deviation | BMD wMean | BMD wSD | Overall Direction | Percent Genes With Overall Direction Up | Percent Genes With Overall Direction Down |
|---|---|---|---|---|---|---|---|---|---|---|---|---|---|---|
| 28Day | Presynaptic phase of homologous DNA pairing and strand exchange | 0.95693 | 0.11619 | 0.18286 | rmi1;rad51d;rad51;brca1;blm | 3513.5312 | 3769.36 | 692.086 | 1790.07678 | 3877.73216 | 1143.86555 | UP | 1 | 0 |
| 28Day | SIRT1 negatively regulates rRNA expression | 0.089621 | 0.98286 | 0.1833 | hist1h4i | 5848.41 | 5848.41 | 5848.41 | | 5848.41 | | DOWN | 0 | 1 |
| 28Day | RNA Polymerase I Promoter Opening | 0.089621 | 0.98286 | 0.1833 | hist1h4i | 5848.41 | 5848.41 | 5848.41 | | 5848.41 | | DOWN | 0 | 1 |
| 90Day | Cell junction organization | 0.085615 | 0.96607 | 0.1837 | arhgef6;afdn;ctnnb1;actn1 | 4037.9335 | 4700.81 | 797.214 | 2295.03793 | 4190.02407 | 2312.13407 | DOWN | 0.25 | 0.75 |
| 90Day | Transcriptional regulation by small RNAs | 0.085615 | 0.96607 | 0.1837 | hist1h4h;hist1h4i;hist1h3c;h2afx | 3214.00725 | 3979.26 | 811.859 | 1602.37406 | 2298.31583 | 1843.92338 | CONFLICT | 0.5 | 0.5 |
| 90Day | MyD88:MAL(TIRAP) cascade initiated on plasma membrane | 0.085615 | 0.96607 | 0.1837 | mapk14;nfkbia;ikbkg;btrc | 4070.33 | 3931.53 | 3265.56 | 831.881085 | 4282.38479 | 1027.24106 | DOWN | 0.25 | 0.75 |
| 90Day | Toll Like Receptor TLR1:TLR2 Cascade | 0.085615 | 0.96607 | 0.1837 | mapk14;nfkbia;ikbkg;btrc | 4070.33 | 3931.53 | 3265.56 | 831.881085 | 4282.38479 | 1027.24106 | DOWN | 0.25 | 0.75 |
| 90Day | Toll Like Receptor TLR6:TLR2 Cascade | 0.085615 | 0.96607 | 0.1837 | mapk14;nfkbia;ikbkg;btrc | 4070.33 | 3931.53 | 3265.56 | 831.881085 | 4282.38479 | 1027.24106 | DOWN | 0.25 | 0.75 |
| 90Day | Toll Like Receptor 2 (TLR2) Cascade | 0.085615 | 0.96607 | 0.1837 | mapk14;nfkbia;ikbkg;btrc | 4070.33 | 3931.53 | 3265.56 | 831.881085 | 4282.38479 | 1027.24106 | DOWN | 0.25 | 0.75 |
| 90Day | Synthesis of DNA | 0.085615 | 0.96607 | 0.1837 | gins1;anapc10;pole4;orc6 | 3885.0525 | 4279.405 | 1127.6 | 1984.54106 | 4057.44037 | 1374.34774 | UP | 0.75 | 0.25 |
| 90Day | Senescence-Associated Secretory Phenotype (SASP) | 0.093851 | 0.9558 | 0.18376 | hist1h4h;anapc10;hist1h4i;hist1h3c;h2afx;cdkn1a | 3026.7015 | 3979.26 | 811.859 | 1683.31454 | 1966.58137 | 1670.51904 | UP | 0.666666667 | 0.333333333 |
| 28Day | Cellular responses to external stimuli | 0.087259 | 0.94296 | 0.18445 | hikeshi;dynll1;gm45902;txnrd1;acd;hist1h4i;map2k4;tubb4b;tubb2a;cdc27;p4hb;mdm2;mapkapk2;gstp1;gstp2;rb1cc1;capza2;bmi1;atg5;tpr | 4149.3983 | 4262.915 | 691.166 | 1621.85619 | 4028.34302 | 1775.09832 | UP | 0.7 | 0.3 |
| 90Day | UCH proteinases | 0.088232 | 0.95884 | 0.18485 | psmd8;mcrs1;psmc4;psmf1;yy1;ino80c | 2661.14467 | 2213.18 | 186.178 | 2068.27993 | 2538.39981 | 2012.24745 | UP | 0.833333333 | 0.166666667 |
| 28Day | Negative epigenetic regulation of rRNA expression | 0.084622 | 0.98404 | 0.18522 | hist1h4i | 5848.41 | 5848.41 | 5848.41 | | 5848.41 | | DOWN | 0 | 1 |
| 28Day | Class B/2 (Secretin family receptors) | 0.084622 | 0.98404 | 0.18522 | gnb5 | 953.648 | 953.648 | 953.648 | | 953.648 | | UP | 1 | 0 |
| 7Day | Transport of bile salts and organic acids, metal ions and amine compounds | 0.10361 | 0.95725 | 0.1854 | slc5a3;slc39a2;slc22a12;slc22a1 | 4744.3375 | 4897.26 | 3194.01 | 1274.2061 | 4760.1461 | 1346.31062 | UP | 0.75 | 0.25 |
| 7Day | Deubiquitination | 0.09411 | 0.94029 | 0.18561 | usp16;babam1;tomm20;psmd5;psmd6;hist2h2ac;taf10;psmc4;ino80c;vdac3;vdac2;uba52;tgfbr1;pten;psmc2;hist2h2aa1;cdc25a | 3774.16353 | 3567.39 | 1811.97 | 1174.89537 | 3578.1711 | 1272.52603 | UP | 0.941176471 | 0.058823529 |
| 7Day | Metabolism of cofactors | 0.94305 | 0.18638 | 0.18638 | hsp90aa1;calm3;calm2 | 2990.83 | 3050.32 | 1005.61 | 1956.15357 | 2746.7427 | 1679.58489 | UP | 0.666666667 | 0.333333333 |
| 7Day | Interleukin-4 and Interleukin-13 signaling | 0.94305 | 0.18638 | 0.18638 | hsp90b1;stat1;jak1 | 3108.04333 | 3554.32 | 1852.94 | 1101.96366 | 3490.72292 | 752.388279 | UP | 1 | 0 |
| 7Day | SCF(Skp2)-mediated degradation of p27/p21 | 0.94305 | 0.18638 | 0.18638 | uba52;cdkn1a;ccne2 | 4059.46 | 4598.19 | 2818.63 | 1077.69047 | 4059.31666 | 1056.86455 | UP | 1 | 0 |
| 7Day | PD-1 signaling | 0.94305 | 0.18638 | 0.18638 | ptpn11;h2-ab1;h2-aa | 2584.69667 | 2261.36 | 1863.06 | 926.627041 | 2807.18587 | 946.421592 | DOWN | 0.333333333 | 0.666666667 |
| 7Day | Metabolism of nitric oxide | 0.94305 | 0.18638 | 0.18638 | hsp90aa1;calm3;calm2 | 2990.83 | 3050.32 | 1005.61 | 1956.15357 | 2746.7427 | 1679.58489 | UP | 0.666666667 | 0.333333333 |
| 7Day | eNOS activation and regulation | 0.94305 | 0.18638 | 0.18638 | hsp90aa1;calm3;calm2 | 2990.83 | 3050.32 | 1005.61 | 1956.15357 | 2746.7427 | 1679.58489 | UP | 0.666666667 | 0.333333333 |
| 7Day | Negative regulation of the PI3K/AKT network | 0.10099 | 0.95162 | 0.18741 | mapk3;ptpn11;pten;ppp2cb;il1rap;fgf1 | 3001.73567 | 3400.86 | 131.024 | 1575.82479 | 2859.8929 | 1611.80192 | CONFLICT | 0.5 | 0.5 |
| 28Day | Activated PKN1 stimulates transcription of AR (androgen receptor) regulated genes KLK2 and KLK3 | 0.079886 | 0.98515 | 0.18767 | hist1h4i | 5848.41 | 5848.41 | 5848.41 | | 5848.41 | | DOWN | 0 | 1 |
| 28Day | Mitochondrial Fatty Acid Beta-Oxidation | 0.95193 | 0.12621 | 0.18828 | echs1;ndufab1;acaa2;acsf2;acadl | 2448.3922 | 2777.52 | 802.301 | 1178.11057 | 1949.93558 | 1216.2426 | DOWN | 0 | 1 |
| 7Day | VEGFR2 mediated vascular permeability | 0.95012 | 0.13186 | 0.1883 | pak2;hsp90aa1;ctnnb1;calm3;calm2 | 2313.04264 | 2538.2 | 54.5232 | 1883.00734 | 2084.58132 | 1819.40898 | UP | 0.6 | 0.4 |
| 7Day | Negative regulation of FGFR1 signaling | 0.95012 | 0.13186 | 0.1883 | mapk3;uba52;ptpn11;ppp2cb;fgf1 | 3893.254 | 3629.67 | 2647.76 | 903.905503 | 3770.28016 | 910.359639 | UP | 0.6 | 0.4 |
| 7Day | Mitotic Spindle Checkpoint | 0.091239 | 0.95697 | 0.18866 | clasp2;cenpk;cdc27;ppp2cb;kif2a;xpo1 | 3765.72 | 3796.245 | 2692.16 | 665.945287 | 3744.07612 | 688.039984 | UP | 0.833333333 | 0.166666667 |
| 90Day | Cytochrome P450 - arranged by substrate type | 0.93537 | 0.11094 | 0.1888 | cyp4f16;cyp3a25;cyp39a1;cyp3a41a;cyp2c54;cyp4a12a;cyp4a12b;cyp2f2;cyp2e1;cyp2d9;cyp2c38;cyp2c37;cyp1a2;cyp2c69;cyp3a41b | 2806.3334 | 3465.22 | 343.937 | 1513.9795 | 2787.20665 | 1535.91861 | CONFLICT | 0.466666667 | 0.533333333 |
| 28Day | Synthesis of (16-20)-hydroxyeicosatetraenoic acids (HETE) | 0.94009 | 0.18894 | 0.18894 | cyp4a12b;cyp2c37;cyp2c29 | 4357.50333 | 4766.57 | 2751.06 | 1445.97832 | 3990.66484 | 1430.78399 | UP | 0.666666667 | 0.333333333 |
| 28Day | Glycolysis | 0.94009 | 0.18894 | 0.18894 | pfkl;gpi1;bpgm | 4249.99333 | 3997.94 | 3982.32 | 450.16425 | 4205.69128 | 429.005103 | DOWN | 0.333333333 | 0.666666667 |

BMD analysis results for functional classification based on dose-responsive genes, using the Reactome database for gene sets in BMDExpress2.2 software.

| Study Day | Gene Set Name | Fisher's Exact Left P-Value | Fisher's Exact Right P-Value | Fisher's Exact Two Tail | Gene Symbols | BMD Mean | BMD Median | BMD Minimum | BMD Standard Deviation | BMD wMean | BMD wSD | Overall Direction | Percent Genes With Overall Direction Up | Percent Genes With Overall Direction Down |
|---|---|---|---|---|---|---|---|---|---|---|---|---|---|---|
| 7Day | Plasma lipoprotein assembly, remodeling, and clearance | 0.93114 | 0.13498 | 0.19063 | npc2;apoa5;angptl8;apob;pcsk5;ldlr;ces3b;apoe;apoc1 | 3412.35067 | 3764.93 | 113.316 | 1492.73573 | 3725.10131 | 1001.45029 | DOWN | 0.222222222 | 0.777777778 |
| 28Day | Electron transport from NADPH to Ferredoxin | 0.98653 | 0.19214 | 0.19214 | fdxr | 5126.12 | 5126.12 | 5126.12 |  | 5126.12 |  | DOWN | 0 | 1 |
| 28Day | Activation of BIM and translocation to mitochondria | 0.98653 | 0.19214 | 0.19214 | dynll1 | 5791.54 | 5791.54 | 5791.54 |  | 5791.54 |  | UP | 1 | 0 |
| 28Day | MASTL Facilitates Mitotic Progression | 0.98653 | 0.19214 | 0.19214 | arpp19 | 2388.34 | 2388.34 | 2388.34 |  | 2388.34 |  | UP | 1 | 0 |
| 28Day | VLDL assembly | 0.98653 | 0.19214 | 0.19214 | apob | 939.205 | 939.205 | 939.205 |  | 939.205 |  | DOWN | 0 | 1 |
| 28Day | Threonine catabolism | 0.98653 | 0.19214 | 0.19214 | sds | 3285.87 | 3285.87 | 3285.87 |  | 3285.87 |  | DOWN | 0 | 1 |
| 28Day | Activation of NIMA Kinases NEK9, NEK6, NEK7 | 0.98653 | 0.19214 | 0.19214 | nek6 | 3203.61 | 3203.61 | 3203.61 |  | 3203.61 |  | UP | 1 | 0 |
| 28Day | Progressive trimming of alpha-1,2-linked mannose residues from Man9/8/7GlcNAc2 to produce Man5GlcNAc2 | 0.98653 | 0.19214 | 0.19214 | man1a | 185.394 | 185.394 | 185.394 |  | 185.394 |  | DOWN | 0 | 1 |
| 28Day | Formation of the active cofactor, UDP-glucuronate | 0.98653 | 0.19214 | 0.19214 | ugdh | 950.22 | 950.22 | 950.22 |  | 950.22 |  | UP | 1 | 0 |
| 28Day | Activation of AMPA receptors | 0.98653 | 0.19214 | 0.19214 | gria3 | 2052.57 | 2052.57 | 2052.57 |  | 2052.57 |  | UP | 1 | 0 |
| 28Day | Interleukin-33 signaling | 0.98653 | 0.19214 | 0.19214 | il1rap | 3705.51 | 3705.51 | 3705.51 |  | 3705.51 |  | DOWN | 0 | 1 |
| 28Day | Abacavir transmembrane transport | 0.98653 | 0.19214 | 0.19214 | slc22a1 | 1681.65 | 1681.65 | 1681.65 |  | 1681.65 |  | DOWN | 0 | 1 |
| 28Day | Hemostasis | 0.092971 | 0.93424 | 0.19294 | spp2;cdc37l1;ola1;f12;abcc4;apob;a2m;tubb4b;tubb2a;trf;tnfrsf10b;serpina1e;serpina1b;proc;pdpk1;itih4;cd74;gnb5;fn1;f7;f5;f2;clu;cdc42;capza2;serpinc1;app;anxa5;jmjd1c;qsox1 | 2816.87093 | 2683.265 | 192.988 | 1800.84791 | 2779.45146 | 1813.3181 | DOWN | 0.3 | 0.7 |
| 90Day | Plasma lipoprotein remodeling | 0.94517 | 0.14315 | 0.19329 | apob;pcsk5;lipc;apoe;apoc3 | 2867.376 | 3093.17 | 175.96 | 2035.57627 | 3179.0703 | 1745.69841 | DOWN | 0 | 1 |
| 90Day | DNA Replication | 0.10062 | 0.94544 | 0.19574 | gins1;anapc10;pole4;psmd8;orc6;dbf4;e2f2;psmc4;psmf1 | 3041.22978 | 3031.27 | 186.178 | 1836.77776 | 2813.06537 | 1625.4728 | UP | 0.888888889 | 0.111111111 |
| 90Day | Signaling by Retinoic Acid | 0.92322 | 0.14852 | 0.19668 | rdh7;pdk4;adh4;aldh1a7;aldh8a1;pdk1;rxrg;rarg;rdh11 | 3921.77556 | 3345.98 | 2740.9 | 1196.95376 | 3809.69662 | 1289.44478 | UP | 0.666666667 | 0.333333333 |
| 28Day | Beta-oxidation of very long chain fatty acids | 0.95556 | 0.19722 | 0.19722 | decr2;acox1 | 2334.455 | 2334.455 | 1680.03 | 925.496711 | 1994.69491 | 790.993253 | DOWN | 0 | 1 |
| 28Day | Ethanol oxidation | 0.95556 | 0.19722 | 0.19722 | adh4;aldh2 | 2764.9895 | 2764.9895 | 541.929 | 3143.88231 | 4119.97938 | 2492.38858 | DOWN | 0 | 1 |
| 28Day | Lysine catabolism | 0.95556 | 0.19722 | 0.19722 | phykpl;aldh7a1 | 3903.99 | 3903.99 | 3472.64 | 610.02102 | 4099.52937 | 543.741075 | CONFLICT | 0.5 | 0.5 |
| 28Day | Triglyceride biosynthesis | 0.95556 | 0.19722 | 0.19722 | dgat2;agmo | 1526.6865 | 1526.6865 | 163.973 | 1927.16791 | 2004.73883 | 1804.69059 | DOWN | 0 | 1 |
| 28Day | IRAK1 recruits IKK complex | 0.95556 | 0.19722 | 0.19722 | ube2n;ikbkg | 5342.195 | 5342.195 | 5266.71 | 106.751911 | 5380.12192 | 92.2987948 | CONFLICT | 0.5 | 0.5 |
| 28Day | IRAK1 recruits IKK complex upon TLR7/8 or 9 stimulation | 0.95556 | 0.19722 | 0.19722 | ube2n;ikbkg | 5342.195 | 5342.195 | 5266.71 | 106.751911 | 5380.12192 | 92.2987948 | CONFLICT | 0.5 | 0.5 |
| 90Day | PIP3 activates AKT signaling | 0.092371 | 0.94333 | 0.19731 | klb;cbx6;irs2;gatad2b;vav1;tgfa;nrg1;pml;mdm2;il1rap;hdac2;gab1;fgf1;cdkn1a;areg | 2221.70409 | 2684.35 | 74.8133 | 1645.65734 | 2027.86438 | 1539.35228 | CONFLICT | 0.533333333 | 0.466666667 |
| 7Day | CLEC7A (Dectin-1) signaling | 0.93674 | 0.1376 | 0.19815 | ube2n;pycard;uba52;cdc34;calm3;calm2;btrc | 3732.51571 | 4207.06 | 1018.89 | 1389.83645 | 3794.07644 | 919.371398 | UP | 0.714285714 | 0.285714286 |
| 90Day | ER to Golgi Anterograde Transport | 0.10211 | 0.93999 | 0.19837 | trappc6b;lman1;tubb6;stx17;dctn3;tubb4b;tubb2a;tuba1b;tgfa;serpina1e;areg;sec13 | 2832.3325 | 2460.705 | 779.791 | 1543.41316 | 2462.75302 | 1445.0997 | UP | 0.75 | 0.25 |
| 90Day | Metabolism of nucleotides | 0.91896 | 0.13468 | 0.19897 | pnp2;dpys;nudt5;txnrd1;dnph1;gmps;txn1;tk1;nudt15;nudt18;pnp;gsr;ak2;adk;atic | 3374.46733 | 3373.77 | 1635.68 | 1137.4905 | 3268.62436 | 1121.40488 | CONFLICT | 0.466666667 | 0.533333333 |
| 28Day | Homologous DNA Pairing and Strand Exchange | 0.9409 | 0.14737 | 0.20118 | rmi1;rad51d;rad51;brca1;blm | 3513.5312 | 3769.36 | 692.086 | 1790.07678 | 3877.73216 | 1143.86555 | UP | 1 | 0 |
| 7Day | C-type lectin receptors (CLRs) | 0.91838 | 0.15494 | 0.20307 | ube2n;pycard;pak2;uba52;cdc34;kras;calm3;calm2;btrc | 3647.16889 | 4158.71 | 1018.89 | 1281.22729 | 3782.27281 | 889.831821 | UP | 0.777777778 | 0.222222222 |
| 90Day | mRNA 3'-end processing | 0.11871 | 0.95592 | 0.20355 | cstf2t;srsf6;thoc7 | 5120.03333 | 5843.41 | 3549.69 | 1361.36044 | 5319.43866 | 1251.94412 | UP | 0.666666667 | 0.333333333 |
| 90Day | Signaling by PDGF | 0.11027 | 0.95966 | 0.20367 | rasa1;sos1;plg | 2899.14333 | 2133.64 | 668.86 | 2695.82055 | 4599.05845 | 2543.65 | DOWN | 0.333333333 | 0.666666667 |
| 90Day | SHC1 events in EGFR signaling | 0.93617 | 0.20368 | 0.20368 | tgfa;sos1;areg | 4009.27667 | 3970.39 | 2162.51 | 1866.51383 | 3698.23096 | 2070.13409 | UP | 0.666666667 | 0.333333333 |
| 90Day | GRB2:SOS provides linkage to MAPK signaling for Integrins | 0.93617 | 0.20368 | 0.20368 | tln1;sos1;fn1 | 4161.30667 | 4478.93 | 2110.06 | 1912.32154 | 4694.64696 | 1722.82421 | DOWN | 0 | 1 |
| 90Day | RNA Polymerase I Transcription | 0.10472 | 0.94716 | 0.20466 | hist1h4h;hist1h4i;hist1h3c;gatad2b;h2afx;hdac2;cdk7 | 2761.40443 | 3141.48 | 202.162 | 1599.6023 | 1901.73792 | 1742.50078 | UP | 0.714285714 | 0.285714286 |

BMD analysis results for functional classification based on dose-responsive genes, using the Reactome database for gene sets in BMDExpress2.2 software.

| Study Day | Gene Set Name | Fisher's Exact Left P-Value | Fisher's Exact Right P-Value | Fisher's Exact Two Tail | Gene Symbols | BMD Mean | BMD Median | BMD Minimum | BMD Standard Deviation | BMD wMean | BMD wSD | Overall Direction | Percent Genes With Overall Direction Up | Percent Genes With Overall Direction Down |
|---|---|---|---|---|---|---|---|---|---|---|---|---|---|---|
| 7Day | COPI-independent Golgi-to-ER retrograde traffic | 0.92975 | 0.14939 | 0.2052 | rab3gap2;tubb4b;tubb2a;tuba4a;rab6a;rab18;capza2 | 2923.54371 | 3113.17 | 919.856 | 1449.40793 | 2603.01544 | 1111.87275 | UP | 1 | 0 |
| 7Day | MAPK1 (ERK2) activation | 0.95455 | 0.20537 | 0.20537 | ptpn11;jak1 | 3591.995 | 3591.995 | 3554.32 | 53.280496 | 3575.77052 | 48.086838 | UP | 1 | 0 |
| 7Day | Interleukin-9 signaling | 0.95455 | 0.20537 | 0.20537 | stat1;jak1 | 3735.595 | 3735.595 | 3554.32 | 256.361564 | 3703.94 | 252.422609 | UP | 1 | 0 |
| 7Day | TP53 Regulates Transcription of Genes Involved in G1 Cell Cycle Arrest | 0.95455 | 0.20537 | 0.20537 | cdkn1a;ccne2 | 3708.41 | 3708.41 | 2818.63 | 1258.33894 | 3837.98107 | 1244.92553 | UP | 1 | 0 |
| 7Day | CLEC7A (Dectin-1) induces NFAT activation | 0.95455 | 0.20537 | 0.20537 | calm3;calm2 | 3983.44 | 3983.44 | 3050.32 | 1319.63096 | 3556.9103 | 1173.69957 | CONFLICT | 0.5 | 0.5 |
| 7Day | Inhibition of replication initiation of damaged DNA by RB1/E2F1 | 0.95455 | 0.20537 | 0.20537 | prim2;ppp2cb | 3816.59 | 3816.59 | 3627.04 | 268.064181 | 3678.94216 | 184.294737 | UP | 1 | 0 |
| 7Day | E2F mediated regulation of DNA replication | 0.95455 | 0.20537 | 0.20537 | prim2;ppp2cb | 3816.59 | 3816.59 | 3627.04 | 268.064181 | 3678.94216 | 184.294737 | UP | 1 | 0 |
| 7Day | Calcineurin activates NFAT | 0.95455 | 0.20537 | 0.20537 | calm3;calm2 | 3983.44 | 3983.44 | 3050.32 | 1319.63096 | 3556.9103 | 1173.69957 | CONFLICT | 0.5 | 0.5 |
| 7Day | Processing of Capped Intron-Containing Pre-mRNA | 0.90921 | 0.13102 | 0.20801 | sf3b1;sf3a3;gm49336;snrpa1;dnajc8;zcrb1;fip1l1;crnkl1;ppih;sf3b6;hnrnpa2b1;cpsf2;prpf19;polr2h;pcbp1;hnrnpul1;prpf38a;zrsr2;snrpc;hnrnpc;dhx9;srsf1;tpr;cstf2;thoc5;snrpd2;sf3b3 | 3697.14907 | 3546.09 | 730.51 | 1304.08807 | 3486.45432 | 1271.82731 | UP | 0.962962963 | 0.037037037 |
| 7Day | Negative regulation of FGFR2 signaling | 0.93404 | 0.16225 | 0.20853 | mapk3;uba52;ptpn11;ppp2cb;fgf1 | 3893.254 | 3629.67 | 2647.76 | 903.905503 | 3770.28016 | 910.359639 | UP | 0.6 | 0.4 |
| 90Day | Signaling by FGFR | 0.099793 | 0.95561 | 0.21093 | hnrnpf;klb;sos1;gab1;fgf1 | 2651.3294 | 3142.57 | 126.428 | 2468.68877 | 3600.8558 | 2042.44758 | DOWN | 0 | 1 |
| 90Day | APC/C-mediated degradation of cell cycle proteins | 0.099793 | 0.95561 | 0.21093 | anapc10;psmd8;psmc4;psmf1;btrc | 2831.1416 | 3031.27 | 186.178 | 2056.6518 | 2996.10829 | 2201.76413 | UP | 0.8 | 0.2 |
| 90Day | Regulation of mitotic cell cycle | 0.099793 | 0.95561 | 0.21093 | anapc10;psmd8;psmc4;psmf1;btrc | 2831.1416 | 3031.27 | 186.178 | 2056.6518 | 2996.10829 | 2201.76413 | UP | 0.8 | 0.2 |
| 7Day | Interferon gamma signaling | 0.93088 | 0.21151 | 0.21151 | stat1;jak1;ifng | 3909.44667 | 3916.87 | 3554.32 | 351.473799 | 3908.88068 | 370.332739 | UP | 1 | 0 |
| 7Day | Platelet sensitization by LDL | 0.93088 | 0.21151 | 0.21151 | apob;ptpn11;ppp2cb | 3085.30667 | 3627.04 | 1999.21 | 940.588224 | 3396.69474 | 696.103131 | UP | 0.666666667 | 0.333333333 |
| 90Day | Metabolism of steroids | 0.10327 | 0.9421 | 0.21231 | osbpl3;cyp39a1;slc27a5;slc27a2;scap;slc10a1;amacr;hsd17b7;hsd11b1;osbpl9 | 3496.525 | 3510.085 | 263.79 | 1503.34531 | 3683.98216 | 1384.69135 | DOWN | 0.1 | 0.9 |
| 90Day | Activation, translocation and oligomerization of BAX | 0.98731 | 0.21268 | 0.21268 | bax | 1844.96 | 1844.96 | 1844.96 |  | 1844.96 |  | UP | 1 | 0 |
| 90Day | RUNX2 regulates osteoblast differentiation | 0.98731 | 0.21268 | 0.21268 | ar | 1998.95 | 1998.95 | 1998.95 |  | 1998.95 |  | DOWN | 0 | 1 |
| 90Day | TICAM1-dependent activation of IRF3/IRF7 | 0.98731 | 0.21268 | 0.21268 | irf7 | 5689.7 | 5689.7 | 5689.7 |  | 5689.7 |  | UP | 1 | 0 |
| 90Day | Signaling by NOTCH4 | 0.98731 | 0.21268 | 0.21268 | ywhaz | 137.958 | 137.958 | 137.958 |  | 137.958 |  | UP | 1 | 0 |
| 90Day | Biosynthesis of DHA-derived sulfido conjugates | 0.98731 | 0.21268 | 0.21268 | gstm4 | 793.669 | 793.669 | 793.669 |  | 793.669 |  | UP | 1 | 0 |
| 90Day | Biosynthesis of maresin conjugates in tissue regeneration (MCTR) | 0.98731 | 0.21268 | 0.21268 | gstm4 | 793.669 | 793.669 | 793.669 |  | 793.669 |  | UP | 1 | 0 |
| 90Day | Interleukin-37 signaling | 0.98731 | 0.21268 | 0.21268 | tbk1 | 1058.39 | 1058.39 | 1058.39 |  | 1058.39 |  | DOWN | 0 | 1 |
| 90Day | NOTCH4 Activation and Transmission of Signal to the Nucleus | 0.98731 | 0.21268 | 0.21268 | ywhaz | 137.958 | 137.958 | 137.958 |  | 137.958 |  | UP | 1 | 0 |
| 90Day | mRNA Editing: A to I Conversion | 0.98731 | 0.21268 | 0.21268 | adar | 5667.94 | 5667.94 | 5667.94 |  | 5667.94 |  | UP | 1 | 0 |
| 90Day | C6 deamination of adenosine | 0.98731 | 0.21268 | 0.21268 | adar | 5667.94 | 5667.94 | 5667.94 |  | 5667.94 |  | UP | 1 | 0 |
| 90Day | Formation of editosomes by ADAR proteins | 0.98731 | 0.21268 | 0.21268 | adar | 5667.94 | 5667.94 | 5667.94 |  | 5667.94 |  | UP | 1 | 0 |
| 90Day | Synthesis of bile acids and bile salts via 24-hydroxycholesterol | 0.98731 | 0.21268 | 0.21268 | cyp39a1 | 4130.84 | 4130.84 | 4130.84 |  | 4130.84 |  | DOWN | 0 | 1 |
| 90Day | DNA Damage Reversal | 0.98731 | 0.21268 | 0.21268 | fto | 4107.48 | 4107.48 | 4107.48 |  | 4107.48 |  | DOWN | 0 | 1 |
| 90Day | Reversal of alkylation damage by DNA dioxygenases | 0.98731 | 0.21268 | 0.21268 | fto | 4107.48 | 4107.48 | 4107.48 |  | 4107.48 |  | DOWN | 0 | 1 |
| 90Day | Biosynthesis of protectins | 0.98731 | 0.21268 | 0.21268 | cyp1a2 | 928.37 | 928.37 | 928.37 |  | 928.37 |  | DOWN | 0 | 1 |
| 90Day | Toll Like Receptor 7/8 (TLR7/8) Cascade | 0.093526 | 0.95884 | 0.21303 | irf7;mapk14;nfkbia;ikbkg;btrc | 4394.204 | 4261.96 | 3265.56 | 1021.51429 | 4535.14678 | 1084.60939 | DOWN | 0.4 | 0.6 |
| 90Day | MyD88 dependent cascade initiated on endosome | 0.093526 | 0.95884 | 0.21303 | irf7;mapk14;nfkbia;ikbkg;btrc | 4394.204 | 4261.96 | 3265.56 | 1021.51429 | 4535.14678 | 1084.60939 | DOWN | 0.4 | 0.6 |
| 7Day | Cell-Cell communication | 0.10563 | 0.95226 | 0.21434 | vasp;flna;prkci;dst;ctnnb1 | 2974.30464 | 3409.24 | 54.5232 | 1777.63271 | 2180.24458 | 1910.18083 | DOWN | 0.4 | 0.6 |
| 7Day | Amplification of signal from the kinetochores | 0.10563 | 0.95226 | 0.21434 | clasp2;cenpk;ppp2cb;kif2a;xpo1 | 3744.748 | 3721.91 | 2692.16 | 742.330938 | 3727.2524 | 745.446361 | UP | 0.8 | 0.2 |

BMD analysis results for functional classification based on dose-responsive genes, using the Reactome database for gene sets in BMDExpress2.2 software.

| Study Day | Gene Set Name | Fisher's Exact Left P-Value | Fisher's Exact Right P-Value | Fisher's Exact Two Tail | Gene Symbols | BMD Mean | BMD Median | BMD Minimum | BMD Standard Deviation | BMD wMean | BMD wSD | Overall Direction | Percent Genes With Overall Direction Up | Percent Genes With Overall Direction Down |
|---|---|---|---|---|---|---|---|---|---|---|---|---|---|---|
| 7Day | Amplification of signal from unattached kinetochores via a MAD2 inhibitory signal | 0.10563 | 0.95226 | 0.21434 | clasp2;cenpk;ppp2cb;kif2a;xpo1 | 3744.748 | 3721.91 | 2692.16 | 742.330938 | 3727.2524 | 745.446361 | UP | 0.8 | 0.2 |
| 28Day | COPI-dependent Golgi-to-ER retrograde traffic | 0.11023 | 0.95899 | 0.21436 | tubb4b;tubb2a;gbf1 | 3055.26667 | 2903.04 | 2359.45 | 783.106406 | 3042.68001 | 716.360849 | UP | 1 | 0 |
| 28Day | Amplification of signal from the kinetochores | 0.10086 | 0.96313 | 0.2165 | zwilch;dynll1;cenpt | 4305.88 | 3567.21 | 3558.89 | 1286.62603 | 4367.29213 | 1311.47892 | UP | 1 | 0 |
| 28Day | Amplification of signal from unattached kinetochores via a MAD2 inhibitory signal | 0.10086 | 0.96313 | 0.2165 | zwilch;dynll1;cenpt | 4305.88 | 3567.21 | 3558.89 | 1286.62603 | 4367.29213 | 1311.47892 | UP | 1 | 0 |
| 28Day | Factors involved in megakaryocyte development and platelet production | 0.11435 | 0.94722 | 0.21899 | tubb4b;tubb2a;cdc42;capza2;jmjd1c | 3799.026 | 2903.04 | 2359.45 | 1693.79969 | 3661.99495 | 1616.51991 | UP | 0.8 | 0.2 |
| 7Day | Downstream TCR signaling | 0.92499 | 0.17841 | 0.22031 | ube2n;uba52;cdc34;pten;btrc | 3321.396 | 3444.79 | 1018.89 | 1431.49909 | 3660.16961 | 864.444638 | UP | 1 | 0 |
| 7Day | Retinoid metabolism and transport | 0.91443 | 0.17431 | 0.22168 | akr1c6;apob;ttr;sdc3;lrp1;apoe;akr1c14 | 2956.06943 | 2842.81 | 113.316 | 1991.38668 | 3428.01601 | 1609.42615 | DOWN | 0.285714286 | 0.714285714 |
| 7Day | HSP90 chaperone cycle for steroid hormone receptors (SHR) | 0.91443 | 0.17431 | 0.22168 | ptges3;tubb4b;tubb2a;tuba4a;stip1;hsp90aa1;capza2 | 1845.66129 | 1815.66 | 832.843 | 994.072057 | 1943.38865 | 1033.81072 | UP | 1 | 0 |
| 28Day | Cell Cycle Checkpoints | 0.10243 | 0.94208 | 0.2223 | ube2n;ube2v2;zwilch;dynll1;cenpt;hist1h4i;cdc6;cdc27;mdm2;brca1 | 4687.953 | 5455.01 | 2266.61 | 1364.22395 | 4423.32685 | 1463.98901 | UP | 0.8 | 0.2 |
| 28Day | TRAF6 mediated NF-kB activation | 0.9451 | 0.22309 | 0.22309 | ikbkg;app | 5024.075 | 5024.075 | 4630.47 | 556.641529 | 5107.68148 | 543.939064 | CONFLICT | 0.5 | 0.5 |
| 7Day | Respiratory electron transport, ATP synthesis by chemiosmotic coupling, and heat production by uncoupling proteins. | 0.92108 | 0.14606 | 0.22325 | ndufaf1;ndufaf4;ndufc2;coq10b;ndufa13;ndufa6;ndufa1;ecsit;ndufa2;atp5j | 3927.71 | 3976.805 | 2874.39 | 629.628907 | 3777.78755 | 683.205285 | UP | 0.6 | 0.4 |
| 90Day | Regulation of RUNX1 Expression and Activity | 0.94825 | 0.22531 | 0.22531 | pml;cbfb | 3837.085 | 3837.085 | 3603.58 | 330.225938 | 3844.42156 | 330.062903 | CONFLICT | 0.5 | 0.5 |
| 90Day | Glutathione synthesis and recycling | 0.94825 | 0.22531 | 0.22531 | gclm;gclc | 1985.395 | 1985.395 | 1419.33 | 800.5368 | 1562.90234 | 532.784267 | UP | 1 | 0 |
| 90Day | SUMOylation of immune response proteins | 0.94825 | 0.22531 | 0.22531 | nfkbia;ikbkg | 3433.33 | 3433.33 | 3265.56 | 237.262609 | 3311.77597 | 163.5322 | CONFLICT | 0.5 | 0.5 |
| 90Day | SUMOylation of ubiquitinylation proteins | 0.94825 | 0.22531 | 0.22531 | pml;mdm2 | 3569.33 | 3569.33 | 3535.08 | 48.4368145 | 3563.16871 | 47.6466363 | CONFLICT | 0.5 | 0.5 |
| 90Day | PLC beta mediated events | 0.13279 | 0.95854 | 0.22653 | camkk2;gnai3 | 3000.5391 | 3000.5391 | 98.0082 | 4104.79856 | 1735.98836 | 3694.75224 | CONFLICT | 0.5 | 0.5 |
| 90Day | Transport of vitamins, nucleosides, and related molecules | 0.13279 | 0.95854 | 0.22653 | slc29a1;slco2b1 | 1533.815 | 1533.815 | 1131.79 | 568.549207 | 1533.23698 | 568.54862 | DOWN | 0 | 1 |
| 90Day | Antigen processing-Cross presentation | 0.13279 | 0.95854 | 0.22653 | tap2;snap23 | 2434.48 | 2434.48 | 544.33 | 2673.07576 | 3329.02624 | 2354.76285 | CONFLICT | 0.5 | 0.5 |
| 90Day | Chromosome Maintenance | 0.13279 | 0.95854 | 0.22653 | cenpu;pole4 | 5799.32 | 5799.32 | 5744.84 | 77.0463549 | 5758.04583 | 50.2894335 | CONFLICT | 0.5 | 0.5 |
| 90Day | TP53 Regulates Transcription of DNA Repair Genes | 0.13279 | 0.95854 | 0.22653 | eloa;cdk7 | 4445.455 | 4445.455 | 3130.16 | 1860.10803 | 4242.37403 | 1837.80252 | UP | 1 | 0 |
| 90Day | Intra-Golgi traffic | 0.12248 | 0.96249 | 0.22688 | stx16;man1a | 4890.04 | 4890.04 | 3931.46 | 1355.63684 | 5316.32153 | 1214.21552 | CONFLICT | 0.5 | 0.5 |
| 90Day | Amine ligand-binding receptors | 0.12248 | 0.96249 | 0.22688 | gpr143;adra1b | 3750.25 | 3750.25 | 2444.64 | 1846.41137 | 4324.10338 | 1658.49919 | CONFLICT | 0.5 | 0.5 |
| 90Day | G-protein mediated events | 0.12248 | 0.96249 | 0.22688 | camkk2;gnai3 | 3000.5391 | 3000.5391 | 98.0082 | 4104.79856 | 1735.98836 | 3694.75224 | CONFLICT | 0.5 | 0.5 |
| 90Day | Switching of origins to a post-replicative state | 0.12248 | 0.96249 | 0.22688 | anapc10;orc6 | 4279.405 | 4279.405 | 4168.34 | 157.069629 | 4206.79823 | 118.858666 | UP | 1 | 0 |
| 90Day | Ca2+ pathway | 0.11288 | 0.96608 | 0.22858 | gng11;ctnnb1 | 4470.64 | 4470.64 | 4087.04 | 542.492323 | 4551.11456 | 530.420221 | CONFLICT | 0.5 | 0.5 |
| 90Day | Retrograde transport at the Trans-Golgi-Network | 0.11288 | 0.96608 | 0.22858 | scoc;stx16 | 5406.6 | 5406.6 | 4964.58 | 625.110679 | 5352.02708 | 620.328102 | UP | 1 | 0 |
| 7Day | TNFR2 non-canonical NF-kB pathway | 0.12015 | 0.96305 | 0.23207 | uba52;btrc | 4484.31 | 4484.31 | 4207.06 | 392.09071 | 4446.04923 | 388.339223 | UP | 1 | 0 |
| 28Day | Membrane Trafficking | 0.11555 | 0.91595 | 0.23273 | pacsin3;trappc8;vps36;ubap1;lman2;dynll1;rab9;rab11a;vps37a;ppp6r3;apob;picalm;tmf1;dennd1a;tubb4b;tubb2a;trf;sec22c;serpina1e;serpina1b;rab18;man1a;hgs;hbegf;ftl1;f5;cux1;capza2;bet1;app;gbf1;tbc1d10a | 3387.70891 | 3377.52 | 185.394 | 1580.83635 | 3222.84678 | 1602.16108 | CONFLICT | 0.46875 | 0.53125 |
| 7Day | Downstream signaling events of B Cell Receptor (BCR) | 0.91527 | 0.19513 | 0.23307 | uba52;kras;calm3;calm2;btrc | 4218.842 | 4207.06 | 3050.32 | 733.237951 | 3970.29285 | 823.83106 | UP | 0.8 | 0.2 |
| 90Day | Sphingolipid metabolism | 0.12672 | 0.93737 | 0.23409 | ormdl2;ppm1l;acer2;sptlc2;psap;gm2a | 3886.44667 | 3669.21 | 3112.61 | 842.476455 | 3660.64044 | 555.904205 | CONFLICT | 0.5 | 0.5 |
| 90Day | MyD88-independent TLR4 cascade | 0.12672 | 0.93737 | 0.23409 | tbk1;irf7;mapk14;nfkbia;ikbkg;btrc | 3838.235 | 3931.53 | 1058.39 | 1639.93973 | 3671.64014 | 1885.92371 | DOWN | 0.333333333 | 0.666666667 |
| 90Day | TRIF(TICAM1)-mediated TLR4 signaling | 0.12672 | 0.93737 | 0.23409 | tbk1;irf7;mapk14;nfkbia;ikbkg;btrc | 3838.235 | 3931.53 | 1058.39 | 1639.93973 | 3671.64014 | 1885.92371 | DOWN | 0.333333333 | 0.666666667 |

BMD analysis results for functional classification based on dose-responsive genes, using the Reactome database for gene sets in BMDExpress2.2 software.

| Study Day | Gene Set Name | Fisher's Exact Left P-Value | Fisher's Exact Right P-Value | Fisher's Exact Two Tail | Gene Symbols | BMD Mean | BMD Median | BMD Minimum | BMD Standard Deviation | BMD wMean | BMD wSD | Overall Direction | Percent Genes With Overall Direction Up | Percent Genes With Overall Direction Down |
|---|---|---|---|---|---|---|---|---|---|---|---|---|---|---|
| 90Day | Mitochondrial translation termination | 0.12672 | 0.93737 | 0.23409 | mrpl58;mrps18b;mrpl54;mrps30;mrps31;mrpl22 | 3388.1725 | 3632.435 | 958.825 | 1571.32063 | 3043.1093 | 1692.27602 | UP | 0.666666667 | 0.333333333 |
| 90Day | Mitochondrial translation | 0.11947 | 0.94153 | 0.23465 | mrpl58;mrps18b;mrpl54;mrps30;mrps31;mrpl22 | 3388.1725 | 3632.435 | 958.825 | 1571.32063 | 3043.1093 | 1692.27602 | UP | 0.666666667 | 0.333333333 |
| 90Day | DDX58/IFIH1-mediated induction of interferon-alpha/beta | 0.91244 | 0.20178 | 0.23678 | tbk1;irf7;pin1;nfkbia;ikbkg | 3712.49 | 3601.1 | 1058.39 | 1781.25687 | 3302.05123 | 1944.70221 | UP | 0.6 | 0.4 |
| 28Day | Loss of Nlp from mitotic centrosomes | 0.1318 | 0.95811 | 0.23725 | dynll1;tubb4b | 4075.495 | 4075.495 | 2359.45 | 2426.85411 | 4561.33816 | 2327.55961 | UP | 1 | 0 |
| 28Day | Loss of proteins required for interphase microtubule organization from the centrosome | 0.1318 | 0.95811 | 0.23725 | dynll1;tubb4b | 4075.495 | 4075.495 | 2359.45 | 2426.85411 | 4561.33816 | 2327.55961 | UP | 1 | 0 |
| 7Day | Beta-catenin phosphorylation cascade | 0.91748 | 0.23731 | 0.23731 | gsk3b;ppp2cb;ctnnb1 | 2727.00107 | 3627.04 | 54.5232 | 2355.18023 | 2722.70432 | 2279.08261 | UP | 0.666666667 | 0.333333333 |
| 7Day | PKA-mediated phosphorylation of CREB | 0.91748 | 0.23731 | 0.23731 | prkar2a;calm3;calm2 | 4011.14667 | 4066.56 | 3050.32 | 934.353205 | 3661.3101 | 940.743026 | DOWN | 0.333333333 | 0.666666667 |
| 7Day | PKA activation | 0.91748 | 0.23731 | 0.23731 | prkar2a;calm3;calm2 | 4011.14667 | 4066.56 | 3050.32 | 934.353205 | 3661.3101 | 940.743026 | DOWN | 0.333333333 | 0.666666667 |
| 7Day | Processing of Intronless Pre-mRNAs | 0.91748 | 0.23731 | 0.23731 | fip1l1;cpsf2;cstf2 | 4141.64667 | 3485.7 | 3207.13 | 1384.4062 | 3620.26137 | 835.420177 | UP | 1 | 0 |
| 28Day | Transcriptional regulation by small RNAs | 0.1256 | 0.96054 | 0.23773 | hist1h4i;polr2a | 5444.54 | 5444.54 | 5040.67 | 571.158431 | 5494.50555 | 566.770537 | CONFLICT | 0.5 | 0.5 |
| 28Day | Visual phototransduction | 0.90524 | 0.16834 | 0.23838 | akr1c6;akr1c12;akr1c19;apob;rdh16f2;lrp1;gpc4;gnb5;apoe;akr1c14 | 3006.0593 | 2943.305 | 939.205 | 1587.10521 | 2423.77594 | 1397.55687 | DOWN | 0.3 | 0.7 |
| 90Day | DNA Double Strand Break Response | 0.13803 | 0.94026 | 0.23848 | hist1h4h;babam1;hist1h4i;h2afx | 4461.0475 | 4046.18 | 3951.81 | 894.337005 | 4412.91487 | 861.771604 | CONFLICT | 0.5 | 0.5 |
| 90Day | PKMTs methylate histone lysines | 0.13803 | 0.94026 | 0.23848 | hist1h4h;atf7ip;hist1h4i;hist1h3c | 2231.928 | 2381.8345 | 157.333 | 2035.38576 | 1872.37212 | 1795.00472 | DOWN | 0.25 | 0.75 |
| 90Day | SUMOylation of DNA damage response and repair proteins | 0.13803 | 0.94026 | 0.23848 | eid3;nup153;pml;sec13 | 3722.275 | 3641.965 | 2758.9 | 857.768881 | 3705.18542 | 766.87462 | UP | 0.75 | 0.25 |
| 90Day | PRC2 methylates histones and DNA | 0.12082 | 0.94904 | 0.23937 | hist1h4h;hist1h4i;hist1h3c;h2afx | 3214.00725 | 3979.26 | 811.859 | 1602.37406 | 2298.31583 | 1843.92338 | CONFLICT | 0.5 | 0.5 |
| 90Day | Peptide hormone metabolism | 0.12082 | 0.94904 | 0.23937 | exoc4;mme;inhbc;ctsd | 3065.9275 | 3132.445 | 2113.16 | 888.35815 | 2926.2467 | 859.013936 | CONFLICT | 0.5 | 0.5 |
| 90Day | Interferon Signaling | 0.12082 | 0.94904 | 0.23937 | usp18;abce1;ifngr2;ifnar1 | 2843.26675 | 3524.105 | 250.557 | 1794.46997 | 2303.69065 | 1986.68488 | CONFLICT | 0.5 | 0.5 |
| 28Day | AURKA Activation by TPX2 | 0.11397 | 0.96499 | 0.24014 | dynll1;tubb4b | 4075.495 | 4075.495 | 2359.45 | 2426.85411 | 4561.33816 | 2327.55961 | UP | 1 | 0 |
| 90Day | Axon guidance | 0.13038 | 0.90883 | 0.24071 | tubb6;pdlim7;ranbp9;irs2;mapk14;tubb4b;tubb2a;tuba1b;tln1;tiam1;rasa1;sos1;siah2;rock2;rock1;myo9b;msn;mmp2;hsp90aa1;gfra1;gab1;cdc42;ap2m1;itga9 | 2507.8766 | 2042.325 | 74.8133 | 1994.3986 | 2237.08825 | 2109.80424 | CONFLICT | 0.416666667 | 0.583333333 |
| 7Day | Nucleotide Excision Repair | 0.11161 | 0.94567 | 0.24099 | ube2n;ube2v2;prpf19;polr2h;ino80c;uba52 | 3622.83333 | 3704.695 | 2423.08 | 931.684013 | 3428.72673 | 879.959361 | UP | 1 | 0 |
| 90Day | Protein-protein interactions at synapses | 0.11292 | 0.95298 | 0.24116 | gria3;ptprd;il1rap;epb41l1 | 2755.46 | 3045.76 | 1097.82 | 1202.43754 | 2533.97991 | 1186.68048 | CONFLICT | 0.5 | 0.5 |
| 90Day | Signaling by FGFR2 | 0.11292 | 0.95298 | 0.24116 | hnrnpf;sos1;gab1;fgf1 | 2351.58925 | 1692.4995 | 126.428 | 2743.52655 | 3545.54798 | 2326.77262 | DOWN | 0 | 1 |
| 7Day | AKT phosphorylates targets in the cytosol | 0.9395 | 0.24158 | 0.24158 | cdkn1a;casp9 | 3233.65 | 3233.65 | 2818.63 | 586.926913 | 3260.0846 | 585.735115 | CONFLICT | 0.5 | 0.5 |
| 7Day | Golgi Cisternae Pericentriolar Stack Reorganization | 0.9395 | 0.24158 | 0.24158 | mapk3;rab1a | 4176.96 | 4176.96 | 3553.68 | 881.451029 | 4087.79673 | 872.385087 | CONFLICT | 0.5 | 0.5 |
| 7Day | Degradation of cysteine and homocysteine | 0.9395 | 0.24158 | 0.24158 | txn2;cdo1 | 4345.35 | 4345.35 | 3081.26 | 1787.69322 | 3978.15605 | 1710.60932 | CONFLICT | 0.5 | 0.5 |
| 7Day | Interleukin-21 signaling | 0.9395 | 0.24158 | 0.24158 | stat1;jak1 | 3735.595 | 3735.595 | 3554.32 | 256.361564 | 3703.94 | 252.422609 | UP | 1 | 0 |
| 7Day | Degradation of DVL | 0.9395 | 0.24158 | 0.24158 | klhl12;uba52 | 4314.45 | 4314.45 | 3867.34 | 632.309026 | 4328.76951 | 631.984657 | UP | 1 | 0 |
| 28Day | Opioid Signalling | 0.10853 | 0.96703 | 0.24204 | gnb5;adcy9 | 2587.124 | 2587.124 | 953.648 | 2310.08391 | 1477.92173 | 1695.82674 | CONFLICT | 0.5 | 0.5 |
| 7Day | RNA Polymerase II Pre-transcription Events | 0.12966 | 0.9442 | 0.2431 | wdr61;polr2h;taf10;ccnk | 3345.3475 | 3655.495 | 2105.8 | 873.384665 | 3595.5247 | 673.466686 | UP | 1 | 0 |
| 90Day | Resolution of Sister Chromatid Cohesion | 0.1177 | 0.93478 | 0.24335 | cenpu;tubb6;tubb4b;tubb2a;tuba1b;kntc1;nudc;sec13;cenpf | 2740.46122 | 2758.9 | 779.791 | 1433.75598 | 2870.13302 | 1732.48579 | UP | 0.888888889 | 0.111111111 |
| 28Day | CLEC7A (Dectin-1) signaling | 0.90725 | 0.20603 | 0.24368 | ube2n;ube2m;ppp3cb;pdpk1;ikbkg | 3581.4416 | 4095.87 | 192.988 | 2143.44278 | 3918.11922 | 1510.6886 | UP | 0.6 | 0.4 |
| 7Day | Global Genome Nucleotide Excision Repair (GG-NER) | 0.12267 | 0.94776 | 0.24392 | ube2n;ube2v2;ino80c;uba52 | 3763.1175 | 3933.915 | 2423.08 | 1053.47331 | 3364.60196 | 1010.9153 | UP | 1 | 0 |
| 28Day | Plasma lipoprotein remodeling | 0.91171 | 0.24406 | 0.24406 | lmf1;apob;apoe | 2386.61833 | 3007.97 | 939.205 | 1257.6687 | 1733.49809 | 1264.85386 | DOWN | 0 | 1 |
| 90Day | Acyl chain remodelling of PG | 0.14742 | 1 | 0.24444 |  |  |  |  |  |  |  |  |  |  |
| 90Day | CRMPs in Sema3A signaling | 0.14742 | 1 | 0.24444 |  |  |  |  |  |  |  |  |  |  |
| 90Day | PKA activation in glucagon signalling | 0.14742 | 1 | 0.24444 |  |  |  |  |  |  |  |  |  |  |
| 7Day | Recruitment of mitotic centrosome proteins and complexes | 0.11601 | 0.95112 | 0.24535 | tubb4b;tuba4a;nedd1;hsp90aa1 | 1703.9565 | 1410.635 | 919.856 | 998.985626 | 1609.23265 | 1031.31055 | UP | 1 | 0 |
| 7Day | Centrosome maturation | 0.11601 | 0.95112 | 0.24535 | tubb4b;tuba4a;nedd1;hsp90aa1 | 1703.9565 | 1410.635 | 919.856 | 998.985626 | 1609.23265 | 1031.31055 | UP | 1 | 0 |
| 90Day | DAG and IP3 signaling | 0.14573 | 0.96896 | 0.24614 | camkk2 | 98.0082 | 98.0082 | 98.0082 |  | 98.0082 |  | DOWN | 0 | 1 |

BMD analysis results for functional classification based on dose-responsive genes, using the Reactome database for gene sets in BMDExpress2.2 software.

| Study Day | Gene Set Name | Fisher's Exact Left P-Value | Fisher's Exact Right P-Value | Fisher's Exact Two Tail | Gene Symbols | BMD Mean | BMD Median | BMD Minimum | BMD Standard Deviation | BMD wMean | BMD wSD | Overall Direction | Percent Genes With Overall Direction Up | Percent Genes With Overall Direction Down |
|---|---|---|---|---|---|---|---|---|---|---|---|---|---|---|
| 90Day | Negative regulation of FGFR1 signaling | 0.14573 | 0.96896 | 0.24614 | fgf1 | 242.429 | 242.429 | 242.429 | | 242.429 | | DOWN | 0 | 1 |
| 90Day | Ovarian tumor domain proteases | 0.14573 | 0.96896 | 0.24614 | ikbkg | 3265.56 | 3265.56 | 3265.56 | | 3265.56 | | UP | 1 | 0 |
| 90Day | Recognition of DNA damage by PCNA-containing replication complex | 0.14573 | 0.96896 | 0.24614 | pole4 | 5853.8 | 5853.8 | 5853.8 | | 5853.8 | | DOWN | 0 | 1 |
| 90Day | Nicotinate metabolism | 0.14573 | 0.96896 | 0.24614 | nmnat3 | 640.772 | 640.772 | 640.772 | | 640.772 | | DOWN | 0 | 1 |
| 90Day | HS-GAG biosynthesis | 0.14573 | 0.96896 | 0.24614 | sdc4 | 630.216 | 630.216 | 630.216 | | 630.216 | | DOWN | 0 | 1 |
| 90Day | mRNA Capping | 0.14573 | 0.96896 | 0.24614 | cdk7 | 3130.16 | 3130.16 | 3130.16 | | 3130.16 | | UP | 1 | 0 |
| 90Day | RNA Polymerase I Promoter Escape | 0.14573 | 0.96896 | 0.24614 | cdk7 | 3130.16 | 3130.16 | 3130.16 | | 3130.16 | | UP | 1 | 0 |
| 7Day | Degradation of beta-catenin by the destruction complex | 0.90489 | 0.21238 | 0.24673 | gsk3b;uba52;ppp2cb;ctnnb1;btrc | 3429.92464 | 4207.06 | 54.5232 | 1933.47127 | 3287.62365 | 1938.69249 | UP | 0.8 | 0.2 |
| 90Day | Formation of Senescence-Associated Heterochromatin Foci (SAHF) | 0.13078 | 1 | 0.24688 | | | | | | | | | | |
| 90Day | Translesion Synthesis by POLH | 0.13078 | 1 | 0.24688 | | | | | | | | | | |
| 90Day | ABC transporters in lipid homeostasis | 0.13078 | 1 | 0.24688 | | | | | | | | | | |
| 90Day | Synthesis, secretion, and deacylation of Ghrelin | 0.13078 | 1 | 0.24688 | | | | | | | | | | |
| 90Day | Activation of SMO | 0.13078 | 1 | 0.24688 | | | | | | | | | | |
| 90Day | Regulation of TNFR1 signaling | 0.13278 | 0.97247 | 0.24697 | ikbkg | 3265.56 | 3265.56 | 3265.56 | | 3265.56 | | UP | 1 | 0 |
| 90Day | DAP12 signaling | 0.13278 | 0.97247 | 0.24697 | sos1 | 5894.93 | 5894.93 | 5894.93 | | 5894.93 | | DOWN | 0 | 1 |
| 90Day | MET activates PTK2 signaling | 0.13278 | 0.97247 | 0.24697 | fn1 | 2110.06 | 2110.06 | 2110.06 | | 2110.06 | | DOWN | 0 | 1 |
| 90Day | Inwardly rectifying K+ channels | 0.13278 | 0.97247 | 0.24697 | kcnj8 | 2260.22 | 2260.22 | 2260.22 | | 2260.22 | | UP | 1 | 0 |
| 90Day | RNA Polymerase I Transcription Termination | 0.13278 | 0.97247 | 0.24697 | cdk7 | 3130.16 | 3130.16 | 3130.16 | | 3130.16 | | UP | 1 | 0 |
| 90Day | Ca-dependent events | 0.13278 | 0.97247 | 0.24697 | camkk2 | 98.0082 | 98.0082 | 98.0082 | | 98.0082 | | DOWN | 0 | 1 |
| 7Day | HDACs deacetylate histones | 0.10966 | 0.95428 | 0.24738 | hist1h4h;hist1h2bc;hist2h2ac;hist2h2a a1 | 4100.405 | 3802.835 | 3406.55 | 933.741438 | 4060.85571 | 1011.0164 | CONFLICT | 0.5 | 0.5 |
| 28Day | Release of apoptotic factors from the mitochondria | 0.97428 | 0.24762 | 0.24762 | 4-Sep | 211.182 | 211.182 | 211.182 | | 211.182 | | UP | 1 | 0 |
| 28Day | Mitochondrial ABC transporters | 0.97428 | 0.24762 | 0.24762 | abcb8 | 3799.52 | 3799.52 | 3799.52 | | 3799.52 | | UP | 1 | 0 |
| 28Day | Axonal growth stimulation | 0.97428 | 0.24762 | 0.24762 | arhgdia | 4971.84 | 4971.84 | 4971.84 | | 4971.84 | | UP | 1 | 0 |
| 28Day | The NLRP1 inflammasome | 0.97428 | 0.24762 | 0.24762 | bcl2l1 | 2151.36 | 2151.36 | 2151.36 | | 2151.36 | | UP | 1 | 0 |
| 28Day | Ubiquinol biosynthesis | 0.97428 | 0.24762 | 0.24762 | coq3 | 1252.61 | 1252.61 | 1252.61 | | 1252.61 | | DOWN | 0 | 1 |
| 28Day | Alternative complement activation | 0.97428 | 0.24762 | 0.24762 | c3 | 2572.88 | 2572.88 | 2572.88 | | 2572.88 | | DOWN | 0 | 1 |
| 28Day | mRNA Editing: C to U Conversion | 0.97428 | 0.24762 | 0.24762 | a1cf | 1306.69 | 1306.69 | 1306.69 | | 1306.69 | | DOWN | 0 | 1 |
| 28Day | Formation of the Editosome | 0.97428 | 0.24762 | 0.24762 | a1cf | 1306.69 | 1306.69 | 1306.69 | | 1306.69 | | DOWN | 0 | 1 |
| 28Day | Conjugation of benzoate with glycine | 0.97428 | 0.24762 | 0.24762 | glyat | 3673.59 | 3673.59 | 3673.59 | | 3673.59 | | UP | 1 | 0 |
| 28Day | Selenoamino acid metabolism | 0.97428 | 0.24762 | 0.24762 | txnrd1 | 3178.52 | 3178.52 | 3178.52 | | 3178.52 | | UP | 1 | 0 |
| 28Day | Activation of AKT2 | 0.97428 | 0.24762 | 0.24762 | pdpk1 | 192.988 | 192.988 | 192.988 | | 192.988 | | DOWN | 0 | 1 |
| 28Day | Fructose catabolism | 0.97428 | 0.24762 | 0.24762 | khk | 3680.34 | 3680.34 | 3680.34 | | 3680.34 | | DOWN | 0 | 1 |
| 28Day | Reuptake of GABA | 0.97428 | 0.24762 | 0.24762 | slc6a13 | 151.142 | 151.142 | 151.142 | | 151.142 | | DOWN | 0 | 1 |
| 28Day | Synthesis of IPs in the nucleus | 0.97428 | 0.24762 | 0.24762 | ippk | 4371.1 | 4371.1 | 4371.1 | | 4371.1 | | UP | 1 | 0 |
| 28Day | Scavenging by Class H Receptors | 0.97428 | 0.24762 | 0.24762 | apob | 939.205 | 939.205 | 939.205 | | 939.205 | | DOWN | 0 | 1 |
| 28Day | Transport of inorganic cations/anions and amino acids/oligopeptides | 0.13846 | 0.93913 | 0.24877 | slc9a5;slc25a10;slc17a8;slc1a2 | 2877.15 | 3000.365 | 1774.78 | 987.277084 | 3012.78763 | 996.593412 | UP | 0.75 | 0.25 |
| 28Day | Formation of ATP by chemiosmotic coupling | 0.93357 | 0.2492 | 0.2492 | atp5g2;atp5j2 | 5554.105 | 5554.105 | 5480.89 | 103.541646 | 5551.28634 | 103.464887 | CONFLICT | 0.5 | 0.5 |
| 28Day | Cristae formation | 0.93357 | 0.2492 | 0.2492 | atp5g2;atp5j2 | 5554.105 | 5554.105 | 5480.89 | 103.541646 | 5551.28634 | 103.464887 | CONFLICT | 0.5 | 0.5 |
| 28Day | TP53 Regulates Transcription of Cell Death Genes | 0.93357 | 0.2492 | 0.2492 | tmem219;bnip3l | 3715.515 | 3715.515 | 1841.2 | 2650.68169 | 2387.84735 | 1871.01861 | DOWN | 0 | 1 |
| 28Day | Synthesis of PIPs at the Golgi membrane | 0.93357 | 0.2492 | 0.2492 | pi4k2b;pi4ka | 4418.385 | 4418.385 | 4173.55 | 346.248978 | 4399.97266 | 345.268484 | CONFLICT | 0.5 | 0.5 |
| 28Day | Microtubule-dependent trafficking of connexons from Golgi to the plasma membrane | 0.93357 | 0.2492 | 0.2492 | tubb4b;tubb2a | 2631.245 | 2631.245 | 2359.45 | 384.376175 | 2702.45657 | 370.948608 | UP | 1 | 0 |
| 28Day | Methylation | 0.93357 | 0.2492 | 0.2492 | ahcy;gm4737 | 2386.29 | 2386.29 | 2114.57 | 384.270109 | 2337.94463 | 378.13882 | DOWN | 0 | 1 |
| 7Day | G beta:gamma signalling through PLC beta | 0.15225 | 1 | 0.24933 | | | | | | | | | | |
| 7Day | RHO GTPases Activate NADPH Oxidases | 0.15225 | 1 | 0.24933 | | | | | | | | | | |

BMD analysis results for functional classification based on dose-responsive genes, using the Reactome database for gene sets in BMDExpress2.2 software.

| Study Day | Gene Set Name | Fisher's Exact Left P-Value | Fisher's Exact Right P-Value | Fisher's Exact Two Tail | Gene Symbols | BMD Mean | BMD Median | BMD Minimum | BMD Standard Deviation | BMD wMean | BMD wSD | Overall Direction | Percent Genes With Overall Direction Up | Percent Genes With Overall Direction Down |
|---|---|---|---|---|---|---|---|---|---|---|---|---|---|---|
| 90Day | Activation of kainate receptors upon glutamate binding | 0.12089 | 0.97558 | 0.24976 | gng11 | 4854.24 | 4854.24 | 4854.24 |  | 4854.24 |  | UP | 1 | 0 |
| 90Day | Neurexins and neuroligins | 0.12089 | 0.97558 | 0.24976 | epb41l1 | 3832.5 | 3832.5 | 3832.5 |  | 3832.5 |  | UP | 1 | 0 |
| 90Day | Transferrin endocytosis and recycling | 0.12089 | 0.97558 | 0.24976 | trf | 368.457 | 368.457 | 368.457 |  | 368.457 |  | DOWN | 0 | 1 |
| 90Day | Negative regulation of FGFR2 signaling | 0.12089 | 0.97558 | 0.24976 | fgf1 | 242.429 | 242.429 | 242.429 |  | 242.429 |  | DOWN | 0 | 1 |
| 90Day | Glucagon signaling in metabolic regulation | 0.12089 | 0.97558 | 0.24976 | gng11 | 4854.24 | 4854.24 | 4854.24 |  | 4854.24 |  | UP | 1 | 0 |
| 90Day | Thrombin signalling through proteinase activated receptors (PARs) | 0.12089 | 0.97558 | 0.24976 | gng11 | 4854.24 | 4854.24 | 4854.24 |  | 4854.24 |  | UP | 1 | 0 |
| 90Day | Disassembly of the destruction complex and recruitment of AXIN to the membrane | 0.12089 | 0.97558 | 0.24976 | ctnnb1 | 4087.04 | 4087.04 | 4087.04 |  | 4087.04 |  | DOWN | 0 | 1 |
| 90Day | Formation of the Early Elongation Complex | 0.12089 | 0.97558 | 0.24976 | cdk7 | 3130.16 | 3130.16 | 3130.16 |  | 3130.16 |  | UP | 1 | 0 |
| 90Day | Smooth Muscle Contraction | 0.12089 | 0.97558 | 0.24976 | tln1 | 4478.93 | 4478.93 | 4478.93 |  | 4478.93 |  | DOWN | 0 | 1 |
| 28Day | Negative regulation of the PI3K/AKT network | 0.12292 | 0.94719 | 0.25016 | phlpp1;il1rap;hbegf;fgf1 | 2439.9445 | 2567.265 | 919.738 | 1456.45266 | 2065.97653 | 1370.40565 | DOWN | 0.25 | 0.75 |
| 7Day | Cell Cycle | 0.12597 | 0.90428 | 0.25054 | ube2n;clasp2;gm49336;pds5a;ube2v2;rnf168;hist1h4h;babam1;hist1h2bc;kmt5a;psmd5;psmd6;cenpk;nek6;arpp19;hist2h2ac;gtse1;mapk3;cop1;psmc4;tubb4b;ywhaz;uba52;tubb2a;tuba4a;tfdp1;cdc27;rab1a;psmc2;prim2;ppp2cb;nedd1;kif2a;hsp90aa1;hist2h2aa1;cdkn1a;cdc25a;ccne2;btrc;abl1;tpr;xpo1 | 3338.35543 | 3521.41 | 707.264 | 1210.81998 | 3295.05526 | 1159.72514 | UP | 0.880952381 | 0.119047619 |
| 7Day | Presynaptic function of Kainate receptors | 0.13787 | 1 | 0.25062 |  |  |  |  |  |  |  |  |  |  |
| 7Day | Phase I - Functionalization of compounds | 0.90818 | 0.14317 | 0.25084 | bphl;cyp3a25;ptges3;cyp39a1;ces2c;nqo2;ncoa2;ncoa1;ces3b;cyp3a11;cyp2e1;cyp2c37;cyp2c29;arnt;aldh2;maob;ces2a;cyp3a41b | 2586.41444 | 3125.9 | 46.9364 | 1865.00344 | 2351.21285 | 1793.97063 | DOWN | 0.388888889 | 0.611111111 |
| 7Day | Platelet Aggregation (Plug Formation) | 0.13406 | 0.97184 | 0.25186 | f2 | 156.627 | 156.627 | 156.627 |  | 156.627 |  | DOWN | 0 | 1 |
| 90Day | Regulation of PTEN stability and activity | 0.11601 | 1 | 0.25267 |  |  |  |  |  |  |  |  |  |  |
| 90Day | Signaling by NOTCH1 | 0.11601 | 1 | 0.25267 |  |  |  |  |  |  |  |  |  |  |
| 90Day | Nicotinamide salvaging | 0.11601 | 1 | 0.25267 |  |  |  |  |  |  |  |  |  |  |
| 90Day | DARPP-32 events | 0.11601 | 1 | 0.25267 |  |  |  |  |  |  |  |  |  |  |
| 90Day | Ephrin signaling | 0.11601 | 1 | 0.25267 |  |  |  |  |  |  |  |  |  |  |
| 90Day | PKA-mediated phosphorylation of CREB | 0.11601 | 1 | 0.25267 |  |  |  |  |  |  |  |  |  |  |
| 90Day | PKA activation | 0.11601 | 1 | 0.25267 |  |  |  |  |  |  |  |  |  |  |
| 28Day | Mitotic Spindle Checkpoint | 0.11341 | 0.95201 | 0.25268 | zwilch;dynll1;cenpt;cdc27 | 4674.6 | 4673.985 | 3558.89 | 1283.51942 | 4611.45147 | 1282.74646 | UP | 1 | 0 |
| 28Day | Formation of the cornified envelope | 0.11341 | 0.95201 | 0.25268 | pkp4;pkp1;krt8;krt18 | 2676.64925 | 2807.215 | 856.847 | 1425.57491 | 2794.74322 | 1223.74793 | UP | 1 | 0 |
| 28Day | COPI-independent Golgi-to-ER retrograde traffic | 0.89949 | 0.2186 | 0.25364 | dynll1;tubb4b;tubb2a;rab18;capza2 | 4334.282 | 5180.95 | 2359.45 | 1581.42285 | 4391.93484 | 1559.12644 | UP | 0.6 | 0.4 |
| 7Day | Adherens junctions interactions | 0.12406 | 0.9745 | 0.25412 | ctnnb1 | 54.5232 | 54.5232 | 54.5232 |  | 54.5232 |  | DOWN | 0 | 1 |
| 7Day | O-glycosylation of TSR domain-containing proteins | 0.12406 | 0.9745 | 0.25412 | adamts7 | 3416.43 | 3416.43 | 3416.43 |  | 3416.43 |  | DOWN | 0 | 1 |
| 7Day | HDR through Single Strand Annealing (SSA) | 0.12406 | 0.9745 | 0.25412 | abl1 | 3368.05 | 3368.05 | 3368.05 |  | 3368.05 |  | DOWN | 0 | 1 |
| 7Day | Translesion synthesis by Y family DNA polymerases bypasses lesions on DNA template | 0.12406 | 0.9745 | 0.25412 | uba52 | 4761.56 | 4761.56 | 4761.56 |  | 4761.56 |  | UP | 1 | 0 |
| 7Day | Activation of ATR in response to replication stress | 0.12406 | 0.9745 | 0.25412 | cdc25a | 5877.76 | 5877.76 | 5877.76 |  | 5877.76 |  | UP | 1 | 0 |
| 90Day | Digestion and absorption | 0.10999 | 0.97834 | 0.25439 | mgam | 2596.25 | 2596.25 | 2596.25 |  | 2596.25 |  | DOWN | 0 | 1 |
| 90Day | G alpha (z) signalling events | 0.10999 | 0.97834 | 0.25439 | gng11 | 4854.24 | 4854.24 | 4854.24 |  | 4854.24 |  | UP | 1 | 0 |
| 90Day | Glucagon-type ligand receptors | 0.10999 | 0.97834 | 0.25439 | gng11 | 4854.24 | 4854.24 | 4854.24 |  | 4854.24 |  | UP | 1 | 0 |

BMD analysis results for functional classification based on dose-responsive genes, using the Reactome database for gene sets in BMDExpress2.2 software.

| Study Day | Gene Set Name | Fisher's Exact Left P-Value | Fisher's Exact Right P-Value | Fisher's Exact Two Tail | Gene Symbols | BMD Mean | BMD Median | BMD Minimum | BMD Standard Deviation | BMD wMean | BMD wSD | Overall Direction | Percent Genes With Overall Direction Up | Percent Genes With Overall Direction Down |
|---|---|---|---|---|---|---|---|---|---|---|---|---|---|---|
| 90Day | HSP90 chaperone cycle for steroid hormone receptors (SHR) | 0.90593 | 0.18125 | 0.25553 | tubb6;dnaja2;dctn3;tubb4b;tubb2a;tuba1b;hsp90aa1;ar | 1572.38525 | 1751.94 | 190.561 | 1127.05582 | 1474.4089 | 1168.2909 | UP | 0.625 | 0.375 |
| 28Day | Digestion | 0.15699 | 1 | 0.25595 | | | | | | | | | | |
| 28Day | SUMOylation of intracellular receptors | 0.15699 | 1 | 0.25595 | | | | | | | | | | |
| 28Day | RNA Polymerase III Transcription Initiation From Type 1 Promoter | 0.14618 | 1 | 0.25638 | | | | | | | | | | |
| 28Day | RNA Polymerase III Transcription Initiation From Type 2 Promoter | 0.14618 | 1 | 0.25638 | | | | | | | | | | |
| 28Day | Platelet calcium homeostasis | 0.14618 | 1 | 0.25638 | | | | | | | | | | |
| 7Day | Inositol transporters | 0.97506 | 0.2569 | 0.2569 | slc5a3 | 5988.82 | 5988.82 | 5988.82 | | 5988.82 | | UP | 1 | 0 |
| 7Day | MASTL Facilitates Mitotic Progression | 0.97506 | 0.2569 | 0.2569 | arpp19 | 1931.08 | 1931.08 | 1931.08 | | 1931.08 | | UP | 1 | 0 |
| 7Day | SMAC (DIABLO) binds to IAPs | 0.97506 | 0.2569 | 0.2569 | xiap | 4874.03 | 4874.03 | 4874.03 | | 4874.03 | | DOWN | 0 | 1 |
| 7Day | SMAC(DIABLO)-mediated dissociation of IAP:caspase complexes | 0.97506 | 0.2569 | 0.2569 | xiap | 4874.03 | 4874.03 | 4874.03 | | 4874.03 | | DOWN | 0 | 1 |
| 7Day | SUMO is conjugated to E1 (UBA2:SAE1) | 0.97506 | 0.2569 | 0.2569 | uba2 | 2542.64 | 2542.64 | 2542.64 | | 2542.64 | | UP | 1 | 0 |
| 7Day | NOTCH2 Activation and Transmission of Signal to the Nucleus | 0.97506 | 0.2569 | 0.2569 | mdk | 4385.8 | 4385.8 | 4385.8 | | 4385.8 | | DOWN | 0 | 1 |
| 7Day | Activation of NIMA Kinases NEK9, NEK6, NEK7 | 0.97506 | 0.2569 | 0.2569 | nek6 | 770.098 | 770.098 | 770.098 | | 770.098 | | UP | 1 | 0 |
| 7Day | Formation of the active cofactor, UDP-glucuronate | 0.97506 | 0.2569 | 0.2569 | ugdh | 654.44 | 654.44 | 654.44 | | 654.44 | | UP | 1 | 0 |
| 7Day | c-src mediated regulation of Cx43 function and closure of gap junctions | 0.97506 | 0.2569 | 0.2569 | gja1 | 4276.18 | 4276.18 | 4276.18 | | 4276.18 | | DOWN | 0 | 1 |
| 7Day | Regulation of gap junction activity | 0.97506 | 0.2569 | 0.2569 | gja1 | 4276.18 | 4276.18 | 4276.18 | | 4276.18 | | DOWN | 0 | 1 |
| 7Day | Activation of AMPA receptors | 0.97506 | 0.2569 | 0.2569 | gria3 | 3853.21 | 3853.21 | 3853.21 | | 3853.21 | | UP | 1 | 0 |
| 7Day | Interleukin-33 signaling | 0.97506 | 0.2569 | 0.2569 | il1rap | 131.024 | 131.024 | 131.024 | | 131.024 | | DOWN | 0 | 1 |
| 7Day | Abacavir transmembrane transport | 0.97506 | 0.2569 | 0.2569 | slc22a1 | 4237.04 | 4237.04 | 4237.04 | | 4237.04 | | DOWN | 0 | 1 |
| 28Day | Inositol phosphate metabolism | 0.1487 | 0.96737 | 0.25729 | ippk | 4371.1 | 4371.1 | 4371.1 | | 4371.1 | | UP | 1 | 0 |
| 7Day | GABA B receptor activation | 0.11474 | 0.97692 | 0.25765 | gnai3 | 794.2 | 794.2 | 794.2 | | 794.2 | | UP | 1 | 0 |
| 7Day | Activation of GABAB receptors | 0.11474 | 0.97692 | 0.25765 | gnai3 | 794.2 | 794.2 | 794.2 | | 794.2 | | UP | 1 | 0 |
| 90Day | Anchoring of the basal body to the plasma membrane | 0.13119 | 0.93144 | 0.25766 | haus7;cep89;dctn3;cntrl;tubb4b;cep76;hsp90aa1 | 3353.60429 | 4147.42 | 426.32 | 1613.41073 | 3557.04342 | 1441.36283 | UP | 1 | 0 |
| 28Day | Signaling by PTK6 | 0.1407 | 0.96962 | 0.2577 | hbegf | 919.738 | 919.738 | 919.738 | | 919.738 | | UP | 1 | 0 |
| 28Day | Signaling by Non-Receptor Tyrosine Kinases | 0.1407 | 0.96962 | 0.2577 | hbegf | 919.738 | 919.738 | 919.738 | | 919.738 | | UP | 1 | 0 |
| 28Day | HDMs demethylate histones | 0.1407 | 0.96962 | 0.2577 | hist1h4i | 5848.41 | 5848.41 | 5848.41 | | 5848.41 | | DOWN | 0 | 1 |
| 28Day | RNA Polymerase III Transcription Initiation From Type 3 Promoter | 0.13612 | 1 | 0.2581 | | | | | | | | | | |
| 28Day | Synthesis of IP3 and IP4 in the cytosol | 0.13612 | 1 | 0.2581 | | | | | | | | | | |
| 28Day | Laminin interactions | 0.13612 | 1 | 0.2581 | | | | | | | | | | |
| 7Day | CD28 dependent PI3K/Akt signaling | 0.11306 | 1 | 0.26016 | | | | | | | | | | |
| 7Day | Adrenaline,noradrenaline inhibits insulin secretion | 0.11306 | 1 | 0.26016 | | | | | | | | | | |
| 7Day | Thromboxane signalling through TP receptor | 0.11306 | 1 | 0.26016 | | | | | | | | | | |
| 7Day | Dopamine Neurotransmitter Release Cycle | 0.11306 | 1 | 0.26016 | | | | | | | | | | |
| 90Day | RNA Polymerase I Promoter Clearance | 0.11734 | 0.93975 | 0.26052 | hist1h4h;hist1h4i;hist1h3c;gatad2b;h2afx;hdac2;cdk7 | 2761.40443 | 3141.48 | 202.162 | 1599.6023 | 1901.73792 | 1742.50078 | UP | 0.714285714 | 0.285714286 |
| 90Day | Plasma lipoprotein clearance | 0.92913 | 0.16074 | 0.26075 | ces3a;apob;lipc;ces3b;apoe;ap2m1 | 2386.01167 | 3015.52 | 175.96 | 1213.11723 | 2683.76947 | 1023.04019 | DOWN | 0.166666667 | 0.833333333 |
| 28Day | Downstream signal transduction | 0.12674 | 1 | 0.26101 | | | | | | | | | | |
| 90Day | Aflatoxin activation and detoxification | 0.94544 | 0.15854 | 0.26146 | cyp3a25;cyp3a41a;cyp1a2;cyp3a41b | 1496.73025 | 871.037 | 343.937 | 1622.60806 | 933.270479 | 1101.72823 | DOWN | 0.25 | 0.75 |
| 90Day | Plasma lipoprotein assembly | 0.94544 | 0.15854 | 0.26146 | apob;bmp1;apoe;apoc3 | 1918.15725 | 970.0945 | 175.96 | 2535.49688 | 1662.93345 | 2515.46435 | DOWN | 0 | 1 |
| 90Day | LDL clearance | 0.94544 | 0.15854 | 0.26146 | ces3a;apob;ces3b;ap2m1 | 2368.27 | 3015.52 | 175.96 | 1466.53733 | 2640.00097 | 1351.10864 | DOWN | 0.25 | 0.75 |
| 7Day | Cell surface interactions at the vascular wall | 0.13971 | 0.92586 | 0.26162 | apob;yes1;sdc3;ptpn11;kras;cd74;f2 | 2984.82957 | 3629.67 | 156.627 | 1444.9241 | 2799.96363 | 1715.23029 | CONFLICT | 0.428571429 | 0.571428571 |
| 28Day | Inwardly rectifying K+ channels | 0.11802 | 1 | 0.26505 | | | | | | | | | | |
| 7Day | HSF1-dependent transactivation | 0.94086 | 0.16562 | 0.268 | hspb8;hsbp1;ptges3;hsp90aa1 | 2848.82 | 3330.73 | 1005.61 | 1252.88568 | 2463.28688 | 1392.96486 | UP | 0.75 | 0.25 |
| 7Day | Transcriptional Regulation by E2F6 | 0.94086 | 0.16562 | 0.268 | pcgf6;suz12;tfdp1;bmi1 | 3451.9685 | 4064.915 | 707.264 | 2009.25089 | 3529.23604 | 1701.83142 | UP | 1 | 0 |

BMD analysis results for functional classification based on dose-responsive genes, using the Reactome database for gene sets in BMDExpress2.2 software.

| Study Day | Gene Set Name | Fisher's Exact Left P-Value | Fisher's Exact Right P-Value | Fisher's Exact Two Tail | Gene Symbols | BMD Mean | BMD Median | BMD Minimum | BMD Standard Deviation | BMD wMean | BMD wSD | Overall Direction | Percent Genes With Overall Direction Up | Percent Genes With Overall Direction Down |
|---|---|---|---|---|---|---|---|---|---|---|---|---|---|---|
| 90Day | Cytosolic sensors of pathogen-associated DNA | 0.91902 | 0.17783 | 0.26872 | tmem173;tbk1;irf7;nfkbia;ikbkg;ctnnb1 | 3626.64667 | 3829.595 | 1058.39 | 1508.72615 | 3285.24843 | 1672.16356 | DOWN | 0.333333333 | 0.666666667 |
| 90Day | Recycling pathway of L1 | 0.91902 | 0.17783 | 0.26872 | tubb6;tubb4b;tubb2a;tuba1b;msn;ap2m1 | 2247.1185 | 1866.255 | 779.791 | 1212.01981 | 1561.1871 | 977.049086 | UP | 0.666666667 | 0.333333333 |
| 90Day | RUNX1 regulates genes involved in megakaryocyte differentiation and platelet function | 0.14539 | 0.93088 | 0.26926 | hist1h4h;hist1h4i;hist1h3c;h2afx;cbfb | 3385.3238 | 4006.71 | 811.859 | 1439.60021 | 2670.8166 | 1780.268 | UP | 0.6 | 0.4 |
| 90Day | Scavenging by Class A Receptors | 0.92872 | 0.26931 | 0.26931 | apob;apoe | 962.89 | 962.89 | 175.96 | 1112.88708 | 1105.17513 | 1094.54444 | DOWN | 0 | 1 |
| 90Day | EGFR interacts with phospholipase C-gamma | 0.92872 | 0.26931 | 0.26931 | tgfa;areg | 3066.45 | 3066.45 | 2162.51 | 1278.36421 | 2568.896 | 1067.28398 | UP | 1 | 0 |
| 90Day | Keratan sulfate degradation | 0.92872 | 0.26931 | 0.26931 | omd;lum | 4004.86 | 4004.86 | 3651.14 | 500.235621 | 4146.75069 | 458.22455 | UP | 1 | 0 |
| 90Day | Regulation of RUNX3 expression and activity | 0.92872 | 0.26931 | 0.26931 | mdm2;cbfb | 3802.835 | 3802.835 | 3535.08 | 378.662752 | 3762.85478 | 374.417741 | UP | 1 | 0 |
| 90Day | IRF3-mediated induction of type I IFN | 0.92872 | 0.26931 | 0.26931 | tmem173;tbk1 | 2558.24 | 2558.24 | 1058.39 | 2121.10821 | 2553.28861 | 2121.09665 | DOWN | 0 | 1 |
| 7Day | TCR signaling | 0.89225 | 0.2004 | 0.2694 | ube2n;pak2;uba52;cdc34;pten;h2-ab1;h2-aa;btrc | 2908.7 | 2856.44 | 1018.89 | 1236.24032 | 3402.87357 | 962.286555 | UP | 0.75 | 0.25 |
| 90Day | Signaling by Insulin receptor | 0.13676 | 0.93571 | 0.27001 | klb;irs2;sos1;gab1;fgf1 | 2037.77806 | 242.429 | 74.8133 | 2687.59133 | 2592.91452 | 2898.02513 | DOWN | 0 | 1 |
| 90Day | Transport of Mature mRNA derived from an Intron-Containing Transcript | 0.13676 | 0.93571 | 0.27001 | srsf6;thoc7;nup153;nxf7;sec13 | 4365.538 | 3680.35 | 2758.9 | 1461.99618 | 4679.90767 | 1460.69593 | UP | 1 | 0 |
| 90Day | Transport of Mature Transcript to Cytoplasm | 0.13676 | 0.93571 | 0.27001 | srsf6;thoc7;nup153;nxf7;sec13 | 4365.538 | 3680.35 | 2758.9 | 1461.99618 | 4679.90767 | 1460.69593 | UP | 1 | 0 |
| 28Day | Disassembly of the destruction complex and recruitment of AXIN to the membrane | 0.10989 | 1 | 0.27014 |  |  |  |  |  |  |  |  |  |  |
| 28Day | Cellular Senescence | 0.12037 | 0.93722 | 0.27076 | acd;hist1h4i;map2k4;cdc27;mdm2;mapkapk2;bmi1 | 4311.00286 | 4371.28 | 2266.61 | 1464.26899 | 3999.04543 | 1655.86208 | CONFLICT | 0.571428571 | 0.428571429 |
| 90Day | mRNA Splicing - Minor Pathway | 0.15826 | 0.93744 | 0.27248 | srsf6;zrsr1;prpf8 | 4512.93667 | 4267.22 | 3549.69 | 1106.75498 | 4550.21269 | 1147.36315 | UP | 0.666666667 | 0.333333333 |
| 90Day | Translation initiation complex formation | 0.14745 | 0.94263 | 0.27257 | eif3m;rps27l;rps12 | 2578.52 | 2517.83 | 1662.63 | 947.693586 | 2378.76706 | 980.623942 | UP | 1 | 0 |
| 90Day | Interleukin-17 signaling | 0.14745 | 0.94263 | 0.27257 | mapk14;ikbkg;btrc | 4226.74 | 4261.96 | 3265.56 | 944.062859 | 4326.22256 | 1102.6478 | DOWN | 0.333333333 | 0.666666667 |
| 90Day | TNFR2 non-canonical NF-kB pathway | 0.14745 | 0.94263 | 0.27257 | eda2r;ube2m;btrc | 2527.68333 | 1752.24 | 678.11 | 2335.9095 | 2635.86595 | 2417.95822 | UP | 0.666666667 | 0.333333333 |
| 90Day | L13a-mediated translational silencing of Ceruloplasmin expression | 0.13727 | 0.94743 | 0.27383 | eif3m;rps27l;rps12 | 2578.52 | 2517.83 | 1662.63 | 947.693586 | 2378.76706 | 980.623942 | UP | 1 | 0 |
| 90Day | Activation of the mRNA upon binding of the cap-binding complex and eIFs, and subsequent binding to 43S | 0.13727 | 0.94743 | 0.27383 | eif3m;rps27l;rps12 | 2578.52 | 2517.83 | 1662.63 | 947.693586 | 2378.76706 | 980.623942 | UP | 1 | 0 |
| 90Day | ABC-family proteins mediated transport | 0.13727 | 0.94743 | 0.27383 | abcb8;rnf5;abca4 | 4273.66 | 3718.83 | 3667.8 | 1005.5108 | 4488.51838 | 1066.58349 | UP | 1 | 0 |
| 90Day | Iron uptake and transport | 0.13727 | 0.94743 | 0.27383 | abcg2;trf;ftl1 | 2195.09567 | 1733.37 | 368.457 | 2095.99746 | 2551.60144 | 2268.40089 | UP | 0.666666667 | 0.333333333 |
| 7Day | Recruitment of NuMA to mitotic centrosomes | 0.14413 | 0.93118 | 0.27403 | tubb4b;tubb2a;tuba4a;nedd1;hsp90aa1 | 1781.9732 | 1815.66 | 919.856 | 882.560048 | 1726.78849 | 899.616232 | UP | 1 | 0 |
| 28Day | mRNA 3'-end processing | 0.91933 | 0.17373 | 0.27418 | cpsf2;u2af2;papola;srsf1;thoc5;bc005561 | 3815.70217 | 4120.91 | 983.533 | 1557.90855 | 4079.59666 | 1475.43623 | CONFLICT | 0.5 | 0.5 |
| 7Day | Post-translational modification: synthesis of GPI-anchored proteins | 0.137 | 0.93519 | 0.27484 | plet1;pigw;ly6e;ly6d;gpaa1 | 4689.798 | 4464.3 | 3178.98 | 1065.1948 | 4804.57437 | 1109.31416 | UP | 0.8 | 0.2 |
| 28Day | snRNP Assembly | 0.92104 | 0.27539 | 0.27539 | snrpd1;smn1 | 1756.176 | 1756.176 | 961.122 | 1124.37615 | 1914.56475 | 1101.83834 | CONFLICT | 0.5 | 0.5 |
| 28Day | Metabolism of non-coding RNA | 0.92104 | 0.27539 | 0.27539 | snrpd1;smn1 | 1756.176 | 1756.176 | 961.122 | 1124.37615 | 1914.56475 | 1101.83834 | CONFLICT | 0.5 | 0.5 |
| 28Day | Phosphorylation of CD3 and TCR zeta chains | 0.92104 | 0.27539 | 0.27539 | h2-ab1;h2-aa | 3461.14 | 3461.14 | 3245.73 | 304.635743 | 3292.13505 | 188.885132 | DOWN | 0 | 1 |
| 28Day | Caspase activation via Death Receptors in the presence of ligand | 0.92104 | 0.27539 | 0.27539 | tnfrsf10b;ly96 | 4300.525 | 4300.525 | 4040.75 | 367.377328 | 4219.52756 | 349.062933 | UP | 1 | 0 |
| 28Day | Transport of connexons to the plasma membrane | 0.92104 | 0.27539 | 0.27539 | tubb4b;tubb2a | 2631.245 | 2631.245 | 2359.45 | 384.376175 | 2702.45657 | 370.948608 | UP | 1 | 0 |
| 28Day | Regulation of necroptotic cell death | 0.92104 | 0.27539 | 0.27539 | tnfrsf10b;birc2 | 4951.5 | 4951.5 | 4040.75 | 1287.995 | 4749.40037 | 1255.8832 | UP | 1 | 0 |
| 28Day | Amino acid synthesis and interconversion (transamination) | 0.93516 | 0.17388 | 0.2762 | serinc1;oat;got2;glul | 2322.7925 | 2161.54 | 1574.09 | 787.273072 | 2374.14146 | 914.935891 | DOWN | 0 | 1 |
| 28Day | Detoxification of Reactive Oxygen Species | 0.93516 | 0.17388 | 0.2762 | txnrd1;p4hb;gstp1;gstp2 | 2875.8315 | 2540.62 | 691.166 | 2157.37958 | 2467.7214 | 2357.58858 | UP | 0.75 | 0.25 |
| 7Day | Gap-filling DNA repair synthesis and ligation in TC-NER | 0.15164 | 0.94019 | 0.27718 | prpf19;polr2h;uba52 | 3815.36333 | 3964.6 | 2719.93 | 1028.96402 | 3913.27434 | 885.21152 | UP | 1 | 0 |

BMD analysis results for functional classification based on dose-responsive genes, using the Reactome database for gene sets in BMDExpress2.2 software.

| Study Day | Gene Set Name | Fisher's Exact Left P-Value | Fisher's Exact Right P-Value | Fisher's Exact Two Tail | Gene Symbols | BMD Mean | BMD Median | BMD Minimum | BMD Standard Deviation | BMD wMean | BMD wSD | Overall Direction | Percent Genes With Overall Direction Up | Percent Genes With Overall Direction Down |
|---|---|---|---|---|---|---|---|---|---|---|---|---|---|---|
| 7Day | Regulation of Hypoxia-inducible Factor (HIF) by oxygen | 0.93085 | 0.18492 | 0.27763 | cul2;uba52;arnt;egln1 | 4260.7 | 4403.685 | 3473.87 | 556.456084 | 4323.49865 | 509.372912 | CONFLICT | 0.5 | 0.5 |
| 7Day | Cellular response to hypoxia | 0.93085 | 0.18492 | 0.27763 | cul2;uba52;arnt;egln1 | 4260.7 | 4403.685 | 3473.87 | 556.456084 | 4323.49865 | 509.372912 | CONFLICT | 0.5 | 0.5 |
| 7Day | Dual incision in TC-NER | 0.14296 | 0.94435 | 0.27794 | prpf19;polr2h;uba52 | 3815.36333 | 3964.6 | 2719.93 | 1028.96402 | 3913.27434 | 885.21152 | UP | 1 | 0 |
| 7Day | Chylomicron assembly | 0.92246 | 0.27804 | 0.27804 | apob;apoe | 1056.263 | 1056.263 | 113.316 | 1333.52844 | 1337.47219 | 1272.84755 | DOWN | 0 | 1 |
| 7Day | Interleukin-27 signaling | 0.92246 | 0.27804 | 0.27804 | stat1;jak1 | 3735.595 | 3735.595 | 3554.32 | 256.361564 | 3703.94 | 252.422609 | UP | 1 | 0 |
| 7Day | Assembly of active LPL and LIPC lipase complexes | 0.92246 | 0.27804 | 0.27804 | angptl8;pcsk5 | 4473.22 | 4473.22 | 4393.36 | 112.939095 | 4482.15982 | 112.229223 | CONFLICT | 0.5 | 0.5 |
| 7Day | p75NTR recruits signalling complexes | 0.92246 | 0.27804 | 0.27804 | uba52;prkci | 4085.4 | 4085.4 | 3409.24 | 956.234642 | 4275.2759 | 917.757582 | UP | 1 | 0 |
| 7Day | Translocation of ZAP-70 to Immunological synapse | 0.92246 | 0.27804 | 0.27804 | h2-ab1;h2-aa | 2062.21 | 2062.21 | 1863.06 | 281.640631 | 2105.93651 | 274.767957 | DOWN | 0 | 1 |
| 90Day | Programmed Cell Death | 0.14928 | 0.91712 | 0.27834 | hmgb2;ywhaz;tnfrsf10b;rock1;bmf;dsg2;ctnnb1;bax | 2260.36 | 2106.36 | 137.958 | 1594.54742 | 2319.13546 | 1448.3806 | UP | 0.625 | 0.375 |
| 7Day | The citric acid (TCA) cycle and respiratory electron transport | 0.8789 | 0.18873 | 0.28029 | ndufaf1;ndufaf4;ndufc2;coq10b;ndufa13;ndufa6;sdha;ndufa1;pdhx;idh2;ecsit;ndufa2;idh3b;dld;atp5j | 3707.30533 | 3920.07 | 114.56 | 1234.07401 | 3744.00079 | 925.90502 | CONFLICT | 0.466666667 | 0.533333333 |
| 28Day | Vesicle-mediated transport | 0.14225 | 0.89335 | 0.28169 | pacsin3;trappc8;vps36;ubap1;lman2;dynll1;rab9;rab11a;vps37a;ppp6r3;apob;picalm;tmf1;dennd1a;tubb4b;tubb2a;trf;sec22c;scarb1;serpina1e;serpina1b;rab18;man1a;lrp1;hgs;hbegf;ftl1;f5;cux1;capza2;bet1;app;apoe;gbf1;tbc1d10a | 3336.57643 | 3278.3 | 185.394 | 1530.92697 | 3185.30924 | 1559.82158 | CONFLICT | 0.428571429 | 0.571428571 |
| 28Day | Sphingolipid metabolism | 0.14304 | 0.94378 | 0.28444 | ormdl2;ormdl3;aldh3a2 | 3690.26 | 3444.81 | 2456.59 | 1372.94999 | 3564.34119 | 1439.47386 | UP | 0.666666667 | 0.333333333 |
| 28Day | Signaling by TGF-beta family members | 0.14304 | 0.94378 | 0.28444 | ube2m;tfdp1;ccnk | 4577.73667 | 5090.85 | 2933.96 | 1456.65483 | 4832.41634 | 1309.22256 | UP | 0.666666667 | 0.333333333 |
| 28Day | Recruitment of NuMA to mitotic centrosomes | 0.13128 | 0.94935 | 0.28722 | dynll1;tubb4b;tubb2a | 3684.67667 | 2903.04 | 2359.45 | 1844.72961 | 3931.15502 | 1868.40338 | UP | 1 | 0 |
| 7Day | Processing of Capped Intronless Pre-mRNA | 0.91996 | 0.20489 | 0.28884 | fip1l1;cpsf2;lsm10;cstf2 | 3832.545 | 3346.415 | 2905.24 | 1288.3694 | 3400.92865 | 758.313332 | UP | 1 | 0 |
| 28Day | Post-translational modification: synthesis of GPI-anchored proteins | 0.12572 | 0.95194 | 0.28919 | pigp;pign;ly6d | 3866.46567 | 5041.89 | 781.797 | 2696.48077 | 4764.57849 | 2265.4523 | UP | 1 | 0 |
| 90Day | Mitochondrial translation elongation | 0.1423 | 0.92826 | 0.29874 | mrpl58;mrps18b;mrpl54;mrps30;mrps31;mrpl22 | 3388.1725 | 3632.435 | 958.825 | 1571.32063 | 3043.1093 | 1692.27602 | UP | 0.666666667 | 0.333333333 |
| 28Day | SMAC, XIAP-regulated apoptotic response | 0.95906 | 0.29929 | 0.29929 | 4-Sep | 211.182 | 211.182 | 211.182 |  | 211.182 |  | UP | 1 | 0 |
| 28Day | Sodium-coupled sulphate, di- and tri-carboxylate transporters | 0.95906 | 0.29929 | 0.29929 | slc13a5 | 4810.3 | 4810.3 | 4810.3 |  | 4810.3 |  | UP | 1 | 0 |
| 28Day | Extrinsic Pathway of Fibrin Clot Formation | 0.95906 | 0.29929 | 0.29929 | f7 | 2170.26 | 2170.26 | 2170.26 |  | 2170.26 |  | DOWN | 0 | 1 |
| 28Day | HDL clearance | 0.95906 | 0.29929 | 0.29929 | scarb1 | 3278.3 | 3278.3 | 3278.3 |  | 3278.3 |  | DOWN | 0 | 1 |
| 28Day | Serotonin and melatonin biosynthesis | 0.95906 | 0.29929 | 0.29929 | ddc | 5580.16 | 5580.16 | 5580.16 |  | 5580.16 |  | DOWN | 0 | 1 |
| 28Day | JNK (c-Jun kinases) phosphorylation and activation mediated by activated human TAK1 | 0.95906 | 0.29929 | 0.29929 | map2k4 | 2616.5 | 2616.5 | 2616.5 |  | 2616.5 |  | UP | 1 | 0 |
| 28Day | Adenosine P1 receptors | 0.95906 | 0.29929 | 0.29929 | adora1 | 907.506 | 907.506 | 907.506 |  | 907.506 |  | UP | 1 | 0 |
| 28Day | Leukotriene receptors | 0.95906 | 0.29929 | 0.29929 | cysltr1 | 4610.42 | 4610.42 | 4610.42 |  | 4610.42 |  | UP | 1 | 0 |
| 28Day | Abacavir transport and metabolism | 0.95906 | 0.29929 | 0.29929 | slc22a1 | 1681.65 | 1681.65 | 1681.65 |  | 1681.65 |  | DOWN | 0 | 1 |
| 28Day | Pre-NOTCH Processing in Golgi | 0.95906 | 0.29929 | 0.29929 | notch1 | 908.573 | 908.573 | 908.573 |  | 908.573 |  | UP | 1 | 0 |
| 28Day | VLDL clearance | 0.95906 | 0.29929 | 0.29929 | apob | 939.205 | 939.205 | 939.205 |  | 939.205 |  | DOWN | 0 | 1 |
| 28Day | N-glycan trimming and elongation in the cis-Golgi | 0.95906 | 0.29929 | 0.29929 | man1a | 185.394 | 185.394 | 185.394 |  | 185.394 |  | DOWN | 0 | 1 |
| 28Day | Synthesis of 15-eicosatetraenoic acid derivatives | 0.95906 | 0.29929 | 0.29929 | gpx4 | 3909.63 | 3909.63 | 3909.63 |  | 3909.63 |  | DOWN | 0 | 1 |
| 28Day | TRAIL signaling | 0.95906 | 0.29929 | 0.29929 | tnfrsf10b | 4040.75 | 4040.75 | 4040.75 |  | 4040.75 |  | UP | 1 | 0 |
| 28Day | Fructose metabolism | 0.95906 | 0.29929 | 0.29929 | khk | 3680.34 | 3680.34 | 3680.34 |  | 3680.34 |  | DOWN | 0 | 1 |
| 28Day | Metabolism of steroids | 0.87553 | 0.20158 | 0.29972 | akr1c6;pmvk;akr1c12;akr1c19;slc10a1;amacr;hsd17b4;hsd17b3;hsd11b1;gc;fdxr;akr1c14 | 3381.83435 | 3383.375 | 67.9262 | 2102.09252 | 3010.03351 | 1961.85968 | DOWN | 0.25 | 0.75 |
| 90Day | RUNX2 regulates bone development | 0.96479 | 0.30141 | 0.30141 | ar | 1998.95 | 1998.95 | 1998.95 |  | 1998.95 |  | DOWN | 0 | 1 |
| 90Day | CREB3 factors activate genes | 0.96479 | 0.30141 | 0.30141 | crebrf | 3847.29 | 3847.29 | 3847.29 |  | 3847.29 |  | UP | 1 | 0 |

BMD analysis results for functional classification based on dose-responsive genes, using the Reactome database for gene sets in BMDExpress2.2 software.

| Study Day | Gene Set Name | Fisher's Exact Left P-Value | Fisher's Exact Right P-Value | Fisher's Exact Two Tail | Gene Symbols | BMD Mean | BMD Median | BMD Minimum | BMD Standard Deviation | BMD wMean | BMD wSD | Overall Direction | Percent Genes With Overall Direction Up | Percent Genes With Overall Direction Down |
|---|---|---|---|---|---|---|---|---|---|---|---|---|---|---|
| 90Day | SUMO is conjugated to E1 (UBA2:SAE1) | 0.96479 | 0.30141 | 0.30141 | sae1 | 3998.58 | 3998.58 | 3998.58 |  | 3998.58 |  | UP | 1 | 0 |
| 90Day | VLDL assembly | 0.96479 | 0.30141 | 0.30141 | apob | 175.96 | 175.96 | 175.96 |  | 175.96 |  | DOWN | 0 | 1 |
| 90Day | Activation of NIMA Kinases NEK9, NEK6, NEK7 | 0.96479 | 0.30141 | 0.30141 | nek6 | 3442.78 | 3442.78 | 3442.78 |  | 3442.78 |  | UP | 1 | 0 |
| 90Day | Progressive trimming of alpha-1,2-linked mannose residues from Man9/8/7GlcNAc2 to produce Man5GlcNAc2 | 0.96479 | 0.30141 | 0.30141 | man1a | 3931.46 | 3931.46 | 3931.46 |  | 3931.46 |  | DOWN | 0 | 1 |
| 90Day | Biosynthesis of E-series 18(S)-resolvins | 0.96479 | 0.30141 | 0.30141 | gpx4 | 2353.96 | 2353.96 | 2353.96 |  | 2353.96 |  | UP | 1 | 0 |
| 90Day | Formation of the active cofactor, UDP-glucuronate | 0.96479 | 0.30141 | 0.30141 | ugdh | 444.891 | 444.891 | 444.891 |  | 444.891 |  | UP | 1 | 0 |
| 90Day | RUNX1 and FOXP3 control the development of regulatory T lymphocytes (Tregs) | 0.96479 | 0.30141 | 0.30141 | cbfb | 4070.59 | 4070.59 | 4070.59 |  | 4070.59 |  | UP | 1 | 0 |
| 90Day | RUNX1 regulates estrogen receptor mediated transcription | 0.96479 | 0.30141 | 0.30141 | cbfb | 4070.59 | 4070.59 | 4070.59 |  | 4070.59 |  | UP | 1 | 0 |
| 90Day | RUNX1 regulates transcription of genes involved in differentiation of myeloid cells | 0.96479 | 0.30141 | 0.30141 | cbfb | 4070.59 | 4070.59 | 4070.59 |  | 4070.59 |  | UP | 1 | 0 |
| 90Day | RUNX1 regulates transcription of genes involved in interleukin signaling | 0.96479 | 0.30141 | 0.30141 | cbfb | 4070.59 | 4070.59 | 4070.59 |  | 4070.59 |  | UP | 1 | 0 |
| 90Day | Activation of BMF and translocation to mitochondria | 0.96479 | 0.30141 | 0.30141 | bmf | 1597.1 | 1597.1 | 1597.1 |  | 1597.1 |  | DOWN | 0 | 1 |
| 90Day | betaKlotho-mediated ligand binding | 0.96479 | 0.30141 | 0.30141 | klb | 3850.29 | 3850.29 | 3850.29 |  | 3850.29 |  | DOWN | 0 | 1 |
| 90Day | FMO oxidises nucleophiles | 0.96479 | 0.30141 | 0.30141 | fmo2 | 4634.02 | 4634.02 | 4634.02 |  | 4634.02 |  | DOWN | 0 | 1 |
| 90Day | Activation of AMPA receptors | 0.96479 | 0.30141 | 0.30141 | gria3 | 1097.82 | 1097.82 | 1097.82 |  | 1097.82 |  | UP | 1 | 0 |
| 90Day | Interleukin-33 signaling | 0.96479 | 0.30141 | 0.30141 | il1rap | 2684.35 | 2684.35 | 2684.35 |  | 2684.35 |  | DOWN | 0 | 1 |
| 90Day | Abacavir transmembrane transport | 0.96479 | 0.30141 | 0.30141 | slc22a1 | 1050.57 | 1050.57 | 1050.57 |  | 1050.57 |  | DOWN | 0 | 1 |
| 7Day | Endogenous sterols | 0.90822 | 0.22546 | 0.30148 | cyp39a1;ncoa2;ncoa1;arnt | 2493.89215 | 3207.45 | 86.7986 | 1611.46881 | 3047.88667 | 868.85147 | CONFLICT | 0.5 | 0.5 |
| 28Day | Metabolism of Angiotensinogen to Angiotensins | 0.90758 | 0.30153 | 0.30153 | mme;agt | 3209.989 | 3209.989 | 776.548 | 3441.40527 | 2561.91124 | 3317.11631 | DOWN | 0 | 1 |
| 28Day | mRNA decay by 3' to 5' exoribonuclease | 0.90758 | 0.30153 | 0.30153 | exosc3;wdr61 | 4156.29 | 4156.29 | 2805.79 | 1909.89542 | 4910.83867 | 1583.98646 | CONFLICT | 0.5 | 0.5 |
| 28Day | Acyl chain remodelling of PE | 0.90758 | 0.30153 | 0.30153 | pnpla8;abhd4 | 4366.025 | 4366.025 | 4305.66 | 85.3690017 | 4370.65129 | 85.1179265 | UP | 1 | 0 |
| 28Day | PD-1 signaling | 0.90758 | 0.30153 | 0.30153 | h2-ab1;h2-aa | 3461.14 | 3461.14 | 3245.73 | 304.635743 | 3292.13505 | 188.885132 | DOWN | 0 | 1 |
| 28Day | Syndecan interactions | 0.90758 | 0.30153 | 0.30153 | vtn;fn1 | 1801.881 | 1801.881 | 447.762 | 1915.01345 | 2418.97549 | 1704.60122 | DOWN | 0 | 1 |
| 7Day | Signaling by Hedgehog | 0.15638 | 0.91939 | 0.30156 | tubb4b;uba52;tubb2a;tuba4a;sel1l;prkar2a | 2980.59933 | 3080.3 | 919.856 | 1567.90875 | 2665.52182 | 1597.68307 | UP | 0.833333333 | 0.166666667 |
| 7Day | Retrograde transport at the Trans-Golgi-Network | 0.88453 | 0.23056 | 0.30176 | cog6;plin3;rab9;cog5;rab6a;igf2r | 3323.49833 | 3535.83 | 1046.66 | 1169.77215 | 3128.60678 | 1189.09328 | DOWN | 0.333333333 | 0.666666667 |
| 28Day | Clathrin-mediated endocytosis | 0.14051 | 0.92844 | 0.31051 | pacsin3;apob;picalm;trf;hgs;hbegf | 2887.5755 | 3153.66 | 919.738 | 1670.43485 | 2099.89084 | 1545.313 | CONFLICT | 0.5 | 0.5 |
| 90Day | PTEN Regulation | 0.16767 | 0.92447 | 0.31115 | cbx6;gatad2b;pml;hdac2 | 1923.04275 | 1943.2145 | 202.162 | 1698.8359 | 1425.49987 | 1661.38348 | UP | 0.75 | 0.25 |
| 90Day | Autodegradation of Cdh1 by Cdh1:APC/C | 0.17863 | 0.91843 | 0.31115 | anapc10;psmd8;psmc4;psmf1 | 2250.752 | 2213.18 | 186.178 | 1842.30153 | 1652.9232 | 1457.31364 | UP | 1 | 0 |
| 90Day | Molecules associated with elastic fibres | 0.18207 | 0.93837 | 0.3112 | vtn;fn1 | 1077.79535 | 1077.79535 | 45.5307 | 1459.84267 | 655.289482 | 1331.96028 | DOWN | 0 | 1 |
| 90Day | Metabolism of polyamines | 0.18207 | 0.93837 | 0.3112 | slc6a12;arg2 | 3788.58 | 3788.58 | 3445.15 | 485.683364 | 3774.75555 | 485.289706 | CONFLICT | 0.5 | 0.5 |
| 90Day | Dual Incision in GG-NER | 0.16847 | 0.94415 | 0.31147 | pole4;polk | 4753.255 | 4753.255 | 3652.71 | 1556.40567 | 3884.77714 | 955.97646 | CONFLICT | 0.5 | 0.5 |
| 90Day | AKT phosphorylates targets in the cytosol | 0.90642 | 0.31325 | 0.31325 | mdm2;cdkn1a | 2224.395 | 2224.395 | 913.71 | 1853.5885 | 2056.00777 | 1838.2279 | UP | 1 | 0 |
| 90Day | Erythropoietin activates RAS | 0.90642 | 0.31325 | 0.31325 | irs2;vav1 | 2117.93165 | 2117.93165 | 74.8133 | 2889.40568 | 1233.22113 | 2604.46535 | DOWN | 0 | 1 |
| 90Day | CS/DS degradation | 0.90642 | 0.31325 | 0.31325 | hyal1;bgn | 2339.1095 | 2339.1095 | 144.869 | 3103.12467 | 3096.28811 | 2912.51504 | DOWN | 0 | 1 |
| 90Day | HDL remodeling | 0.90642 | 0.31325 | 0.31325 | apoe;apoc3 | 3653.15 | 3653.15 | 1749.82 | 2691.7151 | 3933.46099 | 2662.36393 | DOWN | 0 | 1 |
| 90Day | Signaling by NTRK2 (TRKB) | 0.90642 | 0.31325 | 0.31325 | sos1;ntrk2 | 4819.635 | 4819.635 | 3744.34 | 1520.69677 | 5019.62489 | 1494.16424 | DOWN | 0 | 1 |
| 90Day | Glycosphingolipid metabolism | 0.15575 | 0.9494 | 0.31331 | psap;gm2a | 3480.875 | 3480.875 | 3112.61 | 520.805358 | 3533.31507 | 515.498106 | CONFLICT | 0.5 | 0.5 |
| 90Day | Elastic fibre formation | 0.15575 | 0.9494 | 0.31331 | vtn;fn1 | 1077.79535 | 1077.79535 | 45.5307 | 1459.84267 | 655.289482 | 1331.96028 | DOWN | 0 | 1 |
| 90Day | MAP2K and MAPK activation | 0.15575 | 0.9494 | 0.31331 | tln1;fn1 | 3294.495 | 3294.495 | 2110.06 | 1675.04404 | 3616.30164 | 1612.03397 | DOWN | 0 | 1 |
| 90Day | MET promotes cell motility | 0.15575 | 0.9494 | 0.31331 | gab1;fn1 | 1118.244 | 1118.244 | 126.428 | 1402.63964 | 1214.48427 | 1396.02062 | DOWN | 0 | 1 |
| 90Day | Signaling by SCF-KIT | 0.15575 | 0.9494 | 0.31331 | vav1;sos1 | 5027.99 | 5027.99 | 4161.05 | 1226.03831 | 5362.02772 | 1131.37418 | DOWN | 0 | 1 |

BMD analysis results for functional classification based on dose-responsive genes, using the Reactome database for gene sets in BMDExpress2.2 software.

| Study Day | Gene Set Name | Fisher's Exact Left P-Value | Fisher's Exact Right P-Value | Fisher's Exact Two Tail | Gene Symbols | BMD Mean | BMD Median | BMD Minimum | BMD Standard Deviation | BMD wMean | BMD wSD | Overall Direction | Percent Genes With Overall Direction Up | Percent Genes With Overall Direction Down |
|---|---|---|---|---|---|---|---|---|---|---|---|---|---|---|
| 90Day | Recruitment and ATM-mediated phosphorylation of repair and signaling proteins at DNA double strand breaks | 0.14738 | 0.93536 | 0.31414 | hist1h4h;babam1;hist1h4i;h2afx | 4461.0475 | 4046.18 | 3951.81 | 894.337005 | 4412.91487 | 861.771604 | CONFLICT | 0.5 | 0.5 |
| 7Day | ER Quality Control Compartment (ERQC) | 0.90358 | 0.31436 | 0.31436 | uba52;sel1l | 4493.74 | 4493.74 | 4225.92 | 378.754676 | 4638.58379 | 318.583834 | UP | 1 | 0 |
| 7Day | Dectin-1 mediated noncanonical NF-kB signaling | 0.90358 | 0.31436 | 0.31436 | uba52;btrc | 4484.31 | 4484.31 | 4207.06 | 392.09071 | 4446.04923 | 388.339223 | UP | 1 | 0 |
| 7Day | NIK-->noncanonical NF-kB signaling | 0.90358 | 0.31436 | 0.31436 | uba52;btrc | 4484.31 | 4484.31 | 4207.06 | 392.09071 | 4446.04923 | 388.339223 | UP | 1 | 0 |
| 7Day | Regulation of TP53 Activity through Methylation | 0.90358 | 0.31436 | 0.31436 | kmt5a;uba52 | 4125.35 | 4125.35 | 3489.14 | 899.736811 | 3982.64921 | 876.812007 | UP | 1 | 0 |
| 7Day | Interleukin-35 Signalling | 0.90358 | 0.31436 | 0.31436 | stat1;jak1 | 3735.595 | 3735.595 | 3554.32 | 256.361564 | 3703.94 | 252.422609 | UP | 1 | 0 |
| 7Day | MAP3K8 (TPL2)-dependent MAPK1/3 activation | 0.90358 | 0.31436 | 0.31436 | uba52;btrc | 4484.31 | 4484.31 | 4207.06 | 392.09071 | 4446.04923 | 388.339223 | UP | 1 | 0 |
| 7Day | Ionotropic activity of kainate receptors | 0.90358 | 0.31436 | 0.31436 | calm3;calm2 | 3983.44 | 3983.44 | 3050.32 | 1319.63096 | 3556.9103 | 1173.69957 | CONFLICT | 0.5 | 0.5 |
| 7Day | Activation of Ca-permeable Kainate Receptor | 0.90358 | 0.31436 | 0.31436 | calm3;calm2 | 3983.44 | 3983.44 | 3050.32 | 1319.63096 | 3556.9103 | 1173.69957 | CONFLICT | 0.5 | 0.5 |
| 7Day | CD28 dependent Vav1 pathway | 0.90358 | 0.31436 | 0.31436 | pak2;cdc42 | 3567.05 | 3567.05 | 2538.2 | 1455.01362 | 4188.77837 | 1159.29819 | UP | 1 | 0 |
| 7Day | IRAK1 recruits IKK complex | 0.90358 | 0.31436 | 0.31436 | ube2n;uba52 | 4103.175 | 4103.175 | 3444.79 | 931.096996 | 3863.51066 | 867.216021 | UP | 1 | 0 |
| 7Day | TRAF6 mediated IRF7 activation in TLR7/8 or 9 signaling | 0.90358 | 0.31436 | 0.31436 | ube2n;uba52 | 4103.175 | 4103.175 | 3444.79 | 931.096996 | 3863.51066 | 867.216021 | UP | 1 | 0 |
| 7Day | IRAK1 recruits IKK complex upon TLR7/8 or 9 stimulation | 0.90358 | 0.31436 | 0.31436 | ube2n;uba52 | 4103.175 | 4103.175 | 3444.79 | 931.096996 | 3863.51066 | 867.216021 | UP | 1 | 0 |
| 7Day | GP1b-IX-V activation signalling | 0.90358 | 0.31436 | 0.31436 | ywhaz;flna | 3797.385 | 3797.385 | 2726.98 | 1513.78127 | 3602.54505 | 1488.49203 | CONFLICT | 0.5 | 0.5 |
| 7Day | PECAM1 interactions | 0.90358 | 0.31436 | 0.31436 | yes1;ptpn11 | 3825.31 | 3825.31 | 3629.67 | 276.676741 | 3856.08221 | 273.232797 | UP | 1 | 0 |
| 7Day | Negative regulators of DDX58/IFIH1 signaling | 0.90358 | 0.31436 | 0.31436 | tax1bp1;uba52 | 4021.115 | 4021.115 | 3280.67 | 1047.14736 | 4201.81454 | 1015.48656 | UP | 1 | 0 |
| 7Day | AURKA Activation by TPX2 | 0.16979 | 0.92281 | 0.31585 | tubb4b;tuba4a;nedd1;hsp90aa1 | 1703.9565 | 1410.635 | 919.856 | 998.985626 | 1609.23265 | 1031.31055 | UP | 1 | 0 |
| 7Day | Synthesis of PIPs at the plasma membrane | 0.17837 | 0.93945 | 0.31597 | mtmr6;pten | 3141.54 | 3141.54 | 3108.4 | 46.8670375 | 3155.24331 | 42.6726796 | UP | 1 | 0 |
| 90Day | Homology Directed Repair | 0.16007 | 0.90459 | 0.31634 | hist1h4h;babam1;pole4;ppp4c;hist1h4i;polk;rad51;h2afx;brca2;rad51c | 4045.4582 | 4046.18 | 513.022 | 1470.8127 | 3606.13368 | 1521.5189 | UP | 0.7 | 0.3 |
| 7Day | RUNX1 regulates genes involved in megakaryocyte differentiation and platelet function | 0.16104 | 0.9276 | 0.3166 | hist1h4h;hist1h2bc;hist2h2ac;hist2h2aa1 | 4100.405 | 3802.835 | 3406.55 | 933.741438 | 4060.85571 | 1011.0164 | CONFLICT | 0.5 | 0.5 |
| 7Day | PI Metabolism | 0.16104 | 0.9276 | 0.3166 | tnfaip8l1;mtmr7;mtmr6;pten | 3773.97 | 3510.64 | 3108.4 | 861.939561 | 3673.74135 | 722.775577 | UP | 0.75 | 0.25 |
| 7Day | RNA Polymerase II Promoter Escape | 0.16724 | 0.94419 | 0.31663 | polr2h;taf10 | 3661.695 | 3661.695 | 3358.79 | 428.372359 | 3731.6441 | 416.793865 | UP | 1 | 0 |
| 7Day | RNA Polymerase II Transcription Pre-Initiation And Promoter Opening | 0.16724 | 0.94419 | 0.31663 | polr2h;taf10 | 3661.695 | 3661.695 | 3358.79 | 428.372359 | 3731.6441 | 416.793865 | UP | 1 | 0 |
| 7Day | RNA Polymerase II Transcription Initiation | 0.16724 | 0.94419 | 0.31663 | polr2h;taf10 | 3661.695 | 3661.695 | 3358.79 | 428.372359 | 3731.6441 | 416.793865 | UP | 1 | 0 |
| 7Day | RNA Polymerase II Transcription Initiation And Promoter Clearance | 0.16724 | 0.94419 | 0.31663 | polr2h;taf10 | 3661.695 | 3661.695 | 3358.79 | 428.372359 | 3731.6441 | 416.793865 | UP | 1 | 0 |
| 90Day | Formation of Incision Complex in GG-NER | 0.14387 | 0.95419 | 0.31664 | rad23a;cdk7 | 2921.59 | 2921.59 | 2713.02 | 294.962523 | 2994.07751 | 276.57551 | CONFLICT | 0.5 | 0.5 |
| 7Day | Signaling by Insulin receptor | 0.15266 | 0.93213 | 0.31803 | mapk3;ptpn11;fgf1;atp6v1e1 | 3715.1475 | 3706.295 | 2647.76 | 881.029951 | 3601.78694 | 1028.41317 | CONFLICT | 0.5 | 0.5 |
| 7Day | Transport of Mature mRNA derived from an Intron-Containing Transcript | 0.15266 | 0.93213 | 0.31803 | gm49336;srsf1;tpr;thoc5 | 3646.2575 | 3708.43 | 2535 | 938.48001 | 3502.21235 | 1031.06433 | UP | 1 | 0 |
| 7Day | Transport of Mature Transcript to Cytoplasm | 0.15266 | 0.93213 | 0.31803 | gm49336;srsf1;tpr;thoc5 | 3646.2575 | 3708.43 | 2535 | 938.48001 | 3502.21235 | 1031.06433 | UP | 1 | 0 |
| 28Day | Protein ubiquitination | 0.86907 | 0.25107 | 0.3182 | ube2n;ube2v2;ube2g1;wdr61;ube2k;uchl3 | 4568.95833 | 4655.195 | 3288.55 | 901.493696 | 4499.53987 | 938.691394 | CONFLICT | 0.5 | 0.5 |
| 28Day | Cleavage of Growing Transcript in the Termination Region | 0.86907 | 0.25107 | 0.3182 | cpsf2;u2af2;papola;srsf1;thoc5;bc005561 | 3815.70217 | 4120.91 | 983.533 | 1557.90855 | 4079.59666 | 1475.43623 | CONFLICT | 0.5 | 0.5 |
| 28Day | RNA Polymerase II Transcription Termination | 0.86907 | 0.25107 | 0.3182 | cpsf2;u2af2;papola;srsf1;thoc5;bc005561 | 3815.70217 | 4120.91 | 983.533 | 1557.90855 | 4079.59666 | 1475.43623 | CONFLICT | 0.5 | 0.5 |
| 7Day | Cell-cell junction organization | 0.15671 | 0.94858 | 0.31834 | prkci;ctnnb1 | 1731.8816 | 1731.8816 | 54.5232 | 2372.143 | 959.953496 | 2106.01909 | CONFLICT | 0.5 | 0.5 |
| 7Day | IRS-related events triggered by IGF1R | 0.15671 | 0.94858 | 0.31834 | ptpn11;fgf1 | 3138.715 | 3138.715 | 2647.76 | 694.31522 | 2984.26892 | 659.064823 | CONFLICT | 0.5 | 0.5 |
| 7Day | Neurotransmitter release cycle | 0.15671 | 0.94858 | 0.31834 | slc22a1;slc1a2 | 2973.955 | 2973.955 | 1710.87 | 1786.27194 | 2632.70664 | 1719.84492 | DOWN | 0 | 1 |
| 7Day | Aquaporin-mediated transport | 0.15671 | 0.94858 | 0.31834 | rab11a;prkar2a | 4304.455 | 4304.455 | 4066.56 | 336.434335 | 4288.10382 | 335.638705 | CONFLICT | 0.5 | 0.5 |
| 28Day | Cargo concentration in the ER | 0.89343 | 0.24705 | 0.31866 | lman2;serpina1e;serpina1b;f5 | 3322.35775 | 3403.785 | 619.741 | 2143.6356 | 2388.59316 | 2035.76691 | DOWN | 0 | 1 |

BMD analysis results for functional classification based on dose-responsive genes, using the Reactome database for gene sets in BMDExpress2.2 software.

| Study Day | Gene Set Name | Fisher's Exact Left P-Value | Fisher's Exact Right P-Value | Fisher's Exact Two Tail | Gene Symbols | BMD Mean | BMD Median | BMD Minimum | BMD Standard Deviation | BMD wMean | BMD wSD | Overall Direction | Percent Genes With Overall Direction Up | Percent Genes With Overall Direction Down |
|---|---|---|---|---|---|---|---|---|---|---|---|---|---|---|
| 28Day | HDR through Single Strand Annealing (SSA) | 0.89343 | 0.24705 | 0.31866 | rmi1;rad51;brca1;blm | 3449.574 | 3731.45 | 692.086 | 2060.39551 | 3948.89403 | 1514.9493 | UP | 1 | 0 |
| 28Day | Binding and Uptake of Ligands by Scavenger Receptors | 0.89343 | 0.24705 | 0.31866 | apob;scarb1;lrp1;apoe | 2328.17375 | 2547.595 | 939.205 | 1127.37772 | 2051.38533 | 1157.35972 | DOWN | 0 | 1 |
| 7Day | IGF1R signaling cascade | 0.14676 | 0.95264 | 0.32107 | ptpn11;fgf1 | 3138.715 | 3138.715 | 2647.76 | 694.31522 | 2984.26892 | 659.064823 | CONFLICT | 0.5 | 0.5 |
| 28Day | Cellular responses to stress | 0.16828 | 0.88446 | 0.32111 | hikeshi;dynll1;gm45902;txnrd1;acd;hist1h4i;map2k4;tubb4b;tubb2a;cdc27;p4hb;mdm2;mapkapk2;gstp1;gstp2;capza2;bmi1;tpr | 3964.21589 | 4036.505 | 691.166 | 1605.06154 | 3782.47702 | 1758.58395 | UP | 0.666666667 | 0.333333333 |
| 7Day | Transcriptional regulation by RUNX1 | 0.158 | 0.90562 | 0.32113 | pcgf5;hist1h4h;hist1h2bc;hist2h2ac;uba52;ptpn11;hist2h2aa1;csnk2b;bmi1;abl1 | 4031.764 | 3908.47 | 2829.67 | 827.425176 | 4093.68811 | 851.726114 | UP | 0.7 | 0.3 |
| 90Day | S Phase | 0.17168 | 0.90615 | 0.32132 | esco2;gins1;anapc10;pole4;cables1;orc6;cdkn1a | 3442.09 | 4071.91 | 913.71 | 1798.40239 | 2966.13615 | 1623.11377 | UP | 0.714285714 | 0.285714286 |
| 28Day | Signaling by Hedgehog | 0.17448 | 0.91956 | 0.32185 | tubb4b;tubb2a;p4hb;adcy9 | 3803.5025 | 3561.82 | 2359.45 | 1503.88706 | 3496.76486 | 1471.76062 | CONFLICT | 0.5 | 0.5 |
| 28Day | Collagen formation | 0.18117 | 0.9158 | 0.32186 | p4hb;ctss;col8a1;bmp1 | 4192.9125 | 4983.815 | 1023.63 | 2230.98048 | 3878.77064 | 2323.26474 | CONFLICT | 0.5 | 0.5 |
| 28Day | Stimuli-sensing channels | 0.168 | 0.92317 | 0.3222 | ano8;clcn6;sgk3;clcn2 | 3151.355 | 3205.75 | 2316.49 | 647.347601 | 3143.31625 | 644.169192 | DOWN | 0.25 | 0.75 |
| 28Day | Signaling by VEGF | 0.16171 | 0.92663 | 0.3229 | pdpk1;mapkapk2;cdc42;brk1 | 3372.312 | 3919.245 | 192.988 | 2536.00426 | 4213.88679 | 1981.66272 | DOWN | 0.25 | 0.75 |
| 7Day | M Phase | 0.16288 | 0.88324 | 0.32466 | clasp2;gm49336;pds5a;hist1h4h;hist1h2bc;kmt5a;cenpk;nek6;arpp19;hist2h2ac;mapk3;tubb4b;uba52;tubb2a;tuba4a;cdc27;rab1a;ppp2cb;nedd1;kif2a;hsp90aa1;hist2h2aa1;tpr;xpo1 | 3251.11808 | 3521.41 | 770.098 | 1294.16242 | 3190.92806 | 1264.84947 | UP | 0.833333333 | 0.166666667 |
| 7Day | Signaling by Type 1 Insulin-like Growth Factor 1 Receptor (IGF1R) | 0.13737 | 0.95639 | 0.32477 | ptpn11;fgf1 | 3138.715 | 3138.715 | 2647.76 | 694.31522 | 2984.26892 | 659.064823 | CONFLICT | 0.5 | 0.5 |
| 7Day | Glycosaminoglycan metabolism | 0.17429 | 0.90399 | 0.32583 | hs3st3b1;hgsnat;sdc3;hyal1;ext1;bgn;arsb | 3466.58564 | 3370.58 | 34.2395 | 1859.25257 | 3868.38892 | 1587.24792 | DOWN | 0.142857143 | 0.857142857 |
| 28Day | Signaling by FGFR2 | 0.15204 | 0.94994 | 0.32647 | polr2a;fgf1 | 3254.12 | 3254.12 | 1467.57 | 2526.56324 | 2657.99173 | 2381.76069 | CONFLICT | 0.5 | 0.5 |
| 7Day | Role of ABL in ROBO-SLIT signaling | 0.95322 | 0.32694 | 0.32694 | abl1 | 3368.05 | 3368.05 | 3368.05 |  | 3368.05 |  | DOWN | 0 | 1 |
| 7Day | Neurotransmitter uptake and metabolism In glial cells | 0.95322 | 0.32694 | 0.32694 | slc1a2 | 1710.87 | 1710.87 | 1710.87 |  | 1710.87 |  | DOWN | 0 | 1 |
| 7Day | Astrocytic Glutamate-Glutamine Uptake And Metabolism | 0.95322 | 0.32694 | 0.32694 | slc1a2 | 1710.87 | 1710.87 | 1710.87 |  | 1710.87 |  | DOWN | 0 | 1 |
| 7Day | Scavenging by Class B Receptors | 0.95322 | 0.32694 | 0.32694 | apob | 1999.21 | 1999.21 | 1999.21 |  | 1999.21 |  | DOWN | 0 | 1 |
| 7Day | Phosphorylation of proteins involved in G1/S transition by active Cyclin E:Cdk2 complexes | 0.95322 | 0.32694 | 0.32694 | ccne2 | 4598.19 | 4598.19 | 4598.19 |  | 4598.19 |  | UP | 1 | 0 |
| 7Day | Ubiquitin-dependent degradation of Cyclin D1 | 0.95322 | 0.32694 | 0.32694 | uba52 | 4761.56 | 4761.56 | 4761.56 |  | 4761.56 |  | UP | 1 | 0 |
| 7Day | Ubiquitin-dependent degradation of Cyclin D | 0.95322 | 0.32694 | 0.32694 | uba52 | 4761.56 | 4761.56 | 4761.56 |  | 4761.56 |  | UP | 1 | 0 |
| 7Day | Selenoamino acid metabolism | 0.95322 | 0.32694 | 0.32694 | txnrd1 | 2303.89 | 2303.89 | 2303.89 |  | 2303.89 |  | UP | 1 | 0 |
| 7Day | Glycine degradation | 0.95322 | 0.32694 | 0.32694 | dld | 5143.63 | 5143.63 | 5143.63 |  | 5143.63 |  | UP | 1 | 0 |
| 7Day | Cholesterol biosynthesis via desmosterol | 0.95322 | 0.32694 | 0.32694 | ebp | 2966.55 | 2966.55 | 2966.55 |  | 2966.55 |  | DOWN | 0 | 1 |
| 7Day | Organic anion transport | 0.95322 | 0.32694 | 0.32694 | slc22a12 | 3194.01 | 3194.01 | 3194.01 |  | 3194.01 |  | UP | 1 | 0 |
| 7Day | CLEC7A/inflammasome pathway | 0.95322 | 0.32694 | 0.32694 | pycard | 4728.43 | 4728.43 | 4728.43 |  | 4728.43 |  | DOWN | 0 | 1 |
| 7Day | Amine Oxidase reactions | 0.95322 | 0.32694 | 0.32694 | maob | 46.9364 | 46.9364 | 46.9364 |  | 46.9364 |  | DOWN | 0 | 1 |
| 7Day | Advanced glycosylation endproduct receptor signaling | 0.95322 | 0.32694 | 0.32694 | capza2 | 3113.17 | 3113.17 | 3113.17 |  | 3113.17 |  | UP | 1 | 0 |
| 7Day | NGF processing | 0.95322 | 0.32694 | 0.32694 | pcsk5 | 4553.08 | 4553.08 | 4553.08 |  | 4553.08 |  | DOWN | 0 | 1 |
| 7Day | Expression and Processing of Neurotrophins | 0.95322 | 0.32694 | 0.32694 | pcsk5 | 4553.08 | 4553.08 | 4553.08 |  | 4553.08 |  | DOWN | 0 | 1 |
| 7Day | Neurofascin interactions | 0.95322 | 0.32694 | 0.32694 | sdcbp | 3244.26 | 3244.26 | 3244.26 |  | 3244.26 |  | UP | 1 | 0 |
| 7Day | Caspase activation via Dependence Receptors in the absence of ligand | 0.95322 | 0.32694 | 0.32694 | casp9 | 3648.67 | 3648.67 | 3648.67 |  | 3648.67 |  | DOWN | 0 | 1 |
| 7Day | LRR FLII-interacting protein 1 (LRRFIP1) activates type I IFN production | 0.95322 | 0.32694 | 0.32694 | ctnnb1 | 54.5232 | 54.5232 | 54.5232 |  | 54.5232 |  | DOWN | 0 | 1 |
| 7Day | Reelin signalling pathway | 0.95322 | 0.32694 | 0.32694 | reln | 3928.43 | 3928.43 | 3928.43 |  | 3928.43 |  | DOWN | 0 | 1 |
| 7Day | Scavenging by Class H Receptors | 0.95322 | 0.32694 | 0.32694 | apob | 1999.21 | 1999.21 | 1999.21 |  | 1999.21 |  | DOWN | 0 | 1 |

BMD analysis results for functional classification based on dose-responsive genes, using the Reactome database for gene sets in BMDExpress2.2 software.

| Study Day | Gene Set Name | Fisher's Exact Left P-Value | Fisher's Exact Right P-Value | Fisher's Exact Two Tail | Gene Symbols | BMD Mean | BMD Median | BMD Minimum | BMD Standard Deviation | BMD wMean | BMD wSD | Overall Direction | Percent Genes With Overall Direction Up | Percent Genes With Overall Direction Down |
|---|---|---|---|---|---|---|---|---|---|---|---|---|---|---|
| 28Day | ABC transporters in lipid homeostasis | 0.89325 | 0.3275 | 0.3275 | abca3;abcd3 | 1989.92 | 1989.92 | 1485.35 | 713.569737 | 1670.93402 | 552.881235 | DOWN | 0 | 1 |
| 28Day | Synthesis of glycosylphosphatidylinositol (GPI) | 0.89325 | 0.3275 | 0.3275 | pigp;pign | 5408.8 | 5408.8 | 5041.89 | 518.889098 | 5603.60631 | 439.712292 | UP | 1 | 0 |
| 28Day | RIPK1-mediated regulated necrosis | 0.89325 | 0.3275 | 0.3275 | tnfrsf10b;birc2 | 4951.5 | 4951.5 | 4040.75 | 1287.995 | 4749.40037 | 1255.8832 | UP | 1 | 0 |
| 28Day | Regulated Necrosis | 0.89325 | 0.3275 | 0.3275 | tnfrsf10b;birc2 | 4951.5 | 4951.5 | 4040.75 | 1287.995 | 4749.40037 | 1255.8832 | UP | 1 | 0 |
| 7Day | Metabolism of fat-soluble vitamins | 0.89731 | 0.20088 | 0.32938 | akr1c6;apob;ttr;sdc3;lrp1;apoe;akr1c14 | 2956.06943 | 2842.81 | 113.316 | 1991.38668 | 3428.01601 | 1609.42615 | DOWN | 0.285714286 | 0.714285714 |
| 7Day | Xenobiotics | 0.89731 | 0.20088 | 0.32938 | cyp3a25;cyp3a11;cyp2e1;cyp2c37;cyp2c29;arnt;cyp3a41b | 3350.14329 | 3382.64 | 529.743 | 1671.45384 | 3114.36428 | 1507.72766 | DOWN | 0.285714286 | 0.714285714 |
| 7Day | Synthesis of IP3 and IP4 in the cytosol | 0.88227 | 0.26798 | 0.33032 | itpk1;pten;calm3;calm2 | 3684.875 | 3386.31 | 3050.32 | 853.925176 | 3438.70794 | 788.233521 | CONFLICT | 0.5 | 0.5 |
| 28Day | Transport of small molecules | 0.1761 | 0.86409 | 0.3335 | lmf1;atp6v0e2;abcb8;slc35d2;micu2;npc2;rab11a;ano8;slc9a5;abca3;abca8b;slc25a10;clcn6;abcc4;apob;slc13a5;a2m;trf;slc17a8;scarb1;slc22a1;slc1a2;abcd3;abcb4;abcb1b;p4hb;sgk3;gnb5;slc6a13;ftl1;ces3b;clcn2;bmp1;azgp1;atp6v1e1;apoe;adcy9;slco2b1 | 2786.96053 | 2846.515 | 151.142 | 1606.28246 | 2694.95041 | 1574.5074 | CONFLICT | 0.447368421 | 0.552631579 |
| 90Day | RHO GTPases Activate Formins | 0.16072 | 0.90187 | 0.33396 | cenpu;fmnl2;tubb6;tubb4b;tubb2a;tuba1b;kntc1;nudc;cdc42;sec13;cenpf | 2685.02709 | 2758.9 | 156.487 | 1642.73646 | 2833.25496 | 1787.93511 | UP | 0.909090909 | 0.090909091 |
| 90Day | Apoptosis | 0.19162 | 0.88912 | 0.34359 | hmgb2;ywhaz;tnfrsf10b;rock1;bmf;dsg2;ctnnb1;bax | 2260.36 | 2106.36 | 137.958 | 1594.54742 | 2319.13546 | 1448.3806 | UP | 0.625 | 0.375 |
| 7Day | Downstream signal transduction | 0.86814 | 0.28976 | 0.3462 | rasa1;stat1;ptpn11;kras | 4372.8325 | 4037.79 | 3629.67 | 966.662513 | 4569.74061 | 1058.51347 | UP | 0.75 | 0.25 |
| 7Day | ER-Phagosome pathway | 0.86814 | 0.28976 | 0.3462 | tap2;sec22b;h2-t23;h2-q10 | 3670.8125 | 3724.57 | 2584.12 | 941.890827 | 3414.68027 | 934.619277 | DOWN | 0.25 | 0.75 |
| 28Day | Regulation of ornithine decarboxylase (ODC) | 0.94135 | 0.34741 | 0.34741 | odc1 | 2869.35 | 2869.35 | 2869.35 |  | 2869.35 |  | DOWN | 0 | 1 |
| 28Day | Fibronectin matrix formation | 0.94135 | 0.34741 | 0.34741 | fn1 | 3156 | 3156 | 3156 |  | 3156 |  | DOWN | 0 | 1 |
| 28Day | FGFR1b ligand binding and activation | 0.94135 | 0.34741 | 0.34741 | fgf1 | 1467.57 | 1467.57 | 1467.57 |  | 1467.57 |  | DOWN | 0 | 1 |
| 28Day | Glucocorticoid biosynthesis | 0.94135 | 0.34741 | 0.34741 | hsd11b1 | 67.9262 | 67.9262 | 67.9262 |  | 67.9262 |  | DOWN | 0 | 1 |
| 28Day | TP53 Regulates Transcription of Genes Involved in Cytochrome C Release | 0.94135 | 0.34741 | 0.34741 | bnip3l | 1841.2 | 1841.2 | 1841.2 |  | 1841.2 |  | DOWN | 0 | 1 |
| 28Day | mRNA Editing | 0.94135 | 0.34741 | 0.34741 | a1cf | 1306.69 | 1306.69 | 1306.69 |  | 1306.69 |  | DOWN | 0 | 1 |
| 28Day | Regulation of expression of SLITs and ROBOs | 0.94135 | 0.34741 | 0.34741 | dag1 | 5666.49 | 5666.49 | 5666.49 |  | 5666.49 |  | DOWN | 0 | 1 |
| 28Day | Amino Acid conjugation | 0.94135 | 0.34741 | 0.34741 | glyat | 3673.59 | 3673.59 | 3673.59 |  | 3673.59 |  | UP | 1 | 0 |
| 28Day | Conjugation of carboxylic acids | 0.94135 | 0.34741 | 0.34741 | glyat | 3673.59 | 3673.59 | 3673.59 |  | 3673.59 |  | UP | 1 | 0 |
| 28Day | activated TAK1 mediates p38 MAPK activation | 0.94135 | 0.34741 | 0.34741 | mapkapk2 | 5375 | 5375 | 5375 |  | 5375 |  | DOWN | 0 | 1 |
| 28Day | PTK6 promotes HIF1A stabilization | 0.94135 | 0.34741 | 0.34741 | hbegf | 919.738 | 919.738 | 919.738 |  | 919.738 |  | UP | 1 | 0 |
| 28Day | AMPK inhibits chREBP transcriptional activation activity | 0.94135 | 0.34741 | 0.34741 | adipor2 | 2864.86 | 2864.86 | 2864.86 |  | 2864.86 |  | DOWN | 0 | 1 |
| 28Day | Synthesis of 12-eicosatetraenoic acid derivatives | 0.94135 | 0.34741 | 0.34741 | gpx4 | 3909.63 | 3909.63 | 3909.63 |  | 3909.63 |  | DOWN | 0 | 1 |
| 90Day | Response to elevated platelet cytosolic Ca2+ | 0.18291 | 0.88388 | 0.34823 | spp2;trf;tln1;serpina1e;psap;plg;fn1;ecm1;anxa5;ahsg;actn1;sccpdh | 2421.70252 | 2481.665 | 82.4742 | 1669.5291 | 2984.03278 | 1802.70421 | DOWN | 0.083333333 | 0.916666667 |
| 7Day | DNA Replication | 0.16887 | 0.9039 | 0.34942 | psmd5;psmd6;psmc4;uba52;cdc27;psmc2;prim2;ccne2 | 3685.25375 | 3897.135 | 2309.23 | 862.418796 | 3751.9907 | 969.75616 | UP | 1 | 0 |
| 7Day | ERKs are inactivated | 0.88307 | 0.35026 | 0.35026 | mapk3;ppp2cb | 4213.64 | 4213.64 | 3627.04 | 829.577676 | 4084.83206 | 809.330679 | CONFLICT | 0.5 | 0.5 |
| 7Day | Glycogen breakdown (glycogenolysis) | 0.88307 | 0.35026 | 0.35026 | calm3;calm2 | 3983.44 | 3983.44 | 3050.32 | 1319.63096 | 3556.9103 | 1173.69957 | CONFLICT | 0.5 | 0.5 |
| 28Day | COPII-mediated vesicle transport | 0.86649 | 0.24396 | 0.35248 | lman2;ppp6r3;sec22c;serpina1e;serpina1b;f5;bet1 | 3734.47014 | 3497.94 | 619.741 | 1768.65464 | 2866.68484 | 1722.46541 | DOWN | 0.285714286 | 0.714285714 |
| 90Day | APC/C:Cdh1 mediated degradation of Cdc20 and other APC/C:Cdh1 targeted proteins in late mitosis/early G1 | 0.20979 | 0.94986 | 0.35294 | anapc10 | 4390.47 | 4390.47 | 4390.47 |  | 4390.47 |  | UP | 1 | 0 |
| 90Day | Cdc20:Phospho-APC/C mediated degradation of Cyclin A | 0.20979 | 0.94986 | 0.35294 | anapc10 | 4390.47 | 4390.47 | 4390.47 |  | 4390.47 |  | UP | 1 | 0 |
| 90Day | CDK-mediated phosphorylation and removal of Cdc6 | 0.20979 | 0.94986 | 0.35294 | anapc10 | 4390.47 | 4390.47 | 4390.47 |  | 4390.47 |  | UP | 1 | 0 |
| 90Day | Cholesterol biosynthesis | 0.20979 | 0.94986 | 0.35294 | hsd17b7 | 5001.13 | 5001.13 | 5001.13 |  | 5001.13 |  | DOWN | 0 | 1 |
| 90Day | Processing of Capped Intronless Pre-mRNA | 0.20979 | 0.94986 | 0.35294 | cstf2t | 5843.41 | 5843.41 | 5843.41 |  | 5843.41 |  | DOWN | 0 | 1 |

BMD analysis results for functional classification based on dose-responsive genes, using the Reactome database for gene sets in BMDExpress2.2 software.

| Study Day | Gene Set Name | Fisher's Exact Left P-Value | Fisher's Exact Right P-Value | Fisher's Exact Two Tail | Gene Symbols | BMD Mean | BMD Median | BMD Minimum | BMD Standard Deviation | BMD wMean | BMD wSD | Overall Direction | Percent Genes With Overall Direction Up | Percent Genes With Overall Direction Down |
|---|---|---|---|---|---|---|---|---|---|---|---|---|---|---|
| 90Day | WNT ligand biogenesis and trafficking | 0.20979 | 0.94986 | 0.35294 | tmed5 | 3479.95 | 3479.95 | 3479.95 |  | 3479.95 |  | UP | 1 | 0 |
| 7Day | Signaling by TGF-beta family members | 0.15928 | 0.92249 | 0.35301 | uba52;tgfbr1;tfdp1;prkcz;ccnk | 3804.8848 | 4761.56 | 707.264 | 2279.30374 | 4710.02856 | 1911.5824 | UP | 0.8 | 0.2 |
| 28Day | Acyl chain remodelling of PC | 0.87811 | 0.3532 | 0.3532 | pnpla8;pla2g4c | 3890.355 | 3890.355 | 3475.05 | 587.329964 | 3736.74096 | 545.675674 | UP | 1 | 0 |
| 28Day | Metabolism of porphyrins | 0.87811 | 0.3532 | 0.3532 | ugt1a1;fech | 2693.2965 | 2693.2965 | 309.913 | 3370.61327 | 2866.03689 | 3361.74885 | DOWN | 0 | 1 |
| 28Day | Processing of Intronless Pre-mRNAs | 0.87811 | 0.3532 | 0.3532 | cpsf2;papola | 3117.8765 | 3117.8765 | 983.533 | 3018.41752 | 4045.49974 | 2718.43238 | DOWN | 0 | 1 |
| 90Day | Formation of the beta-catenin:TCF transactivating complex | 0.19177 | 0.95552 | 0.35358 | ctnnb1 | 4087.04 | 4087.04 | 4087.04 |  | 4087.04 |  | DOWN | 0 | 1 |
| 90Day | ISG15 antiviral mechanism | 0.19177 | 0.95552 | 0.35358 | usp18 | 4074.3 | 4074.3 | 4074.3 |  | 4074.3 |  | UP | 1 | 0 |
| 90Day | Interleukin receptor SHC signaling | 0.19177 | 0.95552 | 0.35358 | sos1 | 5894.93 | 5894.93 | 5894.93 |  | 5894.93 |  | DOWN | 0 | 1 |
| 90Day | Digestion | 0.19177 | 0.95552 | 0.35358 | mgam | 2596.25 | 2596.25 | 2596.25 |  | 2596.25 |  | DOWN | 0 | 1 |
| 90Day | Endogenous sterols | 0.19177 | 0.95552 | 0.35358 | cyp39a1 | 4130.84 | 4130.84 | 4130.84 |  | 4130.84 |  | DOWN | 0 | 1 |
| 90Day | TNFs bind their physiological receptors | 0.19177 | 0.95552 | 0.35358 | eda2r | 1752.24 | 1752.24 | 1752.24 |  | 1752.24 |  | UP | 1 | 0 |
| 90Day | Beta defensins | 0.19177 | 0.95552 | 0.35358 | defb30 | 5550.64 | 5550.64 | 5550.64 |  | 5550.64 |  | UP | 1 | 0 |
| 90Day | Defensins | 0.19177 | 0.95552 | 0.35358 | defb30 | 5550.64 | 5550.64 | 5550.64 |  | 5550.64 |  | UP | 1 | 0 |
| 90Day | APC:Cdc20 mediated degradation of cell cycle proteins prior to satisfation of the cell cycle checkpoint | 0.19177 | 0.95552 | 0.35358 | anapc10 | 4390.47 | 4390.47 | 4390.47 |  | 4390.47 |  | UP | 1 | 0 |
| 90Day | Negative regulation of FGFR3 signaling | 0.19177 | 0.95552 | 0.35358 | fgf1 | 242.429 | 242.429 | 242.429 |  | 242.429 |  | DOWN | 0 | 1 |
| 28Day | SUMOylation | 0.18145 | 0.8949 | 0.35381 | hist1h4i;rad21;mdm2;ikbkg;brca1;bmi1;blm;tpr | 3945.312 | 4027.865 | 692.086 | 1781.08975 | 3897.46085 | 1655.95085 | UP | 0.875 | 0.125 |
| 90Day | Deadenylation of mRNA | 0.17514 | 0.96055 | 0.35653 | paip1 | 212.512 | 212.512 | 212.512 |  | 212.512 |  | UP | 1 | 0 |
| 90Day | RNA Pol II CTD phosphorylation and interaction with CE | 0.17514 | 0.96055 | 0.35653 | cdk7 | 3130.16 | 3130.16 | 3130.16 |  | 3130.16 |  | UP | 1 | 0 |
| 90Day | Platelet calcium homeostasis | 0.17514 | 0.96055 | 0.35653 | p2rx4 | 185.907 | 185.907 | 185.907 |  | 185.907 |  | DOWN | 0 | 1 |
| 90Day | Sema4D induced cell migration and growth-cone collapse | 0.88169 | 0.35657 | 0.35657 | rock2;rock1 | 2068.101 | 2068.101 | 262.092 | 2554.08242 | 1087.57877 | 2144.87514 | UP | 1 | 0 |
| 90Day | MET activates RAS signaling | 0.88169 | 0.35657 | 0.35657 | ranbp9;sos1 | 4628.24 | 4628.24 | 3361.55 | 1791.37018 | 5369.66555 | 1452.4405 | CONFLICT | 0.5 | 0.5 |
| 90Day | STING mediated induction of host immune responses | 0.88169 | 0.35657 | 0.35657 | tmem173;tbk1 | 2558.24 | 2558.24 | 1058.39 | 2121.10821 | 2553.28861 | 2121.09665 | DOWN | 0 | 1 |
| 90Day | CDC6 association with the ORC:origin complex | 0.88169 | 0.35657 | 0.35657 | orc6;e2f2 | 4208.98 | 4208.98 | 4168.34 | 57.4736392 | 4203.70416 | 56.9872814 | UP | 1 | 0 |
| 90Day | Assembly of active LPL and LIPC lipase complexes | 0.88169 | 0.35657 | 0.35657 | pcsk5;lipc | 3427.31 | 3427.31 | 3093.17 | 472.54532 | 3265.76421 | 413.648394 | DOWN | 0 | 1 |
| 90Day | Signal attenuation | 0.88169 | 0.35657 | 0.35657 | irs2;sos1 | 2984.87165 | 2984.87165 | 74.8133 | 4115.44399 | 2818.21844 | 4108.68989 | DOWN | 0 | 1 |
| 28Day | Metabolism of water-soluble vitamins and cofactors | 0.17087 | 0.91508 | 0.35675 | nudt12;enpp1;pcx;acp5;cyb5a | 3447.1046 | 3121.78 | 201.213 | 2170.0831 | 2762.25847 | 2129.24585 | DOWN | 0.2 | 0.8 |
| 7Day | ROS, RNS production in phagocytes | 0.21115 | 0.94889 | 0.35787 | atp6v1e1 | 3782.92 | 3782.92 | 3782.92 |  | 3782.92 |  | UP | 1 | 0 |
| 7Day | DAP12 signaling | 0.21115 | 0.94889 | 0.35787 | kras | 4158.71 | 4158.71 | 4158.71 |  | 4158.71 |  | UP | 1 | 0 |
| 7Day | EPH-ephrin mediated repulsion of cells | 0.21115 | 0.94889 | 0.35787 | yes1 | 4020.95 | 4020.95 | 4020.95 |  | 4020.95 |  | UP | 1 | 0 |
| 7Day | Termination of translesion DNA synthesis | 0.21115 | 0.94889 | 0.35787 | uba52 | 4761.56 | 4761.56 | 4761.56 |  | 4761.56 |  | UP | 1 | 0 |
| 7Day | G-protein beta:gamma signalling | 0.19604 | 0.95372 | 0.35829 | cdc42 | 4595.9 | 4595.9 | 4595.9 |  | 4595.9 |  | UP | 1 | 0 |
| 7Day | Transferrin endocytosis and recycling | 0.19604 | 0.95372 | 0.35829 | atp6v1e1 | 3782.92 | 3782.92 | 3782.92 |  | 3782.92 |  | UP | 1 | 0 |
| 7Day | Signal amplification | 0.19604 | 0.95372 | 0.35829 | gnai3 | 794.2 | 794.2 | 794.2 |  | 794.2 |  | UP | 1 | 0 |
| 7Day | Sialic acid metabolism | 0.19604 | 0.95372 | 0.35829 | neu1 | 3613.22 | 3613.22 | 3613.22 |  | 3613.22 |  | DOWN | 0 | 1 |
| 7Day | Glucagon signaling in metabolic regulation | 0.19604 | 0.95372 | 0.35829 | prkar2a | 4066.56 | 4066.56 | 4066.56 |  | 4066.56 |  | DOWN | 0 | 1 |
| 7Day | Formation of the Early Elongation Complex | 0.19604 | 0.95372 | 0.35829 | polr2h | 3964.6 | 3964.6 | 3964.6 |  | 3964.6 |  | UP | 1 | 0 |
| 7Day | Amino acid synthesis and interconversion (transamination) | 0.1819 | 0.9581 | 0.36031 | kyat1 | 4788.28 | 4788.28 | 4788.28 |  | 4788.28 |  | DOWN | 0 | 1 |
| 7Day | Resolution of D-loop Structures through Holliday Junction Intermediates | 0.1819 | 0.9581 | 0.36031 | rad51ap1 | 3877.33 | 3877.33 | 3877.33 |  | 3877.33 |  | UP | 1 | 0 |
| 7Day | Digestion and absorption | 0.1819 | 0.9581 | 0.36031 | mgam | 132.859 | 132.859 | 132.859 |  | 132.859 |  | DOWN | 0 | 1 |
| 7Day | Activation of the pre-replicative complex | 0.1819 | 0.9581 | 0.36031 | prim2 | 4006.14 | 4006.14 | 4006.14 |  | 4006.14 |  | UP | 1 | 0 |

BMD analysis results for functional classification based on dose-responsive genes, using the Reactome database for gene sets in BMDExpress2.2 software.

| Study Day | Gene Set Name | Fisher's Exact Left P-Value | Fisher's Exact Right P-Value | Fisher's Exact Two Tail | Gene Symbols | BMD Mean | BMD Median | BMD Minimum | BMD Standard Deviation | BMD wMean | BMD wSD | Overall Direction | Percent Genes With Overall Direction Up | Percent Genes With Overall Direction Down |
|---|---|---|---|---|---|---|---|---|---|---|---|---|---|---|
| 90Day | MAPK6/MAPK4 signaling | 0.15982 | 0.96501 | 0.36161 | cdc42 | 156.487 | 156.487 | 156.487 |  | 156.487 |  | UP | 1 | 0 |
| 90Day | MAPK targets/ Nuclear events mediated by MAP kinases | 0.15982 | 0.96501 | 0.36161 | mapk14 | 4261.96 | 4261.96 | 4261.96 |  | 4261.96 |  | DOWN | 0 | 1 |
| 90Day | Gluconeogenesis | 0.15982 | 0.96501 | 0.36161 | pcx | 410.825 | 410.825 | 410.825 |  | 410.825 |  | DOWN | 0 | 1 |
| 90Day | Endosomal Sorting Complex Required For Transport (ESCRT) | 0.15982 | 0.96501 | 0.36161 | ubap1 | 4451.86 | 4451.86 | 4451.86 |  | 4451.86 |  | UP | 1 | 0 |
| 90Day | TNFR1-induced NFkappaB signaling pathway | 0.15982 | 0.96501 | 0.36161 | ikbkg | 3265.56 | 3265.56 | 3265.56 |  | 3265.56 |  | UP | 1 | 0 |
| 90Day | APC/C:Cdc20 mediated degradation of mitotic proteins | 0.15982 | 0.96501 | 0.36161 | anapc10 | 4390.47 | 4390.47 | 4390.47 |  | 4390.47 |  | UP | 1 | 0 |
| 90Day | Activation of APC/C and APC/C:Cdc20 mediated degradation of mitotic proteins | 0.15982 | 0.96501 | 0.36161 | anapc10 | 4390.47 | 4390.47 | 4390.47 |  | 4390.47 |  | UP | 1 | 0 |
| 90Day | Calmodulin induced events | 0.15982 | 0.96501 | 0.36161 | camkk2 | 98.0082 | 98.0082 | 98.0082 |  | 98.0082 |  | DOWN | 0 | 1 |
| 90Day | CaM pathway | 0.15982 | 0.96501 | 0.36161 | camkk2 | 98.0082 | 98.0082 | 98.0082 |  | 98.0082 |  | DOWN | 0 | 1 |
| 90Day | Signaling by PTK6 | 0.18188 | 0.92571 | 0.36313 | gpnmb;rasa1;nrg1 | 3532.88667 | 3912.34 | 2133.64 | 1253.36637 | 4185.38166 | 823.865612 | UP | 1 | 0 |
| 90Day | Signaling by Non-Receptor Tyrosine Kinases | 0.18188 | 0.92571 | 0.36313 | gpnmb;rasa1;nrg1 | 3532.88667 | 3912.34 | 2133.64 | 1253.36637 | 4185.38166 | 823.865612 | UP | 1 | 0 |
| 90Day | HDMs demethylate histones | 0.18188 | 0.92571 | 0.36313 | hist1h4h;hist1h4i;hist1h3c | 2923.45967 | 3951.81 | 811.859 | 1828.90583 | 2005.0795 | 1880.81489 | DOWN | 0.333333333 | 0.666666667 |
| 90Day | Negative regulation of the PI3K/AKT network | 0.20117 | 0.87896 | 0.36375 | klb;irs2;vav1;tgfa;nrg1;il1rap;gab1;fgf1;areg | 2353.84448 | 2684.35 | 74.8133 | 1778.57928 | 2322.93121 | 1581.92848 | DOWN | 0.333333333 | 0.666666667 |
| 90Day | Mitotic Prophase | 0.20117 | 0.87896 | 0.36375 | smc4;hist1h4h;mastl;nek6;arpp19;hist1h4i;nup153;h2afx;sec13 | 3275.56122 | 3680.35 | 577.791 | 1139.1806 | 3412.99082 | 939.1085 | UP | 0.777777778 | 0.222222222 |
| 7Day | Resolution of D-Loop Structures | 0.16868 | 0.96206 | 0.36381 | rad51ap1 | 3877.33 | 3877.33 | 3877.33 |  | 3877.33 |  | UP | 1 | 0 |
| 28Day | Regulation of PTEN gene transcription | 0.20594 | 0.9499 | 0.36442 | bmi1 | 3918.46 | 3918.46 | 3918.46 |  | 3918.46 |  | UP | 1 | 0 |
| 28Day | PLC beta mediated events | 0.20594 | 0.9499 | 0.36442 | adcy9 | 4220.6 | 4220.6 | 4220.6 |  | 4220.6 |  | DOWN | 0 | 1 |
| 28Day | G-protein mediated events | 0.19521 | 0.95335 | 0.36513 | adcy9 | 4220.6 | 4220.6 | 4220.6 |  | 4220.6 |  | DOWN | 0 | 1 |
| 28Day | Collagen chain trimerization | 0.19521 | 0.95335 | 0.36513 | col8a1 | 4236.71 | 4236.71 | 4236.71 |  | 4236.71 |  | UP | 1 | 0 |
| 28Day | RNA Polymerase I Transcription Initiation | 0.19521 | 0.95335 | 0.36513 | polr1a | 5863.06 | 5863.06 | 5863.06 |  | 5863.06 |  | DOWN | 0 | 1 |
| 90Day | Estrogen-dependent gene expression | 0.17492 | 0.89714 | 0.36535 | hist1h4h;hist1h4i;hist1h3c;nr5a2;yy1;hsp90aa1;h2afx;ddx5;cbfb | 2963.50756 | 3951.81 | 174.249 | 1923.75546 | 2558.29556 | 1937.36612 | CONFLICT | 0.555555556 | 0.444444444 |
| 90Day | Ribosomal scanning and start codon recognition | 0.16973 | 0.93181 | 0.36571 | eif3m;rps27l;rps12 | 2578.52 | 2517.83 | 1662.63 | 947.693586 | 2378.76706 | 980.623942 | UP | 1 | 0 |
| 28Day | Signaling by ERBB2 | 0.18498 | 0.95657 | 0.36666 | hbegf | 919.738 | 919.738 | 919.738 |  | 919.738 |  | UP | 1 | 0 |
| 28Day | Phase 0 - rapid depolarisation | 0.18498 | 0.95657 | 0.36666 | scn7a | 3855.8 | 3855.8 | 3855.8 |  | 3855.8 |  | UP | 1 | 0 |
| 7Day | Synthesis of substrates in N-glycan biosythesis | 0.18039 | 0.92593 | 0.36844 | gnpnat1;neu1;gfpt1 | 3488.70667 | 3613.22 | 3132.03 | 313.545553 | 3454.676 | 347.044078 | UP | 0.666666667 | 0.333333333 |
| 7Day | Fanconi Anemia Pathway | 0.15633 | 0.96565 | 0.36871 | uba52 | 4761.56 | 4761.56 | 4761.56 |  | 4761.56 |  | UP | 1 | 0 |
| 7Day | Glucagon-like Peptide-1 (GLP1) regulates insulin secretion | 0.15633 | 0.96565 | 0.36871 | itpr2 | 4098.21 | 4098.21 | 4098.21 |  | 4098.21 |  | DOWN | 0 | 1 |
| 28Day | TP53 Regulates Metabolic Genes | 0.17523 | 0.95957 | 0.36895 | txnrd1 | 3178.52 | 3178.52 | 3178.52 |  | 3178.52 |  | UP | 1 | 0 |
| 7Day | Neddylation | 0.17947 | 0.87622 | 0.36957 | dcaf8;btbd1;dcun1d5;fbxo22;cul2;fbxo9;psmd5;psmd6;cop1;dcaf10;fem1c;psmc4;nae1;uba52;psmc2;commd1;ccnf;btrc | 3494.13889 | 3634.375 | 1001.32 | 964.08138 | 3461.56237 | 1079.97456 | UP | 0.833333333 | 0.166666667 |
| 28Day | Synthesis of PIPs at the plasma membrane | 0.16595 | 0.96236 | 0.37198 | pi4k2b | 4173.55 | 4173.55 | 4173.55 |  | 4173.55 |  | UP | 1 | 0 |
| 28Day | Signaling by FGFR1 | 0.16595 | 0.96236 | 0.37198 | fgf1 | 1467.57 | 1467.57 | 1467.57 |  | 1467.57 |  | DOWN | 0 | 1 |
| 28Day | Beta-catenin independent WNT signaling | 0.20751 | 0.911 | 0.37249 | ppp3cb;pfn1;gnb5 | 3293.566 | 4095.87 | 953.648 | 2059.51023 | 2775.44284 | 2099.86753 | UP | 1 | 0 |
| 28Day | Integrin cell surface interactions | 0.20751 | 0.911 | 0.37249 | vtn;fn1;col8a1 | 2613.49067 | 3156 | 447.762 | 1951.86296 | 3375.185 | 1506.1754 | DOWN | 0.333333333 | 0.666666667 |
| 90Day | RHO GTPases activate PKNs | 0.20935 | 0.88659 | 0.37295 | hist1h4h;hist1h4i;hist1h3c;ywhaz;h2afx;ar | 2498.82283 | 2975.38 | 137.958 | 1764.78432 | 2050.81594 | 1694.68636 | CONFLICT | 0.5 | 0.5 |
| 90Day | Integrin cell surface interactions | 0.20935 | 0.88659 | 0.37295 | vtn;tnc;lum;icam1;fn1;itga9 | 3345.66678 | 3833.35 | 45.5307 | 2012.35797 | 3331.92876 | 2418.50495 | CONFLICT | 0.5 | 0.5 |
| 90Day | Recruitment of mitotic centrosome proteins and complexes | 0.18811 | 0.90021 | 0.3737 | haus7;dctn3;cntrl;tubb4b;cep76;hsp90aa1 | 3221.30167 | 3997.375 | 426.32 | 1725.30565 | 3467.98166 | 1544.87279 | UP | 1 | 0 |
| 90Day | Centrosome maturation | 0.18811 | 0.90021 | 0.3737 | haus7;dctn3;cntrl;tubb4b;cep76;hsp90aa1 | 3221.30167 | 3997.375 | 426.32 | 1725.30565 | 3467.98166 | 1544.87279 | UP | 1 | 0 |
| 7Day | RHO GTPases Activate WASPs and WAVEs | 0.89386 | 0.23009 | 0.37489 | nckap1;mapk3;cdc42;abl1;brk1 | 3771.484 | 3468.74 | 2624.49 | 909.396614 | 4035.8468 | 882.276231 | UP | 0.6 | 0.4 |

BMD analysis results for functional classification based on dose-responsive genes, using the Reactome database for gene sets in BMDExpress2.2 software.

| Study Day | Gene Set Name | Fisher's Exact Left P-Value | Fisher's Exact Right P-Value | Fisher's Exact Two Tail | Gene Symbols | BMD Mean | BMD Median | BMD Minimum | BMD Standard Deviation | BMD wMean | BMD wSD | Overall Direction | Percent Genes With Overall Direction Up | Percent Genes With Overall Direction Down |
|---|---|---|---|---|---|---|---|---|---|---|---|---|---|---|
| 90Day | HDACs deacetylate histones | 0.17813 | 0.90647 | 0.37522 | hist1h4h;hist1h4i;hist1h3c;gatad2b;hdac3;hdac2 | 2918.02017 | 3546.645 | 202.162 | 2012.29586 | 1830.19513 | 1944.61876 | CONFLICT | 0.5 | 0.5 |
| 28Day | RNA Polymerase II Promoter Escape | 0.15711 | 0.96495 | 0.3757 | polr2a | 5040.67 | 5040.67 | 5040.67 |  | 5040.67 |  | UP | 1 | 0 |
| 28Day | RNA Polymerase II Transcription Pre-Initiation And Promoter Opening | 0.15711 | 0.96495 | 0.3757 | polr2a | 5040.67 | 5040.67 | 5040.67 |  | 5040.67 |  | UP | 1 | 0 |
| 28Day | RNA Polymerase II Transcription Initiation | 0.15711 | 0.96495 | 0.3757 | polr2a | 5040.67 | 5040.67 | 5040.67 |  | 5040.67 |  | UP | 1 | 0 |
| 28Day | RNA Polymerase II Transcription Initiation And Promoter Clearance | 0.15711 | 0.96495 | 0.3757 | polr2a | 5040.67 | 5040.67 | 5040.67 |  | 5040.67 |  | UP | 1 | 0 |
| 28Day | DNA Damage Bypass | 0.15711 | 0.96495 | 0.3757 | pole3 | 805.318 | 805.318 | 805.318 |  | 805.318 |  | UP | 1 | 0 |
| 28Day | Mitotic G1-G1/S phases | 0.1764 | 0.92728 | 0.3759 | pole3;cdc6;tfdp1 | 4127.086 | 5708.4 | 805.318 | 2877.83571 | 4917.81429 | 2323.3286 | UP | 1 | 0 |
| 28Day | Transport of bile salts and organic acids, metal ions and amine compounds | 0.1764 | 0.92728 | 0.3759 | slc13a5;slc22a1;slc6a13 | 2214.364 | 1681.65 | 151.142 | 2374.82136 | 3682.83861 | 2229.861 | DOWN | 0.333333333 | 0.666666667 |
| 90Day | Gap junction assembly | 0.88581 | 0.24465 | 0.37742 | tubb6;tubb4b;tubb2a;tuba1b;gjb2 | 1916.9702 | 1781.5 | 779.791 | 922.579865 | 1733.98302 | 1064.65299 | UP | 0.6 | 0.4 |
| 90Day | Mitotic G1-G1/S phases | 0.16856 | 0.9124 | 0.37746 | pole4;cables1;orc6;dbf4;e2f2;cdkn1a | 3704.34667 | 4120.125 | 913.71 | 1649.0418 | 2970.33065 | 1677.04064 | UP | 0.666666667 | 0.333333333 |
| 90Day | SUMO E3 ligases SUMOylate target proteins | 0.18105 | 0.88134 | 0.37761 | hist1h4h;eid3;park7;hist1h4i;nr5a2;nup153;pml;nfkbia;mdm2;ikbkg;hdac2;ddx5;ar;sec13 | 2821.69924 | 3568.09 | 25.9884 | 1590.20729 | 2400.75322 | 1744.05489 | CONFLICT | 0.5 | 0.5 |
| 28Day | G beta:gamma signalling through CDC42 | 0.86225 | 0.37855 | 0.37855 | gnb5;cdc42 | 1708.569 | 1708.569 | 953.648 | 1067.61952 | 1507.0508 | 1028.87913 | UP | 1 | 0 |
| 28Day | Caspase activation via extrinsic apoptotic signalling pathway | 0.86225 | 0.37855 | 0.37855 | tnfrsf10b;ly96 | 4300.525 | 4300.525 | 4040.75 | 367.377328 | 4219.52756 | 349.062933 | UP | 1 | 0 |
| 28Day | Conversion from APC/C:Cdc20 to APC/C:Cdh1 in late anaphase | 0.86225 | 0.37855 | 0.37855 | cdc14a;cdc27 | 3264.516 | 3264.516 | 748.272 | 3558.50639 | 3689.73493 | 3507.32739 | UP | 1 | 0 |
| 28Day | Purine catabolism | 0.86225 | 0.37855 | 0.37855 | nudt5;pnp | 3241.65 | 3241.65 | 2482 | 1074.30733 | 2885.35398 | 948.81112 | CONFLICT | 0.5 | 0.5 |
| 7Day | Class I MHC mediated antigen processing & presentation | 0.1981 | 0.8541 | 0.37928 | ube2n;btbd1;rnf6;fbxo22;cul2;fbxo9;trim69;ube2v2;ube2k;ube3a;ube2a;ube2e3;uba52;cdc27;cdc34;tap2;sec22b;h2-t23;h2-q10;trip12;ubox5;ube2j2;ccnf;btrc;wwp1 | 3567.1704 | 3369.05 | 1018.89 | 1053.55378 | 3616.27808 | 996.188047 | UP | 0.8 | 0.2 |
| 7Day | Anchoring of the basal body to the plasma membrane | 0.17955 | 0.90508 | 0.37981 | cep89;rab11a;tubb4b;tuba4a;nedd1;hsp90aa1 | 2550.90267 | 2445.18 | 919.856 | 1534.84908 | 2426.2675 | 1534.52335 | UP | 1 | 0 |
| 90Day | Release of apoptotic factors from the mitochondria | 0.93482 | 0.38016 | 0.38016 | bax | 1844.96 | 1844.96 | 1844.96 |  | 1844.96 |  | UP | 1 | 0 |
| 90Day | Lysosomal oligosaccharide catabolism | 0.93482 | 0.38016 | 0.38016 | man2b1 | 677.096 | 677.096 | 677.096 |  | 677.096 |  | DOWN | 0 | 1 |
| 90Day | Mitochondrial ABC transporters | 0.93482 | 0.38016 | 0.38016 | abcb8 | 3667.8 | 3667.8 | 3667.8 |  | 3667.8 |  | UP | 1 | 0 |
| 90Day | SLIT2:ROBO1 increases RHOA activity | 0.93482 | 0.38016 | 0.38016 | myo9b | 5309.89 | 5309.89 | 5309.89 |  | 5309.89 |  | DOWN | 0 | 1 |
| 90Day | Ubiquinol biosynthesis | 0.93482 | 0.38016 | 0.38016 | pdss1 | 5691.78 | 5691.78 | 5691.78 |  | 5691.78 |  | UP | 1 | 0 |
| 90Day | ATF6 (ATF6-alpha) activates chaperones | 0.93482 | 0.38016 | 0.38016 | mbtps2 | 3467.51 | 3467.51 | 3467.51 |  | 3467.51 |  | UP | 1 | 0 |
| 90Day | TRAF6 mediated IRF7 activation | 0.93482 | 0.38016 | 0.38016 | irf7 | 5689.7 | 5689.7 | 5689.7 |  | 5689.7 |  | UP | 1 | 0 |
| 90Day | Scavenging by Class B Receptors | 0.93482 | 0.38016 | 0.38016 | apob | 175.96 | 175.96 | 175.96 |  | 175.96 |  | DOWN | 0 | 1 |
| 90Day | Sulfide oxidation to sulfate | 0.93482 | 0.38016 | 0.38016 | suox | 3807.07 | 3807.07 | 3807.07 |  | 3807.07 |  | DOWN | 0 | 1 |
| 90Day | Alternative complement activation | 0.93482 | 0.38016 | 0.38016 | c3 | 639.57 | 639.57 | 639.57 |  | 639.57 |  | DOWN | 0 | 1 |
| 90Day | ATP sensitive Potassium channels | 0.93482 | 0.38016 | 0.38016 | kcnj8 | 2260.22 | 2260.22 | 2260.22 |  | 2260.22 |  | UP | 1 | 0 |
| 90Day | Interleukin-18 signaling | 0.93482 | 0.38016 | 0.38016 | il18bp | 3115.46 | 3115.46 | 3115.46 |  | 3115.46 |  | DOWN | 0 | 1 |
| 90Day | Selenoamino acid metabolism | 0.93482 | 0.38016 | 0.38016 | txnrd1 | 3099.4 | 3099.4 | 3099.4 |  | 3099.4 |  | UP | 1 | 0 |
| 90Day | Unwinding of DNA | 0.93482 | 0.38016 | 0.38016 | gins1 | 1127.6 | 1127.6 | 1127.6 |  | 1127.6 |  | UP | 1 | 0 |
| 90Day | NGF processing | 0.93482 | 0.38016 | 0.38016 | pcsk5 | 3761.45 | 3761.45 | 3761.45 |  | 3761.45 |  | DOWN | 0 | 1 |
| 90Day | Expression and Processing of Neurotrophins | 0.93482 | 0.38016 | 0.38016 | pcsk5 | 3761.45 | 3761.45 | 3761.45 |  | 3761.45 |  | DOWN | 0 | 1 |
| 90Day | Activated NTRK2 signals through PLCG1 | 0.93482 | 0.38016 | 0.38016 | ntrk2 | 3744.34 | 3744.34 | 3744.34 |  | 3744.34 |  | DOWN | 0 | 1 |
| 90Day | LRR FLII-interacting protein 1 (LRRFIP1) activates type I IFN production | 0.93482 | 0.38016 | 0.38016 | ctnnb1 | 4087.04 | 4087.04 | 4087.04 |  | 4087.04 |  | DOWN | 0 | 1 |
| 90Day | RUNX1 regulates transcription of genes involved in BCR signaling | 0.93482 | 0.38016 | 0.38016 | cbfb | 4070.59 | 4070.59 | 4070.59 |  | 4070.59 |  | UP | 1 | 0 |

BMD analysis results for functional classification based on dose-responsive genes, using the Reactome database for gene sets in BMDExpress2.2 software.

| Study Day | Gene Set Name | Fisher's Exact Left P-Value | Fisher's Exact Right P-Value | Fisher's Exact Two Tail | Gene Symbols | BMD Mean | BMD Median | BMD Minimum | BMD Standard Deviation | BMD wMean | BMD wSD | Overall Direction | Percent Genes With Overall Direction Up | Percent Genes With Overall Direction Down |
|---|---|---|---|---|---|---|---|---|---|---|---|---|---|---|
| 90Day | TRAF3-dependent IRF activation pathway | 0.93482 | 0.38016 | 0.38016 | irf7 | 5689.7 | 5689.7 | 5689.7 |  | 5689.7 |  | UP | 1 | 0 |
| 90Day | Fructose catabolism | 0.93482 | 0.38016 | 0.38016 | tkfc | 1863.37 | 1863.37 | 1863.37 |  | 1863.37 |  | UP | 1 | 0 |
| 90Day | Reuptake of GABA | 0.93482 | 0.38016 | 0.38016 | slc6a12 | 3445.15 | 3445.15 | 3445.15 |  | 3445.15 |  | DOWN | 0 | 1 |
| 90Day | Scavenging by Class H Receptors | 0.93482 | 0.38016 | 0.38016 | apob | 175.96 | 175.96 | 175.96 |  | 175.96 |  | DOWN | 0 | 1 |
| 90Day | HDR through Homologous Recombination (HRR) or Single Strand Annealing (SSA) | 0.2097 | 0.86965 | 0.38215 | hist1h4h;babam1;pole4;ppp4c;hist1h4i;polk;rad51;h2afx;brca2;rad51c | 4045.4582 | 4046.18 | 513.022 | 1470.8127 | 3606.13368 | 1521.5189 | UP | 0.7 | 0.3 |
| 7Day | Recruitment and ATM-mediated phosphorylation of repair and signaling proteins at DNA double strand breaks | 0.86502 | 0.23928 | 0.38224 | ube2n;ube2v2;rnf168;hist1h4h;babam1;hist1h2bc;uba52;abl1 | 3577.685 | 3431.595 | 2423.08 | 684.390117 | 3444.78005 | 685.408558 | UP | 0.75 | 0.25 |
| 90Day | Beta-oxidation of very long chain fatty acids | 0.23799 | 1 | 0.38313 |  |  |  |  |  |  |  |  |  |  |
| 90Day | Regulation of TP53 Activity through Methylation | 0.23799 | 1 | 0.38313 |  |  |  |  |  |  |  |  |  |  |
| 90Day | Interleukin-35 Signalling | 0.23799 | 1 | 0.38313 |  |  |  |  |  |  |  |  |  |  |
| 90Day | Zinc transporters | 0.23799 | 1 | 0.38313 |  |  |  |  |  |  |  |  |  |  |
| 90Day | Pregnenolone biosynthesis | 0.23799 | 1 | 0.38313 |  |  |  |  |  |  |  |  |  |  |
| 90Day | Interleukin-2 signaling | 0.23799 | 1 | 0.38313 |  |  |  |  |  |  |  |  |  |  |
| 90Day | Sodium/Calcium exchangers | 0.23799 | 1 | 0.38313 |  |  |  |  |  |  |  |  |  |  |
| 90Day | Ionotropic activity of kainate receptors | 0.23799 | 1 | 0.38313 |  |  |  |  |  |  |  |  |  |  |
| 90Day | Activation of Ca-permeable Kainate Receptor | 0.23799 | 1 | 0.38313 |  |  |  |  |  |  |  |  |  |  |
| 90Day | Activation of the TFAP2 (AP-2) family of transcription factors | 0.23799 | 1 | 0.38313 |  |  |  |  |  |  |  |  |  |  |
| 90Day | Synthesis of IP2, IP, and Ins in the cytosol | 0.23799 | 1 | 0.38313 |  |  |  |  |  |  |  |  |  |  |
| 28Day | Death Receptor Signalling | 0.20873 | 0.88565 | 0.38317 | tax1bp1;tnfrsf10b;arhgdia;sqstm1;ikbkg;birc2 | 5157.53167 | 5194.76 | 4040.75 | 657.083981 | 5090.48747 | 657.56748 | UP | 0.833333333 | 0.166666667 |
| 90Day | ERKs are inactivated | 0.21114 | 1 | 0.38485 |  |  |  |  |  |  |  |  |  |  |
| 90Day | FGFRL1 modulation of FGFR1 signaling | 0.21114 | 1 | 0.38485 |  |  |  |  |  |  |  |  |  |  |
| 90Day | Notch-HLH transcription pathway | 0.21114 | 1 | 0.38485 |  |  |  |  |  |  |  |  |  |  |
| 90Day | Synthesis of PIPs at the early endosome membrane | 0.21114 | 1 | 0.38485 |  |  |  |  |  |  |  |  |  |  |
| 90Day | mRNA decay by 5' to 3' exoribonuclease | 0.21114 | 1 | 0.38485 |  |  |  |  |  |  |  |  |  |  |
| 90Day | Glycogen breakdown (glycogenolysis) | 0.21114 | 1 | 0.38485 |  |  |  |  |  |  |  |  |  |  |
| 90Day | Glycogen synthesis | 0.21114 | 1 | 0.38485 |  |  |  |  |  |  |  |  |  |  |
| 28Day | Interleukin-1 signaling | 0.883 | 0.24439 | 0.38509 | ube2n;sqstm1;il1rap;ikbkg;app | 4940.87 | 5266.71 | 3705.51 | 791.86401 | 5097.48088 | 859.756978 | DOWN | 0.4 | 0.6 |
| 7Day | PTK6 Regulates RHO GTPases, RAS GTPase and MAP kinases | 0.8611 | 0.38548 | 0.38548 | rasa1;kras | 4972.395 | 4972.395 | 4158.71 | 1150.72436 | 5283.81236 | 1063.11101 | CONFLICT | 0.5 | 0.5 |
| 7Day | KSRP (KHSRP) binds and destabilizes mRNA | 0.8611 | 0.38548 | 0.38548 | dcp2;ywhaz | 3109.105 | 3109.105 | 2726.98 | 540.406358 | 3045.31761 | 532.823957 | UP | 1 | 0 |
| 7Day | Cell-extracellular matrix interactions | 0.8611 | 0.38548 | 0.38548 | vasp;flna | 4212.71 | 4212.71 | 3557.63 | 926.42302 | 4355.77345 | 904.060458 | DOWN | 0 | 1 |
| 7Day | p75NTR signals via NF-kB | 0.8611 | 0.38548 | 0.38548 | uba52;prkci | 4085.4 | 4085.4 | 3409.24 | 956.234642 | 4275.2759 | 917.757582 | UP | 1 | 0 |
| 7Day | Other semaphorin interactions | 0.8611 | 0.38548 | 0.38548 | sema4d;sema4a | 5652.975 | 5652.975 | 5514.77 | 195.451385 | 5725.74518 | 166.163307 | DOWN | 0 | 1 |
| 7Day | Downregulation of TGF-beta receptor signaling | 0.8611 | 0.38548 | 0.38548 | uba52;tgfbr1 | 5206.805 | 5206.805 | 4761.56 | 629.671518 | 5273.58539 | 622.548776 | UP | 1 | 0 |
| 7Day | Methylation | 0.8611 | 0.38548 | 0.38548 | ahcy;gm4737 | 2894.795 | 2894.795 | 2019.09 | 1238.43389 | 3236.60399 | 1140.19811 | DOWN | 0 | 1 |
| 7Day | Reduction of cytosolic Ca++ levels | 0.8611 | 0.38548 | 0.38548 | calm3;calm2 | 3983.44 | 3983.44 | 3050.32 | 1319.63096 | 3556.9103 | 1173.69957 | CONFLICT | 0.5 | 0.5 |
| 7Day | DNA Double Strand Break Response | 0.85521 | 0.25277 | 0.38748 | ube2n;ube2v2;rnf168;hist1h4h;babam1;hist1h2bc;uba52;abl1 | 3577.685 | 3431.595 | 2423.08 | 684.390117 | 3444.78005 | 685.408558 | UP | 0.75 | 0.25 |
| 7Day | WNT5A-dependent internalization of FZD4 | 0.22635 | 1 | 0.38847 |  |  |  |  |  |  |  |  |  |  |
| 7Day | SUMOylation of transcription factors | 0.22635 | 1 | 0.38847 |  |  |  |  |  |  |  |  |  |  |
| 7Day | Insulin processing | 0.22635 | 1 | 0.38847 |  |  |  |  |  |  |  |  |  |  |
| 7Day | Anchoring fibril formation | 0.22635 | 1 | 0.38847 |  |  |  |  |  |  |  |  |  |  |

BMD analysis results for functional classification based on dose-responsive genes, using the Reactome database for gene sets in BMDExpress2.2 software.

| Study Day | Gene Set Name | Fisher's Exact Left P-Value | Fisher's Exact Right P-Value | Fisher's Exact Two Tail | Gene Symbols | BMD Mean | BMD Median | BMD Minimum | BMD Standard Deviation | BMD wMean | BMD wSD | Overall Direction | Percent Genes With Overall Direction Up | Percent Genes With Overall Direction Down |
|---|---|---|---|---|---|---|---|---|---|---|---|---|---|---|
| 90Day | SUMOylation | 0.20912 | 0.85826 | 0.38908 | hist1h4h;eid3;park7;sae1;hist1h4i;nr5a2;nup153;pml;nfkbia;mdm2;ikbkg;hdac2;ddx5;ar;sec13 | 2900.15796 | 3601.1 | 25.9884 | 1562.20041 | 2494.31455 | 1731.99357 | CONFLICT | 0.533333333 | 0.466666667 |
| 7Day | Cellular responses to stress | 0.83657 | 0.21273 | 0.38915 | hspb8;ep400;gm49336;cul2;hist1h4h;hsbp1;hist1h2bc;txn2;ptges3;suz12;txnrd1;hist2h2ac;mapk3;map2k3;dnajb6;tubb4b;uba52;tubb2a;tuba4a;terf2;cdc27;prdx2;stip1;sod1;hsp90aa1;hsph1;hist2h2aa1;gstp1;gstp2;cdkn1a;ccne2;capza2;bmi1;arnt;egln1;tpr | 3303.40881 | 3412.475 | 589.118 | 1315.40316 | 3205.85513 | 1300.74608 | UP | 0.722222222 | 0.277777778 |
| 7Day | SMAC, XIAP-regulated apoptotic response | 0.92684 | 0.39039 | 0.39039 | xiap | 4874.03 | 4874.03 | 4874.03 | | 4874.03 | | DOWN | 0 | 1 |
| 7Day | MET activates PTPN11 | 0.92684 | 0.39039 | 0.39039 | ptpn11 | 3629.67 | 3629.67 | 3629.67 | | 3629.67 | | UP | 1 | 0 |
| 7Day | Sodium-coupled phosphate cotransporters | 0.92684 | 0.39039 | 0.39039 | slc20a1 | 3654.41 | 3654.41 | 3654.41 | | 3654.41 | | UP | 1 | 0 |
| 7Day | Abacavir transport and metabolism | 0.92684 | 0.39039 | 0.39039 | slc22a1 | 4237.04 | 4237.04 | 4237.04 | | 4237.04 | | DOWN | 0 | 1 |
| 7Day | SUMO is transferred from E1 to E2 (UBE2I, UBC9) | 0.92684 | 0.39039 | 0.39039 | uba2 | 2542.64 | 2542.64 | 2542.64 | | 2542.64 | | UP | 1 | 0 |
| 7Day | Activation of RAS in B cells | 0.92684 | 0.39039 | 0.39039 | kras | 4158.71 | 4158.71 | 4158.71 | | 4158.71 | | UP | 1 | 0 |
| 7Day | Formation of xylulose-5-phosphate | 0.92684 | 0.39039 | 0.39039 | dcxr | 5380.13 | 5380.13 | 5380.13 | | 5380.13 | | DOWN | 0 | 1 |
| 7Day | Regulation of cholesterol biosynthesis by SREBP (SREBF) | 0.92684 | 0.39039 | 0.39039 | kpnb1 | 4222.13 | 4222.13 | 4222.13 | | 4222.13 | | UP | 1 | 0 |
| 7Day | Propionyl-CoA catabolism | 0.92684 | 0.39039 | 0.39039 | pccb | 77.8976 | 77.8976 | 77.8976 | | 77.8976 | | DOWN | 0 | 1 |
| 7Day | RUNX3 regulates WNT signaling | 0.92684 | 0.39039 | 0.39039 | ctnnb1 | 54.5232 | 54.5232 | 54.5232 | | 54.5232 | | DOWN | 0 | 1 |
| 7Day | Acyl chain remodeling of CL | 0.92684 | 0.39039 | 0.39039 | hadha | 197.056 | 197.056 | 197.056 | | 197.056 | | DOWN | 0 | 1 |
| 7Day | Cyclin D associated events in G1 | 0.86994 | 0.26666 | 0.39071 | uba52;tfdp1;ppp2cb;cdkn1a;abl1 | 3056.5088 | 3368.05 | 707.264 | 1492.08753 | 3309.31256 | 1223.86398 | UP | 0.8 | 0.2 |
| 7Day | G1 Phase | 0.86994 | 0.26666 | 0.39071 | uba52;tfdp1;ppp2cb;cdkn1a;abl1 | 3056.5088 | 3368.05 | 707.264 | 1492.08753 | 3309.31256 | 1223.86398 | UP | 0.8 | 0.2 |
| 90Day | Eicosanoid ligand-binding receptors | 0.18731 | 1 | 0.39099 | | | | | | | | | | |
| 90Day | Translesion synthesis by REV1 | 0.18731 | 1 | 0.39099 | | | | | | | | | | |
| 90Day | Erythrocytes take up carbon dioxide and release oxygen | 0.18731 | 1 | 0.39099 | | | | | | | | | | |
| 90Day | O2/CO2 exchange in erythrocytes | 0.18731 | 1 | 0.39099 | | | | | | | | | | |
| 90Day | TP53 Regulates Transcription of Cell Death Genes | 0.18731 | 1 | 0.39099 | | | | | | | | | | |
| 90Day | Removal of the Flap Intermediate | 0.18731 | 1 | 0.39099 | | | | | | | | | | |
| 90Day | Reduction of cytosolic Ca++ levels | 0.18731 | 1 | 0.39099 | | | | | | | | | | |
| 7Day | Processing of SMDT1 | 0.20499 | 1 | 0.39137 | | | | | | | | | | |
| 7Day | Nitric oxide stimulates guanylate cyclase | 0.20499 | 1 | 0.39137 | | | | | | | | | | |
| 28Day | POLB-Dependent Long Patch Base Excision Repair | 0.92154 | 0.39224 | 0.39224 | polb | 5853.24 | 5853.24 | 5853.24 | | 5853.24 | | UP | 1 | 0 |
| 28Day | BH3-only proteins associate with and inactivate anti-apoptotic BCL-2 members | 0.92154 | 0.39224 | 0.39224 | bcl2l1 | 2151.36 | 2151.36 | 2151.36 | | 2151.36 | | UP | 1 | 0 |
| 28Day | ChREBP activates metabolic gene expression | 0.92154 | 0.39224 | 0.39224 | acly | 4155.33 | 4155.33 | 4155.33 | | 4155.33 | | DOWN | 0 | 1 |
| 28Day | Heme degradation | 0.92154 | 0.39224 | 0.39224 | ugt1a1 | 309.913 | 309.913 | 309.913 | | 309.913 | | DOWN | 0 | 1 |
| 28Day | Pre-NOTCH Expression and Processing | 0.92154 | 0.39224 | 0.39224 | notch1 | 908.573 | 908.573 | 908.573 | | 908.573 | | UP | 1 | 0 |
| 28Day | Acyl chain remodeling of DAG and TAG | 0.92154 | 0.39224 | 0.39224 | dgat2 | 2889.4 | 2889.4 | 2889.4 | | 2889.4 | | DOWN | 0 | 1 |
| 28Day | Interleukin-36 pathway | 0.92154 | 0.39224 | 0.39224 | il1rap | 3705.51 | 3705.51 | 3705.51 | | 3705.51 | | DOWN | 0 | 1 |
| 28Day | CREB phosphorylation | 0.92154 | 0.39224 | 0.39224 | mapkapk2 | 5375 | 5375 | 5375 | | 5375 | | DOWN | 0 | 1 |
| 28Day | FGFR3b ligand binding and activation | 0.92154 | 0.39224 | 0.39224 | fgf1 | 1467.57 | 1467.57 | 1467.57 | | 1467.57 | | DOWN | 0 | 1 |
| 28Day | Cyclin E associated events during G1/S transition | 0.24079 | 1 | 0.39505 | | | | | | | | | | |
| 28Day | Regulation of lipid metabolism by Peroxisome proliferator-activated receptor alpha (PPARalpha) | 0.24079 | 1 | 0.39505 | | | | | | | | | | |
| 28Day | Lagging Strand Synthesis | 0.24079 | 1 | 0.39505 | | | | | | | | | | |
| 28Day | Cyclin A:Cdk2-associated events at S phase entry | 0.22423 | 1 | 0.39558 | | | | | | | | | | |

BMD analysis results for functional classification based on dose-responsive genes, using the Reactome database for gene sets in BMDExpress2.2 software.

| Study Day | Gene Set Name | Fisher's Exact Left P-Value | Fisher's Exact Right P-Value | Fisher's Exact Two Tail | Gene Symbols | BMD Mean | BMD Median | BMD Minimum | BMD Standard Deviation | BMD wMean | BMD wSD | Overall Direction | Percent Genes With Overall Direction Up | Percent Genes With Overall Direction Down |
|---|---|---|---|---|---|---|---|---|---|---|---|---|---|---|
| 28Day | Regulation of RAS by GAPs | 0.22423 | 1 | 0.39558 | | | | | | | | | | |
| 28Day | NCAM1 interactions | 0.22423 | 1 | 0.39558 | | | | | | | | | | |
| 28Day | Metal ion SLC transporters | 0.22423 | 1 | 0.39558 | | | | | | | | | | |
| 7Day | SHC1 events in ERBB2 signaling | 0.18564 | 1 | 0.39715 | | | | | | | | | | |
| 7Day | G beta:gamma signalling through BTK | 0.18564 | 1 | 0.39715 | | | | | | | | | | |
| 7Day | Synthesis, secretion, and deacylation of Ghrelin | 0.18564 | 1 | 0.39715 | | | | | | | | | | |
| 7Day | Visual phototransduction | 0.83015 | 0.26206 | 0.39773 | akr1c6;metap2;apob;ttr;rdh16f2;sdc3;rgs9;lrp1;calm3;calm2;apoe;akr1c14 | 3329.32883 | 3349.655 | 113.316 | 1742.98114 | 3338.017 | 1322.70907 | DOWN | 0.333333333 | 0.666666667 |
| 28Day | Cellular hexose transport | 0.2088 | 1 | 0.39775 | | | | | | | | | | |
| 28Day | CD209 (DC-SIGN) signaling | 0.2088 | 1 | 0.39775 | | | | | | | | | | |
| 28Day | Transcriptional regulation by the AP-2 (TFAP2) family of transcription factors | 0.2088 | 1 | 0.39775 | | | | | | | | | | |
| 90Day | p75 NTR receptor-mediated signalling | 0.22127 | 0.87328 | 0.39817 | arhgef6;fgd4;vav1;tiam1;sos1;psen2;nfkbia | 4733.14714 | 4586.54 | 3135.19 | 1166.20331 | 4863.56928 | 1187.56504 | DOWN | 0.142857143 | 0.857142857 |
| 90Day | Factors involved in megakaryocyte development and platelet production | 0.19989 | 0.87392 | 0.39958 | tubb6;hist1h3c;tubb4b;tubb2a;tuba1b;hdac2;cdc42;cbx5;rad51c;dock9;kifc1 | 1840.02618 | 1722.38 | 156.487 | 1550.4745 | 1737.85424 | 1637.55179 | UP | 0.818181818 | 0.181818182 |
| 90Day | Import of palmitoyl-CoA into the mitochondrial matrix | 0.16617 | 1 | 0.40088 | | | | | | | | | | |
| 90Day | Translesion synthesis by POLI | 0.16617 | 1 | 0.40088 | | | | | | | | | | |
| 90Day | Asymmetric localization of PCP proteins | 0.16617 | 1 | 0.40088 | | | | | | | | | | |
| 90Day | Processive synthesis on the lagging strand | 0.16617 | 1 | 0.40088 | | | | | | | | | | |
| 28Day | Cobalamin (Cbl, vitamin B12) transport and metabolism | 0.19443 | 1 | 0.40141 | | | | | | | | | | |
| 90Day | Signaling by NTRK1 (TRKA) | 0.22836 | 0.88973 | 0.40228 | irs2;mapk14;sos1;ap2m1 | 3303.81333 | 3622.755 | 74.8133 | 2460.41598 | 2955.19946 | 3083.33332 | DOWN | 0.25 | 0.75 |
| 90Day | CDT1 association with the CDC6:ORC:origin complex | 0.22836 | 0.88973 | 0.40228 | psmd8;orc6;psmc4;psmf1 | 2195.2195 | 2213.18 | 186.178 | 1757.71062 | 2242.33342 | 1753.93797 | UP | 1 | 0 |
| 90Day | SIRT1 negatively regulates rRNA expression | 0.21502 | 0.89763 | 0.40235 | hist1h4h;hist1h4i;hist1h3c;h2afx | 3214.00725 | 3979.26 | 811.859 | 1602.37406 | 2298.31583 | 1843.92338 | CONFLICT | 0.5 | 0.5 |
| 90Day | RNA Polymerase I Promoter Opening | 0.21502 | 0.89763 | 0.40235 | hist1h4h;hist1h4i;hist1h3c;h2afx | 3214.00725 | 3979.26 | 811.859 | 1602.37406 | 2298.31583 | 1843.92338 | CONFLICT | 0.5 | 0.5 |
| 90Day | Nonhomologous End-Joining (NHEJ) | 0.21502 | 0.89763 | 0.40235 | hist1h4h;babam1;hist1h4i;h2afx | 4461.0475 | 4046.18 | 3951.81 | 894.337005 | 4412.91487 | 861.771604 | CONFLICT | 0.5 | 0.5 |
| 7Day | Transport of inorganic cations/anions and amino acids/oligopeptides | 0.20647 | 0.88273 | 0.40294 | slc20a1;slc1a2;slc12a7;slc8b1;calm3;calm2;slc12a6 | 3204.57857 | 3050.32 | 1710.87 | 1160.4099 | 3133.06323 | 998.250535 | DOWN | 0.285714286 | 0.714285714 |
| 90Day | Negative epigenetic regulation of rRNA expression | 0.2023 | 0.90504 | 0.40346 | hist1h4h;hist1h4i;hist1h3c;h2afx | 3214.00725 | 3979.26 | 811.859 | 1602.37406 | 2298.31583 | 1843.92338 | CONFLICT | 0.5 | 0.5 |
| 7Day | Prostacyclin signalling through prostacyclin receptor | 0.16812 | 1 | 0.40543 | | | | | | | | | | |
| 28Day | DNA strand elongation | 0.18105 | 1 | 0.40642 | | | | | | | | | | |
| 28Day | Activation of G protein gated Potassium channels | 0.18105 | 1 | 0.40642 | | | | | | | | | | |
| 28Day | G protein gated Potassium channels | 0.18105 | 1 | 0.40642 | | | | | | | | | | |
| 28Day | Inhibition of voltage gated Ca2+ channels via Gbeta/gamma subunits | 0.18105 | 1 | 0.40642 | | | | | | | | | | |
| 28Day | Regulation of Hypoxia-inducible Factor (HIF) by oxygen | 0.18105 | 1 | 0.40642 | | | | | | | | | | |
| 28Day | Cellular response to hypoxia | 0.18105 | 1 | 0.40642 | | | | | | | | | | |
| 7Day | RMTs methylate histone arginines | 0.21949 | 0.89434 | 0.40686 | prmt3;hist1h4h;hist2h2ac;hist2h2aa1 | 3747.9 | 3796.91 | 2008.38 | 1417.74679 | 3847.08019 | 1329.43276 | CONFLICT | 0.5 | 0.5 |
| 7Day | Signaling by NTRKs | 0.20873 | 0.90068 | 0.40753 | mapk3;ppp2cb;pcsk5;kras | 4284.7675 | 4355.895 | 3627.04 | 511.924296 | 4177.70071 | 574.511106 | CONFLICT | 0.5 | 0.5 |
| 7Day | Biosynthesis of the N-glycan precursor (dolichol lipid-linked oligosaccharide, LLO) and transfer to a nascent protein | 0.20873 | 0.90068 | 0.40753 | gnpnat1;neu1;gfpt1;alg9 | 3673.235 | 3667.045 | 3132.03 | 449.158509 | 3575.95319 | 442.141891 | CONFLICT | 0.5 | 0.5 |
| 7Day | Loss of Nlp from mitotic centrosomes | 0.19839 | 0.90669 | 0.4089 | tubb4b;tuba4a;nedd1;hsp90aa1 | 1703.9565 | 1410.635 | 919.856 | 998.985626 | 1609.23265 | 1031.31055 | UP | 1 | 0 |
| 7Day | Loss of proteins required for interphase microtubule organization from the centrosome | 0.19839 | 0.90669 | 0.4089 | tubb4b;tuba4a;nedd1;hsp90aa1 | 1703.9565 | 1410.635 | 919.856 | 998.985626 | 1609.23265 | 1031.31055 | UP | 1 | 0 |
| 7Day | Synthesis of DNA | 0.18846 | 0.91237 | 0.41095 | uba52;cdc27;prim2;ccne2 | 4309.1175 | 4302.165 | 3870.58 | 436.798058 | 4459.0906 | 388.783432 | UP | 1 | 0 |
| 7Day | Rab regulation of trafficking | 0.84065 | 0.24469 | 0.41158 | rab3gap2;trappc6b;trappc8;trappc13;0610009b22rik;rab9;rab11a;dennd4c;rab6a;rab18;rab10;rab1a;hps4 | 3446.06615 | 3553.68 | 1046.66 | 1001.43544 | 3219.80464 | 836.314437 | UP | 0.846153846 | 0.153846154 |

BMD analysis results for functional classification based on dose-responsive genes, using the Reactome database for gene sets in BMDExpress2.2 software.

| Study Day | Gene Set Name | Fisher's Exact Left P-Value | Fisher's Exact Right P-Value | Fisher's Exact Two Tail | Gene Symbols | BMD Mean | BMD Median | BMD Minimum | BMD Standard Deviation | BMD wMean | BMD wSD | Overall Direction | Percent Genes With Overall Direction Up | Percent Genes With Overall Direction Down |
|---|---|---|---|---|---|---|---|---|---|---|---|---|---|---|
| 90Day | RA biosynthesis pathway | 0.83926 | 0.31261 | 0.41263 | rdh7;adh4;aldh1a7;aldh8a1;rdh11 | 3741.732 | 3277.15 | 2740.9 | 1218.47664 | 3770.57211 | 1434.78885 | UP | 0.8 | 0.2 |
| 28Day | Effects of PIP2 hydrolysis | 0.16859 | 1 | 0.41265 | | | | | | | | | | |
| 28Day | VEGFA-VEGFR2 Pathway | 0.21772 | 0.89454 | 0.41296 | pdpk1;mapkapk2;cdc42;brk1 | 3372.312 | 3919.245 | 192.988 | 2536.00426 | 4213.88679 | 1981.66272 | DOWN | 0.25 | 0.75 |
| 90Day | Regulation of pyruvate dehydrogenase (PDH) complex | 0.90297 | 0.26647 | 0.41389 | pdk4;pdk1;gstz1 | 4115.21 | 3345.98 | 3209.99 | 1451.70948 | 3914.67407 | 1357.04203 | DOWN | 0.333333333 | 0.666666667 |
| 90Day | Syndecan interactions | 0.90297 | 0.26647 | 0.41389 | vtn;sdc4;fn1 | 928.602233 | 630.216 | 45.5307 | 1064.11751 | 649.620371 | 1014.84371 | DOWN | 0 | 1 |
| 90Day | Platelet degranulation | 0.22429 | 0.8532 | 0.41458 | spp2;trf;tln1;serpina1e;psap;plg;fn1;ecm1;anxa5;ahsg;actn1;sccpdh | 2421.70252 | 2481.665 | 82.4742 | 1669.5291 | 2984.03278 | 1802.70421 | DOWN | 0.083333333 | 0.916666667 |
| 28Day | Anchoring of the basal body to the plasma membrane | 0.19516 | 0.9078 | 0.41582 | dynll1;rab11a;tubb4b;ttbk2 | 3168.02 | 2343.81 | 2192.92 | 1750.5057 | 3398.35091 | 1878.93645 | UP | 0.75 | 0.25 |
| 7Day | Plasma lipoprotein assembly | 0.90292 | 0.2636 | 0.41585 | apob;apoe;apoc1 | 1959.152 | 1999.21 | 113.316 | 1826.13655 | 3047.84336 | 1482.79348 | DOWN | 0 | 1 |
| 7Day | Oxygen-dependent proline hydroxylation of Hypoxia-inducible Factor Alpha | 0.90292 | 0.2636 | 0.41585 | cul2;uba52;egln1 | 4522.97667 | 4498.76 | 4308.61 | 227.443973 | 4513.18547 | 247.67794 | UP | 0.666666667 | 0.333333333 |
| 7Day | Post NMDA receptor activation events | 0.90292 | 0.2636 | 0.41585 | prkar2a;calm3;calm2 | 4011.14667 | 4066.56 | 3050.32 | 934.353205 | 3661.3101 | 940.743026 | DOWN | 0.333333333 | 0.666666667 |
| 28Day | ISG15 antiviral mechanism | 0.90104 | 0.26299 | 0.41998 | ube2n;arih1;ppm1b | 4090.57 | 5266.71 | 1290.26 | 2435.46398 | 2838.72879 | 2524.17867 | DOWN | 0.333333333 | 0.666666667 |
| 28Day | TAK1 activates NFkB by phosphorylation and activation of IKKs complex | 0.90104 | 0.26299 | 0.41998 | ube2n;ikbkg;app | 5104.95333 | 5266.71 | 4630.47 | 417.790391 | 5134.26949 | 435.986687 | DOWN | 0.333333333 | 0.666666667 |
| 28Day | Interconversion of nucleotide di- and triphosphates | 0.90104 | 0.26299 | 0.41998 | nme4;txnrd1;guk1 | 4741.02333 | 5240 | 3178.52 | 1382.2958 | 4869.76023 | 1349.71028 | UP | 0.666666667 | 0.333333333 |
| 28Day | Cytosolic sulfonation of small molecules | 0.90104 | 0.26299 | 0.41998 | sult2a8;abhd14b;sult2a7 | 3437.08 | 4127.93 | 1389.09 | 1804.62818 | 3827.35854 | 1658.62082 | DOWN | 0.333333333 | 0.666666667 |
| 7Day | RNA polymerase II transcribes snRNA genes | 0.84443 | 0.25988 | 0.42092 | rprd2;ints13;rprd1b;ssu72;zc3h8;phax;polr2h;ell2;ccnk | 3273.98444 | 3652.28 | 1662.33 | 983.667799 | 3432.99013 | 705.824778 | UP | 1 | 0 |
| 90Day | G2/M Checkpoints | 0.21089 | 0.87589 | 0.42125 | hist1h4h;babam1;orc6;hist1h4i;gtse1;dbf4;ywhaz;h2afx | 3406.016 | 3979.26 | 137.958 | 1687.57608 | 3339.52629 | 1447.23226 | UP | 0.75 | 0.25 |
| 28Day | Apoptosis | 0.85263 | 0.24727 | 0.42176 | dnm1l;dynll1;tnfrsf10b;sept4;pkp1;ly96;kpna1;bcl2l1;birc2 | 4098.76578 | 4560.3 | 211.182 | 1937.78356 | 4222.81278 | 1594.84798 | UP | 1 | 0 |
| 90Day | Oxidative Stress Induced Senescence | 0.20109 | 0.88266 | 0.42251 | hist1h4h;cbx6;hist1h4i;hist1h3c;mapk14;txn1;mdm2;h2afx | 3317.69475 | 3979.26 | 744.949 | 1631.71413 | 2616.77139 | 1797.82337 | CONFLICT | 0.5 | 0.5 |
| 90Day | Plasma lipoprotein assembly, remodeling, and clearance | 0.83324 | 0.27593 | 0.42331 | ces3a;apob;pcsk5;lipc;ces3b;bmp1;apoe;apoc3;ap2m1 | 2647.15211 | 3047.49 | 175.96 | 1714.24418 | 2494.70359 | 1796.92696 | DOWN | 0.111111111 | 0.888888889 |
| 90Day | GPVI-mediated activation cascade | 0.24608 | 0.90912 | 0.42391 | vav1;cdc42 | 2158.7685 | 2158.7685 | 156.487 | 2831.65365 | 2296.14268 | 2824.98125 | CONFLICT | 0.5 | 0.5 |
| 90Day | Degradation of beta-catenin by the destruction complex | 0.24608 | 0.90912 | 0.42391 | ctnnb1;btrc | 4619.87 | 4619.87 | 4087.04 | 753.535412 | 5033.38781 | 475.206971 | DOWN | 0 | 1 |
| 90Day | Glucagon-like Peptide-1 (GLP1) regulates insulin secretion | 0.24608 | 0.90912 | 0.42391 | gng11;kcns3 | 5349.345 | 5349.345 | 4854.24 | 700.184206 | 5679.2676 | 522.072862 | UP | 1 | 0 |
| 90Day | RHO GTPases Activate WASPs and WAVEs | 0.22856 | 0.91746 | 0.42418 | wasf2;cdc42 | 2729.3135 | 2729.3135 | 156.487 | 3638.52613 | 2386.31403 | 3606.04702 | CONFLICT | 0.5 | 0.5 |
| 90Day | SUMOylation of transcription cofactors | 0.22856 | 0.91746 | 0.42418 | park7;ddx5 | 1939.5342 | 1939.5342 | 25.9884 | 2706.16242 | 669.441381 | 2024.11549 | CONFLICT | 0.5 | 0.5 |
| 90Day | Activation of Matrix Metalloproteinases | 0.21208 | 0.92508 | 0.42611 | plg;mmp2 | 3039.485 | 3039.485 | 668.86 | 3352.57003 | 3567.16565 | 3268.4602 | DOWN | 0 | 1 |
| 90Day | Cooperation of PDCL (PhLP1) and TRiC/CCT in G-protein beta folding | 0.21208 | 0.92508 | 0.42611 | gng11;gnai3 | 5378.655 | 5378.655 | 4854.24 | 741.634805 | 5266.80756 | 724.570551 | UP | 1 | 0 |
| 7Day | Receptor-type tyrosine-protein phosphatases | 0.88725 | 0.29022 | 0.42809 | ptprf;ptprd;il1rap | 1132.78467 | 1019.97 | 131.024 | 1062.66875 | 894.670977 | 1177.96202 | DOWN | 0 | 1 |
| 7Day | FRS-mediated FGFR3 signaling | 0.88725 | 0.29022 | 0.42809 | ptpn11;kras;fgf1 | 3478.71333 | 3629.67 | 2647.76 | 766.702949 | 3262.18888 | 788.939216 | UP | 0.666666667 | 0.333333333 |
| 7Day | Citric acid cycle (TCA cycle) | 0.88725 | 0.29022 | 0.42809 | sdha;idh2;idh3b | 2119.2 | 2704.94 | 114.56 | 1785.35012 | 2865.72033 | 1459.09968 | DOWN | 0 | 1 |
| 7Day | Synthesis of Prostaglandins (PG) and Thromboxanes (TX) | 0.88725 | 0.29022 | 0.42809 | akr1c6;ptges3;akr1c14 | 3632.50667 | 3138.45 | 2842.81 | 1121.54702 | 3231.69332 | 834.302096 | UP | 1 | 0 |
| 28Day | Synthesis of Leukotrienes (LT) and Eoxins (EX) | 0.8898 | 0.28209 | 0.42827 | mapkapk2;lta4h;cyp4a12b | 5315.31667 | 5375 | 4766.57 | 521.472889 | 5169.46224 | 585.253197 | DOWN | 0.333333333 | 0.666666667 |
| 7Day | Interleukin-2 family signaling | 0.24385 | 0.90945 | 0.42852 | stat1;jak1 | 3735.595 | 3735.595 | 3554.32 | 256.361564 | 3703.94 | 252.422609 | UP | 1 | 0 |
| 7Day | PCP/CE pathway | 0.24385 | 0.90945 | 0.42852 | uba52;pfn1 | 3933.96 | 3933.96 | 3106.36 | 1170.40314 | 4147.24454 | 1130.86822 | UP | 1 | 0 |
| 7Day | Vasopressin regulates renal water homeostasis via Aquaporins | 0.24385 | 0.90945 | 0.42852 | rab11a;prkar2a | 4304.455 | 4304.455 | 4066.56 | 336.434335 | 4288.10382 | 335.638705 | CONFLICT | 0.5 | 0.5 |
| 7Day | Metabolism of steroid hormones | 0.22937 | 0.91639 | 0.42893 | hsd17b2;hsd11b1 | 2230.17 | 2230.17 | 119.56 | 2984.85329 | 2092.72536 | 2978.5176 | CONFLICT | 0.5 | 0.5 |
| 7Day | Chromosome Maintenance | 0.22937 | 0.91639 | 0.42893 | cenpk;prim2 | 3958.635 | 3958.635 | 3911.13 | 67.1822153 | 3938.19452 | 60.6450649 | UP | 1 | 0 |

BMD analysis results for functional classification based on dose-responsive genes, using the Reactome database for gene sets in BMDExpress2.2 software.

| Study Day | Gene Set Name | Fisher's Exact Left P-Value | Fisher's Exact Right P-Value | Fisher's Exact Two Tail | Gene Symbols | BMD Mean | BMD Median | BMD Minimum | BMD Standard Deviation | BMD wMean | BMD wSD | Overall Direction | Percent Genes With Overall Direction Up | Percent Genes With Overall Direction Down |
|---|---|---|---|---|---|---|---|---|---|---|---|---|---|---|
| 7Day | TP53 Regulates Transcription of DNA Repair Genes | 0.22937 | 0.91639 | 0.42893 | polr2h;ccnk | 3035.2 | 3035.2 | 2105.8 | 1314.37008 | 3590.43465 | 1054.03875 | UP | 1 | 0 |
| 90Day | Signaling by Erythropoietin | 0.8839 | 0.2987 | 0.42948 | irs2;vav1;gab1 | 1454.0971 | 126.428 | 74.8133 | 2344.43203 | 1038.75826 | 2111.79854 | DOWN | 0 | 1 |
| 90Day | GAB1 signalosome | 0.8839 | 0.2987 | 0.42948 | tgfa;gab1;areg | 2086.44267 | 2162.51 | 126.428 | 1923.10963 | 2211.30125 | 1359.24692 | UP | 0.666666667 | 0.333333333 |
| 90Day | Adherens junctions interactions | 0.19659 | 0.93203 | 0.42961 | afdn;ctnnb1 | 2442.127 | 2442.127 | 797.214 | 2326.25827 | 1451.95914 | 1857.58251 | CONFLICT | 0.5 | 0.5 |
| 90Day | O-glycosylation of TSR domain-containing proteins | 0.19659 | 0.93203 | 0.42961 | adamts6;spon2 | 3255.88 | 3255.88 | 2653.16 | 852.374798 | 3005.16209 | 775.128281 | CONFLICT | 0.5 | 0.5 |
| 90Day | Cyclin D associated events in G1 | 0.19659 | 0.93203 | 0.42961 | e2f2;cdkn1a | 2581.665 | 2581.665 | 913.71 | 2358.84458 | 2049.72117 | 2235.66976 | UP | 1 | 0 |
| 90Day | G1 Phase | 0.19659 | 0.93203 | 0.42961 | e2f2;cdkn1a | 2581.665 | 2581.665 | 913.71 | 2358.84458 | 2049.72117 | 2235.66976 | UP | 1 | 0 |
| 90Day | Binding and Uptake of Ligands by Scavenger Receptors | 0.19659 | 0.93203 | 0.42961 | apob;apoe | 962.89 | 962.89 | 175.96 | 1112.88708 | 1105.17513 | 1094.54444 | DOWN | 0 | 1 |
| 90Day | Regulation of mRNA stability by proteins that bind AU-rich elements | 0.19659 | 0.93203 | 0.42961 | exosc9;ywhaz | 1471.424 | 1471.424 | 137.958 | 1885.8057 | 1856.1388 | 1805.61685 | UP | 1 | 0 |
| 90Day | Chaperonin-mediated protein folding | 0.19659 | 0.93203 | 0.42961 | gng11;gnai3 | 5378.655 | 5378.655 | 4854.24 | 741.634805 | 5266.80756 | 724.570551 | UP | 1 | 0 |
| 90Day | Protein folding | 0.19659 | 0.93203 | 0.42961 | gng11;gnai3 | 5378.655 | 5378.655 | 4854.24 | 741.634805 | 5266.80756 | 724.570551 | UP | 1 | 0 |
| 90Day | Translesion synthesis by Y family DNA polymerases bypasses lesions on DNA template | 0.19659 | 0.93203 | 0.42961 | pole4;polk | 4753.255 | 4753.255 | 3652.71 | 1556.40567 | 3884.77714 | 955.97646 | CONFLICT | 0.5 | 0.5 |
| 90Day | Activation of ATR in response to replication stress | 0.19659 | 0.93203 | 0.42961 | orc6;dbf4 | 3568.52 | 3568.52 | 2968.7 | 848.273579 | 3583.49623 | 848.009133 | UP | 1 | 0 |
| 7Day | PI3K Cascade | 0.21561 | 0.92283 | 0.43047 | ptpn11;fgf1 | 3138.715 | 3138.715 | 2647.76 | 694.31522 | 2984.26892 | 659.064823 | CONFLICT | 0.5 | 0.5 |
| 7Day | RNA Polymerase I Transcription Initiation | 0.21561 | 0.92283 | 0.43047 | polr2h;ubtf | 2970.455 | 2970.455 | 1976.31 | 1405.93334 | 3441.15761 | 1238.35644 | UP | 1 | 0 |
| 28Day | SUMO E3 ligases SUMOylate target proteins | 0.2156 | 0.87133 | 0.43085 | hist1h4i;rad21;mdm2;ikbkg;brca1;bmi1;blm;tpr | 3945.312 | 4027.865 | 692.086 | 1781.08975 | 3897.46085 | 1655.95085 | UP | 0.875 | 0.125 |
| 7Day | IRS-mediated signalling | 0.20253 | 0.9288 | 0.43309 | ptpn11;fgf1 | 3138.715 | 3138.715 | 2647.76 | 694.31522 | 2984.26892 | 659.064823 | CONFLICT | 0.5 | 0.5 |
| 7Day | Phase 0 - rapid depolarisation | 0.20253 | 0.9288 | 0.43309 | calm3;calm2 | 3983.44 | 3983.44 | 3050.32 | 1319.63096 | 3556.9103 | 1173.69957 | CONFLICT | 0.5 | 0.5 |
| 28Day | Mitochondrial protein import | 0.90002 | 0.43399 | 0.43399 | otc | 726.832 | 726.832 | 726.832 |  | 726.832 |  | DOWN | 0 | 1 |
| 28Day | Synthesis of UDP-N-acetyl-glucosamine | 0.90002 | 0.43399 | 0.43399 | gfpt1 | 5852.61 | 5852.61 | 5852.61 |  | 5852.61 |  | UP | 1 | 0 |
| 28Day | HuR (ELAVL1) binds and stabilizes mRNA | 0.90002 | 0.43399 | 0.43399 | set | 4060.76 | 4060.76 | 4060.76 |  | 4060.76 |  | UP | 1 | 0 |
| 28Day | Vitamin C (ascorbate) metabolism | 0.90002 | 0.43399 | 0.43399 | cyb5a | 5740.08 | 5740.08 | 5740.08 |  | 5740.08 |  | UP | 1 | 0 |
| 28Day | Stabilization of p53 | 0.90002 | 0.43399 | 0.43399 | mdm2 | 2266.61 | 2266.61 | 2266.61 |  | 2266.61 |  | UP | 1 | 0 |
| 28Day | Activated NOTCH1 Transmits Signal to the Nucleus | 0.90002 | 0.43399 | 0.43399 | notch1 | 908.573 | 908.573 | 908.573 |  | 908.573 |  | UP | 1 | 0 |
| 28Day | SUMOylation of immune response proteins | 0.90002 | 0.43399 | 0.43399 | ikbkg | 5417.68 | 5417.68 | 5417.68 |  | 5417.68 |  | UP | 1 | 0 |
| 28Day | Association of TriC/CCT with target proteins during biosynthesis | 0.90002 | 0.43399 | 0.43399 | cct4 | 5836.87 | 5836.87 | 5836.87 |  | 5836.87 |  | UP | 1 | 0 |
| 28Day | p38MAPK events | 0.90002 | 0.43399 | 0.43399 | mapkapk2 | 5375 | 5375 | 5375 |  | 5375 |  | DOWN | 0 | 1 |
| 28Day | SUMOylation of ubiquitinylation proteins | 0.90002 | 0.43399 | 0.43399 | mdm2 | 2266.61 | 2266.61 | 2266.61 |  | 2266.61 |  | UP | 1 | 0 |
| 28Day | Phosphate bond hydrolysis by NUDT proteins | 0.90002 | 0.43399 | 0.43399 | nudt5 | 2482 | 2482 | 2482 |  | 2482 |  | UP | 1 | 0 |
| 28Day | Receptor Mediated Mitophagy | 0.90002 | 0.43399 | 0.43399 | atg5 | 5747.14 | 5747.14 | 5747.14 |  | 5747.14 |  | UP | 1 | 0 |
| 28Day | Telomere C-strand synthesis initiation | 0.90002 | 0.43399 | 0.43399 | pole3 | 805.318 | 805.318 | 805.318 |  | 805.318 |  | UP | 1 | 0 |
| 28Day | DNA replication initiation | 0.90002 | 0.43399 | 0.43399 | pole3 | 805.318 | 805.318 | 805.318 |  | 805.318 |  | UP | 1 | 0 |
| 28Day | CDT1 association with the CDC6:ORC:origin complex | 0.81587 | 0.33942 | 0.43432 | psmd6;psmd8;cdc6;psmf1;psmb8 | 3966.316 | 4413.43 | 1415.14 | 1680.76279 | 4053.96174 | 1828.75774 | DOWN | 0.4 | 0.6 |
| 28Day | Signaling by the B Cell Receptor (BCR) | 0.22957 | 0.91538 | 0.43521 | ppp3cb;ikbkg | 4756.775 | 4756.775 | 4095.87 | 934.660814 | 4545.37184 | 885.555333 | UP | 1 | 0 |
| 90Day | C-type lectin receptors (CLRs) | 0.24422 | 0.87082 | 0.43594 | ube2m;cdc34;nfkbia;ikbkg;btrc | 2653.3084 | 3265.56 | 569.072 | 1985.29402 | 2657.76128 | 2167.87416 | UP | 0.6 | 0.4 |
| 90Day | HATs acetylate histones | 0.24422 | 0.87082 | 0.43594 | msl1;hist1h4h;mcrs1;hist1h4i;hist1h3c | 3183.1678 | 3951.81 | 811.859 | 2119.24618 | 2113.0481 | 1882.23775 | UP | 0.6 | 0.4 |
| 90Day | Assembly of the pre-replicative complex | 0.24422 | 0.87082 | 0.43594 | psmd8;orc6;e2f2;psmc4;psmf1 | 2606.0996 | 3031.27 | 186.178 | 1777.9967 | 2622.61858 | 1763.81664 | UP | 1 | 0 |
| 28Day | Cap-dependent Translation Initiation | 0.21959 | 0.92011 | 0.4363 | eif3m;eif1ax | 2737.81 | 2737.81 | 1517.45 | 1725.84966 | 2423.68091 | 1667.69388 | CONFLICT | 0.5 | 0.5 |
| 90Day | Toll Like Receptor 3 (TLR3) Cascade | 0.21876 | 0.88708 | 0.43697 | irf7;mapk14;nfkbia;ikbkg;btrc | 4394.204 | 4261.96 | 3265.56 | 1021.51429 | 4535.14678 | 1084.60939 | DOWN | 0.4 | 0.6 |
| 28Day | MAPK6/MAPK4 signaling | 0.87802 | 0.3013 | 0.43742 | sept7;cdc14a;cdc42 | 2996.03733 | 2463.49 | 748.272 | 2555.99239 | 3546.69811 | 2573.36962 | UP | 1 | 0 |
| 28Day | Gluconeogenesis | 0.87802 | 0.3013 | 0.43742 | slc25a10;pcx;pck1 | 3333.02667 | 3209.5 | 3056.49 | 354.811243 | 3331.76336 | 350.089935 | DOWN | 0.333333333 | 0.666666667 |

BMD analysis results for functional classification based on dose-responsive genes, using the Reactome database for gene sets in BMDExpress2.2 software.

| Study Day | Gene Set Name | Fisher's Exact Left P-Value | Fisher's Exact Right P-Value | Fisher's Exact Two Tail | Gene Symbols | BMD Mean | BMD Median | BMD Minimum | BMD Standard Deviation | BMD wMean | BMD wSD | Overall Direction | Percent Genes With Overall Direction Up | Percent Genes With Overall Direction Down |
|---|---|---|---|---|---|---|---|---|---|---|---|---|---|---|
| 28Day | Synthesis of active ubiquitin: roles of E1 and E2 enzymes | 0.87802 | 0.3013 | 0.43742 | ube2g1;ube2k;uchl3 | 4450.56667 | 4043.68 | 4034.64 | 712.591585 | 4474.78803 | 724.761299 | UP | 0.666666667 | 0.333333333 |
| 28Day | DDX58/IFIH1-mediated induction of interferon-alpha/beta | 0.87802 | 0.3013 | 0.43742 | tax1bp1;ikbkg;app | 5005.61333 | 4968.69 | 4630.47 | 394.901754 | 5021.48956 | 301.863796 | DOWN | 0.333333333 | 0.666666667 |
| 28Day | EGFR downregulation | 0.87802 | 0.3013 | 0.43742 | hgs;hbegf;cdc42 | 2201.316 | 2463.49 | 919.738 | 1172.68109 | 2028.69886 | 1124.36761 | UP | 1 | 0 |
| 28Day | Pyruvate metabolism | 0.87802 | 0.3013 | 0.43742 | me1;ldha;gstz1 | 5509.17333 | 5449.12 | 5233.2 | 310.388148 | 5608.35417 | 296.13799 | DOWN | 0 | 1 |
| 28Day | Programmed Cell Death | 0.81693 | 0.2938 | 0.43779 | dnm1l;dynll1;tnfrsf10b;sept4;pkp1;ly96;kpna1;bcl2l1;birc2 | 4098.76578 | 4560.3 | 211.182 | 1937.78356 | 4222.81278 | 1594.84798 | UP | 1 | 0 |
| 28Day | Eukaryotic Translation Initiation | 0.20997 | 0.9246 | 0.43796 | eif3m;eif1ax | 2737.81 | 2737.81 | 1517.45 | 1725.84966 | 2423.68091 | 1667.69388 | CONFLICT | 0.5 | 0.5 |
| 90Day | RMTs methylate histone arginines | 0.2068 | 0.89453 | 0.43878 | smarcd2;hist1h4h;hist1h4i;hist1h3c;smarcb1 | 3700.1278 | 3970.56 | 811.859 | 1789.86064 | 3394.25997 | 2201.30818 | DOWN | 0.4 | 0.6 |
| 28Day | Regulation of actin dynamics for phagocytic cup formation | 0.2007 | 0.92885 | 0.44015 | cdc42;brk1 | 3960.63 | 3960.63 | 2463.49 | 2117.27569 | 4417.2828 | 2016.38111 | CONFLICT | 0.5 | 0.5 |
| 7Day | Beta-catenin independent WNT signaling | 0.24384 | 0.87034 | 0.44033 | uba52;pfn1;ctnnb1;calm3;calm2 | 3177.86464 | 3106.36 | 54.5232 | 1956.25886 | 2843.19005 | 1975.40546 | UP | 0.6 | 0.4 |
| 90Day | Mitochondrial Fatty Acid Beta-Oxidation | 0.85699 | 0.2724 | 0.44087 | acad10;ndufab1;pccb;acaa2;mut;pcca | 1850.32883 | 2143.53 | 105.476 | 1410.64201 | 2371.80545 | 1194.37732 | DOWN | 0.166666667 | 0.833333333 |
| 7Day | Gene Silencing by RNA | 0.22262 | 0.88399 | 0.44117 | hist1h4h;hist1h2bc;hist2h2ac;polr2h;hist2h2aa1 | 4073.244 | 3964.6 | 3406.55 | 810.921331 | 4033.48029 | 829.513011 | UP | 0.6 | 0.4 |
| 7Day | Signaling by FGFR1 | 0.8624 | 0.26295 | 0.44131 | mapk3;uba52;ptpn11;ppp2cb;kras;fgf1 | 3937.49667 | 3894.19 | 2647.76 | 815.708654 | 3810.92898 | 853.996178 | UP | 0.666666667 | 0.333333333 |
| 7Day | CTLA4 inhibitory signaling | 0.87055 | 0.31702 | 0.44187 | yes1;ptpn11;ppp2cb | 3759.22 | 3629.67 | 3627.04 | 226.668643 | 3744.87584 | 220.142069 | UP | 1 | 0 |
| 7Day | Regulation of RAS by GAPs | 0.87055 | 0.31702 | 0.44187 | uba52;rasa1;kras | 4902.11667 | 4761.56 | 4158.71 | 822.739577 | 5136.80433 | 831.742073 | UP | 0.666666667 | 0.333333333 |
| 7Day | Synthesis of epoxy (EET) and dihydroxyeicosatrienoic acids (DHET) | 0.87055 | 0.31702 | 0.44187 | ephx2;cyp2c37;cyp2c29 | 2023.18057 | 2593.25 | 93.6517 | 1717.00186 | 2278.23391 | 1552.8981 | DOWN | 0.333333333 | 0.666666667 |
| 7Day | Common Pathway of Fibrin Clot Formation | 0.87055 | 0.31702 | 0.44187 | f5;f2;serpinc1 | 162.215167 | 156.627 | 85.9375 | 79.2197094 | 194.700484 | 66.2186001 | DOWN | 0 | 1 |
| 28Day | EPH-Ephrin signaling | 0.19178 | 0.93287 | 0.44285 | epha7;cdc42 | 4147.25 | 4147.25 | 2463.49 | 2381.19623 | 4157.06877 | 2381.15574 | UP | 1 | 0 |
| 28Day | HDR through Homologous Recombination (HRR) | 0.86085 | 0.26285 | 0.44604 | rmi1;pole3;rad51d;rad51;brca1;blm | 3062.16233 | 3608.735 | 692.086 | 1945.73971 | 3555.697 | 1478.95115 | UP | 1 | 0 |
| 90Day | Eicosanoids | 0.86335 | 0.33111 | 0.44712 | cyp4f16;cyp4a12a;cyp4a12b | 3624.98 | 3568.65 | 3465.22 | 194.153566 | 3583.99801 | 170.385902 | UP | 1 | 0 |
| 7Day | PIP3 activates AKT signaling | 0.21866 | 0.85238 | 0.44713 | rraga;suz12;mapk3;uba52;ptpn11;pten;ppp2cb;il1rap;fgf1;csnk2b;cdkn1a;casp9;bmi1;xiap | 3449.89529 | 3426.385 | 131.024 | 1256.33563 | 3350.39421 | 1322.94503 | UP | 0.642857143 | 0.357142857 |
| 28Day | ER-Phagosome pathway | 0.86573 | 0.32057 | 0.44732 | tap1;h2-q7;h2-d1 | 3562.11333 | 3718.12 | 1188.24 | 2299.84187 | 3462.70475 | 1959.38094 | DOWN | 0.333333333 | 0.666666667 |
| 28Day | Glyoxylate metabolism and glycine degradation | 0.86573 | 0.32057 | 0.44732 | ndufab1;prodh2;got2 | 2474.68 | 2384.42 | 1721.17 | 802.45623 | 2449.32669 | 832.107975 | DOWN | 0 | 1 |
| 7Day | Vasopressin-like receptors | 0.89697 | 0.44786 | 0.44786 | avpr1a | 836.92 | 836.92 | 836.92 |  | 836.92 |  | UP | 1 | 0 |
| 7Day | Degradation of GLI1 by the proteasome | 0.89697 | 0.44786 | 0.44786 | uba52 | 4761.56 | 4761.56 | 4761.56 |  | 4761.56 |  | UP | 1 | 0 |
| 7Day | Regulation of ornithine decarboxylase (ODC) | 0.89697 | 0.44786 | 0.44786 | nqo1 | 1137.09 | 1137.09 | 1137.09 |  | 1137.09 |  | UP | 1 | 0 |
| 7Day | FGFR1b ligand binding and activation | 0.89697 | 0.44786 | 0.44786 | fgf1 | 2647.76 | 2647.76 | 2647.76 |  | 2647.76 |  | DOWN | 0 | 1 |
| 7Day | Molybdenum cofactor biosynthesis | 0.89697 | 0.44786 | 0.44786 | mocs1 | 3839.03 | 3839.03 | 3839.03 |  | 3839.03 |  | DOWN | 0 | 1 |
| 7Day | Glucocorticoid biosynthesis | 0.89697 | 0.44786 | 0.44786 | hsd11b1 | 119.56 | 119.56 | 119.56 |  | 119.56 |  | DOWN | 0 | 1 |
| 7Day | MET Receptor Activation | 0.89697 | 0.44786 | 0.44786 | hgfac | 186.634 | 186.634 | 186.634 |  | 186.634 |  | DOWN | 0 | 1 |
| 7Day | Attachment of GPI anchor to uPAR | 0.89697 | 0.44786 | 0.44786 | gpaa1 | 5658.97 | 5658.97 | 5658.97 |  | 5658.97 |  | DOWN | 0 | 1 |
| 7Day | Interleukin-10 signaling | 0.89697 | 0.44786 | 0.44786 | jak1 | 3554.32 | 3554.32 | 3554.32 |  | 3554.32 |  | UP | 1 | 0 |
| 7Day | Lipid particle organization | 0.89697 | 0.44786 | 0.44786 | fitm1 | 3812.67 | 3812.67 | 3812.67 |  | 3812.67 |  | UP | 1 | 0 |
| 7Day | Eukaryotic Translation Termination | 0.89697 | 0.44786 | 0.44786 | gspt1 | 5370.24 | 5370.24 | 5370.24 |  | 5370.24 |  | DOWN | 0 | 1 |
| 7Day | mRNA Editing | 0.89697 | 0.44786 | 0.44786 | adar | 3802.37 | 3802.37 | 3802.37 |  | 3802.37 |  | UP | 1 | 0 |
| 7Day | Regulation of expression of SLITs and ROBOs | 0.89697 | 0.44786 | 0.44786 | uba52 | 4761.56 | 4761.56 | 4761.56 |  | 4761.56 |  | UP | 1 | 0 |
| 7Day | activated TAK1 mediates p38 MAPK activation | 0.89697 | 0.44786 | 0.44786 | map2k3 | 2894.34 | 2894.34 | 2894.34 |  | 2894.34 |  | DOWN | 0 | 1 |
| 7Day | TNFR1-mediated ceramide production | 0.89697 | 0.44786 | 0.44786 | smpd2 | 5795.86 | 5795.86 | 5795.86 |  | 5795.86 |  | DOWN | 0 | 1 |
| 7Day | CREB1 phosphorylation through the activation of Adenylate Cyclase | 0.89697 | 0.44786 | 0.44786 | prkar2a | 4066.56 | 4066.56 | 4066.56 |  | 4066.56 |  | DOWN | 0 | 1 |
| 7Day | AMPK inhibits chREBP transcriptional activation activity | 0.89697 | 0.44786 | 0.44786 | adipor2 | 5199.91 | 5199.91 | 5199.91 |  | 5199.91 |  | DOWN | 0 | 1 |

BMD analysis results for functional classification based on dose-responsive genes, using the Reactome database for gene sets in BMDExpress2.2 software.

| Study Day | Gene Set Name | Fisher's Exact Left P-Value | Fisher's Exact Right P-Value | Fisher's Exact Two Tail | Gene Symbols | BMD Mean | BMD Median | BMD Minimum | BMD Standard Deviation | BMD wMean | BMD wSD | Overall Direction | Percent Genes With Overall Direction Up | Percent Genes With Overall Direction Down |
|---|---|---|---|---|---|---|---|---|---|---|---|---|---|---|
| 7Day | Negative feedback regulation of MAPK pathway | 0.89697 | 0.44786 | 0.44786 | mapk3 | 4800.24 | 4800.24 | 4800.24 |  | 4800.24 |  | DOWN | 0 | 1 |
| 7Day | Protein repair | 0.89697 | 0.44786 | 0.44786 | msrb1 | 2837.64 | 2837.64 | 2837.64 |  | 2837.64 |  | DOWN | 0 | 1 |
| 90Day | Gap junction trafficking | 0.84244 | 0.29267 | 0.44841 | tubb6;tubb4b;tubb2a;tuba1b;gjb2;ap2m1 | 2094.7335 | 1866.255 | 779.791 | 933.017487 | 1798.35123 | 1060.01907 | UP | 0.666666667 | 0.333333333 |
| 90Day | GRB7 events in ERBB2 signaling | 0.89934 | 0.45003 | 0.45003 | nrg1 | 3912.34 | 3912.34 | 3912.34 |  | 3912.34 |  | UP | 1 | 0 |
| 90Day | Extrinsic Pathway of Fibrin Clot Formation | 0.89934 | 0.45003 | 0.45003 | f7 | 3350.52 | 3350.52 | 3350.52 |  | 3350.52 |  | DOWN | 0 | 1 |
| 90Day | Activation of C3 and C5 | 0.89934 | 0.45003 | 0.45003 | c3 | 639.57 | 639.57 | 639.57 |  | 639.57 |  | DOWN | 0 | 1 |
| 90Day | MET activates PTPN11 | 0.89934 | 0.45003 | 0.45003 | gab1 | 126.428 | 126.428 | 126.428 |  | 126.428 |  | DOWN | 0 | 1 |
| 90Day | Adenosine P1 receptors | 0.89934 | 0.45003 | 0.45003 | adora1 | 1587.43 | 1587.43 | 1587.43 |  | 1587.43 |  | DOWN | 0 | 1 |
| 90Day | Abacavir transport and metabolism | 0.89934 | 0.45003 | 0.45003 | slc22a1 | 1050.57 | 1050.57 | 1050.57 |  | 1050.57 |  | DOWN | 0 | 1 |
| 90Day | Condensation of Prometaphase Chromosomes | 0.89934 | 0.45003 | 0.45003 | smc4 | 2814.71 | 2814.71 | 2814.71 |  | 2814.71 |  | UP | 1 | 0 |
| 90Day | Synthesis of Lipoxins (LX) | 0.89934 | 0.45003 | 0.45003 | hpgd | 5817.8 | 5817.8 | 5817.8 |  | 5817.8 |  | DOWN | 0 | 1 |
| 90Day | SUMO is transferred from E1 to E2 (UBE2I, UBC9) | 0.89934 | 0.45003 | 0.45003 | sae1 | 3998.58 | 3998.58 | 3998.58 |  | 3998.58 |  | UP | 1 | 0 |
| 90Day | VLDL clearance | 0.89934 | 0.45003 | 0.45003 | apob | 175.96 | 175.96 | 175.96 |  | 175.96 |  | DOWN | 0 | 1 |
| 90Day | Regulation of cholesterol biosynthesis by SREBP (SREBF) | 0.89934 | 0.45003 | 0.45003 | scap | 4410.99 | 4410.99 | 4410.99 |  | 4410.99 |  | DOWN | 0 | 1 |
| 90Day | N-glycan trimming and elongation in the cis-Golgi | 0.89934 | 0.45003 | 0.45003 | man1a | 3931.46 | 3931.46 | 3931.46 |  | 3931.46 |  | DOWN | 0 | 1 |
| 90Day | Transcriptional Regulation by MECP2 | 0.89934 | 0.45003 | 0.45003 | hdac2 | 202.162 | 202.162 | 202.162 |  | 202.162 |  | UP | 1 | 0 |
| 90Day | Synthesis of PIPs at the ER membrane | 0.89934 | 0.45003 | 0.45003 | pi4ka | 3636.02 | 3636.02 | 3636.02 |  | 3636.02 |  | DOWN | 0 | 1 |
| 90Day | Synthesis of 15-eicosatetraenoic acid derivatives | 0.89934 | 0.45003 | 0.45003 | gpx4 | 2353.96 | 2353.96 | 2353.96 |  | 2353.96 |  | UP | 1 | 0 |
| 90Day | Biosynthesis of EPA-derived SPMs | 0.89934 | 0.45003 | 0.45003 | gpx4 | 2353.96 | 2353.96 | 2353.96 |  | 2353.96 |  | UP | 1 | 0 |
| 90Day | TRAIL signaling | 0.89934 | 0.45003 | 0.45003 | tnfrsf10b | 3826.99 | 3826.99 | 3826.99 |  | 3826.99 |  | UP | 1 | 0 |
| 90Day | Activated NTRK2 signals through FYN | 0.89934 | 0.45003 | 0.45003 | ntrk2 | 3744.34 | 3744.34 | 3744.34 |  | 3744.34 |  | DOWN | 0 | 1 |
| 90Day | NTRK2 activates RAC1 | 0.89934 | 0.45003 | 0.45003 | ntrk2 | 3744.34 | 3744.34 | 3744.34 |  | 3744.34 |  | DOWN | 0 | 1 |
| 90Day | RUNX3 regulates WNT signaling | 0.89934 | 0.45003 | 0.45003 | ctnnb1 | 4087.04 | 4087.04 | 4087.04 |  | 4087.04 |  | DOWN | 0 | 1 |
| 90Day | Fructose metabolism | 0.89934 | 0.45003 | 0.45003 | tkfc | 1863.37 | 1863.37 | 1863.37 |  | 1863.37 |  | UP | 1 | 0 |
| 90Day | Regulation of MECP2 expression and activity | 0.89934 | 0.45003 | 0.45003 | hdac2 | 202.162 | 202.162 | 202.162 |  | 202.162 |  | UP | 1 | 0 |
| 90Day | OAS antiviral response | 0.89934 | 0.45003 | 0.45003 | abce1 | 3026.26 | 3026.26 | 3026.26 |  | 3026.26 |  | UP | 1 | 0 |
| 7Day | Intra-Golgi and retrograde Golgi-to-ER traffic | 0.81193 | 0.2591 | 0.45174 | rab3gap2;cog6;plin3;copz1;rab9;cog5;tubb4b;vps45;tubb2a;tuba4a;arcn1;sec22b;rab6a;rab18;rab1a;cyth1;kif2a;kif1c;igf2r;capza2;gbf1 | 3014.27314 | 3251.9 | 919.856 | 1251.48482 | 2885.62196 | 1189.24013 | UP | 0.714285714 | 0.285714286 |
| 7Day | Platelet activation, signaling and aggregation | 0.23938 | 0.82446 | 0.45536 | tmx3;cdc37l1;clec1b;mapk3;abcc4;ywhaz;tuba4a;sod1;ptpn11;flna;lgals3bp;itpr2;gnai3;f5;f2;ecm1;cdc42;calm3;calm2;ahsg;qsox1 | 3246.81448 | 3443.96 | 156.627 | 1742.4818 | 2837.08229 | 1884.89995 | CONFLICT | 0.428571429 | 0.571428571 |
| 7Day | Antigen processing: Ubiquitination & Proteasome degradation | 0.23938 | 0.82446 | 0.45536 | ube2n;btbd1;rnf6;fbxo22;cul2;fbxo9;trim69;ube2v2;ube2k;ube3a;ube2a;ube2e3;uba52;cdc27;cdc34;trip12;ubox5;ube2j2;ccnf;btrc;wwp1 | 3547.42905 | 3369.05 | 1018.89 | 1093.773 | 3640.32488 | 1015.82497 | UP | 0.904761905 | 0.095238095 |
| 7Day | mTORC1-mediated signalling | 0.8529 | 0.34384 | 0.45691 | rps6kb1;rraga;eif4ebp1 | 3455.34333 | 3225.73 | 3116.98 | 494.878532 | 3686.05963 | 493.949394 | UP | 0.666666667 | 0.333333333 |
| 7Day | N-glycan trimming in the ER and Calnexin/Calreticulin cycle | 0.8529 | 0.34384 | 0.45691 | ngly1;uba52;sel1l | 4695.51 | 4761.56 | 4225.92 | 440.296435 | 4822.82749 | 349.287811 | UP | 1 | 0 |
| 7Day | Glycolysis | 0.8529 | 0.34384 | 0.45691 | pfkp;gckr;gpi1 | 3112.06 | 3375.32 | 1853.98 | 1149.29064 | 3116.61725 | 1080.45298 | DOWN | 0 | 1 |
| 7Day | FRS-mediated FGFR4 signaling | 0.8529 | 0.34384 | 0.45691 | ptpn11;kras;fgf1 | 3478.71333 | 3629.67 | 2647.76 | 766.702949 | 3262.18888 | 788.939216 | UP | 0.666666667 | 0.333333333 |
| 28Day | Antiviral mechanism by IFN-stimulated genes | 0.85296 | 0.33985 | 0.45787 | ube2n;arih1;ppm1b | 4090.57 | 5266.71 | 1290.26 | 2435.46398 | 2838.72879 | 2524.17867 | DOWN | 0.333333333 | 0.666666667 |
| 28Day | Regulation of TNFR1 signaling | 0.85296 | 0.33985 | 0.45787 | tax1bp1;ikbkg;birc2 | 5416.20667 | 5417.68 | 4968.69 | 446.781822 | 5309.28907 | 473.741883 | UP | 0.666666667 | 0.333333333 |
| 90Day | ESR-mediated signaling | 0.22849 | 0.85592 | 0.45935 | hist1h4h;ppid;hist1h4i;hist1h3c;nr5a2;yy1;hsp90aa1;h2afx;ddx5;cbfb | 2972.2308 | 3902.445 | 174.249 | 1813.9438 | 2612.30985 | 1823.93818 | UP | 0.6 | 0.4 |
| 90Day | Signaling by MET | 0.24453 | 0.86324 | 0.46451 | ranbp9;hgfac;sos1;sh3gl3;gab1;fn1 | 3111.65133 | 2735.805 | 126.428 | 2182.12293 | 4302.86563 | 2073.75712 | DOWN | 0.333333333 | 0.666666667 |
| 90Day | Fc epsilon receptor (FCERI) signaling | 0.23235 | 0.87143 | 0.46537 | vav1;cdc34;sos1;nfkbia;ikbkg;btrc | 3774.06867 | 3881.075 | 569.072 | 1849.80726 | 3950.01751 | 1961.11201 | DOWN | 0.333333333 | 0.666666667 |
| 90Day | Activation of NF-kappaB in B cells | 0.84146 | 0.36346 | 0.46638 | nfkbia;ikbkg;btrc | 4006.45333 | 3601.1 | 3265.56 | 1006.7561 | 4283.92049 | 1129.74967 | DOWN | 0.333333333 | 0.666666667 |

BMD analysis results for functional classification based on dose-responsive genes, using the Reactome database for gene sets in BMDExpress2.2 software.

| Study Day | Gene Set Name | Fisher's Exact Left P-Value | Fisher's Exact Right P-Value | Fisher's Exact Two Tail | Gene Symbols | BMD Mean | BMD Median | BMD Minimum | BMD Standard Deviation | BMD wMean | BMD wSD | Overall Direction | Percent Genes With Overall Direction Up | Percent Genes With Overall Direction Down |
|---|---|---|---|---|---|---|---|---|---|---|---|---|---|---|
| 90Day | G beta:gamma signalling through CDC42 | 0.84146 | 0.36346 | 0.46638 | arhgef6;gng11;cdc42 | 3654.54233 | 4854.24 | 156.487 | 3078.80769 | 3619.71528 | 3169.47674 | UP | 0.666666667 | 0.333333333 |
| 90Day | Gap junction trafficking and regulation | 0.81143 | 0.33399 | 0.46679 | tubb6;tubb4b;tubb2a;tuba1b;gjb2;ap2m1 | 2094.7335 | 1866.255 | 779.791 | 933.017487 | 1798.35123 | 1060.01907 | UP | 0.666666667 | 0.333333333 |
| 28Day | Phospholipid metabolism | 0.24214 | 0.84447 | 0.46782 | dgat2;pnpla8;pi4k2b;tnfaip8l1;phospho1;pla2g4c;pi4ka;etnk2;ptdss1;abhd4 | 3808.807 | 4014.015 | 2639.44 | 769.146816 | 3817.56261 | 672.152485 | DOWN | 0.4 | 0.6 |
| 28Day | Intra-Golgi and retrograde Golgi-to-ER traffic | 0.2303 | 0.85333 | 0.46857 | dynll1;rab9;tmf1;tubb4b;tubb2a;rab18;man1a;cux1;capza2;gbf1 | 3731.9494 | 4064.745 | 185.394 | 1694.77939 | 4137.04061 | 1320.52339 | CONFLICT | 0.5 | 0.5 |
| 28Day | G-protein beta:gamma signalling | 0.83975 | 0.3591 | 0.46899 | pdpk1;gnb5;cdc42 | 1203.37533 | 953.648 | 192.988 | 1155.66762 | 1408.50452 | 956.075532 | UP | 0.666666667 | 0.333333333 |
| 28Day | NOD1/2 Signaling Pathway | 0.83975 | 0.3591 | 0.46899 | ube2n;ikbkg;birc2 | 5515.54667 | 5417.68 | 5266.71 | 309.597135 | 5632.53274 | 300.031601 | UP | 0.666666667 | 0.333333333 |
| 28Day | Transferrin endocytosis and recycling | 0.83975 | 0.3591 | 0.46899 | atp6v0e2;trf;atp6v1e1 | 3588.84333 | 3086.6 | 2385.58 | 1518.03228 | 2996.26029 | 1240.9233 | DOWN | 0.333333333 | 0.666666667 |
| 28Day | Reactions specific to the complex N-glycan synthesis pathway | 0.87711 | 0.47288 | 0.47288 | mgat2 | 3478.56 | 3478.56 | 3478.56 |  | 3478.56 |  | UP | 1 | 0 |
| 28Day | Apoptotic factor-mediated response | 0.87711 | 0.47288 | 0.47288 | 4-Sep | 211.182 | 211.182 | 211.182 |  | 211.182 |  | UP | 1 | 0 |
| 28Day | Transport of nucleotide sugars | 0.87711 | 0.47288 | 0.47288 | slc35d2 | 3816.75 | 3816.75 | 3816.75 |  | 3816.75 |  | UP | 1 | 0 |
| 28Day | EGFR interacts with phospholipase C-gamma | 0.87711 | 0.47288 | 0.47288 | hbegf | 919.738 | 919.738 | 919.738 |  | 919.738 |  | UP | 1 | 0 |
| 28Day | FGFR2b ligand binding and activation | 0.87711 | 0.47288 | 0.47288 | fgf1 | 1467.57 | 1467.57 | 1467.57 |  | 1467.57 |  | DOWN | 0 | 1 |
| 28Day | Axonal growth inhibition (RHOA activation) | 0.87711 | 0.47288 | 0.47288 | arhgdia | 4971.84 | 4971.84 | 4971.84 |  | 4971.84 |  | UP | 1 | 0 |
| 28Day | Androgen biosynthesis | 0.87711 | 0.47288 | 0.47288 | hsd17b3 | 5151.17 | 5151.17 | 5151.17 |  | 5151.17 |  | UP | 1 | 0 |
| 28Day | Acyl chain remodelling of PI | 0.87711 | 0.47288 | 0.47288 | pla2g4c | 3475.05 | 3475.05 | 3475.05 |  | 3475.05 |  | UP | 1 | 0 |
| 28Day | TP53 Regulates Transcription of Genes Involved in G1 Cell Cycle Arrest | 0.87711 | 0.47288 | 0.47288 | e2f7 | 4451.79 | 4451.79 | 4451.79 |  | 4451.79 |  | UP | 1 | 0 |
| 28Day | TRIF-mediated programmed cell death | 0.87711 | 0.47288 | 0.47288 | ly96 | 4560.3 | 4560.3 | 4560.3 |  | 4560.3 |  | UP | 1 | 0 |
| 28Day | Regulation of RUNX3 expression and activity | 0.87711 | 0.47288 | 0.47288 | mdm2 | 2266.61 | 2266.61 | 2266.61 |  | 2266.61 |  | UP | 1 | 0 |
| 28Day | Serine biosynthesis | 0.87711 | 0.47288 | 0.47288 | serinc1 | 1574.09 | 1574.09 | 1574.09 |  | 1574.09 |  | DOWN | 0 | 1 |
| 28Day | CLEC7A (Dectin-1) induces NFAT activation | 0.87711 | 0.47288 | 0.47288 | ppp3cb | 4095.87 | 4095.87 | 4095.87 |  | 4095.87 |  | UP | 1 | 0 |
| 28Day | Phosphate bond hydrolysis by NTPDase proteins | 0.87711 | 0.47288 | 0.47288 | entpd5 | 1855.96 | 1855.96 | 1855.96 |  | 1855.96 |  | UP | 1 | 0 |
| 28Day | Biotin transport and metabolism | 0.87711 | 0.47288 | 0.47288 | pcx | 3056.49 | 3056.49 | 3056.49 |  | 3056.49 |  | DOWN | 0 | 1 |
| 28Day | Sodium/Proton exchangers | 0.87711 | 0.47288 | 0.47288 | slc9a5 | 3688.09 | 3688.09 | 3688.09 |  | 3688.09 |  | UP | 1 | 0 |
| 28Day | Calcineurin activates NFAT | 0.87711 | 0.47288 | 0.47288 | ppp3cb | 4095.87 | 4095.87 | 4095.87 |  | 4095.87 |  | UP | 1 | 0 |
| 28Day | EGFR Transactivation by Gastrin | 0.87711 | 0.47288 | 0.47288 | hbegf | 919.738 | 919.738 | 919.738 |  | 919.738 |  | UP | 1 | 0 |
| 28Day | Role of LAT2/NTAL/LAB on calcium mobilization | 0.87711 | 0.47288 | 0.47288 | pdpk1 | 192.988 | 192.988 | 192.988 |  | 192.988 |  | DOWN | 0 | 1 |
| 7Day | Generation of second messenger molecules | 0.83438 | 0.37058 | 0.47296 | pak2;h2-ab1;h2-aa | 2220.87333 | 2261.36 | 1863.06 | 339.386038 | 2208.54305 | 306.463493 | DOWN | 0.333333333 | 0.666666667 |
| 7Day | Branched-chain amino acid catabolism | 0.83438 | 0.37058 | 0.47296 | mccc2;dld;bckdha | 3122.99067 | 4026.23 | 199.112 | 2593.05718 | 3005.23722 | 2577.26557 | DOWN | 0.333333333 | 0.666666667 |
| 7Day | FRS-mediated FGFR1 signaling | 0.83438 | 0.37058 | 0.47296 | ptpn11;kras;fgf1 | 3478.71333 | 3629.67 | 2647.76 | 766.702949 | 3262.18888 | 788.939216 | UP | 0.666666667 | 0.333333333 |
| 7Day | RAF-independent MAPK1/3 activation | 0.83438 | 0.37058 | 0.47296 | mapk3;ptpn11;jak1 | 3994.74333 | 3629.67 | 3554.32 | 698.597213 | 3930.59598 | 681.24112 | UP | 0.666666667 | 0.333333333 |
| 7Day | SMAD2/SMAD3:SMAD4 heterotrimer regulates transcription | 0.83438 | 0.37058 | 0.47296 | uba52;tfdp1;ccnk | 2524.87467 | 2105.8 | 707.264 | 2059.38017 | 3053.07053 | 2186.83839 | UP | 1 | 0 |
| 7Day | Cyclin A/B1/B2 associated events during G2/M transition | 0.83438 | 0.37058 | 0.47296 | ppp2cb;cdc25a;xpo1 | 4065.65333 | 3627.04 | 2692.16 | 1637.46697 | 3841.17985 | 1373.84347 | UP | 1 | 0 |
| 7Day | Intrinsic Pathway of Fibrin Clot Formation | 0.83438 | 0.37058 | 0.47296 | f12;f2;serpinc1 | 849.784833 | 156.627 | 85.9375 | 1262.29842 | 372.869706 | 816.971643 | DOWN | 0 | 1 |
| 7Day | VEGFA-VEGFR2 Pathway | 0.8279 | 0.26961 | 0.47491 | nckap1;pak2;rasa1;prkcz;kras;hsp90aa1;cdc42;ctnnb1;calm3;calm2;brk1 | 3454.26211 | 3468.74 | 54.5232 | 1846.95429 | 3559.80325 | 2027.96172 | UP | 0.636363636 | 0.363636364 |
| 90Day | The citric acid (TCA) cycle and respiratory electron transport | 0.24554 | 0.83993 | 0.47517 | ndufab1;ndufc2;sdha;etfdh;ndufaf3;ndufb9;pdk4;pdk1;suclg2;gstz1;atp5k | 3140.79345 | 3209.99 | 105.476 | 1841.10037 | 3749.80618 | 1710.82178 | DOWN | 0.272727273 | 0.727272727 |
| 90Day | RNA Polymerase I Transcription Initiation | 0.27037 | 0.87752 | 0.47531 | gatad2b;hdac2;cdk7 | 2157.934 | 3130.16 | 202.162 | 1693.75769 | 1207.98838 | 1704.99046 | UP | 1 | 0 |
| 90Day | Formation of the ternary complex, and subsequently, the 43S complex | 0.25368 | 0.88712 | 0.4755 | eif3m;rps27l;rps12 | 2578.52 | 2517.83 | 1662.63 | 947.693586 | 2378.76706 | 980.623942 | UP | 1 | 0 |

BMD analysis results for functional classification based on dose-responsive genes, using the Reactome database for gene sets in BMDExpress2.2 software.

| Study Day | Gene Set Name | Fisher's Exact Left P-Value | Fisher's Exact Right P-Value | Fisher's Exact Two Tail | Gene Symbols | BMD Mean | BMD Median | BMD Minimum | BMD Standard Deviation | BMD wMean | BMD wSD | Overall Direction | Percent Genes With Overall Direction Up | Percent Genes With Overall Direction Down |
|---|---|---|---|---|---|---|---|---|---|---|---|---|---|---|
| 90Day | Interleukin-3, Interleukin-5 and GM-CSF signaling | 0.25368 | 0.88712 | 0.4755 | ywhaz;vav1;sos1 | 3397.97933 | 4161.05 | 137.958 | 2953.36914 | 4245.68398 | 2762.84474 | DOWN | 0.333333333 | 0.666666667 |
| 28Day | DNA Repair | 0.2232 | 0.84452 | 0.47622 | ube2n;usp45;rmi1;ube2v2;pole3;hist1h4i;prpf19;ino80c;cenpx;polr2a;rad51d;rad51;polb;lig3;brca1;blm | 4090.84338 | 4527.73 | 692.086 | 1739.90034 | 4395.59369 | 1381.79209 | UP | 0.625 | 0.375 |
| 28Day | Neutrophil degranulation | 0.79216 | 0.26058 | 0.47625 | arhgap45;ndufc2;npc2;cmtm6;ormdl3;psmd6;serpinb1a;golga7;dynll1;hebp2;methig1;iqgap2;clec12a;tubb4b;tnfrsf1b;serpina1e;serpina1b;s100a11;rab18;pnp;pa2g4;pkp1;pfkl;mme;man2b1;lta4h;anpep;h2-q7;h2-d1;gstp1;gstp2;gpi1;gaa;ftl1;ctss;c3;atad3a;acly;qsox1;dnajc3 | 2977.4934 | 3122.575 | 160.43 | 1934.38527 | 2908.55852 | 2001.74707 | DOWN | 0.3 | 0.7 |
| 28Day | Golgi-to-ER retrograde transport | 0.22222 | 0.87673 | 0.47692 | dynll1;tubb4b;tubb2a;rab18;capza2;gbf1 | 4262.45333 | 4542.13 | 2359.45 | 1425.36828 | 4325.76478 | 1432.18749 | UP | 0.666666667 | 0.333333333 |
| 90Day | MAP kinase activation | 0.23778 | 0.89605 | 0.47695 | mapk14;ikbkg;btrc | 4226.74 | 4261.96 | 3265.56 | 944.062859 | 4326.22256 | 1102.6478 | DOWN | 0.333333333 | 0.666666667 |
| 90Day | Nuclear Envelope Breakdown | 0.23778 | 0.89605 | 0.47695 | nek6;nup153;sec13 | 3294.01 | 3442.78 | 2758.9 | 478.400366 | 3382.9906 | 363.640364 | UP | 1 | 0 |
| 90Day | Chondroitin sulfate/dermatan sulfate metabolism | 0.22267 | 0.90433 | 0.47961 | sdc4;hyal1;bgn | 1769.47833 | 630.216 | 144.869 | 2405.85336 | 2565.87271 | 2556.11563 | DOWN | 0 | 1 |
| 90Day | Nucleotide-binding domain, leucine rich repeat containing receptor (NLR) signaling pathways | 0.22267 | 0.90433 | 0.47961 | mapk14;txn1;ikbkg | 4223.68667 | 4261.96 | 3265.56 | 939.574827 | 3938.62375 | 1035.73316 | DOWN | 0.333333333 | 0.666666667 |
| 90Day | Signaling by FGFR1 | 0.22267 | 0.90433 | 0.47961 | sos1;gab1;fgf1 | 2087.929 | 242.429 | 126.428 | 3297.46971 | 3907.43024 | 3338.39856 | DOWN | 0 | 1 |
| 90Day | Arachidonic acid metabolism | 0.80291 | 0.30205 | 0.48018 | cyp4f16;gpx4;cyp2c54;cyp4a12a;pon3;ephx2;cyp4a12b;cyp2c38;cyp2c37;cyp1a2;cyp2c69 | 3044.3 | 3376.53 | 928.37 | 1324.45459 | 3281.65304 | 1143.95283 | CONFLICT | 0.545454545 | 0.454545455 |
| 28Day | Downstream TCR signaling | 0.82612 | 0.37826 | 0.48058 | ube2n;pdpk1;ikbkg | 3625.79267 | 5266.71 | 192.988 | 2973.85422 | 4348.16829 | 2537.13387 | DOWN | 0.333333333 | 0.666666667 |
| 28Day | FCERI mediated NF-kB activation | 0.82612 | 0.37826 | 0.48058 | ube2n;pdpk1;ikbkg | 3625.79267 | 5266.71 | 192.988 | 2973.85422 | 4348.16829 | 2537.13387 | DOWN | 0.333333333 | 0.666666667 |
| 7Day | Intracellular signaling by second messengers | 0.25612 | 0.81682 | 0.48106 | rraga;suz12;mapk3;uba52;ptpn11;pten;prkar2a;ppp2cb;il1rap;fgf1;csnk2b;cdkn1a;casp9;calm3;calm2;bmi1;xiap | 3548.93965 | 3627.04 | 131.024 | 1200.08345 | 3402.72598 | 1247.39608 | CONFLICT | 0.588235294 | 0.411764706 |
| 7Day | Regulation of TP53 Activity through Phosphorylation | 0.22554 | 0.90208 | 0.48367 | taf10;uba52;csnk2b | 3650.00667 | 3358.79 | 2829.67 | 998.326151 | 3713.93443 | 980.911573 | UP | 1 | 0 |
| 7Day | Formation of RNA Pol II elongation complex | 0.22554 | 0.90208 | 0.48367 | wdr61;polr2h;ccnk | 3340.86667 | 3952.2 | 2105.8 | 1069.61708 | 3683.32669 | 810.404723 | UP | 1 | 0 |
| 7Day | RNA Polymerase II Transcription Elongation | 0.22554 | 0.90208 | 0.48367 | wdr61;polr2h;ccnk | 3340.86667 | 3952.2 | 2105.8 | 1069.61708 | 3683.32669 | 810.404723 | UP | 1 | 0 |
| 28Day | Synthesis of DNA | 0.27232 | 0.8744 | 0.48541 | pole3;cdc6;cdc27 | 4151.206 | 5780.76 | 805.318 | 2897.94886 | 4893.04993 | 2396.93088 | UP | 1 | 0 |
| 7Day | Signaling by NTRK1 (TRKA) | 0.21349 | 0.90862 | 0.48662 | mapk3;ppp2cb;kras | 4195.33 | 4158.71 | 3627.04 | 587.456661 | 4099.43077 | 628.875162 | UP | 0.666666667 | 0.333333333 |
| 28Day | PI Metabolism | 0.24287 | 0.89147 | 0.48683 | pi4k2b;tnfaip8l1;pi4ka | 3825.40333 | 4173.55 | 2639.44 | 1055.85318 | 4197.62456 | 743.017577 | DOWN | 0.333333333 | 0.666666667 |
| 90Day | Keratan sulfate biosynthesis | 0.81839 | 0.39555 | 0.48685 | omd;st3gal3;lum | 4411.32667 | 4358.58 | 3651.14 | 787.885329 | 4239.33949 | 529.843763 | UP | 0.666666667 | 0.333333333 |
| 90Day | PI-3K cascade:FGFR4 | 0.81839 | 0.39555 | 0.48685 | klb;gab1;fgf1 | 1406.38233 | 242.429 | 126.428 | 2117.2807 | 2186.59517 | 2243.99506 | DOWN | 0 | 1 |
| 90Day | SHC-mediated cascade:FGFR4 | 0.81839 | 0.39555 | 0.48685 | klb;sos1;fgf1 | 3329.21633 | 3850.29 | 242.429 | 2862.05 | 4571.98571 | 2172.73633 | DOWN | 0 | 1 |
| 28Day | Signaling by MET | 0.23362 | 0.89668 | 0.48817 | ranbp9;hgs;fn1 | 4005.54667 | 3220.72 | 3156 | 1415.7787 | 3669.94431 | 1199.45955 | UP | 0.666666667 | 0.333333333 |
| 90Day | Regulation of PLK1 Activity at G2/M Transition | 0.25567 | 0.84934 | 0.48905 | haus7;dctn3;cntrl;tubb4b;cep76;hsp90aa1;btrc | 3497.21571 | 4266.18 | 426.32 | 1735.93382 | 4002.25491 | 1517.09734 | UP | 0.857142857 | 0.142857143 |
| 7Day | Interleukin-20 family signaling | 0.81508 | 0.3971 | 0.48981 | stat1;ptpn11;jak1 | 3700.28667 | 3629.67 | 3554.32 | 191.312992 | 3689.86935 | 200.012264 | UP | 1 | 0 |
| 7Day | Regulation of IFNA signaling | 0.81508 | 0.3971 | 0.48981 | stat1;ptpn11;jak1 | 3700.28667 | 3629.67 | 3554.32 | 191.312992 | 3689.86935 | 200.012264 | UP | 1 | 0 |
| 7Day | MAPK family signaling cascades | 0.23858 | 0.8294 | 0.49208 | ranbp9;kalrn;mapk3;pebp1;sept7;pak2;uba52;rasa1;ptpn11;ppp2cb;kras;jak1;gfra1;fgf1;cdc42;calm3;calm2;xpo1 | 3682.37111 | 3628.355 | 778.73 | 1160.35694 | 3754.56617 | 1087.58131 | UP | 0.666666667 | 0.333333333 |
| 28Day | Intrinsic Pathway for Apoptosis | 0.81211 | 0.39729 | 0.49256 | dynll1;sept4;bcl2l1 | 2718.02733 | 2151.36 | 211.182 | 2833.00772 | 3821.84553 | 2491.98211 | UP | 1 | 0 |
| 7Day | Apoptosis | 0.26269 | 0.84362 | 0.49302 | ywhaz;dsg1c;kpnb1;ctnnb1;casp9;xiap;dsp | 2684.62517 | 3025.45 | 54.5232 | 1875.07698 | 2538.12877 | 1960.56129 | DOWN | 0.285714286 | 0.714285714 |
| 7Day | RNA Polymerase I Transcription | 0.25264 | 0.85078 | 0.49338 | hist1h4h;hist1h2bc;hist2h2ac;mapk3;polr2h;ubtf;hist2h2aa1 | 3877.53857 | 3964.6 | 1976.31 | 1102.11348 | 3992.99121 | 990.713071 | CONFLICT | 0.571428571 | 0.428571429 |
| 90Day | Retinoid metabolism and transport | 0.81875 | 0.31223 | 0.49411 | apob;ttr;sdc4;rbp1;rdh11;apoe;apoc3 | 2947.38943 | 2528.1 | 175.96 | 2285.35174 | 3535.38245 | 2360.67997 | CONFLICT | 0.428571429 | 0.571428571 |
| 7Day | SUMO E3 ligases SUMOylate target proteins | 0.23894 | 0.84149 | 0.49508 | gm49336;rnf168;hist1h4h;hdac7;nop58;suz12;top2b;ncoa1;hnrnpc;bmi1;uhrf2;tpr | 3370.48792 | 3258.095 | 852.825 | 1076.86867 | 3176.03835 | 1053.06744 | UP | 0.916666667 | 0.083333333 |

BMD analysis results for functional classification based on dose-responsive genes, using the Reactome database for gene sets in BMDExpress2.2 software.

| Study Day | Gene Set Name | Fisher's Exact Left P-Value | Fisher's Exact Right P-Value | Fisher's Exact Two Tail | Gene Symbols | BMD Mean | BMD Median | BMD Minimum | BMD Standard Deviation | BMD wMean | BMD wSD | Overall Direction | Percent Genes With Overall Direction Up | Percent Genes With Overall Direction Down |
|---|---|---|---|---|---|---|---|---|---|---|---|---|---|---|
| 7Day | Cargo recognition for clathrin-mediated endocytosis | 0.23337 | 0.86432 | 0.49543 | ubqln1;slc2a8;apob;picalm;uba52;ldlr;igf2r | 3609.88 | 3459.74 | 1999.21 | 993.723225 | 3580.2941 | 733.778551 | CONFLICT | 0.571428571 | 0.428571429 |
| 28Day | Separation of Sister Chromatids | 0.26035 | 0.8444 | 0.49829 | zwilch;dynll1;cenpt;tubb4b;tubb2a;cdc27;rad21 | 4014.02286 | 3567.21 | 2359.45 | 1333.84151 | 4025.91847 | 1335.86752 | UP | 1 | 0 |
| 7Day | GLI3 is processed to GLI3R by the proteasome | 0.86449 | 0.49992 | 0.49992 | uba52 | 4761.56 | 4761.56 | 4761.56 | | 4761.56 | | UP | 1 | 0 |
| 7Day | Beta-oxidation of pristanoyl-CoA | 0.86449 | 0.49992 | 0.49992 | hsd17b4 | 185.683 | 185.683 | 185.683 | | 185.683 | | DOWN | 0 | 1 |
| 7Day | Pyrimidine catabolism | 0.86449 | 0.49992 | 0.49992 | dpys | 395.538 | 395.538 | 395.538 | | 395.538 | | DOWN | 0 | 1 |
| 7Day | Synthesis of PIPs at the late endosome membrane | 0.86449 | 0.49992 | 0.49992 | mtmr7 | 4966.2 | 4966.2 | 4966.2 | | 4966.2 | | UP | 1 | 0 |
| 7Day | Pre-NOTCH Expression and Processing | 0.86449 | 0.49992 | 0.49992 | prkci | 3409.24 | 3409.24 | 3409.24 | | 3409.24 | | UP | 1 | 0 |
| 7Day | Frs2-mediated activation | 0.86449 | 0.49992 | 0.49992 | mapk3 | 4800.24 | 4800.24 | 4800.24 | | 4800.24 | | DOWN | 0 | 1 |
| 7Day | Acyl chain remodeling of DAG and TAG | 0.86449 | 0.49992 | 0.49992 | dgat2 | 623.511 | 623.511 | 623.511 | | 623.511 | | DOWN | 0 | 1 |
| 7Day | Regulation of gene expression by Hypoxia-inducible Factor | 0.86449 | 0.49992 | 0.49992 | arnt | 3473.87 | 3473.87 | 3473.87 | | 3473.87 | | DOWN | 0 | 1 |
| 7Day | Interleukin-36 pathway | 0.86449 | 0.49992 | 0.49992 | il1rap | 131.024 | 131.024 | 131.024 | | 131.024 | | DOWN | 0 | 1 |
| 7Day | RUNX3 regulates p14-ARF | 0.86449 | 0.49992 | 0.49992 | kras | 4158.71 | 4158.71 | 4158.71 | | 4158.71 | | UP | 1 | 0 |
| 7Day | PTK6 Regulates RTKs and Their Effectors AKT1 and DOK1 | 0.86449 | 0.49992 | 0.49992 | uba52 | 4761.56 | 4761.56 | 4761.56 | | 4761.56 | | UP | 1 | 0 |
| 7Day | Synthesis of Ketone Bodies | 0.86449 | 0.49992 | 0.49992 | hmgcs2 | 3736.33 | 3736.33 | 3736.33 | | 3736.33 | | UP | 1 | 0 |
| 7Day | DEx/H-box helicases activate type I IFN and inflammatory cytokines production | 0.86449 | 0.49992 | 0.49992 | dhx9 | 3100.35 | 3100.35 | 3100.35 | | 3100.35 | | UP | 1 | 0 |
| 7Day | FGFR3b ligand binding and activation | 0.86449 | 0.49992 | 0.49992 | fgf1 | 2647.76 | 2647.76 | 2647.76 | | 2647.76 | | DOWN | 0 | 1 |
| 28Day | Mitotic Anaphase | 0.23911 | 0.85949 | 0.5 | zwilch;dynll1;cenpt;tubb4b;tubb2a;cdc27;rad21 | 4014.02286 | 3567.21 | 2359.45 | 1333.84151 | 4025.91847 | 1335.86752 | UP | 1 | 0 |
| 28Day | Mitotic Metaphase and Anaphase | 0.23231 | 0.86426 | 0.50102 | zwilch;dynll1;cenpt;tubb4b;tubb2a;cdc27;rad21 | 4014.02286 | 3567.21 | 2359.45 | 1333.84151 | 4025.91847 | 1335.86752 | UP | 1 | 0 |
| 90Day | Regulation of RAS by GAPs | 0.29749 | 0.91901 | 0.50319 | rasa1 | 2133.64 | 2133.64 | 2133.64 | | 2133.64 | | UP | 1 | 0 |
| 90Day | Acyl chain remodelling of PS | 0.29749 | 0.91901 | 0.50319 | osbpl10 | 3327.72 | 3327.72 | 3327.72 | | 3327.72 | | UP | 1 | 0 |
| 90Day | PCNA-Dependent Long Patch Base Excision Repair | 0.29749 | 0.91901 | 0.50319 | pole4 | 5853.8 | 5853.8 | 5853.8 | | 5853.8 | | DOWN | 0 | 1 |
| 90Day | IKK complex recruitment mediated by RIP1 | 0.29749 | 0.91901 | 0.50319 | ikbkg | 3265.56 | 3265.56 | 3265.56 | | 3265.56 | | UP | 1 | 0 |
| 90Day | APC/C:Cdc20 mediated degradation of Cyclin B | 0.29749 | 0.91901 | 0.50319 | anapc10 | 4390.47 | 4390.47 | 4390.47 | | 4390.47 | | UP | 1 | 0 |
| 90Day | Nuclear Events (kinase and transcription factor activation) | 0.27306 | 0.92816 | 0.50371 | mapk14 | 4261.96 | 4261.96 | 4261.96 | | 4261.96 | | DOWN | 0 | 1 |
| 90Day | Telomere C-strand (Lagging Strand) Synthesis | 0.27306 | 0.92816 | 0.50371 | pole4 | 5853.8 | 5853.8 | 5853.8 | | 5853.8 | | DOWN | 0 | 1 |
| 90Day | Adrenaline,noradrenaline inhibits insulin secretion | 0.27306 | 0.92816 | 0.50371 | gng11 | 4854.24 | 4854.24 | 4854.24 | | 4854.24 | | UP | 1 | 0 |
| 90Day | Thromboxane signalling through TP receptor | 0.27306 | 0.92816 | 0.50371 | gng11 | 4854.24 | 4854.24 | 4854.24 | | 4854.24 | | UP | 1 | 0 |
| 90Day | Glycolysis | 0.27306 | 0.92816 | 0.50371 | pfkfb3 | 4970.65 | 4970.65 | 4970.65 | | 4970.65 | | UP | 1 | 0 |
| 90Day | Mitochondrial biogenesis | 0.27306 | 0.92816 | 0.50371 | atp5k | 135.802 | 135.802 | 135.802 | | 135.802 | | DOWN | 0 | 1 |
| 28Day | Gamma carboxylation, hypusine formation and arylsulfatase activation | 0.79775 | 0.41617 | 0.50488 | proc;f7;f2 | 2700.24 | 2170.26 | 1340.75 | 1688.07416 | 1850.85737 | 1335.69078 | DOWN | 0 | 1 |
| 7Day | G2/M DNA damage checkpoint | 0.7996 | 0.33507 | 0.50541 | ube2n;ube2v2;rnf168;hist1h4h;babam1;hist1h2bc;ywhaz | 3316.97857 | 3418.4 | 2423.08 | 588.946245 | 3285.99154 | 576.827592 | UP | 0.857142857 | 0.142857143 |
| 90Day | Signaling by ROBO receptors | 0.25036 | 0.93627 | 0.50663 | myo9b | 5309.89 | 5309.89 | 5309.89 | | 5309.89 | | DOWN | 0 | 1 |
| 90Day | Generation of second messenger molecules | 0.25036 | 0.93627 | 0.50663 | h2-aa | 3001.17 | 3001.17 | 3001.17 | | 3001.17 | | DOWN | 0 | 1 |
| 90Day | Role of phospholipids in phagocytosis | 0.25036 | 0.93627 | 0.50663 | fcgr2b | 3055.31 | 3055.31 | 3055.31 | | 3055.31 | | DOWN | 0 | 1 |
| 90Day | SMAD2/SMAD3:SMAD4 heterotrimer regulates transcription | 0.25036 | 0.93627 | 0.50663 | ccnc | 4045.2 | 4045.2 | 4045.2 | | 4045.2 | | UP | 1 | 0 |
| 90Day | Cobalamin (Cbl, vitamin B12) transport and metabolism | 0.25036 | 0.93627 | 0.50663 | mut | 1339.27 | 1339.27 | 1339.27 | | 1339.27 | | DOWN | 0 | 1 |
| 90Day | Cyclin A/B1/B2 associated events during G2/M transition | 0.25036 | 0.93627 | 0.50663 | cdk7 | 3130.16 | 3130.16 | 3130.16 | | 3130.16 | | UP | 1 | 0 |

BMD analysis results for functional classification based on dose-responsive genes, using the Reactome database for gene sets in BMDExpress2.2 software.

| Study Day | Gene Set Name | Fisher's Exact Left P-Value | Fisher's Exact Right P-Value | Fisher's Exact Two Tail | Gene Symbols | BMD Mean | BMD Median | BMD Minimum | BMD Standard Deviation | BMD wMean | BMD wSD | Overall Direction | Percent Genes With Overall Direction Up | Percent Genes With Overall Direction Down |
|---|---|---|---|---|---|---|---|---|---|---|---|---|---|---|
| 90Day | HSF1-dependent transactivation | 0.25036 | 0.93627 | 0.50663 | hsp90aa1 | 426.32 | 426.32 | 426.32 |  | 426.32 |  | UP | 1 | 0 |
| 90Day | APC-Cdc20 mediated degradation of Nek2A | 0.25036 | 0.93627 | 0.50663 | anapc10 | 4390.47 | 4390.47 | 4390.47 |  | 4390.47 |  | UP | 1 | 0 |
| 90Day | Transcriptional Regulation by E2F6 | 0.25036 | 0.93627 | 0.50663 | pcgf6 | 2798.08 | 2798.08 | 2798.08 |  | 2798.08 |  | UP | 1 | 0 |
| 7Day | CDO in myogenesis | 0.79511 | 0.42331 | 0.50726 | cdc42;ctnnb1;abl1 | 2672.8244 | 3368.05 | 54.5232 | 2349.15512 | 2310.38278 | 2623.74558 | DOWN | 0.333333333 | 0.666666667 |
| 7Day | Myogenesis | 0.79511 | 0.42331 | 0.50726 | cdc42;ctnnb1;abl1 | 2672.8244 | 3368.05 | 54.5232 | 2349.15512 | 2310.38278 | 2623.74558 | DOWN | 0.333333333 | 0.666666667 |
| 7Day | FRS-mediated FGFR2 signaling | 0.79511 | 0.42331 | 0.50726 | ptpn11;kras;fgf1 | 3478.71333 | 3629.67 | 2647.76 | 766.702949 | 3262.18888 | 788.939216 | UP | 0.666666667 | 0.333333333 |
| 7Day | Carboxyterminal post-translational modifications of tubulin | 0.79511 | 0.42331 | 0.50726 | tubb4b;tubb2a;tuba4a | 1609.852 | 1815.66 | 919.856 | 613.550908 | 1582.39232 | 663.092821 | UP | 1 | 0 |
| 7Day | CDK-mediated phosphorylation and removal of Cdc6 | 0.79511 | 0.42331 | 0.50726 | uba52;cdc27;ccne2 | 4410.11 | 4598.19 | 3870.58 | 474.333116 | 4498.87719 | 394.432252 | UP | 1 | 0 |
| 7Day | Downstream signaling of activated FGFR3 | 0.79511 | 0.42331 | 0.50726 | ptpn11;kras;fgf1 | 3478.71333 | 3629.67 | 2647.76 | 766.702949 | 3262.18888 | 788.939216 | UP | 0.666666667 | 0.333333333 |
| 7Day | Glycogen metabolism | 0.79511 | 0.42331 | 0.50726 | uba52;calm3;calm2 | 4242.81333 | 4761.56 | 3050.32 | 1035.63339 | 3855.87886 | 1087.62143 | UP | 0.666666667 | 0.333333333 |
| 7Day | Cholesterol biosynthesis | 0.79511 | 0.42331 | 0.50726 | idi1;ebp;acat2 | 2228.13533 | 2966.55 | 41.196 | 1926.93845 | 1932.68892 | 2106.7444 | DOWN | 0.333333333 | 0.666666667 |
| 7Day | Formation of the beta-catenin:TCF transactivating complex | 0.28225 | 0.92398 | 0.50771 | ctnnb1 | 54.5232 | 54.5232 | 54.5232 |  | 54.5232 |  | DOWN | 0 | 1 |
| 7Day | Interleukin receptor SHC signaling | 0.28225 | 0.92398 | 0.50771 | jak1 | 3554.32 | 3554.32 | 3554.32 |  | 3554.32 |  | UP | 1 | 0 |
| 7Day | Netrin-1 signaling | 0.28225 | 0.92398 | 0.50771 | cdc42 | 4595.9 | 4595.9 | 4595.9 |  | 4595.9 |  | UP | 1 | 0 |
| 7Day | Digestion | 0.28225 | 0.92398 | 0.50771 | mgam | 132.859 | 132.859 | 132.859 |  | 132.859 |  | DOWN | 0 | 1 |
| 7Day | Trafficking of AMPA receptors | 0.28225 | 0.92398 | 0.50771 | gria3 | 3853.21 | 3853.21 | 3853.21 |  | 3853.21 |  | UP | 1 | 0 |
| 7Day | Glutamate binding, activation of AMPA receptors and synaptic plasticity | 0.28225 | 0.92398 | 0.50771 | gria3 | 3853.21 | 3853.21 | 3853.21 |  | 3853.21 |  | UP | 1 | 0 |
| 7Day | Resolution of D-loop Structures through Synthesis-Dependent Strand Annealing (SDSA) | 0.28225 | 0.92398 | 0.50771 | rad51ap1 | 3877.33 | 3877.33 | 3877.33 |  | 3877.33 |  | UP | 1 | 0 |
| 90Day | Metabolism of fat-soluble vitamins | 0.7888 | 0.35024 | 0.50849 | apob;ttr;sdc4;rbp1;rdh11;apoe;apoc3 | 2947.38943 | 2528.1 | 175.96 | 2285.35174 | 3535.38245 | 2360.67997 | CONFLICT | 0.428571429 | 0.571428571 |
| 90Day | Bile acid and bile salt metabolism | 0.7888 | 0.35024 | 0.50849 | osbpl3;cyp39a1;slc27a5;slc27a2;slc10a1;amacr;osbpl9 | 3307.29714 | 3419.78 | 263.79 | 1622.33452 | 3906.606 | 1438.56267 | DOWN | 0.142857143 | 0.857142857 |
| 28Day | AKT phosphorylates targets in the cytosol | 0.8531 | 0.5091 | 0.5091 | mdm2 | 2266.61 | 2266.61 | 2266.61 |  | 2266.61 |  | UP | 1 | 0 |
| 28Day | CS/DS degradation | 0.8531 | 0.5091 | 0.5091 | hyal1 | 2376.85 | 2376.85 | 2376.85 |  | 2376.85 |  | DOWN | 0 | 1 |
| 28Day | p75NTR regulates axonogenesis | 0.8531 | 0.5091 | 0.5091 | arhgdia | 4971.84 | 4971.84 | 4971.84 |  | 4971.84 |  | UP | 1 | 0 |
| 28Day | HDR through MMEJ (alt-NHEJ) | 0.8531 | 0.5091 | 0.5091 | lig3 | 5391.42 | 5391.42 | 5391.42 |  | 5391.42 |  | DOWN | 0 | 1 |
| 28Day | PI3K events in ERBB4 signaling | 0.8531 | 0.5091 | 0.5091 | hbegf | 919.738 | 919.738 | 919.738 |  | 919.738 |  | UP | 1 | 0 |
| 28Day | HDL remodeling | 0.8531 | 0.5091 | 0.5091 | apoe | 3212.68 | 3212.68 | 3212.68 |  | 3212.68 |  | DOWN | 0 | 1 |
| 28Day | Interleukin-12 signaling | 0.8531 | 0.5091 | 0.5091 | p4hb | 5730.92 | 5730.92 | 5730.92 |  | 5730.92 |  | DOWN | 0 | 1 |
| 28Day | Synthesis of pyrophosphates in the cytosol | 0.8531 | 0.5091 | 0.5091 | ippk | 4371.1 | 4371.1 | 4371.1 |  | 4371.1 |  | UP | 1 | 0 |
| 28Day | Cohesin Loading onto Chromatin | 0.8531 | 0.5091 | 0.5091 | rad21 | 4137.27 | 4137.27 | 4137.27 |  | 4137.27 |  | UP | 1 | 0 |
| 28Day | Adenylate cyclase activating pathway | 0.8531 | 0.5091 | 0.5091 | adcy9 | 4220.6 | 4220.6 | 4220.6 |  | 4220.6 |  | DOWN | 0 | 1 |
| 28Day | Vitamin D (calciferol) metabolism | 0.8531 | 0.5091 | 0.5091 | gc | 431.226 | 431.226 | 431.226 |  | 431.226 |  | DOWN | 0 | 1 |
| 28Day | Regulation by c-FLIP | 0.8531 | 0.5091 | 0.5091 | tnfrsf10b | 4040.75 | 4040.75 | 4040.75 |  | 4040.75 |  | UP | 1 | 0 |
| 28Day | CASP8 activity is inhibited | 0.8531 | 0.5091 | 0.5091 | tnfrsf10b | 4040.75 | 4040.75 | 4040.75 |  | 4040.75 |  | UP | 1 | 0 |
| 28Day | Dimerization of procaspase-8 | 0.8531 | 0.5091 | 0.5091 | tnfrsf10b | 4040.75 | 4040.75 | 4040.75 |  | 4040.75 |  | UP | 1 | 0 |
| 7Day | Insulin receptor recycling | 0.26279 | 0.93116 | 0.5093 | atp6v1e1 | 3782.92 | 3782.92 | 3782.92 |  | 3782.92 |  | UP | 1 | 0 |
| 7Day | G-protein activation | 0.26279 | 0.93116 | 0.5093 | gnai3 | 794.2 | 794.2 | 794.2 |  | 794.2 |  | UP | 1 | 0 |
| 7Day | RNA Pol II CTD phosphorylation and interaction with CE | 0.26279 | 0.93116 | 0.5093 | polr2h | 3964.6 | 3964.6 | 3964.6 |  | 3964.6 |  | UP | 1 | 0 |
| 7Day | PTEN Regulation | 0.78694 | 0.35088 | 0.51165 | rraga;suz12;uba52;pten;csnk2b;bmi1;xiap | 3856.5 | 3225.73 | 2829.67 | 946.764064 | 3870.44666 | 926.251147 | UP | 0.857142857 | 0.142857143 |
| 7Day | Regulation of actin dynamics for phagocytic cup formation | 0.78694 | 0.35088 | 0.51165 | nckap1;mapk3;myh9;hsp90aa1;cdc42;abl1;brk1 | 3145.07714 | 3368.05 | 1005.61 | 1343.65458 | 3031.74508 | 1474.85132 | CONFLICT | 0.571428571 | 0.428571429 |
| 7Day | RAB geranylgeranylation | 0.78694 | 0.35088 | 0.51165 | rab9;rab11a;rab25;rab6a;rab18;rab10;rab1a | 3525.11714 | 3553.68 | 1046.66 | 1329.4585 | 3611.40244 | 1330.92078 | UP | 0.857142857 | 0.142857143 |
| 90Day | G beta:gamma signalling through PI3Kgamma | 0.22929 | 0.94347 | 0.51173 | gng11 | 4854.24 | 4854.24 | 4854.24 |  | 4854.24 |  | UP | 1 | 0 |
| 90Day | Surfactant metabolism | 0.22929 | 0.94347 | 0.51173 | ctsh | 1857.39 | 1857.39 | 1857.39 |  | 1857.39 |  | DOWN | 0 | 1 |

BMD analysis results for functional classification based on dose-responsive genes, using the Reactome database for gene sets in BMDExpress2.2 software.

| Study Day | Gene Set Name | Fisher's Exact Left P-Value | Fisher's Exact Right P-Value | Fisher's Exact Two Tail | Gene Symbols | BMD Mean | BMD Median | BMD Minimum | BMD Standard Deviation | BMD wMean | BMD wSD | Overall Direction | Percent Genes With Overall Direction Up | Percent Genes With Overall Direction Down |
|---|---|---|---|---|---|---|---|---|---|---|---|---|---|---|
| 90Day | Resolution of AP sites via the multiple-nucleotide patch replacement pathway | 0.22929 | 0.94347 | 0.51173 | pole4 | 5853.8 | 5853.8 | 5853.8 | | 5853.8 | | DOWN | 0 | 1 |
| 90Day | Telomere Maintenance | 0.22929 | 0.94347 | 0.51173 | pole4 | 5853.8 | 5853.8 | 5853.8 | | 5853.8 | | DOWN | 0 | 1 |
| 90Day | Extension of Telomeres | 0.22929 | 0.94347 | 0.51173 | pole4 | 5853.8 | 5853.8 | 5853.8 | | 5853.8 | | DOWN | 0 | 1 |
| 90Day | DNA strand elongation | 0.22929 | 0.94347 | 0.51173 | gins1 | 1127.6 | 1127.6 | 1127.6 | | 1127.6 | | UP | 1 | 0 |
| 90Day | FGFR2 alternative splicing | 0.22929 | 0.94347 | 0.51173 | hnrnpf | 3142.57 | 3142.57 | 3142.57 | | 3142.57 | | DOWN | 0 | 1 |
| 90Day | Orc1 removal from chromatin | 0.22929 | 0.94347 | 0.51173 | orc6 | 4168.34 | 4168.34 | 4168.34 | | 4168.34 | | UP | 1 | 0 |
| 90Day | FGFR1b ligand binding and activation | 0.85999 | 0.51204 | 0.51204 | fgf1 | 242.429 | 242.429 | 242.429 | | 242.429 | | DOWN | 0 | 1 |
| 90Day | RHO GTPases Activate Rhotekin and Rhophilins | 0.85999 | 0.51204 | 0.51204 | rtkn | 3994.23 | 3994.23 | 3994.23 | | 3994.23 | | UP | 1 | 0 |
| 90Day | Glucocorticoid biosynthesis | 0.85999 | 0.51204 | 0.51204 | hsd11b1 | 2402.05 | 2402.05 | 2402.05 | | 2402.05 | | DOWN | 0 | 1 |
| 90Day | MET Receptor Activation | 0.85999 | 0.51204 | 0.51204 | hgfac | 1910.71 | 1910.71 | 1910.71 | | 1910.71 | | DOWN | 0 | 1 |
| 90Day | MET activates PI3K/AKT signaling | 0.85999 | 0.51204 | 0.51204 | gab1 | 126.428 | 126.428 | 126.428 | | 126.428 | | DOWN | 0 | 1 |
| 90Day | Attachment of GPI anchor to uPAR | 0.85999 | 0.51204 | 0.51204 | plaur | 1622.23 | 1622.23 | 1622.23 | | 1622.23 | | DOWN | 0 | 1 |
| 90Day | Synthesis of 5-eicosatetraenoic acids | 0.85999 | 0.51204 | 0.51204 | pon3 | 4320.2 | 4320.2 | 4320.2 | | 4320.2 | | UP | 1 | 0 |
| 90Day | Lipid particle organization | 0.85999 | 0.51204 | 0.51204 | fitm2 | 3161.07 | 3161.07 | 3161.07 | | 3161.07 | | UP | 1 | 0 |
| 90Day | mRNA Editing | 0.85999 | 0.51204 | 0.51204 | adar | 5667.94 | 5667.94 | 5667.94 | | 5667.94 | | UP | 1 | 0 |
| 90Day | activated TAK1 mediates p38 MAPK activation | 0.85999 | 0.51204 | 0.51204 | mapk14 | 4261.96 | 4261.96 | 4261.96 | | 4261.96 | | DOWN | 0 | 1 |
| 90Day | Release of Hh-Np from the secreting cell | 0.85999 | 0.51204 | 0.51204 | notum | 4035.02 | 4035.02 | 4035.02 | | 4035.02 | | DOWN | 0 | 1 |
| 90Day | PTK6 promotes HIF1A stabilization | 0.85999 | 0.51204 | 0.51204 | gpnmb | 4552.68 | 4552.68 | 4552.68 | | 4552.68 | | UP | 1 | 0 |
| 90Day | CaMK IV-mediated phosphorylation of CREB | 0.85999 | 0.51204 | 0.51204 | camkk2 | 98.0082 | 98.0082 | 98.0082 | | 98.0082 | | DOWN | 0 | 1 |
| 90Day | CREB1 phosphorylation through the activation of CaMKII/CaMKK/CaMKIV cascasde | 0.85999 | 0.51204 | 0.51204 | camkk2 | 98.0082 | 98.0082 | 98.0082 | | 98.0082 | | DOWN | 0 | 1 |
| 90Day | Activation of RAC1 downstream of NMDARs | 0.85999 | 0.51204 | 0.51204 | camkk2 | 98.0082 | 98.0082 | 98.0082 | | 98.0082 | | DOWN | 0 | 1 |
| 90Day | Transport and synthesis of PAPS | 0.85999 | 0.51204 | 0.51204 | slc26a2 | 3962.48 | 3962.48 | 3962.48 | | 3962.48 | | DOWN | 0 | 1 |
| 90Day | Protein repair | 0.85999 | 0.51204 | 0.51204 | txn1 | 5143.54 | 5143.54 | 5143.54 | | 5143.54 | | DOWN | 0 | 1 |
| 90Day | Vitamin B2 (riboflavin) metabolism | 0.85999 | 0.51204 | 0.51204 | slc52a3 | 5271 | 5271 | 5271 | | 5271 | | UP | 1 | 0 |
| 90Day | SHC-related events triggered by IGF1R | 0.85999 | 0.51204 | 0.51204 | sos1 | 5894.93 | 5894.93 | 5894.93 | | 5894.93 | | DOWN | 0 | 1 |
| 90Day | Synthesis of 12-eicosatetraenoic acid derivatives | 0.85999 | 0.51204 | 0.51204 | gpx4 | 2353.96 | 2353.96 | 2353.96 | | 2353.96 | | UP | 1 | 0 |
| 90Day | Regulation of PTEN localization | 0.85999 | 0.51204 | 0.51204 | pml | 3603.58 | 3603.58 | 3603.58 | | 3603.58 | | DOWN | 0 | 1 |
| 90Day | IRS activation | 0.85999 | 0.51204 | 0.51204 | irs2 | 74.8133 | 74.8133 | 74.8133 | | 74.8133 | | DOWN | 0 | 1 |
| 90Day | Assembly of the ORC complex at the origin of replication | 0.85999 | 0.51204 | 0.51204 | orc6 | 4168.34 | 4168.34 | 4168.34 | | 4168.34 | | UP | 1 | 0 |
| 7Day | Gluconeogenesis | 0.24448 | 0.93767 | 0.51246 | pgam1 | 4274.34 | 4274.34 | 4274.34 | | 4274.34 | | UP | 1 | 0 |
| 7Day | RNA Polymerase III Transcription Initiation From Type 3 Promoter | 0.24448 | 0.93767 | 0.51246 | polr2h | 3964.6 | 3964.6 | 3964.6 | | 3964.6 | | UP | 1 | 0 |
| 28Day | SUMOylation of transcription cofactors | 0.29651 | 0.9174 | 0.51344 | bmi1 | 3918.46 | 3918.46 | 3918.46 | | 3918.46 | | UP | 1 | 0 |
| 28Day | RUNX1 interacts with co-factors whose precise effect on RUNX1 targets is not known | 0.29651 | 0.9174 | 0.51344 | bmi1 | 3918.46 | 3918.46 | 3918.46 | | 3918.46 | | UP | 1 | 0 |
| 28Day | DNA Damage Recognition in GG-NER | 0.2818 | 0.92309 | 0.51366 | ino80c | 5465.53 | 5465.53 | 5465.53 | | 5465.53 | | DOWN | 0 | 1 |
| 28Day | O-glycosylation of TSR domain-containing proteins | 0.2677 | 0.92839 | 0.51475 | sbspon | 5312.69 | 5312.69 | 5312.69 | | 5312.69 | | UP | 1 | 0 |
| 28Day | Cyclin D associated events in G1 | 0.2677 | 0.92839 | 0.51475 | tfdp1 | 5708.4 | 5708.4 | 5708.4 | | 5708.4 | | UP | 1 | 0 |
| 28Day | G1 Phase | 0.2677 | 0.92839 | 0.51475 | tfdp1 | 5708.4 | 5708.4 | 5708.4 | | 5708.4 | | UP | 1 | 0 |
| 28Day | EPHB-mediated forward signaling | 0.2677 | 0.92839 | 0.51475 | cdc42 | 2463.49 | 2463.49 | 2463.49 | | 2463.49 | | UP | 1 | 0 |
| 28Day | Translesion synthesis by Y family DNA polymerases bypasses lesions on DNA template | 0.2677 | 0.92839 | 0.51475 | pole3 | 805.318 | 805.318 | 805.318 | | 805.318 | | UP | 1 | 0 |
| 28Day | Signaling by FGFR3 | 0.2677 | 0.92839 | 0.51475 | fgf1 | 1467.57 | 1467.57 | 1467.57 | | 1467.57 | | DOWN | 0 | 1 |
| 28Day | Activation of ATR in response to replication stress | 0.2677 | 0.92839 | 0.51475 | cdc6 | 5867.54 | 5867.54 | 5867.54 | | 5867.54 | | UP | 1 | 0 |
| 90Day | Semaphorin interactions | 0.28799 | 0.85255 | 0.51484 | tln1;rock2;rock1;hsp90aa1 | 2260.363 | 2150.215 | 262.092 | 2227.33171 | 2108.65317 | 2313.26435 | UP | 0.75 | 0.25 |

BMD analysis results for functional classification based on dose-responsive genes, using the Reactome database for gene sets in BMDExpress2.2 software.

| Study Day | Gene Set Name | Fisher's Exact Left P-Value | Fisher's Exact Right P-Value | Fisher's Exact Two Tail | Gene Symbols | BMD Mean | BMD Median | BMD Minimum | BMD Standard Deviation | BMD wMean | BMD wSD | Overall Direction | Percent Genes With Overall Direction Up | Percent Genes With Overall Direction Down |
|---|---|---|---|---|---|---|---|---|---|---|---|---|---|---|
| 28Day | GABA B receptor activation | 0.25421 | 0.93333 | 0.51666 | adcy9 | 4220.6 | 4220.6 | 4220.6 |  | 4220.6 |  | DOWN | 0 | 1 |
| 28Day | Activation of GABAB receptors | 0.25421 | 0.93333 | 0.51666 | adcy9 | 4220.6 | 4220.6 | 4220.6 |  | 4220.6 |  | DOWN | 0 | 1 |
| 28Day | Signaling by FGFR4 | 0.25421 | 0.93333 | 0.51666 | fgf1 | 1467.57 | 1467.57 | 1467.57 |  | 1467.57 |  | DOWN | 0 | 1 |
| 7Day | Recognition of DNA damage by PCNA-containing replication complex | 0.22728 | 0.94356 | 0.51705 | uba52 | 4761.56 | 4761.56 | 4761.56 |  | 4761.56 |  | UP | 1 | 0 |
| 7Day | Interleukin-7 signaling | 0.22728 | 0.94356 | 0.51705 | jak1 | 3554.32 | 3554.32 | 3554.32 |  | 3554.32 |  | UP | 1 | 0 |
| 7Day | mRNA Capping | 0.22728 | 0.94356 | 0.51705 | polr2h | 3964.6 | 3964.6 | 3964.6 |  | 3964.6 |  | UP | 1 | 0 |
| 90Day | NoRC negatively regulates rRNA expression | 0.24231 | 0.88129 | 0.51835 | hist1h4h;hist1h4i;hist1h3c;h2afx | 3214.00725 | 3979.26 | 811.859 | 1602.37406 | 2298.31583 | 1843.92338 | CONFLICT | 0.5 | 0.5 |
| 90Day | Regulation of TP53 Activity through Phosphorylation | 0.24231 | 0.88129 | 0.51835 | trp53inp1;mapk14;pin1;mdm2 | 3753.1775 | 3898.52 | 2267.97 | 1145.88415 | 3622.70918 | 1133.0118 | UP | 0.75 | 0.25 |
| 7Day | Costimulation by the CD28 family | 0.77397 | 0.36677 | 0.51842 | yes1;pak2;ptpn11;ppp2cb;h2-ab1;h2-aa;cdc42 | 3219.45429 | 3627.04 | 1863.06 | 1007.7416 | 3600.30516 | 855.55687 | UP | 0.714285714 | 0.285714286 |
| 90Day | CDO in myogenesis | 0.85685 | 0.30897 | 0.51876 | mapk14;mef2a;cdc42;ctnnb1 | 3134.22675 | 4059.23 | 156.487 | 1987.58858 | 2980.93174 | 2048.77964 | DOWN | 0.25 | 0.75 |
| 90Day | Myogenesis | 0.85685 | 0.30897 | 0.51876 | mapk14;mef2a;cdc42;ctnnb1 | 3134.22675 | 4059.23 | 156.487 | 1987.58858 | 2980.93174 | 2048.77964 | DOWN | 0.25 | 0.75 |
| 90Day | Carboxyterminal post-translational modifications of tubulin | 0.85685 | 0.30897 | 0.51876 | tubb6;tubb4b;tubb2a;tuba1b | 1558.67025 | 1751.94 | 779.791 | 528.216289 | 1311.72381 | 614.22224 | UP | 0.75 | 0.25 |
| 7Day | Regulation of HSF1-mediated heat shock response | 0.27969 | 0.85704 | 0.51897 | gm49336;dnajb6;hsph1;tpr | 2911.057 | 3210.97 | 589.118 | 1774.90285 | 2760.63037 | 1688.7125 | UP | 1 | 0 |
| 28Day | mTOR signalling | 0.2413 | 0.93792 | 0.51932 | stradb | 5007.07 | 5007.07 | 5007.07 |  | 5007.07 |  | DOWN | 0 | 1 |
| 28Day | Dual Incision in GG-NER | 0.2413 | 0.93792 | 0.51932 | pole3 | 805.318 | 805.318 | 805.318 |  | 805.318 |  | UP | 1 | 0 |
| 28Day | Deactivation of the beta-catenin transactivating complex | 0.2413 | 0.93792 | 0.51932 | pygo2 | 3936.43 | 3936.43 | 3936.43 |  | 3936.43 |  | DOWN | 0 | 1 |
| 7Day | SUMOylation of DNA damage response and repair proteins | 0.26678 | 0.86529 | 0.51956 | gm49336;rnf168;hdac7;tpr | 3653.6175 | 3723.15 | 2535 | 955.277026 | 3456.68876 | 933.956694 | UP | 1 | 0 |
| 28Day | Toll Like Receptor 9 (TLR9) Cascade | 0.77285 | 0.36599 | 0.52167 | ube2n;map2k4;eea1;mapkapk2;ly96;ikbkg;app | 4767.72571 | 5266.71 | 2616.5 | 1022.82226 | 4879.47107 | 988.613786 | CONFLICT | 0.428571429 | 0.571428571 |
| 28Day | MAP2K and MAPK activation | 0.22896 | 0.9422 | 0.5227 | fn1 | 3156 | 3156 | 3156 |  | 3156 |  | DOWN | 0 | 1 |
| 28Day | MET promotes cell motility | 0.22896 | 0.9422 | 0.5227 | fn1 | 3156 | 3156 | 3156 |  | 3156 |  | DOWN | 0 | 1 |
| 7Day | Interleukin-1 family signaling | 0.24227 | 0.88058 | 0.52272 | ube2n;uba52;il1rap;btrc | 3136.1085 | 3825.925 | 131.024 | 2074.83709 | 2895.88682 | 2054.23699 | UP | 0.75 | 0.25 |
| 7Day | Inactivation, recovery and regulation of the phototransduction cascade | 0.85328 | 0.31177 | 0.52292 | metap2;rgs9;calm3;calm2 | 4272.6525 | 4282.775 | 3050.32 | 1116.94268 | 3771.99798 | 1052.02681 | CONFLICT | 0.5 | 0.5 |
| 7Day | Negative regulation of MAPK pathway | 0.85328 | 0.31177 | 0.52292 | mapk3;pebp1;uba52;kras | 4517.91 | 4556.345 | 4158.71 | 314.067806 | 4543.01794 | 302.022236 | UP | 0.75 | 0.25 |
| 7Day | Gap junction assembly | 0.85328 | 0.31177 | 0.52292 | tubb4b;tubb2a;tuba4a;gja1 | 2276.434 | 1954.85 | 919.856 | 1424.18025 | 1763.60227 | 985.706882 | UP | 0.75 | 0.25 |
| 7Day | Metabolism of vitamins and cofactors | 0.78622 | 0.29132 | 0.52387 | akr1c6;mccc2;nudt12;qprt;pccb;mocs1;btd;naxe;apob;ttr;sdc3;lrp1;hsp90aa1;calm3;calm2;apoe;cyb5a;shmt2;aldh1l1;akr1c14 | 2456.08094 | 2783.725 | 77.8976 | 1883.49191 | 2618.45487 | 1697.27921 | DOWN | 0.3 | 0.7 |
| 28Day | RAB GEFs exchange GTP for GDP on RABs | 0.28761 | 0.85075 | 0.52428 | trappc8;rab9;dennd1a;rab18 | 3404.915 | 2992.42 | 2453.87 | 1213.23951 | 3862.04186 | 1278.52857 | DOWN | 0.25 | 0.75 |
| 28Day | PCP/CE pathway | 0.21718 | 0.94619 | 0.52674 | pfn1 | 4831.18 | 4831.18 | 4831.18 |  | 4831.18 |  | UP | 1 | 0 |
| 28Day | Signaling by NOTCH | 0.21718 | 0.94619 | 0.52674 | notch1 | 908.573 | 908.573 | 908.573 |  | 908.573 |  | UP | 1 | 0 |
| 28Day | SUMOylation of DNA replication proteins | 0.21718 | 0.94619 | 0.52674 | tpr | 3638.67 | 3638.67 | 3638.67 |  | 3638.67 |  | UP | 1 | 0 |
| 90Day | Interconversion of nucleotide di- and triphosphates | 0.83819 | 0.33573 | 0.5275 | txnrd1;txn1;gsr;ak2 | 3060.2 | 2620.955 | 1855.35 | 1487.24137 | 2797.06582 | 1575.60934 | CONFLICT | 0.5 | 0.5 |
| 90Day | Trafficking of AMPA receptors | 0.83819 | 0.33573 | 0.5275 | gria3;mdm2;epb41l1;ap2m1 | 2862.2375 | 3259.315 | 1097.82 | 1227.7367 | 2584.40324 | 1386.19776 | UP | 1 | 0 |
| 90Day | Glutamate binding, activation of AMPA receptors and synaptic plasticity | 0.83819 | 0.33573 | 0.5275 | gria3;mdm2;epb41l1;ap2m1 | 2862.2375 | 3259.315 | 1097.82 | 1227.7367 | 2584.40324 | 1386.19776 | UP | 1 | 0 |
| 90Day | Cytosolic sulfonation of small molecules | 0.83819 | 0.33573 | 0.5275 | abhd14b;sult1b1;bpnt1;slc26a2 | 3219.905 | 3036.205 | 2844.73 | 516.097522 | 3077.28766 | 434.41209 | DOWN | 0.25 | 0.75 |
| 90Day | Signaling by VEGF | 0.27335 | 0.8263 | 0.52936 | mapk14;wasf2;vav1;rasa1;rock2;rock1;hsp90aa1;cdc42;ctnnb1 | 2740.53767 | 3874.11 | 156.487 | 2016.69226 | 2197.99008 | 2124.70017 | CONFLICT | 0.555555556 | 0.444444444 |
| 90Day | PI5P, PP2A and IER3 Regulate PI3K/AKT Signaling | 0.27335 | 0.8263 | 0.52936 | klb;irs2;vav1;tgfa;nrg1;il1rap;gab1;fgf1;areg | 2353.84448 | 2684.35 | 74.8133 | 1778.57928 | 2322.93121 | 1581.92848 | DOWN | 0.333333333 | 0.666666667 |
| 7Day | The phototransduction cascade | 0.83775 | 0.33392 | 0.52996 | metap2;rgs9;calm3;calm2 | 4272.6525 | 4282.775 | 3050.32 | 1116.94268 | 3771.99798 | 1052.02681 | CONFLICT | 0.5 | 0.5 |
| 7Day | Disassembly of the destruction complex and recruitment of AXIN to the membrane | 0.83775 | 0.33392 | 0.52996 | gsk3b;ppp2cb;lrp5;ctnnb1 | 3235.2933 | 4063.24 | 54.5232 | 2175.16894 | 3178.95783 | 2131.91975 | CONFLICT | 0.5 | 0.5 |

BMD analysis results for functional classification based on dose-responsive genes, using the Reactome database for gene sets in BMDExpress2.2 software.

| Study Day | Gene Set Name | Fisher's Exact Left P-Value | Fisher's Exact Right P-Value | Fisher's Exact Two Tail | Gene Symbols | BMD Mean | BMD Median | BMD Minimum | BMD Standard Deviation | BMD wMean | BMD wSD | Overall Direction | Percent Genes With Overall Direction Up | Percent Genes With Overall Direction Down |
|---|---|---|---|---|---|---|---|---|---|---|---|---|---|---|
| 90Day | Visual phototransduction | 0.26209 | 0.83476 | 0.53006 | rdh7;apob;ttr;sdc4;rbp1;rdh11;apoe;apoc3;abca4 | 3292.12178 | 3563.02 | 175.96 | 2145.67605 | 4076.34615 | 2043.87414 | CONFLICT | 0.444444444 | 0.555555556 |
| 28Day | S Phase | 0.23385 | 0.8848 | 0.53012 | pole3;cdc6;cdc27;rad21 | 4147.722 | 4959.015 | 805.318 | 2366.17559 | 4745.67586 | 2056.85116 | UP | 1 | 0 |
| 28Day | Chromosome Maintenance | 0.84152 | 0.32546 | 0.53139 | cenpw;pole3;cenpt;cenpx | 3646.9295 | 4124.75 | 805.318 | 2058.31381 | 4051.51676 | 1870.37166 | CONFLICT | 0.5 | 0.5 |
| 28Day | UCH proteinases | 0.81294 | 0.30655 | 0.53223 | asxl2;psmd6;psmd8;uchl3;psmf1;ino80c;psmb8;hcfc1 | 3618.15388 | 4041.425 | 572.861 | 1783.86457 | 3604.51854 | 1890.72941 | DOWN | 0.375 | 0.625 |
| 7Day | MHC class II antigen presentation | 0.28504 | 0.81669 | 0.53298 | tubb4b;tubb2a;tuba4a;kif2a;cd74;h2-ab1;h2-aa;ctsb;capza2 | 2649.55511 | 2261.36 | 919.856 | 1184.67475 | 2821.27362 | 1222.39151 | UP | 0.666666667 | 0.333333333 |
| 7Day | Homology Directed Repair | 0.25685 | 0.83802 | 0.53452 | ube2n;ube2v2;rnf168;hist1h4h;babam1;hist1h2bc;uba52;rad51ap1;abl1 | 3610.97889 | 3444.79 | 2423.08 | 647.933214 | 3488.58257 | 659.371908 | UP | 0.777777778 | 0.222222222 |
| 28Day | mRNA Splicing - Major Pathway | 0.75772 | 0.34394 | 0.53629 | phf5a;ccar1;sf3b6;cpsf2;prpf19;hnrnpul1;prpf38a;u2af2;snrpd1;polr2a;prpf8;papola;srsf1 | 4273.981 | 4946.8 | 983.533 | 1347.689 | 4407.52389 | 1232.15325 | UP | 0.615384615 | 0.384615385 |
| 90Day | Downstream signaling of activated FGFR4 | 0.81861 | 0.36257 | 0.53771 | klb;sos1;gab1;fgf1 | 2528.51925 | 2046.3595 | 126.428 | 2832.90488 | 3890.50542 | 2640.67822 | DOWN | 0 | 1 |
| 7Day | FCERI mediated NF-kB activation | 0.82159 | 0.35614 | 0.53804 | ube2n;uba52;cdc34;btrc | 3358.075 | 3825.925 | 1018.89 | 1650.23752 | 3816.68588 | 959.204428 | UP | 1 | 0 |
| 7Day | RAF activation | 0.82159 | 0.35614 | 0.53804 | ppp2cb;kras;calm3;calm2 | 3938.1575 | 3892.875 | 3050.32 | 793.927869 | 3662.8258 | 731.819469 | UP | 0.75 | 0.25 |
| 7Day | Golgi-to-ER retrograde transport | 0.78569 | 0.30849 | 0.53909 | rab3gap2;copz1;tubb4b;tubb2a;tuba4a;arcn1;sec22b;rab6a;rab18;rab1a;kif2a;kif1c;capza2;gbf1 | 3009.42471 | 3164.9 | 919.856 | 1239.06258 | 2905.56928 | 1095.93066 | UP | 0.928571429 | 0.071428571 |
| 28Day | RHO GTPases activate KTN1 | 0.82825 | 0.54283 | 0.54283 | cdc42 | 2463.49 | 2463.49 | 2463.49 | | 2463.49 | | UP | 1 | 0 |
| 28Day | Mitochondrial iron-sulfur cluster biogenesis | 0.82825 | 0.54283 | 0.54283 | fdxr | 5126.12 | 5126.12 | 5126.12 | | 5126.12 | | DOWN | 0 | 1 |
| 28Day | NOTCH1 Intracellular Domain Regulates Transcription | 0.82825 | 0.54283 | 0.54283 | notch1 | 908.573 | 908.573 | 908.573 | | 908.573 | | UP | 1 | 0 |
| 28Day | MET activates RAS signaling | 0.82825 | 0.54283 | 0.54283 | ranbp9 | 5639.92 | 5639.92 | 5639.92 | | 5639.92 | | UP | 1 | 0 |
| 28Day | RUNX3 regulates NOTCH signaling | 0.82825 | 0.54283 | 0.54283 | notch1 | 908.573 | 908.573 | 908.573 | | 908.573 | | UP | 1 | 0 |
| 28Day | Establishment of Sister Chromatid Cohesion | 0.82825 | 0.54283 | 0.54283 | rad21 | 4137.27 | 4137.27 | 4137.27 | | 4137.27 | | UP | 1 | 0 |
| 28Day | CDC6 association with the ORC:origin complex | 0.82825 | 0.54283 | 0.54283 | cdc6 | 5867.54 | 5867.54 | 5867.54 | | 5867.54 | | UP | 1 | 0 |
| 28Day | DCC mediated attractive signaling | 0.82825 | 0.54283 | 0.54283 | cdc42 | 2463.49 | 2463.49 | 2463.49 | | 2463.49 | | UP | 1 | 0 |
| 28Day | Assembly of active LPL and LIPC lipase complexes | 0.82825 | 0.54283 | 0.54283 | lmf1 | 3007.97 | 3007.97 | 3007.97 | | 3007.97 | | DOWN | 0 | 1 |
| 28Day | p75NTR recruits signalling complexes | 0.82825 | 0.54283 | 0.54283 | sqstm1 | 5683.98 | 5683.98 | 5683.98 | | 5683.98 | | UP | 1 | 0 |
| 28Day | NF-kB is activated and signals survival | 0.82825 | 0.54283 | 0.54283 | sqstm1 | 5683.98 | 5683.98 | 5683.98 | | 5683.98 | | UP | 1 | 0 |
| 28Day | Heme biosynthesis | 0.82825 | 0.54283 | 0.54283 | fech | 5076.68 | 5076.68 | 5076.68 | | 5076.68 | | DOWN | 0 | 1 |
| 28Day | FGFR1c ligand binding and activation | 0.82825 | 0.54283 | 0.54283 | fgf1 | 1467.57 | 1467.57 | 1467.57 | | 1467.57 | | DOWN | 0 | 1 |
| 28Day | mRNA Splicing | 0.78556 | 0.30738 | 0.54294 | phf5a;ccar1;rnpc3;sf3b6;cpsf2;prpf19;hnrnpul1;prpf38a;u2af2;snrpd1;polr2a;prpf8;papola;srsf1 | 3978.11314 | 4859.02 | 131.831 | 1703.54981 | 3970.57701 | 1778.01563 | UP | 0.642857143 | 0.357142857 |
| 7Day | Downregulation of ERBB2:ERBB3 signaling | 0.83017 | 0.54708 | 0.54708 | uba52 | 4761.56 | 4761.56 | 4761.56 | | 4761.56 | | UP | 1 | 0 |
| 7Day | Negative regulation of TCF-dependent signaling by WNT ligand antagonists | 0.83017 | 0.54708 | 0.54708 | lrp5 | 4760.17 | 4760.17 | 4760.17 | | 4760.17 | | DOWN | 0 | 1 |
| 7Day | Sema4D mediated inhibition of cell attachment and migration | 0.83017 | 0.54708 | 0.54708 | sema4d | 5514.77 | 5514.77 | 5514.77 | | 5514.77 | | DOWN | 0 | 1 |
| 7Day | Regulation of RUNX1 Expression and Activity | 0.83017 | 0.54708 | 0.54708 | ptpn11 | 3629.67 | 3629.67 | 3629.67 | | 3629.67 | | UP | 1 | 0 |
| 7Day | WNT mediated activation of DVL | 0.83017 | 0.54708 | 0.54708 | csnk2b | 2829.67 | 2829.67 | 2829.67 | | 2829.67 | | UP | 1 | 0 |
| 7Day | HuR (ELAVL1) binds and stabilizes mRNA | 0.83017 | 0.54708 | 0.54708 | xpo1 | 2692.16 | 2692.16 | 2692.16 | | 2692.16 | | UP | 1 | 0 |
| 7Day | Vitamin C (ascorbate) metabolism | 0.83017 | 0.54708 | 0.54708 | cyb5a | 2724.64 | 2724.64 | 2724.64 | | 2724.64 | | UP | 1 | 0 |
| 7Day | Signaling by NOTCH2 | 0.83017 | 0.54708 | 0.54708 | mdk | 4385.8 | 4385.8 | 4385.8 | | 4385.8 | | DOWN | 0 | 1 |
| 7Day | The activation of arylsulfatases | 0.83017 | 0.54708 | 0.54708 | arsb | 34.2395 | 34.2395 | 34.2395 | | 34.2395 | | DOWN | 0 | 1 |
| 7Day | Activated NOTCH1 Transmits Signal to the Nucleus | 0.83017 | 0.54708 | 0.54708 | uba52 | 4761.56 | 4761.56 | 4761.56 | | 4761.56 | | UP | 1 | 0 |
| 7Day | IRAK2 mediated activation of TAK1 complex | 0.83017 | 0.54708 | 0.54708 | uba52 | 4761.56 | 4761.56 | 4761.56 | | 4761.56 | | UP | 1 | 0 |
| 7Day | Degradation of AXIN | 0.83017 | 0.54708 | 0.54708 | uba52 | 4761.56 | 4761.56 | 4761.56 | | 4761.56 | | UP | 1 | 0 |

BMD analysis results for functional classification based on dose-responsive genes, using the Reactome database for gene sets in BMDExpress2.2 software.

| Study Day | Gene Set Name | Fisher's Exact Left P-Value | Fisher's Exact Right P-Value | Fisher's Exact Two Tail | Gene Symbols | BMD Mean | BMD Median | BMD Minimum | BMD Standard Deviation | BMD wMean | BMD wSD | Overall Direction | Percent Genes With Overall Direction Up | Percent Genes With Overall Direction Down |
|---|---|---|---|---|---|---|---|---|---|---|---|---|---|---|
| 7Day | FBXL7 down-regulates AURKA during mitotic entry and in early mitosis | 0.83017 | 0.54708 | 0.54708 | uba52 | 4761.56 | 4761.56 | 4761.56 |  | 4761.56 |  | UP | 1 | 0 |
| 7Day | Regulation of RUNX2 expression and activity | 0.83017 | 0.54708 | 0.54708 | uba52 | 4761.56 | 4761.56 | 4761.56 |  | 4761.56 |  | UP | 1 | 0 |
| 7Day | p38MAPK events | 0.83017 | 0.54708 | 0.54708 | kras | 4158.71 | 4158.71 | 4158.71 |  | 4158.71 |  | UP | 1 | 0 |
| 7Day | Transcriptional activation of mitochondrial biogenesis | 0.83017 | 0.54708 | 0.54708 | idh2 | 2704.94 | 2704.94 | 2704.94 |  | 2704.94 |  | DOWN | 0 | 1 |
| 7Day | Zinc influx into cells by the SLC39 gene family | 0.83017 | 0.54708 | 0.54708 | slc39a2 | 5557.48 | 5557.48 | 5557.48 |  | 5557.48 |  | UP | 1 | 0 |
| 7Day | Recycling of eIF2:GDP | 0.83017 | 0.54708 | 0.54708 | eif2s3x | 4962.69 | 4962.69 | 4962.69 |  | 4962.69 |  | UP | 1 | 0 |
| 7Day | Terminal pathway of complement | 0.83017 | 0.54708 | 0.54708 | c8g | 2794.51 | 2794.51 | 2794.51 |  | 2794.51 |  | DOWN | 0 | 1 |
| 7Day | Phosphate bond hydrolysis by NUDT proteins | 0.83017 | 0.54708 | 0.54708 | nudt5 | 1880.13 | 1880.13 | 1880.13 |  | 1880.13 |  | UP | 1 | 0 |
| 7Day | Estrogen biosynthesis | 0.83017 | 0.54708 | 0.54708 | hsd17b2 | 4340.78 | 4340.78 | 4340.78 |  | 4340.78 |  | UP | 1 | 0 |
| 7Day | SLBP independent Processing of Histone Pre-mRNAs | 0.83017 | 0.54708 | 0.54708 | lsm10 | 2905.24 | 2905.24 | 2905.24 |  | 2905.24 |  | UP | 1 | 0 |
| 7Day | Formyl peptide receptors bind formyl peptides and many other ligands | 0.83017 | 0.54708 | 0.54708 | hebp1 | 790.154 | 790.154 | 790.154 |  | 790.154 |  | DOWN | 0 | 1 |
| 7Day | Telomere C-strand synthesis initiation | 0.83017 | 0.54708 | 0.54708 | prim2 | 4006.14 | 4006.14 | 4006.14 |  | 4006.14 |  | UP | 1 | 0 |
| 7Day | DNA replication initiation | 0.83017 | 0.54708 | 0.54708 | prim2 | 4006.14 | 4006.14 | 4006.14 |  | 4006.14 |  | UP | 1 | 0 |
| 90Day | HDR through Homologous Recombination (HRR) | 0.27178 | 0.85262 | 0.54771 | pole4;polk;rad51;brca2;rad51c | 3777.8444 | 4249.95 | 513.022 | 1994.74231 | 3346.62459 | 1844.20396 | UP | 0.8 | 0.2 |
| 90Day | Major pathway of rRNA processing in the nucleolus and cytosol | 0.25884 | 0.83323 | 0.54798 | nop14;riok1;rps27l;rcl1;exosc9;utp4;rps12;emg1;fbl;tsr1 | 2846.4009 | 2776.515 | 591.419 | 1480.39943 | 2670.58313 | 1277.5984 | UP | 0.8 | 0.2 |
| 90Day | rRNA processing | 0.25884 | 0.83323 | 0.54798 | nop14;riok1;rps27l;rcl1;exosc9;utp4;rps12;emg1;fbl;tsr1 | 2846.4009 | 2776.515 | 591.419 | 1480.39943 | 2670.58313 | 1277.5984 | UP | 0.8 | 0.2 |
| 90Day | rRNA processing in the nucleus and cytosol | 0.25884 | 0.83323 | 0.54798 | nop14;riok1;rps27l;rcl1;exosc9;utp4;rps12;emg1;fbl;tsr1 | 2846.4009 | 2776.515 | 591.419 | 1480.39943 | 2670.58313 | 1277.5984 | UP | 0.8 | 0.2 |
| 90Day | EGFR downregulation | 0.79822 | 0.38937 | 0.54919 | tgfa;sh3gl3;cdc42;areg | 2888.90425 | 3066.45 | 156.487 | 2222.23924 | 3335.44859 | 2016.78896 | UP | 1 | 0 |
| 7Day | Opioid Signalling | 0.29061 | 0.83896 | 0.55049 | prkar2a;ppp2cb;gnai3;calm3;calm2 | 3290.936 | 3627.04 | 794.2 | 1553.12577 | 2908.54515 | 1523.23127 | UP | 0.6 | 0.4 |
| 28Day | Nucleotide-binding domain, leucine rich repeat containing receptor (NLR) signaling pathways | 0.79397 | 0.38928 | 0.55523 | ube2n;ikbkg;bcl2l1;birc2 | 4674.5 | 5342.195 | 2151.36 | 1700.98155 | 4096.41432 | 2007.10901 | UP | 0.75 | 0.25 |
| 28Day | Cargo recognition for clathrin-mediated endocytosis | 0.28114 | 0.84438 | 0.55604 | apob;picalm;trf;hgs;hbegf | 2458.9746 | 3086.6 | 919.738 | 1452.65283 | 1857.20336 | 1315.60072 | UP | 0.6 | 0.4 |
| 7Day | Metalloprotease DUBs | 0.78762 | 0.40047 | 0.5568 | babam1;hist2h2ac;uba52;hist2h2aa1 | 4476.405 | 4474.415 | 3567.39 | 779.910371 | 4363.95684 | 884.124588 | UP | 0.75 | 0.25 |
| 90Day | MHC class II antigen presentation | 0.2761 | 0.81636 | 0.56197 | tubb6;dctn3;tubb4b;tubb2a;tuba1b;cd74;h2-aa;ctsh;ctsd;ap2m1;sec13 | 2424.05645 | 2214.7 | 779.791 | 937.752913 | 2264.1907 | 1084.33865 | UP | 0.636363636 | 0.363636364 |
| 7Day | Mitotic Metaphase and Anaphase | 0.30271 | 0.79461 | 0.56466 | clasp2;pds5a;cenpk;tubb4b;uba52;tubb2a;tuba4a;cdc27;ppp2cb;kif2a;xpo1 | 3257.49964 | 3647.06 | 919.856 | 1227.93386 | 3222.5988 | 1220.34245 | UP | 0.909090909 | 0.090909091 |
| 90Day | TP53 Regulates Transcription of Genes Involved in G2 Cell Cycle Arrest | 0.81808 | 0.56706 | 0.56706 | bax | 1844.96 | 1844.96 | 1844.96 |  | 1844.96 |  | UP | 1 | 0 |
| 90Day | HDL assembly | 0.81808 | 0.56706 | 0.56706 | bmp1 | 190.369 | 190.369 | 190.369 |  | 190.369 |  | DOWN | 0 | 1 |
| 90Day | HSF1 activation | 0.81808 | 0.56706 | 0.56706 | hsp90aa1 | 426.32 | 426.32 | 426.32 |  | 426.32 |  | UP | 1 | 0 |
| 90Day | Pyrimidine catabolism | 0.81808 | 0.56706 | 0.56706 | dpys | 1635.68 | 1635.68 | 1635.68 |  | 1635.68 |  | DOWN | 0 | 1 |
| 90Day | BH3-only proteins associate with and inactivate anti-apoptotic BCL-2 members | 0.81808 | 0.56706 | 0.56706 | bmf | 1597.1 | 1597.1 | 1597.1 |  | 1597.1 |  | DOWN | 0 | 1 |
| 90Day | Heme degradation | 0.81808 | 0.56706 | 0.56706 | blvrb | 3840.4 | 3840.4 | 3840.4 |  | 3840.4 |  | UP | 1 | 0 |
| 90Day | Acyl chain remodeling of DAG and TAG | 0.81808 | 0.56706 | 0.56706 | dgat2 | 2903.14 | 2903.14 | 2903.14 |  | 2903.14 |  | DOWN | 0 | 1 |
| 90Day | Interleukin-36 pathway | 0.81808 | 0.56706 | 0.56706 | il1rap | 2684.35 | 2684.35 | 2684.35 |  | 2684.35 |  | DOWN | 0 | 1 |
| 90Day | DEx/H-box helicases activate type I IFN and inflammatory cytokines production | 0.81808 | 0.56706 | 0.56706 | irf7 | 5689.7 | 5689.7 | 5689.7 |  | 5689.7 |  | UP | 1 | 0 |
| 90Day | FGFR3b ligand binding and activation | 0.81808 | 0.56706 | 0.56706 | fgf1 | 242.429 | 242.429 | 242.429 |  | 242.429 |  | DOWN | 0 | 1 |
| 28Day | Neurotransmitter release cycle | 0.76861 | 0.42096 | 0.56966 | lin7c;slc22a1;slc1a2;slc6a13 | 2234.1305 | 1728.215 | 151.142 | 2193.39816 | 3178.351 | 2203.82829 | DOWN | 0 | 1 |
| 90Day | CD28 co-stimulation | 0.32705 | 0.86722 | 0.5717 | vav1;cdc42 | 2158.7685 | 2158.7685 | 156.487 | 2831.65365 | 2296.14268 | 2824.98125 | CONFLICT | 0.5 | 0.5 |
| 90Day | Antiviral mechanism by IFN-stimulated genes | 0.32705 | 0.86722 | 0.5717 | usp18;abce1 | 3550.28 | 3550.28 | 3026.26 | 741.076191 | 3605.64422 | 736.928441 | UP | 1 | 0 |
| 90Day | FCERI mediated Ca+2 mobilization | 0.32705 | 0.86722 | 0.5717 | vav1;sos1 | 5027.99 | 5027.99 | 4161.05 | 1226.03831 | 5362.02772 | 1131.37418 | DOWN | 0 | 1 |

BMD analysis results for functional classification based on dose-responsive genes, using the Reactome database for gene sets in BMDExpress2.2 software.

| Study Day | Gene Set Name | Fisher's Exact Left P-Value | Fisher's Exact Right P-Value | Fisher's Exact Two Tail | Gene Symbols | BMD Mean | BMD Median | BMD Minimum | BMD Standard Deviation | BMD wMean | BMD wSD | Overall Direction | Percent Genes With Overall Direction Up | Percent Genes With Overall Direction Down |
|---|---|---|---|---|---|---|---|---|---|---|---|---|---|---|
| 90Day | EPH-ephrin mediated repulsion of cells | 0.32705 | 0.86722 | 0.5717 | tiam1;mmp2 | 4998.325 | 4998.325 | 4586.54 | 582.351932 | 4881.4162 | 558.389146 | DOWN | 0 | 1 |
| 90Day | Termination of translesion DNA synthesis | 0.32705 | 0.86722 | 0.5717 | pole4;polk | 4753.255 | 4753.255 | 3652.71 | 1556.40567 | 3884.77714 | 955.97646 | CONFLICT | 0.5 | 0.5 |
| 90Day | NOD1/2 Signaling Pathway | 0.30513 | 0.87911 | 0.57205 | mapk14;ikbkg | 3763.76 | 3763.76 | 3265.56 | 704.561197 | 3420.95379 | 511.247768 | CONFLICT | 0.5 | 0.5 |
| 90Day | Sialic acid metabolism | 0.30513 | 0.87911 | 0.57205 | st6galnac6;st3gal3 | 4683.725 | 4683.725 | 4143.19 | 764.431928 | 4469.98451 | 702.129746 | DOWN | 0 | 1 |
| 90Day | Loss of Nlp from mitotic centrosomes | 0.31214 | 0.8156 | 0.57259 | haus7;dctn3;cntrl;tubb4b;cep76;hsp90aa1 | 3221.30167 | 3997.375 | 426.32 | 1725.30565 | 3467.98166 | 1544.87279 | UP | 1 | 0 |
| 90Day | Loss of proteins required for interphase microtubule organization from the centrosome | 0.31214 | 0.8156 | 0.57259 | haus7;dctn3;cntrl;tubb4b;cep76;hsp90aa1 | 3221.30167 | 3997.375 | 426.32 | 1725.30565 | 3467.98166 | 1544.87279 | UP | 1 | 0 |
| 90Day | Cell death signalling via NRAGE, NRIF and NADE | 0.29772 | 0.82606 | 0.57281 | arhgef6;fgd4;vav1;tiam1;sos1;psen2 | 4921.82167 | 5193.43 | 3135.19 | 1154.56154 | 4931.17678 | 1191.79698 | DOWN | 0.166666667 | 0.833333333 |
| 90Day | Regulation of APC/C activators between G1/S and early anaphase | 0.28434 | 0.89001 | 0.57394 | anapc10;btrc | 4771.585 | 4771.585 | 4390.47 | 538.978002 | 5062.49481 | 348.195709 | CONFLICT | 0.5 | 0.5 |
| 28Day | RIP-mediated NFkB activation via ZBP1 | 0.80278 | 0.57425 | 0.57425 | ikbkg | 5417.68 | 5417.68 | 5417.68 |  | 5417.68 |  | UP | 1 | 0 |
| 28Day | Dectin-1 mediated noncanonical NF-kB signaling | 0.80278 | 0.57425 | 0.57425 | ube2m | 2933.96 | 2933.96 | 2933.96 |  | 2933.96 |  | UP | 1 | 0 |
| 28Day | NIK-->noncanonical NF-kB signaling | 0.80278 | 0.57425 | 0.57425 | ube2m | 2933.96 | 2933.96 | 2933.96 |  | 2933.96 |  | UP | 1 | 0 |
| 28Day | Apoptosis induced DNA fragmentation | 0.80278 | 0.57425 | 0.57425 | kpna1 | 5384.85 | 5384.85 | 5384.85 |  | 5384.85 |  | UP | 1 | 0 |
| 28Day | Activation of DNA fragmentation factor | 0.80278 | 0.57425 | 0.57425 | kpna1 | 5384.85 | 5384.85 | 5384.85 |  | 5384.85 |  | UP | 1 | 0 |
| 28Day | Purine ribonucleoside monophosphate biosynthesis | 0.80278 | 0.57425 | 0.57425 | adss | 3213.44 | 3213.44 | 3213.44 |  | 3213.44 |  | UP | 1 | 0 |
| 28Day | MAP3K8 (TPL2)-dependent MAPK1/3 activation | 0.80278 | 0.57425 | 0.57425 | ikbkg | 5417.68 | 5417.68 | 5417.68 |  | 5417.68 |  | UP | 1 | 0 |
| 28Day | Pregnenolone biosynthesis | 0.80278 | 0.57425 | 0.57425 | fdxr | 5126.12 | 5126.12 | 5126.12 |  | 5126.12 |  | DOWN | 0 | 1 |
| 28Day | CD28 dependent Vav1 pathway | 0.80278 | 0.57425 | 0.57425 | cdc42 | 2463.49 | 2463.49 | 2463.49 |  | 2463.49 |  | UP | 1 | 0 |
| 28Day | TRAF6 mediated IRF7 activation in TLR7/8 or 9 signaling | 0.80278 | 0.57425 | 0.57425 | ube2n | 5266.71 | 5266.71 | 5266.71 |  | 5266.71 |  | DOWN | 0 | 1 |
| 28Day | Organic cation transport | 0.80278 | 0.57425 | 0.57425 | slc22a1 | 1681.65 | 1681.65 | 1681.65 |  | 1681.65 |  | DOWN | 0 | 1 |
| 28Day | Negative regulators of DDX58/IFIH1 signaling | 0.80278 | 0.57425 | 0.57425 | tax1bp1 | 4968.69 | 4968.69 | 4968.69 |  | 4968.69 |  | DOWN | 0 | 1 |
| 90Day | Protein localization | 0.27022 | 0.84555 | 0.57529 | gstk1;hacl1;slc27a2;amacr;ephx2;agxt | 3428.52667 | 3398.155 | 2157.32 | 816.22512 | 3062.66676 | 947.203112 | DOWN | 0 | 1 |
| 90Day | Respiratory electron transport, ATP synthesis by chemiosmotic coupling, and heat production by uncoupling proteins. | 0.27022 | 0.84555 | 0.57529 | ndufab1;ndufc2;etfdh;ndufaf3;ndufb9;atp5k | 2794.408 | 3310.375 | 105.476 | 2268.6022 | 4306.21778 | 2218.58014 | DOWN | 0.333333333 | 0.666666667 |
| 90Day | AURKA Activation by TPX2 | 0.27022 | 0.84555 | 0.57529 | haus7;dctn3;cntrl;tubb4b;cep76;hsp90aa1 | 3221.30167 | 3997.375 | 426.32 | 1725.30565 | 3467.98166 | 1544.87279 | UP | 1 | 0 |
| 7Day | RET signaling | 0.32742 | 0.86594 | 0.57562 | ptpn11;gfra1 | 3850.68 | 3850.68 | 3629.67 | 312.555339 | 3903.39421 | 303.534619 | CONFLICT | 0.5 | 0.5 |
| 7Day | DNA Damage Recognition in GG-NER | 0.32742 | 0.86594 | 0.57562 | ino80c;uba52 | 4592.3 | 4592.3 | 4423.04 | 239.369788 | 4648.50109 | 225.789217 | UP | 1 | 0 |
| 7Day | Cargo concentration in the ER | 0.30917 | 0.87594 | 0.57583 | sec22b;f5 | 1730.3555 | 1730.3555 | 244.081 | 2101.90956 | 868.772233 | 1712.70906 | CONFLICT | 0.5 | 0.5 |
| 7Day | Regulation of PLK1 Activity at G2/M Transition | 0.31092 | 0.81559 | 0.57627 | tubb4b;uba52;tuba4a;nedd1;hsp90aa1;btrc | 2630.741 | 2445.18 | 919.856 | 1640.41495 | 2578.74438 | 1683.29047 | UP | 1 | 0 |
| 7Day | Metabolism of polyamines | 0.2917 | 0.88526 | 0.57711 | nqo1;amd1 | 1683.855 | 1683.855 | 1137.09 | 773.242478 | 1840.19108 | 740.96018 | UP | 1 | 0 |
| 7Day | Non-integrin membrane-ECM interactions | 0.2917 | 0.88526 | 0.57711 | ttr;sdc3 | 4752.175 | 4752.175 | 3803.05 | 1342.26545 | 4518.7704 | 1301.04616 | DOWN | 0 | 1 |
| 7Day | NCAM signaling for neurite out-growth | 0.2917 | 0.88526 | 0.57711 | mapk3;kras | 4479.475 | 4479.475 | 4158.71 | 453.630213 | 4552.01512 | 441.878074 | CONFLICT | 0.5 | 0.5 |
| 28Day | HSP90 chaperone cycle for steroid hormone receptors (SHR) | 0.75561 | 0.43666 | 0.57736 | dynll1;tubb4b;tubb2a;capza2 | 4122.615 | 4169.735 | 2359.45 | 1742.36759 | 4179.60212 | 1734.13634 | UP | 0.75 | 0.25 |
| 28Day | Ribosomal scanning and start codon recognition | 0.32314 | 0.8669 | 0.58071 | eif3m;eif1ax | 2737.81 | 2737.81 | 1517.45 | 1725.84966 | 2423.68091 | 1667.69388 | CONFLICT | 0.5 | 0.5 |
| 28Day | Signaling by Type 1 Insulin-like Growth Factor 1 Receptor (IGF1R) | 0.32314 | 0.8669 | 0.58071 | pdpk1;fgf1 | 830.279 | 830.279 | 192.988 | 901.265575 | 1273.10558 | 648.142632 | DOWN | 0 | 1 |
| 28Day | Chemokine receptors bind chemokines | 0.31007 | 0.87412 | 0.58099 | cx3cl1;cxcl9 | 5958.13 | 5958.13 | 5937.6 | 29.0338044 | 5963.10667 | 28.1678407 | CONFLICT | 0.5 | 0.5 |
| 28Day | Condensation of Prophase Chromosomes | 0.31007 | 0.87412 | 0.58099 | set;hist1h4i | 4954.585 | 4954.585 | 4060.76 | 1264.05944 | 4946.81076 | 1264.01162 | CONFLICT | 0.5 | 0.5 |

BMD analysis results for functional classification based on dose-responsive genes, using the Reactome database for gene sets in BMDExpress2.2 software.

| Study Day | Gene Set Name | Fisher's Exact Left P-Value | Fisher's Exact Right P-Value | Fisher's Exact Two Tail | Gene Symbols | BMD Mean | BMD Median | BMD Minimum | BMD Standard Deviation | BMD wMean | BMD wSD | Overall Direction | Percent Genes With Overall Direction Up | Percent Genes With Overall Direction Down |
|---|---|---|---|---|---|---|---|---|---|---|---|---|---|---|
| 28Day | Cell surface interactions at the vascular wall | 0.31652 | 0.81032 | 0.58099 | apob;tnfrsf10b;proc;cd74;fn1;f2 | 3287.43083 | 3598.375 | 939.205 | 1854.98409 | 2882.27048 | 1899.80049 | DOWN | 0.166666667 | 0.833333333 |
| 28Day | Insulin receptor signalling cascade | 0.31007 | 0.87412 | 0.58099 | pdpk1;fgf1 | 830.279 | 830.279 | 192.988 | 901.265575 | 1273.10558 | 648.142632 | DOWN | 0 | 1 |
| 28Day | Heparan sulfate/heparin (HS-GAG) metabolism | 0.31007 | 0.87412 | 0.58099 | hs2st1;gpc4 | 4234.355 | 4234.355 | 3361.03 | 1235.06806 | 4554.00819 | 1149.36364 | DOWN | 0 | 1 |
| 28Day | Formation of TC-NER Pre-Incision Complex | 0.31007 | 0.87412 | 0.58099 | prpf19;polr2a | 4295.465 | 4295.465 | 3550.26 | 1053.87902 | 3967.52849 | 946.348921 | UP | 1 | 0 |
| 28Day | Translation initiation complex formation | 0.29739 | 0.88098 | 0.58181 | eif3m;eif1ax | 2737.81 | 2737.81 | 1517.45 | 1725.84966 | 2423.68091 | 1667.69388 | CONFLICT | 0.5 | 0.5 |
| 28Day | Golgi Associated Vesicle Biogenesis | 0.29739 | 0.88098 | 0.58181 | picalm;ftl1 | 2328.2885 | 2328.2885 | 527.967 | 2546.03908 | 979.680637 | 1686.66199 | UP | 1 | 0 |
| 28Day | L13a-mediated translational silencing of Ceruloplasmin expression | 0.28512 | 0.8875 | 0.58315 | eif3m;eif1ax | 2737.81 | 2737.81 | 1517.45 | 1725.84966 | 2423.68091 | 1667.69388 | CONFLICT | 0.5 | 0.5 |
| 28Day | Activation of the mRNA upon binding of the cap-binding complex and eIFs, and subsequent binding to 43S | 0.28512 | 0.8875 | 0.58315 | eif3m;eif1ax | 2737.81 | 2737.81 | 1517.45 | 1725.84966 | 2423.68091 | 1667.69388 | CONFLICT | 0.5 | 0.5 |
| 28Day | Resolution of Sister Chromatid Cohesion | 0.27443 | 0.84082 | 0.58339 | zwilch;dynll1;cenpt;tubb4b;tubb2a;rad21 | 3719.56667 | 3563.05 | 2359.45 | 1186.01958 | 3809.00797 | 1244.66079 | UP | 1 | 0 |
| 28Day | Kinesins | 0.27324 | 0.89368 | 0.58499 | tubb4b;tubb2a | 2631.245 | 2631.245 | 2359.45 | 384.376175 | 2702.45657 | 370.948608 | UP | 1 | 0 |
| 90Day | Mitotic G2-G2/M phases | 0.30784 | 0.78447 | 0.58722 | haus7;tubb6;dctn3;gtse1;cntrl;tubb4b;cep76;tubb2a;tuba1b;hsp90aa1;cdkn1a;cdk7;btrc | 2700.50008 | 2128.94 | 426.32 | 1618.52744 | 2593.60842 | 1735.8006 | UP | 0.846153846 | 0.153846154 |
| 28Day | G1/S Transition | 0.26175 | 0.89954 | 0.58731 | pole3;cdc6 | 3336.429 | 3336.429 | 805.318 | 3579.5315 | 4404.50906 | 3245.22045 | UP | 1 | 0 |
| 28Day | Homology Directed Repair | 0.76921 | 0.34573 | 0.58937 | ube2n;rmi1;ube2v2;pole3;hist1h4i;rad51d;rad51;lig3;brca1;blm | 3816.8064 | 3892.075 | 692.086 | 1865.9087 | 4049.79857 | 1462.97446 | UP | 0.7 | 0.3 |
| 28Day | The citric acid (TCA) cycle and respiratory electron transport | 0.76921 | 0.34573 | 0.58937 | ndufab1;ndufaf1;ndufc2;atp5g2;etfdh;atp5j2;suclg2;me1;ldha;gstz1 | 4115.695 | 5341.16 | 1023.12 | 1938.77223 | 4052.10752 | 2107.143 | DOWN | 0.2 | 0.8 |
| 7Day | Neutrophil degranulation | 0.74091 | 0.31019 | 0.58967 | faf2;cotl1;ist1;fuca1;tmem30a;arl8a;ndufc2;npc2;ilf2;pycard;psmd6;9130409i23rik;golga7;iqgap2;sdcbp;hgsnat;mgam;tubb4b;ttr;nhlrc3;dsg1c;rab6a;rab18;rab10;psmc2;pa2g4;pgam1;neu1;mme;man2b1;lamp1;kpnb1;igf2r;hsp90aa1;h2-t23;h2-q10;gstp1;gstp2;gpi1;ftl1;ddx3x;ctsb;csnk2b;chil1;cct2;cab39;arsb;ahsg;aga;dsp;mlec;atad3a;qsox1 | 3282.41918 | 3422.8 | 34.2395 | 1455.3462 | 3167.92101 | 1410.26461 | CONFLICT | 0.528301887 | 0.471698113 |
| 7Day | Regulation of localization of FOXO transcription factors | 0.79463 | 0.58979 | 0.58979 | ywhaz | 2726.98 | 2726.98 | 2726.98 |  | 2726.98 |  | UP | 1 | 0 |
| 7Day | Reactions specific to the complex N-glycan synthesis pathway | 0.79463 | 0.58979 | 0.58979 | fuca1 | 2644.02 | 2644.02 | 2644.02 |  | 2644.02 |  | DOWN | 0 | 1 |
| 7Day | Apoptotic factor-mediated response | 0.79463 | 0.58979 | 0.58979 | xiap | 4874.03 | 4874.03 | 4874.03 |  | 4874.03 |  | DOWN | 0 | 1 |
| 7Day | Tight junction interactions | 0.79463 | 0.58979 | 0.58979 | prkci | 3409.24 | 3409.24 | 3409.24 |  | 3409.24 |  | UP | 1 | 0 |
| 7Day | FGFR2b ligand binding and activation | 0.79463 | 0.58979 | 0.58979 | fgf1 | 2647.76 | 2647.76 | 2647.76 |  | 2647.76 |  | DOWN | 0 | 1 |
| 7Day | Axonal growth inhibition (RHOA activation) | 0.79463 | 0.58979 | 0.58979 | lingo1 | 3247.44 | 3247.44 | 3247.44 |  | 3247.44 |  | UP | 1 | 0 |
| 7Day | Josephin domain DUBs | 0.79463 | 0.58979 | 0.58979 | uba52 | 4761.56 | 4761.56 | 4761.56 |  | 4761.56 |  | UP | 1 | 0 |
| 7Day | Regulation of RUNX3 expression and activity | 0.79463 | 0.58979 | 0.58979 | uba52 | 4761.56 | 4761.56 | 4761.56 |  | 4761.56 |  | UP | 1 | 0 |
| 7Day | Phosphate bond hydrolysis by NTPDase proteins | 0.79463 | 0.58979 | 0.58979 | entpd5 | 821.082 | 821.082 | 821.082 |  | 821.082 |  | UP | 1 | 0 |
| 7Day | mitochondrial fatty acid beta-oxidation of saturated fatty acids | 0.79463 | 0.58979 | 0.58979 | hadha | 197.056 | 197.056 | 197.056 |  | 197.056 |  | DOWN | 0 | 1 |
| 7Day | Translocation of SLC2A4 (GLUT4) to the plasma membrane | 0.79463 | 0.58979 | 0.58979 | ywhaz | 2726.98 | 2726.98 | 2726.98 |  | 2726.98 |  | UP | 1 | 0 |
| 7Day | SLBP Dependent Processing of Replication-Dependent Histone Pre-mRNAs | 0.79463 | 0.58979 | 0.58979 | lsm10 | 2905.24 | 2905.24 | 2905.24 |  | 2905.24 |  | UP | 1 | 0 |
| 7Day | EGFR Transactivation by Gastrin | 0.79463 | 0.58979 | 0.58979 | kras | 4158.71 | 4158.71 | 4158.71 |  | 4158.71 |  | UP | 1 | 0 |
| 7Day | SUMOylation | 0.2828 | 0.80419 | 0.59186 | gm49336;rnf168;hist1h4h;hdac7;nop58;suz12;uba2;top2b;ncoa1;hnrnpc;bmi1;uhrf2;tpr | 3306.80731 | 3214.64 | 852.825 | 1056.2797 | 3114.72341 | 1016.19186 | UP | 0.923076923 | 0.076923077 |

BMD analysis results for functional classification based on dose-responsive genes, using the Reactome database for gene sets in BMDExpress2.2 software.

| Study Day | Gene Set Name | Fisher's Exact Left P-Value | Fisher's Exact Right P-Value | Fisher's Exact Two Tail | Gene Symbols | BMD Mean | BMD Median | BMD Minimum | BMD Standard Deviation | BMD wMean | BMD wSD | Overall Direction | Percent Genes With Overall Direction Up | Percent Genes With Overall Direction Down |
|---|---|---|---|---|---|---|---|---|---|---|---|---|---|---|
| 7Day | COPI-dependent Golgi-to-ER retrograde traffic | 0.7418 | 0.37947 | 0.59396 | copz1;tubb4b;tubb2a;tuba4a;arcn1;sec22b;rab1a;kif2a;kif1c;gbf1 | 2649.6696 | 2888.645 | 919.856 | 1184.96711 | 2687.56923 | 1231.98217 | UP | 0.9 | 0.1 |
| 90Day | Global Genome Nucleotide Excision Repair (GG-NER) | 0.32085 | 0.80149 | 0.59459 | pole4;mcrs1;polk;yy1;ino80c;rad23a;cdk7 | 3814.86 | 3652.71 | 1252.26 | 1612.71329 | 3703.59993 | 1422.1654 | CONFLICT | 0.571428571 | 0.428571429 |
| 90Day | RET signaling | 0.78597 | 0.38264 | 0.59472 | pdlim7;irs2;sos1;gfra1;gab1 | 1573.00986 | 218.188 | 74.8133 | 2492.60036 | 1678.27136 | 2433.76832 | DOWN | 0 | 1 |
| 90Day | DNA Replication Pre-Initiation | 0.29361 | 0.82187 | 0.59566 | pole4;psmd8;orc6;dbf4;e2f2;psmc4;psmf1 | 3121.85686 | 3031.27 | 186.178 | 1891.29969 | 2809.12655 | 1647.18856 | UP | 0.857142857 | 0.142857143 |
| 90Day | Fcgamma receptor (FCGR) dependent phagocytosis | 0.28057 | 0.83144 | 0.59705 | wasf2;vav1;myo9b;myo10;hsp90aa1;fcgr2b;cdc42 | 2644.57429 | 3055.31 | 100.823 | 2388.05593 | 3312.00806 | 2193.71301 | DOWN | 0.285714286 | 0.714285714 |
| 7Day | Metabolism of nucleotides | 0.28359 | 0.82846 | 0.6003 | dpys;nudt5;txnrd1;entpd5;ak1;adk;atic | 2189.216 | 1880.13 | 124.762 | 2094.21117 | 2234.18323 | 2040.5626 | UP | 0.714285714 | 0.285714286 |
| 7Day | RNA Polymerase I Promoter Clearance | 0.273 | 0.83618 | 0.60179 | hist1h4h;hist1h2bc;hist2h2ac;mapk3;polr2h;ubtf;hist2h2aa1 | 3877.53857 | 3964.6 | 1976.31 | 1102.11348 | 3992.99121 | 990.713071 | CONFLICT | 0.571428571 | 0.428571429 |
| 90Day | EPHB-mediated forward signaling | 0.76698 | 0.40602 | 0.60261 | tiam1;rasa1;rock2;rock1;cdc42 | 2202.5738 | 2133.64 | 156.487 | 2026.94479 | 1983.44718 | 2199.56514 | UP | 0.8 | 0.2 |
| 7Day | Interleukin-3, Interleukin-5 and GM-CSF signaling | 0.76944 | 0.40096 | 0.60349 | ywhaz;yes1;uba52;ptpn11;jak1 | 3738.696 | 3629.67 | 2726.98 | 740.838803 | 3785.22967 | 622.632352 | UP | 1 | 0 |
| 28Day | Nonsense-Mediated Decay (NMD) | 0.77691 | 0.60352 | 0.60352 | smg5 | 4382.44 | 4382.44 | 4382.44 |  | 4382.44 |  | UP | 1 | 0 |
| 28Day | Nonsense Mediated Decay (NMD) enhanced by the Exon Junction Complex (EJC) | 0.77691 | 0.60352 | 0.60352 | smg5 | 4382.44 | 4382.44 | 4382.44 |  | 4382.44 |  | UP | 1 | 0 |
| 28Day | VEGFR2 mediated cell proliferation | 0.77691 | 0.60352 | 0.60352 | pdpk1 | 192.988 | 192.988 | 192.988 |  | 192.988 |  | DOWN | 0 | 1 |
| 28Day | ZBP1(DAI) mediated induction of type I IFNs | 0.77691 | 0.60352 | 0.60352 | ikbkg | 5417.68 | 5417.68 | 5417.68 |  | 5417.68 |  | UP | 1 | 0 |
| 28Day | GRB2 events in EGFR signaling | 0.77691 | 0.60352 | 0.60352 | hbegf | 919.738 | 919.738 | 919.738 |  | 919.738 |  | UP | 1 | 0 |
| 28Day | Depolymerisation of the Nuclear Lamina | 0.77691 | 0.60352 | 0.60352 | cnep1r1 | 5841.61 | 5841.61 | 5841.61 |  | 5841.61 |  | UP | 1 | 0 |
| 28Day | ERBB2 Activates PTK6 Signaling | 0.77691 | 0.60352 | 0.60352 | hbegf | 919.738 | 919.738 | 919.738 |  | 919.738 |  | UP | 1 | 0 |
| 28Day | Oncogene Induced Senescence | 0.77691 | 0.60352 | 0.60352 | mdm2 | 2266.61 | 2266.61 | 2266.61 |  | 2266.61 |  | UP | 1 | 0 |
| 28Day | Trafficking of GluR2-containing AMPA receptors | 0.77691 | 0.60352 | 0.60352 | gria3 | 2052.57 | 2052.57 | 2052.57 |  | 2052.57 |  | UP | 1 | 0 |
| 28Day | IRAK2 mediated activation of TAK1 complex upon TLR7/8 or 9 stimulation | 0.77691 | 0.60352 | 0.60352 | ly96 | 4560.3 | 4560.3 | 4560.3 |  | 4560.3 |  | UP | 1 | 0 |
| 28Day | Notch-HLH transcription pathway | 0.77691 | 0.60352 | 0.60352 | notch1 | 908.573 | 908.573 | 908.573 |  | 908.573 |  | UP | 1 | 0 |
| 28Day | BBSome-mediated cargo-targeting to cilium | 0.77691 | 0.60352 | 0.60352 | bbs9 | 4941.88 | 4941.88 | 4941.88 |  | 4941.88 |  | DOWN | 0 | 1 |
| 28Day | Apoptotic cleavage of cell adhesion proteins | 0.77691 | 0.60352 | 0.60352 | pkp1 | 3208.19 | 3208.19 | 3208.19 |  | 3208.19 |  | UP | 1 | 0 |
| 28Day | Glycogen breakdown (glycogenolysis) | 0.77691 | 0.60352 | 0.60352 | gaa | 3036.96 | 3036.96 | 3036.96 |  | 3036.96 |  | DOWN | 0 | 1 |
| 28Day | Signalling to RAS | 0.77691 | 0.60352 | 0.60352 | mapkapk2 | 5375 | 5375 | 5375 |  | 5375 |  | DOWN | 0 | 1 |
| 28Day | FGFR3 ligand binding and activation | 0.77691 | 0.60352 | 0.60352 | fgf1 | 1467.57 | 1467.57 | 1467.57 |  | 1467.57 |  | DOWN | 0 | 1 |
| 28Day | FGFR3c ligand binding and activation | 0.77691 | 0.60352 | 0.60352 | fgf1 | 1467.57 | 1467.57 | 1467.57 |  | 1467.57 |  | DOWN | 0 | 1 |
| 28Day | FGFR2c ligand binding and activation | 0.77691 | 0.60352 | 0.60352 | fgf1 | 1467.57 | 1467.57 | 1467.57 |  | 1467.57 |  | DOWN | 0 | 1 |
| 28Day | Phospholipase C-mediated cascade; FGFR3 | 0.77691 | 0.60352 | 0.60352 | fgf1 | 1467.57 | 1467.57 | 1467.57 |  | 1467.57 |  | DOWN | 0 | 1 |
| 28Day | RHO GTPases Activate Formins | 0.29062 | 0.82228 | 0.60405 | zwilch;dynll1;cenpt;tubb4b;tubb2a;pfn1;cdc42 | 3639.25714 | 3558.89 | 2359.45 | 1266.6887 | 3715.75771 | 1282.08584 | UP | 1 | 0 |
| 28Day | TCR signaling | 0.77201 | 0.39514 | 0.60511 | ube2n;pdpk1;ikbkg;h2-ab1;h2-aa | 3559.9316 | 3676.55 | 192.988 | 2110.26973 | 3695.28288 | 1546.16292 | DOWN | 0.2 | 0.8 |
| 28Day | Autodegradation of Cdh1 by Cdh1:APC/C | 0.77201 | 0.39514 | 0.60511 | psmd6;psmd8;psmf1;cdc27;psmb8 | 3948.96 | 4413.43 | 1415.14 | 1656.49498 | 3909.29906 | 1781.98522 | DOWN | 0.4 | 0.6 |
| 7Day | Signaling by VEGF | 0.74868 | 0.36551 | 0.60838 | nckap1;pak2;rasa1;prkcz;kras;hsp90aa1;cdc42;ctnnb1;calm3;calm2;brk1 | 3454.26211 | 3468.74 | 54.5232 | 1846.95429 | 3559.80325 | 2027.96172 | UP | 0.636363636 | 0.363636364 |
| 90Day | Mitochondrial protein import | 0.38412 | 1 | 0.60943 |  |  |  |  |  |  |  |  |  |  |
| 90Day | XBP1(S) activates chaperone genes | 0.38412 | 1 | 0.60943 |  |  |  |  |  |  |  |  |  |  |
| 90Day | Phase 3 - rapid repolarisation | 0.38412 | 1 | 0.60943 |  |  |  |  |  |  |  |  |  |  |
| 90Day | Synthesis of UDP-N-acetyl-glucosamine | 0.38412 | 1 | 0.60943 |  |  |  |  |  |  |  |  |  |  |
| 90Day | WNT mediated activation of DVL | 0.38412 | 1 | 0.60943 |  |  |  |  |  |  |  |  |  |  |
| 90Day | HuR (ELAVL1) binds and stabilizes mRNA | 0.38412 | 1 | 0.60943 |  |  |  |  |  |  |  |  |  |  |
| 90Day | Degradation of AXIN | 0.38412 | 1 | 0.60943 |  |  |  |  |  |  |  |  |  |  |

BMD analysis results for functional classification based on dose-responsive genes, using the Reactome database for gene sets in BMDExpress2.2 software.

| Study Day | Gene Set Name | Fisher's Exact Left P-Value | Fisher's Exact Right P-Value | Fisher's Exact Two Tail | Gene Symbols | BMD Mean | BMD Median | BMD Minimum | BMD Standard Deviation | BMD wMean | BMD wSD | Overall Direction | Percent Genes With Overall Direction Up | Percent Genes With Overall Direction Down |
|---|---|---|---|---|---|---|---|---|---|---|---|---|---|---|
| 90Day | Association of TriC/CCT with target proteins during biosynthesis | 0.38412 | 1 | 0.60943 | | | | | | | | | | |
| 90Day | Zinc influx into cells by the SLC39 gene family | 0.38412 | 1 | 0.60943 | | | | | | | | | | |
| 90Day | Recycling of eIF2:GDP | 0.38412 | 1 | 0.60943 | | | | | | | | | | |
| 90Day | Terminal pathway of complement | 0.38412 | 1 | 0.60943 | | | | | | | | | | |
| 90Day | Receptor Mediated Mitophagy | 0.38412 | 1 | 0.60943 | | | | | | | | | | |
| 90Day | Prostanoid ligand receptors | 0.3408 | 1 | 0.61011 | | | | | | | | | | |
| 90Day | MAPK1 (ERK2) activation | 0.3408 | 1 | 0.61011 | | | | | | | | | | |
| 90Day | Androgen biosynthesis | 0.3408 | 1 | 0.61011 | | | | | | | | | | |
| 90Day | IRE1alpha activates chaperones | 0.3408 | 1 | 0.61011 | | | | | | | | | | |
| 90Day | CLEC7A (Dectin-1) induces NFAT activation | 0.3408 | 1 | 0.61011 | | | | | | | | | | |
| 90Day | Phosphate bond hydrolysis by NTPDase proteins | 0.3408 | 1 | 0.61011 | | | | | | | | | | |
| 90Day | mitochondrial fatty acid beta-oxidation of saturated fatty acids | 0.3408 | 1 | 0.61011 | | | | | | | | | | |
| 90Day | Negative regulation of activity of TFAP2 (AP-2) family transcription factors | 0.3408 | 1 | 0.61011 | | | | | | | | | | |
| 90Day | Processive synthesis on the C-strand of the telomere | 0.3408 | 1 | 0.61011 | | | | | | | | | | |
| 90Day | Removal of the Flap Intermediate from the C-strand | 0.3408 | 1 | 0.61011 | | | | | | | | | | |
| 90Day | Calcineurin activates NFAT | 0.3408 | 1 | 0.61011 | | | | | | | | | | |
| 7Day | MAP kinase activation | 0.7534 | 0.42026 | 0.61038 | mapk3;map2k3;uba52;ppp2cb;btrc | 4058.048 | 4207.06 | 2894.34 | 807.460042 | 3936.95988 | 797.852297 | UP | 0.6 | 0.4 |
| 90Day | Synthesis of bile acids and bile salts | 0.74751 | 0.42928 | 0.61135 | osbpl3;cyp39a1;slc27a2;amacr;osbpl9 | 3411.314 | 3600.39 | 263.79 | 1964.39433 | 4212.33248 | 1569.77619 | DOWN | 0.2 | 0.8 |
| 90Day | Fatty acids | 0.74751 | 0.42928 | 0.61135 | cyp4f16;cyp4a12a;cyp4a12b;cyp2f2;cyp2d9 | 3738.306 | 3841.07 | 3465.22 | 207.288822 | 3648.77843 | 200.303123 | UP | 1 | 0 |
| 7Day | Caspase-mediated cleavage of cytoskeletal proteins | 0.37152 | 1 | 0.6131 | | | | | | | | | | |
| 7Day | Mismatch repair (MMR) directed by MSH2:MSH6 (MutSalpha) | 0.37152 | 1 | 0.6131 | | | | | | | | | | |
| 7Day | Bicarbonate transporters | 0.37152 | 1 | 0.6131 | | | | | | | | | | |
| 7Day | Retrograde neurotrophin signalling | 0.33647 | 1 | 0.61451 | | | | | | | | | | |
| 7Day | Mitochondrial iron-sulfur cluster biogenesis | 0.33647 | 1 | 0.61451 | | | | | | | | | | |
| 7Day | Triglyceride catabolism | 0.33647 | 1 | 0.61451 | | | | | | | | | | |
| 7Day | Hyaluronan metabolism | 0.33647 | 1 | 0.61451 | | | | | | | | | | |
| 7Day | CDC6 association with the ORC:origin complex | 0.33647 | 1 | 0.61451 | | | | | | | | | | |
| 7Day | Mismatch Repair | 0.33647 | 1 | 0.61451 | | | | | | | | | | |
| 7Day | Synthesis of PE | 0.33647 | 1 | 0.61451 | | | | | | | | | | |
| 7Day | Heme biosynthesis | 0.33647 | 1 | 0.61451 | | | | | | | | | | |
| 90Day | AKT phosphorylates targets in the nucleus | 0.30236 | 1 | 0.61561 | | | | | | | | | | |
| 90Day | MAPK3 (ERK1) activation | 0.30236 | 1 | 0.61561 | | | | | | | | | | |
| 90Day | Repression of WNT target genes | 0.30236 | 1 | 0.61561 | | | | | | | | | | |
| 90Day | HDR through MMEJ (alt-NHEJ) | 0.30236 | 1 | 0.61561 | | | | | | | | | | |
| 90Day | Golgi Cisternae Pericentriolar Stack Reorganization | 0.30236 | 1 | 0.61561 | | | | | | | | | | |
| 90Day | Interleukin-12 signaling | 0.30236 | 1 | 0.61561 | | | | | | | | | | |
| 90Day | Interleukin-21 signaling | 0.30236 | 1 | 0.61561 | | | | | | | | | | |
| 90Day | Degradation of DVL | 0.30236 | 1 | 0.61561 | | | | | | | | | | |
| 90Day | Mismatch repair (MMR) directed by MSH2:MSH6 (MutSalpha) | 0.30236 | 1 | 0.61561 | | | | | | | | | | |
| 90Day | Cohesin Loading onto Chromatin | 0.30236 | 1 | 0.61561 | | | | | | | | | | |
| 90Day | Prolonged ERK activation events | 0.30236 | 1 | 0.61561 | | | | | | | | | | |
| 90Day | Ketone body metabolism | 0.30236 | 1 | 0.61561 | | | | | | | | | | |
| 90Day | Bicarbonate transporters | 0.30236 | 1 | 0.61561 | | | | | | | | | | |

BMD analysis results for functional classification based on dose-responsive genes, using the Reactome database for gene sets in BMDExpress2.2 software.

| Study Day | Gene Set Name | Fisher's Exact Left P-Value | Fisher's Exact Right P-Value | Fisher's Exact Two Tail | Gene Symbols | BMD Mean | BMD Median | BMD Minimum | BMD Standard Deviation | BMD wMean | BMD wSD | Overall Direction | Percent Genes With Overall Direction Up | Percent Genes With Overall Direction Down |
|---|---|---|---|---|---|---|---|---|---|---|---|---|---|---|
| 7Day | Programmed Cell Death | 0.33284 | 0.78483 | 0.61684 | ywhaz;uba52;dsg1c;kpnb1;ctnnb1;casp9;xiap;dsp | 2944.24203 | 3337.06 | 54.5232 | 1884.89989 | 2724.23131 | 1970.66225 | DOWN | 0.375 | 0.625 |
| 90Day | Deactivation of the beta-catenin transactivating complex | 0.34528 | 0.83153 | 0.61768 | ywhaz;ctnnb1;btrc | 3125.89933 | 4087.04 | 137.958 | 2641.92219 | 4123.8011 | 2361.37721 | DOWN | 0.333333333 | 0.666666667 |
| 90Day | Apoptotic cleavage of cellular proteins | 0.34528 | 0.83153 | 0.61768 | rock1;dsg2;ctnnb1 | 2769.37067 | 3958.98 | 262.092 | 2172.31088 | 1769.95913 | 2251.57174 | DOWN | 0.333333333 | 0.666666667 |
| 28Day | PTK6 Regulates RHO GTPases, RAS GTPase and MAP kinases | 0.36923 | 1 | 0.61843 | | | | | | | | | | |
| 28Day | Translesion synthesis by REV1 | 0.36923 | 1 | 0.61843 | | | | | | | | | | |
| 28Day | Polymerase switching on the C-strand of the telomere | 0.36923 | 1 | 0.61843 | | | | | | | | | | |
| 28Day | Polymerase switching | 0.36923 | 1 | 0.61843 | | | | | | | | | | |
| 28Day | Leading Strand Synthesis | 0.36923 | 1 | 0.61843 | | | | | | | | | | |
| 28Day | Cell-extracellular matrix interactions | 0.36923 | 1 | 0.61843 | | | | | | | | | | |
| 28Day | Other semaphorin interactions | 0.36923 | 1 | 0.61843 | | | | | | | | | | |
| 28Day | Protein methylation | 0.36923 | 1 | 0.61843 | | | | | | | | | | |
| 28Day | Removal of the Flap Intermediate | 0.36923 | 1 | 0.61843 | | | | | | | | | | |
| 28Day | Reduction of cytosolic Ca++ levels | 0.36923 | 1 | 0.61843 | | | | | | | | | | |
| 7Day | VLDLR internalisation and degradation | 0.30473 | 1 | 0.61909 | | | | | | | | | | |
| 7Day | Pregnenolone biosynthesis | 0.30473 | 1 | 0.61909 | | | | | | | | | | |
| 7Day | WNT5A-dependent internalization of FZD2, FZD5 and ROR2 | 0.30473 | 1 | 0.61909 | | | | | | | | | | |
| 7Day | Regulated proteolysis of p75NTR | 0.30473 | 1 | 0.61909 | | | | | | | | | | |
| 7Day | TNFR1-induced proapoptotic signaling | 0.30473 | 1 | 0.61909 | | | | | | | | | | |
| 28Day | Transcriptional regulation by RUNX2 | 0.34384 | 1 | 0.61924 | | | | | | | | | | |
| 28Day | Calnexin/calreticulin cycle | 0.34384 | 1 | 0.61924 | | | | | | | | | | |
| 28Day | Translesion synthesis by POLK | 0.34384 | 1 | 0.61924 | | | | | | | | | | |
| 28Day | Translesion synthesis by POLI | 0.34384 | 1 | 0.61924 | | | | | | | | | | |
| 28Day | SUMOylation of transcription factors | 0.34384 | 1 | 0.61924 | | | | | | | | | | |
| 28Day | Asymmetric localization of PCP proteins | 0.34384 | 1 | 0.61924 | | | | | | | | | | |
| 28Day | Sema3A PAK dependent Axon repulsion | 0.34384 | 1 | 0.61924 | | | | | | | | | | |
| 28Day | Processive synthesis on the lagging strand | 0.34384 | 1 | 0.61924 | | | | | | | | | | |
| 90Day | Formation of a pool of free 40S subunits | 0.3062 | 0.85613 | 0.61942 | eif3m;rps27l;rps12 | 2578.52 | 2517.83 | 1662.63 | 947.693586 | 2378.76706 | 980.623942 | UP | 1 | 0 |
| 90Day | Interleukin-2 family signaling | 0.3062 | 0.85613 | 0.61942 | sos1;il9r;il15ra | 4914.30333 | 5362.87 | 3485.11 | 1265.98466 | 5245.72554 | 964.055041 | DOWN | 0.333333333 | 0.666666667 |
| 90Day | Signaling by NOTCH | 0.3062 | 0.85613 | 0.61942 | ywhaz;psen2;dll1 | 1908.146 | 2451.29 | 137.958 | 1570.70174 | 2157.20544 | 1492.98733 | DOWN | 0.333333333 | 0.666666667 |
| 90Day | Homologous DNA Pairing and Strand Exchange | 0.3062 | 0.85613 | 0.61942 | rad51;brca2;rad51c | 3127.57067 | 4249.95 | 513.022 | 2271.80208 | 3130.56464 | 2280.41 | UP | 1 | 0 |
| 7Day | Sphingolipid de novo biosynthesis | 0.34163 | 0.83276 | 0.62119 | 9130409i23rik;vapb;sptlc1 | 3872.38 | 3876.31 | 3688.99 | 181.456921 | 3849.15392 | 201.835608 | UP | 0.666666667 | 0.333333333 |
| 28Day | Metabolism of folate and pterines | 0.3202 | 1 | 0.62173 | | | | | | | | | | |
| 28Day | Interleukin-4 and Interleukin-13 signaling | 0.3202 | 1 | 0.62173 | | | | | | | | | | |
| 28Day | SCF(Skp2)-mediated degradation of p27/p21 | 0.3202 | 1 | 0.62173 | | | | | | | | | | |
| 28Day | Metabolism of nitric oxide | 0.3202 | 1 | 0.62173 | | | | | | | | | | |
| 28Day | eNOS activation and regulation | 0.3202 | 1 | 0.62173 | | | | | | | | | | |
| 90Day | Regulation of PTEN gene transcription | 0.28788 | 0.86721 | 0.62187 | cbx6;gatad2b;hdac2 | 1362.86367 | 744.949 | 202.162 | 1564.0529 | 727.677461 | 1043.9247 | UP | 1 | 0 |
| 7Day | Signaling by PTK6 | 0.30927 | 0.85324 | 0.62272 | uba52;rasa1;kras | 4902.11667 | 4761.56 | 4158.71 | 822.739577 | 5136.80433 | 831.742073 | UP | 0.666666667 | 0.333333333 |
| 7Day | Signaling by Non-Receptor Tyrosine Kinases | 0.30927 | 0.85324 | 0.62272 | uba52;rasa1;kras | 4902.11667 | 4761.56 | 4158.71 | 822.739577 | 5136.80433 | 831.742073 | UP | 0.666666667 | 0.333333333 |
| 90Day | P2Y receptors | 0.26825 | 1 | 0.62482 | | | | | | | | | | |
| 90Day | Interleukin-6 signaling | 0.26825 | 1 | 0.62482 | | | | | | | | | | |
| 90Day | Passive transport by Aquaporins | 0.26825 | 1 | 0.62482 | | | | | | | | | | |
| 90Day | Type I hemidesmosome assembly | 0.26825 | 1 | 0.62482 | | | | | | | | | | |
| 90Day | Mitochondrial iron-sulfur cluster biogenesis | 0.26825 | 1 | 0.62482 | | | | | | | | | | |
| 90Day | NOTCH1 Intracellular Domain Regulates Transcription | 0.26825 | 1 | 0.62482 | | | | | | | | | | |
| 90Day | RUNX3 regulates NOTCH signaling | 0.26825 | 1 | 0.62482 | | | | | | | | | | |

BMD analysis results for functional classification based on dose-responsive genes, using the Reactome database for gene sets in BMDExpress2.2 software.

| Study Day | Gene Set Name | Fisher's Exact Left P-Value | Fisher's Exact Right P-Value | Fisher's Exact Two Tail | Gene Symbols | BMD Mean | BMD Median | BMD Minimum | BMD Standard Deviation | BMD wMean | BMD wSD | Overall Direction | Percent Genes With Overall Direction Up | Percent Genes With Overall Direction Down |
|---|---|---|---|---|---|---|---|---|---|---|---|---|---|---|
| 90Day | Triglyceride catabolism | 0.26825 | 1 | 0.62482 | | | | | | | | | | |
| 90Day | Mismatch Repair | 0.26825 | 1 | 0.62482 | | | | | | | | | | |
| 90Day | p75NTR recruits signalling complexes | 0.26825 | 1 | 0.62482 | | | | | | | | | | |
| 90Day | Growth hormone receptor signaling | 0.26825 | 1 | 0.62482 | | | | | | | | | | |
| 90Day | Heme biosynthesis | 0.26825 | 1 | 0.62482 | | | | | | | | | | |
| 90Day | Signaling by EGFR | 0.79506 | 0.35492 | 0.62529 | tgfa;sos1;sh3gl3;gab1;cdc42;areg | 2929.49583 | 3066.45 | 126.428 | 2508.88906 | 3628.85041 | 2226.41237 | UP | 0.666666667 | 0.333333333 |
| 28Day | Formation of Senescence-Associated Heterochromatin Foci (SAHF) | 0.29818 | 1 | 0.62569 | | | | | | | | | | |
| 28Day | Translesion Synthesis by POLH | 0.29818 | 1 | 0.62569 | | | | | | | | | | |
| 28Day | Synthesis, secretion, and deacylation of Ghrelin | 0.29818 | 1 | 0.62569 | | | | | | | | | | |
| 28Day | Interferon gamma signaling | 0.29818 | 1 | 0.62569 | | | | | | | | | | |
| 28Day | Macroautophagy | 0.32716 | 0.84063 | 0.62613 | dynll1;rb1cc1;atg5 | 5807.87333 | 5791.54 | 5747.14 | 70.3369983 | 5786.29948 | 55.9545375 | UP | 1 | 0 |
| 28Day | Peptide hormone metabolism | 0.32716 | 0.84063 | 0.62613 | exoc4;mme;agt | 2953.18267 | 2439.57 | 776.548 | 2473.759 | 2533.74323 | 2521.18437 | DOWN | 0.333333333 | 0.666666667 |
| 28Day | Interferon Signaling | 0.32716 | 0.84063 | 0.62613 | ube2n;arih1;ppm1b | 4090.57 | 5266.71 | 1290.26 | 2435.46398 | 2838.72879 | 2524.17867 | DOWN | 0.333333333 | 0.666666667 |
| 28Day | Collagen biosynthesis and modifying enzymes | 0.32716 | 0.84063 | 0.62613 | p4hb;col8a1;bmp1 | 3663.75333 | 4236.71 | 1023.63 | 2405.38028 | 3386.85404 | 2424.23445 | UP | 0.666666667 | 0.333333333 |
| 28Day | L1CAM interactions | 0.32716 | 0.84063 | 0.62613 | ranbp9;tubb4b;tubb2a | 3634.13667 | 2903.04 | 2359.45 | 1758.19442 | 2994.52802 | 1118.88605 | UP | 1 | 0 |
| 7Day | TRAF6 mediated NF-kB activation | 0.27598 | 1 | 0.62624 | | | | | | | | | | |
| 7Day | LGI-ADAM interactions | 0.27598 | 1 | 0.62624 | | | | | | | | | | |
| 7Day | cGMP effects | 0.27598 | 1 | 0.62624 | | | | | | | | | | |
| 7Day | BBSome-mediated cargo-targeting to cilium | 0.27598 | 1 | 0.62624 | | | | | | | | | | |
| 7Day | Insulin receptor signalling cascade | 0.27915 | 0.8715 | 0.62708 | mapk3;ptpn11;fgf1 | 3692.55667 | 3629.67 | 2647.76 | 1077.61709 | 3582.43453 | 1145.05081 | DOWN | 0.333333333 | 0.666666667 |
| 7Day | Formation of TC-NER Pre-Incision Complex | 0.27915 | 0.8715 | 0.62708 | prpf19;polr2h;uba52 | 3815.36333 | 3964.6 | 2719.93 | 1028.96402 | 3913.27434 | 885.21152 | UP | 1 | 0 |
| 28Day | Collagen degradation | 0.30436 | 0.85499 | 0.62791 | phykpl;tmprss6;col8a1 | 2918.14967 | 4236.71 | 182.399 | 2369.74276 | 3669.8463 | 1804.74723 | UP | 0.666666667 | 0.333333333 |
| 28Day | ER to Golgi Anterograde Transport | 0.74133 | 0.36731 | 0.62837 | lman2;dynll1;ppp6r3;tubb4b;tubb2a;sec22c;serpina1e;serpina1b;f5;capza2;bet1;gbf1 | 3877.92175 | 3700.625 | 619.741 | 1602.85433 | 3499.22612 | 1690.42867 | CONFLICT | 0.5 | 0.5 |
| 28Day | Biosynthesis of the N-glycan precursor (dolichol lipid-linked oligosaccharide, LLO) and transfer to a nascent protein | 0.29339 | 0.86173 | 0.62935 | nanp;gne;gfpt1 | 5085.35667 | 5755.83 | 3647.63 | 1246.04778 | 5180.06702 | 1205.69221 | DOWN | 0.333333333 | 0.666666667 |
| 28Day | Unfolded Protein Response (UPR) | 0.27768 | 1 | 0.63088 | | | | | | | | | | |
| 28Day | DARPP-32 events | 0.27768 | 1 | 0.63088 | | | | | | | | | | |
| 28Day | Ephrin signaling | 0.27768 | 1 | 0.63088 | | | | | | | | | | |
| 28Day | Assembly of collagen fibrils and other multimeric structures | 0.28271 | 0.8682 | 0.63112 | ctss;col8a1;bmp1 | 3680.24333 | 4236.71 | 1023.63 | 2426.71234 | 3369.41807 | 2436.78186 | UP | 0.666666667 | 0.333333333 |
| 7Day | TCF dependent signaling in response to WNT | 0.71383 | 0.39986 | 0.6321 | gsk3b;klhl12;ywhaz;uba52;sox6;ppp2cb;lrp5;csnk2b;ctnnb1;btrc;xiap;xpo1 | 3254.95768 | 3747.19 | 54.5232 | 1671.32215 | 3246.91196 | 1784.39588 | UP | 0.666666667 | 0.333333333 |
| 7Day | HDR through Homologous Recombination (HRR) or Single Strand Annealing (SSA) | 0.31514 | 0.79329 | 0.63373 | ube2n;ube2v2;rnf168;hist1h4h;babam1;hist1h2bc;uba52;rad51ap1;abl1 | 3610.97889 | 3444.79 | 2423.08 | 647.933214 | 3488.58257 | 659.371908 | UP | 0.777777778 | 0.222222222 |
| 7Day | Eicosanoid ligand-binding receptors | 0.24994 | 1 | 0.63543 | | | | | | | | | | |
| 7Day | GRB2:SOS provides linkage to MAPK signaling for Integrins | 0.24994 | 1 | 0.63543 | | | | | | | | | | |
| 7Day | p130Cas linkage to MAPK signaling for integrins | 0.24994 | 1 | 0.63543 | | | | | | | | | | |
| 7Day | Synthesis of PIPs at the Golgi membrane | 0.24994 | 1 | 0.63543 | | | | | | | | | | |
| 7Day | Resolution of Sister Chromatid Cohesion | 0.29486 | 0.80912 | 0.63556 | clasp2;pds5a;cenpk;tubb4b;tubb2a;tuba4a;ppp2cb;kif2a;xpo1 | 3022.26178 | 3627.04 | 919.856 | 1221.78757 | 3036.17958 | 1202.74898 | UP | 0.888888889 | 0.111111111 |
| 90Day | RIP-mediated NFkB activation via ZBP1 | 0.85486 | 0.39885 | 0.63684 | nfkbia;ikbkg | 3433.33 | 3433.33 | 3265.56 | 237.262609 | 3311.77597 | 163.5322 | CONFLICT | 0.5 | 0.5 |
| 90Day | Erythropoietin activates Phosphoinositide-3-kinase (PI3K) | 0.85486 | 0.39885 | 0.63684 | irs2;gab1 | 100.62065 | 100.62065 | 74.8133 | 36.4971044 | 86.6473692 | 30.6844174 | DOWN | 0 | 1 |
| 90Day | Dectin-1 mediated noncanonical NF-kB signaling | 0.85486 | 0.39885 | 0.63684 | ube2m;btrc | 2915.405 | 2915.405 | 678.11 | 3164.01293 | 2982.75275 | 3162.57907 | CONFLICT | 0.5 | 0.5 |
| 90Day | NIK-->noncanonical NF-kB signaling | 0.85486 | 0.39885 | 0.63684 | ube2m;btrc | 2915.405 | 2915.405 | 678.11 | 3164.01293 | 2982.75275 | 3162.57907 | CONFLICT | 0.5 | 0.5 |
| 90Day | Reversible hydration of carbon dioxide | 0.85486 | 0.39885 | 0.63684 | car5a;car3 | 2229.49 | 2229.49 | 859.92 | 1936.86447 | 1474.33408 | 1615.83509 | CONFLICT | 0.5 | 0.5 |

BMD analysis results for functional classification based on dose-responsive genes, using the Reactome database for gene sets in BMDExpress2.2 software.

| Study Day | Gene Set Name | Fisher's Exact Left P-Value | Fisher's Exact Right P-Value | Fisher's Exact Two Tail | Gene Symbols | BMD Mean | BMD Median | BMD Minimum | BMD Standard Deviation | BMD wMean | BMD wSD | Overall Direction | Percent Genes With Overall Direction Up | Percent Genes With Overall Direction Down |
|---|---|---|---|---|---|---|---|---|---|---|---|---|---|---|
| 90Day | Purine ribonucleoside monophosphate biosynthesis | 0.85486 | 0.39885 | 0.63684 | gmps;atic | 3841.07 | 3841.07 | 2515.37 | 1874.82292 | 3607.96146 | 1845.6115 | UP | 1 | 0 |
| 90Day | MAP3K8 (TPL2)-dependent MAPK1/3 activation | 0.85486 | 0.39885 | 0.63684 | ikbkg;btrc | 4209.13 | 4209.13 | 3265.56 | 1334.40949 | 4331.39024 | 1323.16044 | CONFLICT | 0.5 | 0.5 |
| 90Day | Triglyceride biosynthesis | 0.85486 | 0.39885 | 0.63684 | dgat2;agmo | 3065.025 | 3065.025 | 2903.14 | 228.939963 | 3009.70495 | 215.157829 | DOWN | 0 | 1 |
| 90Day | CD28 dependent Vav1 pathway | 0.85486 | 0.39885 | 0.63684 | vav1;cdc42 | 2158.7685 | 2158.7685 | 156.487 | 2831.65365 | 2296.14268 | 2824.98125 | CONFLICT | 0.5 | 0.5 |
| 90Day | Negative regulators of DDX58/IFIH1 signaling | 0.85486 | 0.39885 | 0.63684 | tbk1;pin1 | 3003.045 | 3003.045 | 1058.39 | 2750.15748 | 2467.79178 | 2643.93156 | CONFLICT | 0.5 | 0.5 |
| 7Day | Post-translational protein phosphorylation | 0.75206 | 0.35185 | 0.6369 | apoa5;apob;hsp90b1;nucb1;igfbp5;f5;csf1;c4b;serpinc1;apoe;ahsg;afp;qsox1 | 2429.02581 | 1999.21 | 85.9375 | 2022.85744 | 2176.0983 | 2216.29449 | DOWN | 0.230769231 | 0.769230769 |
| 28Day | ERK/MAPK targets | 0.25858 | 1 | 0.63713 | | | | | | | | | | |
| 28Day | Unblocking of NMDA receptors, glutamate binding and activation | 0.25858 | 1 | 0.63713 | | | | | | | | | | |
| 28Day | Oxygen-dependent proline hydroxylation of Hypoxia-inducible Factor Alpha | 0.25858 | 1 | 0.63713 | | | | | | | | | | |
| 28Day | Signaling by NOTCH3 | 0.25858 | 1 | 0.63713 | | | | | | | | | | |
| 28Day | Regulation of FZD by ubiquitination | 0.25858 | 1 | 0.63713 | | | | | | | | | | |
| 28Day | NOTCH3 Activation and Transmission of Signal to the Nucleus | 0.25858 | 1 | 0.63713 | | | | | | | | | | |
| 28Day | Post NMDA receptor activation events | 0.25858 | 1 | 0.63713 | | | | | | | | | | |
| 90Day | Metabolism of vitamins and cofactors | 0.73926 | 0.33982 | 0.63779 | mccc2;pank1;nmnat3;slc52a3;pccb;pdss1;slc23a2;apob;ttr;pdxk;sdc4;rbp1;pcx;mut;mthfd2;rdh11;hsp90aa1;apoe;apoc3;aox1;hlcs;pcca;aldh1l1 | 2609.66878 | 2679.72 | 175.96 | 1884.21897 | 2916.31643 | 1749.4064 | DOWN | 0.347826087 | 0.652173913 |
| 28Day | Respiratory electron transport, ATP synthesis by chemiosmotic coupling, and heat production by uncoupling proteins. | 0.76649 | 0.38594 | 0.63835 | ndufab1;ndufaf1;ndufc2;atp5g2;etfdh;atp5j2 | 3654.68167 | 3868.245 | 1023.12 | 2215.21614 | 3642.68542 | 2294.18332 | DOWN | 0.333333333 | 0.666666667 |
| 7Day | Metabolism of carbohydrates | 0.33242 | 0.75078 | 0.6389 | man2c1;dcxr;pfkp;hs3st3b1;hgsnat;gckr;uba52;sdc3;pgam1;man2b1;hyal1;gpi1;ext1;calm3;calm2;bgn;arsb;pgd | 3574.79881 | 3642.14 | 34.2395 | 1573.30178 | 3501.90606 | 1542.14129 | DOWN | 0.277777778 | 0.722222222 |
| 7Day | G1/S Transition | 0.74188 | 0.41754 | 0.64308 | uba52;prim2;ppp2cb;cdkn1a;cdc25a;ccne2 | 4281.55333 | 4302.165 | 2818.63 | 1050.99246 | 4140.65106 | 1002.74435 | UP | 1 | 0 |
| 28Day | Receptor-type tyrosine-protein phosphatases | 0.84574 | 0.40347 | 0.64426 | ptprd;il1rap | 3615.755 | 3615.755 | 3526 | 126.932738 | 3624.67675 | 126.304096 | DOWN | 0 | 1 |
| 28Day | Na+/Cl- dependent neurotransmitter transporters | 0.84574 | 0.40347 | 0.64426 | slc22a1;slc6a13 | 916.396 | 916.396 | 151.142 | 1082.23259 | 892.041183 | 1081.68436 | DOWN | 0 | 1 |
| 28Day | Endosomal/Vacuolar pathway | 0.84574 | 0.40347 | 0.64426 | h2-q7;h2-d1 | 4749.05 | 4749.05 | 3718.12 | 1457.95519 | 4309.40997 | 1318.73675 | CONFLICT | 0.5 | 0.5 |
| 28Day | RHO GTPases activate PAKs | 0.84574 | 0.40347 | 0.64426 | cdc42;mylk | 3872.595 | 3872.595 | 2463.49 | 1992.7754 | 3650.52709 | 1967.87334 | UP | 1 | 0 |
| 28Day | VxPx cargo-targeting to cilium | 0.84574 | 0.40347 | 0.64426 | rab11a;exoc4 | 2316.245 | 2316.245 | 2192.92 | 174.407888 | 2290.29724 | 170.50378 | UP | 1 | 0 |
| 7Day | Calnexin/calreticulin cycle | 0.83789 | 0.41985 | 0.6462 | uba52;sel1l | 4493.74 | 4493.74 | 4225.92 | 378.754676 | 4638.58379 | 318.583834 | UP | 1 | 0 |
| 7Day | Phosphorylation of CD3 and TCR zeta chains | 0.83789 | 0.41985 | 0.6462 | h2-ab1;h2-aa | 2062.21 | 2062.21 | 1863.06 | 281.640631 | 2105.93651 | 274.767957 | DOWN | 0 | 1 |
| 7Day | Activation of IRF3/IRF7 mediated by TBK1/IKK epsilon | 0.83789 | 0.41985 | 0.6462 | uba52;ptpn11 | 4195.615 | 4195.615 | 3629.67 | 800.367095 | 4234.65504 | 798.460542 | UP | 1 | 0 |
| 7Day | Sema3A PAK dependent Axon repulsion | 0.83789 | 0.41985 | 0.6462 | pak2;hsp90aa1 | 1771.905 | 1771.905 | 1005.61 | 1083.70478 | 1287.67812 | 839.919468 | UP | 1 | 0 |
| 7Day | Regulation of necroptotic cell death | 0.83789 | 0.41985 | 0.6462 | uba52;xiap | 4817.795 | 4817.795 | 4761.56 | 79.5282997 | 4830.99188 | 77.3074074 | CONFLICT | 0.5 | 0.5 |

BMD analysis results for functional classification based on dose-responsive genes, using the Reactome database for gene sets in BMDExpress2.2 software.

| Study Day | Gene Set Name | Fisher's Exact Left P-Value | Fisher's Exact Right P-Value | Fisher's Exact Two Tail | Gene Symbols | BMD Mean | BMD Median | BMD Minimum | BMD Standard Deviation | BMD wMean | BMD wSD | Overall Direction | Percent Genes With Overall Direction Up | Percent Genes With Overall Direction Down |
|---|---|---|---|---|---|---|---|---|---|---|---|---|---|---|
| 7Day | Metabolism | 0.69987 | 0.33236 | 0.64802 | hadha;ugt1a6a;pla1a;akr1c6;lias;mccc2;fads1;gstk1;dmgdh;man2c1;ugt2b1;amdhd1;kyat1;ndufaf1;elovl5;fitm1;ndufaf4;adipor2;ndufc2;bphl;nudt12;dcxr;coq10b;dgat2;qprt;ndufa13;lipt2;ndufa6;sdha;pccb;crls1;tnfaip8l1;bhmt2;dpys;9130409i23rik;mocs1;txn2;vapb;fads2;pfkp;cyp3a25;ptges3;prodh2;cyp39a1;stard10;hs3st3b1;ndufa1;mtmr7;nudt5;acaa2;hgsnat;txnrd1;ugt1a1;ugt1a9;idi1;pdhx;gcdh;idh2;ecsit;ahcy;sptlc1;slc27a5;decr2;btd;naxe;uroc1;ugt2b35;apob;ces2c;blvrb;ugt2b36;gckr;osbpl2;ugt3a2;ugt2b5;ugdh;uba52;ttr;mtmr6;itpk1;aldh4a1;sdc3;smpd2;smpd1;slc25a17;slc22a1;slc10a2;slc10a1;sardh;pten;ptdss1;prkar2a;ppt1;pgam1;nqo2;nqo1;neu1;ndufa2;ncoa2;ncoa1;man2b1;idh3b;lrp1;phyh;itpr2;kpnb1;hyal1;hsp90aa1;hsd17b4;hsd17b2;hsd11b1;hmgcs2;hao1;h2-ke6;gstp1;gstp2;gstm4;gsta1;gss;gpi1;gnmt;gclc;gc;ext1;ces3b;esd;ephx2;ebp;dld;cyp3a11;cyp2e1;cyp2c37;cyp2c29;elovl3;cdo1;entpd5;calm3;calm2;bgn;bckdha;baat;atp5j;arsb;arnt;apoe;acs | 2811.83118 | 3128.375 | 34.2395 | 1721.84357 | 2825.66182 | 1617.98483 | CONFLICT | 0.422619048 | 0.577380952 |
| 90Day | ZBP1(DAI) mediated induction of type I IFNs | 0.82629 | 0.43979 | 0.65092 | nfkbia;ikbkg | 3433.33 | 3433.33 | 3265.56 | 237.262609 | 3311.77597 | 163.5322 | CONFLICT | 0.5 | 0.5 |
| 90Day | TRAF6 mediated NF-kB activation | 0.82629 | 0.43979 | 0.65092 | nfkbia;ikbkg | 3433.33 | 3433.33 | 3265.56 | 237.262609 | 3311.77597 | 163.5322 | CONFLICT | 0.5 | 0.5 |
| 90Day | Trafficking of GluR2-containing AMPA receptors | 0.82629 | 0.43979 | 0.65092 | gria3;ap2m1 | 2040.685 | 2040.685 | 1097.82 | 1333.41247 | 1421.13725 | 1005.14177 | UP | 1 | 0 |
| 90Day | Apoptotic cleavage of cell adhesion proteins | 0.82629 | 0.43979 | 0.65092 | dsg2;ctnnb1 | 4023.01 | 4023.01 | 3958.98 | 90.5520944 | 4010.29747 | 88.7494518 | DOWN | 0 | 1 |
| 90Day | Signalling to RAS | 0.82629 | 0.43979 | 0.65092 | mapk14;sos1 | 5078.445 | 5078.445 | 4261.96 | 1154.68416 | 5603.32821 | 884.472008 | DOWN | 0 | 1 |
| 90Day | Interleukin-15 signaling | 0.82629 | 0.43979 | 0.65092 | sos1;il15ra | 4690.02 | 4690.02 | 3485.11 | 1704.00006 | 5116.83047 | 1593.51243 | DOWN | 0 | 1 |
| 90Day | Complex I biogenesis | 0.33942 | 0.81812 | 0.65165 | ndufab1;ndufc2;ndufaf3;ndufb9 | 3371.749 | 3776.765 | 105.476 | 2395.08756 | 4696.0207 | 2048.29171 | CONFLICT | 0.5 | 0.5 |
| 28Day | Nucleotide salvage | 0.82865 | 0.42791 | 0.65213 | hprt;adk | 2990.7 | 2990.7 | 2420.29 | 806.681558 | 3160.53958 | 770.093613 | CONFLICT | 0.5 | 0.5 |
| 28Day | Synaptic adhesion-like molecules | 0.82865 | 0.42791 | 0.65213 | gria3;ptprd | 2789.285 | 2789.285 | 2052.57 | 1041.87234 | 2470.20021 | 939.078155 | CONFLICT | 0.5 | 0.5 |
| 28Day | Synthesis of epoxy (EET) and dihydroxyeicosatrienoic acids (DHET) | 0.82865 | 0.42791 | 0.65213 | cyp2c37;cyp2c29 | 4152.97 | 4152.97 | 2751.06 | 1982.60014 | 3551.51531 | 1790.86789 | CONFLICT | 0.5 | 0.5 |
| 28Day | PCNA-Dependent Long Patch Base Excision Repair | 0.82865 | 0.42791 | 0.65213 | pole3;polb | 3329.279 | 3329.279 | 805.318 | 3569.41988 | 4286.22182 | 3302.91979 | UP | 1 | 0 |
| 7Day | RNA Polymerase I Promoter Opening | 0.71164 | 0.4521 | 0.65406 | hist1h4h;hist1h2bc;hist2h2ac;mapk3;ubtf;hist2h2aa1 | 3863.02833 | 3802.835 | 1976.31 | 1206.57215 | 4000.90003 | 1135.9748 | CONFLICT | 0.5 | 0.5 |
| 7Day | Nonhomologous End-Joining (NHEJ) | 0.71164 | 0.4521 | 0.65406 | ube2n;ube2v2;rnf168;hist1h4h;babam1;hist1h2bc | 3415.31167 | 3431.595 | 2423.08 | 578.797266 | 3318.19796 | 582.327022 | UP | 0.833333333 | 0.166666667 |
| 7Day | Negative epigenetic regulation of rRNA expression | 0.35082 | 0.80908 | 0.6546 | hist1h4h;hist1h2bc;hist2h2ac;hist2h2aa1 | 4100.405 | 3802.835 | 3406.55 | 933.741438 | 4060.85571 | 1011.0164 | CONFLICT | 0.5 | 0.5 |
| 90Day | Condensation of Prophase Chromosomes | 0.3045 | 0.84174 | 0.65474 | smc4;hist1h4h;hist1h4i;h2afx | 3714.72 | 3979.26 | 2814.71 | 602.516084 | 3716.61964 | 599.320578 | CONFLICT | 0.5 | 0.5 |
| 90Day | Apoptotic execution phase | 0.3045 | 0.84174 | 0.65474 | hmgb2;rock1;dsg2;ctnnb1 | 2668.968 | 3163.37 | 262.092 | 1785.01517 | 2087.46111 | 1493.84895 | CONFLICT | 0.5 | 0.5 |
| 28Day | Transport to the Golgi and subsequent modification | 0.71862 | 0.38442 | 0.65796 | lman2;dynll1;ppp6r3;tubb4b;tubb2a;mgat2;sec22c;serpina1e;serpina1b;man1a;f5;capza2;bet1;gbf1 | 3585.64393 | 3488.25 | 185.394 | 1772.84744 | 3440.52945 | 1628.71841 | CONFLICT | 0.5 | 0.5 |
| 7Day | mRNA decay by 3' to 5' exoribonuclease | 0.81362 | 0.4532 | 0.65819 | wdr61;hbs1l | 4801.71 | 4801.71 | 3952.2 | 1201.38856 | 4349.57954 | 1017.09909 | UP | 1 | 0 |
| 7Day | Metabolism of folate and pterines | 0.81362 | 0.4532 | 0.65819 | shmt2;aldh1l1 | 2129.5301 | 2129.5301 | 93.0602 | 2880.00335 | 2537.57278 | 2821.59913 | DOWN | 0 | 1 |
| 7Day | Regulation of pyruvate dehydrogenase (PDH) complex | 0.81362 | 0.4532 | 0.65819 | pdhx;dld | 4987.44 | 4987.44 | 4831.25 | 220.886016 | 4979.91771 | 220.629696 | CONFLICT | 0.5 | 0.5 |
| 7Day | Hedgehog ligand biogenesis | 0.81362 | 0.4532 | 0.65819 | uba52;sel1l | 4493.74 | 4493.74 | 4225.92 | 378.754676 | 4638.58379 | 318.583834 | UP | 1 | 0 |
| 7Day | Organic cation/anion/zwitterion transport | 0.81362 | 0.4532 | 0.65819 | slc22a12;slc22a1 | 3715.525 | 3715.525 | 3194.01 | 737.533586 | 3488.48892 | 663.976675 | CONFLICT | 0.5 | 0.5 |

BMD analysis results for functional classification based on dose-responsive genes, using the Reactome database for gene sets in BMDExpress2.2 software.

| Study Day | Gene Set Name | Fisher's Exact Left P-Value | Fisher's Exact Right P-Value | Fisher's Exact Two Tail | Gene Symbols | BMD Mean | BMD Median | BMD Minimum | BMD Standard Deviation | BMD wMean | BMD wSD | Overall Direction | Percent Genes With Overall Direction Up | Percent Genes With Overall Direction Down |
|---|---|---|---|---|---|---|---|---|---|---|---|---|---|---|
| 28Day | Metabolism of vitamins and cofactors | 0.71156 | 0.39228 | 0.65934 | akr1c6;nudt12;akr1c12;akr1c19;apob;coq3;enpp1;pcx;lrp1;gpc4;apoe;acp5;cyb5a;akr1c14 | 3208.65343 | 3167.23 | 201.213 | 1768.46381 | 2676.66634 | 1701.17942 | DOWN | 0.214285714 | 0.785714286 |
| 28Day | Cellular response to heat stress | 0.32799 | 0.8236 | 0.65979 | hikeshi;gm45902;mapkapk2;tpr | 4640.02 | 4764.775 | 3638.67 | 883.900811 | 4474.97086 | 799.34375 | CONFLICT | 0.5 | 0.5 |
| 7Day | Separation of Sister Chromatids | 0.34119 | 0.76327 | 0.66025 | clasp2;pds5a;cenpk;tubb4b;uba52;tubb2a;tuba4a;cdc27;ppp2cb;kif2a;xpo1 | 3257.49964 | 3647.06 | 919.856 | 1227.93386 | 3222.5988 | 1220.34245 | UP | 0.909090909 | 0.090909091 |
| 28Day | Sulfur amino acid metabolism | 0.81106 | 0.4518 | 0.6606 | ahcy;gm4737 | 2386.29 | 2386.29 | 2114.57 | 384.270109 | 2337.94463 | 378.13882 | DOWN | 0 | 1 |
| 28Day | Mitochondrial biogenesis | 0.81106 | 0.4518 | 0.6606 | atp5g2;atp5j2 | 5554.105 | 5554.105 | 5480.89 | 103.541646 | 5551.28634 | 103.464887 | CONFLICT | 0.5 | 0.5 |
| 7Day | Mitotic Anaphase | 0.31208 | 0.78707 | 0.66188 | clasp2;pds5a;cenpk;tubb4b;uba52;tubb2a;tuba4a;cdc27;ppp2cb;kif2a;xpo1 | 3257.49964 | 3647.06 | 919.856 | 1227.93386 | 3222.5988 | 1220.34245 | UP | 0.909090909 | 0.090909091 |
| 28Day | Integration of energy metabolism | 0.30735 | 0.83765 | 0.6619 | adipor2;gnb5;adcy9;acly | 3048.6095 | 3510.095 | 953.648 | 1529.81693 | 2364.85446 | 1615.99454 | DOWN | 0.25 | 0.75 |
| 90Day | KSRP (KHSRP) binds and destabilizes mRNA | 0.79632 | 0.47914 | 0.66645 | exosc9;ywhaz | 1471.424 | 1471.424 | 137.958 | 1885.8057 | 1856.1388 | 1805.61685 | UP | 1 | 0 |
| 90Day | p130Cas linkage to MAPK signaling for integrins | 0.79632 | 0.47914 | 0.66645 | tln1;fn1 | 3294.495 | 3294.495 | 2110.06 | 1675.04404 | 3616.30164 | 1612.03397 | DOWN | 0 | 1 |
| 90Day | SHC1 events in ERBB4 signaling | 0.79632 | 0.47914 | 0.66645 | nrg1;sos1 | 4903.635 | 4903.635 | 3912.34 | 1401.90283 | 5120.14662 | 1368.05592 | CONFLICT | 0.5 | 0.5 |
| 90Day | GRB2 events in ERBB2 signaling | 0.79632 | 0.47914 | 0.66645 | nrg1;sos1 | 4903.635 | 4903.635 | 3912.34 | 1401.90283 | 5120.14662 | 1368.05592 | CONFLICT | 0.5 | 0.5 |
| 90Day | Cell-extracellular matrix interactions | 0.79632 | 0.47914 | 0.66645 | arhgef6;actn1 | 5633.74 | 5633.74 | 5314.58 | 451.360401 | 5440.61636 | 359.350429 | DOWN | 0 | 1 |
| 90Day | Methylation | 0.79632 | 0.47914 | 0.66645 | ahcy;gm4737 | 1523.115 | 1523.115 | 1418.37 | 148.1318 | 1471.13381 | 128.603818 | DOWN | 0 | 1 |
| 90Day | FGFR4 ligand binding and activation | 0.79632 | 0.47914 | 0.66645 | klb;fgf1 | 2046.3595 | 2046.3595 | 242.429 | 2551.14298 | 3002.17622 | 2163.59869 | DOWN | 0 | 1 |
| 28Day | MyD88-independent TLR4 cascade | 0.75369 | 0.38892 | 0.667 | ube2n;map2k4;mapkapk2;ly96;ikbkg;app;birc2 | 4818.41571 | 5266.71 | 2616.5 | 1073.14504 | 4865.34093 | 1108.40121 | CONFLICT | 0.571428571 | 0.428571429 |
| 28Day | TRIF(TICAM1)-mediated TLR4 signaling | 0.75369 | 0.38892 | 0.667 | ube2n;map2k4;mapkapk2;ly96;ikbkg;app;birc2 | 4818.41571 | 5266.71 | 2616.5 | 1073.14504 | 4865.34093 | 1108.40121 | CONFLICT | 0.571428571 | 0.428571429 |
| 28Day | Signaling by ROBO receptors | 0.79303 | 0.47512 | 0.66955 | pfn1;dag1 | 5248.835 | 5248.835 | 4831.18 | 590.653365 | 5394.18337 | 553.731975 | CONFLICT | 0.5 | 0.5 |
| 28Day | Generation of second messenger molecules | 0.79303 | 0.47512 | 0.66955 | h2-ab1;h2-aa | 3461.14 | 3461.14 | 3245.73 | 304.635743 | 3292.13505 | 188.885132 | DOWN | 0 | 1 |
| 28Day | SMAD2/SMAD3:SMAD4 heterotrimer regulates transcription | 0.79303 | 0.47512 | 0.66955 | tfdp1;ccnk | 5399.625 | 5399.625 | 5090.85 | 436.673793 | 5395.60681 | 436.636817 | CONFLICT | 0.5 | 0.5 |
| 28Day | Triglyceride metabolism | 0.79303 | 0.47512 | 0.66955 | dgat2;agmo | 1526.6865 | 1526.6865 | 163.973 | 1927.16791 | 2004.73883 | 1804.69059 | DOWN | 0 | 1 |
| 28Day | Transcriptional Regulation by E2F6 | 0.79303 | 0.47512 | 0.66955 | tfdp1;bmi1 | 4813.43 | 4813.43 | 3918.46 | 1265.67871 | 5237.63724 | 1114.46805 | UP | 1 | 0 |
| 7Day | Regulation of TLR by endogenous ligand | 0.78849 | 0.48543 | 0.67107 | apob;lbp | 3620.015 | 3620.015 | 1999.21 | 2292.16441 | 4179.97575 | 2151.02432 | DOWN | 0 | 1 |
| 7Day | ABC transporters in lipid homeostasis | 0.78849 | 0.48543 | 0.67107 | abcg8;abca3 | 3065.465 | 3065.465 | 2076.62 | 1398.43801 | 3487.61295 | 1264.59918 | DOWN | 0 | 1 |
| 7Day | G0 and Early G1 | 0.78849 | 0.48543 | 0.67107 | tfdp1;ccne2 | 2652.727 | 2652.727 | 707.264 | 2751.30016 | 3693.00674 | 2324.92767 | UP | 1 | 0 |
| 7Day | RIPK1-mediated regulated necrosis | 0.78849 | 0.48543 | 0.67107 | uba52;xiap | 4817.795 | 4817.795 | 4761.56 | 79.5282997 | 4830.99188 | 77.3074074 | CONFLICT | 0.5 | 0.5 |
| 7Day | Regulated Necrosis | 0.78849 | 0.48543 | 0.67107 | uba52;xiap | 4817.795 | 4817.795 | 4761.56 | 79.5282997 | 4830.99188 | 77.3074074 | CONFLICT | 0.5 | 0.5 |
| 7Day | L1CAM interactions | 0.71955 | 0.43053 | 0.6728 | ranbp9;sdcbp;mapk3;tubb4b;tubb2a;tuba4a;csnk2b | 2354.63657 | 2094.04 | 778.73 | 1408.22263 | 2352.67584 | 1511.15062 | UP | 0.857142857 | 0.142857143 |
| 7Day | Signaling by FGFR2 | 0.70542 | 0.4464 | 0.67706 | mapk3;polr2h;uba52;ptpn11;ppp2cb;kras;fgf1 | 3941.36857 | 3964.6 | 2647.76 | 744.707179 | 3839.81356 | 761.564281 | UP | 0.714285714 | 0.285714286 |
| 90Day | Hedgehog 'off' state | 0.36704 | 0.78498 | 0.67737 | tubb6;ift52;tubb4b;tubb2a;tuba1b | 1277.8726 | 1722.38 | 154.682 | 776.85001 | 1233.28221 | 659.90165 | UP | 0.6 | 0.4 |
| 90Day | Signaling by the B Cell Receptor (BCR) | 0.34989 | 0.7977 | 0.67768 | vav1;sos1;nfkbia;ikbkg;btrc | 4415.068 | 4161.05 | 3265.56 | 1093.44984 | 4642.96983 | 1139.53614 | DOWN | 0.2 | 0.8 |
| 90Day | Activated PKN1 stimulates transcription of AR (androgen receptor) regulated genes KLK2 and KLK3 | 0.33323 | 0.80983 | 0.67865 | hist1h4h;hist1h4i;hist1h3c;h2afx;ar | 2970.9958 | 3951.81 | 811.859 | 1490.29352 | 2257.59641 | 1663.47463 | DOWN | 0.4 | 0.6 |

BMD analysis results for functional classification based on dose-responsive genes, using the Reactome database for gene sets in BMDExpress2.2 software.

| Study Day | Gene Set Name | Fisher's Exact Left P-Value | Fisher's Exact Right P-Value | Fisher's Exact Two Tail | Gene Symbols | BMD Mean | BMD Median | BMD Minimum | BMD Standard Deviation | BMD wMean | BMD wSD | Overall Direction | Percent Genes With Overall Direction Up | Percent Genes With Overall Direction Down |
|---|---|---|---|---|---|---|---|---|---|---|---|---|---|---|
| 7Day | Innate Immune System | 0.68012 | 0.36282 | 0.67884 | ube2n;rbsn;faf2;cotl1;ist1;fuca1;tmem30a;c8g;arl8a;ndufc2;npc2;ilf2;pycard;c1rb;psmd6;9130409i23rik;golga7;iqgap2;sdcbp;tax1bp1;hgsnat;c1s1;nckap1;cfhr1;ecsit;mapk3;map2k3;apob;mgam;tubb4b;yes1;pak2;uba52;ttr;hsp90b1;cdc34;nhlrc3;dsg1c;rab6a;rab18;rab10;ptpn11;psmc2;ppp2cb;pa2g4;pgam1;neu1;myh9;mme;man2b1;lbp;lamp1;kras;kpnb1;igf2r;hsp90aa1;h2-t23;h2-q10;gstp1;gstp2;gpi1;ftl1;f2;dhx9;ddx3x;ctsb;csnk2b;chil1;cfh;cdc42;cct2;ctnnb1;casp9;capza2;calm3;calm2;cab39;c4b;c2;c1qb;btrc;atp6v1e1;arsb;ahsg;aga;abl1;dsp;mlec;atad3a;qsox1;brk1 | 3259.52373 | 3422.8 | 34.2395 | 1464.93655 | 3154.0664 | 1455.3492 | CONFLICT | 0.505494505 | 0.494505495 |
| 28Day | G beta:gamma signalling through PI3Kgamma | 0.77463 | 0.49782 | 0.67888 | pdpk1;gnb5 | 573.318 | 573.318 | 192.988 | 537.867844 | 867.34192 | 341.176914 | CONFLICT | 0.5 | 0.5 |
| 28Day | Resolution of AP sites via the multiple-nucleotide patch replacement pathway | 0.77463 | 0.49782 | 0.67888 | pole3;polb | 3329.279 | 3329.279 | 805.318 | 3569.41988 | 4286.22182 | 3302.91979 | UP | 1 | 0 |
| 90Day | G2/M Transition | 0.32932 | 0.76671 | 0.68018 | haus7;tubb6;dctn3;gtse1;cntrl;tubb4b;cep76;tubb2a;tuba1b;hsp90aa1;cdkn1a;cdk7;btrc | 2700.50008 | 2128.94 | 426.32 | 1618.52744 | 2593.60842 | 1735.8006 | UP | 0.846153846 | 0.153846154 |
| 90Day | G2/M DNA damage checkpoint | 0.31709 | 0.82137 | 0.68025 | hist1h4h;babam1;hist1h4i;ywhaz;h2afx | 3596.4296 | 4006.71 | 137.958 | 2082.71447 | 3673.49502 | 1960.51471 | UP | 0.6 | 0.4 |
| 90Day | TCR signaling | 0.31709 | 0.82137 | 0.68025 | cdc34;nfkbia;ikbkg;h2-aa;btrc | 3117.9204 | 3265.56 | 569.072 | 1651.20008 | 3314.96494 | 1742.89169 | DOWN | 0.4 | 0.6 |
| 7Day | trans-Golgi Network Vesicle Budding | 0.3715 | 0.78051 | 0.68037 | picalm;igf2r;ftl1;ap3b1;gbf1 | 2834.5032 | 3321.9 | 720.546 | 1253.27309 | 2750.64336 | 1195.02649 | UP | 0.8 | 0.2 |
| 7Day | Clathrin derived vesicle budding | 0.3715 | 0.78051 | 0.68037 | picalm;igf2r;ftl1;ap3b1;gbf1 | 2834.5032 | 3321.9 | 720.546 | 1253.27309 | 2750.64336 | 1195.02649 | UP | 0.8 | 0.2 |
| 7Day | Cell junction organization | 0.32948 | 0.81154 | 0.68199 | vasp;flna;prkci;dst;ctnnb1 | 2974.30464 | 3409.24 | 54.5232 | 1777.63271 | 2180.24458 | 1910.18083 | DOWN | 0.4 | 0.6 |
| 7Day | Transcriptional regulation by small RNAs | 0.32948 | 0.81154 | 0.68199 | hist1h4h;hist1h2bc;hist2h2ac;polr2h;hist2h2aa1 | 4073.244 | 3964.6 | 3406.55 | 810.921331 | 4033.48029 | 829.513011 | UP | 0.6 | 0.4 |
| 90Day | Transcriptional regulation by RUNX2 | 0.7653 | 0.51675 | 0.68292 | cbfb;ar | 3034.77 | 3034.77 | 1998.95 | 1464.87069 | 3300.56119 | 1415.82352 | CONFLICT | 0.5 | 0.5 |
| 90Day | Sema4D in semaphorin signaling | 0.7653 | 0.51675 | 0.68292 | rock2;rock1 | 2068.101 | 2068.101 | 262.092 | 2554.08242 | 1087.57877 | 2144.87514 | UP | 1 | 0 |
| 90Day | Nucleobase biosynthesis | 0.7653 | 0.51675 | 0.68292 | gmps;atic | 3841.07 | 3841.07 | 2515.37 | 1874.82292 | 3607.96146 | 1845.6115 | UP | 1 | 0 |
| 90Day | Activation of IRF3/IRF7 mediated by TBK1/IKK epsilon | 0.7653 | 0.51675 | 0.68292 | tbk1;irf7 | 3374.045 | 3374.045 | 1058.39 | 3274.83071 | 2689.26313 | 3128.36439 | CONFLICT | 0.5 | 0.5 |
| 90Day | Regulation of innate immune responses to cytosolic DNA | 0.7653 | 0.51675 | 0.68292 | tmem173;tbk1 | 2558.24 | 2558.24 | 1058.39 | 2121.10821 | 2553.28861 | 2121.09665 | DOWN | 0 | 1 |
| 90Day | Phospholipase C-mediated cascade; FGFR4 | 0.7653 | 0.51675 | 0.68292 | klb;fgf1 | 2046.3595 | 2046.3595 | 242.429 | 2551.14298 | 3002.17622 | 2163.59869 | DOWN | 0 | 1 |
| 7Day | Tie2 Signaling | 0.76269 | 0.51644 | 0.68456 | ptpn11;kras | 3894.19 | 3894.19 | 3629.67 | 374.087772 | 3880.93363 | 373.617716 | UP | 1 | 0 |
| 7Day | Metabolism of porphyrins | 0.76269 | 0.51644 | 0.68456 | ugt1a1;blvrb | 2545.203 | 2545.203 | 178.786 | 3346.61902 | 2903.10937 | 3308.12105 | CONFLICT | 0.5 | 0.5 |
| 7Day | Nicotinamide salvaging | 0.76269 | 0.51644 | 0.68456 | nudt12;naxe | 2595.9995 | 2595.9995 | 820.079 | 2511.53086 | 3261.55578 | 2328.48812 | CONFLICT | 0.5 | 0.5 |
| 7Day | DARPP-32 events | 0.76269 | 0.51644 | 0.68456 | prkar2a;ppp2cb | 3846.8 | 3846.8 | 3627.04 | 310.787572 | 3752.6326 | 280.809393 | CONFLICT | 0.5 | 0.5 |
| 7Day | Ephrin signaling | 0.76269 | 0.51644 | 0.68456 | sdcbp;pak2 | 2891.23 | 2891.23 | 2538.2 | 499.259814 | 2954.69377 | 491.126318 | UP | 1 | 0 |
| 7Day | Gastrin-CREB signalling pathway via PKC and MAPK | 0.76269 | 0.51644 | 0.68456 | mapk3;kras | 4479.475 | 4479.475 | 4158.71 | 453.630213 | 4552.01512 | 441.878074 | CONFLICT | 0.5 | 0.5 |
| 7Day | PI-3K cascade:FGFR3 | 0.76269 | 0.51644 | 0.68456 | ptpn11;fgf1 | 3138.715 | 3138.715 | 2647.76 | 694.31522 | 2984.26892 | 659.064823 | CONFLICT | 0.5 | 0.5 |
| 7Day | SHC-mediated cascade:FGFR3 | 0.76269 | 0.51644 | 0.68456 | kras;fgf1 | 3403.235 | 3403.235 | 2647.76 | 1068.40299 | 3131.99117 | 997.165244 | CONFLICT | 0.5 | 0.5 |
| 28Day | Metabolism of carbohydrates | 0.36447 | 0.73532 | 0.68518 | slc25a10;hs2st1;pfkl;pcx;pck1;man2b2;man2b1;khk;hyal1;gpi1;gpc4;gaa;bpgm | 3350.90485 | 3361.03 | 240.253 | 1194.36178 | 3002.02789 | 1341.42233 | DOWN | 0.153846154 | 0.846153846 |
| 28Day | G2/M Checkpoints | 0.32717 | 0.81194 | 0.68608 | ube2n;ube2v2;hist1h4i;cdc6;brca1 | 5182.904 | 5643.31 | 3288.55 | 1086.18586 | 5095.75689 | 1243.24827 | UP | 0.6 | 0.4 |
| 28Day | Oxidative Stress Induced Senescence | 0.31759 | 0.81883 | 0.68711 | hist1h4i;map2k4;mdm2;mapkapk2;bmi1 | 4004.996 | 3918.46 | 2266.61 | 1599.41252 | 3457.62774 | 1668.23985 | UP | 0.6 | 0.4 |
| 28Day | Carboxyterminal post-translational modifications of tubulin | 0.75594 | 0.51989 | 0.68848 | tubb4b;tubb2a | 2631.245 | 2631.245 | 2359.45 | 384.376175 | 2702.45657 | 370.948608 | UP | 1 | 0 |
| 28Day | CDK-mediated phosphorylation and removal of Cdc6 | 0.75594 | 0.51989 | 0.68848 | cdc6;cdc27 | 5824.15 | 5824.15 | 5780.76 | 61.3627265 | 5829.67647 | 60.862965 | UP | 1 | 0 |

BMD analysis results for functional classification based on dose-responsive genes, using the Reactome database for gene sets in BMDExpress2.2 software.

| Study Day | Gene Set Name | Fisher's Exact Left P-Value | Fisher's Exact Right P-Value | Fisher's Exact Two Tail | Gene Symbols | BMD Mean | BMD Median | BMD Minimum | BMD Standard Deviation | BMD wMean | BMD wSD | Overall Direction | Percent Genes With Overall Direction Up | Percent Genes With Overall Direction Down |
|---|---|---|---|---|---|---|---|---|---|---|---|---|---|---|
| 28Day | Processing of Capped Intronless Pre-mRNA | 0.75594 | 0.51989 | 0.68848 | cpsf2;papola | 3117.8765 | 3117.8765 | 983.533 | 3018.41752 | 4045.49974 | 2718.43238 | DOWN | 0 | 1 |
| 28Day | Processing of Capped Intron-Containing Pre-mRNA | 0.69114 | 0.40476 | 0.69144 | phf5a;ccar1;rnpc3;sf3b6;cpsf2;prpf19;hnrnpul1;prpf38a;u2af2;snrpd1;polr2a;prpf8;papola;srsf1;tpr;thoc5;bc005561 | 3965.02082 | 4603.26 | 131.831 | 1550.97798 | 3978.39031 | 1689.41416 | UP | 0.705882353 | 0.294117647 |
| 7Day | DNA Damage/Telomere Stress Induced Senescence | 0.71416 | 0.42642 | 0.69292 | ep400;hist1h4h;hist1h2bc;hist2h2ac;terf2;hist2h2aa1;cdkn1a;ccne2 | 3995.4025 | 3802.835 | 2818.63 | 877.134081 | 4069.18686 | 898.941015 | UP | 0.625 | 0.375 |
| 7Day | Fc epsilon receptor (FCERI) signaling | 0.71416 | 0.42642 | 0.69292 | ube2n;pak2;uba52;cdc34;kras;calm3;calm2;btrc | 3512.01125 | 3801.75 | 1018.89 | 1299.28996 | 3712.1249 | 884.606401 | UP | 0.875 | 0.125 |
| 28Day | Regulation of TP53 Degradation | 0.73701 | 0.5413 | 0.69829 | mdm2;ccng1 | 1695.93 | 1695.93 | 1125.25 | 807.063396 | 1814.89328 | 789.333136 | UP | 1 | 0 |
| 28Day | Regulation of TP53 Expression and Degradation | 0.73701 | 0.5413 | 0.69829 | mdm2;ccng1 | 1695.93 | 1695.93 | 1125.25 | 807.063396 | 1814.89328 | 789.333136 | UP | 1 | 0 |
| 28Day | Integrin alphaIIb beta3 signaling | 0.73701 | 0.5413 | 0.69829 | pdpk1;fn1 | 1674.494 | 1674.494 | 192.988 | 2095.16588 | 2432.121 | 1800.47847 | DOWN | 0 | 1 |
| 28Day | Integrin signaling | 0.73701 | 0.5413 | 0.69829 | pdpk1;fn1 | 1674.494 | 1674.494 | 192.988 | 2095.16588 | 2432.121 | 1800.47847 | DOWN | 0 | 1 |
| 28Day | Trafficking of AMPA receptors | 0.73701 | 0.5413 | 0.69829 | gria3;mdm2 | 2159.59 | 2159.59 | 2052.57 | 151.349135 | 2164.79104 | 151.170299 | UP | 1 | 0 |
| 28Day | Glutamate binding, activation of AMPA receptors and synaptic plasticity | 0.73701 | 0.5413 | 0.69829 | gria3;mdm2 | 2159.59 | 2159.59 | 2052.57 | 151.349135 | 2164.79104 | 151.170299 | UP | 1 | 0 |
| 28Day | The role of GTSE1 in G2/M progression after G2 checkpoint | 0.73701 | 0.5413 | 0.69829 | tubb4b;tubb2a | 2631.245 | 2631.245 | 2359.45 | 384.376175 | 2702.45657 | 370.948608 | UP | 1 | 0 |
| 7Day | ERK/MAPK targets | 0.7364 | 0.54619 | 0.69844 | mapk3;ppp2cb | 4213.64 | 4213.64 | 3627.04 | 829.577676 | 4084.83206 | 809.330679 | CONFLICT | 0.5 | 0.5 |
| 7Day | Regulation of signaling by CBL | 0.7364 | 0.54619 | 0.69844 | yes1;uba52 | 4391.255 | 4391.255 | 4020.95 | 523.690353 | 4358.19543 | 521.59919 | UP | 1 | 0 |
| 7Day | Unblocking of NMDA receptors, glutamate binding and activation | 0.7364 | 0.54619 | 0.69844 | calm3;calm2 | 3983.44 | 3983.44 | 3050.32 | 1319.63096 | 3556.9103 | 1173.69957 | CONFLICT | 0.5 | 0.5 |
| 7Day | Activation of NF-kappaB in B cells | 0.7364 | 0.54619 | 0.69844 | uba52;btrc | 4484.31 | 4484.31 | 4207.06 | 392.09071 | 4446.04923 | 388.339223 | UP | 1 | 0 |
| 7Day | Other interleukin signaling | 0.7364 | 0.54619 | 0.69844 | csf1r;csf1 | 2192.5255 | 2192.5255 | 729.901 | 2068.4634 | 1592.81686 | 1886.5948 | CONFLICT | 0.5 | 0.5 |
| 7Day | Regulation of FZD by ubiquitination | 0.7364 | 0.54619 | 0.69844 | uba52;lrp5 | 4760.865 | 4760.865 | 4760.17 | 0.98287843 | 4760.7558 | 0.97066913 | CONFLICT | 0.5 | 0.5 |
| 90Day | Processing of SMDT1 | 0.73353 | 0.5525 | 0.69992 | afg3l2;micu2 | 3526.375 | 3526.375 | 1479.94 | 2894.09613 | 2753.64746 | 2679.8464 | UP | 1 | 0 |
| 90Day | Metabolism of Angiotensinogen to Angiotensins | 0.73353 | 0.5525 | 0.69992 | mme;ctsd | 3821.095 | 3821.095 | 3756.53 | 91.3086987 | 3803.24857 | 87.7512875 | CONFLICT | 0.5 | 0.5 |
| 90Day | Metabolism of folate and pterines | 0.73353 | 0.5525 | 0.69992 | mthfd2;aldh1l1 | 2812.785 | 2812.785 | 2673.17 | 197.445427 | 2817.17769 | 197.347675 | CONFLICT | 0.5 | 0.5 |
| 90Day | PI3K events in ERBB2 signaling | 0.73353 | 0.5525 | 0.69992 | nrg1;gab1 | 2019.384 | 2019.384 | 126.428 | 2677.04405 | 2617.01628 | 2540.12522 | CONFLICT | 0.5 | 0.5 |
| 90Day | Metabolism of cofactors | 0.73353 | 0.5525 | 0.69992 | pdss1;hsp90aa1 | 3059.05 | 3059.05 | 426.32 | 3723.24247 | 3544.99278 | 3659.26956 | UP | 1 | 0 |
| 90Day | p53-Dependent G1 DNA Damage Response | 0.73353 | 0.5525 | 0.69992 | mdm2;cdkn1a | 2224.395 | 2224.395 | 913.71 | 1853.5885 | 2056.00777 | 1838.2279 | UP | 1 | 0 |
| 90Day | p53-Dependent G1/S DNA damage checkpoint | 0.73353 | 0.5525 | 0.69992 | mdm2;cdkn1a | 2224.395 | 2224.395 | 913.71 | 1853.5885 | 2056.00777 | 1838.2279 | UP | 1 | 0 |
| 90Day | Norepinephrine Neurotransmitter Release Cycle | 0.73353 | 0.5525 | 0.69992 | unc13b;slc22a1 | 2810.74 | 2810.74 | 1050.57 | 2489.25629 | 3149.81569 | 2442.63223 | CONFLICT | 0.5 | 0.5 |
| 90Day | Signaling by NTRKs | 0.327 | 0.80465 | 0.7008 | irs2;mapk14;sos1;pcsk5;ntrk2;ap2m1 | 3453.50722 | 3752.895 | 74.8133 | 1919.8951 | 3207.75314 | 2451.07586 | DOWN | 0.166666667 | 0.833333333 |
| 7Day | Arachidonic acid metabolism | 0.34856 | 0.78745 | 0.70184 | akr1c6;ptges3;ephx2;cyp2c37;cyp2c29;akr1c14 | 2827.84362 | 2990.63 | 93.6517 | 1568.23608 | 2653.56942 | 1284.27005 | UP | 0.666666667 | 0.333333333 |
| 7Day | DNA Replication Pre-Initiation | 0.34856 | 0.78745 | 0.70184 | psmd5;psmd6;psmc4;uba52;psmc2;prim2 | 3502.21 | 3625.07 | 2309.23 | 909.674091 | 3376.05087 | 1015.17591 | UP | 1 | 0 |
| 28Day | Toll Like Receptor 4 (TLR4) Cascade | 0.68699 | 0.45459 | 0.70228 | ube2n;map2k4;mapkapk2;ly96;lbp;ikbkg;app;birc2 | 4941.99375 | 5320.855 | 2616.5 | 1053.22955 | 4922.34751 | 1090.07569 | CONFLICT | 0.5 | 0.5 |
| 28Day | Nucleotide Excision Repair | 0.68699 | 0.45459 | 0.70228 | ube2n;usp45;ube2v2;pole3;prpf19;ino80c;polr2a;lig3 | 3831.411 | 4295.465 | 805.318 | 1777.30939 | 4077.8285 | 1518.49647 | CONFLICT | 0.5 | 0.5 |
| 7Day | RNA Polymerase I Chain Elongation | 0.32317 | 0.80656 | 0.70406 | hist1h4h;hist1h2bc;hist2h2ac;polr2h;ubtf;hist2h2aa1 | 3723.755 | 3691.5 | 1976.31 | 1122.02054 | 3843.70217 | 1012.37228 | UP | 0.666666667 | 0.333333333 |
| 28Day | Mitotic Prophase | 0.37212 | 0.76792 | 0.7046 | nek6;arpp19;set;cnep1r1;hist1h4i;tpr | 4163.56667 | 3849.715 | 2388.34 | 1415.17198 | 4048.58649 | 1299.74126 | UP | 0.833333333 | 0.166666667 |
| 28Day | Rab regulation of trafficking | 0.35299 | 0.78278 | 0.70516 | trappc8;rab9;rab11a;dennd1a;rab18;tbc1d10a | 3353.03333 | 2992.42 | 2192.92 | 1155.84614 | 3498.40632 | 1290.04174 | DOWN | 0.333333333 | 0.666666667 |
| 7Day | Positive epigenetic regulation of rRNA expression | 0.73465 | 0.39474 | 0.70567 | sf3b1;hist1h4h;hist1h2bc;gsk3b;ddx21;hist2h2ac;polr2h;mybbp1a;hist2h2aa1 | 3817.88444 | 3439.85 | 2845.95 | 780.915516 | 3713.87572 | 783.361635 | UP | 0.777777778 | 0.222222222 |
| 7Day | B-WICH complex positively regulates rRNA expression | 0.73465 | 0.39474 | 0.70567 | sf3b1;hist1h4h;hist1h2bc;gsk3b;ddx21;hist2h2ac;polr2h;mybbp1a;hist2h2aa1 | 3817.88444 | 3439.85 | 2845.95 | 780.915516 | 3713.87572 | 783.361635 | UP | 0.777777778 | 0.222222222 |
| 28Day | Insulin receptor recycling | 0.71791 | 0.56203 | 0.70822 | atp6v0e2;atp6v1e1 | 3839.965 | 3839.965 | 2385.58 | 2056.81099 | 2967.18762 | 1645.29352 | CONFLICT | 0.5 | 0.5 |

BMD analysis results for functional classification based on dose-responsive genes, using the Reactome database for gene sets in BMDExpress2.2 software.

| Study Day | Gene Set Name | Fisher's Exact Left P-Value | Fisher's Exact Right P-Value | Fisher's Exact Two Tail | Gene Symbols | BMD Mean | BMD Median | BMD Minimum | BMD Standard Deviation | BMD wMean | BMD wSD | Overall Direction | Percent Genes With Overall Direction Up | Percent Genes With Overall Direction Down |
|---|---|---|---|---|---|---|---|---|---|---|---|---|---|---|
| 28Day | Deadenylation of mRNA | 0.71791 | 0.56203 | 0.70822 | cnot1;paip1 | 3500.885 | 3500.885 | 3132.16 | 521.455896 | 3494.40951 | 521.375476 | UP | 1 | 0 |
| 90Day | SHC1 events in ERBB2 signaling | 0.41366 | 0.86922 | 0.71236 | nrg1 | 3912.34 | 3912.34 | 3912.34 | | 3912.34 | | UP | 1 | 0 |
| 90Day | Regulation of TLR by endogenous ligand | 0.41366 | 0.86922 | 0.71236 | apob | 175.96 | 175.96 | 175.96 | | 175.96 | | DOWN | 0 | 1 |
| 90Day | G beta:gamma signalling through BTK | 0.41366 | 0.86922 | 0.71236 | gng11 | 4854.24 | 4854.24 | 4854.24 | | 4854.24 | | UP | 1 | 0 |
| 90Day | Synthesis of glycosylphosphatidylinositol (GPI) | 0.41366 | 0.86922 | 0.71236 | pigp | 3011.39 | 3011.39 | 3011.39 | | 3011.39 | | UP | 1 | 0 |
| 90Day | Interferon gamma signaling | 0.41366 | 0.86922 | 0.71236 | ifngr2 | 4021.95 | 4021.95 | 4021.95 | | 4021.95 | | DOWN | 0 | 1 |
| 90Day | Serotonin Neurotransmitter Release Cycle | 0.41366 | 0.86922 | 0.71236 | unc13b | 4570.91 | 4570.91 | 4570.91 | | 4570.91 | | UP | 1 | 0 |
| 90Day | GABA synthesis, release, reuptake and degradation | 0.41366 | 0.86922 | 0.71236 | slc6a12 | 3445.15 | 3445.15 | 3445.15 | | 3445.15 | | DOWN | 0 | 1 |
| 90Day | RIPK1-mediated regulated necrosis | 0.41366 | 0.86922 | 0.71236 | tnfrsf10b | 3826.99 | 3826.99 | 3826.99 | | 3826.99 | | UP | 1 | 0 |
| 90Day | Regulated Necrosis | 0.41366 | 0.86922 | 0.71236 | tnfrsf10b | 3826.99 | 3826.99 | 3826.99 | | 3826.99 | | UP | 1 | 0 |
| 7Day | RUNX1 regulates transcription of genes involved in differentiation of HSCs | 0.70978 | 0.57463 | 0.7125 | uba52;abl1 | 4064.805 | 4064.805 | 3368.05 | 985.360371 | 4326.32968 | 913.315248 | CONFLICT | 0.5 | 0.5 |
| 7Day | TGF-beta receptor signaling activates SMADs | 0.70978 | 0.57463 | 0.7125 | uba52;tgfbr1 | 5206.805 | 5206.805 | 4761.56 | 629.671518 | 5273.58539 | 622.548776 | UP | 1 | 0 |
| 7Day | Interleukin-12 family signaling | 0.70978 | 0.57463 | 0.7125 | stat1;jak1 | 3735.595 | 3735.595 | 3554.32 | 256.361564 | 3703.94 | 252.422609 | UP | 1 | 0 |
| 7Day | Regulation of lipid metabolism by Peroxisome proliferator-activated receptor alpha (PPARalpha) | 0.70978 | 0.57463 | 0.7125 | ncoa2;ncoa1 | 1694.1743 | 1694.1743 | 86.7986 | 2273.17251 | 2801.46736 | 1647.76134 | UP | 1 | 0 |
| 7Day | APC/C:Cdc20 mediated degradation of Securin | 0.70978 | 0.57463 | 0.7125 | uba52;cdc27 | 4316.07 | 4316.07 | 3870.58 | 630.018 | 4393.04009 | 620.543222 | UP | 1 | 0 |
| 7Day | HS-GAG degradation | 0.70978 | 0.57463 | 0.7125 | hgsnat;sdc3 | 3460.675 | 3460.675 | 3118.3 | 484.191368 | 3385.715 | 472.443943 | DOWN | 0 | 1 |
| 7Day | Endosomal/Vacuolar pathway | 0.70978 | 0.57463 | 0.7125 | h2-t23;h2-q10 | 3617.055 | 3617.055 | 2584.12 | 1460.79069 | 2959.99285 | 1127.14155 | DOWN | 0 | 1 |
| 7Day | Signal transduction by L1 | 0.70978 | 0.57463 | 0.7125 | mapk3;csnk2b | 3814.955 | 3814.955 | 2829.67 | 1393.40341 | 4062.18886 | 1348.82315 | CONFLICT | 0.5 | 0.5 |
| 7Day | PI-3K cascade:FGFR4 | 0.70978 | 0.57463 | 0.7125 | ptpn11;fgf1 | 3138.715 | 3138.715 | 2647.76 | 694.31522 | 2984.26892 | 659.064823 | CONFLICT | 0.5 | 0.5 |
| 7Day | SHC-mediated cascade:FGFR4 | 0.70978 | 0.57463 | 0.7125 | kras;fgf1 | 3403.235 | 3403.235 | 2647.76 | 1068.40299 | 3131.99117 | 997.165244 | CONFLICT | 0.5 | 0.5 |
| 28Day | HDR through Homologous Recombination (HRR) or Single Strand Annealing (SSA) | 0.70907 | 0.42191 | 0.7127 | ube2n;rmi1;ube2v2;pole3;hist1h4i;rad51d;rad51;brca1;blm | 3641.84933 | 3769.36 | 692.086 | 1890.0939 | 3817.81985 | 1459.82142 | UP | 0.777777778 | 0.222222222 |
| 90Day | Negative regulation of MET activity | 0.38176 | 0.88399 | 0.71287 | sh3gl3 | 5266.23 | 5266.23 | 5266.23 | | 5266.23 | | UP | 1 | 0 |
| 90Day | Phospholipase C-mediated cascade; FGFR2 | 0.38176 | 0.88399 | 0.71287 | fgf1 | 242.429 | 242.429 | 242.429 | | 242.429 | | DOWN | 0 | 1 |
| 90Day | Prostacyclin signalling through prostacyclin receptor | 0.38176 | 0.88399 | 0.71287 | gng11 | 4854.24 | 4854.24 | 4854.24 | | 4854.24 | | UP | 1 | 0 |
| 90Day | Beta-catenin phosphorylation cascade | 0.38176 | 0.88399 | 0.71287 | ctnnb1 | 4087.04 | 4087.04 | 4087.04 | | 4087.04 | | DOWN | 0 | 1 |
| 90Day | Metabolism of porphyrins | 0.38176 | 0.88399 | 0.71287 | blvrb | 3840.4 | 3840.4 | 3840.4 | | 3840.4 | | UP | 1 | 0 |
| 90Day | Deposition of new CENPA-containing nucleosomes at the centromere | 0.38176 | 0.88399 | 0.71287 | cenpu | 5744.84 | 5744.84 | 5744.84 | | 5744.84 | | UP | 1 | 0 |
| 90Day | Nucleosome assembly | 0.38176 | 0.88399 | 0.71287 | cenpu | 5744.84 | 5744.84 | 5744.84 | | 5744.84 | | UP | 1 | 0 |
| 90Day | Gastrin-CREB signalling pathway via PKC and MAPK | 0.38176 | 0.88399 | 0.71287 | sos1 | 5894.93 | 5894.93 | 5894.93 | | 5894.93 | | DOWN | 0 | 1 |
| 90Day | Processing of Intronless Pre-mRNAs | 0.38176 | 0.88399 | 0.71287 | cstf2t | 5843.41 | 5843.41 | 5843.41 | | 5843.41 | | DOWN | 0 | 1 |
| 90Day | FOXO-mediated transcription | 0.35178 | 0.89708 | 0.71525 | ywhaz | 137.958 | 137.958 | 137.958 | | 137.958 | | UP | 1 | 0 |
| 90Day | ERK/MAPK targets | 0.35178 | 0.89708 | 0.71525 | mapk14 | 4261.96 | 4261.96 | 4261.96 | | 4261.96 | | DOWN | 0 | 1 |
| 90Day | G beta:gamma signalling through PLC beta | 0.35178 | 0.89708 | 0.71525 | gng11 | 4854.24 | 4854.24 | 4854.24 | | 4854.24 | | UP | 1 | 0 |
| 90Day | Regulation of signaling by CBL | 0.35178 | 0.89708 | 0.71525 | vav1 | 4161.05 | 4161.05 | 4161.05 | | 4161.05 | | DOWN | 0 | 1 |
| 90Day | FGFR2 ligand binding and activation | 0.35178 | 0.89708 | 0.71525 | fgf1 | 242.429 | 242.429 | 242.429 | | 242.429 | | DOWN | 0 | 1 |
| 90Day | Caspase activation via extrinsic apoptotic signalling pathway | 0.35178 | 0.89708 | 0.71525 | tnfrsf10b | 3826.99 | 3826.99 | 3826.99 | | 3826.99 | | UP | 1 | 0 |
| 90Day | Conversion from APC/C:Cdc20 to APC/C:Cdh1 in late anaphase | 0.35178 | 0.89708 | 0.71525 | anapc10 | 4390.47 | 4390.47 | 4390.47 | | 4390.47 | | UP | 1 | 0 |
| 90Day | Regulation of FZD by ubiquitination | 0.35178 | 0.89708 | 0.71525 | lgr4 | 5316.37 | 5316.37 | 5316.37 | | 5316.37 | | UP | 1 | 0 |
| 90Day | Signaling by Hippo | 0.35178 | 0.89708 | 0.71525 | wwc1 | 5949.63 | 5949.63 | 5949.63 | | 5949.63 | | DOWN | 0 | 1 |
| 90Day | Post NMDA receptor activation events | 0.35178 | 0.89708 | 0.71525 | camkk2 | 98.0082 | 98.0082 | 98.0082 | | 98.0082 | | DOWN | 0 | 1 |
| 7Day | Nucleotide salvage | 0.39825 | 0.87515 | 0.71527 | adk | 124.762 | 124.762 | 124.762 | | 124.762 | | DOWN | 0 | 1 |
| 7Day | Acyl chain remodelling of PS | 0.39825 | 0.87515 | 0.71527 | pla1a | 3489.79 | 3489.79 | 3489.79 | | 3489.79 | | DOWN | 0 | 1 |

BMD analysis results for functional classification based on dose-responsive genes, using the Reactome database for gene sets in BMDExpress2.2 software.

| Study Day | Gene Set Name | Fisher's Exact Left P-Value | Fisher's Exact Right P-Value | Fisher's Exact Two Tail | Gene Symbols | BMD Mean | BMD Median | BMD Minimum | BMD Standard Deviation | BMD wMean | BMD wSD | Overall Direction | Percent Genes With Overall Direction Up | Percent Genes With Overall Direction Down |
|---|---|---|---|---|---|---|---|---|---|---|---|---|---|---|
| 7Day | ADP signalling through P2Y purinoceptor 12 | 0.39825 | 0.87515 | 0.71527 | gnai3 | 794.2 | 794.2 | 794.2 |  | 794.2 |  | UP | 1 | 0 |
| 7Day | Metal ion SLC transporters | 0.39825 | 0.87515 | 0.71527 | slc39a2 | 5557.48 | 5557.48 | 5557.48 |  | 5557.48 |  | UP | 1 | 0 |
| 7Day | Telomere C-strand (Lagging Strand) Synthesis | 0.37246 | 0.88694 | 0.71631 | prim2 | 4006.14 | 4006.14 | 4006.14 |  | 4006.14 |  | UP | 1 | 0 |
| 7Day | Cellular hexose transport | 0.37246 | 0.88694 | 0.71631 | slc2a8 | 3236.88 | 3236.88 | 3236.88 |  | 3236.88 |  | DOWN | 0 | 1 |
| 28Day | TNFR1-induced NFkappaB signaling pathway | 0.6987 | 0.58209 | 0.71821 | ikbkg;birc2 | 5639.965 | 5639.965 | 5417.68 | 314.358462 | 5681.7264 | 308.760771 | UP | 1 | 0 |
| 7Day | Glutamate Neurotransmitter Release Cycle | 0.34799 | 0.89762 | 0.71857 | slc1a2 | 1710.87 | 1710.87 | 1710.87 |  | 1710.87 |  | DOWN | 0 | 1 |
| 7Day | Triglyceride metabolism | 0.34799 | 0.89762 | 0.71857 | dgat2 | 623.511 | 623.511 | 623.511 |  | 623.511 |  | DOWN | 0 | 1 |
| 7Day | S Phase | 0.35263 | 0.77603 | 0.71906 | pds5a;uba52;cdc27;prim2;cdkn1a;cdc25a;ccne2 | 4225.70286 | 4006.14 | 2818.63 | 969.895529 | 4116.90686 | 941.177518 | UP | 1 | 0 |
| 28Day | VEGFR2 mediated vascular permeability | 0.39854 | 0.87326 | 0.71911 | pdpk1 | 192.988 | 192.988 | 192.988 |  | 192.988 |  | DOWN | 0 | 1 |
| 28Day | Energy dependent regulation of mTOR by LKB1-AMPK | 0.39854 | 0.87326 | 0.71911 | stradb | 5007.07 | 5007.07 | 5007.07 |  | 5007.07 |  | DOWN | 0 | 1 |
| 28Day | DAG and IP3 signaling | 0.39854 | 0.87326 | 0.71911 | adcy9 | 4220.6 | 4220.6 | 4220.6 |  | 4220.6 |  | DOWN | 0 | 1 |
| 28Day | Negative regulation of FGFR1 signaling | 0.39854 | 0.87326 | 0.71911 | fgf1 | 1467.57 | 1467.57 | 1467.57 |  | 1467.57 |  | DOWN | 0 | 1 |
| 28Day | Ovarian tumor domain proteases | 0.39854 | 0.87326 | 0.71911 | ikbkg | 5417.68 | 5417.68 | 5417.68 |  | 5417.68 |  | UP | 1 | 0 |
| 28Day | Signaling by ERBB4 | 0.39854 | 0.87326 | 0.71911 | hbegf | 919.738 | 919.738 | 919.738 |  | 919.738 |  | UP | 1 | 0 |
| 28Day | Recognition of DNA damage by PCNA-containing replication complex | 0.39854 | 0.87326 | 0.71911 | pole3 | 805.318 | 805.318 | 805.318 |  | 805.318 |  | UP | 1 | 0 |
| 28Day | Nicotinate metabolism | 0.39854 | 0.87326 | 0.71911 | nudt12 | 5115.96 | 5115.96 | 5115.96 |  | 5115.96 |  | DOWN | 0 | 1 |
| 28Day | mRNA Capping | 0.39854 | 0.87326 | 0.71911 | polr2a | 5040.67 | 5040.67 | 5040.67 |  | 5040.67 |  | UP | 1 | 0 |
| 28Day | RNA Polymerase I Promoter Escape | 0.39854 | 0.87326 | 0.71911 | polr1a | 5863.06 | 5863.06 | 5863.06 |  | 5863.06 |  | DOWN | 0 | 1 |
| 90Day | Chondroitin sulfate biosynthesis | 0.32371 | 0.9087 | 0.71926 | bgn | 4533.35 | 4533.35 | 4533.35 |  | 4533.35 |  | DOWN | 0 | 1 |
| 90Day | Presynaptic function of Kainate receptors | 0.32371 | 0.9087 | 0.71926 | gng11 | 4854.24 | 4854.24 | 4854.24 |  | 4854.24 |  | UP | 1 | 0 |
| 90Day | TGF-beta receptor signaling activates SMADs | 0.32371 | 0.9087 | 0.71926 | ube2m | 678.11 | 678.11 | 678.11 |  | 678.11 |  | UP | 1 | 0 |
| 90Day | Interleukin-12 family signaling | 0.32371 | 0.9087 | 0.71926 | crlf1 | 3200.93 | 3200.93 | 3200.93 |  | 3200.93 |  | UP | 1 | 0 |
| 90Day | Regulation of lipid metabolism by Peroxisome proliferator-activated receptor alpha (PPARalpha) | 0.32371 | 0.9087 | 0.71926 | hdac3 | 5394.1 | 5394.1 | 5394.1 |  | 5394.1 |  | DOWN | 0 | 1 |
| 90Day | Inhibition of the proteolytic activity of APC/C required for the onset of anaphase by mitotic spindle checkpoint components | 0.32371 | 0.9087 | 0.71926 | anapc10 | 4390.47 | 4390.47 | 4390.47 |  | 4390.47 |  | UP | 1 | 0 |
| 90Day | Inactivation of APC/C via direct inhibition of the APC/C complex | 0.32371 | 0.9087 | 0.71926 | anapc10 | 4390.47 | 4390.47 | 4390.47 |  | 4390.47 |  | UP | 1 | 0 |
| 90Day | APC/C:Cdc20 mediated degradation of Securin | 0.32371 | 0.9087 | 0.71926 | anapc10 | 4390.47 | 4390.47 | 4390.47 |  | 4390.47 |  | UP | 1 | 0 |
| 90Day | HS-GAG degradation | 0.32371 | 0.9087 | 0.71926 | sdc4 | 630.216 | 630.216 | 630.216 |  | 630.216 |  | DOWN | 0 | 1 |
| 90Day | Signal transduction by L1 | 0.32371 | 0.9087 | 0.71926 | itga9 | 4436.62 | 4436.62 | 4436.62 |  | 4436.62 |  | DOWN | 0 | 1 |
| 90Day | RHO GTPases activate PAKs | 0.32371 | 0.9087 | 0.71926 | cdc42 | 156.487 | 156.487 | 156.487 |  | 156.487 |  | UP | 1 | 0 |
| 90Day | VxPx cargo-targeting to cilium | 0.32371 | 0.9087 | 0.71926 | exoc4 | 2113.16 | 2113.16 | 2113.16 |  | 2113.16 |  | UP | 1 | 0 |
| 28Day | Regulation of TP53 Activity through Acetylation | 0.37985 | 0.88198 | 0.7197 | meaf6 | 2859.88 | 2859.88 | 2859.88 |  | 2859.88 |  | DOWN | 0 | 1 |
| 28Day | Inactivation, recovery and regulation of the phototransduction cascade | 0.37985 | 0.88198 | 0.7197 | gnb5 | 953.648 | 953.648 | 953.648 |  | 953.648 |  | UP | 1 | 0 |
| 28Day | FCERI mediated Ca+2 mobilization | 0.37985 | 0.88198 | 0.7197 | ppp3cb | 4095.87 | 4095.87 | 4095.87 |  | 4095.87 |  | UP | 1 | 0 |
| 28Day | MET activates PTK2 signaling | 0.37985 | 0.88198 | 0.7197 | fn1 | 3156 | 3156 | 3156 |  | 3156 |  | DOWN | 0 | 1 |
| 28Day | EPH-ephrin mediated repulsion of cells | 0.37985 | 0.88198 | 0.7197 | epha7 | 5831.01 | 5831.01 | 5831.01 |  | 5831.01 |  | UP | 1 | 0 |
| 28Day | Downstream signaling of activated FGFR2 | 0.37985 | 0.88198 | 0.7197 | fgf1 | 1467.57 | 1467.57 | 1467.57 |  | 1467.57 |  | DOWN | 0 | 1 |
| 28Day | Termination of translesion DNA synthesis | 0.37985 | 0.88198 | 0.7197 | pole3 | 805.318 | 805.318 | 805.318 |  | 805.318 |  | UP | 1 | 0 |

BMD analysis results for functional classification based on dose-responsive genes, using the Reactome database for gene sets in BMDExpress2.2 software.

| Study Day | Gene Set Name | Fisher's Exact Left P-Value | Fisher's Exact Right P-Value | Fisher's Exact Two Tail | Gene Symbols | BMD Mean | BMD Median | BMD Minimum | BMD Standard Deviation | BMD wMean | BMD wSD | Overall Direction | Percent Genes With Overall Direction Up | Percent Genes With Overall Direction Down |
|---|---|---|---|---|---|---|---|---|---|---|---|---|---|---|
| 28Day | RNA Polymerase I Transcription Termination | 0.37985 | 0.88198 | 0.7197 | polr1a | 5863.06 | 5863.06 | 5863.06 | | 5863.06 | | DOWN | 0 | 1 |
| 28Day | Ca-dependent events | 0.37985 | 0.88198 | 0.7197 | adcy9 | 4220.6 | 4220.6 | 4220.6 | | 4220.6 | | DOWN | 0 | 1 |
| 28Day | Activation of kainate receptors upon glutamate binding | 0.36185 | 0.89011 | 0.72094 | gnb5 | 953.648 | 953.648 | 953.648 | | 953.648 | | UP | 1 | 0 |
| 28Day | The phototransduction cascade | 0.36185 | 0.89011 | 0.72094 | gnb5 | 953.648 | 953.648 | 953.648 | | 953.648 | | UP | 1 | 0 |
| 28Day | Neurexins and neuroligins | 0.36185 | 0.89011 | 0.72094 | epb41l3 | 5896.01 | 5896.01 | 5896.01 | | 5896.01 | | DOWN | 0 | 1 |
| 28Day | Signal amplification | 0.36185 | 0.89011 | 0.72094 | gnb5 | 953.648 | 953.648 | 953.648 | | 953.648 | | UP | 1 | 0 |
| 28Day | Downstream signaling of activated FGFR1 | 0.36185 | 0.89011 | 0.72094 | fgf1 | 1467.57 | 1467.57 | 1467.57 | | 1467.57 | | DOWN | 0 | 1 |
| 28Day | Negative regulation of FGFR2 signaling | 0.36185 | 0.89011 | 0.72094 | fgf1 | 1467.57 | 1467.57 | 1467.57 | | 1467.57 | | DOWN | 0 | 1 |
| 28Day | G alpha (12/13) signalling events | 0.36185 | 0.89011 | 0.72094 | gnb5 | 953.648 | 953.648 | 953.648 | | 953.648 | | UP | 1 | 0 |
| 28Day | Glucagon signaling in metabolic regulation | 0.36185 | 0.89011 | 0.72094 | adcy9 | 4220.6 | 4220.6 | 4220.6 | | 4220.6 | | DOWN | 0 | 1 |
| 28Day | Formation of the Early Elongation Complex | 0.36185 | 0.89011 | 0.72094 | polr2a | 5040.67 | 5040.67 | 5040.67 | | 5040.67 | | UP | 1 | 0 |
| 28Day | DNA Replication | 0.38497 | 0.74891 | 0.72143 | psmd6;pole3;psmd8;cdc6;psmf1;cdc27;psmb8 | 3773.95114 | 4413.43 | 805.318 | 2013.49365 | 4057.3808 | 1993.62148 | CONFLICT | 0.571428571 | 0.428571429 |
| 7Day | Synthesis of PC | 0.32482 | 0.90729 | 0.72192 | stard10 | 4547.5 | 4547.5 | 4547.5 | | 4547.5 | | UP | 1 | 0 |
| 7Day | Surfactant metabolism | 0.32482 | 0.90729 | 0.72192 | abca3 | 2076.62 | 2076.62 | 2076.62 | | 2076.62 | | DOWN | 0 | 1 |
| 7Day | Antigen activates B Cell Receptor (BCR) leading to generation of second messengers | 0.32482 | 0.90729 | 0.72192 | itpr2 | 4098.21 | 4098.21 | 4098.21 | | 4098.21 | | DOWN | 0 | 1 |
| 7Day | Telomere Maintenance | 0.32482 | 0.90729 | 0.72192 | prim2 | 4006.14 | 4006.14 | 4006.14 | | 4006.14 | | UP | 1 | 0 |
| 7Day | Extension of Telomeres | 0.32482 | 0.90729 | 0.72192 | prim2 | 4006.14 | 4006.14 | 4006.14 | | 4006.14 | | UP | 1 | 0 |
| 7Day | DNA strand elongation | 0.32482 | 0.90729 | 0.72192 | prim2 | 4006.14 | 4006.14 | 4006.14 | | 4006.14 | | UP | 1 | 0 |
| 7Day | Scavenging of heme from plasma | 0.32482 | 0.90729 | 0.72192 | lrp1 | 1316.54 | 1316.54 | 1316.54 | | 1316.54 | | DOWN | 0 | 1 |
| 7Day | FGFR2 alternative splicing | 0.32482 | 0.90729 | 0.72192 | polr2h | 3964.6 | 3964.6 | 3964.6 | | 3964.6 | | UP | 1 | 0 |
| 7Day | Orc1 removal from chromatin | 0.32482 | 0.90729 | 0.72192 | uba52 | 4761.56 | 4761.56 | 4761.56 | | 4761.56 | | UP | 1 | 0 |
| 7Day | Cytochrome P450 - arranged by substrate type | 0.71882 | 0.40566 | 0.7226 | cyp3a25;cyp39a1;ncoa2;ncoa1;cyp3a11;cyp2e1;cyp2c37;cyp2c29;arnt;cyp3a41b | 2995.27016 | 3207.45 | 86.7986 | 1706.55759 | 3069.02013 | 1300.90994 | DOWN | 0.4 | 0.6 |
| 28Day | Glucagon-type ligand receptors | 0.34452 | 0.89768 | 0.72278 | gnb5 | 953.648 | 953.648 | 953.648 | | 953.648 | | UP | 1 | 0 |
| 28Day | Regulation of APC/C activators between G1/S and early anaphase | 0.34452 | 0.89768 | 0.72278 | cdc27 | 5780.76 | 5780.76 | 5780.76 | | 5780.76 | | UP | 1 | 0 |
| 28Day | RAF activation | 0.34452 | 0.89768 | 0.72278 | map3k11 | 4123.28 | 4123.28 | 4123.28 | | 4123.28 | | DOWN | 0 | 1 |
| 7Day | N-glycan antennae elongation in the medial/trans-Golgi | 0.30291 | 0.91605 | 0.72623 | fuca1 | 2644.02 | 2644.02 | 2644.02 | | 2644.02 | | DOWN | 0 | 1 |
| 7Day | Effects of PIP2 hydrolysis | 0.30291 | 0.91605 | 0.72623 | itpr2 | 4098.21 | 4098.21 | 4098.21 | | 4098.21 | | DOWN | 0 | 1 |
| 7Day | COPI-mediated anterograde transport | 0.69526 | 0.43188 | 0.72632 | cog6;copz1;cog5;tubb4b;tubb2a;tuba4a;arcn1;rab1a;capza2;gbf1 | 2848.0736 | 3070.085 | 919.856 | 994.927228 | 2795.54103 | 958.513638 | UP | 0.9 | 0.1 |
| 28Day | Metalloprotease DUBs | 0.31186 | 0.91129 | 0.72803 | brca1 | 5643.31 | 5643.31 | 5643.31 | | 5643.31 | | UP | 1 | 0 |
| 28Day | Fanconi Anemia Pathway | 0.31186 | 0.91129 | 0.72803 | cenpx | 5532.9 | 5532.9 | 5532.9 | | 5532.9 | | DOWN | 0 | 1 |
| 28Day | Cytosolic sensors of pathogen-associated DNA | 0.31186 | 0.91129 | 0.72803 | ikbkg | 5417.68 | 5417.68 | 5417.68 | | 5417.68 | | UP | 1 | 0 |
| 28Day | Glucagon-like Peptide-1 (GLP1) regulates insulin secretion | 0.31186 | 0.91129 | 0.72803 | gnb5 | 953.648 | 953.648 | 953.648 | | 953.648 | | UP | 1 | 0 |
| 7Day | G2/M Checkpoints | 0.68329 | 0.44496 | 0.72855 | ube2n;ube2v2;rnf168;hist1h4h;babam1;hist1h2bc;gtse1;ywhaz;uba52;cdc25a | 3819.2 | 3506.09 | 2423.08 | 1013.09681 | 3600.20171 | 917.409884 | UP | 0.9 | 0.1 |
| 90Day | Keratan sulfate/keratin metabolism | 0.76935 | 0.45823 | 0.73129 | omd;st3gal3;lum | 4411.32667 | 4358.58 | 3651.14 | 787.885329 | 4239.33949 | 529.843763 | UP | 0.666666667 | 0.333333333 |
| 90Day | Synthesis of very long-chain fatty acyl-CoAs | 0.76935 | 0.45823 | 0.73129 | acsl4;acsl1;elovl3 | 4415.75 | 4450.55 | 3817.19 | 581.940912 | 4378.99247 | 653.984583 | UP | 0.666666667 | 0.333333333 |
| 90Day | FRS-mediated FGFR4 signaling | 0.76935 | 0.45823 | 0.73129 | klb;sos1;fgf1 | 3329.21633 | 3850.29 | 242.429 | 2862.05 | 4571.98571 | 2172.73633 | DOWN | 0 | 1 |
| 7Day | Regulation of TP53 Degradation | 0.77454 | 0.44912 | 0.73137 | uba52;ppp2cb;ccng1 | 3207.74333 | 3627.04 | 1234.63 | 1800.46274 | 2951.96869 | 1731.17243 | UP | 1 | 0 |
| 7Day | Regulation of TP53 Expression and Degradation | 0.77454 | 0.44912 | 0.73137 | uba52;ppp2cb;ccng1 | 3207.74333 | 3627.04 | 1234.63 | 1800.46274 | 2951.96869 | 1731.17243 | UP | 1 | 0 |
| 28Day | Antigen Presentation: Folding, assembly and peptide loading of class I MHC | 0.76813 | 0.4533 | 0.7351 | tap1;h2-q7;h2-d1 | 3562.11333 | 3718.12 | 1188.24 | 2299.84187 | 3462.70475 | 1959.38094 | DOWN | 0.333333333 | 0.666666667 |

BMD analysis results for functional classification based on dose-responsive genes, using the Reactome database for gene sets in BMDExpress2.2 software.

| Study Day | Gene Set Name | Fisher's Exact Left P-Value | Fisher's Exact Right P-Value | Fisher's Exact Two Tail | Gene Symbols | BMD Mean | BMD Median | BMD Minimum | BMD Standard Deviation | BMD wMean | BMD wSD | Overall Direction | Percent Genes With Overall Direction Up | Percent Genes With Overall Direction Down |
|---|---|---|---|---|---|---|---|---|---|---|---|---|---|---|
| 28Day | Platelet Aggregation (Plug Formation) | 0.76813 | 0.4533 | 0.7351 | pdpk1;fn1;f2 | 1563.246 | 1340.75 | 192.988 | 1493.98406 | 1721.26663 | 1119.56706 | DOWN | 0 | 1 |
| 90Day | Fatty acid metabolism | 0.67012 | 0.41346 | 0.73519 | acad10;ndufab1;cyp4f16;pccb;gpx4;hacl1;acaa2;acsl4;cyp2c54;cyp4a12a;pon3;slc27a2;slc25a17;scd1;mut;acsl1;ephx2;cyp4a12b;cyp2c38;cyp2c37;cyp1a2;elovl3;pcca;cyp2c69 | 2894.76238 | 3148.415 | 105.476 | 1486.54079 | 3095.7356 | 1281.543 | CONFLICT | 0.458333333 | 0.541666667 |
| 7Day | RNA Polymerase III Transcription Initiation From Type 1 Promoter | 0.75348 | 0.47444 | 0.73723 | brf1;gtf3c6;polr2h | 2841.95 | 2665.35 | 1895.9 | 1045.59581 | 3394.41506 | 909.790933 | UP | 0.666666667 | 0.333333333 |
| 7Day | RNA Polymerase III Transcription Initiation From Type 2 Promoter | 0.75348 | 0.47444 | 0.73723 | brf1;gtf3c6;polr2h | 2841.95 | 2665.35 | 1895.9 | 1045.59581 | 3394.41506 | 909.790933 | UP | 0.666666667 | 0.333333333 |
| 7Day | Interleukin-6 family signaling | 0.75348 | 0.47444 | 0.73723 | stat1;ptpn11;jak1 | 3700.28667 | 3629.67 | 3554.32 | 191.312992 | 3689.86935 | 200.012264 | UP | 1 | 0 |
| 7Day | Downstream signaling of activated FGFR4 | 0.75348 | 0.47444 | 0.73723 | ptpn11;kras;fgf1 | 3478.71333 | 3629.67 | 2647.76 | 766.702949 | 3262.18888 | 788.939216 | UP | 0.666666667 | 0.333333333 |
| 7Day | Platelet calcium homeostasis | 0.75348 | 0.47444 | 0.73723 | itpr2;calm3;calm2 | 4021.69667 | 4098.21 | 3050.32 | 935.469749 | 3605.92075 | 987.837442 | DOWN | 0.333333333 | 0.666666667 |
| 90Day | Branched-chain amino acid catabolism | 0.74372 | 0.48852 | 0.73888 | mccc2;ivd;aldh6a1 | 2901.54 | 2782.05 | 2413.93 | 557.051067 | 2905.96425 | 437.440481 | DOWN | 0 | 1 |
| 28Day | Base Excision Repair | 0.75295 | 0.4715 | 0.7392 | pole3;polb;lig3 | 4016.65933 | 5391.42 | 805.318 | 2790.67273 | 4750.69575 | 2278.10973 | UP | 0.666666667 | 0.333333333 |
| 28Day | Resolution of Abasic Sites (AP sites) | 0.75295 | 0.4715 | 0.7392 | pole3;polb;lig3 | 4016.65933 | 5391.42 | 805.318 | 2790.67273 | 4750.69575 | 2278.10973 | UP | 0.666666667 | 0.333333333 |
| 28Day | Toll-like Receptor Cascades | 0.69115 | 0.42871 | 0.7413 | ube2n;map2k4;apob;eea1;mapkapk2;ly96;lbp;ikbkg;ctss;app;birc2 | 4705.72409 | 5375 | 939.205 | 1555.50389 | 4457.55552 | 1860.88208 | DOWN | 0.363636364 | 0.636363636 |
| 7Day | Mitotic Prophase | 0.67062 | 0.45252 | 0.74228 | gm49336;hist1h4h;hist1h2bc;kmt5a;nek6;arpp19;hist2h2ac;mapk3;rab1a;hist2h2aa1;tpr | 3464.91164 | 3489.14 | 770.098 | 1336.66819 | 3385.40368 | 1262.79732 | UP | 0.727272727 | 0.272727273 |
| 90Day | VEGFA-VEGFR2 Pathway | 0.37426 | 0.7464 | 0.74297 | mapk14;wasf2;vav1;rasa1;rock2;rock1;hsp90aa1;cdc42;ctnnb1 | 2740.53767 | 3874.11 | 156.487 | 2016.69226 | 2197.99008 | 2124.70017 | CONFLICT | 0.555555556 | 0.444444444 |
| 28Day | Metabolism of polyamines | 0.73755 | 0.48941 | 0.74362 | otc;odc1;ass1 | 1555.824 | 1071.29 | 726.832 | 1150.51108 | 2152.64352 | 1141.9296 | DOWN | 0 | 1 |
| 28Day | Fatty acids | 0.73755 | 0.48941 | 0.74362 | cyp4a12b;cyp2a5;cyp2a4 | 3719.93667 | 4062.67 | 2330.57 | 1253.64413 | 3560.79952 | 1366.51391 | UP | 1 | 0 |
| 7Day | CYP2E1 reactions | 0.73202 | 0.49922 | 0.7437 | cyp2e1;cyp2c37;cyp2c29 | 2168.54433 | 2593.25 | 529.743 | 1473.10438 | 2359.55856 | 1350.29483 | DOWN | 0.333333333 | 0.666666667 |
| 7Day | Endosomal Sorting Complex Required For Transport (ESCRT) | 0.73202 | 0.49922 | 0.7437 | chmp5;ubap1;uba52 | 4748.63667 | 4761.56 | 4143.71 | 598.569641 | 4466.39253 | 497.911596 | UP | 0.666666667 | 0.333333333 |
| 7Day | Calmodulin induced events | 0.73202 | 0.49922 | 0.7437 | prkar2a;calm3;calm2 | 4011.14667 | 4066.56 | 3050.32 | 934.353205 | 3661.3101 | 940.743026 | DOWN | 0.333333333 | 0.666666667 |
| 7Day | CaM pathway | 0.73202 | 0.49922 | 0.7437 | prkar2a;calm3;calm2 | 4011.14667 | 4066.56 | 3050.32 | 934.353205 | 3661.3101 | 940.743026 | DOWN | 0.333333333 | 0.666666667 |
| 7Day | Estrogen-dependent gene expression | 0.38074 | 0.74008 | 0.74512 | hist1h4h;hist1h2bc;ptges3;hist2h2ac;polr2h;ncoa2;ncoa1;hsp90aa1;hist2h2aa1 | 3099.84762 | 3406.55 | 86.7986 | 1615.33069 | 3333.02753 | 1366.62708 | UP | 0.777777778 | 0.222222222 |
| 28Day | Cargo trafficking to the periciliary membrane | 0.72198 | 0.50703 | 0.74833 | rab11a;bbs9;exoc4 | 3191.45667 | 2439.57 | 2192.92 | 1520.91927 | 2895.01352 | 1368.7554 | UP | 0.666666667 | 0.333333333 |
| 7Day | DAG and IP3 signaling | 0.71024 | 0.52339 | 0.75067 | prkar2a;calm3;calm2 | 4011.14667 | 4066.56 | 3050.32 | 934.353205 | 3661.3101 | 940.743026 | DOWN | 0.333333333 | 0.666666667 |
| 7Day | Signaling by ERBB4 | 0.71024 | 0.52339 | 0.75067 | uba52;kras;wwp1 | 3915.25667 | 4158.71 | 2825.5 | 990.724091 | 3677.90484 | 1055.68644 | UP | 1 | 0 |
| 7Day | Nicotinate metabolism | 0.71024 | 0.52339 | 0.75067 | nudt12;qprt;naxe | 1773.19433 | 820.079 | 127.584 | 2277.04164 | 1305.01876 | 2232.32789 | DOWN | 0.333333333 | 0.666666667 |
| 7Day | HS-GAG biosynthesis | 0.71024 | 0.52339 | 0.75067 | hs3st3b1;sdc3;ext1 | 4352.01 | 3803.05 | 3370.58 | 1342.88039 | 4460.9593 | 1397.14798 | DOWN | 0.333333333 | 0.666666667 |
| 7Day | Interferon alpha/beta signaling | 0.71024 | 0.52339 | 0.75067 | stat1;ptpn11;jak1 | 3700.28667 | 3629.67 | 3554.32 | 191.312992 | 3689.86935 | 200.012264 | UP | 1 | 0 |
| 28Day | TNF signaling | 0.70627 | 0.52433 | 0.75329 | tax1bp1;ikbkg;birc2 | 5416.20667 | 5417.68 | 4968.69 | 446.781822 | 5309.28907 | 473.741883 | UP | 0.666666667 | 0.333333333 |
| 90Day | Downstream signaling of activated FGFR3 | 0.69103 | 0.54646 | 0.75626 | sos1;gab1;fgf1 | 2087.929 | 242.429 | 126.428 | 3297.46971 | 3907.43024 | 3338.39856 | DOWN | 0 | 1 |
| 7Day | Regulation of TNFR1 signaling | 0.68823 | 0.5469 | 0.75805 | tax1bp1;uba52;xiap | 4305.42 | 4761.56 | 3280.67 | 889.239449 | 4538.5068 | 745.308274 | UP | 0.666666667 | 0.333333333 |
| 7Day | Downstream signaling of activated FGFR2 | 0.68823 | 0.5469 | 0.75805 | ptpn11;kras;fgf1 | 3478.71333 | 3629.67 | 2647.76 | 766.702949 | 3262.18888 | 788.939216 | UP | 0.666666667 | 0.333333333 |
| 7Day | Ca-dependent events | 0.68823 | 0.5469 | 0.75805 | prkar2a;calm3;calm2 | 4011.14667 | 4066.56 | 3050.32 | 934.353205 | 3661.3101 | 940.743026 | DOWN | 0.333333333 | 0.666666667 |
| 28Day | E3 ubiquitin ligases ubiquitinate target proteins | 0.69044 | 0.54128 | 0.75846 | ube2n;ube2v2;wdr61 | 4687.35 | 5266.71 | 3288.55 | 1217.32932 | 4527.85068 | 1325.9576 | DOWN | 0.333333333 | 0.666666667 |
| 28Day | Formation of Incision Complex in GG-NER | 0.69044 | 0.54128 | 0.75846 | ube2n;usp45;ube2v2 | 3466.03 | 3288.55 | 1842.83 | 1718.82603 | 3280.75322 | 1178.82295 | DOWN | 0.333333333 | 0.666666667 |
| 28Day | Vasopressin regulates renal water homeostasis via Aquaporins | 0.69044 | 0.54128 | 0.75846 | rab11a;gnb5;adcy9 | 2455.72267 | 2192.92 | 953.648 | 1649.25522 | 1742.1359 | 1240.36097 | UP | 0.666666667 | 0.333333333 |
| 28Day | Signaling by Nuclear Receptors | 0.37449 | 0.73889 | 0.75896 | akr1c6;ppid;akr1c12;akr1c19;hist1h4i;adh4;aldh8a1;rdh16f2;polr2a;akr1c14 | 4222.7323 | 5014.36 | 912.843 | 1695.66273 | 3921.62892 | 1559.28116 | DOWN | 0.4 | 0.6 |
| 7Day | Factors involved in megakaryocyte development and platelet production | 0.67047 | 0.44262 | 0.7613 | rbsn;mfn1;tubb4b;vps45;tubb2a;tuba4a;itpk1;prkar2a;kif2a;kif1c;cdc42;cbx5;capza2 | 3141.45738 | 3597.94 | 919.856 | 1608.01789 | 2958.75896 | 1521.1747 | UP | 0.615384615 | 0.384615385 |
| 90Day | Regulation of TP53 Degradation | 0.42605 | 0.80823 | 0.76178 | mdm2;ccng1 | 2199.502 | 2199.502 | 863.924 | 1888.79252 | 3071.06832 | 1431.18185 | UP | 1 | 0 |

BMD analysis results for functional classification based on dose-responsive genes, using the Reactome database for gene sets in BMDExpress2.2 software.

| Study Day | Gene Set Name | Fisher's Exact Left P-Value | Fisher's Exact Right P-Value | Fisher's Exact Two Tail | Gene Symbols | BMD Mean | BMD Median | BMD Minimum | BMD Standard Deviation | BMD wMean | BMD wSD | Overall Direction | Percent Genes With Overall Direction Up | Percent Genes With Overall Direction Down |
|---|---|---|---|---|---|---|---|---|---|---|---|---|---|---|
| 90Day | Regulation of TP53 Expression and Degradation | 0.42605 | 0.80823 | 0.76178 | mdm2;ccng1 | 2199.502 | 2199.502 | 863.924 | 1888.79252 | 3071.06832 | 1431.18185 | UP | 1 | 0 |
| 90Day | TAK1 activates NFkB by phosphorylation and activation of IKKs complex | 0.42605 | 0.80823 | 0.76178 | nfkbia;ikbkg | 3433.33 | 3433.33 | 3265.56 | 237.262609 | 3311.77597 | 163.5322 | CONFLICT | 0.5 | 0.5 |
| 90Day | SUMOylation of intracellular receptors | 0.42605 | 0.80823 | 0.76178 | nr5a2;ar | 1086.5995 | 1086.5995 | 174.249 | 1290.25845 | 1071.30871 | 1290.07723 | DOWN | 0 | 1 |
| 90Day | A tetrasaccharide linker sequence is required for GAG synthesis | 0.42605 | 0.80823 | 0.76178 | sdc4;bgn | 2581.783 | 2581.783 | 630.216 | 2759.93252 | 3403.41741 | 2503.40993 | DOWN | 0 | 1 |
| 90Day | Interleukin-6 family signaling | 0.39963 | 0.82486 | 0.7622 | lifr;crlf1 | 3403.375 | 3403.375 | 3200.93 | 286.300465 | 3314.11858 | 256.971864 | CONFLICT | 0.5 | 0.5 |
| 90Day | G-protein activation | 0.39963 | 0.82486 | 0.7622 | gng11;gnai3 | 5378.655 | 5378.655 | 4854.24 | 741.634805 | 5266.80756 | 724.570551 | UP | 1 | 0 |
| 90Day | Synthesis of active ubiquitin: roles of E1 and E2 enzymes | 0.37431 | 0.84018 | 0.76367 | ube2k;cdc34 | 2429.116 | 2429.116 | 569.072 | 2630.49945 | 1344.2356 | 2136.72563 | UP | 1 | 0 |
| 90Day | Synthesis of bile acids and bile salts via 7alpha-hydroxycholesterol | 0.37431 | 0.84018 | 0.76367 | slc27a2;amacr | 3510.085 | 3510.085 | 3419.78 | 127.710556 | 3490.24552 | 124.590434 | DOWN | 0 | 1 |
| 90Day | Negative regulation of FGFR4 signaling | 0.37431 | 0.84018 | 0.76367 | klb;fgf1 | 2046.3595 | 2046.3595 | 242.429 | 2551.14298 | 3002.17622 | 2163.59869 | DOWN | 0 | 1 |
| 28Day | Antigen processing-Cross presentation | 0.67454 | 0.55788 | 0.76382 | tap1;h2-q7;h2-d1 | 3562.11333 | 3718.12 | 1188.24 | 2299.84187 | 3462.70475 | 1959.38094 | DOWN | 0.333333333 | 0.666666667 |
| 28Day | Metabolism of steroid hormones | 0.67454 | 0.55788 | 0.76382 | hsd17b3;hsd11b1;fdxr | 3448.4054 | 5126.12 | 67.9262 | 2927.60766 | 3847.46522 | 2710.49219 | DOWN | 0.333333333 | 0.666666667 |
| 7Day | Activation of kainate receptors upon glutamate binding | 0.43028 | 0.80396 | 0.7642 | calm3;calm2 | 3983.44 | 3983.44 | 3050.32 | 1319.63096 | 3556.9103 | 1173.69957 | CONFLICT | 0.5 | 0.5 |
| 7Day | Thrombin signalling through proteinase activated receptors (PARs) | 0.43028 | 0.80396 | 0.7642 | mapk3;f2 | 2478.4335 | 2478.4335 | 156.627 | 3283.53024 | 2159.69073 | 3252.44169 | DOWN | 0 | 1 |
| 7Day | Intrinsic Pathway for Apoptosis | 0.38684 | 0.83132 | 0.76518 | ywhaz;xiap | 3800.505 | 3800.505 | 2726.98 | 1518.19361 | 4303.76091 | 1341.03648 | CONFLICT | 0.5 | 0.5 |
| 7Day | TBC/RABGAPs | 0.38684 | 0.83132 | 0.76518 | rab11a;rab6a | 4298.915 | 4298.915 | 4055.48 | 344.269079 | 4355.93759 | 334.690971 | UP | 1 | 0 |
| 7Day | RHO GTPases Activate Formins | 0.3822 | 0.72879 | 0.76558 | clasp2;cenpk;tubb4b;tubb2a;tuba4a;ppp2cb;pfn2;pfn1;kif2a;cdc42;xpo1 | 3175.61509 | 3627.04 | 919.856 | 1191.81016 | 3128.68157 | 1280.33364 | UP | 0.909090909 | 0.090909091 |
| 90Day | Downstream signal transduction | 0.35011 | 0.85427 | 0.76611 | rasa1;sos1 | 4014.285 | 4014.285 | 2133.64 | 2659.63367 | 5271.62423 | 1977.83907 | CONFLICT | 0.5 | 0.5 |
| 90Day | Signaling by ERBB4 | 0.35011 | 0.85427 | 0.76611 | nrg1;sos1 | 4903.635 | 4903.635 | 3912.34 | 1401.90283 | 5120.14662 | 1368.05592 | CONFLICT | 0.5 | 0.5 |
| 90Day | ER-Phagosome pathway | 0.35011 | 0.85427 | 0.76611 | tap2;snap23 | 2434.48 | 2434.48 | 544.33 | 2673.07576 | 3329.02624 | 2354.76285 | CONFLICT | 0.5 | 0.5 |
| 90Day | Interleukin-7 signaling | 0.35011 | 0.85427 | 0.76611 | irs2;hist1h3c | 443.33615 | 443.33615 | 74.8133 | 521.170013 | 516.773173 | 510.717328 | CONFLICT | 0.5 | 0.5 |
| 7Day | Gamma carboxylation, hypusine formation and arylsulfatase activation | 0.36626 | 0.84367 | 0.76673 | f2;arsb | 95.43325 | 95.43325 | 34.2395 | 86.5410312 | 126.416077 | 74.6289419 | DOWN | 0 | 1 |
| 28Day | Intra-Golgi traffic | 0.42588 | 0.80479 | 0.76729 | man1a;cux1 | 2205.787 | 2205.787 | 185.394 | 2857.26718 | 3712.11899 | 1904.18057 | DOWN | 0 | 1 |
| 28Day | PI3K Cascade | 0.42588 | 0.80479 | 0.76729 | pdpk1;fgf1 | 830.279 | 830.279 | 192.988 | 901.265575 | 1273.10558 | 648.142632 | DOWN | 0 | 1 |
| 28Day | Switching of origins to a post-replicative state | 0.42588 | 0.80479 | 0.76729 | cdc6;cdc27 | 5824.15 | 5824.15 | 5780.76 | 61.3627265 | 5829.67647 | 60.862965 | UP | 1 | 0 |
| 28Day | Formation of the ternary complex, and subsequently, the 43S complex | 0.41002 | 0.81502 | 0.76741 | eif3m;eif1ax | 2737.81 | 2737.81 | 1517.45 | 1725.84966 | 2423.68091 | 1667.69388 | CONFLICT | 0.5 | 0.5 |
| 28Day | Ca2+ pathway | 0.41002 | 0.81502 | 0.76741 | ppp3cb;gnb5 | 2524.759 | 2524.759 | 953.648 | 2221.88648 | 2301.60545 | 2199.36003 | UP | 1 | 0 |
| 28Day | IRS-mediated signalling | 0.41002 | 0.81502 | 0.76741 | pdpk1;fgf1 | 830.279 | 830.279 | 192.988 | 901.265575 | 1273.10558 | 648.142632 | DOWN | 0 | 1 |
| 28Day | Retrograde transport at the Trans-Golgi-Network | 0.41002 | 0.81502 | 0.76741 | rab9;tmf1 | 3666.6 | 3666.6 | 2900.88 | 1082.89161 | 3862.31598 | 1046.92156 | CONFLICT | 0.5 | 0.5 |
| 28Day | Chondroitin sulfate/dermatan sulfate metabolism | 0.37947 | 0.83405 | 0.76875 | hyal1;gpc4 | 2868.94 | 2868.94 | 2376.85 | 695.920352 | 2635.93564 | 612.962541 | DOWN | 0 | 1 |
| 90Day | Regulation of TP53 Activity through Acetylation | 0.75535 | 0.44236 | 0.76941 | pin1;gatad2b;pml;hdac2 | 2973.7305 | 3372.53 | 202.162 | 2000.2498 | 2520.57141 | 2294.44974 | UP | 0.75 | 0.25 |
| 90Day | Metabolism of water-soluble vitamins and cofactors | 0.64977 | 0.46152 | 0.77049 | mccc2;pank1;nmnat3;slc52a3;pccb;slc23a2;pdxk;pcx;mut;mthfd2;aox1;hlcs;pcca;aldh1l1 | 2376.61114 | 2730.885 | 338.932 | 1542.82357 | 2731.93797 | 1506.15671 | DOWN | 0.214285714 | 0.785714286 |
| 28Day | IRS-related events triggered by IGF1R | 0.3505 | 0.8513 | 0.77146 | pdpk1;fgf1 | 830.279 | 830.279 | 192.988 | 901.265575 | 1273.10558 | 648.142632 | DOWN | 0 | 1 |
| 7Day | Fatty acyl-CoA biosynthesis | 0.7518 | 0.44424 | 0.77166 | elovl5;ppt1;h2-ke6;elovl3 | 2943.36225 | 3453.59 | 212.399 | 1928.833 | 2974.02822 | 1575.38039 | CONFLICT | 0.5 | 0.5 |
| 28Day | IGF1R signaling cascade | 0.33662 | 0.8593 | 0.77328 | pdpk1;fgf1 | 830.279 | 830.279 | 192.988 | 901.265575 | 1273.10558 | 648.142632 | DOWN | 0 | 1 |
| 90Day | G alpha (12/13) signalling events | 0.73309 | 0.46835 | 0.77349 | gng11;rock2;rock1;adra1b | 2858.7705 | 3159.375 | 262.092 | 1993.91208 | 2150.48638 | 1967.48202 | UP | 0.75 | 0.25 |
| 7Day | Binding and Uptake of Ligands by Scavenger Receptors | 0.73334 | 0.46576 | 0.77494 | apob;hsp90b1;lrp1;apoe | 1320.5015 | 1584.74 | 113.316 | 856.630708 | 1503.0686 | 778.63729 | DOWN | 0.25 | 0.75 |
| 7Day | EPHB-mediated forward signaling | 0.73334 | 0.46576 | 0.77494 | kalrn;yes1;rasa1;cdc42 | 4449.69 | 4308.425 | 3395.83 | 1016.81766 | 4753.88739 | 995.095429 | CONFLICT | 0.5 | 0.5 |
| 7Day | Regulation of mRNA stability by proteins that bind AU-rich elements | 0.73334 | 0.46576 | 0.77494 | dcp2;ywhaz;uba52;xpo1 | 3417.9825 | 3109.105 | 2692.16 | 968.653438 | 3487.09233 | 1071.329 | UP | 1 | 0 |
| 28Day | Apoptotic execution phase | 0.72908 | 0.46766 | 0.77773 | dnm1l;pkp1;kpna1;birc2 | 5033.44 | 5531.66 | 3208.19 | 1232.6146 | 4608.97876 | 1444.68139 | UP | 1 | 0 |
| 28Day | ECM proteoglycans | 0.72908 | 0.46766 | 0.77773 | vtn;fn1;dag1;app | 3475.1805 | 3893.235 | 447.762 | 2265.95602 | 4422.97912 | 1870.22533 | DOWN | 0 | 1 |

BMD analysis results for functional classification based on dose-responsive genes, using the Reactome database for gene sets in BMDExpress2.2 software.

| Study Day | Gene Set Name | Fisher's Exact Left P-Value | Fisher's Exact Right P-Value | Fisher's Exact Two Tail | Gene Symbols | BMD Mean | BMD Median | BMD Minimum | BMD Standard Deviation | BMD wMean | BMD wSD | Overall Direction | Percent Genes With Overall Direction Up | Percent Genes With Overall Direction Down |
|---|---|---|---|---|---|---|---|---|---|---|---|---|---|---|
| 28Day | Pyruvate metabolism and Citric Acid (TCA) cycle | 0.72908 | 0.46766 | 0.77773 | suclg2;me1;ldha;gstz1 | 4807.215 | 5341.16 | 2701.34 | 1426.60759 | 5227.92689 | 1161.60616 | DOWN | 0 | 1 |
| 90Day | Downstream TCR signaling | 0.7104 | 0.49389 | 0.77823 | cdc34;nfkbia;ikbkg;btrc | 3147.108 | 3433.33 | 569.072 | 1905.15166 | 3410.68987 | 2043.61215 | CONFLICT | 0.5 | 0.5 |
| 90Day | FCERI mediated NF-kB activation | 0.7104 | 0.49389 | 0.77823 | cdc34;nfkbia;ikbkg;btrc | 3147.108 | 3433.33 | 569.072 | 1905.15166 | 3410.68987 | 2043.61215 | CONFLICT | 0.5 | 0.5 |
| 7Day | Metabolism of lipids | 0.38976 | 0.66291 | 0.78122 | hadha;pla1a;akr1c6;fads1;elovl5;fitm1;dgat2;pccb;crls1;tnfaip8l1;9130409i23rik;vapb;fads2;cyp3a25;ptges3;cyp39a1;stard10;mtmr7;acaa2;idi1;sptlc1;slc27a5;decr2;osbpl2;mtmr6;smpd2;smpd1;slc25a17;slc10a2;slc10a1;pten;ptdss1;ppt1;neu1;ncoa2;ncoa1;phyh;kpnb1;hsd17b4;hsd17b2;hsd11b1;hmgcs2;h2-ke6;gstm4;gc;ephx2;ebp;cyp3a11;cyp2e1;cyp2c37;cyp2c29;elovl3;baat;arsb;pecr;acat2;akr1c14;hsd3b7;cyp3a41b | 2746.25929 | 3174.68 | 34.2395 | 1719.82553 | 2844.91315 | 1560.56945 | CONFLICT | 0.457627119 | 0.542372881 |
| 7Day | mTOR signalling | 0.69561 | 0.50785 | 0.78285 | rps6kb1;rraga;eif4ebp1;cab39 | 3640.5775 | 3624.525 | 3116.98 | 548.193968 | 3866.9375 | 468.42227 | UP | 0.75 | 0.25 |
| 7Day | Formation of Fibrin Clot (Clotting Cascade) | 0.69561 | 0.50785 | 0.78285 | f12;f5;f2;serpinc1 | 698.358875 | 200.354 | 85.9375 | 1074.23654 | 310.699694 | 558.93663 | DOWN | 0 | 1 |
| 28Day | Iron uptake and transport | 0.70197 | 0.49802 | 0.78314 | atp6v0e2;trf;ftl1;atp6v1e1 | 2823.62425 | 2736.09 | 527.967 | 1969.39643 | 2135.74969 | 1654.17081 | CONFLICT | 0.5 | 0.5 |
| 90Day | TP53 Regulates Transcription of Cell Cycle Genes | 0.68739 | 0.51889 | 0.78356 | plk2;cdkn1a;btg2;bax | 2194.0025 | 1943.11 | 913.71 | 1285.83436 | 1710.06551 | 1075.88404 | UP | 1 | 0 |
| 28Day | Innate Immune System | 0.64699 | 0.40447 | 0.78438 | ube2n;atp6v0e2;arhgap45;c8g;ndufc2;npc2;cmtm6;ormdl3;psmd6;serpinb1a;golga7;dynll1;hebp2;methig1;iqgap2;tax1bp1;map2k4;apob;clec12a;tubb4b;vtn;ube2m;tnfrsf1b;eea1;serpina1e;serpina1b;s100a11;rab18;ppp3cb;pnp;pa2g4;pkp1;pfkl;pdpk1;mme;mapkapk2;man2b1;ly96;lta4h;lbp;anpep;ikbkg;h2-q7;h2-d1;gstp1;gstp2;gpi1;gaa;ftl1;f2;ctss;clu;cdc42;capza2;c4b;c3;c2;bcl2l1;atp6v1e1;app;birc2;atad3a;acly;qsox1;brk1;dnajc3 | 3190.72403 | 3171.82 | 160.43 | 1921.18708 | 3116.35917 | 1948.69713 | DOWN | 0.318181818 | 0.681818182 |
| 28Day | Respiratory electron transport | 0.68825 | 0.51292 | 0.78616 | ndufab1;ndufaf1;ndufc2;etfdh | 2704.97 | 1988.385 | 1023.12 | 2137.1137 | 2428.10357 | 2123.03848 | DOWN | 0.25 | 0.75 |
| 7Day | Glycosphingolipid metabolism | 0.67644 | 0.52833 | 0.78738 | smpd2;smpd1;neu1;arsb | 3517.87488 | 4120.7 | 34.2395 | 2487.75667 | 4054.00508 | 2446.20526 | DOWN | 0 | 1 |
| 7Day | TNF signaling | 0.67644 | 0.52833 | 0.78738 | tax1bp1;uba52;smpd2;xiap | 4678.03 | 4817.795 | 3280.67 | 1040.44095 | 4863.61056 | 877.60986 | CONFLICT | 0.5 | 0.5 |
| 7Day | Gap junction trafficking | 0.67644 | 0.52833 | 0.78738 | tubb4b;tubb2a;tuba4a;gja1 | 2276.434 | 1954.85 | 919.856 | 1424.18025 | 1763.60227 | 985.706882 | UP | 0.75 | 0.25 |
| 7Day | Signaling by SCF-KIT | 0.67644 | 0.52833 | 0.78738 | yes1;stat1;ptpn11;kras | 3931.55 | 3968.91 | 3629.67 | 224.307128 | 3931.63954 | 198.580589 | UP | 1 | 0 |
| 28Day | Formation of RNA Pol II elongation complex | 0.67444 | 0.52762 | 0.78937 | iws1;wdr61;polr2a;ccnk | 4124.69025 | 5065.76 | 860.451 | 2186.16416 | 4389.08607 | 2021.74453 | CONFLICT | 0.5 | 0.5 |
| 28Day | RNA Polymerase II Transcription Elongation | 0.67444 | 0.52762 | 0.78937 | iws1;wdr61;polr2a;ccnk | 4124.69025 | 5065.76 | 860.451 | 2186.16416 | 4389.08607 | 2021.74453 | CONFLICT | 0.5 | 0.5 |
| 7Day | Signaling by NOTCH | 0.65715 | 0.54838 | 0.79223 | ywhaz;uba52;prkci;mdk | 3820.895 | 3897.52 | 2726.98 | 925.576967 | 4101.75459 | 806.418941 | UP | 0.75 | 0.25 |
| 90Day | Antigen Presentation: Folding, assembly and peptide loading of class I MHC | 0.4099 | 0.78792 | 0.79254 | erap1;tap2;sec13 | 3293.66667 | 2797.47 | 2758.9 | 893.048687 | 3139.69012 | 789.484091 | DOWN | 0.333333333 | 0.666666667 |
| 90Day | SUMOylation of chromatin organization proteins | 0.4099 | 0.78792 | 0.79254 | hist1h4h;hist1h4i;hdac2 | 2720.22733 | 3951.81 | 202.162 | 2180.88131 | 1950.71221 | 2307.88021 | DOWN | 0.333333333 | 0.666666667 |
| 90Day | Platelet Aggregation (Plug Formation) | 0.4099 | 0.78792 | 0.79254 | tln1;sos1;fn1 | 4161.30667 | 4478.93 | 2110.06 | 1912.32154 | 4694.64696 | 1722.82421 | DOWN | 0 | 1 |
| 28Day | Deadenylation-dependent mRNA decay | 0.66058 | 0.5421 | 0.79274 | exosc3;wdr61;cnot1;paip1 | 3828.5875 | 3500.885 | 2805.79 | 1204.04491 | 4227.20544 | 1273.09992 | UP | 0.75 | 0.25 |
| 90Day | Signaling by FGFR3 | 0.38758 | 0.80341 | 0.7936 | sos1;gab1;fgf1 | 2087.929 | 242.429 | 126.428 | 3297.46971 | 3907.43024 | 3338.39856 | DOWN | 0 | 1 |
| 7Day | Regulation of PTEN gene transcription | 0.43202 | 0.77063 | 0.79423 | rraga;suz12;bmi1 | 3785.18667 | 3225.73 | 3193.23 | 997.285596 | 3681.52085 | 944.533221 | UP | 1 | 0 |
| 7Day | Switching of origins to a post-replicative state | 0.41291 | 0.78439 | 0.7945 | uba52;cdc27;ccne2 | 4410.11 | 4598.19 | 3870.58 | 474.333116 | 4498.87719 | 394.432252 | UP | 1 | 0 |
| 7Day | Ub-specific processing proteases | 0.39179 | 0.70614 | 0.79473 | usp16;tomm20;psmd5;psmd6;hist2h2ac;taf10;psmc4;vdac3;vdac2;uba52;tgfbr1;pten;psmc2;hist2h2aa1;cdc25a | 3744.69 | 3548.46 | 1811.97 | 1242.38365 | 3552.48514 | 1367.78801 | UP | 0.933333333 | 0.066666667 |
| 7Day | Ca2+ pathway | 0.39429 | 0.79747 | 0.79525 | ctnnb1;calm3;calm2 | 2673.80107 | 3050.32 | 54.5232 | 2452.7893 | 2387.26243 | 2186.51911 | DOWN | 0.333333333 | 0.666666667 |

BMD analysis results for functional classification based on dose-responsive genes, using the Reactome database for gene sets in BMDExpress2.2 software.

| Study Day | Gene Set Name | Fisher's Exact Left P-Value | Fisher's Exact Right P-Value | Fisher's Exact Two Tail | Gene Symbols | BMD Mean | BMD Median | BMD Minimum | BMD Standard Deviation | BMD wMean | BMD wSD | Overall Direction | Percent Genes With Overall Direction Up | Percent Genes With Overall Direction Down |
|---|---|---|---|---|---|---|---|---|---|---|---|---|---|---|
| 90Day | Presynaptic phase of homologous DNA pairing and strand exchange | 0.36604 | 0.81793 | 0.79532 | rad51;brca2;rad51c | 3127.57067 | 4249.95 | 513.022 | 2271.80208 | 3130.56464 | 2280.41 | UP | 1 | 0 |
| 28Day | Nonhomologous End-Joining (NHEJ) | 0.64667 | 0.55634 | 0.79627 | ube2n;ube2v2;hist1h4i;brca1 | 5011.745 | 5455.01 | 3288.55 | 1173.78176 | 4729.48604 | 1369.44158 | CONFLICT | 0.5 | 0.5 |
| 7Day | Nuclear Envelope Breakdown | 0.3762 | 0.80987 | 0.79646 | gm49336;nek6;tpr | 2646.08933 | 2535 | 770.098 | 1933.93044 | 2710.863 | 1721.80663 | UP | 1 | 0 |
| 28Day | Synthesis of substrates in N-glycan biosythesis | 0.4159 | 0.78041 | 0.7971 | nanp;gne;gfpt1 | 5085.35667 | 5755.83 | 3647.63 | 1246.04778 | 5180.06702 | 1205.69221 | DOWN | 0.333333333 | 0.666666667 |
| 28Day | Signaling by TGF-beta Receptor Complex | 0.4159 | 0.78041 | 0.7971 | ube2m;tfdp1;ccnk | 4577.73667 | 5090.85 | 2933.96 | 1456.65483 | 4832.41634 | 1309.22256 | UP | 0.666666667 | 0.333333333 |
| 28Day | Dual incision in TC-NER | 0.36352 | 0.81681 | 0.80021 | pole3;prpf19;polr2a | 3132.08267 | 3550.26 | 805.318 | 2148.41938 | 3348.7397 | 1703.23431 | UP | 1 | 0 |
| 28Day | C-type lectin receptors (CLRs) | 0.71318 | 0.46404 | 0.80304 | ube2n;ube2m;ppp3cb;pdpk1;ikbkg | 3581.4416 | 4095.87 | 192.988 | 2143.44278 | 3918.11922 | 1510.6886 | UP | 0.6 | 0.4 |
| 28Day | HATs acetylate histones | 0.71318 | 0.46404 | 0.80304 | msl1;meaf6;hist1h4i;kat7;hcfc1 | 4539.96 | 5043.8 | 2859.88 | 1234.05187 | 4409.47817 | 1273.01653 | DOWN | 0.4 | 0.6 |
| 28Day | Assembly of the pre-replicative complex | 0.71318 | 0.46404 | 0.80304 | psmd6;psmd8;cdc6;psmf1;psmb8 | 3966.316 | 4413.43 | 1415.14 | 1680.76279 | 4053.96174 | 1828.75774 | DOWN | 0.4 | 0.6 |
| 28Day | Platelet activation, signaling and aggregation | 0.64418 | 0.44965 | 0.80465 | spp2;cdc37l1;ola1;abcc4;a2m;trf;serpina1e;serpina1b;pdpk1;itih4;gnb5;fn1;f5;f2;clu;cdc42;app;anxa5;qsox1 | 2518.72995 | 2463.49 | 192.988 | 1720.69751 | 2423.18308 | 1716.29855 | DOWN | 0.263157895 | 0.736842105 |
| 28Day | Interleukin-1 family signaling | 0.70103 | 0.47757 | 0.80473 | ube2n;sqstm1;il1rap;ikbkg;app | 4940.87 | 5266.71 | 3705.51 | 791.86401 | 5097.48088 | 859.756978 | DOWN | 0.4 | 0.6 |
| 28Day | Toll Like Receptor 3 (TLR3) Cascade | 0.68878 | 0.49099 | 0.8066 | ube2n;map2k4;mapkapk2;ikbkg;app | 4661.272 | 5266.71 | 2616.5 | 1186.39761 | 4522.68638 | 1287.59598 | DOWN | 0.4 | 0.6 |
| 7Day | Fatty acid metabolism | 0.65828 | 0.43334 | 0.80668 | hadha;akr1c6;fads1;elovl5;pccb;fads2;ptges3;acaa2;decr2;slc25a17;ppt1;phyh;hsd17b4;h2-ke6;ephx2;cyp2c37;cyp2c29;elovl3;pecr;akr1c14 | 2020.81211 | 2641.18 | 55.2305 | 1724.8506 | 2170.46283 | 1464.92174 | DOWN | 0.4 | 0.6 |
| 28Day | trans-Golgi Network Vesicle Budding | 0.67644 | 0.50428 | 0.80864 | picalm;hgs;ftl1;app;gbf1 | 3282.2154 | 3903.31 | 527.967 | 1620.92556 | 2497.62022 | 1908.50446 | UP | 0.8 | 0.2 |
| 28Day | Clathrin derived vesicle budding | 0.67644 | 0.50428 | 0.80864 | picalm;hgs;ftl1;app;gbf1 | 3282.2154 | 3903.31 | 527.967 | 1620.92556 | 2497.62022 | 1908.50446 | UP | 0.8 | 0.2 |
| 7Day | Condensation of Prophase Chromosomes | 0.65206 | 0.53239 | 0.81154 | hist1h4h;hist1h2bc;kmt5a;hist2h2ac;hist2h2aa1 | 3978.152 | 3489.14 | 3406.55 | 853.600483 | 3909.52678 | 885.518779 | UP | 0.6 | 0.4 |
| 7Day | Heparan sulfate/heparin (HS-GAG) metabolism | 0.65206 | 0.53239 | 0.81154 | hs3st3b1;hgsnat;sdc3;ext1;bgn | 3828.584 | 3370.58 | 2968.59 | 1190.86868 | 4003.60067 | 1265.31843 | DOWN | 0.2 | 0.8 |
| 7Day | Pyruvate metabolism and Citric Acid (TCA) cycle | 0.65206 | 0.53239 | 0.81154 | sdha;pdhx;idh2;idh3b;dld | 3266.496 | 3538.1 | 114.56 | 2018.40912 | 3640.89587 | 1559.57539 | DOWN | 0.2 | 0.8 |
| 28Day | Toll Like Receptor 10 (TLR10) Cascade | 0.65159 | 0.53043 | 0.81314 | ube2n;map2k4;mapkapk2;ikbkg;app | 4661.272 | 5266.71 | 2616.5 | 1186.39761 | 4522.68638 | 1287.59598 | DOWN | 0.4 | 0.6 |
| 28Day | Toll Like Receptor 5 (TLR5) Cascade | 0.65159 | 0.53043 | 0.81314 | ube2n;map2k4;mapkapk2;ikbkg;app | 4661.272 | 5266.71 | 2616.5 | 1186.39761 | 4522.68638 | 1287.59598 | DOWN | 0.4 | 0.6 |
| 28Day | MyD88 cascade initiated on plasma membrane | 0.65159 | 0.53043 | 0.81314 | ube2n;map2k4;mapkapk2;ikbkg;app | 4661.272 | 5266.71 | 2616.5 | 1186.39761 | 4522.68638 | 1287.59598 | DOWN | 0.4 | 0.6 |
| 90Day | Signaling by ERBB2 | 0.43732 | 0.74632 | 0.81326 | nrg1;sos1;hsp90aa1;gab1 | 2590.0045 | 2169.33 | 126.428 | 2794.15124 | 3580.82543 | 2756.86322 | CONFLICT | 0.5 | 0.5 |
| 90Day | TP53 Regulates Metabolic Genes | 0.41661 | 0.76222 | 0.81359 | txnrd1;ywhaz;txn1;gsr | 2630.852 | 2620.955 | 137.958 | 2080.55574 | 3004.54948 | 2352.81113 | UP | 0.75 | 0.25 |
| 7Day | Cell Cycle Checkpoints | 0.39779 | 0.69086 | 0.81501 | ube2n;clasp2;ube2v2;rnf168;hist1h4h;babam1;hist1h2bc;cenpk;gtse1;cop1;ywhaz;uba52;cdc27;ppp2cb;kif2a;cdkn1a;cdc25a;ccne2;xpo1 | 3780.57105 | 3627.71 | 2423.08 | 852.712829 | 3670.51007 | 817.173885 | UP | 0.894736842 | 0.105263158 |
| 7Day | Interleukin-17 signaling | 0.63469 | 0.55017 | 0.81509 | mapk3;map2k3;uba52;ppp2cb;btrc | 4058.048 | 4207.06 | 2894.34 | 807.460042 | 3936.95988 | 797.852297 | UP | 0.6 | 0.4 |
| 7Day | Semaphorin interactions | 0.63469 | 0.55017 | 0.81509 | gsk3b;pak2;sema4d;sema4a;hsp90aa1 | 3869.84 | 4499.44 | 1005.61 | 2047.60939 | 3962.70312 | 2199.68011 | UP | 0.6 | 0.4 |
| 7Day | Iron uptake and transport | 0.43239 | 0.74875 | 0.81512 | abcg2;uba52;ftl1;atp6v1e1 | 3576.0815 | 4272.24 | 720.546 | 1978.48703 | 3616.39084 | 2146.03772 | UP | 0.75 | 0.25 |
| 28Day | MyD88:MAL(TIRAP) cascade initiated on plasma membrane | 0.6391 | 0.54327 | 0.8156 | ube2n;map2k4;mapkapk2;ikbkg;app | 4661.272 | 5266.71 | 2616.5 | 1186.39761 | 4522.68638 | 1287.59598 | DOWN | 0.4 | 0.6 |
| 28Day | Toll Like Receptor TLR1:TLR2 Cascade | 0.6391 | 0.54327 | 0.8156 | ube2n;map2k4;mapkapk2;ikbkg;app | 4661.272 | 5266.71 | 2616.5 | 1186.39761 | 4522.68638 | 1287.59598 | DOWN | 0.4 | 0.6 |
| 28Day | Toll Like Receptor TLR6:TLR2 Cascade | 0.6391 | 0.54327 | 0.8156 | ube2n;map2k4;mapkapk2;ikbkg;app | 4661.272 | 5266.71 | 2616.5 | 1186.39761 | 4522.68638 | 1287.59598 | DOWN | 0.4 | 0.6 |
| 28Day | Toll Like Receptor 2 (TLR2) Cascade | 0.6391 | 0.54327 | 0.8156 | ube2n;map2k4;mapkapk2;ikbkg;app | 4661.272 | 5266.71 | 2616.5 | 1186.39761 | 4522.68638 | 1287.59598 | DOWN | 0.4 | 0.6 |
| 90Day | Sphingolipid de novo biosynthesis | 0.37683 | 0.79167 | 0.81574 | ormdl2;ppm1l;acer2;sptlc2 | 4089.2325 | 3669.21 | 3502.64 | 963.349978 | 3708.02376 | 627.838636 | CONFLICT | 0.5 | 0.5 |
| 7Day | NoRC negatively regulates rRNA expression | 0.39859 | 0.77446 | 0.81613 | hist1h4h;hist1h2bc;hist2h2ac;hist2h2aa1 | 4100.405 | 3802.835 | 3406.55 | 933.741438 | 4060.85571 | 1011.0164 | CONFLICT | 0.5 | 0.5 |
| 7Day | Intraflagellar transport | 0.39859 | 0.77446 | 0.81613 | hspb11;tubb4b;tubb2a;tuba4a | 2178.474 | 1954.85 | 919.856 | 1242.69347 | 2388.51606 | 1364.4516 | UP | 1 | 0 |
| 7Day | Signaling by PDGF | 0.38226 | 0.78651 | 0.81713 | rasa1;stat1;ptpn11;kras | 4372.8325 | 4037.79 | 3629.67 | 966.662513 | 4569.74061 | 1058.51347 | UP | 0.75 | 0.25 |
| 28Day | Transcription-Coupled Nucleotide Excision Repair (TC-NER) | 0.40711 | 0.76638 | 0.81809 | pole3;prpf19;polr2a;lig3 | 3696.917 | 4295.465 | 805.318 | 2086.45358 | 3989.40693 | 1722.6516 | UP | 0.75 | 0.25 |
| 28Day | Signaling by Insulin receptor | 0.40711 | 0.76638 | 0.81809 | atp6v0e2;pdpk1;fgf1;atp6v1e1 | 2335.122 | 1926.575 | 192.988 | 2168.02221 | 2304.43263 | 1455.8728 | DOWN | 0.25 | 0.75 |
| 7Day | SIRT1 negatively regulates rRNA expression | 0.36634 | 0.79805 | 0.81844 | hist1h4h;hist1h2bc;hist2h2ac;hist2h2aa1 | 4100.405 | 3802.835 | 3406.55 | 933.741438 | 4060.85571 | 1011.0164 | CONFLICT | 0.5 | 0.5 |
| 7Day | Signaling by the B Cell Receptor (BCR) | 0.69622 | 0.46922 | 0.82004 | uba52;kras;itpr2;calm3;calm2;btrc | 4198.73667 | 4182.885 | 3050.32 | 657.674434 | 3976.2843 | 788.611862 | UP | 0.666666667 | 0.333333333 |

BMD analysis results for functional classification based on dose-responsive genes, using the Reactome database for gene sets in BMDExpress2.2 software.

| Study Day | Gene Set Name | Fisher's Exact Left P-Value | Fisher's Exact Right P-Value | Fisher's Exact Two Tail | Gene Symbols | BMD Mean | BMD Median | BMD Minimum | BMD Standard Deviation | BMD wMean | BMD wSD | Overall Direction | Percent Genes With Overall Direction Up | Percent Genes With Overall Direction Down |
|---|---|---|---|---|---|---|---|---|---|---|---|---|---|---|
| 28Day | RNA Polymerase II Pre-transcription Events | 0.37193 | 0.79249 | 0.82026 | iws1;wdr61;polr2a;ccnk | 4124.69025 | 5065.76 | 860.451 | 2186.16416 | 4389.08607 | 2021.74453 | CONFLICT | 0.5 | 0.5 |
| 28Day | TRAF6 mediated induction of NFkB and MAP kinases upon TLR7/8 or 9 activation | 0.69072 | 0.47296 | 0.82248 | ube2n;map2k4;mapkapk2;ly96;ikbkg;app | 4644.44333 | 4948.59 | 2616.5 | 1061.94664 | 4533.01649 | 1074.62366 | CONFLICT | 0.5 | 0.5 |
| 28Day | APC/C-mediated degradation of cell cycle proteins | 0.69072 | 0.47296 | 0.82248 | psmd6;psmd8;cdc14a;psmf1;cdc27;psmb8 | 3415.512 | 3894.855 | 748.272 | 1975.49515 | 3457.19909 | 2020.42083 | CONFLICT | 0.5 | 0.5 |
| 28Day | Regulation of mitotic cell cycle | 0.69072 | 0.47296 | 0.82248 | psmd6;psmd8;cdc14a;psmf1;cdc27;psmb8 | 3415.512 | 3894.855 | 748.272 | 1975.49515 | 3457.19909 | 2020.42083 | CONFLICT | 0.5 | 0.5 |
| 90Day | Metabolism of amino acids and derivatives | 0.63212 | 0.45352 | 0.82316 | mccc2;dmgdh;amdhd1;ndufab1;hoga1;asrgl1;serinc1;ivd;txnrd1;ahcy;tst;slc25a21;suox;sardh;oat;hpd;gstz1;glul;slc6a12;cdo1;arg2;gm4737;agxt;aldh6a1 | 2656.47342 | 2998.6 | 105.476 | 1333.22225 | 2688.41813 | 1392.52728 | DOWN | 0.208333333 | 0.791666667 |
| 28Day | Toll Like Receptor 7/8 (TLR7/8) Cascade | 0.67949 | 0.48515 | 0.82379 | ube2n;map2k4;mapkapk2;ly96;ikbkg;app | 4644.44333 | 4948.59 | 2616.5 | 1061.94664 | 4533.01649 | 1074.62366 | CONFLICT | 0.5 | 0.5 |
| 28Day | MyD88 dependent cascade initiated on endosome | 0.67949 | 0.48515 | 0.82379 | ube2n;map2k4;mapkapk2;ly96;ikbkg;app | 4644.44333 | 4948.59 | 2616.5 | 1061.94664 | 4533.01649 | 1074.62366 | CONFLICT | 0.5 | 0.5 |
| 28Day | DNA Replication Pre-Initiation | 0.67949 | 0.48515 | 0.82379 | psmd6;pole3;psmd8;cdc6;psmf1;psmb8 | 3439.483 | 3894.855 | 805.318 | 1981.23419 | 3717.90337 | 2013.21092 | CONFLICT | 0.5 | 0.5 |
| 7Day | Autodegradation of Cdh1 by Cdh1:APC/C | 0.66493 | 0.50298 | 0.82404 | psmd5;psmd6;psmc4;uba52;cdc27;psmc2 | 3479.61667 | 3598.515 | 2309.23 | 896.239144 | 3408.72083 | 977.398512 | UP | 1 | 0 |
| 7Day | EPH-Ephrin signaling | 0.63323 | 0.53594 | 0.82899 | kalrn;sdcbp;yes1;pak2;rasa1;cdc42 | 3930.20333 | 3708.39 | 2538.2 | 1147.99056 | 4503.50691 | 1119.22462 | UP | 0.666666667 | 0.333333333 |
| 7Day | Cleavage of Growing Transcript in the Termination Region | 0.63323 | 0.53594 | 0.82899 | fip1l1;cpsf2;lsm10;srsf1;cstf2;thoc5 | 3791.17333 | 3366.41 | 2905.24 | 1041.714 | 3506.15051 | 699.668867 | UP | 1 | 0 |
| 7Day | RNA Polymerase II Transcription Termination | 0.63323 | 0.53594 | 0.82899 | fip1l1;cpsf2;lsm10;srsf1;cstf2;thoc5 | 3791.17333 | 3366.41 | 2905.24 | 1041.714 | 3506.15051 | 699.668867 | UP | 1 | 0 |
| 90Day | NRAGE signals death through JNK | 0.4403 | 0.72787 | 0.82899 | arhgef6;fgd4;vav1;tiam1;sos1 | 5279.148 | 5800.32 | 4161.05 | 841.81329 | 5353.08411 | 810.835565 | DOWN | 0.2 | 0.8 |
| 90Day | Respiratory electron transport | 0.42133 | 0.7431 | 0.82929 | ndufab1;ndufc2;etfdh;ndufaf3;ndufb9 | 3326.1292 | 3477.1 | 105.476 | 2076.71355 | 4597.15369 | 1965.30097 | DOWN | 0.4 | 0.6 |
| 90Day | Kinesins | 0.42133 | 0.7431 | 0.82929 | tubb6;tubb4b;tubb2a;tuba1b;kifc1 | 1389.634 | 1722.38 | 713.489 | 593.401723 | 1135.0221 | 585.08693 | UP | 0.8 | 0.2 |
| 90Day | G1/S Transition | 0.40278 | 0.75769 | 0.82998 | pole4;cables1;orc6;dbf4;cdkn1a | 3595.292 | 4071.91 | 913.71 | 1819.33413 | 2719.27209 | 1739.06073 | UP | 0.6 | 0.4 |
| 90Day | Intraflagellar transport | 0.40278 | 0.75769 | 0.82998 | tubb6;ift52;tubb4b;tubb2a;tuba1b | 1277.8726 | 1722.38 | 154.682 | 776.85001 | 1233.28221 | 659.90165 | UP | 0.6 | 0.4 |
| 28Day | Processing of DNA double-strand break ends | 0.63401 | 0.53295 | 0.83032 | ube2n;rmi1;ube2v2;hist1h4i;brca1;blm | 4031.196 | 4357.41 | 692.086 | 1973.26334 | 4212.5832 | 1623.69045 | UP | 0.666666667 | 0.333333333 |
| 7Day | PKMTs methylate histone lysines | 0.43206 | 0.73322 | 0.83073 | hist1h4h;kmt5a;suz12;setd2;kmt5b | 3441.166 | 3406.55 | 3159.12 | 320.71106 | 3391.94842 | 276.159994 | UP | 0.6 | 0.4 |
| 7Day | HATs acetylate histones | 0.41647 | 0.74569 | 0.83109 | hist1h4h;hist1h2bc;kat7;ncoa2;ncoa1 | 2713.08172 | 3352.11 | 86.7986 | 1468.87603 | 3226.13378 | 748.206477 | UP | 0.8 | 0.2 |
| 7Day | Assembly of the pre-replicative complex | 0.41647 | 0.74569 | 0.83109 | psmd5;psmd6;psmc4;uba52;psmc2 | 3401.424 | 3326.45 | 2309.23 | 978.876936 | 3327.35463 | 1056.01708 | UP | 1 | 0 |
| 7Day | PRC2 methylates histones and DNA | 0.40117 | 0.75773 | 0.8317 | hist1h4h;hist1h2bc;suz12;hist2h2ac;hist2h2aa1 | 3918.97 | 3418.4 | 3193.23 | 904.708849 | 3846.64569 | 946.911026 | UP | 0.6 | 0.4 |
| 7Day | Protein-protein interactions at synapses | 0.38618 | 0.76934 | 0.83257 | gria3;ptprf;ptprd;il1rap;flot2 | 2550.5868 | 2247.36 | 131.024 | 2161.76821 | 2088.5953 | 1959.99374 | DOWN | 0.2 | 0.8 |
| 7Day | Asparagine N-linked glycosylation | 0.40069 | 0.67929 | 0.83345 | trappc6b;fuca1;cog6;0610009b22rik;ngly1;copz1;gnpnat1;ppp6r1;cog5;tubb4b;uba52;tubb2a;tuba4a;arcn1;sel1l;sec22b;rab1a;neu1;gfpt1;f5;capza2;asgr1;gbf1;alg9 | 3351.56737 | 3410.995 | 244.081 | 1310.67174 | 3049.41852 | 1353.91995 | UP | 0.708333333 | 0.291666667 |
| 7Day | Toll Like Receptor 10 (TLR10) Cascade | 0.66214 | 0.49341 | 0.83656 | ube2n;ecsit;mapk3;map2k3;uba52;ppp2cb;btrc | 3993.80429 | 4207.06 | 2894.34 | 704.971717 | 3855.96351 | 691.922621 | CONFLICT | 0.571428571 | 0.428571429 |
| 7Day | Toll Like Receptor 5 (TLR5) Cascade | 0.66214 | 0.49341 | 0.83656 | ube2n;ecsit;mapk3;map2k3;uba52;ppp2cb;btrc | 3993.80429 | 4207.06 | 2894.34 | 704.971717 | 3855.96351 | 691.922621 | CONFLICT | 0.571428571 | 0.428571429 |
| 7Day | MyD88 cascade initiated on plasma membrane | 0.66214 | 0.49341 | 0.83656 | ube2n;ecsit;mapk3;map2k3;uba52;ppp2cb;btrc | 3993.80429 | 4207.06 | 2894.34 | 704.971717 | 3855.96351 | 691.922621 | CONFLICT | 0.571428571 | 0.428571429 |
| 7Day | MyD88:MAL(TIRAP) cascade initiated on plasma membrane | 0.64749 | 0.50882 | 0.8383 | ube2n;ecsit;mapk3;map2k3;uba52;ppp2cb;btrc | 3993.80429 | 4207.06 | 2894.34 | 704.971717 | 3855.96351 | 691.922621 | CONFLICT | 0.571428571 | 0.428571429 |
| 7Day | Toll Like Receptor TLR1:TLR2 Cascade | 0.64749 | 0.50882 | 0.8383 | ube2n;ecsit;mapk3;map2k3;uba52;ppp2cb;btrc | 3993.80429 | 4207.06 | 2894.34 | 704.971717 | 3855.96351 | 691.922621 | CONFLICT | 0.571428571 | 0.428571429 |
| 7Day | Toll Like Receptor TLR6:TLR2 Cascade | 0.64749 | 0.50882 | 0.8383 | ube2n;ecsit;mapk3;map2k3;uba52;ppp2cb;btrc | 3993.80429 | 4207.06 | 2894.34 | 704.971717 | 3855.96351 | 691.922621 | CONFLICT | 0.571428571 | 0.428571429 |
| 7Day | Toll Like Receptor 2 (TLR2) Cascade | 0.64749 | 0.50882 | 0.8383 | ube2n;ecsit;mapk3;map2k3;uba52;ppp2cb;btrc | 3993.80429 | 4207.06 | 2894.34 | 704.971717 | 3855.96351 | 691.922621 | CONFLICT | 0.571428571 | 0.428571429 |

BMD analysis results for functional classification based on dose-responsive genes, using the Reactome database for gene sets in BMDExpress2.2 software.

| Study Day | Gene Set Name | Fisher's Exact Left P-Value | Fisher's Exact Right P-Value | Fisher's Exact Two Tail | Gene Symbols | BMD Mean | BMD Median | BMD Minimum | BMD Standard Deviation | BMD wMean | BMD wSD | Overall Direction | Percent Genes With Overall Direction Up | Percent Genes With Overall Direction Down |
|---|---|---|---|---|---|---|---|---|---|---|---|---|---|---|
| 90Day | Regulation of actin dynamics for phagocytic cup formation | 0.619 | 0.53966 | 0.84112 | wasf2;vav1;myo9b;myo10;hsp90aa1;fcgr2b;cdc42 | 2644.57429 | 3055.31 | 100.823 | 2388.05593 | 3312.00806 | 2193.71301 | DOWN | 0.285714286 | 0.714285714 |
| 90Day | EPH-Ephrin signaling | 0.44242 | 0.71364 | 0.8413 | tiam1;rasa1;rock2;rock1;mmp2;cdc42 | 2737.16317 | 3003.875 | 156.487 | 2236.40759 | 2441.83028 | 2378.23325 | UP | 0.666666667 | 0.333333333 |
| 7Day | RHO GTPase Effectors | 0.59957 | 0.47881 | 0.84152 | clasp2;myh14;hist1h4h;hist1h2bc;cenpk;iqgap2;nckap1;hist2h2ac;mapk3;tubb4b;ywhaz;pak2;tubb2a;tuba4a;flna;ppp2cb;pfn2;pfn1;ncoa2;myh9;kif2a;hist2h2aa1;cdc42;ctnnb1;calm3;calm2;abl1;xpo1;brk1 | 3174.79406 | 3406.55 | 54.5232 | 1375.89626 | 3213.28147 | 1370.13031 | UP | 0.620689655 | 0.379310345 |
| 7Day | COPII-mediated vesicle transport | 0.44599 | 0.70939 | 0.8428 | trappc6b;0610009b22rik;ppp6r1;sec22b;rab1a;f5 | 3049.9035 | 3385.155 | 244.081 | 1691.22153 | 2500.88926 | 1631.85364 | UP | 0.666666667 | 0.333333333 |
| 7Day | Signaling by MET | 0.43133 | 0.72163 | 0.84296 | ranbp10;ranbp9;hgfac;uba52;ptpn11;kras | 2747.02567 | 3298.26 | 186.634 | 1860.55789 | 2417.40203 | 1865.94033 | UP | 0.666666667 | 0.333333333 |
| 90Day | Peroxisomal protein import | 0.39066 | 0.75578 | 0.84305 | gstk1;hacl1;slc27a2;amacr;ephx2;agxt | 3428.52667 | 3398.155 | 2157.32 | 816.22512 | 3062.66676 | 947.203112 | DOWN | 0 | 1 |
| 90Day | L1CAM interactions | 0.67586 | 0.47009 | 0.84422 | tubb6;ranbp9;tubb4b;tubb2a;tuba1b;msn;ap2m1;itga9 | 2660.11012 | 2467.28 | 779.791 | 1310.19834 | 1803.37656 | 1184.81498 | UP | 0.625 | 0.375 |
| 7Day | RHO GTPases activate PKNs | 0.38877 | 0.75616 | 0.84467 | hist1h4h;hist1h2bc;hist2h2ac;ywhaz;ncoa2;hist2h2aa1 | 3202.56643 | 3412.475 | 86.7986 | 1776.19071 | 3725.32417 | 1328.83106 | UP | 0.666666667 | 0.333333333 |
| 7Day | Platelet homeostasis | 0.38877 | 0.75616 | 0.84467 | apob;ptpn11;ppp2cb;itpr2;calm3;calm2 | 3553.50167 | 3628.355 | 1999.21 | 983.347249 | 3501.98056 | 773.659418 | CONFLICT | 0.5 | 0.5 |
| 28Day | Metabolism of RNA | 0.62327 | 0.45133 | 0.8461 | las1l;a1cf;phf5a;ccar1;rnpc3;exosc3;wdr61;pno1;sf3b6;set;cpsf2;prpf19;cnot1;hnrnpul1;prpf38a;smg5;u2af2;paip1;wdr18;dhx37;snrpd1;smn1;polr2a;prpf8;papola;fbl;bop1;srsf1;tpr;thoc5;bc005561 | 3604.15581 | 3919.15 | 131.831 | 1610.53153 | 3719.0459 | 1653.32351 | UP | 0.64516129 | 0.35483871 |
| 7Day | Mitotic G1-G1/S phases | 0.63295 | 0.51386 | 0.84959 | uba52;tfdp1;prim2;ppp2cb;cdkn1a;cdc25a;ccne2;abl1 | 3720.57925 | 3816.59 | 707.264 | 1540.65955 | 3868.29641 | 1301.93724 | UP | 0.875 | 0.125 |
| 7Day | Fcgamma receptor (FCGR) dependent phagocytosis | 0.63295 | 0.51386 | 0.84959 | nckap1;mapk3;yes1;myh9;hsp90aa1;cdc42;abl1;brk1 | 3254.56125 | 3418.395 | 1005.61 | 1281.94634 | 3162.32786 | 1406.29011 | UP | 0.625 | 0.375 |
| 7Day | Cellular response to heat stress | 0.63295 | 0.51386 | 0.84959 | hspb8;gm49336;hsbp1;ptges3;dnajb6;hsp90aa1;hsph1;tpr | 2879.9385 | 3330.73 | 589.118 | 1422.66123 | 2634.35759 | 1461.94836 | UP | 0.875 | 0.125 |
| 7Day | Processing of DNA double-strand break ends | 0.44405 | 0.70102 | 0.85268 | ube2n;ube2v2;rnf168;hist1h4h;babam1;hist1h2bc;uba52 | 3607.63286 | 3444.79 | 2423.08 | 733.542077 | 3447.91192 | 706.296567 | UP | 0.857142857 | 0.142857143 |
| 7Day | Mitochondrial translation elongation | 0.44405 | 0.70102 | 0.85268 | mrpl16;mrpl1;mrpl47;mrps17;mrps36;mrps31;mrpl2 | 4077.59429 | 3969.79 | 3223.73 | 605.190521 | 4004.64794 | 651.515278 | UP | 1 | 0 |
| 90Day | COPII-mediated vesicle transport | 0.39536 | 0.74285 | 0.85281 | trappc6b;lman1;stx17;tgfa;serpina1e;areg;sec13 | 3432.10557 | 3798.74 | 959.779 | 1610.18273 | 3119.79648 | 1439.58855 | UP | 0.714285714 | 0.285714286 |
| 7Day | Sphingolipid metabolism | 0.41687 | 0.724 | 0.85325 | 9130409i23rik;vapb;sptlc1;smpd2;smpd1;neu1;arsb | 3669.80564 | 3876.31 | 34.2395 | 1772.38512 | 3960.10113 | 1691.87893 | DOWN | 0.285714286 | 0.714285714 |
| 7Day | MyD88-independent TLR4 cascade | 0.41687 | 0.724 | 0.85325 | ube2n;mapk3;map2k3;uba52;ptpn11;ppp2cb;btrc | 3909.24286 | 3629.67 | 2894.34 | 708.585348 | 3806.22655 | 683.032185 | UP | 0.714285714 | 0.285714286 |
| 7Day | TRIF(TICAM1)-mediated TLR4 signaling | 0.41687 | 0.724 | 0.85325 | ube2n;mapk3;map2k3;uba52;ptpn11;ppp2cb;btrc | 3909.24286 | 3629.67 | 2894.34 | 708.585348 | 3806.22655 | 683.032185 | UP | 0.714285714 | 0.285714286 |
| 7Day | Mitochondrial translation termination | 0.41687 | 0.724 | 0.85325 | mrpl16;mrpl1;mrpl47;mrps17;mrps36;mrps31;mrpl2 | 4077.59429 | 3969.79 | 3223.73 | 605.190521 | 4004.64794 | 651.515278 | UP | 1 | 0 |
| 7Day | Mitochondrial translation | 0.40358 | 0.73503 | 0.85378 | mrpl16;mrpl1;mrpl47;mrps17;mrps36;mrps31;mrpl2 | 4077.59429 | 3969.79 | 3223.73 | 605.190521 | 4004.64794 | 651.515278 | UP | 1 | 0 |
| 28Day | Glycerophospholipid biosynthesis | 0.45251 | 0.69221 | 0.85444 | dgat2;pnpla8;phospho1;pla2g4c;etnk2;ptdss1;abhd4 | 3801.69429 | 3854.48 | 2889.4 | 718.035407 | 3698.35911 | 647.344505 | CONFLICT | 0.428571429 | 0.571428571 |
| 7Day | Cellular responses to external stimuli | 0.60364 | 0.465 | 0.86009 | hspb8;ep400;gm49336;cul2;hist1h4h;rraga;hsbp1;hist1h2bc;txn2;ptges3;suz12;txnrd1;hist2h2ac;mapk3;map2k3;atg4c;dnajb6;tubb4b;uba52;tubb2a;tuba4a;terf2;cdc27;prdx2;stip1;sod1;hsp90aa1;hsph1;hist2h2aa1;gstp1;gstp2;cdkn1a;ccne2;capza2;bmi1;arnt;egln1;tpr | 3243.93466 | 3392.01 | 589.118 | 1327.40568 | 3113.54853 | 1326.53415 | UP | 0.736842105 | 0.263157895 |
| 7Day | Oxidative Stress Induced Senescence | 0.40399 | 0.727 | 0.86201 | hist1h4h;hist1h2bc;suz12;hist2h2ac;map2k3;uba52;hist2h2aa1;bmi1 | 4023.41875 | 3802.835 | 2894.34 | 924.438937 | 3897.23919 | 961.420058 | UP | 0.625 | 0.375 |

BMD analysis results for functional classification based on dose-responsive genes, using the Reactome database for gene sets in BMDExpress2.2 software.

| Study Day | Gene Set Name | Fisher's Exact Left P-Value | Fisher's Exact Right P-Value | Fisher's Exact Two Tail | Gene Symbols | BMD Mean | BMD Median | BMD Minimum | BMD Standard Deviation | BMD wMean | BMD wSD | Overall Direction | Percent Genes With Overall Direction Up | Percent Genes With Overall Direction Down |
|---|---|---|---|---|---|---|---|---|---|---|---|---|---|---|
| 28Day | Degradation of the extracellular matrix | 0.45106 | 0.68523 | 0.8625 | phykpl;tmprss6;a2m;fn1;ctss;col8a1;capn5;bmp1 | 3632.22238 | 4286.025 | 182.399 | 2059.39605 | 3939.4751 | 1801.13642 | UP | 0.625 | 0.375 |
| 7Day | Epigenetic regulation of gene expression | 0.6468 | 0.48397 | 0.86343 | sf3b1;hist1h4h;hist1h2bc;gsk3b;ddx21;suz12;hist2h2ac;polr2h;mybbp1a;hist2h2aa1 | 3755.419 | 3429.125 | 2845.95 | 762.292318 | 3660.16077 | 755.922136 | UP | 0.8 | 0.2 |
| 90Day | Recruitment of NuMA to mitotic centrosomes | 0.44602 | 0.68517 | 0.86659 | haus7;tubb6;dctn3;cntrl;tubb4b;cep76;tubb2a;tuba1b;hsp90aa1 | 2642.33233 | 1951.01 | 426.32 | 1646.5088 | 2407.21003 | 1637.1364 | UP | 0.888888889 | 0.111111111 |
| 7Day | Toll Like Receptor 4 (TLR4) Cascade | 0.44025 | 0.68916 | 0.8679 | ube2n;ecsit;mapk3;map2k3;uba52;ptpn11;ppp2cb;lbp;btrc | 4091.90222 | 4207.06 | 2894.34 | 756.880427 | 3950.90744 | 747.335692 | CONFLICT | 0.555555556 | 0.444444444 |
| 7Day | ESR-mediated signaling | 0.46202 | 0.66377 | 0.87377 | hist1h4h;hist1h2bc;ppid;ptges3;hist2h2ac;polr2h;ncoa2;ncoa1;hsp90aa1;hist2h2aa1 | 2897.57586 | 3354.05 | 86.7986 | 1651.82033 | 3175.19169 | 1443.43193 | UP | 0.8 | 0.2 |
| 7Day | Metabolism of water-soluble vitamins and cofactors | 0.43841 | 0.68486 | 0.87394 | mccc2;nudt12;qprt;pccb;mocs1;btd;naxe;cyb5a;shmt2;aldh1l1 | 1945.66428 | 1772.3595 | 77.8976 | 1848.22599 | 2127.08921 | 1776.81271 | DOWN | 0.2 | 0.8 |
| 28Day | Ub-specific processing proteases | 0.43866 | 0.67829 | 0.88054 | tomm20;psmd6;psmd8;psmf1;usp12;polb;mdm2;psmb8;ikbkg;hgs;birc2 | 3729.44755 | 3654.44 | 784.943 | 1731.84434 | 3412.99335 | 1936.53099 | UP | 0.727272727 | 0.272727273 |
| 7Day | Platelet degranulation | 0.59477 | 0.52152 | 0.88291 | tmx3;cdc37l1;abcc4;tuba4a;sod1;flna;lgals3bp;f5;ecm1;calm3;calm2;ahsg;qsox1 | 3320.20592 | 3190.96 | 244.081 | 1797.47619 | 2990.51446 | 1857.71969 | DOWN | 0.384615385 | 0.615384615 |
| 7Day | Regulation of Insulin-like Growth Factor (IGF) transport and uptake by Insulin-like Growth Factor Binding Proteins (IGFBPs) | 0.59477 | 0.52152 | 0.88291 | apoa5;apob;hsp90b1;nucb1;igfbp5;f5;csf1;c4b;serpinc1;apoe;ahsg;afp;qsox1 | 2429.02581 | 1999.21 | 85.9375 | 2022.85744 | 2176.0983 | 2216.29449 | DOWN | 0.230769231 | 0.769230769 |
| 7Day | Mitotic G2-G2/M phases | 0.46744 | 0.64879 | 0.88362 | gtse1;tubb4b;uba52;tubb2a;tuba4a;ppp2cb;nedd1;hsp90aa1;cdkn1a;cdc25a;btrc;xpo1 | 3102.3255 | 2946.665 | 919.856 | 1524.03417 | 2964.09012 | 1451.34659 | UP | 1 | 0 |
| 90Day | Post-translational protein phosphorylation | 0.61197 | 0.50087 | 0.88489 | notum;spp2;apob;trf;tnc;serpina1e;itih2;igfbp4;fn1;csf1;c3;apoe;ahsg;golm1 | 2072.66716 | 1808.155 | 82.4742 | 1716.50033 | 2402.55112 | 1823.09973 | DOWN | 0.142857143 | 0.857142857 |
| 7Day | ER to Golgi Anterograde Transport | 0.6212 | 0.48655 | 0.88908 | trappc6b;cog6;0610009b22rik;copz1;ppp6r1;cog5;tubb4b;tubb2a;tuba4a;arcn1;sec22b;rab1a;f5;capza2;gbf1 | 2881.76513 | 3113.17 | 244.081 | 1280.05518 | 2587.34367 | 1266.21649 | UP | 0.8 | 0.2 |
| 7Day | Cellular Senescence | 0.42144 | 0.68282 | 0.89208 | ep400;hist1h4h;hist1h2bc;suz12;hist2h2ac;mapk3;map2k3;uba52;terf2;cdc27;hist2h2aa1;cdkn1a;ccne2;bmi1 | 4029.98357 | 4028.925 | 2818.63 | 848.565347 | 4022.93412 | 881.356636 | UP | 0.642857143 | 0.357142857 |
| 7Day | Signaling by Nuclear Receptors | 0.459 | 0.64527 | 0.89479 | akr1c6;hist1h4h;hist1h2bc;ppid;ptges3;hist2h2ac;pdhx;polr2h;rdh16f2;ncoa2;ncoa1;hsp90aa1;hist2h2aa1;dld;akr1c14 | 3258.57057 | 3406.55 | 86.7986 | 1603.45202 | 3238.65029 | 1384.02731 | UP | 0.733333333 | 0.266666667 |
| 7Day | Transport to the Golgi and subsequent modification | 0.42807 | 0.67068 | 0.89832 | trappc6b;fuca1;cog6;0610009b22rik;copz1;ppp6r1;cog5;tubb4b;tubb2a;tuba4a;arcn1;sec22b;rab1a;f5;capza2;gbf1 | 2866.90606 | 3070.085 | 244.081 | 1238.07829 | 2588.85654 | 1246.45916 | UP | 0.75 | 0.25 |
| 28Day | Deubiquitination | 0.46061 | 0.63976 | 0.89888 | asxl2;tomm20;psmd6;psmd8;uchl3;psmf1;ino80c;usp12;polb;mdm2;psmb8;ikbkg;hgs;hcfc1;brca1;birc2 | 3853.0265 | 4041.425 | 572.861 | 1803.26965 | 3618.32643 | 1970.31024 | UP | 0.6875 | 0.3125 |
| 7Day | Signaling by WNT | 0.42646 | 0.66946 | 0.90116 | tmed5;gsk3b;vps29;klhl12;ywhaz;uba52;sox6;ppp2cb;pfn1;lrp5;csnk2b;ctnnb1;calm3;calm2;btrc;xiap;xpo1 | 3368.88013 | 3627.04 | 54.5232 | 1460.48609 | 3362.34156 | 1535.85026 | UP | 0.705882353 | 0.294117647 |
| 28Day | Asparagine N-linked glycosylation | 0.57907 | 0.51673 | 0.90366 | nanp;lman2;ngly1;dynll1;ppp6r3;gne;tubb4b;tubb2a;mgat2;sec22c;serpina1e;serpina1b;man1a;gfpt1;f5;capza2;bet1;asgr1;gbf1 | 4033.60763 | 3903.31 | 185.394 | 1747.19849 | 3926.40047 | 1680.86707 | CONFLICT | 0.473684211 | 0.526315789 |
| 7Day | Response to elevated platelet cytosolic Ca2+ | 0.53999 | 0.57586 | 1 | tmx3;cdc37l1;abcc4;tuba4a;sod1;flna;lgals3bp;f5;ecm1;calm3;calm2;ahsg;qsox1 | 3320.20592 | 3190.96 | 244.081 | 1797.47619 | 2990.51446 | 1857.71969 | DOWN | 0.384615385 | 0.615384615 |
| 7Day | Purine salvage | 0.72196 | 0.66353 | 1 | adk | 124.762 | 124.762 | 124.762 |  | 124.762 |  | DOWN | 0 | 1 |
| 7Day | Activation of BAD and translocation to mitochondria | 0.68564 | 0.69527 | 1 | ywhaz | 2726.98 | 2726.98 | 2726.98 |  | 2726.98 |  | UP | 1 | 0 |
| 7Day | Activation of BH3-only proteins | 0.45381 | 0.84775 | 1 | ywhaz | 2726.98 | 2726.98 | 2726.98 |  | 2726.98 |  | UP | 1 | 0 |
| 7Day | Signaling by ERBB2 | 0.59904 | 0.60571 | 1 | yes1;uba52;kras;hsp90aa1 | 3486.7075 | 4089.83 | 1005.61 | 1685.04165 | 3246.78653 | 1805.94232 | UP | 1 | 0 |
| 7Day | CD28 co-stimulation | 0.4531 | 0.78885 | 1 | pak2;cdc42 | 3567.05 | 3567.05 | 2538.2 | 1455.01362 | 4188.77837 | 1159.29819 | UP | 1 | 0 |

BMD analysis results for functional classification based on dose-responsive genes, using the Reactome database for gene sets in BMDExpress2.2 software.

| Study Day | Gene Set Name | Fisher's Exact Left P-Value | Fisher's Exact Right P-Value | Fisher's Exact Two Tail | Gene Symbols | BMD Mean | BMD Median | BMD Minimum | BMD Standard Deviation | BMD wMean | BMD wSD | Overall Direction | Percent Genes With Overall Direction Up | Percent Genes With Overall Direction Down |
|---|---|---|---|---|---|---|---|---|---|---|---|---|---|---|
| 7Day | TP53 Regulates Metabolic Genes | 0.57974 | 0.6238 | 1 | rraga;txnrd1;ywhaz;prdx2 | 3021.79 | 2976.355 | 2303.89 | 657.772449 | 3146.44726 | 649.412862 | UP | 0.75 | 0.25 |
| 7Day | Downregulation of ERBB2 signaling | 0.6029 | 0.67518 | 1 | uba52;hsp90aa1 | 2883.585 | 2883.585 | 1005.61 | 2655.85771 | 2564.36068 | 2617.20688 | UP | 1 | 0 |
| 7Day | Transcriptional regulation by RUNX2 | 0.58015 | 0.77365 | 1 | uba52 | 4761.56 | 4761.56 | 4761.56 |  | 4761.56 |  | UP | 1 | 0 |
| 7Day | FOXO-mediated transcription | 0.45381 | 0.84775 | 1 | ywhaz | 2726.98 | 2726.98 | 2726.98 |  | 2726.98 |  | UP | 1 | 0 |
| 7Day | G2/M Transition | 0.4896 | 0.62828 | 1 | gtse1;tubb4b;uba52;tubb2a;tuba4a;ppp2cb;nedd1;hsp90aa1;cdkn1a;cdc25a;btrc;xpo1 | 3102.3255 | 2946.665 | 919.856 | 1524.03417 | 2964.09012 | 1451.34659 | UP | 1 | 0 |
| 7Day | Energy dependent regulation of mTOR by LKB1-AMPK | 0.47661 | 0.77272 | 1 | rraga;cab39 | 3711.005 | 3711.005 | 3225.73 | 686.282486 | 3826.89474 | 666.425379 | UP | 1 | 0 |
| 7Day | Antigen Presentation: Folding, assembly and peptide loading of class I MHC | 0.55576 | 0.67258 | 1 | tap2;h2-t23;h2-q10 | 3822.20667 | 4232.51 | 2584.12 | 1092.34442 | 3453.18156 | 1077.07007 | DOWN | 0 | 1 |
| 7Day | Prostanoid ligand receptors | 0.41021 | 1 | 1 |  |  |  |  |  |  |  |  |  |  |
| 7Day | Activated PKN1 stimulates transcription of AR (androgen receptor) regulated genes KLK2 and KLK3 | 0.51381 | 0.66427 | 1 | hist1h4h;hist1h2bc;hist2h2ac;ncoa2;hist2h2aa1 | 3297.68372 | 3418.4 | 86.7986 | 1968.68283 | 3851.16831 | 1376.36603 | UP | 0.6 | 0.4 |
| 7Day | UCH proteinases | 0.48168 | 0.65952 | 1 | psmd5;psmd6;hist2h2ac;psmc4;ino80c;uba52;psmc2;hist2h2aa1 | 3875.85375 | 4055.48 | 2309.23 | 1045.086 | 3896.76234 | 1200.81492 | UP | 0.875 | 0.125 |
| 7Day | Chondroitin sulfate/dermatan sulfate metabolism | 0.56056 | 0.64136 | 1 | sdc3;hyal1;bgn;arsb | 2973.70488 | 3385.82 | 34.2395 | 2144.95655 | 3428.03796 | 1961.6416 | DOWN | 0 | 1 |
| 7Day | Chondroitin sulfate biosynthesis | 0.42537 | 0.86213 | 1 | bgn | 2968.59 | 2968.59 | 2968.59 |  | 2968.59 |  | DOWN | 0 | 1 |
| 7Day | Toll Like Receptor 9 (TLR9) Cascade | 0.59137 | 0.55595 | 1 | ube2n;rbsn;ecsit;mapk3;map2k3;uba52;ppp2cb;btrc | 4237.3375 | 4214.33 | 2894.34 | 948.922894 | 3958.31477 | 823.420852 | CONFLICT | 0.5 | 0.5 |
| 7Day | Toll Like Receptor 3 (TLR3) Cascade | 0.5536 | 0.61382 | 1 | ube2n;mapk3;map2k3;uba52;ppp2cb;btrc | 3955.83833 | 3917.05 | 2894.34 | 764.378356 | 3822.84942 | 721.933719 | UP | 0.666666667 | 0.333333333 |
| 7Day | Toll Like Receptor 7/8 (TLR7/8) Cascade | 0.50046 | 0.65144 | 1 | ube2n;ecsit;mapk3;map2k3;uba52;ppp2cb;btrc | 3993.80429 | 4207.06 | 2894.34 | 704.971717 | 3855.96351 | 691.922621 | CONFLICT | 0.571428571 | 0.428571429 |
| 7Day | Toll-like Receptor Cascades | 0.47509 | 0.63751 | 1 | ube2n;rbsn;ecsit;mapk3;map2k3;apob;uba52;hsp90b1;ptpn11;ppp2cb;lbp;ctsb;btrc | 3884.85385 | 3881.76 | 1852.94 | 1186.21385 | 3883.96422 | 915.388264 | CONFLICT | 0.538461538 | 0.461538462 |
| 7Day | Nuclear Events (kinase and transcription factor activation) | 0.65616 | 0.62754 | 1 | mapk3;ppp2cb | 4213.64 | 4213.64 | 3627.04 | 829.577676 | 4084.83206 | 809.330679 | CONFLICT | 0.5 | 0.5 |
| 7Day | MAPK targets/ Nuclear events mediated by MAP kinases | 0.50078 | 0.75552 | 1 | mapk3;ppp2cb | 4213.64 | 4213.64 | 3627.04 | 829.577676 | 4084.83206 | 809.330679 | CONFLICT | 0.5 | 0.5 |
| 7Day | TRAF6 mediated induction of NFkB and MAP kinases upon TLR7/8 or 9 activation | 0.51491 | 0.63831 | 1 | ube2n;ecsit;mapk3;map2k3;uba52;ppp2cb;btrc | 3993.80429 | 4207.06 | 2894.34 | 704.971717 | 3855.96351 | 691.922621 | CONFLICT | 0.571428571 | 0.428571429 |
| 7Day | MyD88 dependent cascade initiated on endosome | 0.50046 | 0.65144 | 1 | ube2n;ecsit;mapk3;map2k3;uba52;ppp2cb;btrc | 3993.80429 | 4207.06 | 2894.34 | 704.971717 | 3855.96351 | 691.922621 | CONFLICT | 0.571428571 | 0.428571429 |
| 7Day | Intracellular oxygen transport | 0.7431 | 1 | 1 |  |  |  |  |  |  |  |  |  |  |
| 7Day | Axon guidance | 0.53171 | 0.5529 | 1 | ranbp9;gsk3b;kalrn;sdcbp;mapk3;tubb4b;yes1;pak2;vasp;uba52;tubb2a;tuba4a;rasa1;sema4d;sema4a;reln;ptpn11;pfn2;pfn1;kras;hsp90aa1;gfra1;csnk2b;cdc42;abl1 | 3515.54904 | 3629.67 | 778.73 | 1414.19868 | 3659.18086 | 1592.19662 | UP | 0.64 | 0.36 |
| 7Day | Glucose metabolism | 0.48569 | 0.70607 | 1 | pfkp;gckr;pgam1;gpi1 | 3402.63 | 3741.1 | 1853.98 | 1103.76765 | 3416.45976 | 1054.46301 | DOWN | 0.25 | 0.75 |
| 7Day | snRNP Assembly | 0.58015 | 0.77365 | 1 | snrpd2 | 5726.15 | 5726.15 | 5726.15 |  | 5726.15 |  | UP | 1 | 0 |
| 7Day | Metabolism of non-coding RNA | 0.58015 | 0.77365 | 1 | snrpd2 | 5726.15 | 5726.15 | 5726.15 |  | 5726.15 |  | UP | 1 | 0 |
| 7Day | Beta-oxidation of very long chain fatty acids | 0.68564 | 0.69527 | 1 | decr2 | 3510.23 | 3510.23 | 3510.23 |  | 3510.23 |  | UP | 1 | 0 |
| 7Day | Mitochondrial calcium ion transport | 0.51457 | 0.81436 | 1 | slc8b1 | 2876.78 | 2876.78 | 2876.78 |  | 2876.78 |  | DOWN | 0 | 1 |
| 7Day | Trafficking and processing of endosomal TLR | 0.62942 | 0.65201 | 1 | hsp90b1;ctsb | 2867.35 | 2867.35 | 1852.94 | 1434.59238 | 3470.67949 | 1153.27462 | UP | 1 | 0 |
| 7Day | Intra-Golgi traffic | 0.6184 | 0.58709 | 1 | cog6;cog5;vps45;cyth1 | 3305.2525 | 3897.525 | 1099.15 | 1502.79538 | 2991.04604 | 1609.07416 | CONFLICT | 0.5 | 0.5 |
| 7Day | RNA Polymerase III Transcription | 0.57754 | 0.65355 | 1 | brf1;gtf3c6;polr2h | 2841.95 | 2665.35 | 1895.9 | 1045.59581 | 3394.41506 | 909.790933 | UP | 0.666666667 | 0.333333333 |
| 7Day | RNA Polymerase III Transcription Initiation | 0.57754 | 0.65355 | 1 | brf1;gtf3c6;polr2h | 2841.95 | 2665.35 | 1895.9 | 1045.59581 | 3394.41506 | 909.790933 | UP | 0.666666667 | 0.333333333 |
| 7Day | Metabolism of Angiotensinogen to Angiotensins | 0.5468 | 0.79501 | 1 | mme | 2165.57 | 2165.57 | 2165.57 |  | 2165.57 |  | DOWN | 0 | 1 |

BMD analysis results for functional classification based on dose-responsive genes, using the Reactome database for gene sets in BMDExpress2.2 software.

| Study Day | Gene Set Name | Fisher's Exact Left P-Value | Fisher's Exact Right P-Value | Fisher's Exact Two Tail | Gene Symbols | BMD Mean | BMD Median | BMD Minimum | BMD Standard Deviation | BMD wMean | BMD wSD | Overall Direction | Percent Genes With Overall Direction Up | Percent Genes With Overall Direction Down |
|---|---|---|---|---|---|---|---|---|---|---|---|---|---|---|
| 7Day | Formation of Incision Complex in GG-NER | 0.45162 | 0.75615 | 1 | ube2n;ube2v2;uba52 | 3543.14333 | 3444.79 | 2423.08 | 1172.33835 | 3265.85323 | 1041.89728 | UP | 1 | 0 |
| 7Day | G-protein mediated events | 0.6184 | 0.58709 | 1 | prkar2a;gnai3;calm3;calm2 | 3206.91 | 3558.44 | 794.2 | 1780.22388 | 2668.09864 | 1730.81535 | CONFLICT | 0.5 | 0.5 |
| 7Day | PLC beta mediated events | 0.63779 | 0.56798 | 1 | prkar2a;gnai3;calm3;calm2 | 3206.91 | 3558.44 | 794.2 | 1780.22388 | 2668.09864 | 1730.81535 | CONFLICT | 0.5 | 0.5 |
| 7Day | Inositol phosphate metabolism | 0.52268 | 0.67483 | 1 | itpk1;pten;calm3;calm2 | 3684.875 | 3386.31 | 3050.32 | 853.925176 | 3438.70794 | 788.233521 | CONFLICT | 0.5 | 0.5 |
| 7Day | Hedgehog 'off' state | 0.5479 | 0.63366 | 1 | tubb4b;uba52;tubb2a;tuba4a;prkar2a | 2731.5352 | 2094.04 | 919.856 | 1614.82979 | 2575.30579 | 1620.66012 | UP | 0.8 | 0.2 |
| 7Day | Pentose phosphate pathway | 0.5468 | 0.79501 | 1 | pgd | 4459.38 | 4459.38 | 4459.38 |  | 4459.38 |  | UP | 1 | 0 |
| 7Day | SUMOylation of transcription cofactors | 0.57754 | 0.65355 | 1 | ncoa1;bmi1;uhrf2 | 4116.22333 | 4110.52 | 3301.55 | 817.539921 | 4021.24749 | 882.151957 | UP | 1 | 0 |
| 7Day | ZBP1(DAI) mediated induction of type I IFNs | 0.64974 | 0.72402 | 1 | dhx9 | 3100.35 | 3100.35 | 3100.35 |  | 3100.35 |  | UP | 1 | 0 |
| 7Day | DDX58/IFIH1-mediated induction of interferon-alpha/beta | 0.50078 | 0.75552 | 1 | tax1bp1;uba52 | 4021.115 | 4021.115 | 3280.67 | 1047.14736 | 4201.81454 | 1015.48656 | UP | 1 | 0 |
| 7Day | RIP-mediated NFkB activation via ZBP1 | 0.68564 | 0.69527 | 1 | dhx9 | 3100.35 | 3100.35 | 3100.35 |  | 3100.35 |  | UP | 1 | 0 |
| 7Day | Cytosolic sensors of pathogen-associated DNA | 0.59953 | 0.63374 | 1 | uba52;dhx9;ctnnb1 | 2638.81107 | 3100.35 | 54.5232 | 2387.21857 | 2223.71515 | 2513.95685 | UP | 0.666666667 | 0.333333333 |
| 7Day | TAK1 activates NFkB by phosphorylation and activation of IKKs complex | 0.55088 | 0.71775 | 1 | ube2n;uba52 | 4103.175 | 4103.175 | 3444.79 | 931.096996 | 3863.51066 | 867.216021 | UP | 1 | 0 |
| 7Day | Interleukin-1 signaling | 0.50406 | 0.69073 | 1 | ube2n;uba52;il1rap;btrc | 3136.1085 | 3825.925 | 131.024 | 2074.83709 | 2895.88682 | 2054.23699 | UP | 0.75 | 0.25 |
| 7Day | GPVI-mediated activation cascade | 0.59953 | 0.63374 | 1 | clec1b;ptpn11;cdc42 | 4148.05667 | 4218.6 | 3629.67 | 486.962396 | 4208.40007 | 528.675569 | UP | 0.666666667 | 0.333333333 |
| 7Day | NOD1/2 Signaling Pathway | 0.66608 | 0.56972 | 1 | ube2n;uba52;casp9 | 3951.67333 | 3648.67 | 3444.79 | 708.751771 | 3792.89388 | 627.63501 | UP | 0.666666667 | 0.333333333 |
| 7Day | Nucleotide-binding domain, leucine rich repeat containing receptor (NLR) signaling pathways | 0.56056 | 0.64136 | 1 | ube2n;pycard;uba52;casp9 | 4145.8625 | 4188.55 | 3444.79 | 696.938863 | 3907.68166 | 657.882053 | CONFLICT | 0.5 | 0.5 |
| 7Day | The canonical retinoid cycle in rods (twilight vision) | 0.6029 | 0.67518 | 1 | ttr;rdh16f2 | 3935.075 | 3935.075 | 2168.85 | 2497.81935 | 3201.02358 | 2271.87996 | DOWN | 0 | 1 |
| 7Day | Activation of NMDA receptors and postsynaptic events | 0.57754 | 0.65355 | 1 | prkar2a;calm3;calm2 | 4011.14667 | 4066.56 | 3050.32 | 934.353205 | 3661.3101 | 940.743026 | DOWN | 0.333333333 | 0.666666667 |
| 7Day | Deadenylation-dependent mRNA decay | 0.56513 | 0.61774 | 1 | dcp2;wdr61;hbs1l;cnot1;eif4a2 | 3863.62 | 3491.23 | 2781.97 | 1082.84387 | 3360.85733 | 718.959455 | UP | 1 | 0 |
| 7Day | Butyrate Response Factor 1 (BRF1) binds and destabilizes mRNA | 0.5468 | 0.79501 | 1 | dcp2 | 3491.23 | 3491.23 | 3491.23 |  | 3491.23 |  | UP | 1 | 0 |
| 7Day | Interconversion of nucleotide di- and triphosphates | 0.55088 | 0.71775 | 1 | txnrd1;ak1 | 4121.665 | 4121.665 | 2303.89 | 2570.72206 | 4649.3665 | 2460.01507 | UP | 1 | 0 |
| 7Day | Digestion of dietary carbohydrate | 0.61452 | 0.75006 | 1 | mgam | 132.859 | 132.859 | 132.859 |  | 132.859 |  | DOWN | 0 | 1 |
| 7Day | SUMOylation of chromatin organization proteins | 0.55576 | 0.67258 | 1 | hist1h4h;suz12;bmi1 | 3845.46 | 3406.55 | 3193.23 | 950.95543 | 3682.31274 | 838.77756 | UP | 0.666666667 | 0.333333333 |
| 7Day | Sema4D in semaphorin signaling | 0.58015 | 0.77365 | 1 | sema4d | 5514.77 | 5514.77 | 5514.77 |  | 5514.77 |  | DOWN | 0 | 1 |
| 7Day | TP53 Regulates Transcription of Cell Cycle Genes | 0.62166 | 0.61316 | 1 | cnot1;cdkn1a;ccne2 | 3399.59667 | 2818.63 | 2781.97 | 1038.17411 | 3426.27872 | 1052.18962 | UP | 1 | 0 |
| 7Day | Apoptosis induced DNA fragmentation | 0.68564 | 0.69527 | 1 | kpnb1 | 4222.13 | 4222.13 | 4222.13 |  | 4222.13 |  | UP | 1 | 0 |
| 7Day | Activation of DNA fragmentation factor | 0.68564 | 0.69527 | 1 | kpnb1 | 4222.13 | 4222.13 | 4222.13 |  | 4222.13 |  | UP | 1 | 0 |
| 7Day | Formation of Senescence-Associated Heterochromatin Foci (SAHF) | 0.51457 | 0.81436 | 1 | ep400 | 3377.47 | 3377.47 | 3377.47 |  | 3377.47 |  | DOWN | 0 | 1 |
| 7Day | Apoptotic execution phase | 0.46761 | 0.72085 | 1 | dsg1c;kpnb1;ctnnb1;dsp | 1885.67405 | 1633.0215 | 54.5232 | 2067.00433 | 1763.10246 | 1971.21268 | DOWN | 0.25 | 0.75 |
| 7Day | FCERI mediated MAPK activation | 0.57669 | 0.69709 | 1 | pak2;kras | 3348.455 | 3348.455 | 2538.2 | 1145.87361 | 3692.75181 | 1037.27805 | UP | 1 | 0 |
| 7Day | FCERI mediated Ca+2 mobilization | 0.4531 | 0.78885 | 1 | calm3;calm2 | 3983.44 | 3983.44 | 3050.32 | 1319.63096 | 3556.9103 | 1173.69957 | CONFLICT | 0.5 | 0.5 |
| 7Day | Antigen processing-Cross presentation | 0.63779 | 0.56798 | 1 | tap2;sec22b;h2-t23;h2-q10 | 3670.8125 | 3724.57 | 2584.12 | 941.890827 | 3414.68027 | 934.619277 | DOWN | 0.25 | 0.75 |
| 7Day | Signaling by EGFR | 0.6184 | 0.58709 | 1 | uba52;ptpn11;kras;cdc42 | 4286.46 | 4377.305 | 3629.67 | 506.34846 | 4337.45426 | 495.668123 | UP | 1 | 0 |
| 7Day | GRB2 events in EGFR signaling | 0.64974 | 0.72402 | 1 | kras | 4158.71 | 4158.71 | 4158.71 |  | 4158.71 |  | UP | 1 | 0 |
| 7Day | GAB1 signalosome | 0.51457 | 0.81436 | 1 | ptpn11 | 3629.67 | 3629.67 | 3629.67 |  | 3629.67 |  | UP | 1 | 0 |
| 7Day | SHC1 events in EGFR signaling | 0.61452 | 0.75006 | 1 | kras | 4158.71 | 4158.71 | 4158.71 |  | 4158.71 |  | UP | 1 | 0 |
| 7Day | EGFR downregulation | 0.50078 | 0.75552 | 1 | uba52;cdc42 | 4678.73 | 4678.73 | 4595.9 | 117.139309 | 4668.27085 | 116.201678 | UP | 1 | 0 |
| 7Day | Signaling by TGF-beta Receptor Complex | 0.51381 | 0.66427 | 1 | uba52;tgfbr1;tfdp1;prkcz;ccnk | 3804.8848 | 4761.56 | 707.264 | 2279.30374 | 4710.02856 | 1911.5824 | UP | 0.8 | 0.2 |
| 7Day | Fibronectin matrix formation | 0.55214 | 1 | 1 |  |  |  |  |  |  |  |  |  |  |
| 7Day | MAP2K and MAPK activation | 0.47167 | 0.74095 | 1 | mapk3;pebp1;kras | 4436.69333 | 4351.13 | 4158.71 | 329.212695 | 4476.19461 | 324.644236 | UP | 0.666666667 | 0.333333333 |
| 7Day | EPHA-mediated growth cone collapse | 0.45381 | 0.84775 | 1 | yes1 | 4020.95 | 4020.95 | 4020.95 |  | 4020.95 |  | UP | 1 | 0 |

BMD analysis results for functional classification based on dose-responsive genes, using the Reactome database for gene sets in BMDExpress2.2 software.

| Study Day | Gene Set Name | Fisher's Exact Left P-Value | Fisher's Exact Right P-Value | Fisher's Exact Two Tail | Gene Symbols | BMD Mean | BMD Median | BMD Minimum | BMD Standard Deviation | BMD wMean | BMD wSD | Overall Direction | Percent Genes With Overall Direction Up | Percent Genes With Overall Direction Down |
|---|---|---|---|---|---|---|---|---|---|---|---|---|---|---|
| 7Day | Ion homeostasis | 0.44983 | 0.73508 | 1 | itpr2;dmpk;calm3;calm2 | 3890.9575 | 3798.475 | 3050.32 | 807.324813 | 3574.7767 | 786.454883 | DOWN | 0.25 | 0.75 |
| 7Day | Negative regulation of MET activity | 0.48356 | 0.83188 | 1 | uba52 | 4761.56 | 4761.56 | 4761.56 |  | 4761.56 |  | UP | 1 | 0 |
| 7Day | Signaling by FGFR | 0.51491 | 0.63831 | 1 | mapk3;polr2h;uba52;ptpn11;ppp2cb;kras;fgf1 | 3941.36857 | 3964.6 | 2647.76 | 744.707179 | 3839.81356 | 761.564281 | UP | 0.714285714 | 0.285714286 |
| 7Day | FGFR2 ligand binding and activation | 0.45381 | 0.84775 | 1 | fgf1 | 2647.76 | 2647.76 | 2647.76 |  | 2647.76 |  | DOWN | 0 | 1 |
| 7Day | FGFR1 ligand binding and activation | 0.58015 | 0.77365 | 1 | fgf1 | 2647.76 | 2647.76 | 2647.76 |  | 2647.76 |  | DOWN | 0 | 1 |
| 7Day | Phospholipase C-mediated cascade: FGFR1 | 0.5468 | 0.79501 | 1 | fgf1 | 2647.76 | 2647.76 | 2647.76 |  | 2647.76 |  | DOWN | 0 | 1 |
| 7Day | Phospholipase C-mediated cascade; FGFR2 | 0.48356 | 0.83188 | 1 | fgf1 | 2647.76 | 2647.76 | 2647.76 |  | 2647.76 |  | DOWN | 0 | 1 |
| 7Day | Downstream signaling of activated FGFR1 | 0.66608 | 0.56972 | 1 | ptpn11;kras;fgf1 | 3478.71333 | 3629.67 | 2647.76 | 766.702949 | 3262.18888 | 788.939216 | UP | 0.666666667 | 0.333333333 |
| 7Day | SHC-mediated cascade:FGFR1 | 0.68298 | 0.60175 | 1 | kras;fgf1 | 3403.235 | 3403.235 | 2647.76 | 1068.40299 | 3131.99117 | 997.165244 | CONFLICT | 0.5 | 0.5 |
| 7Day | PI-3K cascade:FGFR1 | 0.68298 | 0.60175 | 1 | ptpn11;fgf1 | 3138.715 | 3138.715 | 2647.76 | 694.31522 | 2984.26892 | 659.064823 | CONFLICT | 0.5 | 0.5 |
| 7Day | PI-3K cascade:FGFR2 | 0.62942 | 0.65201 | 1 | ptpn11;fgf1 | 3138.715 | 3138.715 | 2647.76 | 694.31522 | 2984.26892 | 659.064823 | CONFLICT | 0.5 | 0.5 |
| 7Day | SHC-mediated cascade:FGFR2 | 0.62942 | 0.65201 | 1 | kras;fgf1 | 3403.235 | 3403.235 | 2647.76 | 1068.40299 | 3131.99117 | 997.165244 | CONFLICT | 0.5 | 0.5 |
| 7Day | mRNA 3'-end processing | 0.58246 | 0.60141 | 1 | fip1l1;cpsf2;srsf1;cstf2;thoc5 | 3968.36 | 3485.7 | 3207.13 | 1058.77133 | 3686.98511 | 697.626174 | UP | 1 | 0 |
| 7Day | Synthesis of very long-chain fatty acyl-CoAs | 0.65616 | 0.62754 | 1 | elovl5;elovl3 | 1653.9245 | 1653.9245 | 212.399 | 2038.62491 | 2396.21501 | 1747.57007 | CONFLICT | 0.5 | 0.5 |
| 7Day | p75NTR regulates axonogenesis | 0.75842 | 0.62848 | 1 | lingo1 | 3247.44 | 3247.44 | 3247.44 |  | 3247.44 |  | UP | 1 | 0 |
| 7Day | Sema4D induced cell migration and growth-cone collapse | 0.72196 | 0.66353 | 1 | sema4d | 5514.77 | 5514.77 | 5514.77 |  | 5514.77 |  | DOWN | 0 | 1 |
| 7Day | RHO GTPases activate CIT | 0.45292 | 1 | 1 |  |  |  |  |  |  |  |  |  |  |
| 7Day | RHO GTPases activate KTN1 | 0.72196 | 0.66353 | 1 | cdc42 | 4595.9 | 4595.9 | 4595.9 |  | 4595.9 |  | UP | 1 | 0 |
| 7Day | RHO GTPases Activate ROCKs | 0.60961 | 1 | 1 |  |  |  |  |  |  |  |  |  |  |
| 7Day | Ovarian tumor domain proteases | 0.47661 | 0.77272 | 1 | uba52;pten | 3968.12 | 3968.12 | 3174.68 | 1122.09361 | 3805.44643 | 1098.25711 | UP | 1 | 0 |
| 7Day | Activation of the AP-1 family of transcription factors | 0.75842 | 0.62848 | 1 | mapk3 | 4800.24 | 4800.24 | 4800.24 |  | 4800.24 |  | DOWN | 0 | 1 |
| 7Day | IL-6-type cytokine receptor ligand interactions | 0.42537 | 0.86213 | 1 | jak1 | 3554.32 | 3554.32 | 3554.32 |  | 3554.32 |  | UP | 1 | 0 |
| 7Day | Adenylate cyclase inhibitory pathway | 0.61452 | 0.75006 | 1 | gnai3 | 794.2 | 794.2 | 794.2 |  | 794.2 |  | UP | 1 | 0 |
| 7Day | Inhibition of adenylate cyclase pathway | 0.61452 | 0.75006 | 1 | gnai3 | 794.2 | 794.2 | 794.2 |  | 794.2 |  | UP | 1 | 0 |
| 7Day | GRB7 events in ERBB2 signaling | 0.60961 | 1 | 1 |  |  |  |  |  |  |  |  |  |  |
| 7Day | Inflammasomes | 0.58015 | 0.77365 | 1 | pycard | 4728.43 | 4728.43 | 4728.43 |  | 4728.43 |  | DOWN | 0 | 1 |
| 7Day | Kinesins | 0.59985 | 0.58469 | 1 | tubb4b;tubb2a;tuba4a;kif2a;kif1c | 2136.1572 | 1815.66 | 919.856 | 1552.81607 | 2213.42063 | 1590.85728 | UP | 0.8 | 0.2 |
| 7Day | SUMO is proteolytically processed | 0.55214 | 1 | 1 |  |  |  |  |  |  |  |  |  |  |
| 7Day | Processing and activation of SUMO | 0.75842 | 0.62848 | 1 | uba2 | 2542.64 | 2542.64 | 2542.64 |  | 2542.64 |  | UP | 1 | 0 |
| 7Day | Tryptophan catabolism | 0.72196 | 0.66353 | 1 | kyat1 | 4788.28 | 4788.28 | 4788.28 |  | 4788.28 |  | DOWN | 0 | 1 |
| 7Day | Androgen biosynthesis | 0.41021 | 1 | 1 |  |  |  |  |  |  |  |  |  |  |
| 7Day | Senescence-Associated Secretory Phenotype (SASP) | 0.49512 | 0.64737 | 1 | hist1h4h;hist1h2bc;hist2h2ac;mapk3;uba52;cdc27;hist2h2aa1;cdkn1a | 4081.57875 | 4028.925 | 2818.63 | 864.824131 | 4038.51343 | 934.807892 | UP | 0.625 | 0.375 |
| 7Day | Oncogene Induced Senescence | 0.64974 | 0.72402 | 1 | uba52 | 4761.56 | 4761.56 | 4761.56 |  | 4761.56 |  | UP | 1 | 0 |
| 7Day | Type I hemidesmosome assembly | 0.72196 | 0.66353 | 1 | dst | 2982.34 | 2982.34 | 2982.34 |  | 2982.34 |  | UP | 1 | 0 |
| 7Day | Gap junction trafficking and regulation | 0.63779 | 0.56798 | 1 | tubb4b;tubb2a;tuba4a;gja1 | 2276.434 | 1954.85 | 919.856 | 1424.18025 | 1763.60227 | 985.706882 | UP | 0.75 | 0.25 |
| 7Day | RUNX1 interacts with co-factors whose precise effect on RUNX1 targets is not known | 0.57754 | 0.65355 | 1 | pcgf5;csnk2b;bmi1 | 4052.24667 | 4390.47 | 2829.67 | 1093.42799 | 4167.82963 | 1022.92134 | UP | 1 | 0 |
| 7Day | Translesion synthesis by REV1 | 0.61452 | 0.75006 | 1 | uba52 | 4761.56 | 4761.56 | 4761.56 |  | 4761.56 |  | UP | 1 | 0 |
| 7Day | Translesion Synthesis by POLH | 0.51457 | 0.81436 | 1 | uba52 | 4761.56 | 4761.56 | 4761.56 |  | 4761.56 |  | UP | 1 | 0 |
| 7Day | Polymerase switching on the C-strand of the telomere | 0.61452 | 0.75006 | 1 | prim2 | 4006.14 | 4006.14 | 4006.14 |  | 4006.14 |  | UP | 1 | 0 |
| 7Day | Translesion synthesis by POLK | 0.58015 | 0.77365 | 1 | uba52 | 4761.56 | 4761.56 | 4761.56 |  | 4761.56 |  | UP | 1 | 0 |
| 7Day | Translesion synthesis by POLI | 0.58015 | 0.77365 | 1 | uba52 | 4761.56 | 4761.56 | 4761.56 |  | 4761.56 |  | UP | 1 | 0 |
| 7Day | Gap-filling DNA repair synthesis and ligation in GG-NER | 0.42537 | 0.86213 | 1 | uba52 | 4761.56 | 4761.56 | 4761.56 |  | 4761.56 |  | UP | 1 | 0 |
| 7Day | Polymerase switching | 0.61452 | 0.75006 | 1 | prim2 | 4006.14 | 4006.14 | 4006.14 |  | 4006.14 |  | UP | 1 | 0 |
| 7Day | Leading Strand Synthesis | 0.61452 | 0.75006 | 1 | prim2 | 4006.14 | 4006.14 | 4006.14 |  | 4006.14 |  | UP | 1 | 0 |
| 7Day | Lagging Strand Synthesis | 0.42537 | 0.86213 | 1 | prim2 | 4006.14 | 4006.14 | 4006.14 |  | 4006.14 |  | UP | 1 | 0 |

BMD analysis results for functional classification based on dose-responsive genes, using the Reactome database for gene sets in BMDExpress2.2 software.

| Study Day | Gene Set Name | Fisher's Exact Left P-Value | Fisher's Exact Right P-Value | Fisher's Exact Two Tail | Gene Symbols | BMD Mean | BMD Median | BMD Minimum | BMD Standard Deviation | BMD wMean | BMD wSD | Overall Direction | Percent Genes With Overall Direction Up | Percent Genes With Overall Direction Down |
|---|---|---|---|---|---|---|---|---|---|---|---|---|---|---|
| 7Day | TP53 regulates transcription of additional cell cycle genes whose exact role in the p53 pathway remain uncertain | 0.51457 | 0.81436 | 1 | cnot1 | 2781.97 | 2781.97 | 2781.97 |  | 2781.97 |  | UP | 1 | 0 |
| 7Day | Transcriptional activity of SMAD2/SMAD3:SMAD4 heterotrimer | 0.51302 | 0.7083 | 1 | uba52;tfdp1;ccnk | 2524.87467 | 2105.8 | 707.264 | 2059.38017 | 3053.07053 | 2186.83839 | UP | 1 | 0 |
| 7Day | Extrinsic Pathway of Fibrin Clot Formation | 0.60961 | 1 | 1 |  |  |  |  |  |  |  |  |  |  |
| 7Day | Gamma-carboxylation of protein precursors | 0.72196 | 0.66353 | 1 | f2 | 156.627 | 156.627 | 156.627 |  | 156.627 |  | DOWN | 0 | 1 |
| 7Day | Transport of gamma-carboxylated protein precursors from the endoplasmic reticulum to the Golgi apparatus | 0.72196 | 0.66353 | 1 | f2 | 156.627 | 156.627 | 156.627 |  | 156.627 |  | DOWN | 0 | 1 |
| 7Day | Removal of aminoterminal propeptides from gamma-carboxylated proteins | 0.68564 | 0.69527 | 1 | f2 | 156.627 | 156.627 | 156.627 |  | 156.627 |  | DOWN | 0 | 1 |
| 7Day | Gamma-carboxylation, transport, and amino-terminal cleavage of proteins | 0.64974 | 0.72402 | 1 | f2 | 156.627 | 156.627 | 156.627 |  | 156.627 |  | DOWN | 0 | 1 |
| 7Day | Zinc transporters | 0.68564 | 0.69527 | 1 | slc39a2 | 5557.48 | 5557.48 | 5557.48 |  | 5557.48 |  | UP | 1 | 0 |
| 7Day | Miscellaneous substrates | 0.57754 | 0.65355 | 1 | cyp3a25;cyp3a11;cyp3a41b | 4490.5 | 5106.56 | 2813.51 | 1469.25114 | 4069.13875 | 1571.9222 | DOWN | 0.333333333 | 0.666666667 |
| 7Day | Synthesis of (16-20)-hydroxyeicosatetraenoic acids (HETE) | 0.65616 | 0.62754 | 1 | cyp2c37;cyp2c29 | 2987.945 | 2987.945 | 2593.25 | 558.183022 | 2960.06961 | 556.789198 | CONFLICT | 0.5 | 0.5 |
| 7Day | SHC1 events in ERBB4 signaling | 0.61452 | 0.75006 | 1 | kras | 4158.71 | 4158.71 | 4158.71 |  | 4158.71 |  | UP | 1 | 0 |
| 7Day | GRB2 events in ERBB2 signaling | 0.61452 | 0.75006 | 1 | kras | 4158.71 | 4158.71 | 4158.71 |  | 4158.71 |  | UP | 1 | 0 |
| 7Day | G beta:gamma signalling through CDC42 | 0.45381 | 0.84775 | 1 | cdc42 | 4595.9 | 4595.9 | 4595.9 |  | 4595.9 |  | UP | 1 | 0 |
| 7Day | Purine ribonucleoside monophosphate biosynthesis | 0.68564 | 0.69527 | 1 | atic | 3859.67 | 3859.67 | 3859.67 |  | 3859.67 |  | UP | 1 | 0 |
| 7Day | Nucleobase biosynthesis | 0.58015 | 0.77365 | 1 | atic | 3859.67 | 3859.67 | 3859.67 |  | 3859.67 |  | UP | 1 | 0 |
| 7Day | HDL assembly | 0.50008 | 1 | 1 |  |  |  |  |  |  |  |  |  |  |
| 7Day | HDL clearance | 0.60961 | 1 | 1 |  |  |  |  |  |  |  |  |  |  |
| 7Day | HDL remodeling | 0.75842 | 0.62848 | 1 | apoe | 113.316 | 113.316 | 113.316 |  | 113.316 |  | DOWN | 0 | 1 |
| 7Day | Deadenylation of mRNA | 0.52556 | 0.73721 | 1 | cnot1;eif4a2 | 3111.725 | 3111.725 | 2781.97 | 466.343993 | 3093.7181 | 465.648175 | UP | 1 | 0 |
| 7Day | AUF1 (hnRNP D0) binds and destabilizes mRNA | 0.75842 | 0.62848 | 1 | uba52 | 4761.56 | 4761.56 | 4761.56 |  | 4761.56 |  | UP | 1 | 0 |
| 7Day | Electron transport from NADPH to Ferredoxin | 0.7431 | 1 | 1 |  |  |  |  |  |  |  |  |  |  |
| 7Day | Signaling by NOTCH1 | 0.48356 | 0.83188 | 1 | uba52 | 4761.56 | 4761.56 | 4761.56 |  | 4761.56 |  | UP | 1 | 0 |
| 7Day | Sulfide oxidation to sulfate | 0.67306 | 1 | 1 |  |  |  |  |  |  |  |  |  |  |
| 7Day | Interleukin-12 signaling | 0.75842 | 0.62848 | 1 | jak1 | 3554.32 | 3554.32 | 3554.32 |  | 3554.32 |  | UP | 1 | 0 |
| 7Day | Synthesis of glycosylphosphatidylinositol (GPI) | 0.51457 | 0.81436 | 1 | pigw | 4464.3 | 4464.3 | 4464.3 |  | 4464.3 |  | UP | 1 | 0 |
| 7Day | Acyl chain remodelling of PG | 0.5468 | 0.79501 | 1 | crls1 | 4148.47 | 4148.47 | 4148.47 |  | 4148.47 |  | UP | 1 | 0 |
| 7Day | Interleukin-2 signaling | 0.68564 | 0.69527 | 1 | jak1 | 3554.32 | 3554.32 | 3554.32 |  | 3554.32 |  | UP | 1 | 0 |
| 7Day | Nucleobase catabolism | 0.55576 | 0.67258 | 1 | dpys;nudt5;entpd5 | 1032.25 | 821.082 | 395.538 | 764.491527 | 1229.95011 | 711.717804 | UP | 0.666666667 | 0.333333333 |
| 7Day | Ethanol oxidation | 0.68564 | 0.69527 | 1 | aldh2 | 303.779 | 303.779 | 303.779 |  | 303.779 |  | DOWN | 0 | 1 |
| 7Day | Trafficking of GluR2-containing AMPA receptors | 0.64974 | 0.72402 | 1 | gria3 | 3853.21 | 3853.21 | 3853.21 |  | 3853.21 |  | UP | 1 | 0 |
| 7Day | Recycling pathway of L1 | 0.59953 | 0.63374 | 1 | tubb4b;tubb2a;tuba4a | 1609.852 | 1815.66 | 919.856 | 613.550908 | 1582.39232 | 663.092821 | UP | 1 | 0 |
| 7Day | TNFR1-induced NFkappaB signaling pathway | 0.50078 | 0.75552 | 1 | uba52;xiap | 4817.795 | 4817.795 | 4761.56 | 79.5282997 | 4830.99188 | 77.3074074 | CONFLICT | 0.5 | 0.5 |
| 7Day | Synthesis of pyrophosphates in the cytosol | 0.75842 | 0.62848 | 1 | itpk1 | 3597.94 | 3597.94 | 3597.94 |  | 3597.94 |  | DOWN | 0 | 1 |
| 7Day | Adrenoceptors | 0.41021 | 1 | 1 |  |  |  |  |  |  |  |  |  |  |
| 7Day | Alternative complement activation | 0.67306 | 1 | 1 |  |  |  |  |  |  |  |  |  |  |
| 7Day | Post-transcriptional silencing by small RNAs | 0.50008 | 1 | 1 |  |  |  |  |  |  |  |  |  |  |
| 7Day | MET activates STAT3 | 0.7431 | 1 | 1 |  |  |  |  |  |  |  |  |  |  |
| 7Day | Na+/Cl- dependent neurotransmitter transporters | 0.42537 | 0.86213 | 1 | slc22a1 | 4237.04 | 4237.04 | 4237.04 |  | 4237.04 |  | DOWN | 0 | 1 |

BMD analysis results for functional classification based on dose-responsive genes, using the Reactome database for gene sets in BMDExpress2.2 software.

| Study Day | Gene Set Name | Fisher's Exact Left P-Value | Fisher's Exact Right P-Value | Fisher's Exact Two Tail | Gene Symbols | BMD Mean | BMD Median | BMD Minimum | BMD Standard Deviation | BMD wMean | BMD wSD | Overall Direction | Percent Genes With Overall Direction Up | Percent Genes With Overall Direction Down |
|---|---|---|---|---|---|---|---|---|---|---|---|---|---|---|
| 7Day | Apoptotic cleavage of cellular proteins | 0.49215 | 0.725 | 1 | dsg1c;ctnnb1;dsp | 1106.8554 | 240.593 | 54.5232 | 1664.15427 | 1209.2455 | 1689.05741 | DOWN | 0 | 1 |
| 7Day | Golgi Associated Vesicle Biogenesis | 0.44983 | 0.73508 | 1 | picalm;igf2r;ftl1;ap3b1 | 2855.5565 | 3390.82 | 720.546 | 1446.1338 | 2750.71883 | 1359.65521 | UP | 0.75 | 0.25 |
| 7Day | Downregulation of SMAD2/3:SMAD4 transcriptional activity | 0.42537 | 0.86213 | 1 | uba52 | 4761.56 | 4761.56 | 4761.56 |  | 4761.56 |  | UP | 1 | 0 |
| 7Day | Transcriptional regulation by RUNX3 | 0.55576 | 0.67258 | 1 | uba52;kras;ctnnb1 | 2991.59773 | 4158.71 | 54.5232 | 2561.37895 | 2455.7853 | 2724.14338 | UP | 0.666666667 | 0.333333333 |
| 7Day | Mitochondrial biogenesis | 0.65616 | 0.62754 | 1 | idh2;atp5j | 3837.36 | 3837.36 | 2704.94 | 1601.48372 | 4362.13372 | 1419.14594 | CONFLICT | 0.5 | 0.5 |
| 7Day | Formation of ATP by chemiosmotic coupling | 0.61452 | 0.75006 | 1 | atp5j | 4969.78 | 4969.78 | 4969.78 |  | 4969.78 |  | UP | 1 | 0 |
| 7Day | Cristae formation | 0.61452 | 0.75006 | 1 | atp5j | 4969.78 | 4969.78 | 4969.78 |  | 4969.78 |  | UP | 1 | 0 |
| 7Day | Regulation of KIT signaling | 0.61452 | 0.75006 | 1 | yes1 | 4020.95 | 4020.95 | 4020.95 |  | 4020.95 |  | UP | 1 | 0 |
| 7Day | Caspase activation via extrinsic apoptotic signalling pathway | 0.45381 | 0.84775 | 1 | casp9 | 3648.67 | 3648.67 | 3648.67 |  | 3648.67 |  | DOWN | 0 | 1 |
| 7Day | IKK complex recruitment mediated by RIP1 | 0.68298 | 0.60175 | 1 | ube2n;uba52 | 4103.175 | 4103.175 | 3444.79 | 931.096996 | 3863.51066 | 867.216021 | UP | 1 | 0 |
| 7Day | TRAF6-mediated induction of TAK1 complex within TLR4 complex | 0.61452 | 0.75006 | 1 | uba52 | 4761.56 | 4761.56 | 4761.56 |  | 4761.56 |  | UP | 1 | 0 |
| 7Day | IRAK2 mediated activation of TAK1 complex upon TLR7/8 or 9 stimulation | 0.64974 | 0.72402 | 1 | uba52 | 4761.56 | 4761.56 | 4761.56 |  | 4761.56 |  | UP | 1 | 0 |
| 7Day | ChREBP activates metabolic gene expression | 0.50008 | 1 | 1 |  |  |  |  |  |  |  |  |  |  |
| 7Day | Inhibition of the proteolytic activity of APC/C required for the onset of anaphase by mitotic spindle checkpoint components | 0.42537 | 0.86213 | 1 | cdc27 | 3870.58 | 3870.58 | 3870.58 |  | 3870.58 |  | UP | 1 | 0 |
| 7Day | Inactivation of APC/C via direct inhibition of the APC/C complex | 0.42537 | 0.86213 | 1 | cdc27 | 3870.58 | 3870.58 | 3870.58 |  | 3870.58 |  | UP | 1 | 0 |
| 7Day | APC/C:Cdc20 mediated degradation of Cyclin B | 0.68298 | 0.60175 | 1 | uba52;cdc27 | 4316.07 | 4316.07 | 3870.58 | 630.018 | 4393.04009 | 620.543222 | UP | 1 | 0 |
| 7Day | APC/C-mediated degradation of cell cycle proteins | 0.51491 | 0.63831 | 1 | psmd5;psmd6;psmc4;uba52;cdc27;psmc2;btrc | 3583.53714 | 3870.58 | 2309.23 | 863.11457 | 3583.52534 | 923.347336 | UP | 1 | 0 |
| 7Day | APC/C:Cdh1 mediated degradation of Cdc20 and other APC/C:Cdh1 targeted proteins in late mitosis/early G1 | 0.57669 | 0.69709 | 1 | uba52;cdc27 | 4316.07 | 4316.07 | 3870.58 | 630.018 | 4393.04009 | 620.543222 | UP | 1 | 0 |
| 7Day | Cdc20:Phospho-APC/C mediated degradation of Cyclin A | 0.57669 | 0.69709 | 1 | uba52;cdc27 | 4316.07 | 4316.07 | 3870.58 | 630.018 | 4393.04009 | 620.543222 | UP | 1 | 0 |
| 7Day | Conversion from APC/C:Cdc20 to APC/C:Cdh1 in late anaphase | 0.45381 | 0.84775 | 1 | cdc27 | 3870.58 | 3870.58 | 3870.58 |  | 3870.58 |  | UP | 1 | 0 |
| 7Day | Regulation of APC/C activators between G1/S and early anaphase | 0.64386 | 0.59181 | 1 | uba52;cdc27;btrc | 4279.73333 | 4207.06 | 3870.58 | 449.91377 | 4311.88815 | 418.982594 | UP | 1 | 0 |
| 7Day | APC/C:Cdc20 mediated degradation of mitotic proteins | 0.50078 | 0.75552 | 1 | uba52;cdc27 | 4316.07 | 4316.07 | 3870.58 | 630.018 | 4393.04009 | 620.543222 | UP | 1 | 0 |
| 7Day | Phosphorylation of the APC/C | 0.5468 | 0.79501 | 1 | cdc27 | 3870.58 | 3870.58 | 3870.58 |  | 3870.58 |  | UP | 1 | 0 |
| 7Day | Activation of APC/C and APC/C:Cdc20 mediated degradation of mitotic proteins | 0.50078 | 0.75552 | 1 | uba52;cdc27 | 4316.07 | 4316.07 | 3870.58 | 630.018 | 4393.04009 | 620.543222 | UP | 1 | 0 |
| 7Day | APC-Cdc20 mediated degradation of Nek2A | 0.62942 | 0.65201 | 1 | uba52;cdc27 | 4316.07 | 4316.07 | 3870.58 | 630.018 | 4393.04009 | 620.543222 | UP | 1 | 0 |
| 7Day | APC:Cdc20 mediated degradation of cell cycle proteins prior to satisfation of the cell cycle checkpoint | 0.55088 | 0.71775 | 1 | uba52;cdc27 | 4316.07 | 4316.07 | 3870.58 | 630.018 | 4393.04009 | 620.543222 | UP | 1 | 0 |
| 7Day | Regulation of mitotic cell cycle | 0.51491 | 0.63831 | 1 | psmd5;psmd6;psmc4;uba52;cdc27;psmc2;btrc | 3583.53714 | 3870.58 | 2309.23 | 863.11457 | 3583.52534 | 923.347336 | UP | 1 | 0 |
| 7Day | Dissolution of Fibrin Clot | 0.51457 | 0.81436 | 1 | serpinb8 | 2712.82 | 2712.82 | 2712.82 |  | 2712.82 |  | DOWN | 0 | 1 |
| 7Day | Phenylalanine and tyrosine catabolism | 0.68564 | 0.69527 | 1 | kyat1 | 4788.28 | 4788.28 | 4788.28 |  | 4788.28 |  | DOWN | 0 | 1 |
| 7Day | Gap junction degradation | 0.72196 | 0.66353 | 1 | gja1 | 4276.18 | 4276.18 | 4276.18 |  | 4276.18 |  | DOWN | 0 | 1 |
| 7Day | Formation of annular gap junctions | 0.75842 | 0.62848 | 1 | gja1 | 4276.18 | 4276.18 | 4276.18 |  | 4276.18 |  | DOWN | 0 | 1 |
| 7Day | RNA Polymerase I Promoter Escape | 0.47661 | 0.77272 | 1 | polr2h;ubtf | 2970.455 | 2970.455 | 1976.31 | 1405.93334 | 3441.15761 | 1238.35644 | UP | 1 | 0 |
| 7Day | RNA Polymerase I Transcription Termination | 0.4531 | 0.78885 | 1 | polr2h;ubtf | 2970.455 | 2970.455 | 1976.31 | 1405.93334 | 3441.15761 | 1238.35644 | UP | 1 | 0 |
| 7Day | Pyruvate metabolism | 0.50078 | 0.75552 | 1 | pdhx;dld | 4987.44 | 4987.44 | 4831.25 | 220.886016 | 4979.91771 | 220.629696 | CONFLICT | 0.5 | 0.5 |
| 7Day | Hyaluronan uptake and degradation | 0.50008 | 1 | 1 |  |  |  |  |  |  |  |  |  |  |

BMD analysis results for functional classification based on dose-responsive genes, using the Reactome database for gene sets in BMDExpress2.2 software.

| Study Day | Gene Set Name | Fisher's Exact Left P-Value | Fisher's Exact Right P-Value | Fisher's Exact Two Tail | Gene Symbols | BMD Mean | BMD Median | BMD Minimum | BMD Standard Deviation | BMD wMean | BMD wSD | Overall Direction | Percent Genes With Overall Direction Up | Percent Genes With Overall Direction Down |
|---|---|---|---|---|---|---|---|---|---|---|---|---|---|---|
| 7Day | A tetrasaccharide linker sequence is required for GAG synthesis | 0.55088 | 0.71775 | 1 | sdc3;bgn | 3385.82 | 3385.82 | 2968.59 | 590.052325 | 3628.87151 | 479.597402 | DOWN | 0 | 1 |
| 7Day | Serine biosynthesis | 0.41021 | 1 | 1 | | | | | | | | | | |
| 7Day | Regulation of innate immune responses to cytosolic DNA | 0.58015 | 0.77365 | 1 | uba52 | 4761.56 | 4761.56 | 4761.56 | | 4761.56 | | UP | 1 | 0 |
| 7Day | The NLRP3 inflammasome | 0.75842 | 0.62848 | 1 | pycard | 4728.43 | 4728.43 | 4728.43 | | 4728.43 | | DOWN | 0 | 1 |
| 7Day | Deposition of new CENPA-containing nucleosomes at the centromere | 0.48356 | 0.83188 | 1 | cenpk | 3911.13 | 3911.13 | 3911.13 | | 3911.13 | | UP | 1 | 0 |
| 7Day | Nucleosome assembly | 0.48356 | 0.83188 | 1 | cenpk | 3911.13 | 3911.13 | 3911.13 | | 3911.13 | | UP | 1 | 0 |
| 7Day | Triglyceride biosynthesis | 0.68564 | 0.69527 | 1 | dgat2 | 623.511 | 623.511 | 623.511 | | 623.511 | | DOWN | 0 | 1 |
| 7Day | Miscellaneous transport and binding events | 0.62942 | 0.65201 | 1 | nipa2;azgp1 | 1792.7206 | 1792.7206 | 73.2912 | 2431.64038 | 2195.51779 | 2363.97626 | CONFLICT | 0.5 | 0.5 |
| 7Day | Establishment of Sister Chromatid Cohesion | 0.72196 | 0.66353 | 1 | pds5a | 3647.06 | 3647.06 | 3647.06 | | 3647.06 | | UP | 1 | 0 |
| 7Day | CDT1 association with the CDC6:ORC:origin complex | 0.56513 | 0.61774 | 1 | psmd5;psmd6;psmc4;uba52;psmc2 | 3401.424 | 3326.45 | 2309.23 | 978.876936 | 3327.35463 | 1056.01708 | UP | 1 | 0 |
| 7Day | DCC mediated attractive signaling | 0.72196 | 0.66353 | 1 | cdc42 | 4595.9 | 4595.9 | 4595.9 | | 4595.9 | | UP | 1 | 0 |
| 7Day | Asymmetric localization of PCP proteins | 0.58015 | 0.77365 | 1 | uba52 | 4761.56 | 4761.56 | 4761.56 | | 4761.56 | | UP | 1 | 0 |
| 7Day | mRNA decay by 5' to 3' exoribonuclease | 0.64974 | 0.72402 | 1 | dcp2 | 3491.23 | 3491.23 | 3491.23 | | 3491.23 | | UP | 1 | 0 |
| 7Day | FCGR activation | 0.61452 | 0.75006 | 1 | yes1 | 4020.95 | 4020.95 | 4020.95 | | 4020.95 | | UP | 1 | 0 |
| 7Day | CD22 mediated BCR regulation | 0.55214 | 1 | 1 | | | | | | | | | | |
| 7Day | Interleukin-23 signaling | 0.45292 | 1 | 1 | | | | | | | | | | |
| 7Day | Mitochondrial Fatty Acid Beta-Oxidation | 0.49215 | 0.725 | 1 | hadha;pccb;acaa2 | 144.187867 | 157.61 | 77.8976 | 60.7025232 | 152.608919 | 42.1833052 | DOWN | 0 | 1 |
| 7Day | Purine catabolism | 0.45381 | 0.84775 | 1 | nudt5 | 1880.13 | 1880.13 | 1880.13 | | 1880.13 | | UP | 1 | 0 |
| 7Day | Signaling by Retinoic Acid | 0.59985 | 0.58469 | 1 | akr1c6;pdhx;rdh16f2;dld;akr1c14 | 3980.56 | 4831.25 | 2168.85 | 1371.92456 | 3373.89278 | 1403.06273 | UP | 0.6 | 0.4 |
| 7Day | RA biosynthesis pathway | 0.62166 | 0.61316 | 1 | akr1c6;rdh16f2;akr1c14 | 3309.30667 | 2842.81 | 2168.85 | 1431.87981 | 2672.74701 | 975.286841 | UP | 0.666666667 | 0.333333333 |
| 7Day | Signaling by NOTCH3 | 0.45381 | 0.84775 | 1 | uba52 | 4761.56 | 4761.56 | 4761.56 | | 4761.56 | | UP | 1 | 0 |
| 7Day | NF-kB is activated and signals survival | 0.72196 | 0.66353 | 1 | uba52 | 4761.56 | 4761.56 | 4761.56 | | 4761.56 | | UP | 1 | 0 |
| 7Day | MicroRNA (miRNA) biogenesis | 0.50008 | 1 | 1 | | | | | | | | | | |
| 7Day | Small interfering RNA (siRNA) biogenesis | 0.41021 | 1 | 1 | | | | | | | | | | |
| 7Day | Interleukin-37 signaling | 0.82042 | 1 | 1 | | | | | | | | | | |
| 7Day | Cohesin Loading onto Chromatin | 0.75842 | 0.62848 | 1 | pds5a | 3647.06 | 3647.06 | 3647.06 | | 3647.06 | | UP | 1 | 0 |
| 7Day | Mitotic Telophase/Cytokinesis | 0.61452 | 0.75006 | 1 | pds5a | 3647.06 | 3647.06 | 3647.06 | | 3647.06 | | UP | 1 | 0 |
| 7Day | Dermatan sulfate biosynthesis | 0.72196 | 0.66353 | 1 | bgn | 2968.59 | 2968.59 | 2968.59 | | 2968.59 | | DOWN | 0 | 1 |
| 7Day | Smooth Muscle Contraction | 0.66608 | 0.56972 | 1 | pak2;calm3;calm2 | 3501.69333 | 3050.32 | 2538.2 | 1251.77973 | 3460.1468 | 1033.85516 | UP | 0.666666667 | 0.333333333 |
| 7Day | CD209 (DC-SIGN) signaling | 0.65616 | 0.62754 | 1 | pak2;kras | 3348.455 | 3348.455 | 2538.2 | 1145.87361 | 3692.75181 | 1037.27805 | UP | 1 | 0 |
| 7Day | Beta oxidation of lauroyl-CoA to decanoyl-CoA-CoA | 0.7431 | 1 | 1 | | | | | | | | | | |
| 7Day | Prolonged ERK activation events | 0.75842 | 0.62848 | 1 | mapk3 | 4800.24 | 4800.24 | 4800.24 | | 4800.24 | | DOWN | 0 | 1 |
| 7Day | Signalling to ERKs | 0.62942 | 0.65201 | 1 | mapk3;kras | 4479.475 | 4479.475 | 4158.71 | 453.630213 | 4552.01512 | 441.878074 | CONFLICT | 0.5 | 0.5 |
| 7Day | VxPx cargo-targeting to cilium | 0.42537 | 0.86213 | 1 | rab11a | 4542.35 | 4542.35 | 4542.35 | | 4542.35 | | UP | 1 | 0 |
| 7Day | Rap1 signalling | 0.61452 | 0.75006 | 1 | ywhaz | 2726.98 | 2726.98 | 2726.98 | | 2726.98 | | UP | 1 | 0 |
| 7Day | Synthesis of dolichyl-phosphate-glucose | 0.82042 | 1 | 1 | | | | | | | | | | |
| 7Day | NOTCH3 Activation and Transmission of Signal to the Nucleus | 0.45381 | 0.84775 | 1 | uba52 | 4761.56 | 4761.56 | 4761.56 | | 4761.56 | | UP | 1 | 0 |
| 7Day | CRMPs in Sema3A signaling | 0.5468 | 0.79501 | 1 | gsk3b | 4499.44 | 4499.44 | 4499.44 | | 4499.44 | | UP | 1 | 0 |
| 7Day | SUMOylation of SUMOylation proteins | 0.55214 | 1 | 1 | | | | | | | | | | |
| 7Day | Signalling to RAS | 0.64974 | 0.72402 | 1 | kras | 4158.71 | 4158.71 | 4158.71 | | 4158.71 | | UP | 1 | 0 |
| 7Day | Nuclear Pore Complex (NPC) Disassembly | 0.64386 | 0.59181 | 1 | gm49336;nek6;tpr | 2646.08933 | 2535 | 770.098 | 1933.93044 | 2710.863 | 1721.80663 | UP | 1 | 0 |
| 7Day | SUMOylation of DNA replication proteins | 0.45162 | 0.75615 | 1 | gm49336;top2b;tpr | 3332.64 | 2829.75 | 2535 | 1135.89309 | 3116.87225 | 994.282581 | UP | 1 | 0 |
| 7Day | Breakdown of the nuclear lamina | 0.7431 | 1 | 1 | | | | | | | | | | |
| 7Day | Release of Hh-Np from the secreting cell | 0.55214 | 1 | 1 | | | | | | | | | | |

BMD analysis results for functional classification based on dose-responsive genes, using the Reactome database for gene sets in BMDExpress2.2 software.

| Study Day | Gene Set Name | Fisher's Exact Left P-Value | Fisher's Exact Right P-Value | Fisher's Exact Two Tail | Gene Symbols | BMD Mean | BMD Median | BMD Minimum | BMD Standard Deviation | BMD wMean | BMD wSD | Overall Direction | Percent Genes With Overall Direction Up | Percent Genes With Overall Direction Down |
|---|---|---|---|---|---|---|---|---|---|---|---|---|---|---|
| 7Day | PKA activation in glucagon signalling | 0.5468 | 0.79501 | 1 | prkar2a | 4066.56 | 4066.56 | 4066.56 |  | 4066.56 |  | DOWN | 0 | 1 |
| 7Day | Nuclear signaling by ERBB4 | 0.55214 | 1 | 1 |  |  |  |  |  |  |  |  |  |  |
| 7Day | Sodium/Proton exchangers | 0.41021 | 1 | 1 |  |  |  |  |  |  |  |  |  |  |
| 7Day | Norepinephrine Neurotransmitter Release Cycle | 0.5468 | 0.79501 | 1 | slc22a1 | 4237.04 | 4237.04 | 4237.04 |  | 4237.04 |  | DOWN | 0 | 1 |
| 7Day | Glycogen synthesis | 0.64974 | 0.72402 | 1 | uba52 | 4761.56 | 4761.56 | 4761.56 |  | 4761.56 |  | UP | 1 | 0 |
| 7Day | Regulation of FOXO transcriptional activity by acetylation | 0.50008 | 1 | 1 |  |  |  |  |  |  |  |  |  |  |
| 7Day | PTK6 Activates STAT3 | 0.67306 | 1 | 1 |  |  |  |  |  |  |  |  |  |  |
| 7Day | Removal of the Flap Intermediate | 0.61452 | 0.75006 | 1 | prim2 | 4006.14 | 4006.14 | 4006.14 |  | 4006.14 |  | UP | 1 | 0 |
| 7Day | Processive synthesis on the lagging strand | 0.58015 | 0.77365 | 1 | prim2 | 4006.14 | 4006.14 | 4006.14 |  | 4006.14 |  | UP | 1 | 0 |
| 7Day | NRIF signals cell death from the nucleus | 0.61452 | 0.75006 | 1 | uba52 | 4761.56 | 4761.56 | 4761.56 |  | 4761.56 |  | UP | 1 | 0 |
| 7Day | Telomere Extension By Telomerase | 0.82042 | 1 | 1 |  |  |  |  |  |  |  |  |  |  |
| 7Day | N-glycan trimming and elongation in the cis-Golgi | 0.60961 | 1 | 1 |  |  |  |  |  |  |  |  |  |  |
| 7Day | Progressive trimming of alpha-1,2-linked mannose residues from Man9/8/7GlcNAc2 to produce Man5GlcNAc2 | 0.7431 | 1 | 1 |  |  |  |  |  |  |  |  |  |  |
| 7Day | Chk1/Chk2(Cds1) mediated inactivation of Cyclin B:Cdk1 complex | 0.72196 | 0.66353 | 1 | ywhaz | 2726.98 | 2726.98 | 2726.98 |  | 2726.98 |  | UP | 1 | 0 |
| 7Day | CREB phosphorylation | 0.50008 | 1 | 1 |  |  |  |  |  |  |  |  |  |  |
| 7Day | ARL13B-mediated ciliary trafficking of INPP5E | 0.7431 | 1 | 1 |  |  |  |  |  |  |  |  |  |  |
| 7Day | Beta oxidation of butanoyl-CoA to acetyl-CoA | 0.90577 | 1 | 1 |  |  |  |  |  |  |  |  |  |  |
| 7Day | Elevation of cytosolic Ca2+ levels | 0.64974 | 0.72402 | 1 | itpr2 | 4098.21 | 4098.21 | 4098.21 |  | 4098.21 |  | DOWN | 0 | 1 |
| 7Day | Vitamin D (calciferol) metabolism | 0.75842 | 0.62848 | 1 | gc | 739.513 | 739.513 | 739.513 |  | 739.513 |  | DOWN | 0 | 1 |
| 7Day | WNT ligand biogenesis and trafficking | 0.57669 | 0.69709 | 1 | tmed5;vps29 | 3569.115 | 3569.115 | 3021.31 | 774.713261 | 3835.69635 | 676.793471 | UP | 1 | 0 |
| 7Day | Signal attenuation | 0.72196 | 0.66353 | 1 | mapk3 | 4800.24 | 4800.24 | 4800.24 |  | 4800.24 |  | DOWN | 0 | 1 |
| 7Day | Syndecan interactions | 0.5468 | 0.79501 | 1 | sdc3 | 3803.05 | 3803.05 | 3803.05 |  | 3803.05 |  | DOWN | 0 | 1 |
| 7Day | Ketone body metabolism | 0.75842 | 0.62848 | 1 | hmgcs2 | 3736.33 | 3736.33 | 3736.33 |  | 3736.33 |  | UP | 1 | 0 |
| 7Day | Formation of apoptosome | 0.82042 | 1 | 1 |  |  |  |  |  |  |  |  |  |  |
| 7Day | Cytochrome c-mediated apoptotic response | 0.82042 | 1 | 1 |  |  |  |  |  |  |  |  |  |  |
| 7Day | Regulation of the apoptosome activity | 0.82042 | 1 | 1 |  |  |  |  |  |  |  |  |  |  |
| 7Day | Ion influx/efflux at host-pathogen interface | 0.67306 | 1 | 1 |  |  |  |  |  |  |  |  |  |  |
| 7Day | Organic cation transport | 0.68564 | 0.69527 | 1 | slc22a1 | 4237.04 | 4237.04 | 4237.04 |  | 4237.04 |  | DOWN | 0 | 1 |
| 7Day | Cross-presentation of particulate exogenous antigens (phagosomes) | 0.45292 | 1 | 1 |  |  |  |  |  |  |  |  |  |  |
| 7Day | Biosynthesis of protectins | 0.82042 | 1 | 1 |  |  |  |  |  |  |  |  |  |  |
| 7Day | Aromatic amines can be N-hydroxylated or N-dealkylated by CYP1A2 | 0.90577 | 1 | 1 |  |  |  |  |  |  |  |  |  |  |
| 7Day | Interleukin-15 signaling | 0.64974 | 0.72402 | 1 | jak1 | 3554.32 | 3554.32 | 3554.32 |  | 3554.32 |  | UP | 1 | 0 |
| 7Day | FGFR3 ligand binding and activation | 0.64974 | 0.72402 | 1 | fgf1 | 2647.76 | 2647.76 | 2647.76 |  | 2647.76 |  | DOWN | 0 | 1 |
| 7Day | FGFR4 ligand binding and activation | 0.61452 | 0.75006 | 1 | fgf1 | 2647.76 | 2647.76 | 2647.76 |  | 2647.76 |  | DOWN | 0 | 1 |
| 7Day | FGFR3c ligand binding and activation | 0.64974 | 0.72402 | 1 | fgf1 | 2647.76 | 2647.76 | 2647.76 |  | 2647.76 |  | DOWN | 0 | 1 |
| 7Day | FGFR1c ligand binding and activation | 0.72196 | 0.66353 | 1 | fgf1 | 2647.76 | 2647.76 | 2647.76 |  | 2647.76 |  | DOWN | 0 | 1 |
| 7Day | FGFR2c ligand binding and activation | 0.64974 | 0.72402 | 1 | fgf1 | 2647.76 | 2647.76 | 2647.76 |  | 2647.76 |  | DOWN | 0 | 1 |
| 7Day | Phospholipase C-mediated cascade; FGFR3 | 0.64974 | 0.72402 | 1 | fgf1 | 2647.76 | 2647.76 | 2647.76 |  | 2647.76 |  | DOWN | 0 | 1 |
| 7Day | Phospholipase C-mediated cascade; FGFR4 | 0.58015 | 0.77365 | 1 | fgf1 | 2647.76 | 2647.76 | 2647.76 |  | 2647.76 |  | DOWN | 0 | 1 |
| 7Day | Synthesis of IPs in the nucleus | 0.67306 | 1 | 1 |  |  |  |  |  |  |  |  |  |  |
| 7Day | Assembly of the ORC complex at the origin of replication | 0.55214 | 1 | 1 |  |  |  |  |  |  |  |  |  |  |
| 7Day | PKB-mediated events | 0.90577 | 1 | 1 |  |  |  |  |  |  |  |  |  |  |

BMD analysis results for functional classification based on dose-responsive genes, using the Reactome database for gene sets in BMDExpress2.2 software.

| Study Day | Gene Set Name | Fisher's Exact Left P-Value | Fisher's Exact Right P-Value | Fisher's Exact Two Tail | Gene Symbols | BMD Mean | BMD Median | BMD Minimum | BMD Standard Deviation | BMD wMean | BMD wSD | Overall Direction | Percent Genes With Overall Direction Up | Percent Genes With Overall Direction Down |
|---|---|---|---|---|---|---|---|---|---|---|---|---|---|---|
| 7Day | PDE3B signalling | 0.90577 | 1 | 1 | | | | | | | | | | |
| 7Day | Signaling by Leptin | 0.82042 | 1 | 1 | | | | | | | | | | |
| 7Day | PKA-mediated phosphorylation of key metabolic factors | 0.90577 | 1 | 1 | | | | | | | | | | |
| 28Day | CDO in myogenesis | 0.48011 | 0.83141 | 1 | cdc42 | 2463.49 | 2463.49 | 2463.49 | | 2463.49 | | UP | 1 | 0 |
| 28Day | Myogenesis | 0.48011 | 0.83141 | 1 | cdc42 | 2463.49 | 2463.49 | 2463.49 | | 2463.49 | | UP | 1 | 0 |
| 28Day | Activation of BH3-only proteins | 0.62145 | 0.74142 | 1 | dynll1 | 5791.54 | 5791.54 | 5791.54 | | 5791.54 | | UP | 1 | 0 |
| 28Day | Costimulation by the CD28 family | 0.57711 | 0.6238 | 1 | pdpk1;h2-ab1;h2-aa;cdc42 | 2394.6895 | 2854.61 | 192.988 | 1551.3069 | 2791.05227 | 959.057983 | DOWN | 0.25 | 0.75 |
| 28Day | CD28 co-stimulation | 0.66015 | 0.62015 | 1 | pdpk1;cdc42 | 1328.239 | 1328.239 | 192.988 | 1605.48736 | 2052.23855 | 1236.62402 | CONFLICT | 0.5 | 0.5 |
| 28Day | CD28 dependent PI3K/Akt signaling | 0.5482 | 0.7912 | 1 | pdpk1 | 192.988 | 192.988 | 192.988 | | 192.988 | | DOWN | 0 | 1 |
| 28Day | Downregulation of ERBB2 signaling | 0.50218 | 0.81895 | 1 | hbegf | 919.738 | 919.738 | 919.738 | | 919.738 | | UP | 1 | 0 |
| 28Day | Sphingolipid de novo biosynthesis | 0.59484 | 0.63522 | 1 | ormdl2;ormdl3;aldh3a2 | 3690.26 | 3444.81 | 2456.59 | 1372.94999 | 3564.34119 | 1439.47386 | UP | 0.666666667 | 0.333333333 |
| 28Day | Formation of a pool of free 40S subunits | 0.45872 | 0.78282 | 1 | eif3m;eif1ax | 2737.81 | 2737.81 | 1517.45 | 1725.84966 | 2423.68091 | 1667.69388 | CONFLICT | 0.5 | 0.5 |
| 28Day | Lysosome Vesicle Biogenesis | 0.62174 | 0.65548 | 1 | hgs;app | 3925.595 | 3925.595 | 3220.72 | 996.843785 | 3872.79325 | 994.042998 | CONFLICT | 0.5 | 0.5 |
| 28Day | N-glycan antennae elongation in the medial/trans-Golgi | 0.48011 | 0.83141 | 1 | mgat2 | 3478.56 | 3478.56 | 3478.56 | | 3478.56 | | UP | 1 | 0 |
| 28Day | MHC class II antigen presentation | 0.5482 | 0.59626 | 1 | dynll1;tubb4b;tubb2a;cd74;h2-ab1;h2-aa;ctss;capza2 | 4356.4125 | 4556.49 | 2359.45 | 1451.31924 | 4308.08647 | 1498.46386 | DOWN | 0.375 | 0.625 |
| 28Day | Eicosanoid ligand-binding receptors | 0.7508 | 0.63077 | 1 | cysltr1 | 4610.42 | 4610.42 | 4610.42 | | 4610.42 | | UP | 1 | 0 |
| 28Day | Formation of the beta-catenin:TCF transactivating complex | 0.4587 | 0.84301 | 1 | pygo2 | 3936.43 | 3936.43 | 3936.43 | | 3936.43 | | DOWN | 0 | 1 |
| 28Day | Nuclear Events (kinase and transcription factor activation) | 0.5482 | 0.7912 | 1 | mapkapk2 | 5375 | 5375 | 5375 | | 5375 | | DOWN | 0 | 1 |
| 28Day | ERKs are inactivated | 0.39648 | 1 | 1 | | | | | | | | | | |
| 28Day | Interleukin-17 signaling | 0.51707 | 0.70261 | 1 | map2k4;mapkapk2;ikbkg | 4469.72667 | 5375 | 2616.5 | 1605.08324 | 4378.98863 | 1647.6138 | UP | 0.666666667 | 0.333333333 |
| 28Day | MAPK targets/ Nuclear events mediated by MAP kinases | 0.41791 | 0.86388 | 1 | mapkapk2 | 5375 | 5375 | 5375 | | 5375 | | DOWN | 0 | 1 |
| 28Day | MAP kinase activation | 0.62665 | 0.60545 | 1 | map2k4;mapkapk2;ikbkg | 4469.72667 | 5375 | 2616.5 | 1605.08324 | 4378.98863 | 1647.6138 | UP | 0.666666667 | 0.333333333 |
| 28Day | DNA Double-Strand Break Repair | 0.53551 | 0.59406 | 1 | ube2n;rmi1;ube2v2;pole3;hist1h4i;rad51d;rad51;lig3;brca1;blm | 3816.8064 | 3892.075 | 692.086 | 1865.9087 | 4049.79857 | 1462.97446 | UP | 0.7 | 0.3 |
| 28Day | Recruitment and ATM-mediated phosphorylation of repair and signaling proteins at DNA double strand breaks | 0.56331 | 0.63648 | 1 | ube2n;ube2v2;hist1h4i;brca1 | 5011.745 | 5455.01 | 3288.55 | 1173.78176 | 4729.48604 | 1369.44158 | CONFLICT | 0.5 | 0.5 |
| 28Day | DNA Double Strand Break Response | 0.54959 | 0.64888 | 1 | ube2n;ube2v2;hist1h4i;brca1 | 5011.745 | 5455.01 | 3288.55 | 1173.78176 | 4729.48604 | 1369.44158 | CONFLICT | 0.5 | 0.5 |
| 28Day | G2/M DNA damage checkpoint | 0.60486 | 0.5976 | 1 | ube2n;ube2v2;hist1h4i;brca1 | 5011.745 | 5455.01 | 3288.55 | 1173.78176 | 4729.48604 | 1369.44158 | CONFLICT | 0.5 | 0.5 |
| 28Day | RHO GTPases Activate WASPs and WAVEs | 0.56515 | 0.70349 | 1 | cdc42;brk1 | 3960.63 | 3960.63 | 2463.49 | 2117.27569 | 4417.2828 | 2016.38111 | CONFLICT | 0.5 | 0.5 |
| 28Day | RUNX1 regulates transcription of genes involved in differentiation of HSCs | 0.59653 | 0.75921 | 1 | tal1 | 1424.03 | 1424.03 | 1424.03 | | 1424.03 | | DOWN | 0 | 1 |
| 28Day | Mitochondrial calcium ion transport | 0.6725 | 0.70182 | 1 | micu2 | 5256.23 | 5256.23 | 5256.23 | | 5256.23 | | DOWN | 0 | 1 |
| 28Day | Processing of SMDT1 | 0.69847 | 0.6798 | 1 | micu2 | 5256.23 | 5256.23 | 5256.23 | | 5256.23 | | DOWN | 0 | 1 |
| 28Day | Trafficking and processing of endosomal TLR | 0.52488 | 0.80557 | 1 | ctss | 5780.39 | 5780.39 | 5780.39 | | 5780.39 | | DOWN | 0 | 1 |
| 28Day | Complex I biogenesis | 0.56334 | 0.66338 | 1 | ndufab1;ndufaf1;ndufc2 | 2854.76 | 1721.17 | 1023.12 | 2591.57484 | 2475.6788 | 2540.36649 | DOWN | 0.333333333 | 0.666666667 |
| 28Day | COPI-mediated anterograde transport | 0.49757 | 0.66308 | 1 | dynll1;tubb4b;tubb2a;capza2;bet1;gbf1 | 3921.455 | 3519.135 | 2359.45 | 1406.29296 | 3960.61037 | 1431.19614 | UP | 0.833333333 | 0.166666667 |
| 28Day | Global Genome Nucleotide Excision Repair (GG-NER) | 0.53932 | 0.63939 | 1 | ube2n;usp45;ube2v2;pole3;ino80c | 3333.7876 | 3288.55 | 805.318 | 2055.39985 | 3663.82139 | 1926.19448 | DOWN | 0.4 | 0.6 |
| 28Day | G beta:gamma signalling through PLC beta | 0.62145 | 0.74142 | 1 | gnb5 | 953.648 | 953.648 | 953.648 | | 953.648 | | UP | 1 | 0 |
| 28Day | Presynaptic function of Kainate receptors | 0.59653 | 0.75921 | 1 | gnb5 | 953.648 | 953.648 | 953.648 | | 953.648 | | UP | 1 | 0 |
| 28Day | Synthesis of PC | 0.50218 | 0.81895 | 1 | phospho1 | 4698.14 | 4698.14 | 4698.14 | | 4698.14 | | DOWN | 0 | 1 |
| 28Day | Hedgehog 'off' state | 0.44366 | 0.76008 | 1 | tubb4b;tubb2a;adcy9 | 3161.03 | 2903.04 | 2359.45 | 957.020878 | 2870.18918 | 656.933577 | UP | 0.666666667 | 0.333333333 |
| 28Day | Elastic fibre formation | 0.47567 | 0.77104 | 1 | vtn;fn1 | 1801.881 | 1801.881 | 447.762 | 1915.01345 | 2418.97549 | 1704.60122 | DOWN | 0 | 1 |
| 28Day | Molecules associated with elastic fibres | 0.51059 | 0.74579 | 1 | vtn;fn1 | 1801.881 | 1801.881 | 447.762 | 1915.01345 | 2418.97549 | 1704.60122 | DOWN | 0 | 1 |
| 28Day | Surfactant metabolism | 0.50218 | 0.81895 | 1 | abca3 | 2494.49 | 2494.49 | 2494.49 | | 2494.49 | | DOWN | 0 | 1 |

BMD analysis results for functional classification based on dose-responsive genes, using the Reactome database for gene sets in BMDExpress2.2 software.

| Study Day | Gene Set Name | Fisher's Exact Left P-Value | Fisher's Exact Right P-Value | Fisher's Exact Two Tail | Gene Symbols | BMD Mean | BMD Median | BMD Minimum | BMD Standard Deviation | BMD wMean | BMD wSD | Overall Direction | Percent Genes With Overall Direction Up | Percent Genes With Overall Direction Down |
|---|---|---|---|---|---|---|---|---|---|---|---|---|---|---|
| 28Day | Regulation of HSF1-mediated heat shock response | 0.56331 | 0.63648 | 1 | hikeshi;gm45902;mapkapk2;tpr | 4640.02 | 4764.775 | 3638.67 | 883.900811 | 4474.97086 | 799.34375 | CONFLICT | 0.5 | 0.5 |
| 28Day | N-glycan trimming in the ER and Calnexin/Calreticulin cycle | 0.5482 | 0.7912 | 1 | ngly1 | 5615.31 | 5615.31 | 5615.31 | | 5615.31 | | DOWN | 0 | 1 |
| 28Day | ER Quality Control Compartment (ERQC) | 0.42575 | 1 | 1 | | | | | | | | | | |
| 28Day | GPVI-mediated activation cascade | 0.58383 | 0.68814 | 1 | pdpk1;cdc42 | 1328.239 | 1328.239 | 192.988 | 1605.48736 | 2052.23855 | 1236.62402 | CONFLICT | 0.5 | 0.5 |
| 28Day | Netrin-1 signaling | 0.4587 | 0.84301 | 1 | cdc42 | 2463.49 | 2463.49 | 2463.49 | | 2463.49 | | UP | 1 | 0 |
| 28Day | Protein-protein interactions at synapses | 0.50901 | 0.68439 | 1 | gria3;ptprd;il1rap;epb41l3 | 3795.0225 | 3615.755 | 2052.57 | 1584.36894 | 3120.2557 | 1402.73545 | DOWN | 0.25 | 0.75 |
| 28Day | The canonical retinoid cycle in rods (twilight vision) | 0.50218 | 0.81895 | 1 | rdh16f2 | 2673.93 | 2673.93 | 2673.93 | | 2673.93 | | DOWN | 0 | 1 |
| 28Day | ROS, RNS production in phagocytes | 0.66015 | 0.62015 | 1 | atp6v0e2;atp6v1e1 | 3839.965 | 3839.965 | 2385.58 | 2056.81099 | 2967.18762 | 1645.29352 | CONFLICT | 0.5 | 0.5 |
| 28Day | TBC/RABGAPs | 0.60271 | 0.67214 | 1 | rab11a;tbc1d10a | 3249.27 | 3249.27 | 2192.92 | 1493.9045 | 2704.58757 | 1279.99717 | CONFLICT | 0.5 | 0.5 |
| 28Day | RAB geranylgeranylation | 0.59096 | 0.61083 | 1 | rab9;rab11a;rab29;rab18 | 3519.6475 | 3352.36 | 2192.92 | 1288.89752 | 3601.15039 | 1504.38651 | CONFLICT | 0.5 | 0.5 |
| 28Day | Butyrate Response Factor 1 (BRF1) binds and destabilizes mRNA | 0.69847 | 0.6798 | 1 | exosc3 | 2805.79 | 2805.79 | 2805.79 | | 2805.79 | | UP | 1 | 0 |
| 28Day | Regulation of mRNA stability by proteins that bind AU-rich elements | 0.5285 | 0.7323 | 1 | exosc3;set | 3433.275 | 3433.275 | 2805.79 | 887.397797 | 3679.80909 | 816.037216 | UP | 1 | 0 |
| 28Day | KSRP (KHSRP) binds and destabilizes mRNA | 0.7508 | 0.63077 | 1 | exosc3 | 2805.79 | 2805.79 | 2805.79 | | 2805.79 | | UP | 1 | 0 |
| 28Day | Major pathway of rRNA processing in the nucleolus and cytosol | 0.48288 | 0.66555 | 1 | las1l;exosc3;pno1;wdr18;dhx37;fbl;bop1 | 3014.84343 | 3919.15 | 185.964 | 1717.0495 | 3391.14106 | 1585.91685 | CONFLICT | 0.571428571 | 0.428571429 |
| 28Day | rRNA processing | 0.48288 | 0.66555 | 1 | las1l;exosc3;pno1;wdr18;dhx37;fbl;bop1 | 3014.84343 | 3919.15 | 185.964 | 1717.0495 | 3391.14106 | 1585.91685 | CONFLICT | 0.571428571 | 0.428571429 |
| 28Day | rRNA processing in the nucleus and cytosol | 0.48288 | 0.66555 | 1 | las1l;exosc3;pno1;wdr18;dhx37;fbl;bop1 | 3014.84343 | 3919.15 | 185.964 | 1717.0495 | 3391.14106 | 1585.91685 | CONFLICT | 0.571428571 | 0.428571429 |
| 28Day | Nucleotide-like (purinergic) receptors | 0.69847 | 0.6798 | 1 | adora1 | 907.506 | 907.506 | 907.506 | | 907.506 | | UP | 1 | 0 |
| 28Day | ADP signalling through P2Y purinoceptor 1 | 0.50218 | 0.81895 | 1 | gnb5 | 953.648 | 953.648 | 953.648 | | 953.648 | | UP | 1 | 0 |
| 28Day | Signaling by Activin | 0.39648 | 1 | 1 | | | | | | | | | | |
| 28Day | Antagonism of Activin by Follistatin | 0.75238 | 1 | 1 | | | | | | | | | | |
| 28Day | SUMOylation of chromatin organization proteins | 0.5467 | 0.7182 | 1 | hist1h4i;bmi1 | 4883.435 | 4883.435 | 3918.46 | 1364.68073 | 5169.0195 | 1303.54765 | CONFLICT | 0.5 | 0.5 |
| 28Day | Recycling of bile acids and salts | 0.62145 | 0.74142 | 1 | slc10a1 | 2878.3 | 2878.3 | 2878.3 | | 2878.3 | | DOWN | 0 | 1 |
| 28Day | TNFR2 non-canonical NF-kB pathway | 0.51707 | 0.70261 | 1 | ube2m;tnfrsf1b;birc2 | 3321.17667 | 2933.96 | 1167.32 | 2371.29595 | 2952.86511 | 2468.02167 | UP | 0.666666667 | 0.333333333 |
| 28Day | TNF receptor superfamily (TNFSF) members mediating non-canonical NF-kB pathway | 0.6725 | 0.70182 | 1 | birc2 | 5862.25 | 5862.25 | 5862.25 | | 5862.25 | | UP | 1 | 0 |
| 28Day | TP53 Regulates Transcription of Cell Cycle Genes | 0.60271 | 0.67214 | 1 | e2f7;cnot1 | 3791.975 | 3791.975 | 3132.16 | 933.119322 | 3822.04232 | 932.149978 | UP | 1 | 0 |
| 28Day | Histidine catabolism | 0.56601 | 1 | 1 | | | | | | | | | | |
| 28Day | Fc epsilon receptor (FCERI) signaling | 0.57652 | 0.60482 | 1 | ube2n;map2k4;ppp3cb;pdpk1;ikbkg | 3517.9496 | 4095.87 | 192.988 | 2171.92953 | 3919.16084 | 1585.36842 | UP | 0.6 | 0.4 |
| 28Day | FCERI mediated MAPK activation | 0.48011 | 0.83141 | 1 | map2k4 | 2616.5 | 2616.5 | 2616.5 | | 2616.5 | | UP | 1 | 0 |
| 28Day | Sialic acid metabolism | 0.6409 | 0.63815 | 1 | nanp;gne | 4701.73 | 4701.73 | 3647.63 | 1490.72252 | 4718.87066 | 1490.52542 | DOWN | 0 | 1 |
| 28Day | Transport of vitamins, nucleosides, and related molecules | 0.44212 | 0.79406 | 1 | slc35d2;slco2b1 | 3128.045 | 3128.045 | 2439.34 | 973.975951 | 3030.48208 | 964.153571 | CONFLICT | 0.5 | 0.5 |
| 28Day | SHC1 events in ERBB2 signaling | 0.6725 | 0.70182 | 1 | hbegf | 919.738 | 919.738 | 919.738 | | 919.738 | | UP | 1 | 0 |
| 28Day | Multifunctional anion exchangers | 0.56601 | 1 | 1 | | | | | | | | | | |
| 28Day | Nuclear Receptor transcription pathway | 0.53234 | 0.68993 | 1 | nr1d2;rorc;nrbp1 | 4105.93333 | 3736.79 | 3688.98 | 681.199256 | 3809.92148 | 421.24327 | UP | 0.666666667 | 0.333333333 |
| 28Day | Signaling by EGFR | 0.65859 | 0.57412 | 1 | hgs;hbegf;cdc42 | 2201.316 | 2463.49 | 919.738 | 1172.68109 | 2028.69886 | 1124.36761 | UP | 1 | 0 |
| 28Day | GAB1 signalosome | 0.6725 | 0.70182 | 1 | hbegf | 919.738 | 919.738 | 919.738 | | 919.738 | | UP | 1 | 0 |
| 28Day | SHC1 events in EGFR signaling | 0.7508 | 0.63077 | 1 | hbegf | 919.738 | 919.738 | 919.738 | | 919.738 | | UP | 1 | 0 |
| 28Day | RNA polymerase II transcribes snRNA genes | 0.60153 | 0.58077 | 1 | ints14;ell3;rpap2;polr2a;ccnk | 4003.346 | 3559.08 | 2852.38 | 1007.63001 | 3883.3938 | 943.742673 | UP | 0.6 | 0.4 |
| 28Day | TGF-beta receptor signaling activates SMADs | 0.59653 | 0.75921 | 1 | ube2m | 2933.96 | 2933.96 | 2933.96 | | 2933.96 | | UP | 1 | 0 |
| 28Day | Non-integrin membrane-ECM interactions | 0.51059 | 0.74579 | 1 | vtn;fn1 | 1801.881 | 1801.881 | 447.762 | 1915.01345 | 2418.97549 | 1704.60122 | DOWN | 0 | 1 |

BMD analysis results for functional classification based on dose-responsive genes, using the Reactome database for gene sets in BMDExpress2.2 software.

| Study Day | Gene Set Name | Fisher's Exact Left P-Value | Fisher's Exact Right P-Value | Fisher's Exact Two Tail | Gene Symbols | BMD Mean | BMD Median | BMD Minimum | BMD Standard Deviation | BMD wMean | BMD wSD | Overall Direction | Percent Genes With Overall Direction Up | Percent Genes With Overall Direction Down |
|---|---|---|---|---|---|---|---|---|---|---|---|---|---|---|
| 28Day | GRB2:SOS provides linkage to MAPK signaling for Integrins | 0.7508 | 0.63077 | 1 | fn1 | 3156 | 3156 | 3156 | | 3156 | | DOWN | 0 | 1 |
| 28Day | p130Cas linkage to MAPK signaling for integrins | 0.7508 | 0.63077 | 1 | fn1 | 3156 | 3156 | 3156 | | 3156 | | DOWN | 0 | 1 |
| 28Day | EPHA-mediated growth cone collapse | 0.62145 | 0.74142 | 1 | epha7 | 5831.01 | 5831.01 | 5831.01 | | 5831.01 | | UP | 1 | 0 |
| 28Day | Branched-chain amino acid catabolism | 0.52488 | 0.80557 | 1 | aldh6a1 | 2600.38 | 2600.38 | 2600.38 | | 2600.38 | | DOWN | 0 | 1 |
| 28Day | Peptide hormone biosynthesis | 0.45717 | 1 | 1 | | | | | | | | | | |
| 28Day | Negative regulation of MET activity | 0.6468 | 0.72232 | 1 | hgs | 3220.72 | 3220.72 | 3220.72 | | 3220.72 | | UP | 1 | 0 |
| 28Day | FGFR2 ligand binding and activation | 0.62145 | 0.74142 | 1 | fgf1 | 1467.57 | 1467.57 | 1467.57 | | 1467.57 | | DOWN | 0 | 1 |
| 28Day | FGFR1 ligand binding and activation | 0.72461 | 0.65616 | 1 | fgf1 | 1467.57 | 1467.57 | 1467.57 | | 1467.57 | | DOWN | 0 | 1 |
| 28Day | Phospholipase C-mediated cascade: FGFR1 | 0.69847 | 0.6798 | 1 | fgf1 | 1467.57 | 1467.57 | 1467.57 | | 1467.57 | | DOWN | 0 | 1 |
| 28Day | Phospholipase C-mediated cascade; FGFR2 | 0.6468 | 0.72232 | 1 | fgf1 | 1467.57 | 1467.57 | 1467.57 | | 1467.57 | | DOWN | 0 | 1 |
| 28Day | SHC-mediated cascade:FGFR1 | 0.57209 | 0.77577 | 1 | fgf1 | 1467.57 | 1467.57 | 1467.57 | | 1467.57 | | DOWN | 0 | 1 |
| 28Day | PI-3K cascade:FGFR1 | 0.57209 | 0.77577 | 1 | fgf1 | 1467.57 | 1467.57 | 1467.57 | | 1467.57 | | DOWN | 0 | 1 |
| 28Day | FRS-mediated FGFR1 signaling | 0.52488 | 0.80557 | 1 | fgf1 | 1467.57 | 1467.57 | 1467.57 | | 1467.57 | | DOWN | 0 | 1 |
| 28Day | PI-3K cascade:FGFR2 | 0.52488 | 0.80557 | 1 | fgf1 | 1467.57 | 1467.57 | 1467.57 | | 1467.57 | | DOWN | 0 | 1 |
| 28Day | SHC-mediated cascade:FGFR2 | 0.52488 | 0.80557 | 1 | fgf1 | 1467.57 | 1467.57 | 1467.57 | | 1467.57 | | DOWN | 0 | 1 |
| 28Day | FRS-mediated FGFR2 signaling | 0.48011 | 0.83141 | 1 | fgf1 | 1467.57 | 1467.57 | 1467.57 | | 1467.57 | | DOWN | 0 | 1 |
| 28Day | FGFRL1 modulation of FGFR1 signaling | 0.39648 | 1 | 1 | | | | | | | | | | |
| 28Day | Transport of Mature mRNA derived from an Intron-Containing Transcript | 0.58901 | 0.59289 | 1 | u2af2;srsf1;tpr;thoc5;bc005561 | 4059.426 | 3638.67 | 3469.84 | 668.012629 | 4008.58851 | 597.208978 | UP | 0.8 | 0.2 |
| 28Day | Transport of Mature Transcript to Cytoplasm | 0.58901 | 0.59289 | 1 | u2af2;srsf1;tpr;thoc5;bc005561 | 4059.426 | 3638.67 | 3469.84 | 668.012629 | 4008.58851 | 597.208978 | UP | 0.8 | 0.2 |
| 28Day | ERBB2 Regulates Cell Motility | 0.72461 | 0.65616 | 1 | hbegf | 919.738 | 919.738 | 919.738 | | 919.738 | | UP | 1 | 0 |
| 28Day | SUMOylation of DNA damage response and repair proteins | 0.54959 | 0.64888 | 1 | rad21;brca1;blm;tpr | 3527.834 | 3887.97 | 692.086 | 2073.67647 | 4059.64798 | 1691.6082 | UP | 1 | 0 |
| 28Day | Downstream signaling events of B Cell Receptor (BCR) | 0.60271 | 0.67214 | 1 | ppp3cb;ikbkg | 4756.775 | 4756.775 | 4095.87 | 934.660814 | 4545.37184 | 885.555333 | UP | 1 | 0 |
| 28Day | Activation of NF-kappaB in B cells | 0.62145 | 0.74142 | 1 | ikbkg | 5417.68 | 5417.68 | 5417.68 | | 5417.68 | | UP | 1 | 0 |
| 28Day | Nuclear Envelope Breakdown | 0.62665 | 0.60545 | 1 | nek6;cnep1r1;tpr | 4227.96333 | 3638.67 | 3203.61 | 1414.28815 | 3739.88139 | 1152.28749 | UP | 1 | 0 |
| 28Day | Interleukin-12 family signaling | 0.59653 | 0.75921 | 1 | p4hb | 5730.92 | 5730.92 | 5730.92 | | 5730.92 | | DOWN | 0 | 1 |
| 28Day | Interleukin-6 family signaling | 0.43797 | 0.85382 | 1 | lifr | 727.581 | 727.581 | 727.581 | | 727.581 | | DOWN | 0 | 1 |
| 28Day | IL-6-type cytokine receptor ligand interactions | 0.59653 | 0.75921 | 1 | lifr | 727.581 | 727.581 | 727.581 | | 727.581 | | DOWN | 0 | 1 |
| 28Day | Interleukin-35 Signalling | 0.42575 | 1 | 1 | | | | | | | | | | |
| 28Day | Interleukin-27 signaling | 0.45717 | 1 | 1 | | | | | | | | | | |
| 28Day | Adenylate cyclase inhibitory pathway | 0.7508 | 0.63077 | 1 | adcy9 | 4220.6 | 4220.6 | 4220.6 | | 4220.6 | | DOWN | 0 | 1 |
| 28Day | G-protein activation | 0.43797 | 0.85382 | 1 | gnb5 | 953.648 | 953.648 | 953.648 | | 953.648 | | UP | 1 | 0 |
| 28Day | Chaperonin-mediated protein folding | 0.5285 | 0.7323 | 1 | gnb5;cct4 | 3395.259 | 3395.259 | 953.648 | 3452.95939 | 3138.05293 | 3433.74702 | UP | 1 | 0 |
| 28Day | Protein folding | 0.5285 | 0.7323 | 1 | gnb5;cct4 | 3395.259 | 3395.259 | 953.648 | 3452.95939 | 3138.05293 | 3433.74702 | UP | 1 | 0 |
| 28Day | ADP signalling through P2Y purinoceptor 12 | 0.57209 | 0.77577 | 1 | gnb5 | 953.648 | 953.648 | 953.648 | | 953.648 | | UP | 1 | 0 |
| 28Day | Cooperation of PDCL (PhLP1) and TRiC/CCT in G-protein beta folding | 0.5467 | 0.7182 | 1 | gnb5;cct4 | 3395.259 | 3395.259 | 953.648 | 3452.95939 | 3138.05293 | 3433.74702 | UP | 1 | 0 |
| 28Day | Inhibition of adenylate cyclase pathway | 0.7508 | 0.63077 | 1 | adcy9 | 4220.6 | 4220.6 | 4220.6 | | 4220.6 | | DOWN | 0 | 1 |
| 28Day | PI3K events in ERBB2 signaling | 0.69847 | 0.6798 | 1 | hbegf | 919.738 | 919.738 | 919.738 | | 919.738 | | UP | 1 | 0 |
| 28Day | Inflammasomes | 0.72461 | 0.65616 | 1 | bcl2l1 | 2151.36 | 2151.36 | 2151.36 | | 2151.36 | | UP | 1 | 0 |
| 28Day | SUMO is proteolytically processed | 0.65259 | 1 | 1 | | | | | | | | | | |
| 28Day | Processing and activation of SUMO | 0.4909 | 1 | 1 | | | | | | | | | | |
| 28Day | Aquaporin-mediated transport | 0.57904 | 0.6495 | 1 | rab11a;gnb5;adcy9 | 2455.72267 | 2192.92 | 953.648 | 1649.25522 | 1742.1359 | 1240.36097 | UP | 0.666666667 | 0.333333333 |
| 28Day | Endogenous sterols | 0.4587 | 0.84301 | 1 | fdxr | 5126.12 | 5126.12 | 5126.12 | | 5126.12 | | DOWN | 0 | 1 |
| 28Day | Gap junction trafficking and regulation | 0.44212 | 0.79406 | 1 | tubb4b;tubb2a | 2631.245 | 2631.245 | 2359.45 | 384.376175 | 2702.45657 | 370.948608 | UP | 1 | 0 |
| 28Day | Gap junction trafficking | 0.47567 | 0.77104 | 1 | tubb4b;tubb2a | 2631.245 | 2631.245 | 2359.45 | 384.376175 | 2702.45657 | 370.948608 | UP | 1 | 0 |
| 28Day | Gap junction assembly | 0.66015 | 0.62015 | 1 | tubb4b;tubb2a | 2631.245 | 2631.245 | 2359.45 | 384.376175 | 2702.45657 | 370.948608 | UP | 1 | 0 |
| 28Day | Metabolism of cofactors | 0.69847 | 0.6798 | 1 | coq3 | 1252.61 | 1252.61 | 1252.61 | | 1252.61 | | DOWN | 0 | 1 |

BMD analysis results for functional classification based on dose-responsive genes, using the Reactome database for gene sets in BMDExpress2.2 software.

| Study Day | Gene Set Name | Fisher's Exact Left P-Value | Fisher's Exact Right P-Value | Fisher's Exact Two Tail | Gene Symbols | BMD Mean | BMD Median | BMD Minimum | BMD Standard Deviation | BMD wMean | BMD wSD | Overall Direction | Percent Genes With Overall Direction Up | Percent Genes With Overall Direction Down |
|---|---|---|---|---|---|---|---|---|---|---|---|---|---|---|
| 28Day | Telomere Maintenance | 0.50218 | 0.81895 | 1 | pole3 | 805.318 | 805.318 | 805.318 | | 805.318 | | UP | 1 | 0 |
| 28Day | Telomere C-strand (Lagging Strand) Synthesis | 0.5482 | 0.7912 | 1 | pole3 | 805.318 | 805.318 | 805.318 | | 805.318 | | UP | 1 | 0 |
| 28Day | Extension of Telomeres | 0.50218 | 0.81895 | 1 | pole3 | 805.318 | 805.318 | 805.318 | | 805.318 | | UP | 1 | 0 |
| 28Day | Gap-filling DNA repair synthesis and ligation in GG-NER | 0.59653 | 0.75921 | 1 | pole3 | 805.318 | 805.318 | 805.318 | | 805.318 | | UP | 1 | 0 |
| 28Day | Gap-filling DNA repair synthesis and ligation in TC-NER | 0.57711 | 0.6238 | 1 | pole3;prpf19;polr2a;lig3 | 3696.917 | 4295.465 | 805.318 | 2086.45358 | 3989.40693 | 1722.6516 | UP | 0.75 | 0.25 |
| 28Day | TNFs bind their physiological receptors | 0.4587 | 0.84301 | 1 | tnfrsf1b | 1167.32 | 1167.32 | 1167.32 | | 1167.32 | | DOWN | 0 | 1 |
| 28Day | TP53 regulates transcription of additional cell cycle genes whose exact role in the p53 pathway remain uncertain | 0.6725 | 0.70182 | 1 | cnot1 | 3132.16 | 3132.16 | 3132.16 | | 3132.16 | | UP | 1 | 0 |
| 28Day | Transcriptional activity of SMAD2/SMAD3:SMAD4 heterotrimer | 0.51059 | 0.74579 | 1 | tfdp1;ccnk | 5399.625 | 5399.625 | 5090.85 | 436.673793 | 5395.60681 | 436.636817 | CONFLICT | 0.5 | 0.5 |
| 28Day | Zinc transporters | 0.42575 | 1 | 1 | | | | | | | | | | |
| 28Day | Eicosanoids | 0.6468 | 0.72232 | 1 | cyp4a12b | 4766.57 | 4766.57 | 4766.57 | | 4766.57 | | UP | 1 | 0 |
| 28Day | Intraflagellar transport | 0.47238 | 0.73825 | 1 | dynll1;tubb4b;tubb2a | 3684.67667 | 2903.04 | 2359.45 | 1844.72961 | 3931.15502 | 1868.40338 | UP | 1 | 0 |
| 28Day | SHC1 events in ERBB4 signaling | 0.7508 | 0.63077 | 1 | hbegf | 919.738 | 919.738 | 919.738 | | 919.738 | | UP | 1 | 0 |
| 28Day | GRB2 events in ERBB2 signaling | 0.7508 | 0.63077 | 1 | hbegf | 919.738 | 919.738 | 919.738 | | 919.738 | | UP | 1 | 0 |
| 28Day | Prostacyclin signalling through prostacyclin receptor | 0.6468 | 0.72232 | 1 | gnb5 | 953.648 | 953.648 | 953.648 | | 953.648 | | UP | 1 | 0 |
| 28Day | Adrenaline,noradrenaline inhibits insulin secretion | 0.5482 | 0.7912 | 1 | gnb5 | 953.648 | 953.648 | 953.648 | | 953.648 | | UP | 1 | 0 |
| 28Day | G alpha (z) signalling events | 0.62174 | 0.65548 | 1 | gnb5;adcy9 | 2587.124 | 2587.124 | 953.648 | 2310.08391 | 1477.92173 | 1695.82674 | CONFLICT | 0.5 | 0.5 |
| 28Day | Thromboxane signalling through TP receptor | 0.5482 | 0.7912 | 1 | gnb5 | 953.648 | 953.648 | 953.648 | | 953.648 | | UP | 1 | 0 |
| 28Day | Thrombin signalling through proteinase activated receptors (PARs) | 0.6409 | 0.63815 | 1 | gnb5;f2 | 1147.199 | 1147.199 | 953.648 | 273.722449 | 1145.11067 | 273.706516 | CONFLICT | 0.5 | 0.5 |
| 28Day | G beta:gamma signalling through BTK | 0.6725 | 0.70182 | 1 | gnb5 | 953.648 | 953.648 | 953.648 | | 953.648 | | UP | 1 | 0 |
| 28Day | Nucleobase biosynthesis | 0.72461 | 0.65616 | 1 | adss | 3213.44 | 3213.44 | 3213.44 | | 3213.44 | | UP | 1 | 0 |
| 28Day | ATF6 (ATF6-alpha) activates chaperones | 0.75238 | 1 | 1 | | | | | | | | | | |
| 28Day | Activation of IRF3/IRF7 mediated by TBK1/IKK epsilon | 0.72461 | 0.65616 | 1 | ly96 | 4560.3 | 4560.3 | 4560.3 | | 4560.3 | | UP | 1 | 0 |
| 28Day | Platelet Adhesion to exposed collagen | 0.45717 | 1 | 1 | | | | | | | | | | |
| 28Day | Scavenging of heme from plasma | 0.50218 | 0.81895 | 1 | lrp1 | 1882.51 | 1882.51 | 1882.51 | | 1882.51 | | DOWN | 0 | 1 |
| 28Day | Tetrahydrobiopterin (BH4) synthesis, recycling, salvage and regulation | 0.45717 | 1 | 1 | | | | | | | | | | |
| 28Day | Signaling by NOTCH1 | 0.6468 | 0.72232 | 1 | notch1 | 908.573 | 908.573 | 908.573 | | 908.573 | | UP | 1 | 0 |
| 28Day | Amine-derived hormones | 0.69847 | 0.6798 | 1 | ddc | 5580.16 | 5580.16 | 5580.16 | | 5580.16 | | DOWN | 0 | 1 |
| 28Day | Recycling pathway of L1 | 0.58383 | 0.68814 | 1 | tubb4b;tubb2a | 2631.245 | 2631.245 | 2359.45 | 384.376175 | 2702.45657 | 370.948608 | UP | 1 | 0 |
| 28Day | WNT5A-dependent internalization of FZD2, FZD5 and ROR2 | 0.42575 | 1 | 1 | | | | | | | | | | |
| 28Day | Adrenoceptors | 0.52712 | 1 | 1 | | | | | | | | | | |
| 28Day | TP53 Regulates Transcription of DNA Repair Genes | 0.44212 | 0.79406 | 1 | polr2a;ccnk | 5065.76 | 5065.76 | 5040.67 | 35.4826183 | 5074.14393 | 33.4430194 | CONFLICT | 0.5 | 0.5 |
| 28Day | MET Receptor Activation | 0.65259 | 1 | 1 | | | | | | | | | | |
| 28Day | GABA A receptor activation | 0.39648 | 1 | 1 | | | | | | | | | | |
| 28Day | Apoptotic cleavage of cellular proteins | 0.49297 | 0.7587 | 1 | pkp1;birc2 | 4535.22 | 4535.22 | 3208.19 | 1876.70382 | 4209.41526 | 1819.26353 | UP | 1 | 0 |
| 28Day | HS-GAG biosynthesis | 0.67943 | 0.60146 | 1 | hs2st1;gpc4 | 4234.355 | 4234.355 | 3361.03 | 1235.06806 | 4554.00819 | 1149.36364 | DOWN | 0 | 1 |
| 28Day | Transcriptional regulation by RUNX3 | 0.5467 | 0.7182 | 1 | notch1;mdm2 | 1587.5915 | 1587.5915 | 908.573 | 960.277172 | 1863.66593 | 877.32438 | UP | 1 | 0 |
| 28Day | p53-Dependent G1 DNA Damage Response | 0.69847 | 0.6798 | 1 | mdm2 | 2266.61 | 2266.61 | 2266.61 | | 2266.61 | | UP | 1 | 0 |
| 28Day | p53-Dependent G1/S DNA damage checkpoint | 0.69847 | 0.6798 | 1 | mdm2 | 2266.61 | 2266.61 | 2266.61 | | 2266.61 | | UP | 1 | 0 |
| 28Day | G1/S DNA Damage Checkpoints | 0.62145 | 0.74142 | 1 | mdm2 | 2266.61 | 2266.61 | 2266.61 | | 2266.61 | | UP | 1 | 0 |
| 28Day | Glutamate Neurotransmitter Release Cycle | 0.52488 | 0.80557 | 1 | slc1a2 | 1774.78 | 1774.78 | 1774.78 | | 1774.78 | | DOWN | 0 | 1 |
| 28Day | Attachment of GPI anchor to uPAR | 0.65259 | 1 | 1 | | | | | | | | | | |

BMD analysis results for functional classification based on dose-responsive genes, using the Reactome database for gene sets in BMDExpress2.2 software.

| Study Day | Gene Set Name | Fisher's Exact Left P-Value | Fisher's Exact Right P-Value | Fisher's Exact Two Tail | Gene Symbols | BMD Mean | BMD Median | BMD Minimum | BMD Standard Deviation | BMD wMean | BMD wSD | Overall Direction | Percent Genes With Overall Direction Up | Percent Genes With Overall Direction Down |
|---|---|---|---|---|---|---|---|---|---|---|---|---|---|---|
| 28Day | TRAF6-mediated induction of TAK1 complex within TLR4 complex | 0.7508 | 0.63077 | 1 | ly96 | 4560.3 | 4560.3 | 4560.3 | | 4560.3 | | UP | 1 | 0 |
| 28Day | Inhibition of the proteolytic activity of APC/C required for the onset of anaphase by mitotic spindle checkpoint components | 0.59653 | 0.75921 | 1 | cdc27 | 5780.76 | 5780.76 | 5780.76 | | 5780.76 | | UP | 1 | 0 |
| 28Day | Inactivation of APC/C via direct inhibition of the APC/C complex | 0.59653 | 0.75921 | 1 | cdc27 | 5780.76 | 5780.76 | 5780.76 | | 5780.76 | | UP | 1 | 0 |
| 28Day | APC/C:Cdc20 mediated degradation of Cyclin B | 0.57209 | 0.77577 | 1 | cdc27 | 5780.76 | 5780.76 | 5780.76 | | 5780.76 | | UP | 1 | 0 |
| 28Day | APC/C:Cdc20 mediated degradation of Securin | 0.59653 | 0.75921 | 1 | cdc27 | 5780.76 | 5780.76 | 5780.76 | | 5780.76 | | UP | 1 | 0 |
| 28Day | APC/C:Cdh1 mediated degradation of Cdc20 and other APC/C:Cdh1 targeted proteins in late mitosis/early G1 | 0.48011 | 0.83141 | 1 | cdc27 | 5780.76 | 5780.76 | 5780.76 | | 5780.76 | | UP | 1 | 0 |
| 28Day | Cdc20:Phospho-APC/C mediated degradation of Cyclin A | 0.48011 | 0.83141 | 1 | cdc27 | 5780.76 | 5780.76 | 5780.76 | | 5780.76 | | UP | 1 | 0 |
| 28Day | APC/C:Cdc20 mediated degradation of mitotic proteins | 0.41791 | 0.86388 | 1 | cdc27 | 5780.76 | 5780.76 | 5780.76 | | 5780.76 | | UP | 1 | 0 |
| 28Day | Phosphorylation of the APC/C | 0.69847 | 0.6798 | 1 | cdc27 | 5780.76 | 5780.76 | 5780.76 | | 5780.76 | | UP | 1 | 0 |
| 28Day | Activation of APC/C and APC/C:Cdc20 mediated degradation of mitotic proteins | 0.41791 | 0.86388 | 1 | cdc27 | 5780.76 | 5780.76 | 5780.76 | | 5780.76 | | UP | 1 | 0 |
| 28Day | APC-Cdc20 mediated degradation of Nek2A | 0.52488 | 0.80557 | 1 | cdc27 | 5780.76 | 5780.76 | 5780.76 | | 5780.76 | | UP | 1 | 0 |
| 28Day | APC:Cdc20 mediated degradation of cell cycle proteins prior to satisfation of the cell cycle checkpoint | 0.4587 | 0.84301 | 1 | cdc27 | 5780.76 | 5780.76 | 5780.76 | | 5780.76 | | UP | 1 | 0 |
| 28Day | HS-GAG degradation | 0.59653 | 0.75921 | 1 | gpc4 | 3361.03 | 3361.03 | 3361.03 | | 3361.03 | | DOWN | 0 | 1 |
| 28Day | FRS-mediated FGFR3 signaling | 0.59653 | 0.75921 | 1 | fgf1 | 1467.57 | 1467.57 | 1467.57 | | 1467.57 | | DOWN | 0 | 1 |
| 28Day | Downstream signaling of activated FGFR3 | 0.48011 | 0.83141 | 1 | fgf1 | 1467.57 | 1467.57 | 1467.57 | | 1467.57 | | DOWN | 0 | 1 |
| 28Day | FRS-mediated FGFR4 signaling | 0.5482 | 0.7912 | 1 | fgf1 | 1467.57 | 1467.57 | 1467.57 | | 1467.57 | | DOWN | 0 | 1 |
| 28Day | Downstream signaling of activated FGFR4 | 0.43797 | 0.85382 | 1 | fgf1 | 1467.57 | 1467.57 | 1467.57 | | 1467.57 | | DOWN | 0 | 1 |
| 28Day | Nicotinamide salvaging | 0.6468 | 0.72232 | 1 | nudt12 | 5115.96 | 5115.96 | 5115.96 | | 5115.96 | | DOWN | 0 | 1 |
| 28Day | Triglyceride catabolism | 0.45717 | 1 | 1 | | | | | | | | | | |
| 28Day | FGFR2 alternative splicing | 0.50218 | 0.81895 | 1 | polr2a | 5040.67 | 5040.67 | 5040.67 | | 5040.67 | | UP | 1 | 0 |
| 28Day | RNA Pol II CTD phosphorylation and interaction with CE | 0.43797 | 0.85382 | 1 | polr2a | 5040.67 | 5040.67 | 5040.67 | | 5040.67 | | UP | 1 | 0 |
| 28Day | Regulation of pyruvate dehydrogenase (PDH) complex | 0.69847 | 0.6798 | 1 | gstz1 | 5233.2 | 5233.2 | 5233.2 | | 5233.2 | | DOWN | 0 | 1 |
| 28Day | Hyaluronan metabolism | 0.45717 | 1 | 1 | | | | | | | | | | |
| 28Day | Hyaluronan uptake and degradation | 0.60776 | 1 | 1 | | | | | | | | | | |
| 28Day | A tetrasaccharide linker sequence is required for GAG synthesis | 0.4587 | 0.84301 | 1 | gpc4 | 3361.03 | 3361.03 | 3361.03 | | 3361.03 | | DOWN | 0 | 1 |
| 28Day | Transport of nucleosides and free purine and pyrimidine bases across the plasma membrane | 0.56601 | 1 | 1 | | | | | | | | | | |
| 28Day | The NLRP3 inflammasome | 0.4909 | 1 | 1 | | | | | | | | | | |
| 28Day | G0 and Early G1 | 0.6725 | 0.70182 | 1 | tfdp1 | 5708.4 | 5708.4 | 5708.4 | | 5708.4 | | UP | 1 | 0 |
| 28Day | Glycoprotein hormones | 0.52712 | 1 | 1 | | | | | | | | | | |
| 28Day | Miscellaneous transport and binding events | 0.52488 | 0.80557 | 1 | azgp1 | 190.758 | 190.758 | 190.758 | | 190.758 | | DOWN | 0 | 1 |
| 28Day | Orc1 removal from chromatin | 0.50218 | 0.81895 | 1 | cdc6 | 5867.54 | 5867.54 | 5867.54 | | 5867.54 | | UP | 1 | 0 |
| 28Day | Activation of the pre-replicative complex | 0.62174 | 0.65548 | 1 | pole3;cdc6 | 3336.429 | 3336.429 | 805.318 | 3579.5315 | 4404.50906 | 3245.22045 | UP | 1 | 0 |
| 28Day | Sodium/Calcium exchangers | 0.42575 | 1 | 1 | | | | | | | | | | |
| 28Day | Ionotropic activity of kainate receptors | 0.42575 | 1 | 1 | | | | | | | | | | |
| 28Day | Activation of Ca-permeable Kainate Receptor | 0.42575 | 1 | 1 | | | | | | | | | | |

BMD analysis results for functional classification based on dose-responsive genes, using the Reactome database for gene sets in BMDExpress2.2 software.

| Study Day | Gene Set Name | Fisher's Exact Left P-Value | Fisher's Exact Right P-Value | Fisher's Exact Two Tail | Gene Symbols | BMD Mean | BMD Median | BMD Minimum | BMD Standard Deviation | BMD wMean | BMD wSD | Overall Direction | Percent Genes With Overall Direction Up | Percent Genes With Overall Direction Down |
|---|---|---|---|---|---|---|---|---|---|---|---|---|---|---|
| 28Day | SUMOylation of RNA binding proteins | 0.65259 | 1 | 1 | | | | | | | | | | |
| 28Day | SUMOylation of DNA methylation proteins | 0.75238 | 1 | 1 | | | | | | | | | | |
| 28Day | p75NTR signals via NF-kB | 0.7508 | 0.63077 | 1 | sqstm1 | 5683.98 | 5683.98 | 5683.98 | | 5683.98 | | UP | 1 | 0 |
| 28Day | Regulated proteolysis of p75NTR | 0.42575 | 1 | 1 | | | | | | | | | | |
| 28Day | Citric acid cycle (TCA cycle) | 0.59653 | 0.75921 | 1 | suclg2 | 2701.34 | 2701.34 | 2701.34 | | 2701.34 | | DOWN | 0 | 1 |
| 28Day | Small interfering RNA (siRNA) biogenesis | 0.52712 | 1 | 1 | | | | | | | | | | |
| 28Day | SUMO is conjugated to E1 (UBA2:SAE1) | 0.80786 | 1 | 1 | | | | | | | | | | |
| 28Day | SUMO is transferred from E1 to E2 (UBE2I, UBC9) | 0.70071 | 1 | 1 | | | | | | | | | | |
| 28Day | Mitotic Telophase/Cytokinesis | 0.7508 | 0.63077 | 1 | rad21 | 4137.27 | 4137.27 | 4137.27 | | 4137.27 | | UP | 1 | 0 |
| 28Day | Dopamine Neurotransmitter Release Cycle | 0.5482 | 0.7912 | 1 | lin7c | 5328.95 | 5328.95 | 5328.95 | | 5328.95 | | DOWN | 0 | 1 |
| 28Day | Smooth Muscle Contraction | 0.6409 | 0.63815 | 1 | cald1;mylk | 4008.765 | 4008.765 | 2735.83 | 1800.20194 | 3689.60129 | 1742.69793 | UP | 1 | 0 |
| 28Day | Hedgehog ligand biogenesis | 0.69847 | 0.6798 | 1 | p4hb | 5730.92 | 5730.92 | 5730.92 | | 5730.92 | | DOWN | 0 | 1 |
| 28Day | Signalling to ERKs | 0.52488 | 0.80557 | 1 | mapkapk2 | 5375 | 5375 | 5375 | | 5375 | | DOWN | 0 | 1 |
| 28Day | Insulin processing | 0.72461 | 0.65616 | 1 | exoc4 | 2439.57 | 2439.57 | 2439.57 | | 2439.57 | | UP | 1 | 0 |
| 28Day | Gastrin-CREB signalling pathway via PKC and MAPK | 0.6468 | 0.72232 | 1 | hbegf | 919.738 | 919.738 | 919.738 | | 919.738 | | UP | 1 | 0 |
| 28Day | Activation of RAS in B cells | 0.70071 | 1 | 1 | | | | | | | | | | |
| 28Day | Transport of organic anions | 0.72461 | 0.65616 | 1 | slco2b1 | 2439.34 | 2439.34 | 2439.34 | | 2439.34 | | DOWN | 0 | 1 |
| 28Day | Calcitonin-like ligand receptors | 0.4909 | 1 | 1 | | | | | | | | | | |
| 28Day | Glycogen metabolism | 0.48011 | 0.83141 | 1 | gaa | 3036.96 | 3036.96 | 3036.96 | | 3036.96 | | DOWN | 0 | 1 |
| 28Day | SUMOylation of SUMOylation proteins | 0.65259 | 1 | 1 | | | | | | | | | | |
| 28Day | Negative regulation of FGFR3 signaling | 0.4587 | 0.84301 | 1 | fgf1 | 1467.57 | 1467.57 | 1467.57 | | 1467.57 | | DOWN | 0 | 1 |
| 28Day | Negative regulation of FGFR4 signaling | 0.41791 | 0.86388 | 1 | fgf1 | 1467.57 | 1467.57 | 1467.57 | | 1467.57 | | DOWN | 0 | 1 |
| 28Day | Nuclear Pore Complex (NPC) Disassembly | 0.62174 | 0.65548 | 1 | nek6;tpr | 3421.14 | 3421.14 | 3203.61 | 307.633876 | 3334.60261 | 282.243091 | UP | 1 | 0 |
| 28Day | Anchoring fibril formation | 0.72461 | 0.65616 | 1 | bmp1 | 1023.63 | 1023.63 | 1023.63 | | 1023.63 | | UP | 1 | 0 |
| 28Day | GP1b-IX-V activation signalling | 0.42575 | 1 | 1 | | | | | | | | | | |
| 28Day | eNOS activation | 0.42575 | 1 | 1 | | | | | | | | | | |
| 28Day | Vitamins B6 activation to pyridoxal phosphate | 0.80786 | 1 | 1 | | | | | | | | | | |
| 28Day | PKA-mediated phosphorylation of CREB | 0.6468 | 0.72232 | 1 | adcy9 | 4220.6 | 4220.6 | 4220.6 | | 4220.6 | | DOWN | 0 | 1 |
| 28Day | Calmodulin induced events | 0.41791 | 0.86388 | 1 | adcy9 | 4220.6 | 4220.6 | 4220.6 | | 4220.6 | | DOWN | 0 | 1 |
| 28Day | CaM pathway | 0.41791 | 0.86388 | 1 | adcy9 | 4220.6 | 4220.6 | 4220.6 | | 4220.6 | | DOWN | 0 | 1 |
| 28Day | PKA activation | 0.6468 | 0.72232 | 1 | adcy9 | 4220.6 | 4220.6 | 4220.6 | | 4220.6 | | DOWN | 0 | 1 |
| 28Day | PKA activation in glucagon signalling | 0.69847 | 0.6798 | 1 | adcy9 | 4220.6 | 4220.6 | 4220.6 | | 4220.6 | | DOWN | 0 | 1 |
| 28Day | Regulation of cholesterol biosynthesis by SREBP (SREBF) | 0.70071 | 1 | 1 | | | | | | | | | | |
| 28Day | Norepinephrine Neurotransmitter Release Cycle | 0.69847 | 0.6798 | 1 | slc22a1 | 1681.65 | 1681.65 | 1681.65 | | 1681.65 | | DOWN | 0 | 1 |
| 28Day | Transcriptional activation of mitochondrial biogenesis | 0.56601 | 1 | 1 | | | | | | | | | | |
| 28Day | CaMK IV-mediated phosphorylation of CREB | 0.65259 | 1 | 1 | | | | | | | | | | |
| 28Day | CREB1 phosphorylation through the activation of CaMKII/CaMKK/CaMKIV cascasde | 0.65259 | 1 | 1 | | | | | | | | | | |
| 28Day | Activation of RAC1 downstream of NMDARs | 0.65259 | 1 | 1 | | | | | | | | | | |
| 28Day | Cholesterol biosynthesis | 0.48011 | 0.83141 | 1 | pmvk | 3381.92 | 3381.92 | 3381.92 | | 3381.92 | | DOWN | 0 | 1 |
| 28Day | Negative regulation of activity of TFAP2 (AP-2) family transcription factors | 0.52712 | 1 | 1 | | | | | | | | | | |

BMD analysis results for functional classification based on dose-responsive genes, using the Reactome database for gene sets in BMDExpress2.2 software.

| Study Day | Gene Set Name | Fisher's Exact Left P-Value | Fisher's Exact Right P-Value | Fisher's Exact Two Tail | Gene Symbols | BMD Mean | BMD Median | BMD Minimum | BMD Standard Deviation | BMD wMean | BMD wSD | Overall Direction | Percent Genes With Overall Direction Up | Percent Genes With Overall Direction Down |
|---|---|---|---|---|---|---|---|---|---|---|---|---|---|---|
| 28Day | Zinc influx into cells by the SLC39 gene family | 0.56601 | 1 | 1 | | | | | | | | | | |
| 28Day | Processive synthesis on the C-strand of the telomere | 0.52712 | 1 | 1 | | | | | | | | | | |
| 28Day | Removal of the Flap Intermediate from the C-strand | 0.52712 | 1 | 1 | | | | | | | | | | |
| 28Day | Organic cation/anion/zwitterion transport | 0.69847 | 0.6798 | 1 | slc22a1 | 1681.65 | 1681.65 | 1681.65 | | 1681.65 | | DOWN | 0 | 1 |
| 28Day | GABA synthesis, release, reuptake and degradation | 0.6725 | 0.70182 | 1 | slc6a13 | 151.142 | 151.142 | 151.142 | | 151.142 | | DOWN | 0 | 1 |
| 28Day | PI-3K cascade:FGFR3 | 0.6468 | 0.72232 | 1 | fgf1 | 1467.57 | 1467.57 | 1467.57 | | 1467.57 | | DOWN | 0 | 1 |
| 28Day | PI-3K cascade:FGFR4 | 0.59653 | 0.75921 | 1 | fgf1 | 1467.57 | 1467.57 | 1467.57 | | 1467.57 | | DOWN | 0 | 1 |
| 28Day | NRIF signals cell death from the nucleus | 0.7508 | 0.63077 | 1 | sqstm1 | 5683.98 | 5683.98 | 5683.98 | | 5683.98 | | UP | 1 | 0 |
| 28Day | CLEC7A/inflammasome pathway | 0.75238 | 1 | 1 | | | | | | | | | | |
| 28Day | Glycerophospholipid catabolism | 0.80786 | 1 | 1 | | | | | | | | | | |
| 28Day | Propionyl-CoA catabolism | 0.70071 | 1 | 1 | | | | | | | | | | |
| 28Day | Protein repair | 0.65259 | 1 | 1 | | | | | | | | | | |
| 28Day | Beta oxidation of palmitoyl-CoA to myristoyl-CoA | 0.93135 | 1 | 1 | | | | | | | | | | |
| 28Day | Beta oxidation of butanoyl-CoA to acetyl-CoA | 0.93135 | 1 | 1 | | | | | | | | | | |
| 28Day | Transcriptional Regulation by MECP2 | 0.70071 | 1 | 1 | | | | | | | | | | |
| 28Day | NGF processing | 0.75238 | 1 | 1 | | | | | | | | | | |
| 28Day | Expression and Processing of Neurotrophins | 0.75238 | 1 | 1 | | | | | | | | | | |
| 28Day | Regulation of IFNG signaling | 0.45717 | 1 | 1 | | | | | | | | | | |
| 28Day | Cam-PDE 1 activation | 0.65259 | 1 | 1 | | | | | | | | | | |
| 28Day | Long-term potentiation | 0.75238 | 1 | 1 | | | | | | | | | | |
| 28Day | Biosynthesis of protectins | 0.86741 | 1 | 1 | | | | | | | | | | |
| 28Day | Aromatic amines can be N-hydroxylated or N-dealkylated by CYP1A2 | 0.93135 | 1 | 1 | | | | | | | | | | |
| 28Day | Synthesis of dolichyl-phosphate mannose | 0.80786 | 1 | 1 | | | | | | | | | | |
| 28Day | Regulation of MECP2 expression and activity | 0.70071 | 1 | 1 | | | | | | | | | | |
| 28Day | FGFR4 ligand binding and activation | 0.7508 | 0.63077 | 1 | fgf1 | 1467.57 | 1467.57 | 1467.57 | | 1467.57 | | DOWN | 0 | 1 |
| 28Day | Phospholipase C-mediated cascade; FGFR4 | 0.72461 | 0.65616 | 1 | fgf1 | 1467.57 | 1467.57 | 1467.57 | | 1467.57 | | DOWN | 0 | 1 |
| 28Day | SHC-mediated cascade:FGFR3 | 0.6468 | 0.72232 | 1 | fgf1 | 1467.57 | 1467.57 | 1467.57 | | 1467.57 | | DOWN | 0 | 1 |
| 28Day | SHC-mediated cascade:FGFR4 | 0.59653 | 0.75921 | 1 | fgf1 | 1467.57 | 1467.57 | 1467.57 | | 1467.57 | | DOWN | 0 | 1 |
| 28Day | Platelet sensitization by LDL | 0.6725 | 0.70182 | 1 | apob | 939.205 | 939.205 | 939.205 | | 939.205 | | DOWN | 0 | 1 |
| 28Day | Assembly of the ORC complex at the origin of replication | 0.65259 | 1 | 1 | | | | | | | | | | |
| 28Day | SDK interactions | 0.86741 | 1 | 1 | | | | | | | | | | |
| 90Day | Purine salvage | 0.64343 | 0.73175 | 1 | adk | 2663.49 | 2663.49 | 2663.49 | | 2663.49 | | DOWN | 0 | 1 |
| 90Day | Nucleotide salvage | 0.5728 | 0.70251 | 1 | tk1;adk | 3584.32 | 3584.32 | 2663.49 | 1302.25027 | 4057.93025 | 1116.80009 | DOWN | 0 | 1 |
| 90Day | Regulation of Insulin-like Growth Factor (IGF) transport and uptake by Insulin-like Growth Factor Binding Proteins (IGFBPs) | 0.53277 | 0.57618 | 1 | notum;spp2;apob;trf;tnc;serpina1e;mmp2;itih2;igfbp4;fn1;csf1;c3;apoe;ahsg;golm1 | 2295.16335 | 1866.49 | 82.4742 | 1865.07009 | 2483.87114 | 1863.40676 | DOWN | 0.133333333 | 0.866666667 |
| 90Day | Intrinsic Pathway for Apoptosis | 0.48111 | 0.73533 | 1 | ywhaz;bmf;bax | 1193.33933 | 1597.1 | 137.958 | 922.350781 | 1275.32396 | 881.071038 | UP | 0.666666667 | 0.333333333 |
| 90Day | Activation of BAD and translocation to mitochondria | 0.60115 | 0.76201 | 1 | ywhaz | 137.958 | 137.958 | 137.958 | | 137.958 | | UP | 1 | 0 |
| 90Day | Activation of BH3-only proteins | 0.63654 | 0.64822 | 1 | ywhaz;bmf | 867.529 | 867.529 | 137.958 | 1031.7692 | 957.421294 | 1023.90744 | CONFLICT | 0.5 | 0.5 |
| 90Day | Downregulation of ERBB2:ERBB3 signaling | 0.77469 | 0.61588 | 1 | nrg1 | 3912.34 | 3912.34 | 3912.34 | | 3912.34 | | UP | 1 | 0 |
| 90Day | G-protein beta:gamma signalling | 0.53165 | 0.69487 | 1 | arhgef6;gng11;cdc42 | 3654.54233 | 4854.24 | 156.487 | 3078.80769 | 3619.71528 | 3169.47674 | UP | 0.666666667 | 0.333333333 |
| 90Day | VEGFR2 mediated vascular permeability | 0.584 | 0.64989 | 1 | vav1;hsp90aa1;ctnnb1 | 2891.47 | 4087.04 | 426.32 | 2135.20321 | 2629.79926 | 2233.41338 | DOWN | 0.333333333 | 0.666666667 |

BMD analysis results for functional classification based on dose-responsive genes, using the Reactome database for gene sets in BMDExpress2.2 software.

| Study Day | Gene Set Name | Fisher's Exact Left P-Value | Fisher's Exact Right P-Value | Fisher's Exact Two Tail | Gene Symbols | BMD Mean | BMD Median | BMD Minimum | BMD Standard Deviation | BMD wMean | BMD wSD | Overall Direction | Percent Genes With Overall Direction Up | Percent Genes With Overall Direction Down |
|---|---|---|---|---|---|---|---|---|---|---|---|---|---|---|
| 90Day | Cyclin E associated events during G1/S transition | 0.60445 | 0.67629 | 1 | cables1;cdkn1a | 2492.81 | 2492.81 | 913.71 | 2233.18464 | 1416.85383 | 1634.54894 | CONFLICT | 0.5 | 0.5 |
| 90Day | Cyclin A:Cdk2-associated events at S phase entry | 0.5728 | 0.70251 | 1 | cables1;cdkn1a | 2492.81 | 2492.81 | 913.71 | 2233.18464 | 1416.85383 | 1634.54894 | CONFLICT | 0.5 | 0.5 |
| 90Day | Downregulation of ERBB2 signaling | 0.48204 | 0.77071 | 1 | nrg1;hsp90aa1 | 2169.33 | 2169.33 | 426.32 | 2464.98838 | 2502.38562 | 2419.56931 | UP | 1 | 0 |
| 90Day | Regulation of localization of FOXO transcription factors | 0.73069 | 0.6592 | 1 | ywhaz | 137.958 | 137.958 | 137.958 |  | 137.958 |  | UP | 1 | 0 |
| 90Day | Peroxisomal lipid metabolism | 0.61063 | 0.62569 | 1 | hacl1;slc27a2;slc25a17 | 3683.26 | 3419.78 | 2910.82 | 932.527616 | 3761.45897 | 916.721686 | DOWN | 0.333333333 | 0.666666667 |
| 90Day | Nonsense-Mediated Decay (NMD) | 0.56021 | 0.78886 | 1 | smg5 | 2531.67 | 2531.67 | 2531.67 |  | 2531.67 |  | UP | 1 | 0 |
| 90Day | Nonsense Mediated Decay (NMD) enhanced by the Exon Junction Complex (EJC) | 0.56021 | 0.78886 | 1 | smg5 | 2531.67 | 2531.67 | 2531.67 |  | 2531.67 |  | UP | 1 | 0 |
| 90Day | Cargo concentration in the ER | 0.59398 | 0.61242 | 1 | lman1;tgfa;serpina1e;areg | 3227.46225 | 3066.45 | 959.779 | 2124.07144 | 2615.34503 | 1585.21285 | CONFLICT | 0.5 | 0.5 |
| 90Day | Signaling by Nuclear Receptors | 0.54559 | 0.55191 | 1 | hist1h4h;ppid;rdh7;hist1h4i;hist1h3c;pdk4;adh4;nr5a2;aldh1a7;aldh8a1;pdk1;yy1;rxrg;rarg;rdh11;hsp90aa1;h2afx;ddx5;cbfb | 3422.01516 | 3563.02 | 174.249 | 1587.20613 | 3203.98005 | 1657.68063 | UP | 0.631578947 | 0.368421053 |
| 90Day | Role of ABL in ROBO-SLIT signaling | 0.61984 | 1 | 1 |  |  |  |  |  |  |  |  |  |  |
| 90Day | RUNX1 regulates transcription of genes involved in differentiation of HSCs | 0.60445 | 0.67629 | 1 | cdk7;cbfb | 3600.375 | 3600.375 | 3130.16 | 664.98443 | 3784.03771 | 612.160364 | UP | 1 | 0 |
| 90Day | Amino acid synthesis and interconversion (transamination) | 0.50611 | 0.71566 | 1 | serinc1;oat;glul | 3429.27667 | 2970.16 | 1556.81 | 2139.29899 | 3287.57914 | 2457.41055 | DOWN | 0.333333333 | 0.666666667 |
| 90Day | Mitochondrial calcium ion transport | 0.7013 | 0.58634 | 1 | afg3l2;micu2 | 3526.375 | 3526.375 | 1479.94 | 2894.09613 | 2753.64746 | 2679.8464 | UP | 1 | 0 |
| 90Day | Complement cascade | 0.51976 | 0.66058 | 1 | cpn2;c5ar2;vtn;crp;c3 | 1958.91334 | 639.57 | 45.5307 | 2312.16663 | 1418.61854 | 1923.42509 | DOWN | 0.2 | 0.8 |
| 90Day | Regulation of Complement cascade | 0.45854 | 0.72963 | 1 | cpn2;c5ar2;vtn;c3 | 1482.31668 | 433.493 | 45.5307 | 2369.3579 | 696.504019 | 1435.23764 | DOWN | 0.25 | 0.75 |
| 90Day | Mitophagy | 0.51148 | 0.74964 | 1 | tomm20;tomm70a | 3015.0435 | 3015.0435 | 786.107 | 3152.19223 | 2376.38885 | 3020.02588 | UP | 1 | 0 |
| 90Day | Pink/Parkin Mediated Mitophagy | 0.63654 | 0.64822 | 1 | tomm20;tomm70a | 3015.0435 | 3015.0435 | 786.107 | 3152.19223 | 2376.38885 | 3020.02588 | UP | 1 | 0 |
| 90Day | Pentose phosphate pathway | 0.4475 | 0.85258 | 1 | rpe | 54.2263 | 54.2263 | 54.2263 |  | 54.2263 |  | DOWN | 0 | 1 |
| 90Day | Resolution of D-Loop Structures | 0.48111 | 0.73533 | 1 | rad51;brca2;rad51c | 3127.57067 | 4249.95 | 513.022 | 2271.80208 | 3130.56464 | 2280.41 | UP | 1 | 0 |
| 90Day | Resolution of D-loop Structures through Holliday Junction Intermediates | 0.50611 | 0.71566 | 1 | rad51;brca2;rad51c | 3127.57067 | 4249.95 | 513.022 | 2271.80208 | 3130.56464 | 2280.41 | UP | 1 | 0 |
| 90Day | Regulation of ornithine decarboxylase (ODC) | 0.48796 | 1 | 1 |  |  |  |  |  |  |  |  |  |  |
| 90Day | Synthesis of PI | 0.54997 | 1 | 1 |  |  |  |  |  |  |  |  |  |  |
| 90Day | Lectin pathway of complement activation | 0.69859 | 1 | 1 |  |  |  |  |  |  |  |  |  |  |
| 90Day | Initial triggering of complement | 0.66889 | 0.61824 | 1 | crp;c3 | 2252.435 | 2252.435 | 639.57 | 2280.93556 | 1977.85009 | 2247.63726 | DOWN | 0 | 1 |
| 90Day | Creation of C4 and C2 activators | 0.60115 | 0.76201 | 1 | crp | 3865.3 | 3865.3 | 3865.3 |  | 3865.3 |  | DOWN | 0 | 1 |
| 90Day | N-glycan trimming in the ER and Calnexin/Calreticulin cycle | 0.54177 | 0.72694 | 1 | ngly1;rnf5 | 4475.645 | 4475.645 | 3718.83 | 1070.29804 | 4617.15875 | 1051.42075 | UP | 1 | 0 |
| 90Day | ER Quality Control Compartment (ERQC) | 0.60115 | 0.76201 | 1 | rnf5 | 3718.83 | 3718.83 | 3718.83 |  | 3718.83 |  | UP | 1 | 0 |
| 90Day | Calnexin/calreticulin cycle | 0.48325 | 0.83383 | 1 | rnf5 | 3718.83 | 3718.83 | 3718.83 |  | 3718.83 |  | UP | 1 | 0 |
| 90Day | VEGFR2 mediated cell proliferation | 0.56021 | 0.78886 | 1 | rasa1 | 2133.64 | 2133.64 | 2133.64 |  | 2133.64 |  | UP | 1 | 0 |
| 90Day | PTK6 Regulates RHO GTPases, RAS GTPase and MAP kinases | 0.52086 | 0.81269 | 1 | rasa1 | 2133.64 | 2133.64 | 2133.64 |  | 2133.64 |  | UP | 1 | 0 |
| 90Day | Interleukin-1 family signaling | 0.52991 | 0.62587 | 1 | irak3;tbk1;nfkbia;il1rap;ikbkg;il18bp;btrc | 2734.35957 | 3115.46 | 262.957 | 1630.24673 | 2470.42611 | 1941.7124 | DOWN | 0.142857143 | 0.857142857 |
| 90Day | Interleukin-1 signaling | 0.51976 | 0.66058 | 1 | irak3;nfkbia;il1rap;ikbkg;btrc | 2993.3334 | 3265.56 | 262.957 | 1778.81827 | 2754.88632 | 2105.90813 | DOWN | 0.2 | 0.8 |
| 90Day | Antigen activates B Cell Receptor (BCR) leading to generation of second messengers | 0.48204 | 0.77071 | 1 | vav1;sos1 | 5027.99 | 5027.99 | 4161.05 | 1226.03831 | 5362.02772 | 1131.37418 | DOWN | 0 | 1 |
| 90Day | PI3K Cascade | 0.45854 | 0.72963 | 1 | klb;irs2;gab1;fgf1 | 1073.49008 | 184.4285 | 74.8133 | 1852.5264 | 1155.9193 | 1943.48751 | DOWN | 0 | 1 |
| 90Day | IRS-mediated signalling | 0.62406 | 0.56268 | 1 | klb;irs2;sos1;gab1;fgf1 | 2037.77806 | 242.429 | 74.8133 | 2687.59133 | 2592.91452 | 2898.02513 | DOWN | 0 | 1 |
| 90Day | PI3K/AKT activation | 0.73069 | 0.6592 | 1 | irs2 | 74.8133 | 74.8133 | 74.8133 |  | 74.8133 |  | DOWN | 0 | 1 |
| 90Day | Tie2 Signaling | 0.66889 | 0.61824 | 1 | tek;sos1 | 3169.313 | 3169.313 | 443.696 | 3854.60453 | 4968.4106 | 2895.59523 | DOWN | 0 | 1 |
| 90Day | Signaling by Type 1 Insulin-like Growth Factor 1 Receptor (IGF1R) | 0.49942 | 0.67836 | 1 | klb;irs2;sos1;gab1;fgf1 | 2037.77806 | 242.429 | 74.8133 | 2687.59133 | 2592.91452 | 2898.02513 | DOWN | 0 | 1 |
| 90Day | IGF1R signaling cascade | 0.51976 | 0.66058 | 1 | klb;irs2;sos1;gab1;fgf1 | 2037.77806 | 242.429 | 74.8133 | 2687.59133 | 2592.91452 | 2898.02513 | DOWN | 0 | 1 |

BMD analysis results for functional classification based on dose-responsive genes, using the Reactome database for gene sets in BMDExpress2.2 software.

| Study Day | Gene Set Name | Fisher's Exact Left P-Value | Fisher's Exact Right P-Value | Fisher's Exact Two Tail | Gene Symbols | BMD Mean | BMD Median | BMD Minimum | BMD Standard Deviation | BMD wMean | BMD wSD | Overall Direction | Percent Genes With Overall Direction Up | Percent Genes With Overall Direction Down |
|---|---|---|---|---|---|---|---|---|---|---|---|---|---|---|
| 90Day | IRS-related events triggered by IGF1R | 0.54033 | 0.64218 | 1 | klb;irs2;sos1;gab1;fgf1 | 2037.77806 | 242.429 | 74.8133 | 2687.59133 | 2592.91452 | 2898.02513 | DOWN | 0 | 1 |
| 90Day | Insulin receptor signalling cascade | 0.47938 | 0.6955 | 1 | klb;irs2;sos1;gab1;fgf1 | 2037.77806 | 242.429 | 74.8133 | 2687.59133 | 2592.91452 | 2898.02513 | DOWN | 0 | 1 |
| 90Day | Netrin-1 signaling | 0.66427 | 0.57395 | 1 | mapk14;siah2;cdc42 | 1520.492 | 156.487 | 143.029 | 2374.19047 | 944.958876 | 1990.34255 | DOWN | 0.333333333 | 0.666666667 |
| 90Day | DSCAM interactions | 0.73069 | 0.6592 | 1 | mapk14 | 4261.96 | 4261.96 | 4261.96 |  | 4261.96 |  | DOWN | 0 | 1 |
| 90Day | MET receptor recycling | 0.68675 | 0.69764 | 1 | gab1 | 126.428 | 126.428 | 126.428 |  | 126.428 |  | DOWN | 0 | 1 |
| 90Day | LGI-ADAM interactions | 0.56021 | 0.78886 | 1 | stx1b | 328.2 | 328.2 | 328.2 |  | 328.2 |  | DOWN | 0 | 1 |
| 90Day | Synaptic adhesion-like molecules | 0.5728 | 0.70251 | 1 | gria3;ptprd | 2252.495 | 2252.495 | 1097.82 | 1632.95705 | 2230.33073 | 1632.65618 | CONFLICT | 0.5 | 0.5 |
| 90Day | Apoptotic factor-mediated response | 0.73069 | 0.6592 | 1 | bax | 1844.96 | 1844.96 | 1844.96 |  | 1844.96 |  | UP | 1 | 0 |
| 90Day | mRNA decay by 3' to 5' exoribonuclease | 0.4475 | 0.85258 | 1 | exosc9 | 2804.89 | 2804.89 | 2804.89 |  | 2804.89 |  | UP | 1 | 0 |
| 90Day | Butyrate Response Factor 1 (BRF1) binds and destabilizes mRNA | 0.4475 | 0.85258 | 1 | exosc9 | 2804.89 | 2804.89 | 2804.89 |  | 2804.89 |  | UP | 1 | 0 |
| 90Day | Digestion of dietary carbohydrate | 0.52086 | 0.81269 | 1 | mgam | 2596.25 | 2596.25 | 2596.25 |  | 2596.25 |  | DOWN | 0 | 1 |
| 90Day | Signal amplification | 0.53165 | 0.69487 | 1 | gng11;mapk14;gnai3 | 5006.42333 | 4854.24 | 4261.96 | 831.071798 | 4956.1591 | 771.687345 | UP | 0.666666667 | 0.333333333 |
| 90Day | Nucleotide-like (purinergic) receptors | 0.4475 | 0.85258 | 1 | adora1 | 1587.43 | 1587.43 | 1587.43 |  | 1587.43 |  | DOWN | 0 | 1 |
| 90Day | ADP signalling through P2Y purinoceptor 1 | 0.48204 | 0.77071 | 1 | gng11;mapk14 | 4558.1 | 4558.1 | 4261.96 | 418.805204 | 4602.80994 | 414.004639 | CONFLICT | 0.5 | 0.5 |
| 90Day | Synthesis of PS | 0.78732 | 1 | 1 |  |  |  |  |  |  |  |  |  |  |
| 90Day | YAP1- and WWTR1 (TAZ)-stimulated gene expression | 0.43294 | 1 | 1 |  |  |  |  |  |  |  |  |  |  |
| 90Day | Recycling of bile acids and salts | 0.63654 | 0.64822 | 1 | slc27a5;slc10a1 | 3047.255 | 3047.255 | 2758.21 | 408.771359 | 2997.14048 | 402.580545 | DOWN | 0 | 1 |
| 90Day | CLEC7A (Dectin-1) signaling | 0.58201 | 0.60356 | 1 | ube2m;cdc34;nfkbia;ikbkg;btrc | 2653.3084 | 3265.56 | 569.072 | 1985.29402 | 2657.76128 | 2167.87416 | UP | 0.6 | 0.4 |
| 90Day | Histidine, lysine, phenylalanine, tyrosine, proline and tryptophan catabolism | 0.62406 | 0.56268 | 1 | amdhd1;asrgl1;slc25a21;hpd;gstz1 | 2628.7694 | 3209.99 | 932.277 | 1194.08148 | 2495.47326 | 1167.59929 | DOWN | 0 | 1 |
| 90Day | Histidine catabolism | 0.77469 | 0.61588 | 1 | amdhd1 | 3887.79 | 3887.79 | 3887.79 |  | 3887.79 |  | DOWN | 0 | 1 |
| 90Day | Apoptosis induced DNA fragmentation | 0.60115 | 0.76201 | 1 | hmgb2 | 2367.76 | 2367.76 | 2367.76 |  | 2367.76 |  | UP | 1 | 0 |
| 90Day | Activation of DNA fragmentation factor | 0.60115 | 0.76201 | 1 | hmgb2 | 2367.76 | 2367.76 | 2367.76 |  | 2367.76 |  | UP | 1 | 0 |
| 90Day | FCERI mediated MAPK activation | 0.45354 | 0.79021 | 1 | vav1;sos1 | 5027.99 | 5027.99 | 4161.05 | 1226.03831 | 5362.02772 | 1131.37418 | DOWN | 0 | 1 |
| 90Day | SEMA3A-Plexin repulsion signaling by inhibiting Integrin adhesion | 0.68675 | 0.69764 | 1 | tln1 | 4478.93 | 4478.93 | 4478.93 |  | 4478.93 |  | DOWN | 0 | 1 |
| 90Day | Multifunctional anion exchangers | 0.77469 | 0.61588 | 1 | slc26a2 | 3962.48 | 3962.48 | 3962.48 |  | 3962.48 |  | DOWN | 0 | 1 |
| 90Day | Nuclear Receptor transcription pathway | 0.47938 | 0.6955 | 1 | nr5a2;esrrg;rxrg;rarg;ar | 1966.2334 | 1998.95 | 174.249 | 1868.5268 | 2021.14167 | 1818.34825 | DOWN | 0.2 | 0.8 |
| 90Day | Non-integrin membrane-ECM interactions | 0.57072 | 0.63396 | 1 | vtn;ttr;sdc4;fn1 | 1730.32918 | 1370.138 | 45.5307 | 1823.72195 | 1054.70846 | 1572.60387 | DOWN | 0.25 | 0.75 |
| 90Day | ECM proteoglycans | 0.47938 | 0.6955 | 1 | vtn;tnc;fn1;bgn;itga9 | 3388.13014 | 4436.62 | 45.5307 | 2297.14105 | 3504.64194 | 2580.55043 | DOWN | 0.2 | 0.8 |
| 90Day | Integrin alphaIIb beta3 signaling | 0.66427 | 0.57395 | 1 | tln1;sos1;fn1 | 4161.30667 | 4478.93 | 2110.06 | 1912.32154 | 4694.64696 | 1722.82421 | DOWN | 0 | 1 |
| 90Day | Integrin signaling | 0.66427 | 0.57395 | 1 | tln1;sos1;fn1 | 4161.30667 | 4478.93 | 2110.06 | 1912.32154 | 4694.64696 | 1722.82421 | DOWN | 0 | 1 |
| 90Day | Organic anion transporters | 0.68675 | 0.69764 | 1 | slc17a8 | 2572.47 | 2572.47 | 2572.47 |  | 2572.47 |  | UP | 1 | 0 |
| 90Day | Retrograde neurotrophin signalling | 0.64343 | 0.73175 | 1 | ap2m1 | 2983.55 | 2983.55 | 2983.55 |  | 2983.55 |  | UP | 1 | 0 |
| 90Day | Receptor-type tyrosine-protein phosphatases | 0.60445 | 0.67629 | 1 | ptprd;il1rap | 3045.76 | 3045.76 | 2684.35 | 511.110924 | 3054.7998 | 510.951015 | DOWN | 0 | 1 |
| 90Day | Carnitine synthesis | 0.61984 | 1 | 1 |  |  |  |  |  |  |  |  |  |  |
| 90Day | Neurotransmitter release cycle | 0.54033 | 0.64218 | 1 | lin7c;unc13b;slc22a1;slc1a2;slc6a12 | 2723.9178 | 3445.15 | 777.189 | 1704.97764 | 3301.41504 | 1207.79029 | DOWN | 0.4 | 0.6 |
| 90Day | Acetylcholine Neurotransmitter Release Cycle | 0.4475 | 0.85258 | 1 | unc13b | 4570.91 | 4570.91 | 4570.91 |  | 4570.91 |  | UP | 1 | 0 |
| 90Day | Peptide hormone biosynthesis | 0.64343 | 0.73175 | 1 | inhbc | 2508.36 | 2508.36 | 2508.36 |  | 2508.36 |  | DOWN | 0 | 1 |
| 90Day | Pyrimidine salvage | 0.68675 | 0.69764 | 1 | tk1 | 4505.15 | 4505.15 | 4505.15 |  | 4505.15 |  | DOWN | 0 | 1 |
| 90Day | FGFR1 ligand binding and activation | 0.48325 | 0.83383 | 1 | fgf1 | 242.429 | 242.429 | 242.429 |  | 242.429 |  | DOWN | 0 | 1 |
| 90Day | FGFR2b ligand binding and activation | 0.73069 | 0.6592 | 1 | fgf1 | 242.429 | 242.429 | 242.429 |  | 242.429 |  | DOWN | 0 | 1 |
| 90Day | Phospholipase C-mediated cascade: FGFR1 | 0.4475 | 0.85258 | 1 | fgf1 | 242.429 | 242.429 | 242.429 |  | 242.429 |  | DOWN | 0 | 1 |
| 90Day | Downstream signaling of activated FGFR1 | 0.53165 | 0.69487 | 1 | sos1;gab1;fgf1 | 2087.929 | 242.429 | 126.428 | 3297.46971 | 3907.43024 | 3338.39856 | DOWN | 0 | 1 |
| 90Day | SHC-mediated cascade:FGFR1 | 0.5728 | 0.70251 | 1 | sos1;fgf1 | 3068.6795 | 3068.6795 | 242.429 | 3996.92179 | 4960.29053 | 2969.67998 | DOWN | 0 | 1 |
| 90Day | PI-3K cascade:FGFR1 | 0.5728 | 0.70251 | 1 | gab1;fgf1 | 184.4285 | 184.4285 | 126.428 | 82.0250937 | 169.646309 | 79.3163895 | DOWN | 0 | 1 |
| 90Day | FRS-mediated FGFR1 signaling | 0.51148 | 0.74964 | 1 | sos1;fgf1 | 3068.6795 | 3068.6795 | 242.429 | 3996.92179 | 4960.29053 | 2969.67998 | DOWN | 0 | 1 |
| 90Day | PI-3K cascade:FGFR2 | 0.51148 | 0.74964 | 1 | gab1;fgf1 | 184.4285 | 184.4285 | 126.428 | 82.0250937 | 169.646309 | 79.3163895 | DOWN | 0 | 1 |

BMD analysis results for functional classification based on dose-responsive genes, using the Reactome database for gene sets in BMDExpress2.2 software.

| Study Day | Gene Set Name | Fisher's Exact Left P-Value | Fisher's Exact Right P-Value | Fisher's Exact Two Tail | Gene Symbols | BMD Mean | BMD Median | BMD Minimum | BMD Standard Deviation | BMD wMean | BMD wSD | Overall Direction | Percent Genes With Overall Direction Up | Percent Genes With Overall Direction Down |
|---|---|---|---|---|---|---|---|---|---|---|---|---|---|---|
| 90Day | Downstream signaling of activated FGFR2 | 0.55764 | 0.67295 | 1 | sos1;gab1;fgf1 | 2087.929 | 242.429 | 126.428 | 3297.46971 | 3907.43024 | 3338.39856 | DOWN | 0 | 1 |
| 90Day | SHC-mediated cascade:FGFR2 | 0.51148 | 0.74964 | 1 | sos1;fgf1 | 3068.6795 | 3068.6795 | 242.429 | 3996.92179 | 4960.29053 | 2969.67998 | DOWN | 0 | 1 |
| 90Day | FRS-mediated FGFR2 signaling | 0.45354 | 0.79021 | 1 | sos1;fgf1 | 3068.6795 | 3068.6795 | 242.429 | 3996.92179 | 4960.29053 | 2969.67998 | DOWN | 0 | 1 |
| 90Day | Fatty acyl-CoA biosynthesis | 0.61736 | 0.5901 | 1 | acsl4;scd1;acsl1;elovl3 | 3458.811 | 4133.87 | 587.994 | 1971.97849 | 3579.47816 | 1867.87989 | UP | 0.75 | 0.25 |
| 90Day | RHO GTPases activate KTN1 | 0.64343 | 0.73175 | 1 | cdc42 | 156.487 | 156.487 | 156.487 |  | 156.487 |  | UP | 1 | 0 |
| 90Day | ERBB2 Regulates Cell Motility | 0.48325 | 0.83383 | 1 | nrg1 | 3912.34 | 3912.34 | 3912.34 |  | 3912.34 |  | UP | 1 | 0 |
| 90Day | DNA Damage Recognition in GG-NER | 0.61736 | 0.5901 | 1 | mcrs1;yy1;ino80c;rad23a | 3516.8375 | 3761.895 | 1252.26 | 1879.48684 | 3649.65772 | 1980.59354 | CONFLICT | 0.5 | 0.5 |
| 90Day | Sodium-coupled sulphate, di- and tri-carboxylate transporters | 0.54997 | 1 | 1 |  |  |  |  |  |  |  |  |  |  |
| 90Day | Activation of the AP-1 family of transcription factors | 0.68675 | 0.69764 | 1 | mapk14 | 4261.96 | 4261.96 | 4261.96 |  | 4261.96 |  | DOWN | 0 | 1 |
| 90Day | Lysosphingolipid and LPA receptors | 0.52086 | 0.81269 | 1 | lpar3 | 5175 | 5175 | 5175 |  | 5175 |  | UP | 1 | 0 |
| 90Day | Downstream signaling events of B Cell Receptor (BCR) | 0.48111 | 0.73533 | 1 | nfkbia;ikbkg;btrc | 4006.45333 | 3601.1 | 3265.56 | 1006.7561 | 4283.92049 | 1129.74967 | DOWN | 0.333333333 | 0.666666667 |
| 90Day | WNT5A-dependent internalization of FZD4 | 0.48325 | 0.83383 | 1 | ap2m1 | 2983.55 | 2983.55 | 2983.55 |  | 2983.55 |  | UP | 1 | 0 |
| 90Day | IL-6-type cytokine receptor ligand interactions | 0.60445 | 0.67629 | 1 | lifr;crlf1 | 3403.375 | 3403.375 | 3200.93 | 286.300465 | 3314.11858 | 256.971864 | CONFLICT | 0.5 | 0.5 |
| 90Day | Interleukin-27 signaling | 0.64343 | 0.73175 | 1 | crlf1 | 3200.93 | 3200.93 | 3200.93 |  | 3200.93 |  | UP | 1 | 0 |
| 90Day | Adenylate cyclase inhibitory pathway | 0.52086 | 0.81269 | 1 | gnai3 | 5903.07 | 5903.07 | 5903.07 |  | 5903.07 |  | UP | 1 | 0 |
| 90Day | ADP signalling through P2Y purinoceptor 12 | 0.5728 | 0.70251 | 1 | gng11;gnai3 | 5378.655 | 5378.655 | 4854.24 | 741.634805 | 5266.80756 | 724.570551 | UP | 1 | 0 |
| 90Day | Inhibition of adenylate cyclase pathway | 0.52086 | 0.81269 | 1 | gnai3 | 5903.07 | 5903.07 | 5903.07 |  | 5903.07 |  | UP | 1 | 0 |
| 90Day | ERBB2 Activates PTK6 Signaling | 0.56021 | 0.78886 | 1 | nrg1 | 3912.34 | 3912.34 | 3912.34 |  | 3912.34 |  | UP | 1 | 0 |
| 90Day | Inflammasomes | 0.48325 | 0.83383 | 1 | txn1 | 5143.54 | 5143.54 | 5143.54 |  | 5143.54 |  | DOWN | 0 | 1 |
| 90Day | The NLRP1 inflammasome | 0.61984 | 1 | 1 |  |  |  |  |  |  |  |  |  |  |
| 90Day | SUMO is proteolytically processed | 0.48796 | 1 | 1 |  |  |  |  |  |  |  |  |  |  |
| 90Day | Processing and activation of SUMO | 0.68675 | 0.69764 | 1 | sae1 | 3998.58 | 3998.58 | 3998.58 |  | 3998.58 |  | UP | 1 | 0 |
| 90Day | Molybdenum cofactor biosynthesis | 0.48796 | 1 | 1 |  |  |  |  |  |  |  |  |  |  |
| 90Day | POLB-Dependent Long Patch Base Excision Repair | 0.43294 | 1 | 1 |  |  |  |  |  |  |  |  |  |  |
| 90Day | Phosphorylation of CD3 and TCR zeta chains | 0.48325 | 0.83383 | 1 | h2-aa | 3001.17 | 3001.17 | 3001.17 |  | 3001.17 |  | DOWN | 0 | 1 |
| 90Day | Oncogene Induced Senescence | 0.56021 | 0.78886 | 1 | mdm2 | 3535.08 | 3535.08 | 3535.08 |  | 3535.08 |  | UP | 1 | 0 |
| 90Day | RUNX1 interacts with co-factors whose precise effect on RUNX1 targets is not known | 0.64078 | 0.56705 | 1 | smarcd2;cbx6;smarcb1;cbfb | 3636.44975 | 4020.575 | 744.949 | 2095.15915 | 3779.92877 | 2174.25311 | UP | 0.75 | 0.25 |
| 90Day | Translesion synthesis by POLK | 0.48325 | 0.83383 | 1 | polk | 3652.71 | 3652.71 | 3652.71 |  | 3652.71 |  | UP | 1 | 0 |
| 90Day | Gap-filling DNA repair synthesis and ligation in GG-NER | 0.60445 | 0.67629 | 1 | pole4;polk | 4753.255 | 4753.255 | 3652.71 | 1556.40567 | 3884.77714 | 955.97646 | CONFLICT | 0.5 | 0.5 |
| 90Day | TP53 regulates transcription of additional cell cycle genes whose exact role in the p53 pathway remain uncertain | 0.7013 | 0.58634 | 1 | plk2;btg2 | 3008.67 | 3008.67 | 2041.26 | 1368.12434 | 2563.00625 | 1214.30303 | UP | 1 | 0 |
| 90Day | Gamma-carboxylation of protein precursors | 0.64343 | 0.73175 | 1 | f7 | 3350.52 | 3350.52 | 3350.52 |  | 3350.52 |  | DOWN | 0 | 1 |
| 90Day | Transport of gamma-carboxylated protein precursors from the endoplasmic reticulum to the Golgi apparatus | 0.64343 | 0.73175 | 1 | f7 | 3350.52 | 3350.52 | 3350.52 |  | 3350.52 |  | DOWN | 0 | 1 |
| 90Day | Removal of aminoterminal propeptides from gamma-carboxylated proteins | 0.60115 | 0.76201 | 1 | f7 | 3350.52 | 3350.52 | 3350.52 |  | 3350.52 |  | DOWN | 0 | 1 |
| 90Day | Gamma-carboxylation, transport, and amino-terminal cleavage of proteins | 0.56021 | 0.78886 | 1 | f7 | 3350.52 | 3350.52 | 3350.52 |  | 3350.52 |  | DOWN | 0 | 1 |
| 90Day | Synthesis of Leukotrienes (LT) and Eoxins (EX) | 0.63743 | 0.60037 | 1 | cyp4f16;cyp4a12a;cyp4a12b | 3624.98 | 3568.65 | 3465.22 | 194.153566 | 3583.99801 | 170.385902 | UP | 1 | 0 |
| 90Day | PI3K events in ERBB4 signaling | 0.68675 | 0.69764 | 1 | nrg1 | 3912.34 | 3912.34 | 3912.34 |  | 3912.34 |  | UP | 1 | 0 |
| 90Day | Unfolded Protein Response (UPR) | 0.66889 | 0.61824 | 1 | crebrf;mbtps2 | 3657.4 | 3657.4 | 3467.51 | 268.545013 | 3577.10508 | 243.355453 | UP | 1 | 0 |

BMD analysis results for functional classification based on dose-responsive genes, using the Reactome database for gene sets in BMDExpress2.2 software.

| Study Day | Gene Set Name | Fisher's Exact Left P-Value | Fisher's Exact Right P-Value | Fisher's Exact Two Tail | Gene Symbols | BMD Mean | BMD Median | BMD Minimum | BMD Standard Deviation | BMD wMean | BMD wSD | Overall Direction | Percent Genes With Overall Direction Up | Percent Genes With Overall Direction Down |
|---|---|---|---|---|---|---|---|---|---|---|---|---|---|---|
| 90Day | Josephin domain DUBs | 0.73069 | 0.6592 | 1 | rad23a | 2713.02 | 2713.02 | 2713.02 |  | 2713.02 |  | DOWN | 0 | 1 |
| 90Day | G2/M DNA replication checkpoint | 0.61984 | 1 | 1 |  |  |  |  |  |  |  |  |  |  |
| 90Day | alpha-linolenic (omega3) and linoleic (omega6) acid metabolism | 0.73069 | 0.6592 | 1 | acsl1 | 4979.51 | 4979.51 | 4979.51 |  | 4979.51 |  | DOWN | 0 | 1 |
| 90Day | alpha-linolenic acid (ALA) metabolism | 0.77469 | 0.61588 | 1 | acsl1 | 4979.51 | 4979.51 | 4979.51 |  | 4979.51 |  | DOWN | 0 | 1 |
| 90Day | Beta-oxidation of pristanoyl-CoA | 0.43294 | 1 | 1 |  |  |  |  |  |  |  |  |  |  |
| 90Day | HDL clearance | 0.54997 | 1 | 1 |  |  |  |  |  |  |  |  |  |  |
| 90Day | VLDLR internalisation and degradation | 0.60115 | 0.76201 | 1 | ap2m1 | 2983.55 | 2983.55 | 2983.55 |  | 2983.55 |  | UP | 1 | 0 |
| 90Day | Tetrahydrobiopterin (BH4) synthesis, recycling, salvage and regulation | 0.64343 | 0.73175 | 1 | hsp90aa1 | 426.32 | 426.32 | 426.32 |  | 426.32 |  | UP | 1 | 0 |
| 90Day | Attenuation phase | 0.56021 | 0.78886 | 1 | hsp90aa1 | 426.32 | 426.32 | 426.32 |  | 426.32 |  | UP | 1 | 0 |
| 90Day | Electron transport from NADPH to Ferredoxin | 0.69859 | 1 | 1 |  |  |  |  |  |  |  |  |  |  |
| 90Day | Interleukin-9 signaling | 0.73069 | 0.6592 | 1 | il9r | 5362.87 | 5362.87 | 5362.87 |  | 5362.87 |  | UP | 1 | 0 |
| 90Day | WNT5A-dependent internalization of FZD2, FZD5 and ROR2 | 0.60115 | 0.76201 | 1 | ap2m1 | 2983.55 | 2983.55 | 2983.55 |  | 2983.55 |  | UP | 1 | 0 |
| 90Day | Adrenoceptors | 0.73069 | 0.6592 | 1 | adra1b | 2444.64 | 2444.64 | 2444.64 |  | 2444.64 |  | DOWN | 0 | 1 |
| 90Day | JNK (c-Jun kinases) phosphorylation and activation mediated by activated human TAK1 | 0.54997 | 1 | 1 |  |  |  |  |  |  |  |  |  |  |
| 90Day | Post-transcriptional silencing by small RNAs | 0.43294 | 1 | 1 |  |  |  |  |  |  |  |  |  |  |
| 90Day | MET activates RAP1 and RAC1 | 0.68675 | 0.69764 | 1 | gab1 | 126.428 | 126.428 | 126.428 |  | 126.428 |  | DOWN | 0 | 1 |
| 90Day | Na+/Cl- dependent neurotransmitter transporters | 0.60445 | 0.67629 | 1 | slc22a1;slc6a12 | 2247.86 | 2247.86 | 1050.57 | 1693.22376 | 3017.91745 | 1296.54531 | DOWN | 0 | 1 |
| 90Day | GABA A receptor activation | 0.56021 | 0.78886 | 1 | gabrb3 | 4201.91 | 4201.91 | 4201.91 |  | 4201.91 |  | DOWN | 0 | 1 |
| 90Day | Transcriptional regulation by RUNX3 | 0.61736 | 0.5901 | 1 | mdm2;brd2;cbfb;ctnnb1 | 4263.645 | 4078.815 | 3535.08 | 775.750103 | 3966.25751 | 640.611894 | UP | 0.75 | 0.25 |
| 90Day | Formation of ATP by chemiosmotic coupling | 0.52086 | 0.81269 | 1 | atp5k | 135.802 | 135.802 | 135.802 |  | 135.802 |  | DOWN | 0 | 1 |
| 90Day | Cristae formation | 0.52086 | 0.81269 | 1 | atp5k | 135.802 | 135.802 | 135.802 |  | 135.802 |  | DOWN | 0 | 1 |
| 90Day | SCF(Skp2)-mediated degradation of p27/p21 | 0.4475 | 0.85258 | 1 | cdkn1a | 913.71 | 913.71 | 913.71 |  | 913.71 |  | UP | 1 | 0 |
| 90Day | TP53 Regulates Transcription of Genes Involved in G1 Cell Cycle Arrest | 0.73069 | 0.6592 | 1 | cdkn1a | 913.71 | 913.71 | 913.71 |  | 913.71 |  | UP | 1 | 0 |
| 90Day | G1/S DNA Damage Checkpoints | 0.63654 | 0.64822 | 1 | mdm2;cdkn1a | 2224.395 | 2224.395 | 913.71 | 1853.5885 | 2056.00777 | 1838.2279 | UP | 1 | 0 |
| 90Day | Lysine catabolism | 0.60115 | 0.76201 | 1 | slc25a21 | 3224.71 | 3224.71 | 3224.71 |  | 3224.71 |  | DOWN | 0 | 1 |
| 90Day | Glutamate Neurotransmitter Release Cycle | 0.51148 | 0.74964 | 1 | unc13b;slc1a2 | 2674.0495 | 2674.0495 | 777.189 | 2682.56585 | 3235.52021 | 2562.35454 | CONFLICT | 0.5 | 0.5 |
| 90Day | Regulation of KIT signaling | 0.52086 | 0.81269 | 1 | sos1 | 5894.93 | 5894.93 | 5894.93 |  | 5894.93 |  | DOWN | 0 | 1 |
| 90Day | Proline catabolism | 0.69859 | 1 | 1 |  |  |  |  |  |  |  |  |  |  |
| 90Day | Caspase activation via Death Receptors in the presence of ligand | 0.48325 | 0.83383 | 1 | tnfrsf10b | 3826.99 | 3826.99 | 3826.99 |  | 3826.99 |  | UP | 1 | 0 |
| 90Day | ChREBP activates metabolic gene expression | 0.43294 | 1 | 1 |  |  |  |  |  |  |  |  |  |  |
| 90Day | Vitamin B5 (pantothenate) metabolism | 0.56021 | 0.78886 | 1 | pank1 | 2679.72 | 2679.72 | 2679.72 |  | 2679.72 |  | DOWN | 0 | 1 |
| 90Day | Phosphorylation of the APC/C | 0.4475 | 0.85258 | 1 | anapc10 | 4390.47 | 4390.47 | 4390.47 |  | 4390.47 |  | UP | 1 | 0 |
| 90Day | Dissolution of Fibrin Clot | 0.7013 | 0.58634 | 1 | plg;plaur | 1145.545 | 1145.545 | 668.86 | 674.134392 | 1394.68147 | 574.734041 | DOWN | 0 | 1 |
| 90Day | TP53 Regulates Transcription of Genes Involved in Cytochrome C Release | 0.48796 | 1 | 1 |  |  |  |  |  |  |  |  |  |  |
| 90Day | Vitamin C (ascorbate) metabolism | 0.77469 | 0.61588 | 1 | slc23a2 | 338.932 | 338.932 | 338.932 |  | 338.932 |  | DOWN | 0 | 1 |
| 90Day | Stabilization of p53 | 0.77469 | 0.61588 | 1 | mdm2 | 3535.08 | 3535.08 | 3535.08 |  | 3535.08 |  | UP | 1 | 0 |
| 90Day | Gap junction degradation | 0.64343 | 0.73175 | 1 | ap2m1 | 2983.55 | 2983.55 | 2983.55 |  | 2983.55 |  | UP | 1 | 0 |
| 90Day | Formation of annular gap junctions | 0.68675 | 0.69764 | 1 | ap2m1 | 2983.55 | 2983.55 | 2983.55 |  | 2983.55 |  | UP | 1 | 0 |
| 90Day | FRS-mediated FGFR3 signaling | 0.60445 | 0.67629 | 1 | sos1;fgf1 | 3068.6795 | 3068.6795 | 242.429 | 3996.92179 | 4960.29053 | 2969.67998 | DOWN | 0 | 1 |
| 90Day | Signaling by FGFR4 | 0.57072 | 0.63396 | 1 | klb;sos1;gab1;fgf1 | 2528.51925 | 2046.3595 | 126.428 | 2832.90488 | 3890.50542 | 2640.67822 | DOWN | 0 | 1 |
| 90Day | Triglyceride metabolism | 0.51148 | 0.74964 | 1 | dgat2;agmo | 3065.025 | 3065.025 | 2903.14 | 228.939963 | 3009.70495 | 215.157829 | DOWN | 0 | 1 |
| 90Day | Pyruvate metabolism | 0.61063 | 0.62569 | 1 | pdk4;pdk1;gstz1 | 4115.21 | 3345.98 | 3209.99 | 1451.70948 | 3914.67407 | 1357.04203 | DOWN | 0.333333333 | 0.666666667 |
| 90Day | Pyruvate metabolism and Citric Acid (TCA) cycle | 0.47938 | 0.6955 | 1 | sdha;pdk4;pdk1;suclg2;gstz1 | 3556.456 | 3209.99 | 2609.96 | 1282.57086 | 3264.47055 | 1059.70182 | DOWN | 0.2 | 0.8 |

BMD analysis results for functional classification based on dose-responsive genes, using the Reactome database for gene sets in BMDExpress2.2 software.

| Study Day | Gene Set Name | Fisher's Exact Left P-Value | Fisher's Exact Right P-Value | Fisher's Exact Two Tail | Gene Symbols | BMD Mean | BMD Median | BMD Minimum | BMD Standard Deviation | BMD wMean | BMD wSD | Overall Direction | Percent Genes With Overall Direction Up | Percent Genes With Overall Direction Down |
|---|---|---|---|---|---|---|---|---|---|---|---|---|---|---|
| 90Day | Transport of nucleosides and free purine and pyrimidine bases across the plasma membrane | 0.77469 | 0.61588 | 1 | slc29a1 | 1131.79 | 1131.79 | 1131.79 |  | 1131.79 |  | DOWN | 0 | 1 |
| 90Day | Serine biosynthesis | 0.73069 | 0.6592 | 1 | serinc1 | 2970.16 | 2970.16 | 2970.16 |  | 2970.16 |  | UP | 1 | 0 |
| 90Day | The NLRP3 inflammasome | 0.68675 | 0.69764 | 1 | txn1 | 5143.54 | 5143.54 | 5143.54 |  | 5143.54 |  | DOWN | 0 | 1 |
| 90Day | Termination of O-glycan biosynthesis | 0.4475 | 0.85258 | 1 | st3gal3 | 5224.26 | 5224.26 | 5224.26 |  | 5224.26 |  | DOWN | 0 | 1 |
| 90Day | Glycoprotein hormones | 0.73069 | 0.6592 | 1 | inhbc | 2508.36 | 2508.36 | 2508.36 |  | 2508.36 |  | DOWN | 0 | 1 |
| 90Day | Establishment of Sister Chromatid Cohesion | 0.64343 | 0.73175 | 1 | esco2 | 3568.8 | 3568.8 | 3568.8 |  | 3568.8 |  | UP | 1 | 0 |
| 90Day | Activation of the pre-replicative complex | 0.50611 | 0.71566 | 1 | pole4;orc6;dbf4 | 4330.28 | 4168.34 | 2968.7 | 1449.35121 | 3793.77257 | 1067.30893 | UP | 0.666666667 | 0.333333333 |
| 90Day | Synthesis of PIPs at the Golgi membrane | 0.52086 | 0.81269 | 1 | pi4ka | 3636.02 | 3636.02 | 3636.02 |  | 3636.02 |  | DOWN | 0 | 1 |
| 90Day | DCC mediated attractive signaling | 0.64343 | 0.73175 | 1 | cdc42 | 156.487 | 156.487 | 156.487 |  | 156.487 |  | UP | 1 | 0 |
| 90Day | Classical antibody-mediated complement activation | 0.73069 | 0.6592 | 1 | crp | 3865.3 | 3865.3 | 3865.3 |  | 3865.3 |  | DOWN | 0 | 1 |
| 90Day | FCGR activation | 0.52086 | 0.81269 | 1 | fcgr2b | 3055.31 | 3055.31 | 3055.31 |  | 3055.31 |  | DOWN | 0 | 1 |
| 90Day | Interleukin-10 signaling | 0.48796 | 1 | 1 |  |  |  |  |  |  |  |  |  |  |
| 90Day | Interferon alpha/beta signaling | 0.584 | 0.64989 | 1 | usp18;abce1;ifnar1 | 2450.37233 | 3026.26 | 250.557 | 1975.8511 | 2122.02408 | 2095.71228 | UP | 0.666666667 | 0.333333333 |
| 90Day | Regulation of IFNA signaling | 0.48204 | 0.77071 | 1 | usp18;ifnar1 | 2162.4285 | 2162.4285 | 250.557 | 2703.7946 | 1821.52235 | 2660.46448 | CONFLICT | 0.5 | 0.5 |
| 90Day | Glucuronidation | 0.48204 | 0.77071 | 1 | ugt2b35;ugdh | 497.0045 | 497.0045 | 444.891 | 73.6996185 | 491.891363 | 73.344021 | UP | 1 | 0 |
| 90Day | Signaling by NOTCH3 | 0.63654 | 0.64822 | 1 | psen2;dll1 | 2793.24 | 2793.24 | 2451.29 | 483.590328 | 2851.27329 | 476.575156 | DOWN | 0 | 1 |
| 90Day | SUMOylation of RNA binding proteins | 0.48796 | 1 | 1 |  |  |  |  |  |  |  |  |  |  |
| 90Day | Other interleukin signaling | 0.63654 | 0.64822 | 1 | stx3;csf1 | 4961.12 | 4961.12 | 4474.79 | 687.774482 | 4742.6821 | 614.49451 | DOWN | 0 | 1 |
| 90Day | p75NTR signals via NF-kB | 0.52086 | 0.81269 | 1 | nfkbia | 3601.1 | 3601.1 | 3601.1 |  | 3601.1 |  | DOWN | 0 | 1 |
| 90Day | Regulated proteolysis of p75NTR | 0.60115 | 0.76201 | 1 | psen2 | 3135.19 | 3135.19 | 3135.19 |  | 3135.19 |  | DOWN | 0 | 1 |
| 90Day | NF-kB is activated and signals survival | 0.64343 | 0.73175 | 1 | nfkbia | 3601.1 | 3601.1 | 3601.1 |  | 3601.1 |  | DOWN | 0 | 1 |
| 90Day | Citric acid cycle (TCA cycle) | 0.60445 | 0.67629 | 1 | sdha;suclg2 | 2718.325 | 2718.325 | 2609.96 | 153.251253 | 2737.61233 | 150.804323 | DOWN | 0 | 1 |
| 90Day | PI5P Regulates TP53 Acetylation | 0.68675 | 0.69764 | 1 | pin1 | 4947.7 | 4947.7 | 4947.7 |  | 4947.7 |  | UP | 1 | 0 |
| 90Day | Mitotic Telophase/Cytokinesis | 0.52086 | 0.81269 | 1 | nudc | 3184.54 | 3184.54 | 3184.54 |  | 3184.54 |  | UP | 1 | 0 |
| 90Day | Dermatan sulfate biosynthesis | 0.64343 | 0.73175 | 1 | bgn | 4533.35 | 4533.35 | 4533.35 |  | 4533.35 |  | DOWN | 0 | 1 |
| 90Day | COPI-independent Golgi-to-ER retrograde traffic | 0.5611 | 0.62317 | 1 | tubb6;dctn3;tubb4b;tubb2a;tuba1b | 1992.6502 | 1781.5 | 779.791 | 1072.82446 | 1774.95351 | 1190.4266 | UP | 0.8 | 0.2 |
| 90Day | Dopamine Neurotransmitter Release Cycle | 0.54177 | 0.72694 | 1 | lin7c;unc13b | 4173.34 | 4173.34 | 3775.77 | 562.248886 | 4004.12754 | 508.780988 | UP | 1 | 0 |
| 90Day | Sema3A PAK dependent Axon repulsion | 0.48325 | 0.83383 | 1 | hsp90aa1 | 426.32 | 426.32 | 426.32 |  | 426.32 |  | UP | 1 | 0 |
| 90Day | Hedgehog ligand biogenesis | 0.4475 | 0.85258 | 1 | notum | 4035.02 | 4035.02 | 4035.02 |  | 4035.02 |  | DOWN | 0 | 1 |
| 90Day | Beta oxidation of lauroyl-CoA to decanoyl-CoA-CoA | 0.69859 | 1 | 1 |  |  |  |  |  |  |  |  |  |  |
| 90Day | Frs2-mediated activation | 0.43294 | 1 | 1 |  |  |  |  |  |  |  |  |  |  |
| 90Day | Signalling to ERKs | 0.51148 | 0.74964 | 1 | mapk14;sos1 | 5078.445 | 5078.445 | 4261.96 | 1154.68416 | 5603.32821 | 884.472008 | DOWN | 0 | 1 |
| 90Day | Insulin processing | 0.48325 | 0.83383 | 1 | exoc4 | 2113.16 | 2113.16 | 2113.16 |  | 2113.16 |  | UP | 1 | 0 |
| 90Day | IRAK1 recruits IKK complex | 0.60115 | 0.76201 | 1 | ikbkg | 3265.56 | 3265.56 | 3265.56 |  | 3265.56 |  | UP | 1 | 0 |
| 90Day | TRAF6 mediated IRF7 activation in TLR7/8 or 9 signaling | 0.60115 | 0.76201 | 1 | irf7 | 5689.7 | 5689.7 | 5689.7 |  | 5689.7 |  | UP | 1 | 0 |
| 90Day | IRAK1 recruits IKK complex upon TLR7/8 or 9 stimulation | 0.60115 | 0.76201 | 1 | ikbkg | 3265.56 | 3265.56 | 3265.56 |  | 3265.56 |  | UP | 1 | 0 |
| 90Day | The retinoid cycle in cones (daylight vision) | 0.54997 | 1 | 1 |  |  |  |  |  |  |  |  |  |  |
| 90Day | Opsins | 0.77469 | 0.61588 | 1 | opn3 | 5797.17 | 5797.17 | 5797.17 |  | 5797.17 |  | UP | 1 | 0 |
| 90Day | Resolution of D-loop Structures through Synthesis-Dependent Strand Annealing (SDSA) | 0.66427 | 0.57395 | 1 | rad51;brca2;rad51c | 3127.57067 | 4249.95 | 513.022 | 2271.80208 | 3130.56464 | 2280.41 | UP | 1 | 0 |
| 90Day | Activation of RAS in B cells | 0.54997 | 1 | 1 |  |  |  |  |  |  |  |  |  |  |
| 90Day | Rap1 signalling | 0.52086 | 0.81269 | 1 | ywhaz | 137.958 | 137.958 | 137.958 |  | 137.958 |  | UP | 1 | 0 |
| 90Day | Transport of organic anions | 0.48325 | 0.83383 | 1 | slco2b1 | 1935.84 | 1935.84 | 1935.84 |  | 1935.84 |  | DOWN | 0 | 1 |
| 90Day | Urea cycle | 0.73069 | 0.6592 | 1 | arg2 | 4132.01 | 4132.01 | 4132.01 |  | 4132.01 |  | UP | 1 | 0 |
| 90Day | Protein methylation | 0.52086 | 0.81269 | 1 | etfbkmt | 3942.91 | 3942.91 | 3942.91 |  | 3942.91 |  | UP | 1 | 0 |
| 90Day | SCF-beta-TrCP mediated degradation of Emi1 | 0.77469 | 0.61588 | 1 | btrc | 5152.7 | 5152.7 | 5152.7 |  | 5152.7 |  | DOWN | 0 | 1 |

BMD analysis results for functional classification based on dose-responsive genes, using the Reactome database for gene sets in BMDExpress2.2 software.

| Study Day | Gene Set Name | Fisher's Exact Left P-Value | Fisher's Exact Right P-Value | Fisher's Exact Two Tail | Gene Symbols | BMD Mean | BMD Median | BMD Minimum | BMD Standard Deviation | BMD wMean | BMD wSD | Overall Direction | Percent Genes With Overall Direction Up | Percent Genes With Overall Direction Down |
|---|---|---|---|---|---|---|---|---|---|---|---|---|---|---|
| 90Day | Regulation of expression of SLITs and ROBOs | 0.48796 | 1 | 1 | | | | | | | | | | |
| 90Day | NOTCH3 Activation and Transmission of Signal to the Nucleus | 0.63654 | 0.64822 | 1 | psen2;dll1 | 2793.24 | 2793.24 | 2451.29 | 483.590328 | 2851.27329 | 476.575156 | DOWN | 0 | 1 |
| 90Day | TFAP2 (AP-2) family regulates transcription of cell cycle factors | 0.69859 | 1 | 1 | | | | | | | | | | |
| 90Day | p38MAPK events | 0.77469 | 0.61588 | 1 | mapk14 | 4261.96 | 4261.96 | 4261.96 | | 4261.96 | | DOWN | 0 | 1 |
| 90Day | Metabolism of ingested SeMet, Sec, MeSec into H2Se | 0.78732 | 1 | 1 | | | | | | | | | | |
| 90Day | Creatine metabolism | 0.68675 | 0.69764 | 1 | slc6a12 | 3445.15 | 3445.15 | 3445.15 | | 3445.15 | | DOWN | 0 | 1 |
| 90Day | Nuclear Pore Complex (NPC) Disassembly | 0.50611 | 0.71566 | 1 | nek6;nup153;sec13 | 3294.01 | 3442.78 | 2758.9 | 478.400366 | 3382.9906 | 363.640364 | UP | 1 | 0 |
| 90Day | Coenzyme A biosynthesis | 0.77469 | 0.61588 | 1 | pank1 | 2679.72 | 2679.72 | 2679.72 | | 2679.72 | | DOWN | 0 | 1 |
| 90Day | Anchoring fibril formation | 0.48325 | 0.83383 | 1 | bmp1 | 190.369 | 190.369 | 190.369 | | 190.369 | | DOWN | 0 | 1 |
| 90Day | GP1b-IX-V activation signalling | 0.60115 | 0.76201 | 1 | ywhaz | 137.958 | 137.958 | 137.958 | | 137.958 | | UP | 1 | 0 |
| 90Day | PD-1 signaling | 0.4475 | 0.85258 | 1 | h2-aa | 3001.17 | 3001.17 | 3001.17 | | 3001.17 | | DOWN | 0 | 1 |
| 90Day | Metabolism of nitric oxide | 0.4475 | 0.85258 | 1 | hsp90aa1 | 426.32 | 426.32 | 426.32 | | 426.32 | | UP | 1 | 0 |
| 90Day | eNOS activation | 0.60115 | 0.76201 | 1 | hsp90aa1 | 426.32 | 426.32 | 426.32 | | 426.32 | | UP | 1 | 0 |
| 90Day | eNOS activation and regulation | 0.4475 | 0.85258 | 1 | hsp90aa1 | 426.32 | 426.32 | 426.32 | | 426.32 | | UP | 1 | 0 |
| 90Day | Glyoxylate metabolism and glycine degradation | 0.584 | 0.64989 | 1 | ndufab1;hoga1;agxt | 2143.492 | 3027.04 | 105.476 | 1770.16421 | 2350.01449 | 1669.89196 | DOWN | 0.333333333 | 0.666666667 |
| 90Day | TNFR1-mediated ceramide production | 0.48796 | 1 | 1 | | | | | | | | | | |
| 90Day | Regulation of gene expression by Hypoxia-inducible Factor | 0.43294 | 1 | 1 | | | | | | | | | | |
| 90Day | Translocation of SLC2A4 (GLUT4) to the plasma membrane | 0.73069 | 0.6592 | 1 | ywhaz | 137.958 | 137.958 | 137.958 | | 137.958 | | UP | 1 | 0 |
| 90Day | TP53 regulates transcription of several additional cell death genes whose specific roles in p53-dependent apoptosis remain uncertain | 0.69859 | 1 | 1 | | | | | | | | | | |
| 90Day | Nuclear signaling by ERBB4 | 0.48796 | 1 | 1 | | | | | | | | | | |
| 90Day | RUNX3 regulates YAP1-mediated transcription | 0.61984 | 1 | 1 | | | | | | | | | | |
| 90Day | Synthesis of bile acids and bile salts via 27-hydroxycholesterol | 0.48796 | 1 | 1 | | | | | | | | | | |
| 90Day | Mismatch repair (MMR) directed by MSH2:MSH3 (MutSbeta) | 0.48796 | 1 | 1 | | | | | | | | | | |
| 90Day | Aryl hydrocarbon receptor signalling | 0.43294 | 1 | 1 | | | | | | | | | | |
| 90Day | Phosphorylation of Emi1 | 0.54997 | 1 | 1 | | | | | | | | | | |
| 90Day | AMPK inhibits chREBP transcriptional activation activity | 0.48796 | 1 | 1 | | | | | | | | | | |
| 90Day | RHO GTPases Activate NADPH Oxidases | 0.63654 | 0.64822 | 1 | mapk14;pin1 | 4604.83 | 4604.83 | 4261.96 | 484.891404 | 4787.23244 | 410.582968 | CONFLICT | 0.5 | 0.5 |
| 90Day | Organic cation/anion/zwitterion transport | 0.4475 | 0.85258 | 1 | slc22a1 | 1050.57 | 1050.57 | 1050.57 | | 1050.57 | | DOWN | 0 | 1 |
| 90Day | PI-3K cascade:FGFR3 | 0.66889 | 0.61824 | 1 | gab1;fgf1 | 184.4285 | 184.4285 | 126.428 | 82.0250937 | 169.646309 | 79.3163895 | DOWN | 0 | 1 |
| 90Day | NRIF signals cell death from the nucleus | 0.52086 | 0.81269 | 1 | psen2 | 3135.19 | 3135.19 | 3135.19 | | 3135.19 | | DOWN | 0 | 1 |
| 90Day | Telomere Extension By Telomerase | 0.78732 | 1 | 1 | | | | | | | | | | |
| 90Day | Chk1/Chk2(Cds1) mediated inactivation of Cyclin B:Cdk1 complex | 0.64343 | 0.73175 | 1 | ywhaz | 137.958 | 137.958 | 137.958 | | 137.958 | | UP | 1 | 0 |
| 90Day | ARMS-mediated activation | 0.54997 | 1 | 1 | | | | | | | | | | |
| 90Day | CREB phosphorylation | 0.43294 | 1 | 1 | | | | | | | | | | |
| 90Day | Beta oxidation of butanoyl-CoA to acetyl-CoA | 0.88732 | 1 | 1 | | | | | | | | | | |
| 90Day | Elevation of cytosolic Ca2+ levels | 0.56021 | 0.78886 | 1 | p2rx4 | 185.907 | 185.907 | 185.907 | | 185.907 | | DOWN | 0 | 1 |
| 90Day | Neurotransmitter clearance | 0.43294 | 1 | 1 | | | | | | | | | | |
| 90Day | Advanced glycosylation endproduct receptor signaling | 0.61984 | 1 | 1 | | | | | | | | | | |
| 90Day | PTK6 Regulates RTKs and Their Effectors AKT1 and DOK1 | 0.43294 | 1 | 1 | | | | | | | | | | |

BMD analysis results for functional classification based on dose-responsive genes, using the Reactome database for gene sets in BMDExpress2.2 software.

| Study Day | Gene Set Name | Fisher's Exact Left P-Value | Fisher's Exact Right P-Value | Fisher's Exact Two Tail | Gene Symbols | BMD Mean | BMD Median | BMD Minimum | BMD Standard Deviation | BMD wMean | BMD wSD | Overall Direction | Percent Genes With Overall Direction Up | Percent Genes With Overall Direction Down |
|---|---|---|---|---|---|---|---|---|---|---|---|---|---|---|
| 90Day | Neurofascin interactions | 0.61984 | 1 | 1 | | | | | | | | | | |
| 90Day | Regulation of IFNG signaling | 0.64343 | 0.73175 | 1 | ifngr2 | 4021.95 | 4021.95 | 4021.95 | | 4021.95 | | DOWN | 0 | 1 |
| 90Day | Synthesis of Ketone Bodies | 0.43294 | 1 | 1 | | | | | | | | | | |
| 90Day | Regulation by c-FLIP | 0.68675 | 0.69764 | 1 | tnfrsf10b | 3826.99 | 3826.99 | 3826.99 | | 3826.99 | | UP | 1 | 0 |
| 90Day | CASP8 activity is inhibited | 0.68675 | 0.69764 | 1 | tnfrsf10b | 3826.99 | 3826.99 | 3826.99 | | 3826.99 | | UP | 1 | 0 |
| 90Day | Regulation of necroptotic cell death | 0.48325 | 0.83383 | 1 | tnfrsf10b | 3826.99 | 3826.99 | 3826.99 | | 3826.99 | | UP | 1 | 0 |
| 90Day | Dimerization of procaspase-8 | 0.68675 | 0.69764 | 1 | tnfrsf10b | 3826.99 | 3826.99 | 3826.99 | | 3826.99 | | UP | 1 | 0 |
| 90Day | Formation of apoptosome | 0.78732 | 1 | 1 | | | | | | | | | | |
| 90Day | Cytochrome c-mediated apoptotic response | 0.78732 | 1 | 1 | | | | | | | | | | |
| 90Day | Regulation of the apoptosome activity | 0.78732 | 1 | 1 | | | | | | | | | | |
| 90Day | Prolactin receptor signaling | 0.73069 | 0.6592 | 1 | btrc | 5152.7 | 5152.7 | 5152.7 | | 5152.7 | | DOWN | 0 | 1 |
| 90Day | Cam-PDE 1 activation | 0.48796 | 1 | 1 | | | | | | | | | | |
| 90Day | Long-term potentiation | 0.61984 | 1 | 1 | | | | | | | | | | |
| 90Day | Caspase activation via Dependence Receptors in the absence of ligand | 0.61984 | 1 | 1 | | | | | | | | | | |
| 90Day | Organic cation transport | 0.60115 | 0.76201 | 1 | slc22a1 | 1050.57 | 1050.57 | 1050.57 | | 1050.57 | | DOWN | 0 | 1 |
| 90Day | Transfer of LPS from LBP carrier to CD14 | 0.78732 | 1 | 1 | | | | | | | | | | |
| 90Day | Translocation of ZAP-70 to Immunological synapse | 0.64343 | 0.73175 | 1 | h2-aa | 3001.17 | 3001.17 | 3001.17 | | 3001.17 | | DOWN | 0 | 1 |
| 90Day | Enzymatic degradation of dopamine by COMT | 0.78732 | 1 | 1 | | | | | | | | | | |
| 90Day | Dopamine clearance from the synaptic cleft | 0.69859 | 1 | 1 | | | | | | | | | | |
| 90Day | Ligand-receptor interactions | 0.43294 | 1 | 1 | | | | | | | | | | |
| 90Day | Synthesis of dolichyl-phosphate mannose | 0.69859 | 1 | 1 | | | | | | | | | | |
| 90Day | EGFR Transactivation by Gastrin | 0.73069 | 0.6592 | 1 | sos1 | 5894.93 | 5894.93 | 5894.93 | | 5894.93 | | DOWN | 0 | 1 |
| 90Day | Interconversion of 2-oxoglutarate and 2-hydroxyglutarate | 0.69859 | 1 | 1 | | | | | | | | | | |
| 90Day | Oxygen-dependent asparagine hydroxylation of Hypoxia-inducible Factor Alpha | 0.69859 | 1 | 1 | | | | | | | | | | |
| 90Day | FGFR3 ligand binding and activation | 0.56021 | 0.78886 | 1 | fgf1 | 242.429 | 242.429 | 242.429 | | 242.429 | | DOWN | 0 | 1 |
| 90Day | FGFR3c ligand binding and activation | 0.56021 | 0.78886 | 1 | fgf1 | 242.429 | 242.429 | 242.429 | | 242.429 | | DOWN | 0 | 1 |
| 90Day | FGFR1c ligand binding and activation | 0.64343 | 0.73175 | 1 | fgf1 | 242.429 | 242.429 | 242.429 | | 242.429 | | DOWN | 0 | 1 |
| 90Day | FGFR2c ligand binding and activation | 0.56021 | 0.78886 | 1 | fgf1 | 242.429 | 242.429 | 242.429 | | 242.429 | | DOWN | 0 | 1 |
| 90Day | Phospholipase C-mediated cascade; FGFR3 | 0.56021 | 0.78886 | 1 | fgf1 | 242.429 | 242.429 | 242.429 | | 242.429 | | DOWN | 0 | 1 |
| 90Day | SHC-mediated cascade:FGFR3 | 0.66889 | 0.61824 | 1 | sos1;fgf1 | 3068.6795 | 3068.6795 | 242.429 | 3996.92179 | 4960.29053 | 2969.67998 | DOWN | 0 | 1 |
| 90Day | Platelet sensitization by LDL | 0.7013 | 0.58634 | 1 | mapk14;apob | 2218.96 | 2218.96 | 175.96 | 2889.23831 | 1673.63662 | 2784.41068 | DOWN | 0 | 1 |
| 90Day | Neurophilin interactions with VEGF and VEGFR | 0.61984 | 1 | 1 | | | | | | | | | | |
| 90Day | Formyl peptide receptors bind formyl peptides and many other ligands | 0.77469 | 0.61588 | 1 | hebp1 | 2191.05 | 2191.05 | 2191.05 | | 2191.05 | | DOWN | 0 | 1 |
| 90Day | Role of LAT2/NTAL/LAB on calcium mobilization | 0.73069 | 0.6592 | 1 | sos1 | 5894.93 | 5894.93 | 5894.93 | | 5894.93 | | DOWN | 0 | 1 |
| 90Day | Regulation of commissural axon pathfinding by SLIT and ROBO | 0.69859 | 1 | 1 | | | | | | | | | | |
| 90Day | Degradation of GABA | 0.78732 | 1 | 1 | | | | | | | | | | |
| 90Day | Beta oxidation of decanoyl-CoA to octanoyl-CoA-CoA | 0.88732 | 1 | 1 | | | | | | | | | | |
| 90Day | Telomere C-strand synthesis initiation | 0.77469 | 0.61588 | 1 | pole4 | 5853.8 | 5853.8 | 5853.8 | | 5853.8 | | DOWN | 0 | 1 |
| 90Day | DNA replication initiation | 0.77469 | 0.61588 | 1 | pole4 | 5853.8 | 5853.8 | 5853.8 | | 5853.8 | | DOWN | 0 | 1 |
| 90Day | Rhesus glycoproteins mediate ammonium transport. | 0.69859 | 1 | 1 | | | | | | | | | | |
| 90Day | Signaling by Leptin | 0.78732 | 1 | 1 | | | | | | | | | | |
| 90Day | PKA-mediated phosphorylation of key metabolic factors | 0.88732 | 1 | 1 | | | | | | | | | | |

# THE DOW CHEMICAL COMPANY
# BIOCHEMICAL RESEARCH LABORATORY

FILE
K NO.
CHG. 7901059
REF.
SOURCE H. G. Hughes
SUB. BY T. R. Torkelson
REP'T. BY **
CHECKED BY P. J. Gehring
DATE March 10, 1971

## THE CHRONIC TOXICITY OF 1,4-DIOXANE:

## CONTINUOUS EXPOSURE OF SHERMAN RATS TO VARIOUS CONCENTRATIONS OF 1,4-DIOXANE IN DRINKING WATER FOR TWO YEARS

R. J. Kociba
**Reported by: R. J. Kociba, T. R. Torkelson, A. Clashman, S. McCollister and P. J. Gehring

LAB CODE LETTERS AND REPORT NO.

INFORMATIVE SUMMARY WITH CONCLUSIONS-BASED ON THE SAMPLE RECEIVED.

A two year toxicopathologic study of the effects of drinking water containing 1,4-dioxane has been performed using rats. Four groups of rats, 60/sex/level, received 1.0%, 0.1%, 0.01% or 0% 1,4-dioxane in their drinking water for 714-716 days. Parameters which were evaluated were survival rates, water consumption, hematological studies, organ weight-body weight ratios, and pathologic alterations. Special emphasis was given to tumor induction.

Daily dosages of 1,4-dioxane for male and female rats receiving 1.0% dioxane in their drinking water were approximately 1015 and 1599 mg/kg, respectively. Both male and female rats receiving 1.0% dioxane in the drinking water showed significantly decreased body weight gains, survival rates and water consumption. Renal tubular epithelial sloughing and hepatic degenerative alterations were also noted in both sexes at this level. When compared to controls, female rats receiving this treatment had a higher incidence of focal gastritis, an increased terminal liver weight and a significant increase in hepatocellular hyperplastic nodule formation. Both male and female rats receiving water containing 1.0% dioxane had a significant increase in the occurrence of hepatocellular carcinoma. This type of hepatic tumor accounted for a significant increase in the total number of tumors and tumor bearing animals in male rats receiving water containing 1.0% dioxane.

Male and female rats receiving 0.1% dioxane in their drinking water received approximately 94 and 148 mg/kg/day, respectively. Both sexes exhibited inconsistent degrees of renal tubular sloughing and hepatocellular degenerative changes. No significant increase in neoplasia was detected in these rats.

Male and female rats receiving drinking water containing 0.01% dioxane received approximately 9.6 and 19.0 mg/kg/day, respectively. No increase in tumor incidence or compound related hepatic alterations were observed in these rats. Renal tubular epithelial

Over

sloughing was observed in one female rat which died spontaneously from widespread leukemia. Since no other female or male rats in this treatment group was similarly affected, it is concluded that the response of this one rat was not related to treatment.

# TABLE OF CONTENTS

## TABLES

## FIGURES

# THE CHRONIC TOXICITY OF 1,4-DIOXANE:

## CONTINUOUS EXPOSURE OF SHERMAN RATS TO VARIOUS CONCENTRATIONS OF 1,4-DIOXANE IN DRINKING WATER FOR TWO YEARS

Richard J. Kociba, D.V.M., Ph.D., T. R. Torkelson, D.Sc.,
Aileen Clashman, B.S., Susan McCollister, B.S. and
P. J. Gehring, D.V.M., Ph.D.

March 9, 1971

Toxicology Unit, Chemical Biology Research
The Dow Chemical Company
Midland, Michigan 48640 USA

## I. INTRODUCTION

Argus, et al. (1965) reported the occurrence of hepatic tumors in rats administered 1.0% of 1,4-dioxane in the drinking water for 63 weeks. Unfortunately, this report did not include data which could be used to establish a dose-response relationship.

A two year study of rats given 1,4-dioxane in drinking water has been conducted to fulfill the following objectives:

1. Confirm or negate the results of Argus, et al. (1965).
2. Assuming hepatic tumors are induced by drinking water containing 1,4-dioxane, determine whether this effect is related to dose.
3. Obtain data which will be useful in establishing tolerance limits for Dow Chemical Company personnel.
4. Determine whether untoward effects other than hepatic carcinogenesis are associated with the consumption of water containing 1,4-dioxane.

## II. EXPERIMENTAL PROCEDURES

### A. Experimental Animals

Weanling Sherman rats, 45-60 days of age and weighing approximately 150 grams (male) and 125 grams (female), were used to initiate this study. The rats originated from a stock colony formerly maintained by the Toxicology Section of Chemical Biology Research. The rats were divided into four well-matched groups, each consisting of 60 males and 60 females. They were caged in a room with controlled temperature and humidity and fed Purina Laboratory Chow *ad libitum*.

B. Test Chemical

Thirty, one quart bottles of 1,4-Dioxane (Sample B-91768) were supplied by H. G. Hughes, Solvents Laboratories, B-1510 Building, Texas Division, The Dow Chemical Company, Freeport, Texas. This sample was utilized for the first 17 months of the study. A second sample (TB-012870), also supplied by H. G. Hughes, was utilized for the remainder of the study. The results of analyses for impurities in these samples are shown in Table 1. All stock samples were stored in amber-colored bottles and were padded with nitrogen until they were opened for use. Generally, they were used within one week after opening.

## C. Treatment

A 1.0% aqueous solution of dioxane was prepared by combining 60 ml of dioxane with 5940 ml of water. Portions of this solution were diluted to provide solutions containing 0.1% and 0.01% dioxane. Fresh solutions were prepared twice weekly during the first year of the study and weekly during the second year. The respective solutions of dioxane were supplied as the sole source of drinking water as follows:

| Sex | No. Rats | Dioxane Concentration in drinking water |
|---|---|---|
| M | 60 | 0 (Control) |
| M | 60 | 1.0% |
| M | 60 | 0.1% |
| M | 60 | 0.01% |
| F | 60 | 0 (Control) |
| F | 60 | 1.0% |
| F | 60 | 0.1% |
| F | 60 | 0.01% |

Water intake was recorded during 3 different time periods of the 2 year study. Periodically, samples were collected from individual water dispensers, as well as storage vessels, and analyzed for dioxane content (Table 3).

## D. Clinical Observations

The behavior and physical condition of the rats were observed daily. Individual body weights were recorded twice weekly the first month, weekly during months 2-7, and biweekly thereafter.

## E. Clinical Laboratory Studies

Hematology - During the 4th, 6th, 12th and 18th months of the study, blood samples were obtained from a minimum of 5 male and 5 female rats receiving 1.0% dioxane in their drinking water. Blood samples were obtained from all rats during the 24th month. The following determinations were made on each blood sample: packed cell volume (PCV), total erythrocyte counts (RBC), hemoglobin (Hgb), total leukocytes (WBC), and a differential white blood cell count.

## F. Postmortem and Histopathologic Studies

During the course of the study a necropsy was conducted on rats that died or appeared moribund. After 714 days, all surviving rats were fasted overnight and killed by decapitation. A complete gross pathological examination was conducted. Representative specimens of the tissues indicated below, as well as gross lesions, were collected and placed in buffered 10% formalin.

brain
pituitary gland
mesenteric lymph nodes
pancreas
prostate
duodenum
jejunum
spinal cord
bone marrow
sternum
heart
spleen
colon
kidneys
testes
adrenal gland
ovaries
uterus
liver
stomach
trachea
esophagus
lungs
thyroid gland
parathyroid gland
nasal mucosa

Conventional techniques were used to prepare specimens for microscopic examination. Hematoxylin and eosin were used for staining.

Additional specimens of liver were preserved in 95% alcohol and stained with Best's Carmine for glycogen. Frozen specimens of liver were sectioned with a cryostat and stained with Oil Red O to evaluate fat content. Selected liver sections were stained with the Periodic acid - Schiff technique before and after digestion with diastase for evaluation of digestible glycogen content.

## G. Organ Weights and Ratios

At the termination of the experiment, organ weights were determined for all surviving rats. Organ weight-body weight ratios were calculated for brain, liver, kidneys, testes, spleen and heart.

## H. Statistical Analyses

The Chi-Square method of analysis, using the Yates correction factor when the sample size was too small, was used to analyze the ratio of tumor incidence in treated and control rats. Survival rates were also analyzed in this manner.

The Student-Fisher "t" test was used to analyze the hematologic, body weight, organ weight-body weight and water consumption data.

## III. RESULTS AND DISCUSSION

### A. Water Intake and Dosage of 1,4-Dioxane

Table 2 lists the average water intake during 3 different periods of the study. Initially, both sexes were considered together in the comparison of water intake from day 1 to day 113. During this time period, rats receiving water containing 1.0% dioxane consumed less than controls, $P<0.001$. Subsequently, water consumption by male and female rats was analyzed separately.

From day 114 to day 198, male and female rats receiving 1.0% dioxane in their drinking water consumed less water than controls, $P<0.001$ and $P<0.05$, respectively. Females receiving water containing 0.1% dioxane consumed less than controls, $P<0.01$, while those given water containing 0.01% dioxane consumed more than controls, $P<0.01$. There was no significant difference in the water consumption of males receiving water containing 0.1% or 0.01% dioxane.

From day 446 to day 460, male and female rats receiving water containing 1.0% dioxane drank comparable amounts of water as the controls.

The approximate daily dose of dioxane for the time period, day 114 to day 198, was 1015 and 1599 mg/kg/day for male and female rats drinking water containing 1.0% dioxane, respectively. The lower dosage levels were approximately 0.1 and 0.01 of these dosages.

Table 3 lists the content of dioxane in the water dispensers as determined by analysis at various time intervals during the study. Examination of these data reveal that the content of dioxane in water as determined by analysis closely agrees with the desired concentration.

B. Survival Rates

Figures 1 and 2 show the survival rates for male and female rats, respectively. Both sexes of rats receiving drinking water containing 1.0% dioxane had a significant decrease in the number of survivors at 4 months (males $P<0.01$; females $P<0.005$). The rats succumbing during this early period of high mortality (1.0% dioxane) had evidence of both hepatic and renal pathology which will be described later.

From the 5th to the 24th month, the mortality rate of the rats receiving 1.0% dioxane paralleled that of other groups.

C. Body Weights

Male and female rats drinking water containing 1.0% dioxane had a decreased rate of weight gain, Figures 3 and 4, respectively. The body weights were significantly depressed ($P<0.001$) by day 2 of the study in both sexes and remained depressed throughout the study in the female rats. Since only one male rat was alive during the last 60 days of the study, the apparent upward direction of the body weight curve for male rats drinking water containing 1.0% dioxane during this period was of no significance. The body weights of both male and female rats receiving 0.1% or 0.01% dioxane were not significantly different than those of controls.

D. Terminal Body-Organ Weights and Ratios

The mean terminal body weight, organ weights, and organ weight per 100 g body weight for the various groups are presented in Table 4. The average body weight of the three surviving female rats given drinking water containing 1.0% dioxane was significantly depressed. The absolute liver weight and liver weight per 100 g body weight of this group were increased. The pathological changes seen in the livers of these debilitated rats are described later.

The only other significant alteration was an increase of the average brain weight of males receiving 0.1% dioxane in the drinking water ($P \leq 0.05$). Since this manifestation is not related to either dose or detectible pathological changes, it is of no toxicological importance.

## E. Hematology

The hematologic data are summarized in Table 5. There is a significant elevation ($P<0.05$) of PCV (packed cell volume) in female rats which had been drinking water containing 1.0% dioxane for 4 months. After 6 months, there was a significant depression ($P \leq 0.01$) of the RBC (red blood cell count) and Hgb (hemoglobin) in male rats receiving water containing 1.0% dioxane. These manifestations are of questionable importance because the same changes were not found later in the study.

In the 24th month, there was an elevation of RBC in female rats receiving water containing 1.0% dioxane and a depression of RBC in female rats receiving water containing 0.1% dioxane. This change was not dose related and did not occur in the males. It is probably a reflection of the degree of hydration at the time of sampling.

## F. Gross Pathological and Histopathological Studies

### 1. Hepatic Lesions

Table 6 is a compilation of the hepatic alterations observed in the gross and histological examination of the livers. Since some of the lesions described herein may be unfamiliar to the reader, they are described and/or illustrated in an appendix, Appendix 1.

Examination of the data in Table 6 suggests there may be a dose-response relationship for the occurrence of the following lesions: elevated nodular formations, discrete pale foci, hepatocellular anisonucleosis and bile duct epithelial hyperplasia. There is no apparent dose-response relationship for the other manifestations listed in Table 6; hence, their toxicological significance is questionable. Hepatic tumors are covered in a following section.

As indicated in Appendix 1, histological examination of the pale foci which were observed grossly in the liver revealed hepatocellular cytoplasmic vacuolar degeneration. The production of this lesion by dioxane has been previously reported (De Navasquez, 1935; Kesten, et al, 1939; and Laug et al., 1939). However, no mention of this lesion was made in a recent report by Argus, et al., 1965.

A variety of nonspecific lesions found in the livers of both control and treated rats are not referred to in Table 6. These included (1) irregular, fine clumping of the cytoplasm and darker staining of the hepatocytes; (2) isolated small foci of necrobiosis; (3) irregular and minimal degrees of fatty metamorphosis; and (4) passive hyperemia. Infiltration of the liver with lymphoid metatases from other organs has also been excluded.

2. Renal Lesions

Table 7 is a compilation of the renal alterations observed in the gross and histological examination of the kidneys. Some of these alterations are described in Appendix 2.

The surface of the kidneys of rats in all groups appeared mottled, contracted or granular. These lesions were observed most frequently in males and in groups with the largest number of survivors. The disease, chronic nephritis, leading to the development of these lesions occurs spontaneously in old rats (Snell, 1967). A dose-response relationship was not established for the following lesions; glomerular alterations, tubular dilatation and cast formation or interstitial fibrosis. Since rats receiving 1.0% dioxane in their drinking water did not have as many survivors after 24 months of treatment, it cannot be concluded that this level of dioxane does not increase the severity of these lesions.

The occurrence of renal tubular epithelial vacuolization and sloughing as well as the regeneration activity of tubular cells appears to be compound related. These manifestations were observed with the greatest frequency in rats receiving water containing 1.0% dioxane, less frequently in those receiving water containing 0.1% dioxane, and rarely in control rats or rats receiving 0.01% dioxane in their water.

Nephrocalcinosis also appeared to be related to treatment. This lesions was observed most frequently in males receiving 1.0% or 0.1% dioxane in their drinking water. Renal tubular epithelial degeneration and necrosis has been previously reported to be induced by dioxane (De Navasquez, 1935; Kesten et al., 1939 and Laug et al., 1939). In a recent report, dioxane induced glomerular alterations received more emphasis (Argus et al., 1965).

In addition to the lesions previously discussed, there were others which occurred in isolated single cases and were not related to treatment; renal infarction, perirenal capsulitis; three neoplasms were found. These will be discussed below.

3. Additional Pathological Alterations

Table 8 is a compilation of various pathological alterations observed in the rats used in this study. Most of the various degenerative and inflammatory lesions referred to in this table are similar to those found by Berg (1967) in his study of aging rats. With one possible exception, these alterations do not appear to be related to treatment. In female rats, dioxane treatment appears to have increased the incidence of gastritis. However, the significance of this observation is questionable because in male rats the controls had the greatest frequency of this lesion. Subjectively, rats receiving water containing 1.0% dioxane appeared to have more severe pneumonic lesions.

4. Tumor Incidence

A total of 132 tumors were found in 112 rats (Table 9). The morphological type and the location of the tumors are indicated in the table. Although not considered to be neoplastic, the frequency of hepatocellular hyperplastic nodules is also shown in the table.

Table 10 shows the statistical evaluation of the total number of tumors, tumor bearing animals, hepatocellular carcinmas and combined hepatic tumors. In male rats receiving water containing 1.0% dioxane, the total number of tumors as well as the number of tumor bearing animals was increased. The total number of hepatic tumors was increased significantly ($P<0.05$) in both male and female rats receiving water containing 1.0% dioxane.

In males, all of the hepatic tumors were hepatocellular carcinomas while in females four of the six hepatic tumors were of this type. The incidence of hepatic tumors was not significantly increased in the other treatment groups.

Argus et al. (1965) reported that 7 of 26 rats given 1.0% dioxane in their drinking water for 63 weeks developed hepatic tumors. Since they did not define their criteria for classification of hepatic tumors, Argus, et al. (1965) may not have differentiated hepatic hyperplasia and neoplasia. In the study reported herein, hepatocellular hyperplasia was not considered to be neoplasia. Hepatocellular hyperplasia has been frequently observed in rats treated with hepatotoxic agents (Popper and Schaffner, 1957; Reuber, 1965; Firminger and Reuber, 1961; Popper, et al. 1960; Merkow, et al., 1969).

Although spontaneous tumors of the nasal cavity of rats are rare, 3 squamous cell carcinomas were found in the nasal mucosa of treated rats in this study. Recently, Hoch-Ligeti, et al. (1970) reported the occurrence of nasal carcinomas in rats receiving dioxane. Thus, it is concluded that the occurrence of this malignancy may be related to treatment with dioxane.

The other neoplasms observed in this study are not considered to be related to dioxane treatment. Most of these neoplasms have been reported to occur spontaneously in rats (Bullock and Curtis, 1930; Thompson et al., 1961; Davis et al. 1956; and Gilber and Gilman, 1958). Furthermore, the frequency of occurrence of these tumors in treated rats was essentially the same as that in control rats.

## IV. SUMMARY

A two year toxicopathologic study of the effects of drinking water containing 1,4-dioxane has been performed using rats. Four groups of rats, 60/sex/level, received 1.0%, 0.1%, 0.01% and 0% 1,4-dioxane in their drinking water for 714-716 days. Parameters which were evaluated were survival rates, water consumption, hematologic studies, organ weight-body weight ratios, and pathologic alterations. Special emphasis was given to tumor induction.

Daily dosages of 1,4-dioxane for male and female rats receiving 1.0% dioxane in their drinking water were approximately 1015 and 1599 mg/kg, respectively. Both male and female rats receiving 1.0% dioxane in the drinking water showed significantly decreased body weight gains, survival rates and water consumption. Renal tubular epithelial sloughing and hepatic degenerative alterations were also noted in both sexes at this level. When compared to controls, female rats receiving this treatment had a higher incidence of focal gastritis, an increased terminal liver weight and a significant increase in hepatocellular hyperplastic nodule formation. Both male and female rats receiving water containing 1.0% dioxane had significant increase in the occurrence of hepatocellular carcinoma. This type of hepatic tumor accounted for a significant increase in the total number of tumors and tumor bearing animals in male rats receiving water containing 1.0% dioxane.

Male and female rats receiving 0.1% dioxane in their drinking water received approximately 94 and 148 mg/kg/day, respectively. Both sexes exhibited inconsistent degrees of renal tubular sloughing and hepatocellular degenerative changes. No significant increase in neoplasia was detected in these rats.

Male and female rats receiving drinking water containing 0.01% dioxane received approximately 9.6 and 19.0 mg/kg/day, respectively. No increase in tumor incidence or compound related hepatic alterations were observed in these rats. Renal tubular epithelial sloughing was observed in one female rat which died spontaneously from widespread leukemia. Since no other female or male rats in this treatment group was similarly affected, it is concluded that the response of this one rat was not related to treatment.

## REFERENCES

Argus, M. F., Arcos, J. C., and Hoch-Ligeti, C.: Studies on the Carcinogenic Activity of Protein-Denaturing Agents: Hepatocarcinogenicity of Dioxane. J. Nat. Cancer Institute, 35, 949-958, 1965.

Berg, B. N.: Longevity Studies in Rats II. Pathology of Ageing Rats. Chapter in Pathology of Laboratory Rats and Mice, Edited by E. Cotchin and F. Roe. Blackwell Scientific Publications, Oxford, England, 1967.

Bullock, F. D., and Curtis, M. R.: Spontaneous Tumors of the Rat. J. of Cancer Research, 14, 1-115, 1930.

Davis, R. K., Stevenson, G. T., and Busch, K. A.: Tumor Incidence in Normal Sprague-Dawley Female Rats. Cancer Research, 16, 194-197, 1956.

DeNavasquez, S.: Experimental Tubular Necrosis of the Kidney Accompanied by Liver Changes due to Dioxane Poisoning. J. Hygiene, 35, 540-548, 1935.

Firminger, H. I., and Reuber, M. D.: Influence of Adrenocortical, Androgenic, and Anabolic Hormones on the Development of Carcinoma and Cirrhosis of the Liver in AXC Rats Fed N-2-Fluorenyldiacetamide. J. Nat. Cancer Institute, 27, 555-595, 1961.

Gilbert, C., and Gillman, J.: Spontaneous Neoplasms in the Albino Rat. S. Afr. J. Med. Sci., 23, 257-272, 1958.

Hoch-Ligeti, C., Argus, M. F., and Arcos, J. C.: Induction of Carcinomas in the Nasal Cavity of Rats by Dioxane. Brit. J. Cancer, 26, 164-170, 1970.

Kesten, M. G., Mulinos, M. G., and Pomerantz, L.: Pathologic Effects of Certain Glycols and Related Compounds. Arch. Path., 27, 447-465, 1939.

Laug, E. P., Calvery, H. O., Morris, H. J., and Woodard, G.: The Toxicology of Some Glycols and Derivatives. J. Indust. Hyg. and Toxicol., 21, 173-201, 1939.

Merkow, L. P., Epstein, S. M., Farber, E., Pardo, M., and Bartus, B.: Cellular Analysis of Liver Carcinogenesis III. Comparison of the Ultrastructure of Hyperplastic Liver Nodules and Hepatocellular Carcinomas Induced in Rat Liver by 2-Fluorenylacetamide. J. Nat. Cancer Institute, 43, 37-63, 1969.

Popper, H., and Schaffner, F.: Liver: Structure and Function. McGraw-Hill Book Company, New York, 1957.

Popper, H., Sternberg, S. S., Oser, B. L., and Oser, M.: The Carcinogenic Effect of Aramite in Rats. A Study of Hepatic Nodules. Cancer, 13, 1035-1046, 1960.

Reuber, M. D.: Development of Preneoplastic and Neoplastic Lesions of the Liver in Male Rats Given 0.025% N-2-Fluorenyldiacetamide. J. Nat. Cancer Institute, 34, 697-724, 1965.

Snell, K. C.: Renal Disease of the Rat. Chapter in Pathology of Laboratory Rats and Mice, Edited by E. Cotchin and F. Roe. Blackwell Scientific Publications, Oxford, England, 1967.

Thompson, S.W., Huseby, R. A., Fox, M. A., Davis, C. L., and Hunt, R. D.: Spontaneous tumors in the Sprague-Dawley rat. J. Nat. Cancer Inst., 27:1037-1057, 1961.

APPENDIX 1. Description of the Hepatic Lesions Referred to in this report.

Elevated Nodular Formation - This term refers to the presence of grossly visible irregularly elevated nodules in the liver. Histologically, the lesion was associated with the occurrence of hepatic tumors and hepatocellular hyperplastic nodule formations.

Discrete Pale Foci - These lesions were observed by gross examination of the liver. Histologically they consist of areas of hepatocellular cytoplasmic vacuolar degeneration and necrosis.

Hepatocellular Anisonucleosis - This term refers to a variation in the size and shape of nuclei.

Hepatocellular Cytoplasmic Degeneration - This term refers to the presence of areas, sometimes confined to the central zone of the lobule, where the lobular arrangement had become distorted by marked swelling of the hepatocytes. The cytoplasm often appears vacuolated. In most cases, nuclei are retained.

Hepatocellular Necrosis - This term refers to the presence of areas where degeneration had progressed to the point of complete disintegration of the hepatocyte with loss of nuclei (Figure 5).

Hepatocellular Hyperplastic Nodule Formation - This term refers to well defined nodules of parenchymal cells with distinct compression of surrounding parenchyma, Figure 6 (Popper, et al., 1960; Reuber, 1965). The architecture in these nodules varies from well organized hepatic cords to a more disorderly pattern. At times, atypical cells of such a degree not to be considered malignant are present.

Hepatocellular Carcinoma - This term refers to malignant tumors of parenchymal cells which are either well or poorly differentiated anaplastic growths with occasional cholangiomatous areas (Reuber, 1965; Firminger and Reuber, 1961). As a rule, the liver cells are enlarged and contain large nuclei with multiple nucleoli (Figures 7 and 8).

In these lesions, mitotic figures are frequently observed. Occasionally, metastatic cells are observed in the hepatic vessels and/or lung. Widening of the hepatic cords due to an increased number of cells was observed in some areas. In some cases, the malignant cells were proliferating in the form of extended fingerlike projections into accompanying areas of hepatic hemorrhage.

Bile Duct Epithelial Hyperplasia - This term refers to an increased number of bile ducts and ductular epithelial cells. These flat to cuboidal cells contain vesicular nuclei. The most pronounced degree of hyperplasia was seen in the portal triad areas.

Cholangioma - This term refers to the rather disorderly proliferation of the larger bile ducts and ductular cells without atypical cytological morphology. Frequently, these cells formed papillary projections extending into enclosed cystic spaces.

Cholangiocarcinoma - This lesion was observed in one control female rat. The term refers to a proliferation of atypical epithelial cells which resemble anaplastic bile duct epithelial cells. The large number of mitotic figures seen in these cells suggested a high rate of mitotic activity. In one area it appeared that these cells were forming a cystic structure enclosed by these anaplastic cells.

## APPENDIX 2. Description of the Renal Lesions Referred to in This Report.

Renal Glomerular Alterations - This designation is used to indicate that one or more of the following morphological changes was observed: adhesions between the parietal and visceral layers of Bowman's capsule; sharp delineation of capillary loops of the glomeruli; atrophy of the glomerular tufts; an increased density of the mesangium; a thickening of the parietal layer of Bowman's capsule.

Renal Tubular Dilatation and Proteinaceous Cast Formation - Renal tubular dilatation indicates that the cells of the cortical tubules were atrophied and the tubules were dilated. Most of the tubules were distended with acidophilic proteinaceous material, casts.

Renal Interstitial Fibrosis and Lymphocytosis - This term indicates that the interstitial area was fibrotic and sometimes infiltrated with lymphocytes.

Renal Tubular Vacuolization and Sloughing - This term applies to those cases in which vacuolar degeneration of the proximal tubular epithelial cells was sufficiently severe to cause sloughing into the lumen of the tubules. Occasionally, only the basalmembrane remained.

Increased Renal Tubular Regeneration Activity - In this case, there were epithelial cells present which appeared to be in the process of regeneration. These flattened squamoid-appearing cells located along the basement membrane contained oval, hyperchromatic nuclei and occasionally mitotic figures.

Table 1

ANALYSES OF IMPURITIES PRESENT IN SAMPLES OF 1,4-DIOXANE USED IN TWO YEAR DRINKING WATER STUDY

| | Sample B-91768 | | | | | Sample TB-012870 | |
|---|---|---|---|---|---|---|---|
| | | | | (Midland) 2/70 | | | |
| Impurities Present in Sample | (Texas) 9/68 | (Texas) 7/69 | (Midland) 2/70 | Amber Collection Bottle | Clear Collection Bottle | (Texas) 1/70 | (Midland) 2/70 |
| Peroxide (mg/ml as $H_2O_2$) | 0.01 | 0.326 | 0.30 | 0.34 | 0.34 | 0 | 0.03 |
| Acidity (meq/ml) | 0.001 | 0.0031 | 0.0035 | 0.0042 | 0.0039 | 0.00087 | 0.0006 |
| Acetaldehyde (ppm) | -- | -- | <6 | -- | -- | -- | <6 |
| Crotonaldehyde (ppm) | 1320 | 1340 | 820 | -- | -- | 360 | 220 |
| 2-Methyl-1,4-Dioxolane (ppm) | 108 | 100 | 60 | -- | -- | None Reported | 6 |
| $H_2O$ (ppm) | 15 | 90 | -- | -- | -- | 10 | -- |

### Table 2

### IMBIBITION OF WATER CONTAINING 1,4-DIOXANE BY RATS DURING VARIOUS PERIODS OF A TWO YEAR STUDY

| Time Period | Sex | Dioxane Level | Average Daily Water Consumption (ml/day/rat) | Estimated Daily Dose of Dioxane† (mg/kg/day) | |
|---|---|---|---|---|---|
| Days 1-113 | | 0 (Control) | 39.5 + 3.2 | | |
| | | 1.0% (Both sexes combined) | 34.9 ± 3.3*** | | |
| Days 114-198 | M | 0 (Control) | 43.1 ± 4.6 | | |
| | M | 1.0 % | 38.1 ± 5.5*** | 1015 | 914-1229 |
| | M | 0.1 % | 41.2 ± 6.8 | 94 | 59- 113 |
| | M | 0.01% | 43.0 ± 9.2 | 9.6 | 10- 12 |
| | F | 0 (Control) | 39.5 ± 4.0 | | |
| | F | 1.0 % | 35.5 ± 5.8* | 1599 | 1416-2149 |
| | F | 0.1 % | 36.4 ± 4.2** | 148 | 130- 168 |
| | F | 0.01% | 45.3 ± 3.8** | 19 | 18- 20 |
| Days 446-460 | M | 0 (Control) | 44.9 ± 10.8 | | |
| | M | 1.0% | 42.4 ± 12.1 | 1046 | 869-1231 |
| | F | 0 (Control) | 30.3 ± 3.4 | | |
| | F | 1.0% | 27.3 ± 4.3 | 1078 | 1019-1176 |

Means marked with asterisks differ significantly from controls: $*P<0.05$; $**P<0.01$; $***P<0.001$.

†Listed are the average values and ranges, based on daily water intake and coinciding average body weights. For discussion purposes, the more complete data for Days 114-198 will be used.

TABLE 3

RESULTS OF ANALYSES FOR 1,4-DIOXANE CONTENT OF WATER SUPPLY ADMINISTERED TO RATS FOR TWO YEARS

| Dosage Level | Source of Sample | Day of Study | | | | | | | | | | | |
|---|---|---|---|---|---|---|---|---|---|---|---|---|---|
| | | $14^1$ | $14^0$ | $19^0$ | $19^1$ | 42 | 49 | 84 | $125^2$ | $125^3$ | $253^0$ | $253^1$ | 615 |
| 0 (Control) | Supply Tank | .02 | < .01 | <.01 | <.01 | .005 | .001 | <.01 | <.01 | < .01 | -- | <.005 | < .001 |
| 0 (Control) | Top of Rack | <.01 | < .01 | <.01 | <.01 | .002 | .001 | <.01 | <.01 | < .01 | -- | <.005 | < .001 |
| 0 (Control) | Bottom of Rack | <.01 | < .01 | <.01 | <.01 | -- | -- | <.01 | <.01 | < .01 | -- | <.005 | < .001 |
| 1.0 % | Supply Tank | .83 | .93 | .82 | .76 | 1.044 | 1.026 | .89 | .88 | 1.06 | 1.17 | .99 | .77 |
| 1.0 % | Top of Rack | .87 | .95 | .78 | .84 | 1.058 | .938 | .89 | .88 | 1.05 | 1.11 | .99 | .84 |
| 1.0 % | Bottom of Rack | .87 | -- | .74 | .89 | .701 | 1.010 | .66 | .90 | 1.00 | .94 | .59 | .83 |
| 1.0 % | P. E. Bottles | .99 | 1.01 | .87 | .93 | 1.141 | 1.106 | .65 | -- | -- | -- | -- | 1.01 |
| 0.1 % | Supply Tank | .09 | .09 | .08 | .08 | .088 | .097 | .05 | .10 | .10 | .10 | .098 | .094 |
| 0.1 % | Top of Rack | .09 | .10 | .08 | .07 | .100 | .093 | .09 | .10 | .09 | .11 | .095 | .096 |
| 0.1 % | Bottom of Rack | .09 | -- | .08 | .09 | .019 | .096 | .05 | .09 | .09 | .089 | .079 | .095 |
| 0.1 % | P. E. Bottles | .10 | .10 | .09 | .10 | .093 | .093 | .1 | .10 | -- | -- | -- | .10 |
| 0.01% | Supply Tank | .01 | .01 | .01 | .01 | .0102 | .003 | .01 | .01 | .01 | .01 | <.005 | .013 |
| 0.01% | Top of Rack | .01 | .01 | .01 | .01 | .013 | .008 | .01 | .01 | .01 | .01 | <.005 | .023 |
| 0.01% | Bottom of Rack | .01 | -- | <.01 | .01 | .008 | .008 | .01 | .01 | .01 | < .005 | <.011 | .012 |
| 0.01% | P. E. Bottles | .01 | .01 | .01 | .01 | .009 | .010 | .01 | .01 | -- | -- | -- | .0097 |

On days 14, 19 and 253 analyses were conducted on both fresh$^0$ and 2-3 day old water supplies$^1$ prior to replenishment.

-- Data not available

Water samples were those supplied to male rats$^2$ and female rats$^3$

P. E. Bottles - polyethylene bottles used in sample preparation

All values expressed as actual percentage (%) of water supply as analyzed by gas liquid chromatography. Limits of accuracy are assumed to be indicated by Minimal Values listed for control samples on the respective days.

## TABLE 4

### BODY AND ORGAN WEIGHTS OF MALE AND FEMALE RATS AT TERMINATION OF TWO YEAR 1,4-DIOXANE IN WATER STUDY

| Dosage Level (mg/kg/day) | No. of Rats | Sex | Av. Body Wt. (g) | Average Organ Weights (grams and grams/100 grams) | | | | | | | | | | | |
|---|---|---|---|---|---|---|---|---|---|---|---|---|---|---|---|
| | | | | Brain | | Heart | | Liver | | Kidney | | Spleen | | Testes | |
| | | | | g | g/100g | g | g/100g | g | g/100g | g | g/100g | g | g/100g | g | g/100g |
| Control 0 | 20 | M | 378±40 | 1.78±0.15§ | 0.48±0.05 | 1.56±0.25 | 0.42±0.08 | 9.58±1.39 | 2.54±0.32 | 3.01±0.41 | 0.80±0.13 | 0.70±0.23 | 0.19±0.07 | 2.93±0.40 | 0.78±0.09 |
| 1.0 % | 1† | M | 377 | 1.80 | 0.47 | 1.25 | 0.33 | 15.10 | 4.00 | 3.00 | 0.79 | 0.95 | 0.25 | 3.10 | 0.82 |
| 0.1 % | 14 | M | 377±57 | 1.77±0.06 | 0.48±0.07 | 1.64±0.28 | 0.44±0.08 | 10.23±1.81 | 2.74±0.49 | 3.03±0.29 | 0.82±0.12 | 0.51±0.17 | 0.14±0.04 | 2.87±0.45 | 0.79±0.09 |
| 0.01% | 24 | M | 378±68 | 1.87±0.13* | 0.50±0.09 | 1.52±0.25 | 0.40±0.07 | 9.69±1.55 | 2.56±0.31 | 3.04±0.48 | 0.80±0.08 | 0.68±0.24 | 0.18±0.06 | 2.82±0.78 | 0.74±0.17 |
| Control 0 | 37 | F | 285±47 | 1.72±0.12 | 0.61±0.08 | 1.23±0.23 | 0.44±0.09 | 8.16±1.83 | 2.89±0.68 | 2.16±0.34 | 0.77±0.11 | 0.65±0.25 | 0.23±0.09 | | |
| 1.0 % | 3 | F | 212±42** | 1.58±0.20 | 0.78±0.24 | 1.03±0.31 | 0.48±0.06 | 12.60±5.16*** | 5.76±1.50* | 2.10±0.40 | 0.99±0.09 | 0.45±0.25 | 0.20±0.09 | | |
| 0.1 % | 32 | F | 280±47 | 1.77±0.13 | 0.65±0.11 | 1.32±0.25 | 0.48±0.10 | 8.35±1.53 | 2.99±0.38 | 2.17±0.29 | 0.79±0.12 | 0.72±0.33 | 0.26±0.13 | | |
| 0.01% | 36 | F | 289±42 | 1.75±0.09 | 0.62±0.08 | 1.24±1.24 | 0.43±0.07 | 8.36±1.89 | 2.90±0.53 | 2.27±0.38 | 0.79±0.11 | 0.76±0.45 | 0.26±0.16 | | |

Means marked with asterisks differ significantly from controls: *$P<0.05$; **$P<0.01$; ***$P<0.001$

§Standard Deviation.

†Too few in this group for statistical analysis.

TABLE 5

SUMMARY OF HEMATOLOGIC DATA COMPILED DURING TWO YEAR PERIOD OF ADMINISTRATION OF 1,4-DIOXANE IN THE WATER SUPPLY

| Month of Study | Dosage Level | Number/ Group | Sex | PCV % | RBC x $10^6/mm^3$ | Hemoglobin g/100 cc | WBC x$10^3/mm^3$ | WBC Differential (%)† | | | | |
|---|---|---|---|---|---|---|---|---|---|---|---|---|
| | | | | | | | | Neut | Lymph | Mono | Eosin | Baso |
| 4 | 0 (Control) | 5 | M | 42.7 ± 3.4 | 7.46 ± 0.5 | 11.8 ± 2.8 | 14.8 ± 0.7 | 21 | 76 | 1 | 2 | 0 |
| | 1.0 % | 15 | M | 44.4 ± 1.8 | 7.34 ± 0.3 | 12.4 ± 2.5 | 15.1 ± 0.5 | 24 | 75 | 0.5 | 0.5 | 0 |
| | 0 (Control) | 5 | F | 46.6 ± 2.5 | 6.63 ± 0.3 | 14.5 ± 0.8 | 12.1 ± 1.8 | 23 | 73 | 2 | 1.5 | 0.5 |
| | 1.0 % | 15 | F | 50.3 ± 3.3* | 6.89 ± 0.6 | 15.0 ± 0.8 | 13.2 ± 2.4 | 30 | 66 | 2 | 2 | 0 |
| 6 | 0 (Control) | 5 | M | 50.0 ± 2.0 | 8.13 ± 0.18 | 16.4 ± 0.38 | 19.7 ± 5.1 | 30 | 62 | 6 | 2 | 0 |
| | 1.0 % | 5 | M | 48.9 ± 2.8 | 7.57 ± 0.32** | 15.5 ± 0.41** | 26.1 ± 4.7 | 33 | 60 | 3 | 4 | 0 |
| | 0 (Control) | 5 | F | 47.5 ± 3.5 | 7.38 ± 0.39 | 16.0 ± 1.1 | 22.0 ± 8.7 | 32 | 63 | 2 | 3 | 0 |
| | 1.0 % | 5 | F | 48.3 ± 3.4 | 7.38 ± 0.17 | 15.6 ± 0.5 | 18.2 ± 1.7 | 29 | 65 | 2 | 4 | 0 |
| 12 | 0 (Control) | 5 | M | 50.3 ± 4.1 | 7.88 ± 0.84 | 16.0 ± 1.1 | 15.4 ± 4.5 | 41 | 52 | 4 | 3 | 0 |
| | 1.0 % | 5 | M | 53.2 ± 2.4 | 7.84 ± 0.26 | 16.5 ± 0.6 | 17.2 ± 3.0 | 30 | 62 | 4 | 3.5 | 0.5 |
| | 0 (Control) | 5 | F | 50.7 ± 3.1 | 7.18 ± 0.60 | 16.7 ± 0.9 | 12.1 ± 3.0 | 23 | 64 | 4 | 9 | 0 |
| | 1.0 % | 5 | F | 53.3 ± 2.7 | 7.39 ± 0.60 | 16.8 ± 0.5 | 12.8 ± 3.0 | 31 | 60 | 6 | 2.5 | 0.5 |
| 18 | 0 (Control) | 38 | M | 50.8 ± 5.8 | 6.50 ± 1.08 | 15.6 ± 2.2 | 20.9 ± 5.7 | 42 | 52 | 3 | 3 | 0 |
| | 1.0 % | 22 | M | 50.6 ± 5.8 | 6.99 ± 1.04 | 15.6 ± 1.8 | 21.0 ± 7.6 | 45 | 48 | 3 | 4 | 0 |
| | 0 (Control) | 48 | F | 50.1 ± 4.5 | 7.14 ± 0.80 | 15.7 ± 1.3 | 19.4 ± 9.8 | 40 | 53 | 4 | 3 | 0 |
| | 1.0 % | 15 | F | 51.7 ± 3.8 | 7.42 ± 0.70 | 15.4 ± 1.2 | 22.6 ± 5.6 | 42 | 52 | 3 | 3 | 0 |
| 24 | 0 (Control) | 22 | M | 50.7 ± 7.1 | 7.98 ± 1.7 | 15.1 ± 3.2 | 25.9 ± 7.2 | 37 | 57 | 3 | 3 | 0 |
| | 1.0 % | 1[1] | M | 51.5 | 9.00 | 15.4 | 21.3 | 50 | 44 | 6 | 0 | 0 |
| | 0.1 % | 15 | M | 53.4 ± 8.1 | 8.2 ± 1.3 | 15.7 ± 2.2 | 22.5 ± 5.8 | 47 | 49 | 2.5 | 1.5 | 0 |
| | 0.01% | 25 | M | 48.4 ± 6.3 | 7.8 ± 1.3 | 14.0 ± 2.6 | 24.1 ± 7.2 | 41 | 50 | 4 | 5 | 0 |
| | 0 (Control) | 37 | F | 51.5 ± 6.5 | 7.9 ± 1.0 | 16.1 ± 1.98 | 18.2 ± 4.7 | 38 | 56 | 4 | 2 | 0 |
| | 1.0 % | 4 | F | 53.4 ± 8.5 | 9.1 ± 1.0* | 17.2 ± 2.1 | 18.7 ± 3.4 | 38 | 54 | 7 | 1 | 0 |
| | 0.1 % | 32 | F | 49.9 ± 6.8 | 7.5 ± 1.1 | 15.6 ± 2.3 | 19.5 ± 8.8 | 34 | 62 | 2 | 2 | 0 |
| | 0.01% | 36 | F | 49.2 ± 6.0 | 7.2 ± 1.2* | 15.2 ± 1.9 | 18.0 ± 6.7 | 39 | 55 | 3 | 3 | 0 |

†WBC differential counts were not statistically analyzed.

Neut = Neutrophil; Lymph = Lymphocyte; Mono = Monocyte; Eosin = Eosinophil; Baso = Basophil.
PCV = Packed Cell Volume; RBC = Red Blood Cells; WBC = White Blood Cells.

[1] Too few per group for analysis.

Means marked with asterisks differ significantly from controls: $*P<0.05$; $**P<0.01$.

## TABLE 6

## HEPATIC ALTERATIONS OBSERVED IN RATS ADMINISTERED 1,4-DIOXANE IN DRINKING WATER FOR TWO YEARS[1]

| | Sex | No. Rats (Initial) | No. Rats Alive (Termination) | Generalized Hepatic Paleness | Hepatomegaly | Discrete Pale Foci | Elevated Nodular Formation | | Hemangiectasis | Hepatocellular Cytoplasmic Vacuolar Degeneration | | | Hepatocellular Necrosis | | | Hepatocellular Anisonucleosis | Bile Duct Epithelial Hyperplasia | Focal Mononuclear Cell Accumulations | Focal Pleocellular Accumulations | Focal Hepatic Fibrosis | Hepatocellular Hyperplastic Nodule Formation | Hepatocellular Carcinoma | Cholangiocarcinoma | Cholangioma |
|---|---|---|---|---|---|---|---|---|---|---|---|---|---|---|---|---|---|---|---|---|---|---|---|---|
| | | | | | | | | | | Min. | Mod. | Sev. | Min. | Mod. | Sev. | | | | | | | | | |
| 0 | M | 60 | 20 | 5 | 1 | 3 | 1 | | 1 | 4 | 0 | 0 | 1 | 1 | 0 | 1 | 4 | 5 | 2 | 1 | 1 | 1 | 0 | 0 |
| 1.0 % | M | 60 | 1 | 8 | 0 | 14 | 7 | | 1 | 5 | 12 | 0 | 11 | 8 | 5 | 15 | 10 | 0 | 2 | 1 | 1 | 6 | 0 | 0 |
| 0.1 % | M | 60 | 14 | 11 | 2 | 7 | 2 | | 0 | 11 | 1 | 2 | 6 | 4 | 2 | 0 | 3 | 4 | 1 | 1 | 2 | 0 | 0 | 0 |
| 0.01% | M | 60 | 24 | 8 | 0 | 3 | 1 | | 0 | 1 | 0 | 0 | 5 | 1 | 0 | 1 | 0 | 4 | 3 | 0 | 1 | 0 | 0 | 0 |
| 0 | F | 60 | 37 | 6 | 1 | 2 | 0 | | 1 | 4 | 1 | 0 | 0 | 0 | 1 | 0 | 6 | 14 | 5 | 2 | 0 | 0 | 1 | 0 |
| 1.0 % | F | 60 | 3 | 10 | 3 | 17 | 12 | | 0 | 11 | 9 | 5 | 8 | 16 | 7 | 19 | 13 | 1 | 0 | 5 | 8 | 4 | 0 | 2 |
| 0.1 % | F | 60 | 32 | 5 | 0 | 7 | 2 | | 0 | 10 | 4 | 0 | 8 | 3 | 0 | 2 | 6 | 10 | 2 | 3 | 1 | 1 | 0 | 0 |
| 0.01% | F | 60 | 36 | 6 | 0 | 2 | 0 | | 1 | 4 | 0 | 0 | 2 | 0 | 0 | 0 | 1 | 1 | 1 | 1 | 0 | 0 | 0 | 0 |

[1] Appendix 1 contains a description of the more pertinent hepatic alterations.

## TABLE 7

## RENAL ALTERATIONS OBSERVED IN RATS ADMINISTERED 1,4-DIOXANE IN THE DRINKING WATER FOR TWO YEARS[1]

| Level of Dioxane in Water | Sex | No. Rats (Initial) | No. Rats Alive at Termination | Mottling, Contraction or Granularity of Renal Surface (Gross) | Renal Glomerular Alterations | | | Renal Tubular Dilatation and Proteinaceous Cast Formation | | | Renal Interstitial Fibrosis ± Lymphocytosis | | | Nephrocalcinosis | Hydronephrosis | Purulent Nephritis ± Abscess Formation | Renal Tubular Epithelial Vacuolization and Sloughing | Increased Renal Tubular Regeneration Activity | Renal Cyst Formation | Renal Neoplasms |
|---|---|---|---|---|---|---|---|---|---|---|---|---|---|---|---|---|---|---|---|---|
| | | | | | Min. | Mod. | Sev. | Min. | Mod. | Sev. | Min. | Mod. | Sev. | | | | | | | |
| (Control) 0 | M | 60 | 20 | 17 | 16 | 9 | 9 | 12 | 17 | 11 | 7 | 11 | 6 | 1 | 0 | 3 | 0 | 0 | 1 | 0 |
| 1.0 % | M | 60 | 1 | 12 | 13 | 13 | 1 | 5 | 8 | 0 | 1 | 1 | 1 | 4 | 1 | 3 | 19 | 11 | 2 | 1* |
| 0.1 % | M | 60 | 14 | 20 | 11 | 20 | 5 | 8 | 24 | 5 | 9 | 11 | 7 | 6 | 1 | 3 | 6 | 1 | 2 | 1** |
| 0.01% | M | 60 | 24 | 19 | 16 | 16 | 4 | 17 | 17 | 4 | 14 | 7 | 4 | 1 | 0 | 3 | 0 | 0 | 3 | 0 |
| (Control) 0 | F | 60 | 37 | 8 | 19 | 22 | 2 | 20 | 12 | 4 | 11 | 7 | 2 | 0 | 0 | 2 | 0 | 0 | 1 | 0 |
| 1.0 % | F | 60 | 3 | 8 | 11 | 16 | 0 | 10 | 10 | 1 | 3 | 0 | 1 | 5 | 0 | 1 | 18 | 12 | 2 | 0 |
| 0.1 % | F | 60 | 32 | 7 | 20 | 22 | 2 | 14 | 15 | 2 | 6 | 7 | 1 | 0 | 0 | 0 | 3 | 1 | 0 | 0 |
| 0.01% | F | 60 | 36 | 10 | 27 | 21 | 3 | 23 | 14 | 2 | 10 | 5 | 2 | 0 | 0 | 0 | 1 | 0 | 1 | 1** |

*Transitional cell carcinoma of renal pelvis.

**Renal carcinoma.

[1] Appendix 2 contains a description of the more pertinent renal alterations.

### TABLE 8

### PATHOLOGIC ALTERATIONS FOUND IN RATS RECEIVING 1,4-DIOXANE IN DRINKING WATER*

|  | Sex | No. Rats (Original) | No. Rats (Terminal) | Hypophyseal Hemangiectasis ± Effusion | Adrenal Gland Hemangiectasis ± Effusion | Lymph Node Hyperplasia | Otitis Media/Interna | Meningitis/Encephalitis | Periarteritis/Sclerosis of Mesenteric Vessels | Depletion of Mesenteric Fat | Myocardial Degeneration/ Inflammation | Pericarditis | Pleuritis | Murine Pneumonia |  |  | Gastritis | Enteritis | Colonic Fecal Impaction | Colitis | Pancreatitis | Subcutaneous Cellulitis | Ovarian Cyst Formation | Metritis | Urocystitis | Prostatitis/Seminal Vesiculitis/Orchitis | Testicular Atrophy |
|---|---|---|---|---|---|---|---|---|---|---|---|---|---|---|---|---|---|---|---|---|---|---|---|---|---|---|---|
|  |  |  |  |  |  |  |  |  |  |  |  |  |  | Min. | Mod. | Sev. |  |  |  |  |  |  |  |  |  |  |  |
| 0 | M | 60 | 20 | 0 | 5 | 1 | 6 | 4 | 7 | 11 | 17 | 2 | 2 | 18 | 18 | 13 | 5 | 2 | 0 | 1 | 2 | 2 | - | - | 1 | 1 | 11 |
| 1.0 % | M | 60 | 1 | 0 | 1 | 0 | 4 | 2 | 0 | 13 | 1 | 2 | 4 | 3 | 24 | 19 | 4 | 1 | 0 | 1 | 2 | 2 | - | - | 1 | 0 | 7 |
| 0.1 % | M | 60 | 14 | 2 | 1 | 1 | 8 | 1 | 1 | 12 | 13 | 0 | 3 | 13 | 22 | 12 | 3 | 0 | 2 | 0 | 1 | 2 | - | - | 0 | 1 | 13 |
| 0.01% | M | 60 | 24 | 0 | 4 | 2 | 8 | 0 | 1 | 18 | 17 | 0 | 1 | 15 | 17 | 15 | 3 | 3 | 1 | 2 | 1 | 0 | - | - | 1 | 2 | 13 |
| 0 | F | 60 | 37 | 7 | 15 | 1 | 7 | 3 | 2 | 7 | 13 | 0 | 2 | 24 | 20 | 7 | 0 | 0 | 1 | 1 | 1 | 2 | 2 | 5 | 1 | - | -- |
| 1.0 % | F | 60 | 3 | 1 | 3 | 1 | 5 | 1 | 1 | 10 | 3 | 2 | 2 | 9 | 15 | 30 | 7 | 0 | 0 | 0 | 0 | 0 | 0 | 2 | 0 | - | -- |
| 0.1 % | F | 60 | 32 | 1 | 7 | 1 | 10 | 2 | 1 | 7 | 9 | 2 | 0 | 22 | 16 | 9 | 2 | 2 | 0 | 0 | 0 | 1 | 2 | 6 | 1 | - | -- |
| 0.01% | F | 60 | 36 | 3 | 6 | 2 | 7 | 3 | 2 | 7 | 11 | 0 | 1 | 23 | 16 | 4 | 1 | 1 | 1 | 1 | 0 | 0 | 0 | 7 | 1 | - | -- |

*Excluding hepatic, renal and neoplastic findings compiled separately.
Not included are additional pathologic alterations, such as colonic nematodiasis, urocystic nematodiasis, variable degrees of splenic hematopoiesis, oophoritis, panophthalmitis, etc. The occurrence of these unlisted alterations was scattered, and showed no dose-response relationship.
Values listed indicate number of rats in which the alteration was observed.

## TABLE 9

## MORPHOLOGIC CLASSIFICATION OF TUMORS AND HEPATOCELLULAR HYPERPLASTIC NODULES OCCURRING IN RATS RECEIVING 1,4-DIOXANE IN DRINKING WATER FOR TWO YEARS

| | Females | | | | Males | | | |
|---|---|---|---|---|---|---|---|---|
| Location and Classification | 0 | 1.0% | 0.1% | 0.01% | 0 | 1.0% | 0.1% | 0.01% |
| Mammary Gland | | | | | | | | |
| Fibroadenoma | 13 | 2 | 12 | 7 | | | | |
| Cystaadenoma | | | 1 | | | | | |
| Adenocarcinoma | | 1 | | | | | | |
| Hypophysis (Anterior) | | | | | | | | |
| Adenoma | 7 | | 5 | 9 | | | | |
| Lymphoreticular & Hematopoietic | | | | | | | | |
| Generalized Lymphosarcoma | | | 1 | 3 | | | | 2 |
| Pulmonary Lymphosarcoma | 2 | | 1 | 1 | 2 | | 2 | 1 |
| Reticulum Cell Sarcoma | | | 1 | 1 | | | | |
| Myelogenous Leukemia | 1 | 1 | | 1 | | | 1 | |
| Plasma Cell Myeloma | | | 1 | | | | | |
| Adrenal | | | | | | | | |
| Cortical Adenoma | | | | 1 | | | | |
| Uterus | | | | | | | | |
| Fibroma | | | | 2 | | | | |
| Myoma | | | | 1 | | | | |
| Adenomatous Polyp | 1 | | | | | | | |
| Fibroadenoma | 1 | | | | | | | |
| Thyroid | | | | | | | | |
| Adenoma | 1 | | | 1 | | 1 | | |
| Carcinoma | | | | | | | | 1 |
| Kidney | | | | | | | | |
| Renal Carcinoma | | | | 1 | | | 1 | |
| Transitional Cell Carcinoma | | | | | | 1 | | |
| Pancreas | | | | | | | | |
| Islet Cell Tumor | 1 | | | | | | | 3 |
| Subcutaneous Tissue | | | | | | | | |
| Undifferentiated Sarcoma | | | | | | | | 1 |
| Fibrosarcoma | 1 | | | | | | | |
| Fibroma | | 1 | | | | | 1 | |
| Pelvic Limb | | | | | | | | |
| Osteosarcoma | | | | 1 | | | | |
| Abdominal Cavity | | | | | | | | |
| Undifferentiated Carcinoma | | | | | | | 1 | |
| Hemangioma | | | | | 1 | | | |
| Undifferentiated Sarcoma | | | | | | | 1 | 1 |
| Leiomyosarcoma | | | | | | | | 1 |
| Central Nervous System | | | | | | | | |
| Glioma | | | | | | | | 2 |
| Thoracic Cavity | | | | | | | | |
| Carcinoma | 1 | | | | | | | |
| Thymus | | | | | | | | |
| Thymoma | | | 2 | | | | | 1 |
| Lung | | | | | | | | |
| Bronchiogenic Carcinoma | | | | | | | 1 | |
| Ovary | | | | | | | | |
| Fibroma | | | 1 | | | | | |
| Nasal Mucosa | | | | | | | | |
| Squamous Cell Carcinoma | | 1 | | 1 | | 1 | | |
| Liver | | | | | | | | |
| Hepatocellular Carcinoma | | 4 | 1 | | 1 | 6 | | |
| Cholangiocarcinoma | 1 | | | | | | | |
| Cholangioma | | 2 | | | | | | |
| Hepatocellular Hyperplastic Nodule Formation | 0 | 8<br>P<.05 | 1 | 0 | 1 | 1 | 2 | 1 |

Statistical analysis of Tumor Incidence has been included in Table 10.

## TABLE 10

## STATISTICAL EVALUATION OF TUMORS IN RATS RECEIVING DIOXANE IN DRINKING WATER FOR TWO YEARS

| Level of Dioxane in Drinking Water | Sex | Rats Surviving at Months |  |  |  |  |  |  |  |  |  |  |  |  | Total Tumors (No.) | TBA | Tumors/ TBA | Total Hepatic Tumors | Hepatocellular Carcinomas |
|---|---|---|---|---|---|---|---|---|---|---|---|---|---|---|---|---|---|---|---|
|  |  | 0 | 2 | 4 | 6 | 8 | 10 | 12 | 14 | 16 | 18 | 20 | 22 | 24 |  |  |  |  |  |
| 0 | M | 60 | 57 | 50 | 50 | 50 | 50 | 49 | 48 | 47 | 38 | 34 | 30 | 20 | 4 | 3 | 1.33 | 1 | 1 |
| 1.0 % | M | 60 | 58 | 43 | 33 | 32 | 32 | 31 | 30 | 28 | 22 | 12 | 3 | 1 | 9*** | 9** | 1.00 | 6** | 6** |
| 0.1 % | M | 60 | 60 | 57 | 55 | 55 | 54 | 52 | 51 | 50 | 40 | 31 | 24 | 14 | 8 | 7 | 1.14 | 0 | 0 |
| 0.01% | M | 60 | 60 | 57 | 54 | 53 | 53 | 53 | 51 | 48 | 42 | 35 | 27 | 24 | 13 | 11 | 1.18 | 0 | 0 |
| 0 | F | 60 | 60 | 59 | 59 | 59 | 59 | 57 | 55 | 53 | 51 | 46 | 43 | 37 | 30 | 27 | 1.11 | 1 | 0 |
| 1.0 % | F | 60 | 58 | 45 | 36 | 35 | 35 | 35 | 31 | 28 | 16 | 14 | 6 | 3 | 12 | 10 | 1.20 | 6** | 4* |
| 0.1 % | F | 60 | 60 | 60 | 56 | 56 | 54 | 54 | 54 | 54 | 51 | 47 | 37 | 32 | 26 | 21 | 1.24 | 1 | 1 |
| 0.01% | F | 60 | 60 | 59 | 59 | 59 | 59 | 57 | 56 | 56 | 50 | 48 | 45 | 36 | 30 | 24 | 1.25 | 0 | 0 |

TBA = Tumor Bearing Animals.

128/132 tumors occurred in rats which were necropsied from the 12th to the 24th month. Therefore statistical analyses are corrected for the numbers of rats surviving in each group at 12 months, when the first hepatic tumor was found.

*$P<0.10$; **$P<0.05$; ***$P<0.01$.

FIGURE 1

SURVIVAL RATES OF MALE RATS RECEIVING 1,4-DIOXANE IN DRINKING WATER

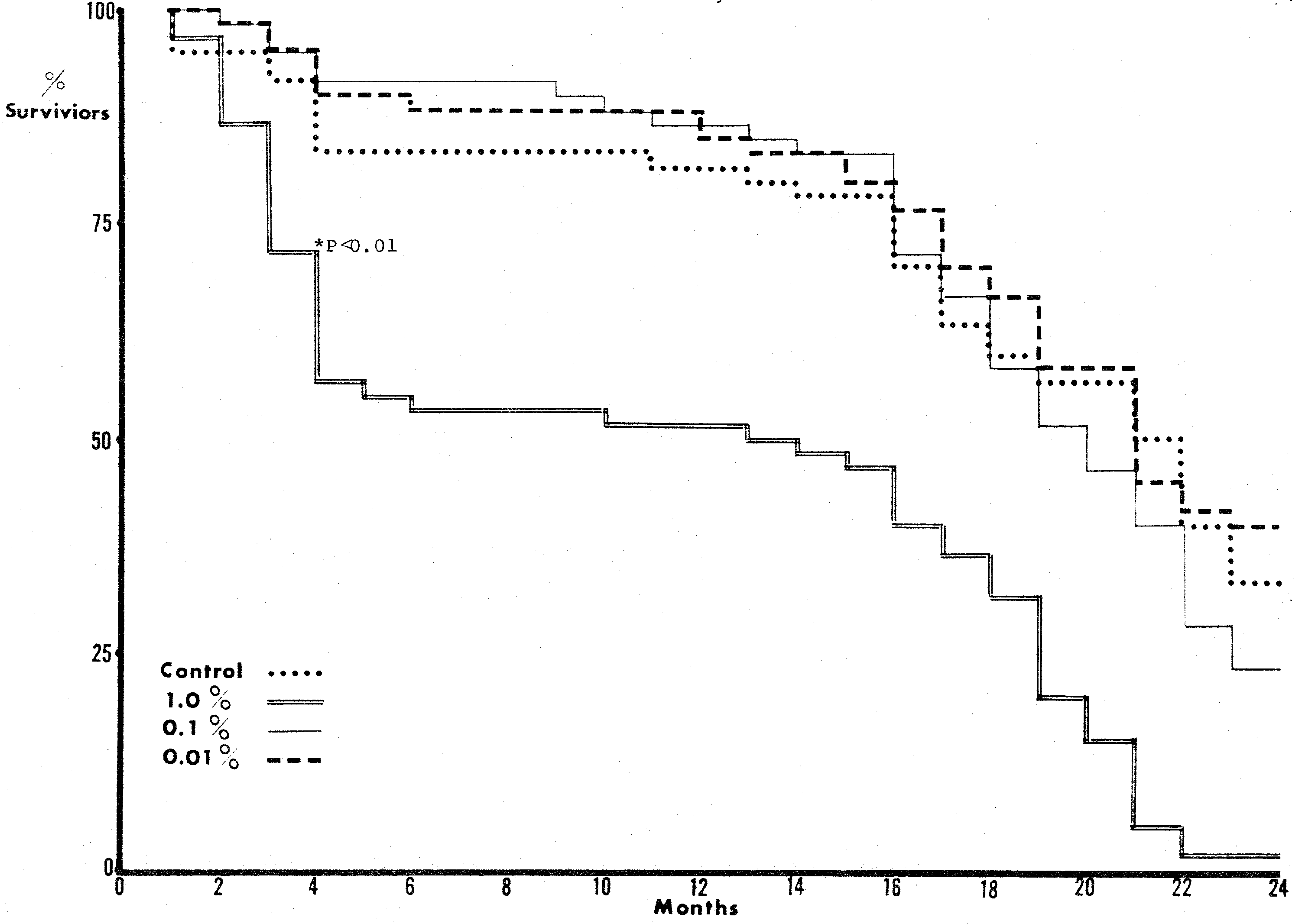

FIGURE 2

SURVIVAL RATES OF FEMALE RATS RECEIVING 1,4-DIOXANE IN DRINKING WATER

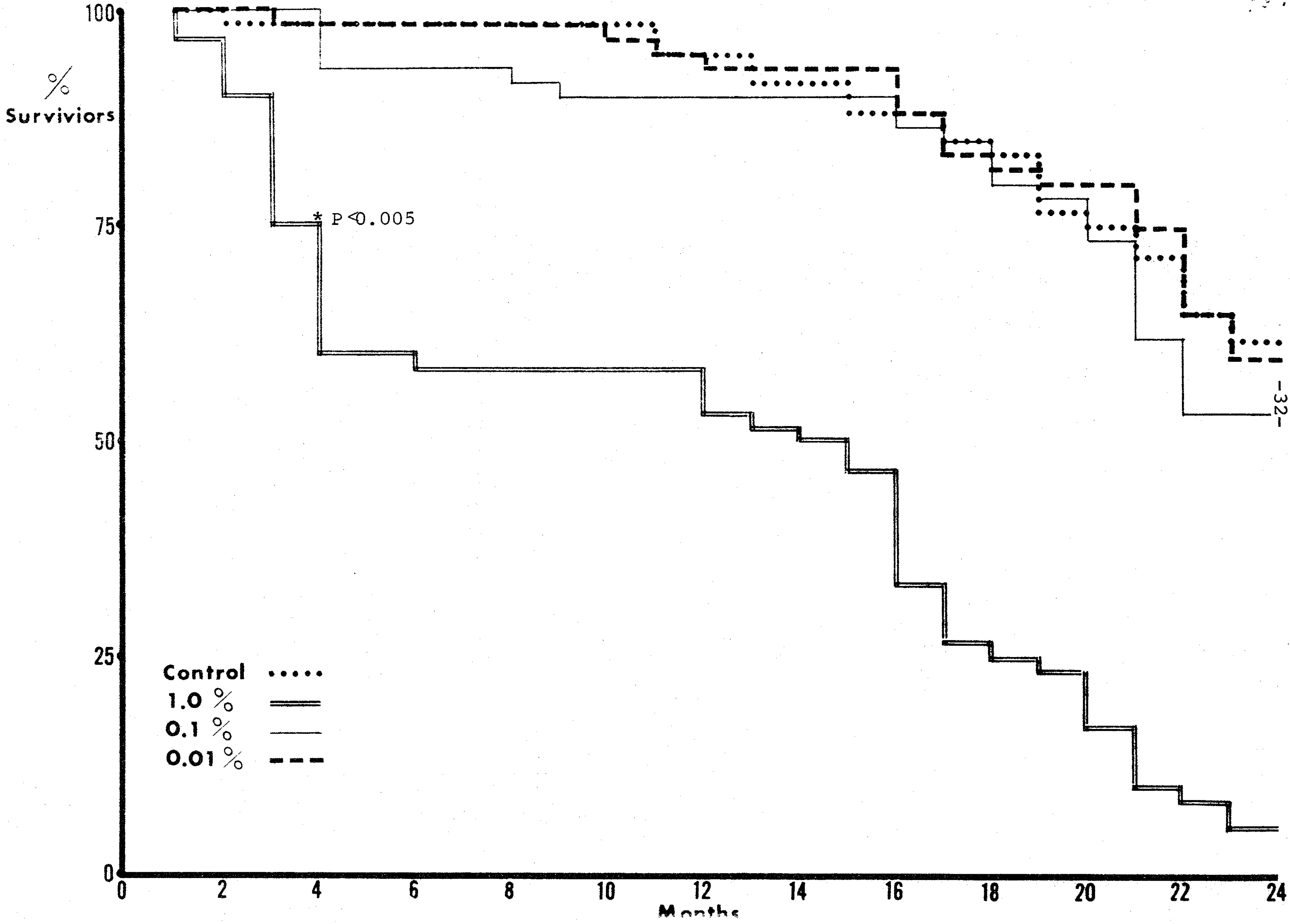

FIGURE 3

BODY WEIGHT GAINS FOR MALE RATS RECEIVING 1,4-DIOXANE IN DRINKING WATER FOR TWO YEARS

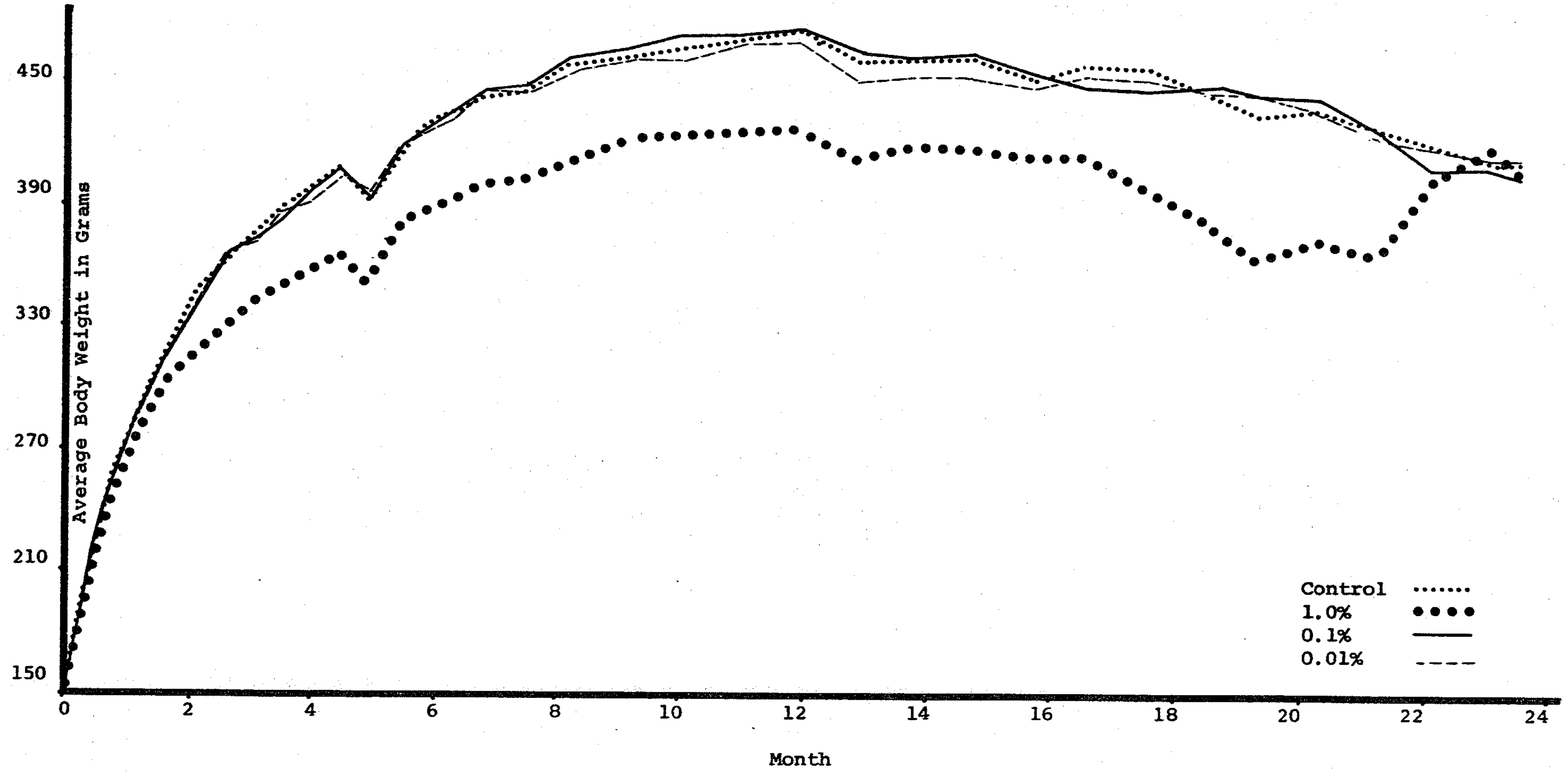

FIGURE 4

BODY WEIGHT GAINS FOR FEMALE RATS RECEIVING 1,4-DIOXANE IN DRINKING WATER FOR TWO YEARS

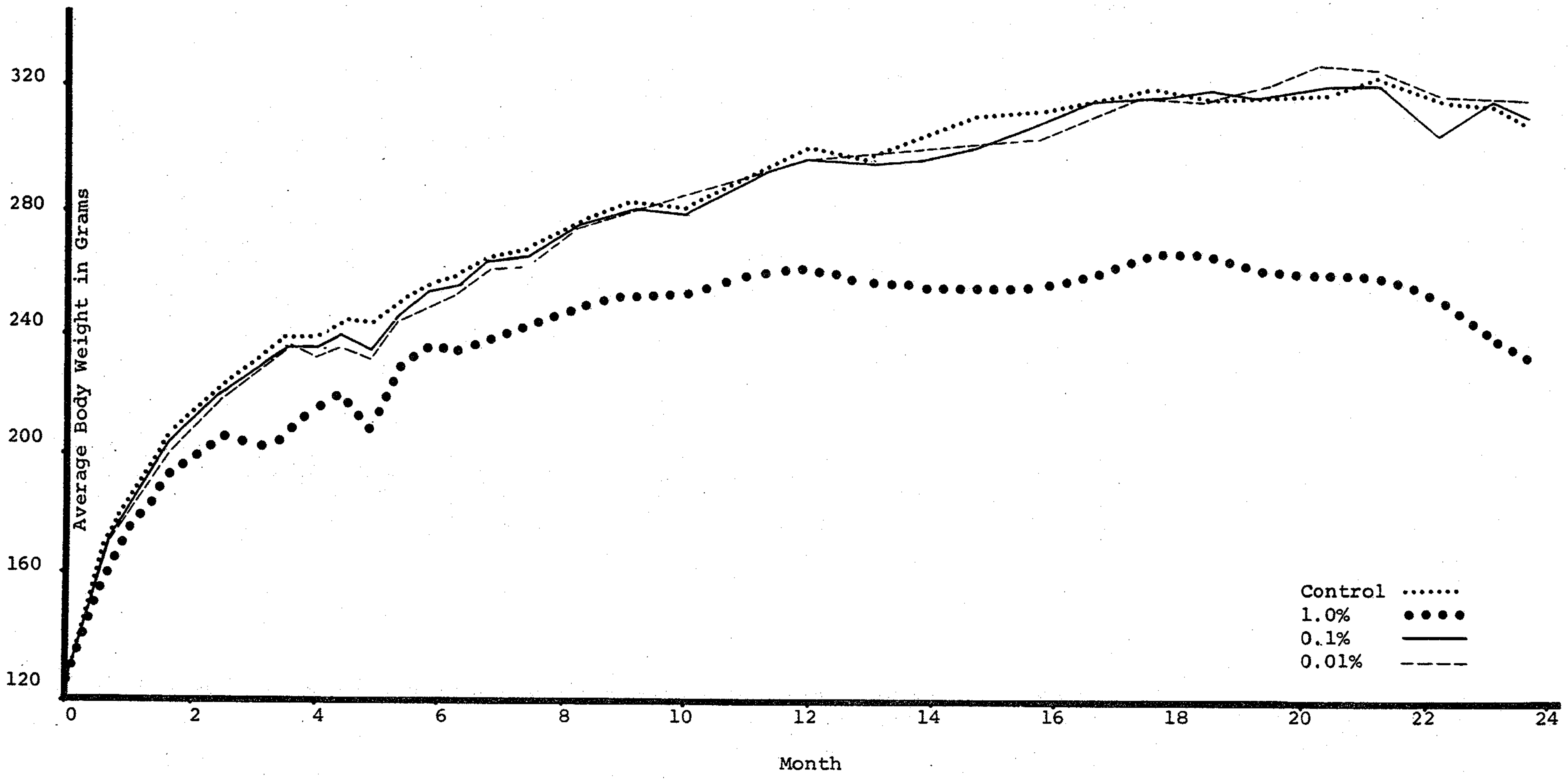

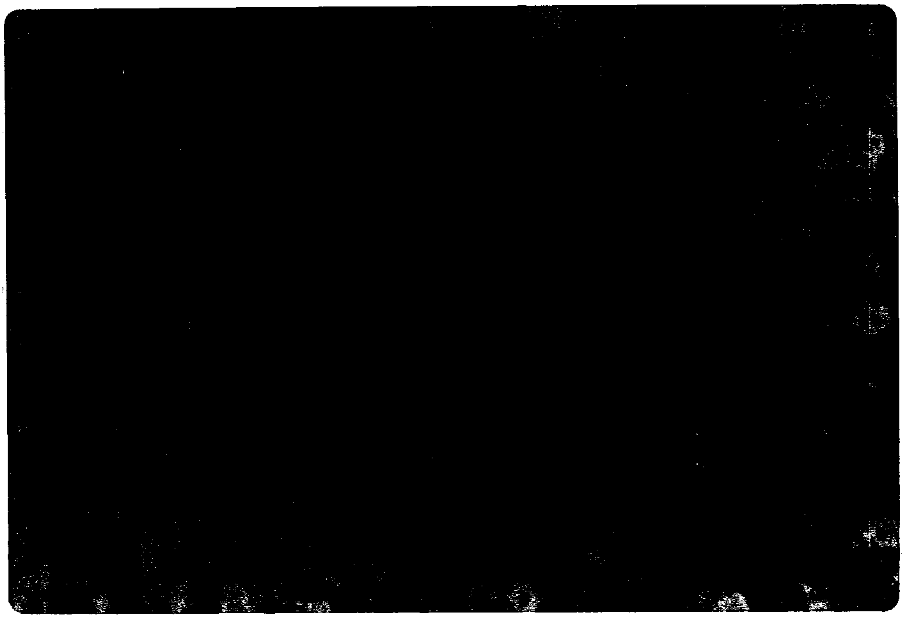

Figure 5. Hepatocellular vacuolar degeneration and necrosis in liver of rat receiving 1.0% dioxane. Note more pronounced change in centrilobular area. (arrow) H&E stain. x 125.

Figure 6. Hepatocellular hyperplastic nodule formation in liver of rat receiving 1.0% dioxane. Note compression of adjacent parenchyma by well defined nodule (upper right). H&E stain. x 125

Figure 7. Hepatocellular carcinoma (cholangiomatous area) in liver of rat receiving 1.0% dioxane. Note irregular proliferation of malignant cells. H&E stain. x 125.

Figure 8. Higher magnification of hepatocellular carcinoma in liver of rat receiving 1.0% dioxane. Note anaplastic appearance of cells with multiple nuclei and nucleoli present. H&E stain. x 630.